Synthesis and Screening of Diverse and Three-Dimensional Libraries for Fragment-Based Drug Discovery

Troelsen, Nikolaj Sten

Publication date:
2020

Document Version
Publisher's PDF, also known as Version of record

Synthesis and Screening of Diverse and Three-Dimensional Libraries for Fragment-Based Drug Discovery

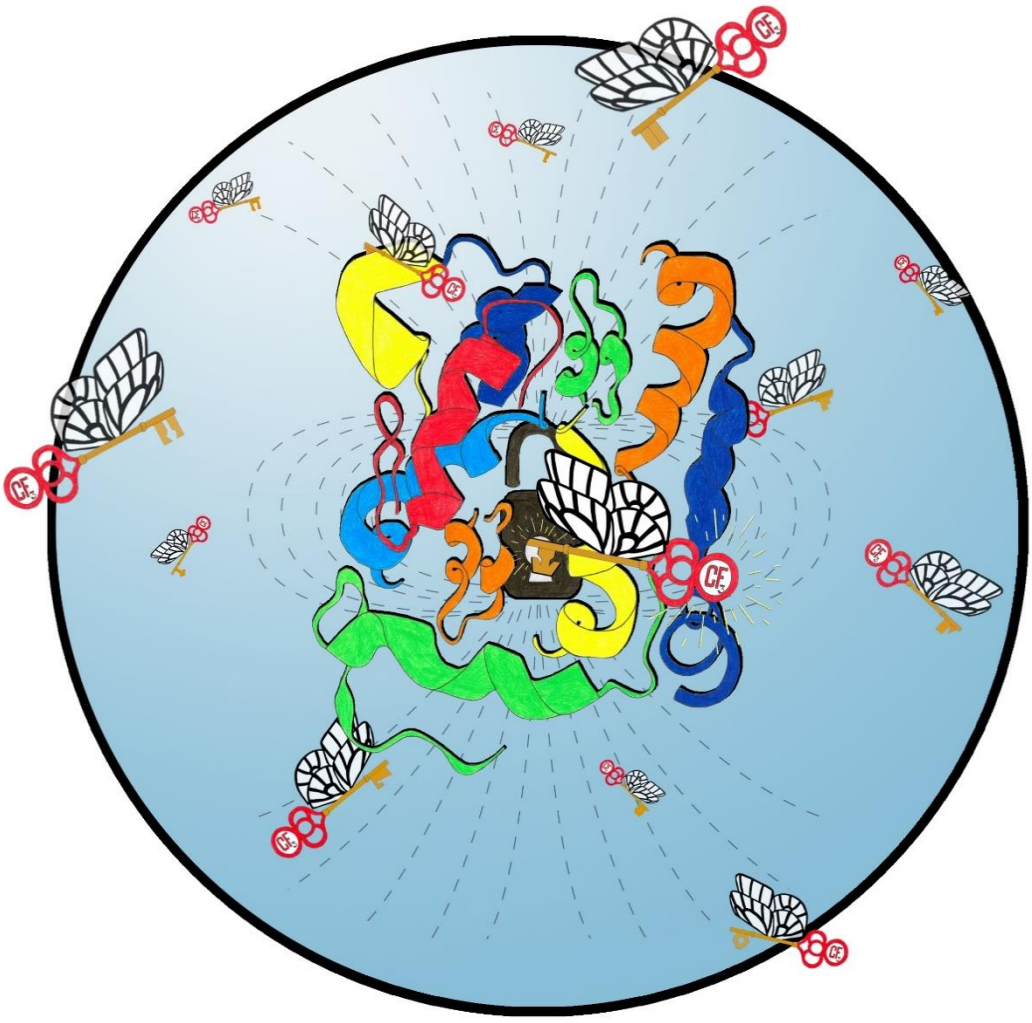

PhD Thesis by
Nikolaj Sten Troelsen
February 2020

DTU

Synthesis and Screening of Diverse and Three-Dimensional Libraries for Fragment-Based Drug Discovery

PhD Thesis by
Nikolaj Sten Troelsen
February 2020

DTU Chemistry
Technical University of Denmark
Kemitorvet, building 206
2800 Kgs. Lyngby
Denmark

PhD Supervisors:
Professor Mads H. Clausen
Associate Professor Charlotte H. Gotfredsen

Form follows function – that has been misunderstood.
Form and function should be one, joined in a spiritual union.

architect Frank Lloyd Wright, 1908

Preface

The work presented in this thesis is the result of my PhD studies at the Technical University of Denmark (DTU) from January 2017 to February 2020 under supervision of Professor Mads H. Clausen and Associate Professor Charlotte H. Gotfredsen. A five month external stay was conducted at the University of Cambridge, UK in the laboratory of Professor David R. Spring.

This thesis is divided into three parts – Part I provides a general introduction to fragment-based drug discovery, biophysical screening techniques, library synthesis, and fluorine. Part II describes the synthesis and biological evaluation of a fluorinated fragment library and was performed at DTU. Part III covers the synthesis of diverse and natural product-like small molecules for fragment-based drug discovery and was undertaken at the University of Cambridge. A list of publications authored during the PhD program is provided on page *ix* with publications related to work described herein highlighted in bold. Highlighted publications are attached in the appendix of this thesis.

A number people have contributed to the work presented in Part II of this thesis. Under my co-supervision, a group of MSc and BSc students have helped synthesize some of the compounds presented herein. The majority of chemistry presented in Part II was developed by myself and the students have primarily helped with synthesis of additional analogues or optimization of reaction conditions. These students are listed in the acknowledgements and are credited for the synthesis of individual compounds in the experimental section at the end of the thesis. In addition, collaboration partners at the Max-Planck Institute (MPI) of Colloids and Interfaces in Potsdam and the Centro Nacional de Biotecnología (CNB)/Consejo Superior de Investigaciones Científicas (CSIC) in Madrid have contributed with work related to certain of the protein targets presented.

In this thesis, absolute and relative stereochemistry is differentiated by the use of wedged (,) and unwedged (,) bonds, respectively. Diastereoselectivity, reported either as diastereomeric ratio (*dr*) or ratio of *endo*/*exo*, were calculated using crude ^{1}H or ^{19}F NMR. Generally, all new compounds (excluding byproducts) have been fully characterized with melting point (if applicable), ^{1}H NMR, ^{13}C NMR, ^{19}F NMR (if applicable), IR, and HRMS. Experimentals for both parts can be found at the end of the thesis. Analytical data including fully assigned NMR spectra and NMR screening data can be found in the separate Supporting Information.

Nikolaj Sten Troelsen

Acknowledgements

I am truly grateful to my supervisor Professor Mads H. Clausen. His mentorship since the beginning of my MSc studies at DTU has been much appreciated and a tremendous learning experience. I thank him for his trust and the independence that he inspire. It has been a most pleasurable collaboration. I would also sincerely like to thank my co-supervisor Associate Professor Charlotte H. Gotfredsen for her enormous support and training in NMR spectroscopy. Her insights have been absolute key to the fruitful results of this thesis and I am grateful for all her dedication and patience.

I am thankful to Professor David R. Spring for accepting me in his laboratory at the University of Cambridge for my external research stay. I thank Abi Hanby and Dr. Thomas J. Osberger for their supervision during this stay. The entire Spring group is also thanked for their warm and humorous mood with a special thanks to Hikaru Seki, Dr. Stephen Walsh, and Dr. Kim T. Mortensen for their help and good company.

The technical staff of the department, namely Philip Charlie Johansen, Brian L. Dideriksen, Anne Hector, and Kasper Enemark-Rasmussen are gratefully acknowledge for their technical expertise and tremendous effort in keeping the department afloat. Johanne M. Nielsen and Lisbeth Riber are thanked for their assistance with ordering chemicals and cleaning glassware, respectively. Jette B. Nestén is also thanked for her always helpful attitude with various practical matters.

I would like to extend my gratitude to collaboration partners for productive partnerships: Elena Shanina, Hengxi Zhang, and Dr. Christoph Rademacher at the Max-Planck Institute of Colloids and Interfaces (Potsdam) and Diego Gonzalez-Romero, Dr. Juan J. Sanz-Ezquerro, and Dr. Ana Cuenda from the Centro Nacional de Biotecnología/Consejo Superior de Investigaciones Científicas (Madrid).

Professor Pernille Harris is thanked for her expertise in X-ray crystallography and her help with obtaining crystal structures. I would also like to thank Professor Ruth Brenk from the University of Bergen for her invitation to visit her lab and Illimar H. Rekand for taking the time to introduce me to their screening facilities. Dr. Chris Empson, Dr. Gauthier M. L. Scavée, and Caspar A. B. Jespersen are thanked for their help regarding PMI analysis and Python programming.

Current and former members of the Clausen group are gratefully acknowledged for creating a fun and ambitious working environment. I would like to thank Dr. Faranak Nami for her assistance with NMR screening along with Dr. Jorge Peiró and Dr. Viola Previtali for many fun hours of writing a review article. Dr. Cecilia Romanó, Dr. Faranak Nami, Dr. Hao Jiang, and Dr. Ulrik B Keiding are thanked for their feedback and valuable discussions during the writing of my thesis. I also owe great thanks to the many talented students who have contributed to my research. These include MSc students Daniela Danková, Ida S. A. Jensen, Katarzyna J. Śniady, and Ana Laura da Silva and BSc students Anastasia E. Richter, Mie A.

Larsen, Sanne L. Møller, Thomas P. Klevin, Joakim M. Svensson, Julie Forchhammer, and Pernille V. Christensen.

The Department of Chemistry at DTU is thanked for the awarded Excellence Scholarship to fund my PhD studies. Biorender.com is acknowledged for its use in creating Figure 1.7, Figure 1.12, Figure 1.16, and Figure 1.18.

I would also like to show my gratitude to the other member of the Lunch Club, Kristoffer H. Møller, for valuable discussions over lunch. Finally, I am thankful to my friends and family for all their support and affection. In particular, I would like to thank my wife, Kathrin, for all her love and patience as well as valued scientific discussions throughout my PhD studies.

Abstract

Fragment-based drug discovery (FBDD) has become a powerful strategy for the discovery of new pharmaceuticals. However, in spite of its success, FBDD still suffers from a limited diversity of fragments libraries applied and by cumbersome screening workflows. To address these challenges, two novel fragment libraries were constructed following different strategies.

The first approach describes the design and synthesis of a fluorinated Fsp^3-rich fragment (3F) library – the first synthetic fragment library tailor-made for efficient ^{19}F NMR screening (Figure i). A total of 115 diverse fragments were synthesized in a minimal number of steps from a group of similar fluorinated starting materials. With a low average AlogP and a high degree of shape diversity, the 3F library demonstrated significant improvements over commercial fragment collections. As a proof-of-concept, biological evaluation of the 3F library was performed using ^{19}F NMR-based screening against seven protein targets affording hit rates of 3–15%.

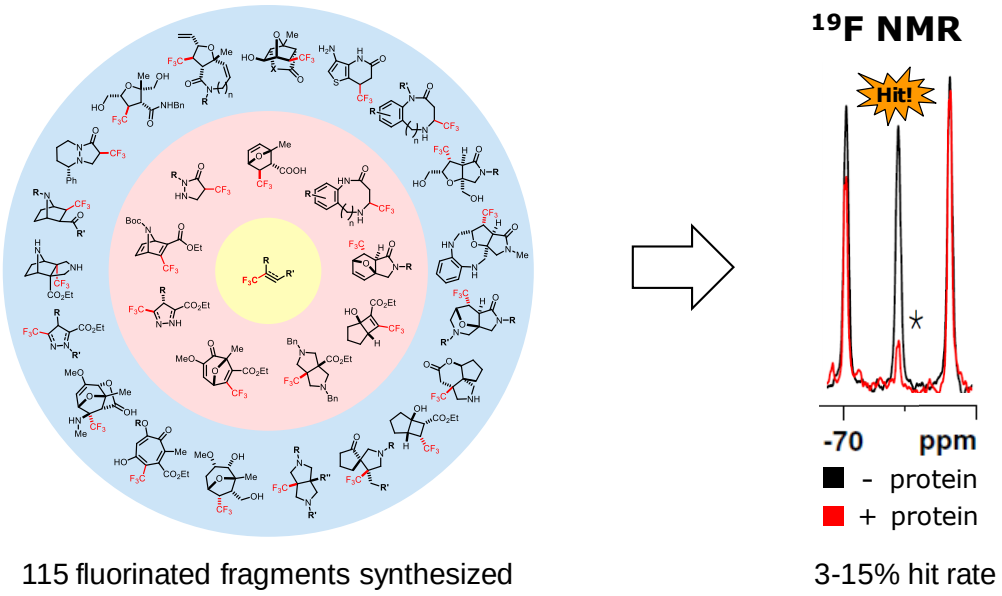

Figure i. Synthesis and biological evaluation using ^{19}F NMR of the fluorinated Fsp^3-rich fragment (3F) library. Adapted with permission from reference.[1] Copyright (2020) John Wiley and Sons.

In the second approach, a small library of natural product-like fragments bearing quaternary carbon atoms was synthesized. Using diversity-oriented synthesis from a pair of diastereomeric building blocks, the library was constructed in an efficient manner. The structurally diverse fragments exhibited highly desirable properties including a high degree of three-dimensionality and incorporation of multiple exit vectors for later fragment optimization (Figure ii).

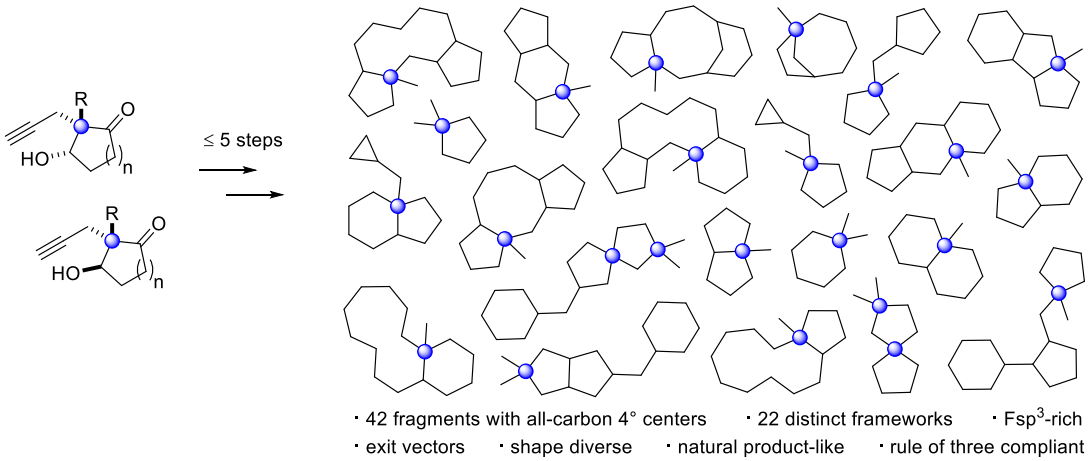

Figure ii. Diversity-oriented synthesis of 42 natural product-like and diverse fragments containing all-carbon quaternary centers for increased three-dimensionality.

Resumé

Fragment-baseret lægemiddeludvikling er blevet en effektiv tilgang til udvikling af nye lægemidler. På trods af metodens succes lider fragment-baseret lægemiddeludvikling stadig af en begrænset tilgang til forskelligartede fragmenter samt tidskrævende screeningsprocesser. I et forsøg på at imødekomme disse udfordringer er to nye fragment biblioteker blevet fremstillet via forskellige strategier.

I den første tilgang beskrives designet og syntese af et fluoreret Fsp^3-rigt fragment (3F) bibliotek – det første syntetiske fragment bibliotek skræddersyet til effektivt screening med ^{19}F NMR (Figur i). I alt blev 115 diverse fragmenter syntetiseret i få trin fra en gruppe af beslægtede fluorerede startmaterialer. Med en lav gennemsnitlig AlogP og en høj grad af formdiversitet udviser 3F biblioteket betydelige forbedringer over kommercielle fragment samlinger. Som demonstration bibliotekets brugbarhed blev fragmenterne screenet mod forskellige sygdomsrelevante proteiner med ^{19}F NMR og resulterede i hit rater mellem 3–15%.

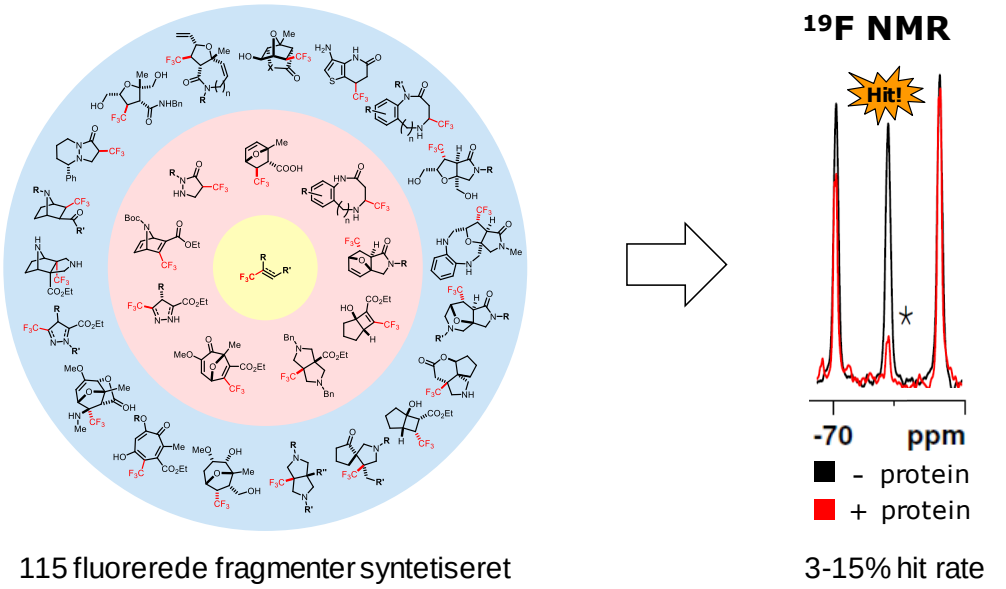

Figur i. Syntese og biologisk evaluering med ^{19}F NMR af det fluorinerede Fsp^3-rige fragment (3F) bibliotek. Tilrettet med tilladelse fra reference.[1] Copyright (2020) John Wiley and Sons.

Det andet bibliotek bestod af 42 naturprodukt-lignende fragmenter med kvarternære kulstofcentre. Biblioteket blev syntetiseret ved brug af diversitets-orienteret syntese fra to diastereomeriske byggeblokke. De forskelligartede fragmenter udviste fremragende egenskaber heriblandt en høj grad af tredimensionalitet samt tilstedeværelse af flere exit vektorer til senere fragmentoptimering (Figur ii).

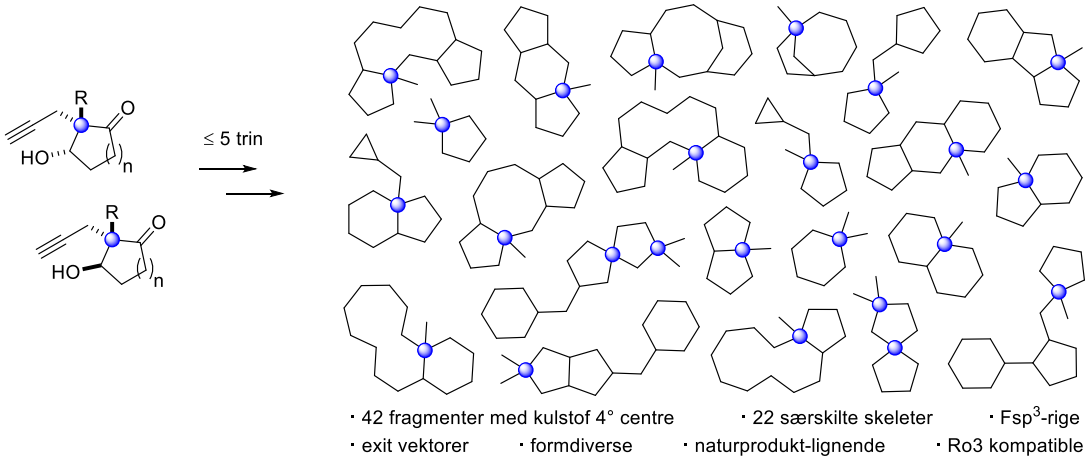

Figur ii. Diversitets-orienteret syntese af 42 naturprodukt-lignende and diverse fragmenter med kulstof kvarternære centre til forøgelse af tredimensionalitet.

List of Publications

1. **The 3F Library: Fluorinated Fsp^3-rich Fragments for Expeditious ^{19}F NMR-based Screening.** Troelsen, N. S., Shanina, E. Gonzalez-Romero, D. Danková, D. Jensen, I. S. A., Śniady, K. J., Nami, F., Zhang, H., Rademacher, C., Cuenda, A., Gotfredsen, C. H., Clausen, M. H., *Angew. Chem. Int. Ed.,* **2020**, *59*, 2204 (frontispiece).*

2. **Fsp^3-rich and Diverse Fragments Inspired by Natural Products as a Collection to Enhance Fragment-Based Drug Discovery.** Hanby, A. R., Troelsen, N. S., Osberger, T. J., Kidd, S. L., Mortensen, K. T., Spring, D. R., *Chem. Commun.*, **2020**, *56*, 2280.*

3. **Library Design Strategies to Accelerate Fragment-Based Drug Discovery**. Troelsen, N. S., Clausen, M. H., *manuscript submitted to Chem. – Eur. J.*, **2020**.*

4. Auxiliary *in vitro* and *in vivo* biological evaluation of hydrogen peroxide sensitive prodrugs of methotrexate and aminopterin for the treatment of rheumatoid arthritis. Previtali, V., Petrovic, K., Cadahía, J. P., Troelsen, N. S., Clausen, M. H., *Bioorg. Med. Chem.*, **2020**, *28*, 115247.

5. Prodrug Strategies for Targeted Therapy Triggered by Reactive Oxygen Species. Cadahía, J. P.,† Previtali, V.,† Troelsen, N. S.,† Clausen, M. H., *MedChemComm*, **2019**, *10*, 1531 (inside front cover).

6. Heteropolycyclic Scaffold Library Generation from a Highly Diastereoselective Petasis/Diels-Alder and ROM-RCM Reaction Sequence. Flagstad, T., Azevedo, C. M. G., Troelsen, N. S., Ming, G. K., Nielsen, T. E., Clausen, M. H., *Eur. J. Org. Chem.*, **2019**, *2019*, 1061.

7. Methotrexate Prodrugs Sensitive to Reactive Oxygen Species for the Improved Treatment of Rheumatoid Arthritis. Andersen, N. S.,‡ Cadahía, J. P., Hansen, A. E., Clausen, M. H., *Eur. J. Med. Chem.*, **2018**, *156*, 738.

8. Prodrugs til Forbedret Behandling af Leddegigt. Andersen, N. S.,‡ Cadahía, J. P., Previtali, V., Clausen, M. H.. *Dansk Kemi*, **2018**, *99*, 10 (popular science).

9. Synthesis and Formulation Studies of Griseofulvin Analogues with Improved Solubility and Metabolic Stability. Petersen, A. B., Andersen, N. S.,‡ Konotop, G.; Hanafiah, N. H. B.; Raab, M. S., Krämer, A., Clausen, M. H. *Eur. J. Med. Chem.*, **2017**, *130*, 240.

---

* Related to work described herein. Attached in the appendix (p. 299).
† Authors have contributed equally to this work.
‡ Name change from *Andersen* to *Troelsen* in 2018.

Table of Contents

Abbreviations xiii
Introduction 1

Part I 3

1.1. Fragment-Based Drug Discovery 5
1.1.1. What is a Fragment? 6
1.2. Fragment-Based Screening 7
1.2.1. Ligand-Observed NMR Spectroscopy 8
1.2.2. Protein-Observed NMR Spectroscopy 11
1.2.3. X-Ray Crystallography 12
1.2.4. Surface Plasmon Resonance 14
1.2.5. Isothermal Titration Calorimetry 15
1.2.6. Mass Spectrometry 16
1.2.7. Fluorescence-Based Thermal Shift Assay 16
1.2.8. Virtual Screening 17
1.2.9. Microscale Thermophoresis 18
1.2.10. Affinity-based Separation 19
1.2.11. Other Techniques 20
1.3. Fragment Elaboration 21
1.3.1. Case Studies 22
1.4. Fragment Library Design 25
1.4.1. Unsuitable Functional Groups and PAINS 25
1.4.2. Library Diversity 27
1.4.3. Molecular shape diversity 28
1.4.4. Library construction 30
1.5. Diversity-Oriented Synthesis 31
1.5.1. Applications in FBDD 33
1.6. Fluorine 36
1.6.1. Properties of Fluorine 36
1.6.2. Fluorine in Medicinal Chemistry 38
1.6.3. ^{19}F NMR Spectroscopy 40
1.6.4. ^{19}F NMR-Based Screening 42
1.6.5. Fluorine Moieties for ^{19}F NMR 43

Part II 45

2.1. Project Outline 47
2.2. Library Design 48
2.3. Library Synthesis 50
2.3.1. Furan Diels-Alder 50

2.3.2. Intramolecular Diels-Alder ... 58
2.3.3. Pyrrole Diels-Alder ... 63
2.3.4. [5+2] Cycloaddition ... 68
2.3.5. [2+2] Cycloaddition ... 74
2.3.6. Double [3+2] cycloaddition – Pyrrolidine ... 80
2.3.7. [3+2] Cycloaddition – Dihydropyrazole ... 82
2.3.8. Dinucleophile Cyclization ... 86
2.3.9. Hydrazine Cyclization – Pyrazolidinone ... 90
2.3.10. Other Scaffolds ... 94
2.4. Chemoinformatic Library Analysis ... 98
2.4.1. Physicochemical Properties ... 98
2.4.2. PMI Analysis ... 101
2.4.3. Natural Product-Likeness ... 102
2.5. NMR-Based Screening ... 105
2.5.1. Quality Control ... 105
2.5.2. Protein Targets ... 107
2.5.3. Primary ^{19}F NMR-Based Screening ... 108
2.5.4. Validation by ^{1}H NMR ... 110
2.5.5. Further Studies ... 111
2.5.6. Analysis and Discussion ... 114
2.6. Conclusion ... 117
2.7. Future Perspectives ... 118
Part III ... 121
3.1. Project Outline ... 123
3.2. Library Synthesis ... 127
3.2.1. Building Block Synthesis ... 127
3.2.2. *Anti* Building Block Chemistry ... 128
3.2.3. *Syn* Building Block Chemistry ... 137
3.2.4. Building Block Derivatives ... 145
3.3. Chemoinformatic Library Analysis ... 146
3.3.1. Physicochemical Properties ... 147
3.3.2. PMI Analysis ... 147
3.3.3. Natural Product-Likeness ... 149
3.4. Conclusion ... 151
3.5. Future Perspectives ... 152
Experimentals ... 155
4.1. Part II ... 157
4.2. Part III ... 245
References ... 275
Appendix ... 299

Abbreviations

2D	two-dimensional
3D	three-dimensional
3F	fluorinated Fsp^3-rich fragment
Aβ	amyloid β
AAC	azide alkyne cycloaddition
Ac	acetyl
AD	Alzheimer's disease
AIBN	α,α′-azoisobutyronitrile
Ala	alanine
All	allyl
AlogP	atomic partition coefficient
aq.	aqueous
Arg	arginine
At	7-azabenzotriazole
ATF2	activating transcription factor 2
BACE1	β-site APP-cleaving enzyme 1
BCL2	B-cell lymphoma 2
BDE	bond dissociation energy
BIOS	biology-oriented synthesis
Bn	benzyl
Boc	*tert*-butyloxycarbonyl
br.	broad
brsm	based on recovered starting material
Bt	benzotriazole
BTFFH	fluoro-dipyrrolidinocarbenium hexafluorophosphate
Bu	butyl
BVO	Baeyer-Villiger oxidation
B/C/P	build/couple/pair
calcd	calculated
Cbz	benzyloxy carbamate
CDK2	cyclin-dependent kinase 2
CE	capillary electrophoresis
cm	centimeter
CNB	Centro Nacional de Biotecnología
CNS	central nervous system
cod	1,5-cyclooctadiene

CPMG	Carr-Purcell-Meibom-Gill
Cp	cyclopentadienyl
Cp*	pentamethylcyclopentadienyl
CSA	chemical shift anisotropy
CSIC	Consejo Superior de Investigaciones Científicas
CuAAC	copper(I)-catalyzed alkyne azide cycloaddition
Cy	cyclohexyl
d	doublet
D	debey
Da	dalton
DA	Diels-Alder
DABCO	1,4-diazabicyclo[2.2.2]octane
DBU	1,8-diazabicyclo[5.4.0]undec-7-ene
DCC	dicyclohexylcarbodiimide
DCE	1,2-dichloroethane
DC-SIGN	dendritic cell-specific intercellular adhesion molecules-3-grabbing non-integrin
dCSP	differential chemical shift perturbation
dd	doublet of doublets
ddd	doublet of doublet of doublets
dddd	doublet of doublet of doublet of doublets
ddt	doublet of doublet of triplets
DEAD	diethyl azodicarboxylate
DIAD	diisopropyl azodicarboxylate
DIBAL	diisobutylaluminum
DIPEA	*N*,*N*-diisopropylethylamine
DMAD	dimethyl acetylenedicarboxylate
DMAP	4-(dimethylamino)pyridine
DMF	*N*,*N*-dimethylformamide
DMPO	5,5-dimethyl-1-pyrroline *N*-oxide
DMSO	dimethyl sulfoxide
DNA	deoxyribonucleic acid
DOI	digital object identifier
DOS	diversity-oriented synthesis
dq	doublet of quartets
dr	diastereomeric ratio
DSF	differential scanning fluorimetry
dt	doublet of triplets
DTT	dithiothreitol
DTU	Technical University of Denmark

E. coli	*Escherichia coli*
EDC	*N*-ethyl-*N*′-(3-dimethylaminopropyl)carbodiimide
EDTA	ethylenediaminetetraacetic acid
EGTA	ethylene glycol-bis(2-aminoethylether)-*N*,*N*,*N*′,*N*′-tetraacetic acid
EM	electron microscopy
eq.	equation
equiv.	equivalents
er	enantiomeric ratio
ESI	electron spray ionization
Et	ethyl
etc.	*et cetera*
EWG	electron withdrawing group
EYCM	enyne cross-metathesis
e.g.	*exempli gratia*
FAXS	fluorine chemical shift anisotropy and exchange for screening
FBDD	fragment-based drug discovery
FBS	fragment-based screening
FDA	Food and Drug Administration
Fsp^3	fraction of sp^3-hybridized carbons
FT	Fourier transform
g	gram
GABA	γ-aminobutyric acid
Gly	glycine
Grubbs II	Grubbs 2nd generation catalyst
GST	glutathione-S-transferase
h	hour
HAC	heavy atom count
HATU	1-[bis(dimethylamino)methylene]-1*H*-1,2,3-triazolo[4,5-*b*]pyridinium 3-oxid hexafluorophosphate
HBA	hydrogen-bond acceptor
HBD	hydrogen-bond donor
HEPES	4-(2-hydroxyethyl)piperazine-1-ethanesulfonic acid
hept	heptet
Het	heteroatom
HG II	Hoveyda-Grubbs 2nd generation catalyst
HIV	human immunodeficiency virus
HMBC	heteronuclear multiple bond correlation spectroscopy
HMDS	hexamethyldisilazane
HOMO	highest occupied molecular orbital

HPLC	high-performance liquid chromatography
HRMS	high-resolution mass spectrometry
HSA	human serum albumin
HSQC	heteronuclear single quantum coherence
I	moment of inertia
IBX	2-iodoxybenzoic acid
IC_{50}	half maximal inhibitory concentration
ICAM	intercellular adhesion molecule
ID_{50}	half maximal infectious dose
IMDA	intramolecular Diels-Alder
^{i}Pr	isopropyl
IR	infrared
ITC	isothermal titration calorimetry
i.e.	*id est*
J	coupling constant
K_d	dissociation constant
kJ	kilojoule
L	liter
LCMS	liquid chromatography mass spectrometry
LDA	lithium diisopropylamide
LE	ligand efficiency
LLE	ligand-lipophilicity efficiency
LOGSY	ligand observed *via* gradient spectroscopy
LOS	lead-oriented synthesis
LUMO	lowest unoccupied molecular orbital
m	multiplet
m	*meta*
M	molar
MAPK	mitogen-activated protein kinase
MBP	Myelin basic protein
*m*CPBA	*meta*-chloroperoxybenzoic acid
Me	methyl
MHz	mega hertz
Min.	minutes
MMP	matrix metalloproteinase
m.p.	melting point
MPI	Max Planck Institute
ms	millisecond
Ms	methanesulfonyl

MS	molecular sieves or mass spectrometry
MST	microscale thermophoresis
MW	molecular weight
n	normal
NA	not applicable
NADPH	nicotinamide adenine dinucleotide phosphate
ND	not determined
NHS	*N*-hydroxysuccinimide
nm	nanometer
NMM	*N*-methylmorpholine
NMR	nuclear magnetic resonance
NMRAL1	nitrogen metabolite repression A-like redox sensor 1
NOE	nuclear Overhauser effect
NOESY	nuclear Overhauser effect spectroscopy
NP	natural product
nROT	number of rotatable bonds
o	*ortho*
p	*para*
p	pentet
p70S6K1	ribosomal protein S6 kinase beta-1
P-gp	P-glycoprotein
PAINS	pan-assay interference compounds
PBF	plane of best fit
PBS	phosphate buffered saline
PDA	photodiode array
PDB	protein data bank
PDK1	3-phosphoinositide-dependent protein kinase-1
pDOS	privileged-substructure-based diversity-oriented synthesis
Ph	phenyl
PMB	*para*-methoxybenzyl
PMI	principal moment of inertia
PMSF	phenylmethylsulfonyl fluoride
PPI	protein-protein interaction
ppm	parts per million
Pr	propyl
Pro	proline
PSA	polar surface area
PyBOP	benzotriazol-1-yl-oxytripyrrolidinophosphonium hexafluorophosphate
PyBroP	bromotripyrrolidinophosphonium hexafluorophosphate
q	quartet

qd	quartet of doublets
QF	quaternary fragment
qq	quartet of quartets
RCEYM	ring-closing enyne metathesis
RCM	ring-closing metathesis
R_f	retention factor
RNA	ribonucleic Acid
Ro3	rule of three
Ro5	rule of five
ROE	rotating-frame Overhauser enhancement
ROESY	rotating-frame Overhauser enhancement spectroscopy
ROM	ring-opening metathesis
RP	reversed phase
rpm	revolutions per minute
R_t	retention time
s	singlet
SAR	structure-activity relationship
sat.	saturated
SD	standard deviation
SEM	standard error mean
sept	septet
SPhos	2-dicyclohexylphosphino-2′,6′-dimethoxybiphenyl
STD	saturation-transfer difference
t	triplet
$t_{1/2}$	half-life
T_2	transverse relaxation
TBAF	tetra-*n*-butylammonium fluoride
TBAI	tetra-*n*-butylammonium iodide
TBHP	*tert*-butyl hydroperoxide
TBS	*tert*-butyldimethylsilyl
^{t}Bu	*tert*-butyl
td	triplet of doublets
tdd	triplet of doublet of doublets
Tf	trifluoromethanesulfonate
TFA	trifluoroacetic acid
THF	tetrahydrofuran
Thr	threonine
TLC	thin layer chromatography
T_m	unfolding temperature
TM	trademark

TMS	trimethylsilyl
Tris	2-amino-2-(hydroxymethyl)-1,3-propanediol
Ts	toluenesulfonyl
TS	thermal shift
UPLC	ultra-performance liquid chromatography
UV	ultraviolet
V	volume
vdW	van der Waals
WAC	weak affinity chromatography
WLOGSY	water-ligand observed *via* gradient spectroscopy
wt	weight
Å	angstrom
γ	magnetogyric ratio
δ	chemical shift
λ	wavelength
µs	microsecond
µW	microwave
τ_c	rotational correlation time

Introduction

Fragment-based drug discovery (FBDD) has emerged as a powerful tool for the discovery of new drug leads.[2–4] By screening smaller molecules (fragments), FBDD offers increased hit rates and superior sampling of chemical space as compared to the traditional high-throughput screening (HTS). The methodology relies on sensitive biophysical techniques such as X-ray crystallography and NMR spectroscopy to detect the generally weaker binding of fragments. However, in spite of the success of FBDD, the approach still suffers from laborious workflows of many screening platforms and a low diversity of the fragments applied. Thus, in an effort to address these shortcomings, new approaches to the design and synthesis of fragment libraries are addressed in this thesis.

The thesis has been divided into three parts. Part I will provide a general introduction to FBDD with an overview of the major biophysical screening techniques available with emphasis on NMR methods. Fragment library design is discussed with focus on library diversity and how to achieve this with synthesis. The final chapter is dedicated to fluorine and its unique properties regarding medicinal chemistry and NMR-based screening.

Part II is titled "The 3F Library: Fluorinated Fsp^3-rich Fragments for Expeditious ^{19}F NMR-based Screening" and describes a library design strategy to improve both fragment diversity and subsequent screening workflows. Herein, the design and synthesis of a novel and diverse library of fluorinated fragments is presented followed by its biological evaluation using ^{19}F NMR-based screening.

Finally, Part III describes a different synthetic approach to obtaining structural diversity of fragments and is entitled "Fsp^3-rich and Diverse Fragments Inspired by Natural Products as a Collection to Enhance Fragment-Based Drug Discovery". Quaternary stereocenters are useful for generating three-dimensionality and metabolic stability but are underrepresented in fragment collections. Consequently, a library methodology to access such fragment entities is reported in this part.

Part I

Background

1.1. Fragment-Based Drug Discovery

The discovery of hit molecules is key to the development of new drugs. Over the past decades, the pharmaceutical industry has primarily relied on HTS where tens of thousands to millions of compounds are screened to find new hit compounds.[5] While HTS has successfully produced a number of approved drugs, in particular against established targets,[5] the method suffers from a series of drawbacks. Hit rates of HTS campaigns are extremely low (~0.01%) and are often accompanied by significant proportions of false positives. In fact, about half of HTS campaigns fail to produce any usable hits and is often the case against newer or more difficult targets.[2,3,6–8] Moreover, maintaining the quality and performing screening of these enormous libraries is costly. In contrast, FBDD involves the screening of smaller collections of smaller molecules, so-called fragments (typically molecular weight < 300 Da), that can be elaborated into larger and more potent compounds (Figure 1.1).[2,3,9] Due to the smaller size of fragments, FBDD offers significantly higher hit rates (~1–10%)[10] and superior sampling of chemical space.[11]

The chemical space, which encompasses all theoretically possible molecules,[12] is incomprehensibly large. For drug-like molecules (heavy atom count, HAC < 36) this has been estimated to consist of at least 10^{60} compounds.[13,14] In comparison, fragment-like space (HAC < 17) is significantly smaller with an estimated size of 10^{11} molecules.[15] While both numbers are astronomically high, it is nonetheless easier to sample fragment-like space.

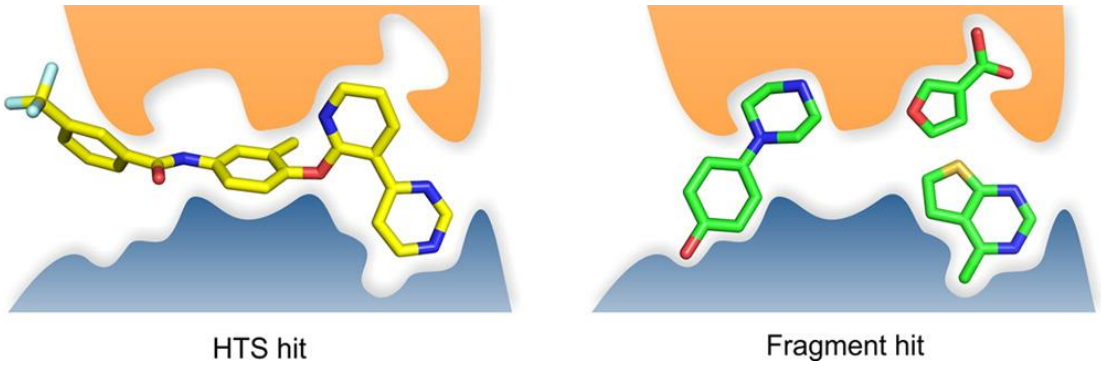

Figure 1.1. Illustrative comparison between hits obtained from high-throughput screening (HTS) and fragment-based screening. HTS hits often bind through numerous suboptimal interactions while fragment hits are more ligand efficient with involve fewer but more optimized interactions. Reprinted with permission from reference.[2] Copyright (2012) American Chemical Society.

The origins of FBDD can be traced back to a seminal paper by Jencks from 1981 where it is proposed that small “fragments”, although weakly binding, can form high-quality interactions that can be optimized into larger, potent molecules.[16] However, it was not until a decade later that the first reports on this approach appeared.[17] FBDD became truly established

through pioneering work at Abbott Laboratories (using NMR spectroscopy[18] and X-ray crystallography[19]) and at Astex Pharmaceuticals (using X-ray crystallography).[20] Since then, the method has been employed with great success and has even proven effective against targets that have previously been reported poorly druggable by HTS.[21,22] These include protein-protein interactions (PPIs), transcription factors, protein chaperones, and RNA.[23–30]

In 2011, an important landmark was reached with the FDA-approval of the first drug developed using FBDD: vemurafenib, a BRAF-V600E inhibitor against melanoma.[31,32] To date, three fragment-based drugs have been approved for the clinic: vemurafenib, the BCL-2 inhibitor venetoclax used for the treatment of chronic lymphocytic leukemia,[33] and most recently erdafitinib for treatment of urothelial carcinoma (Figure 1.2).[34] Furthermore, approximately 30 fragment-based drug candidates are currently in clinical trials.[3]

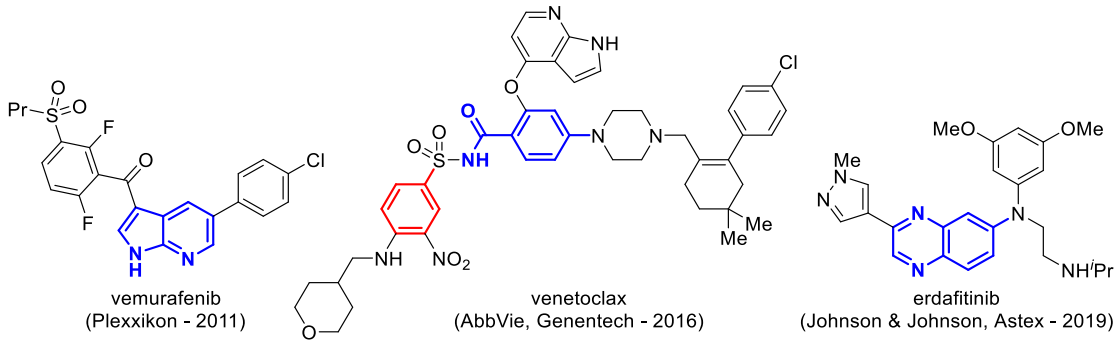

Figure 1.2. Approved fragment-based drugs. Initial fragment entities are highlighted in blue and red.[31–34]

1.1.1. What is a Fragment?

Fragments typically conform to the 'Rule of Three' (Ro3) in which molecular weight < 300 Da, ClogP ≤ 3, hydrogen-bond donors (HBD) ≤ 3, and hydrogen-bond acceptors (HBA) ≤ 3.[3,35,36] These properties were proposed by researchers at Astex after analysis of various fragment screening campaigns where fragment hits, on average, were found to followed this Ro3.[35] In addition, the study suggested other useful parameters including the number of rotatable bonds (nROT) ≤ 3 and polar surface area (PSA) ≤ 60 Å^2. However, like Lipinski's Rule of Five (Ro5),[37] the Ro3 should be viewed as a set of guidelines rather than actual rules and many examples of non-Ro3 compatible fragment hits have been identified.[38]

1.2. Fragment-Based Screening

Because of their smaller size, fragment hits generally bind weaker with typical binding affinities in the range of 0.1–10 mM (Figure 1.3). Compared to HTS hits, fragment hits make fewer but more optimized binding interactions. For this reason, fragments are generally considered more 'atom efficient' binders, which is demonstrated by a higher ligand efficiency (LE = -ΔG/HAC).[39] In order to detect this weaker binding, sensitive biophysical screening techniques are necessary as most cellular or biochemical assays used for HTS are not sensitive enough.[2,9,40]

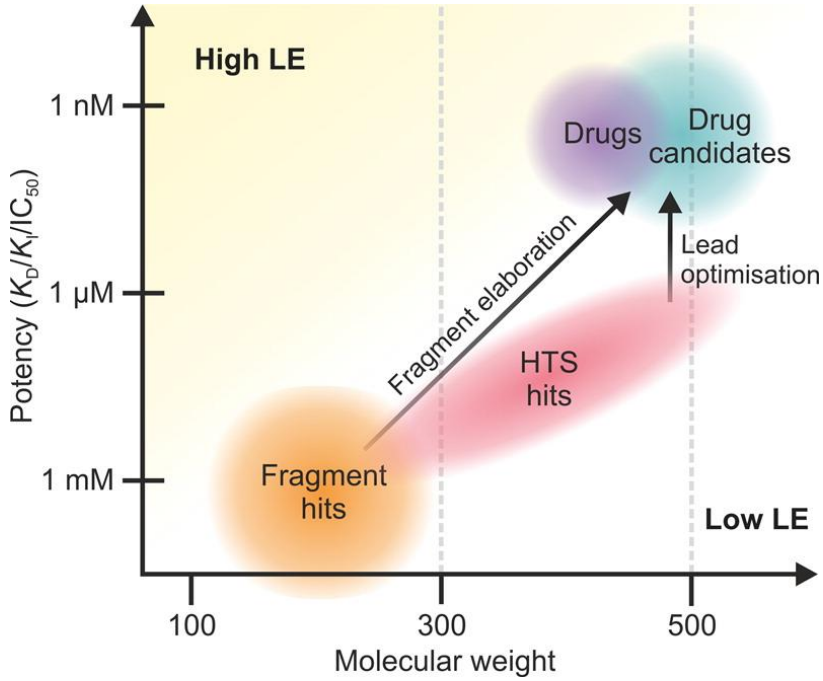

Figure 1.3. Comparison of MW vs. potency of typical HTS and fragment hits. The smaller fragment hits are less potent than HTS hits but generally exhibit higher ligand efficiency. Reprinted with permission from reference.[2] Copyright (2012) American Chemical Society.

Over the years, a range of biophysical techniques have been adopted for fragment screening with the most widespread being fluorescent-based thermal shift (TS), X-ray crystallography, NMR spectroscopy, and surface plasmon resonance (SPR).[10] X-ray crystallography is generally accepted as the most powerful technique and gives the most detailed structural information on the mode of binding. However, the method has a relatively low sample throughput, requires protein crystallization, and depends on expensive infrastructure. For these reasons, less resource intensive and higher throughput methods such as TS, SPR, and NMR are often

initially used to discover hits before X-ray crystallography is employed for determining the exact mode of binding.[2,3,9,40] An overview of the most widely used screening methods for FBDD is given in Table 1.1.

1.2.1. Ligand-Observed NMR Spectroscopy

NMR spectroscopy was the first method to be successfully used for screening of fragments[18] and has since evolved into a valuable tool for FBDD. It is considered the most robust screening technique for weaker binding ligands and has become the most widely adopted method for fragment screening.[10] NMR-based screening is divided into ligand- and protein-observed methods with each their advantages and limitations.

Ligand-based NMR offers relatively high sensitivity and is ideally suited for weak to medium binders. However, strong binders can also be detected using more careful experimental design. The method has a decent sample throughput relying on 1D experiments with fast acquisition times combined with screening of multiple fragments at the same time in "cocktails". A key advantage is the simultaneous quality control of fragments from 1D spectra, which can identify compound degradation or aggregation and helps to avoid false positives. The technique works best for medium to large proteins (> 15 kDa) with larger proteins giving the best results (fragments experience a greater difference upon binding). Disadvantages include a relatively high protein consumption compared to other methods such as SPR or TS. Furthermore, binding information is typically limited, although some information may be obtained depending on the experiment or by addition of a displacer ligand.[2,40–42]

The simplest and most useful 1D NMR experiments for fragment screening include saturation transfer difference (STD),[43] water-ligand observed *via* gradient spectroscopy (WaterLOGSY),[44] and transverse (T_2)-relaxation-based experiments. All three experiments rely on a fast exchange between bound and unbound ligands to affect a large proportion of the ligand population and are thus ideally suited for weak to medium binders.[45]

The ^{1}H NMR experiment STD is based on an intermolecular nuclear Overhauser effect (NOE) between protein and ligand (Figure 1.4). The protein is selectively saturated by irradiation of protein-associated signals (often from 0 to –1 ppm) to give an *on-resonance* spectrum. In the event of ligand binding, the saturation is transferred from the protein to the ligand causing a reduction of ligand signals. The *on-resonance* spectrum is subtracted from a reference spectrum (*off-resonance*) to afford a difference spectrum where only signals from binders will appear. Ligand protons closest to the protein are affected the most and the method can therefore be used to determine binding epitopes ligands.[43]

Table 1.1. Summary of the most widely used screening methods for FBDD.[2,10,40]

Method	Sensitivity	Throughput	Pros	Cons
Ligand-observed NMR	10 mM – 100 nM	Medium	Robust and sensitive Some binding information	High protein consumption Medium FPs
Protein-observed NMR	5 mM lower limit	Low	Binding information Determination of K_d Few FP	Isotopically labeled protein <40 kDa proteins
X-ray crystallography	All	Low	Binding information Few FP	Crystallization required Equipment demanding Many FNs
Surface plasmon resonance	500 µM lower limit	Medium	Measurement of kinetics Low protein consumption	Immobilization and integrity of protein Many FPs
Fluorescent-Based Thermal shift	500 µM lower limit	High	Inexpensive and fast Reliable for K_d < 10 µM Low protein consumption	Many FPs/FNs
Isothermal titration calorimetry	1 mM – 10 nM	Low	Robust method for K_d measurements	High protein consumption Low throughput
Mass spectrometry	200 µM lower limit	Medium/ high	Covalent inhibitors Low protein consumption	Requires ionizable system Difficult for weak binders
Microscale thermophoresis	pM – mM	Medium	Large dynamic range Determination of K_d	Specialized equipment Often requires labeling
Weak-affinity chromatography	1 µM upper limit	Medium	Simple Inexpensive	Immobilization and integrity of protein
Enzymatic assays	100 µM lower limit	High	Effective for well-defined active sites (*e.g.* kinases)	High fragment conc. Low sensitivity Many FPs/FNs

FP: false positive; FN: false negative

WaterLOGSY is also an NOE-based experiment but relies on intermolecular transfer of magnetization *via* bulk water. Due to a large difference in correlation times between target-bound water and solvent water, NOEs experienced by binders and non-binders will be of opposite signs.[44] A comparison between STD and WaterLOGSY spectra is shown in Figure 1.5.

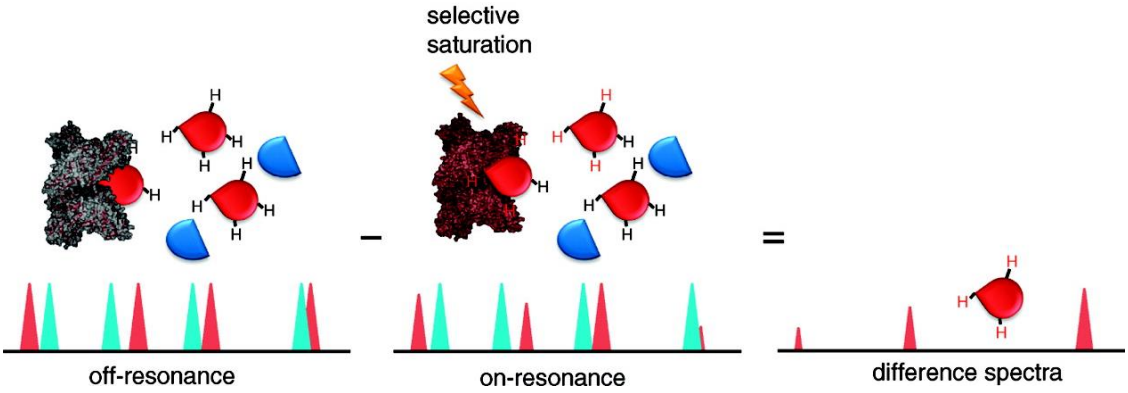

Figure 1.4. Schematic illustration of saturation transfer difference NMR. Ligand binding is detected as an intermolecular transfer of magnetization from protein to ligand causing a reduction of ligand signals. Reprinted with permission from reference.[46] Copyright (2011) of American Chemical Society.

In T_2-relaxation-based experiments, a difference in tumbling rates between large biomolecules and fragments is exploited. Due to their slow rotational correlation time (long τ_c), large biomolecules have shorter T_2-relaxation times than those of fragments. Consequently, binding of a fragment results in a significant reduction of its T_2-relaxtion and is observed by peak broadening of the fragment signals. This effect is easily visualized when applying a T_2-filter such as the Carr–Purcell–Meibom–Gill (CPMG) scheme (Figure 1.6).[47–50] This spin-echo pulse sequence adds a relaxation delay (one or several trains of hard 180° pulses) before signal detection and results in a reduction of signal intensities from broadened peaks. Due to the large chemical shift anisotropy (CSA) of fluorine, this approach is in particularly useful for ^{19}F NMR (*vide infra*).[50]

Another useful NMR approach is competition ligand-based NMR experiments, which also allow for the efficient detection of strong binders. These assays rely on the displacement of a known binder, the spy molecule, and only identifies specific binding ligands. A particular simple and effective methods is the ^{19}F NMR-based "fluorine chemical shift anisotropy and exchange for screening" (FAXS) experiment.[50–52] FAXS is also based on a CPMG spin-echo scheme and monitors the displacement of a fluorinated ligand (Figure 1.7). The approach draws on the increased simplicity and relative sensitivity of ^{19}F NMR without the need of fluorinated fragments. While effective, competition experiments require a known weak-to-medium binder to work. Furthermore, as binding is observed indirectly, deconvolution of screening cocktails is necessary for identifying new binders.

1.2.2. Protein-Observed NMR Spectroscopy

Compared to ligand-observed experiments, protein-based NMR screening typically relies on more complex 2D protein-detected $^{1}H–^{15}N$ heteronuclear single quantum coherence (HSQC) experiments. Fragment binding is detected as perturbations in chemical shifts of $^{1}H–^{15}N$ amide cross peaks of a ^{15}N-labeled protein (Figure 1.8). The method easily distinguishes between nonspecific and specific binding while providing valuable structural information about the site of binding (requires a solved NMR structure). Protein-observed experiments are highly sensitive and have a larger detectable affinity range as compared to ligand-observed techniques, particularly in the high-affinity end.[2,9,40,53] The method was used in one of the first published examples of FBDD under the name "structure-activity relationship (SAR) by NMR"[18] and has successfully been employed in several campaigns since then.[54–56]

Because the method relies mainly on changes in NH backbone chemical shifts, protein-observed NMR screening is limited to relatively small proteins (<30–40 kDa). ^{13}C-labeling, deuteration, and/or amino acid-selective labeling can extend the size of the protein but the faster relaxation properties of larger proteins may be a concern. Furthermore, large quantities of protein is needed and since isotopic labeling is required, the method is costly. Consequently, X-ray crystallography has become the preferred approach for obtaining structural information on fragment binding.[2,9,40,53]

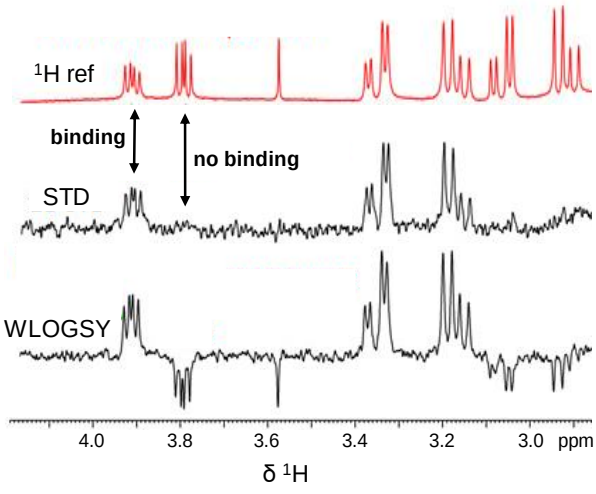

Figure 1.5. Detection of ligand binding using STD and WaterLOGSY ^{1}H NMR experiments. Spectra are both phased so that positive signals indicate binding. Negative signals in the WaterLOGSY spectrum originates from NOEs of solvated water. Figure adapted from reference.[364]

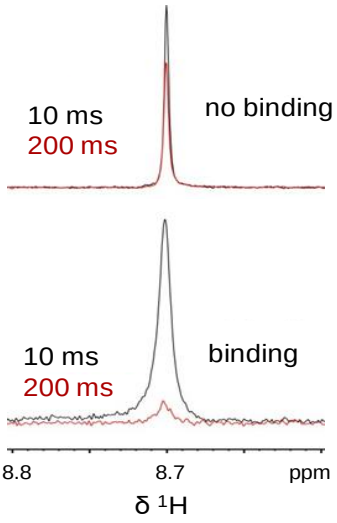

Figure 1.6. Example of how a T_2-based relaxation experiment can be used to identify binding. Spectra recorded using 10 ms (black) and 200 ms (red) relaxation delays, respectively. Figure adapted from reference.[364]

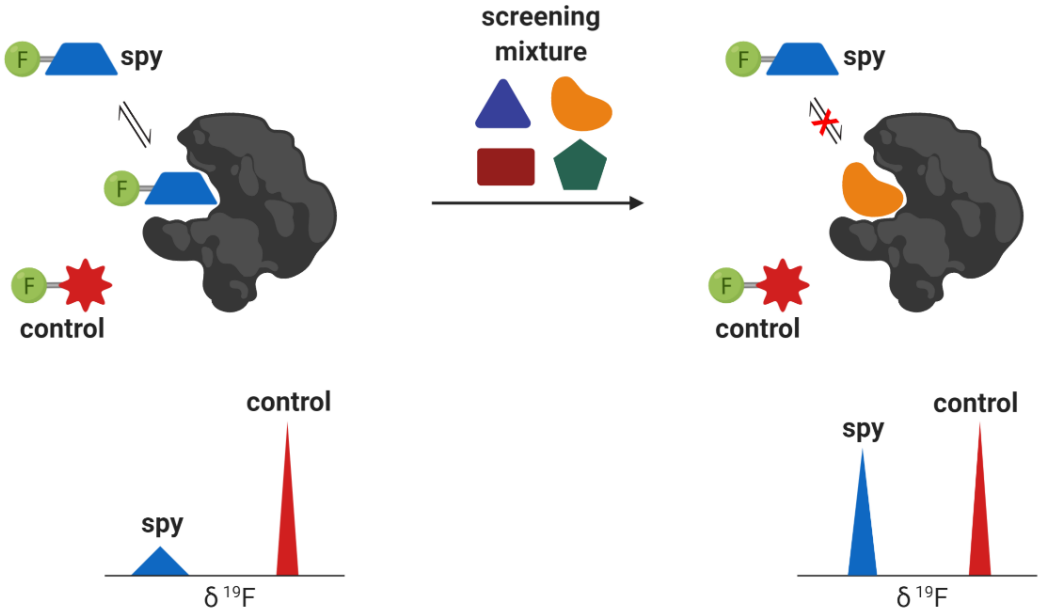

Figure 1.7. Screening by FAXS NMR. A mixture of non-fluorinated compounds is screened against a known fluorinated ligand, the spy molecule (S). The broad signal of the spy molecule becomes sharper upon displacement by another binder. Deconvolution of the screening mixture is then required to determine the identity of the binder. A control molecule (C) is typically added as an internal reference.

1.2.3. X-Ray Crystallography

The routine application of X-ray crystallographic screening was pioneered at both Abbott[19] and Astex[20] and is today considered the most powerful tool for fragment screening (Figure 1.9). The technique can provide detailed information on the mode of binding with a low number of false positives and, in contrast to protein-observed NMR, works for larger proteins as well. As previously stated, the method is generally used as a secondary screening assay due to the relative low sample throughput and dependence on expensive infrastructure.[2,9,40,57] However, it should be noted that recent advances in high-throughput setups can now facilitate primary screens by X-ray crystallography.[10,58]

Obtaining high quality crystals of protein-ligand complexes can be both difficult and time consuming. Crystal soaking is the most resource-effective approach in which a protein crystal (*apo*-form or with a weakly bound ligand) is soaked with fragment cocktails or individual fragments in high concentrations (up to 50 mM). This method requires the binding site to be solvent-exposed and/or unhindered for binding to occur. The high fragment concentration is needed to achieve high fragment occupancy in the protein in order to obtain sufficient electron density maps and detect binding. Consequently, X-ray crystallography is prone to many false

negatives if high protein occupancy is not achieved.[2,9,40,57] However, the use of halogenated (typically brominated) fragments may aid in achieving better crystallographic data and thus higher hit rates *via* heavy atom anomalous scattering.[59,60]

For more difficult systems, in which the protein does not crystallize without a ligand or if ligand binding induces larges conformational changes that cracks the crystal, co-crystallization can be attempted instead. Here, the protein-ligand complex is prepared in an aqueous media preceding crystallization. However, this method normally requires different crystallization conditions for each fragment and therefore has an even lower sample throughput.[2,9,40,57]

While crystallographic data is considered the gold standard of structural information, it is important to note that crystallographic models are still *models*. Models can be misleading and in particular lower resolution structures may have the position or conformation of ligands mis-assigned. In severe cases, the ligand itself could be incorrect or entirely absent.[61] More frequently, fragment binding may occur through crystal contacts, *i.e.* interactions only present in the crystalline state of the protein and not in solution. This has been estimated to apply for as many as a third of structures published in the PDB database.[62] Finally, crystallographic data provides only limited information on binding affinity and should therefore be correlated with other screening methods.[9]

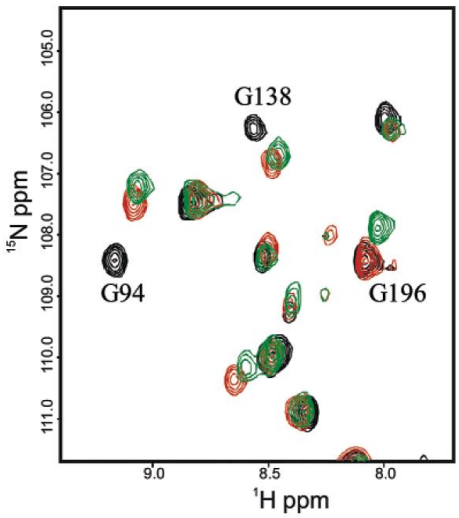

Figure 1.8. Selected region of a ^{1}H–^{15}N HSQC spectrum from a protein-observed NMR screen. ^{15}N-labeled protein alone (black) and two examples of fragment binding (red and green). Reprinted with permission from reference.[90] Copyright (2012) American Chemical Society.

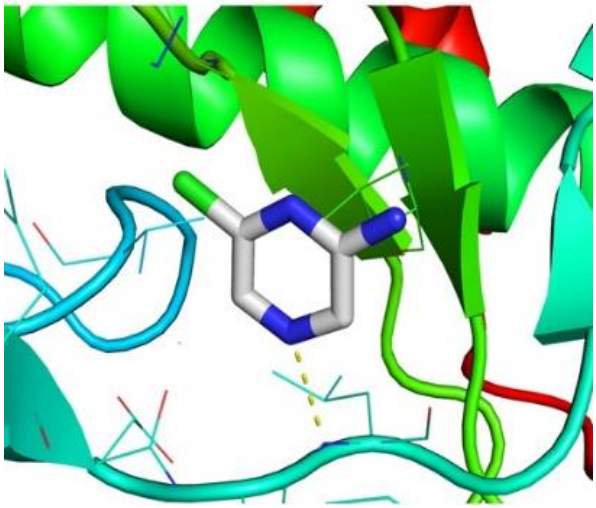

Figure 1.9. X-ray crystallography is a powerful method for determining the binding mode of fragment hits, which is vital for structure-based drug design. The technique typically has a relatively low sample throughput and is therefore primarily used as a secondary assay. Reprinted with permission from reference.[2] Copyright (2012) American Chemical Society.

1.2.4. Surface Plasmon Resonance

Surface plasmon resonance (SPR) is one of the major screening techniques for FBDD. The main advantages include information on binding kinetics and thermodynamics while only requiring relatively small amounts of protein. SPR works by immobilizing a target biomolecule on a gold chip and sequentially passing solutions of single fragments over it. As fragment binding causes an increase of surface mass, binding can be detected in real-time as a change of refractive index (Figure 1.10). Binding kinetics can then be measured from the time-dependent fragment association−dissociation response and be used to calculate binding affinity. Recent developments in biosensors and instrumentation have enabled the method to detect binding of molecules down to 100 Da and allow for significantly higher sample throughput than previously possible.[2,9,40,63,64]

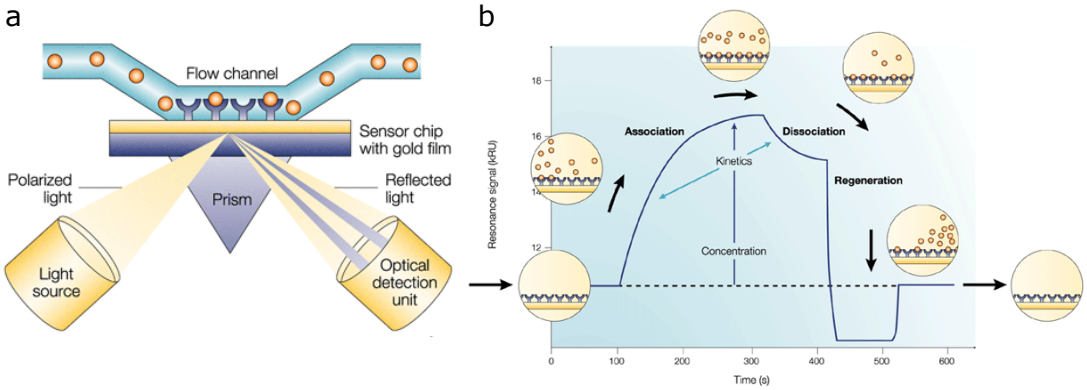

Figure 1.10. Illustration of surface plasmon resonance (SPR). (**a**) Ligand binding to a surface-immobilized biomolecule is detected as a change in refractive index (proportional to change in surface mass). (**b**) SPR sensorgram of a typical binding cycle. Ligand binding results in an increase of the resonance signal until an equilibrium is reached (related to the ligand concentration). The solution of ligand is replace with buffer and the biomolecule–ligand complex is allowed to dissociate. Based on the association and dissociation kinetics, the binding affinity can then be calculated ($K_d = k_{diss}/k_{ass}$**)**. Reprinted with permission from reference.[63] Copyright (2002) of Springer Nature.

Immobilization of the target biomolecule to the sensor surface is a central element in SPR. The process must preserve the integrity and activity of the protein while producing high protein density on the sensor surface. Typically, immobilization of proteins is performed covalently using amide couplings between lysine side chains of the protein and carboxylic acids on the surface of the sensor chip. The approach requires no biomolecular engineering or chemical modifications of the protein but does give a heterogeneous mixture of immobilized proteins,

which can lead to loss of activity. Another disadvantage is potential lack of regenerative properties of the chip following a screen. Promiscuous binders have been shown difficult to remove and may significantly affect subsequent screens. Alternatively, capturing of histidine-tagged proteins can be used and enables full regeneration of the surface. However, protein leakage can be a concern and much larger quantities of protein is needed.[40,63,65]

SPR is generally easier to set up and run compared to NMR spectroscopy and X-ray crystallography. However, because fragment binding is weak the method requires high fragment concentrations and is relatively susceptible to unspecific binding. Furthermore, experiments can easily be set up or interpreted incorrectly. As an example, an extensive review article from 2008 concluded that less than 30% of the 1400 SPR experiments reviewed had been conducted and reported in an appropriate manner.[66]

1.2.5. Isothermal Titration Calorimetry

Isothermal titration calorimetry (ITC) provides quantitative binding data with high sensitivity and full thermodynamic characterization over a large dynamic range of K_d-values.[67] The methods works by measuring the heat released (or absorbed) when a ligand binds to a protein through a series of titrations (Figure 1.11). It is the most robust method for measuring K_d-values but requires large quantities of protein and has a low sample throughput. Consequently, ITC is better suited as a secondary screening technique.[2,40]

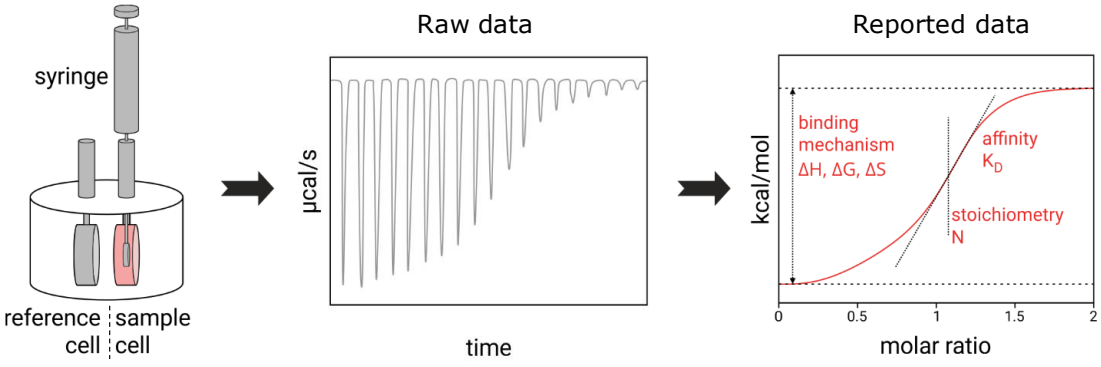

Figure 1.11. Isothermal titration calorimetry is a robust method for measuring binding affinity. Small, successive aliquots of ligand are titrated into a solution of protein and the amount of heat released is measured as a function of time. Concurrent with binding, protein sites become progressively occupied and less heat is released upon injection of additional ligand. Figure adapted from reference.[68]

1.2.6. Mass Spectrometry

Although less established, native-protein mass spectrometry (MS) has become increasingly useful as a complementary screening technique.[69] The method relies on soft electrospray ionization (ESI) to detect target–ligand complexes and enables direct deconvolution of screening mixtures with fragments of different masses (Figure 1.12).[69,70] Importantly, native-protein MS requires only small quantities of protein and is often rapid and automated. However, it is a challenge to achieve detectable target occupancy with weakly binding fragments. As the target–ligand complex must survive in the gas phase, screening by MS is best suited for covalent interactions.[2,9]

An interesting covalent approach is *tethering*, in which a natural or engineered reactive functionality in a protein is used to capture fragments binding in the vicinity.[71] The earliest example of this approach exploits a native cysteine to covalently link to thiol-containing fragments.[72]

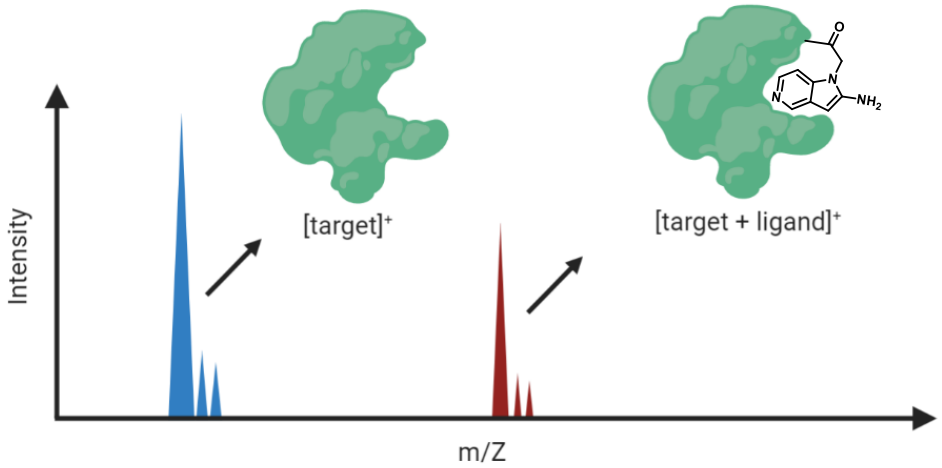

Figure 1.12. Native-protein mass spectrometry using soft electrospray ionization can be used to detect fragment binding. Binding is detected as a corresponding increase in mass of the protein and allows for direct deconvolution of screening mixtures (assuming unique molecular weights of fragments). As protein–ligand interactions must survive in the gas phase, the method works best for covalent binders.

1.2.7. Fluorescence-Based Thermal Shift Assay

Fluorescence-based thermal shift (TS) or differential scanning fluorimetry (DSF) is perhaps the fastest screening method for fragments and is relatively inexpensive, requiring affordable equipment and only little protein and. The technique is based on an increase in the unfolding temperature (ΔT_m) of a protein as a result of stabilization by fragment binding (Figure 1.13). The assay is typically carried out in a plate-based format using an exogenous environmentally sensitive fluorescent dye to monitor the unfolding process. Because fragment binding is weak,

temperature shifts are consequently also small, $\Delta T_m \approx 0.5\text{-}2$ °C. Unfortunately, the method is prone to many false positives and negatives and results are not always reproducible. Thus, TS is often used as a preliminary screening assay prior to more accurate methods such as NMR or SPR.[2,40,73,74]

1.2.8. Virtual Screening

In silico techniques are becoming increasingly sophisticated and available for use in FBDD (Figure 1.14). Generally, computational methods are employed in one of two ways: Virtual screening of large libraries or as a tool for producing modes of binding for hits in the absence of structural information. While several successful examples on the use of *in silico* methods for fragments exist, there are still many limitations for effective implementation in early stage drug discovery. The major challenges in regards to FBDD lie with the smaller size of fragments. Possible docking modes are significantly increased while the weaker binding interactions make changes more subtle. Consequently, computational techniques continue to find more application in later stages of drug development and they will undoubtedly play an increasingly important role in the future.[2,9,75,76]

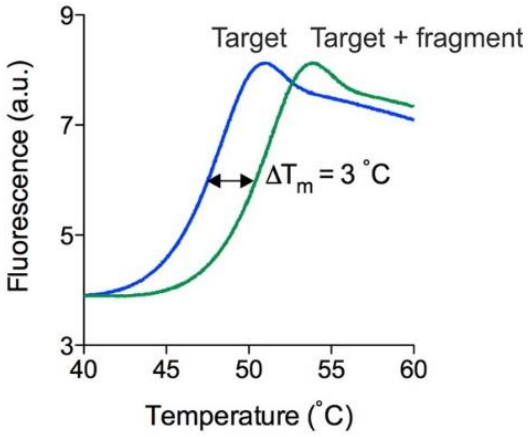

Figure 1.13. Illustration of data output from a fluorescence-based thermal shift assays. Binding is observed as an increase in the melting temperature of a protein in the presence of a fragment. Reprinted with permission from reference.[2] Copyright (2012) American Chemical Society.

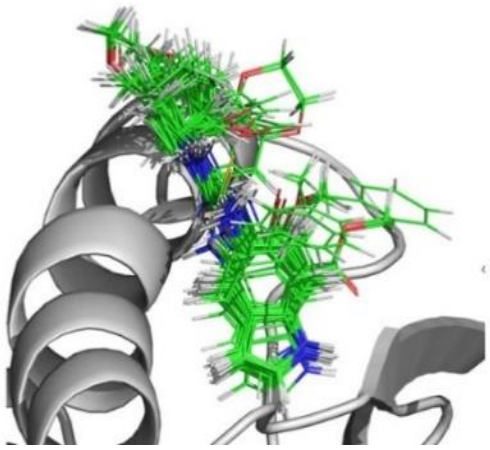

Figure 1.14. Computational methods can be used to screen virtual libraries or finding binding modes of ligands. However, it is generally difficult to apply for fragments due to their small size. Reprinted with permission from reference.[2] Copyright (2012) American Chemical Society.

1.2.9. Microscale Thermophoresis

Microscale thermophoresis (MST) is an immobilization-free technique that is slowly becoming increasingly popular for fragment-based screening (Figure 1.15).[77] The technique relies on the physical phenomenon of thermophoresis, which describes molecular migration in the presence of a temperature gradient (either towards or away from higher temperatures). Ligand binding affects the migratory behavior of proteins *via* alteration of charge, size, or shell hydration and this can be monitored using fluorescent detection. This is typically performed using a fluorescently labeled protein but can also be done label-free *via* native tryptophan residues. MST enables measurement of binding affinity as well as direct detection of protein denaturation or aggregation, which helps to avoid false positives. While this method has previously suffered from a low sample throughput, recent technological advances now enable higher throughput screening in an automated setting.[78] However, such specialized equipment is relatively expensive.

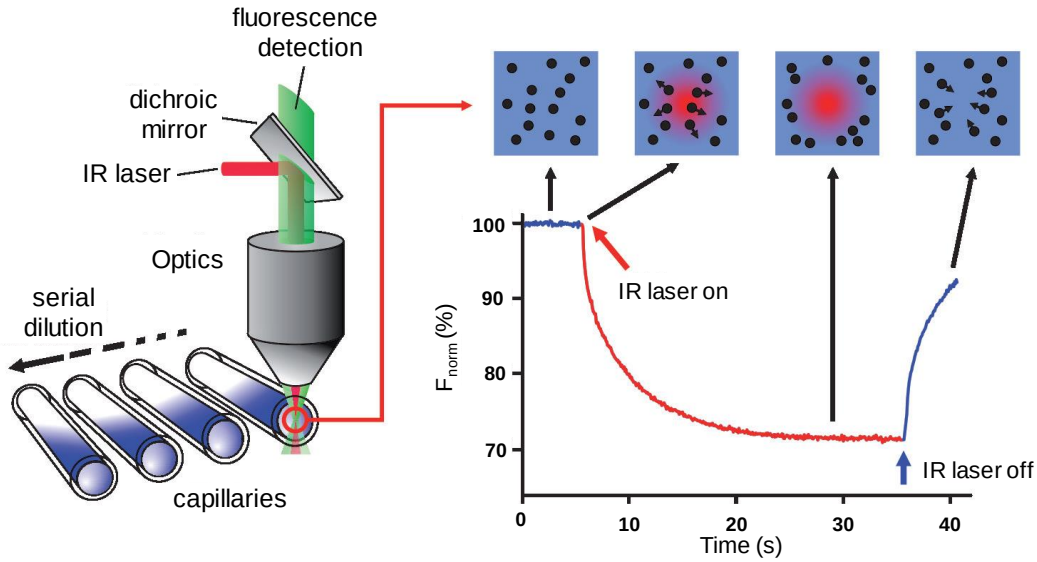

Figure 1.15. Microscale thermophoresis detects the flow of molecules in the presence of a temperature gradient generated by an IR laser. Ligand binding affects the chemical microenvironment around the protein and thus migratory behavior, which is monitored by fluorescence. Changes in the thermophoretic profile of a protein at varying ligand concentrations enable measurement of K_d-values. Figure adapted from reference.[79]

1.2.10. Affinity-based Separation

Techniques based on affinity-based separation are relatively simple and inexpensive but are generally not widely applied. A few examples of such methods are briefly described here and includes capillary electrophoresis, weak-affinity chromatography (WAC), and ultrafiltration.

CE involves the application of high voltage across a liquid-filled capillary with analysis of analyte migration. The method relies on a reporter ligand whose mobility is decreased in the presence of a protein target in the buffer (Figure 1.16). Screening of fragments can then be performed and binding is detected as a change in the retention time of the reporter ligand. The method has a low consumption of unmodified protein and a similar throughput comparable to many other biophysical techniques.[80–82]

Ultrafiltration is an exceptionally simple approach and relies on centrifugation of screening mixtures through a membrane that only retains macromolecules (along with bound fragments). The composition of the filtrate is compared to that of the initial mixture and depletion of any signals are attributed to target binding.[83]

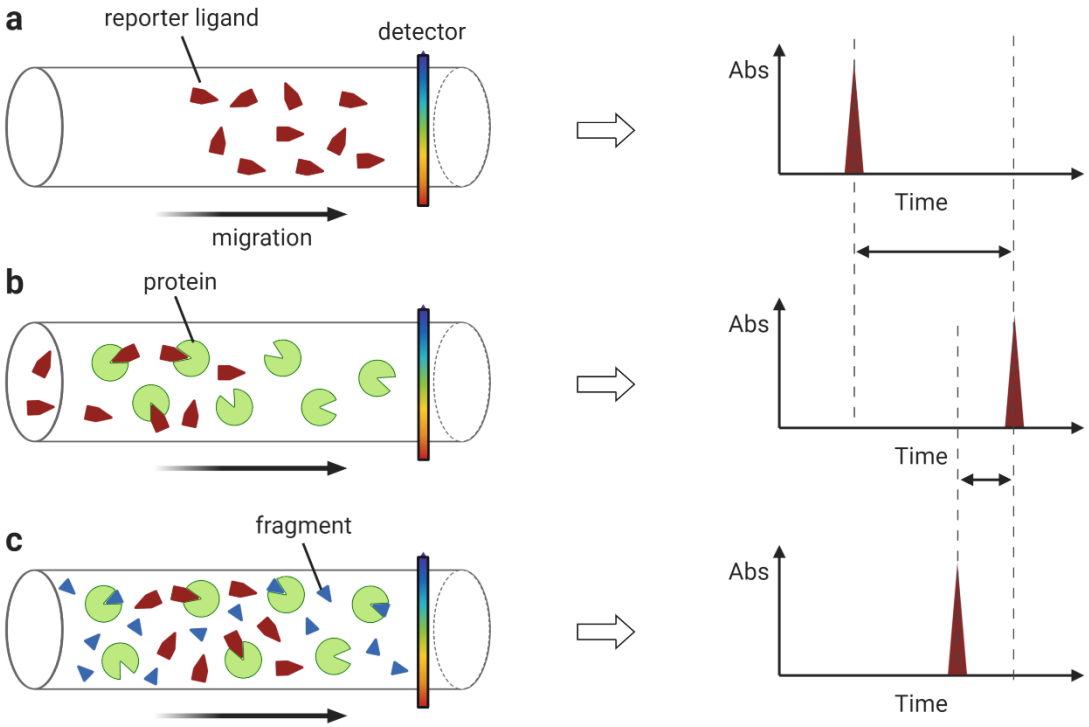

Figure 1.16. Schematic illustration of fragment screening using capillary electrophoresis. (**a, b**) In a capillary exposed to a high voltage gradient, the mobility of a reporter ligand is reduced upon addition of the protein target in the buffer. (**c**) Fragment screening is then performed by addition of a fragment to the buffer. Fragment binding is detected as a change in the retention time of the reporter ligand due to competitive binding of the protein.

In WAC, fragments are passed through a chromatography column containing a covalently immobilized protein (similarly to SPR) and binding is detected as an increase in retention time compared to a non-derivatized column. WAC can advantageously be performed using high-performance liquid chromatography (HPLC), which in combination with MS also facilitates screening of fragment mixtures. The main challenges of using WAC are related to the immobilization, integrity, and stability of the protein on the chromatography column.[84]

1.2.11. Other Techniques

In addition to the well-established techniques described so far, a number of other techniques have also been adapted for fragment-based screening, *e.g.* fluorescence anisotropy, fluorescence correlation spectroscopy, and biolayer interferometry. However, these methods are only rarely employed for screening of fragment and are for that reason not described herein.[10]

To end with, advances in electron cryogenic electron microscopy (cryo-EM) has now made this technology competitive with X-ray crystallography and have led to the first examples of its use in FBDD. Researchers at Astex recently reported high quality cryo-EM maps showing fragments binding in two different proteins (Figure 1.17). While throughput is still a major limitation, the technique could potentially open thousands of uncrystallized proteins for structure-based design.[85]

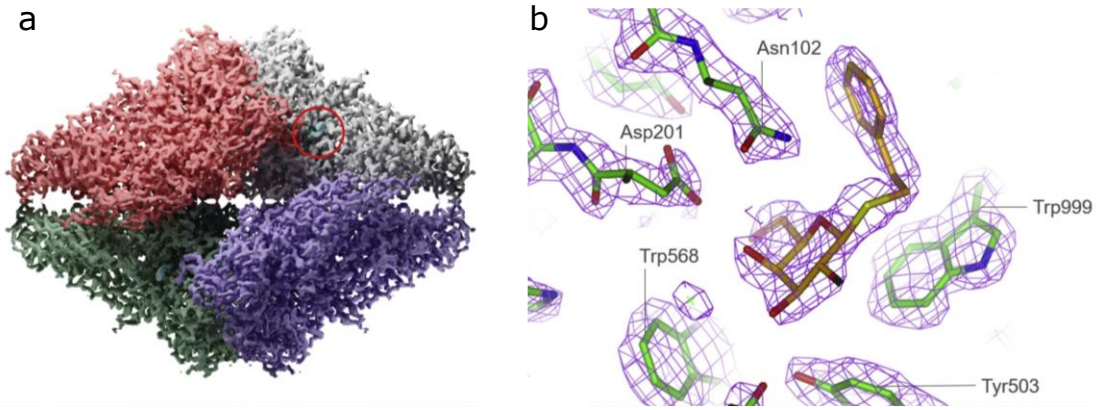

Figure 1.17. Cryo-EM structure of β-galactosidase with a bound ligand at 2.2–2.3 Å resolution. (**a**) Tetrameric structure of β-galactosidase with the active site marked with a red ring. (**b**) Zoom in on the active site shows clear density of the bound ligand (orange). Adapted with permission from reference.[85] Copyright (2020) Elsevier.

1.3. Fragment Elaboration

Due to the issues of false positives (and false negatives), it is recommended to perform fragment screening using orthogonal techniques – at least as a measure to validate hits.[10] Once validated, hits are synthetically elaborated into more potent compounds by iterative cycles. While more conventional medicinal chemistry can be performed (*e.g.* by SAR), structural binding information is typically key for successful fragment elaboration. Thus, many companies only pursue hits that can be characterized crystallographically.[9]

The simpler structures and higher LE of fragment hits can make optimization efforts easier compared to HTS campaigns. One exceptional example is the development of vemurafenib, which took only 6 years from project initiation to FDA approval. Unfortunately, this is not always the case and for conventional targets optimization from HTS hits can be equally fast. Nonetheless, many fragment screens lead to identification of new chemotypes that may offer better selectivity and new intellectual property.[3] In FBDD, there are three main strategies for hit-to-lead optimization of fragments: linking, merging, and growing (Figure 1.18).

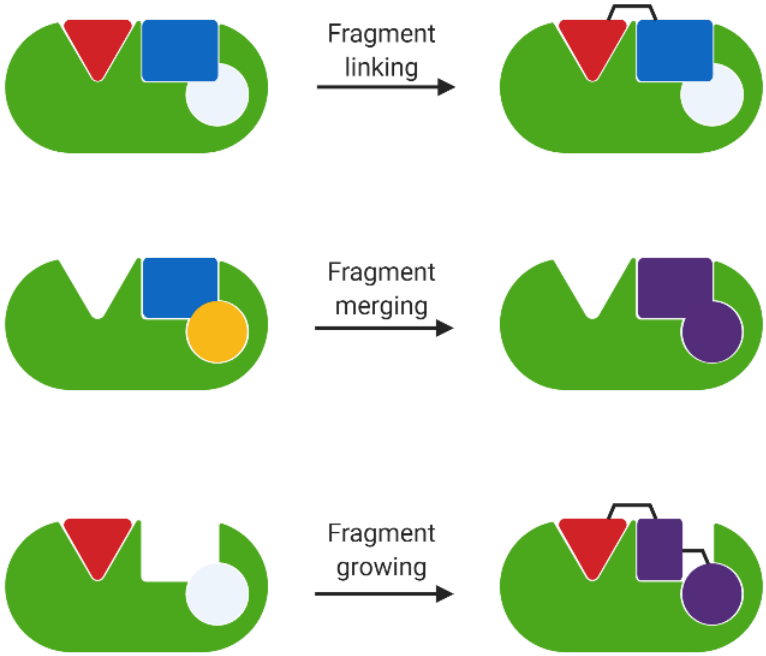

Figure 1.18. The three main fragment elaboration strategies: growing, linking, and merging.

Fragment linking is conceptually an attractive approach. Two or more fragments are identified to bind in adjacent sites and are then linked together to form a high-affinity com-

pound.[18,86,87] Ideally, the linker should allow the fragments to adopt their preferred orientations, make additional binding interactions, and contribute with only little entropic penalty. However, in practice fragment linking is often challenging. Finding a suitable linker is difficult and even small deficiencies in geometry or linker length can dramatically reduce affinity. Furthermore, highly flexible linkers may allow the molecule to undergo 'hydrophobic collapse' causing hydrophobic surfaces to be intramolecularly buried. [2,3,9,30,40] Thus, while there are impressive examples of fragment linking, these tend to be the exception.[18,88–92]

Fragment merging, on the other hand, has proven more successful and easier to implement. Similar to linking, fragment merging consists of the combination of fragments but is achieved through merging of overlapping structural motifs (Figure 1.18). The approach draws on information derived from hits, the literature, and known substrates and relies heavily on crystal structures to identify overlapping structures.[2,3,9,30,40]

Finally, fragment growing is the simplest and most popular strategy for hit elaboration. One fragment hit provides the central scaffold for further optimizations. Typically, similar fragments are initially tested to determine the ideal core scaffold. Then, growing of the fragment by chemical synthesis is performed. This can be done either through classical SAR by derivatization of possible vectors or more often by structure-guided design. In the latter, the fragment hit is slowly and iteratively grown to pick up specific binding interactions.[2,3,9,30,40]

1.3.1. Case Studies

Fragment growing was used in the development of **1.4**, a nanomolar inhibitor of the oncology-related kinases Aurora A and B (Figure 1.19).[93] Based on a pyrazole-benzimidazole fragment hit (**1.1**), crystal structures showed two main growth vectors that were used to grow the fragment and achieving nanomolar potency. Due to poor pharmacokinetic properties of **1.3**, a urea-linked cyclopropyl was incorporated instead of the benzamide to afford the best combination of potency and pharmacokinetic properties. Interestingly, **1.1** was originally identified as a hit against cyclin-dependent kinase 2 (CDK2) during another screening campaign. However, good selectivity against Aurora A and B was successfully achieved during fragment elaboration. Unlike many cases, crystal structures showed good overlap between the initial fragment hit **1.1** and the final drug candidate. Compound **1.4** underwent phase II clinical trials against metastatic solid tumors and hematological malignancies but was discontinued due to poor clinical responses.[94,95]

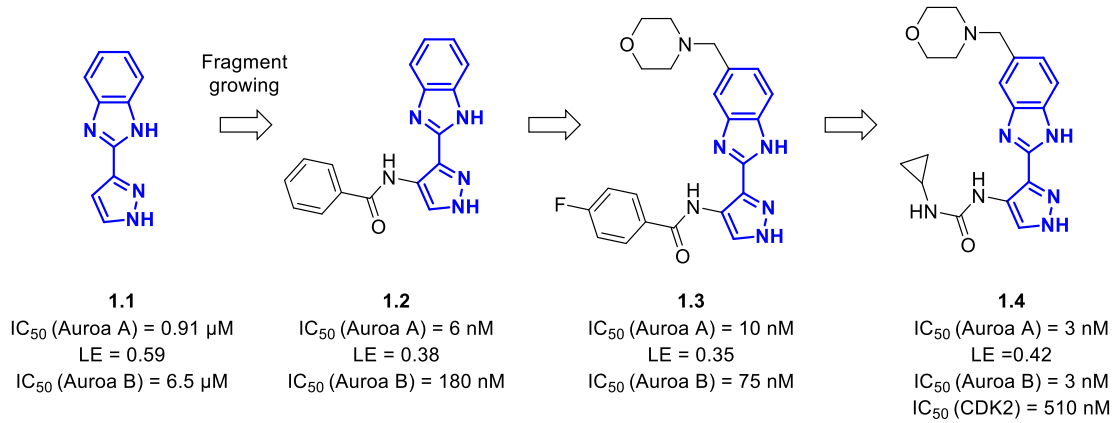

Figure 1.19. Fragment growing was used in the development of **1.4**, an ATP binding site inhibitor of the Aurora A and B kinases.[93]

Researchers at Vernalis demonstrated the power of fragment merging in the development of a 3-phosphoinositide-dependent protein kinase-1 (PDK1) inhibitor.[96] Fragment hit **1.5** was initially optimized to compound **1.6** to occupy an adjacent hydrophilic pocket. Based on multiple crystal structures, **1.5** was merged with two other fragment hits, **1.7** and **1.8**. Superpositioning of the three fragment binders afforded a number of combinations, among which compound **1.9** exhibited the best mix of affinity, kinase selectivity, and *in vivo* efficacy (Figure 1.20).

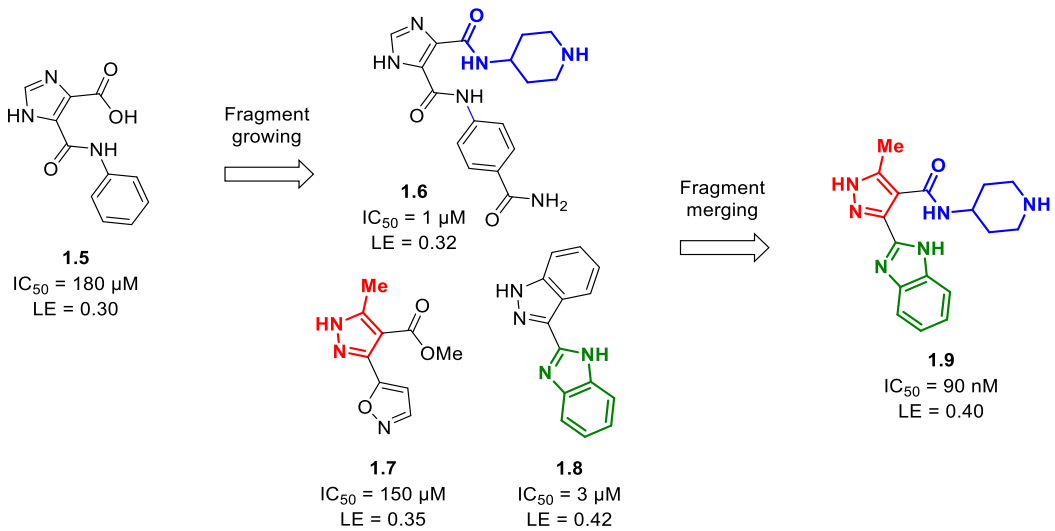

Figure 1.20. An example of fragment merging. Fragment hit **1.5** was initially optimized to **1.6**, which was merged with two other fragment hits, **1.7** and **1.8**, around a common pyrazole scaffold to form the nM inhibitor **1.9**.[96]

An elegant example of fragment linking was performed at Abbott using SAR by NMR.[88] Screening against stromelysin, a zinc-dependent matrix metalloproteinase (MMP) resulted in two promising fragments hits – the zinc-binding acetohydroxamic acid **1.10** and a simple biphenyl derivative **1.11** occupying a proximal hydrophobic pocket. Using a flexible alkoxy-linker, the two fragments were combined to form the non-peptidic MMP inhibitor **1.13** with low nanomolar affinity (Figure 1.21).

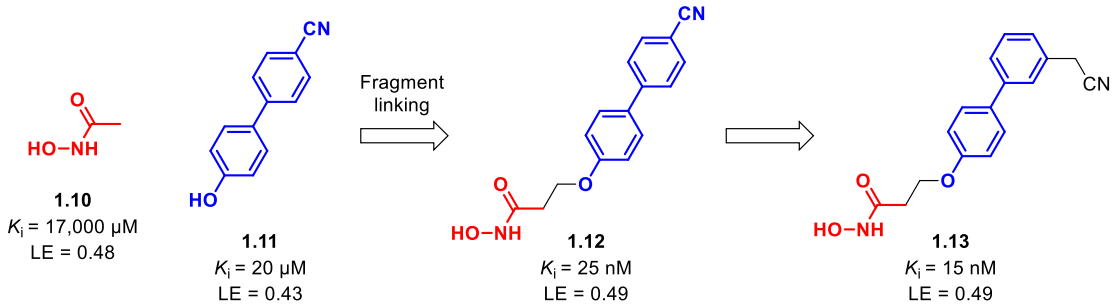

Figure 1.21. Fragment linking demonstrated in the development of stromelysin inhibitor **1.13**.[88]

1.4. Fragment Library Design

Construction of a suitable fragment library is essential for successful FBDD.[8] As it is not synthetically feasible to access all theoretically possible small molecules, libraries should ideally be as diverse as possible to best sample chemical space. Nonetheless, focused libraries can in some cases be advantageous to increase hit rates as demonstrated for protein-protein interactions[97,98] and against various kinases.[99] Library size can vary from less than a hundred to several thousands of fragments and are thus significantly smaller than typical HTS collections (~10^4–10^6 compounds).[5] Generally, the Ro3 is considered a useful set of guidelines for fragments but a number of influential papers have also been published on fragment library design dealing with more complex properties such as diversity and unwanted functionalities.[8,100–103] Recently, researchers at Astex published an updated list of criteria for their fragment libraries including properties such as aqueous solubility, complexity, synthetic feasibility, and vectors for later elaboration.[104]

1.4.1. Unsuitable Functional Groups and PAINS

Unfortunately, many hits turn out to be false positives due to non-specific interactions between compound and protein. If these artefacts are not correctly recognized, efforts to optimize potency are consequently wasted. Thus, to deal with this challenge, many functional groups have been flagged as undesirable for screening purposes, primarily due to unwanted reactivity that may lead to false positives (Figure 1.22).[101,105,106]

In addition to unsuitable functional groups, many compound classes have also been found to exhibit unspecific activity against a range of targets. Interference in assays may occur through various mechanisms including covalent modifications, chelation, redox activity, stability issues, or aggregation. These compounds are termed pan-assay interference compounds (PAINS) and show promising activity but lead to unfruitful hit optimizations. Roughly 480 compound classes have been identified to give rise to PAINS but of these, 15 classes account for more than half of observed artefacts (Figure 1.23).[101,106,107]

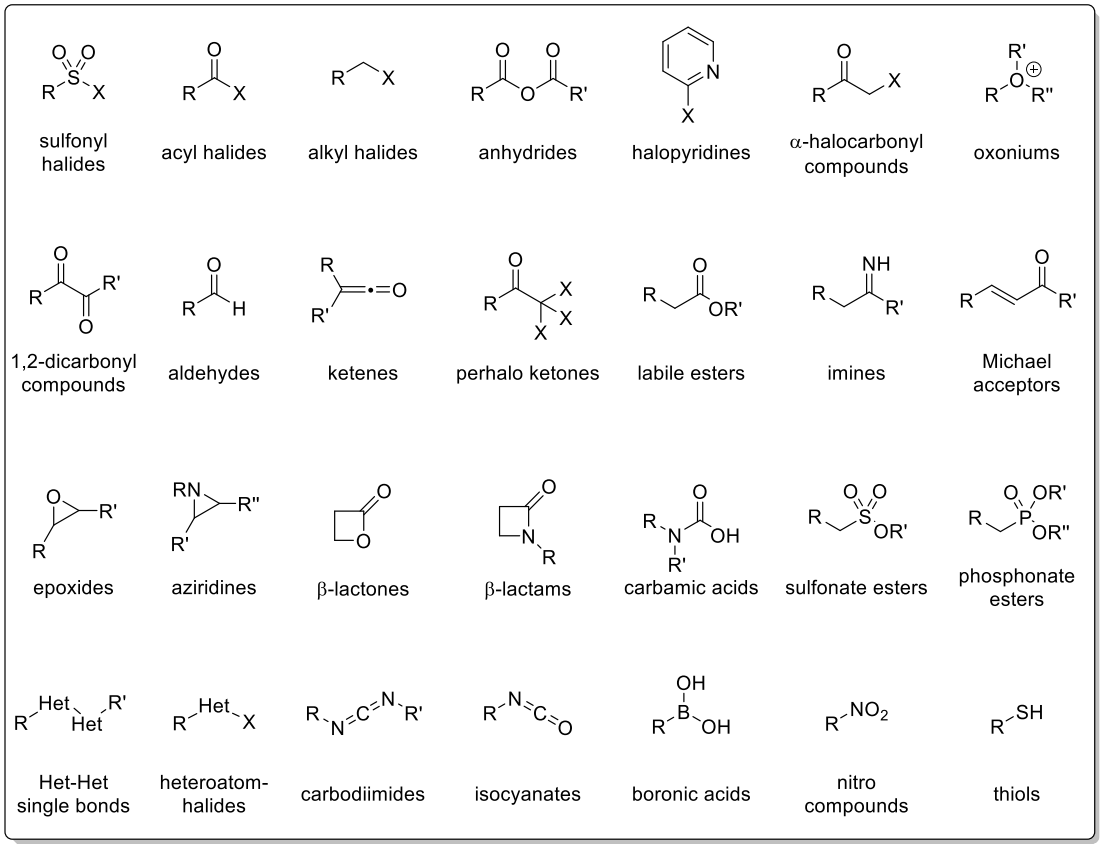

Figure 1.22. Unstable or reactive functional groups generally considered unsuitable for screening compounds. X = halogen; Het = heteroatom (N, S, O).[105,106]

The apparent activity of PAINS is often seductive and has led to numerous publications falsely claiming these artefacts as promising inhibitors – something one should be mindful of. It is estimated that as many as 5 –12% of compounds in academic screening libraries are PAINS,[106] and it is therefore important to be aware of these potential 'bad-actors'. While learning the most disreputable structures is highly recommended, hits should be crosschecked in the literature and ideally confirmed by orthogonal methods in order to validate them.

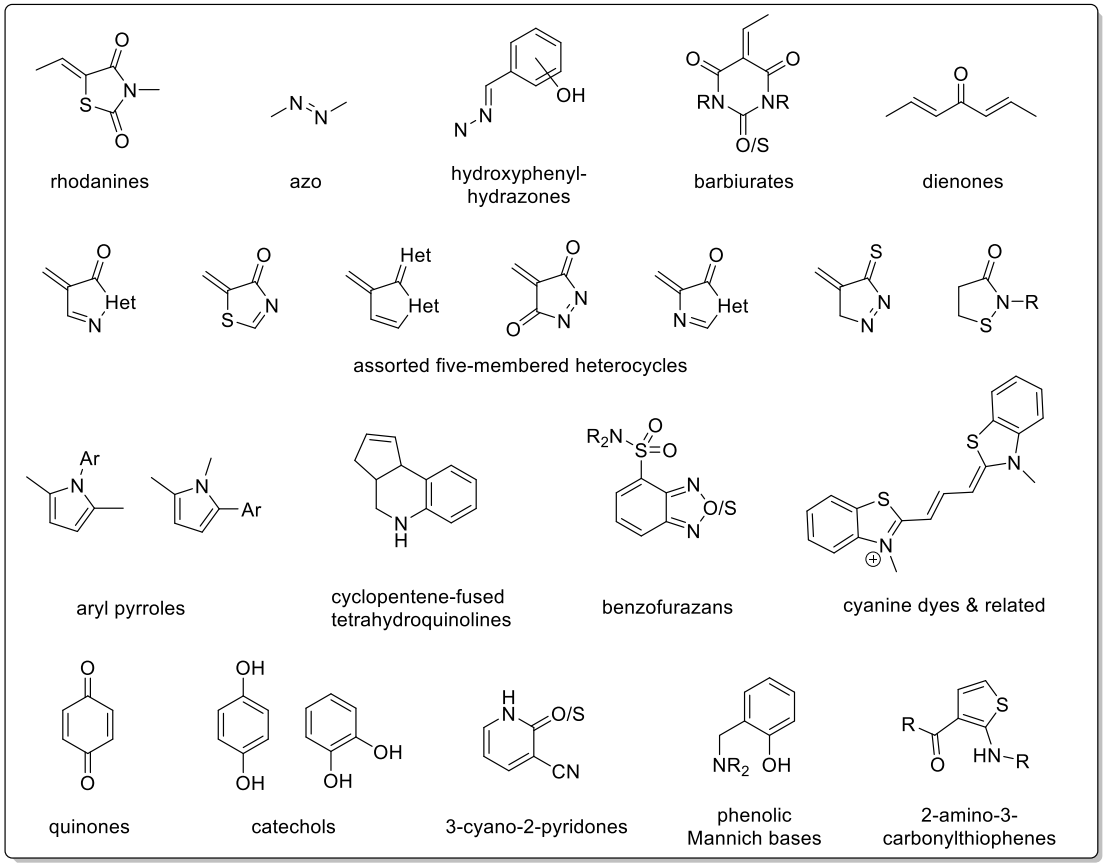

Figure 1.23. A list of the 'worst offenders' among recognized PAINS. Around 15 compound classes (out of 480 known) have been identified to account for up to 60% of nuisance compounds. Many compounds are covalent modifiers (*e.g.* α,β-unsaturated systems and catechols) or metal complexers (*e.g.* hydroxyphenylhydrazines and phenolic Mannich bases). Others are prone to chemical decomposition (*e.g.* aryl pyrroles), can function as redox cyclers (*e.g.* quinones and catechols), or are simply promiscuous/nonspecific (*e.g.* 2-amino-3-carbonylthiophenes). Het = heteroatom (N, S, O).[106,107]

1.4.2. Library Diversity

Diversity is a somewhat subjective term and may refer to a number of properties such as functional groups, pharmacophores, scaffolds, side chains, stereochemistry, shape, and more. As nature recognizes molecules as three-dimensional (3D) surfaces of chemical information, the overall shape of a small molecules is arguably the most fundamental factor controlling its biological effects.[108–111] Indeed, extensive 'shape space' coverage has been correlated with a broad biological activity and has been identified as the most important property for overall functional diversity.[108,109,111–115] Interestingly, the main factor for determining the shape of small molecules is their central scaffolds and thus, shape diversity is ultimately linked to scaffold diversity.[112]

In recent years, 'three-dimensionality' has received increasing attention as an important physical property.[116–118] The vast majority of small drug-like molecules synthesized to date are dominated by aromatic moieties and flat topologies.[118–120] However, compounds with higher fractions of sp^3-hybridized carbons (Fsp^3) tend to perform better in drug discovery campaigns partly due to higher aqueous solubility and lower off-target binding.[121–124] Additionally, more 3D hits may offer alternative growth vectors for later optimization whereas aromatic moieties limits elaboration to the plane of ring systems.[125] Interestingly, natural products tend to have significantly higher 3D character with greater degrees of carbon saturation.[117,126] Thus, there has been a push towards exploring more natural product-like and 'three-dimensional' structures to improve the shape diversity of current screening collections.

1.4.3. Molecular shape diversity

The simplest approach to estimate 'three-dimensionality' is by looking at the Fsp^3 as saturation tend to result in higher degrees of complexity and 3D shape.[121,127] However, it is a crude approach and 3D conformers can also be generated from sp^2-rich molecules.[118] Consequently, more elaborate models have been developed for determining molecular shape.[112,120,128–131] For library analysis, the principal moment of inertia (PMI) plot is probably the most widely used method. Although fairly basic, PMI analysis provide an easy way to visualize and compare the shape diversity of large numbers of compounds (Figure 1.24).[112]

Moment of inertia or rotational inertia (I) is a measurement of how resistant a body is to changes in rotational motion about an axis.[132] Based on the lowest energy conformer of a compound, its three PMIs (I_x, I_y, and I_z) around orthogonal axes going through the center of gravity are calculated. For a molecule, the moment of inertia is defined as the *product sum of atomic mass and atomic distance squared* for each heavy atom (eq. 1).

$$I = \sum_{i=1}^{HAC} m_i r_i^2, \qquad (1)$$

where m is atomic mass and r is the distance of the atom from the center of gravity in the molecule.

The PMIs are then normalized by dividing the two lower values with the highest value to generate two size independent and normalized PMI ratios, NPR1 and NPR2. The two values are plotted in a ternary plot with each corner representing a geometrical extreme – a rod, disc, or sphere, respectively (Figure 1.24).[112]

Because PMI is calculated from the distribution of mass rather than volume, the method is slightly biased towards high-density atoms or functional groups. For instance, while chlorine and methyl substituents have similar Van der Waals (VdW) volumes,[133,134] chlorine has a larger influence on the calculated PMI due to its larger mass.

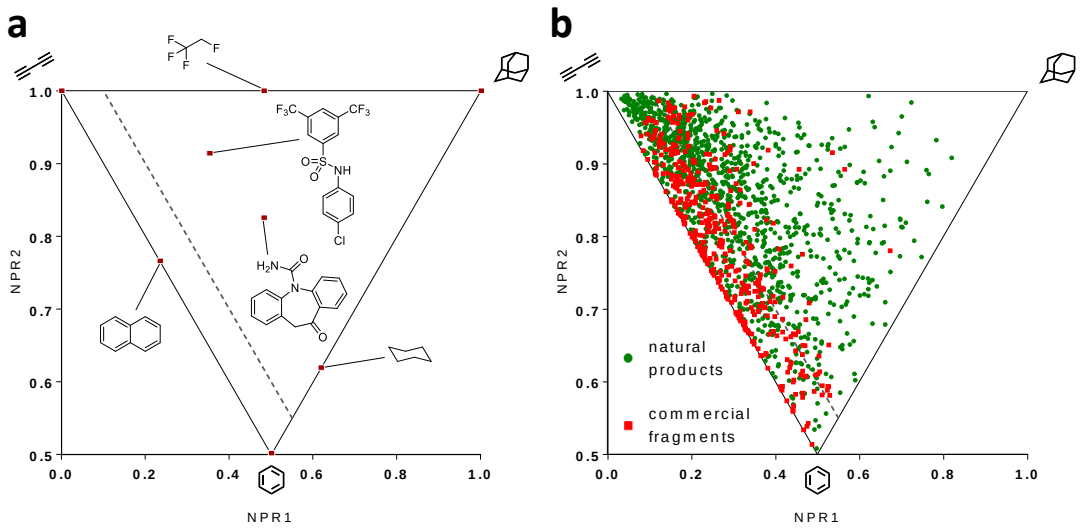

Figure 1.24. Principle moment of inertia (PMI) plot with normalized axes. Each corner of the ternary plot represents molecular extremes – rod-like [0,1], disk-like [½,½], and sphere-like [1,1] geometries, repsectively. "Flatland" is situated below the dashed line (NPR1 + NPR2 < 1.1).[118] (**a**) Examples of five intermediate geometries including two non-planar molecules with $Fsp^3 = 0$. (**b**) Comparison between a typical commercial fragment library (red) and a collection of 1356 natural products (green).[135] NPR = normalized PMI ratios. Coordinates were calculated using open-source software.[136]

Another interesting method for evaluating structural shape is the plane of best fit (PBF). The PBF of a molecule is calculated to afford the lowest average distance of each heavy atom to this plane (Figure 1.25). The method can profitably be used in combination with PMI analysis for more detailed analysis and has shown to be able to differentiate between closely clustered molecules in NPR space.[120]

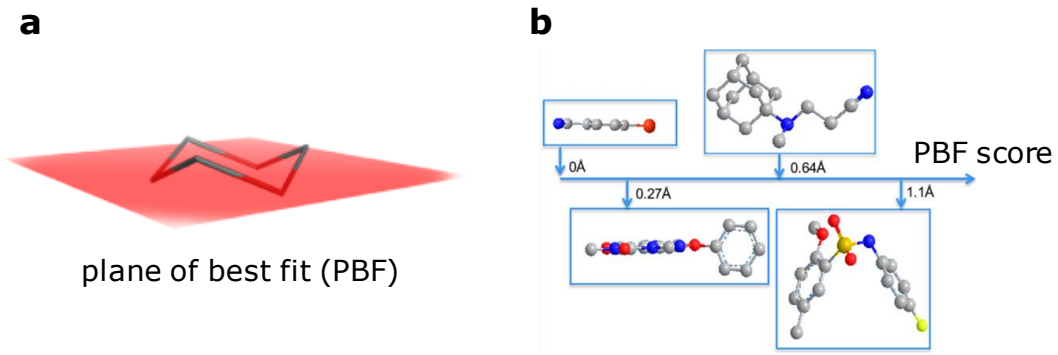

Figure 1.25. Principle of the plane of best fit (PBF) for characterization of molecular three-dimensionality. (**a**) Example of a PBF for cyclohexane. (**b**) Molecules are assigned a PBF score equal to the average atomic distance in Å from the PBF. Figure adapted from reference.[120]

1.4.4. Library construction

Generally, small molecules can be obtained from three distinct sources – natural products, commercial sources, and synthesis. Natural products possess enormous structural diversity and have been a major source of drugs and lead compounds over the years. However, their use is associated with multiple challenges including purification, availability, and chemical modification. Commercially available libraries comprise millions of compounds and offer an easy and important source of small molecules. Unfortunately, these collections typically consist of structurally simple and similar compounds with flat topologies (low Fsp^3). While such compounds have proven successful for the discovery of numerous bioactive molecules, this lack of diversity is a drawback in respect to the identification of novel bioactive chemotypes. Finally, synthesis of new compound collections can aid in accessing new and diverse structures. Several synthetic strategies have been developed for this purpose, however, it remains a formidable challenge to efficiently access large numbers of diverse molecules.[2,109,119]

1.5. Diversity-Oriented Synthesis

Traditionally, combinatorial library synthesis has been the dominating approach for construction of screening collections.[137] This strategy seeks to achieve library diversity through variation of side chains around a limited number of central scaffolds. In contrast, diversity-oriented synthesis (DOS) is a newer synthetic philosophy that aims to efficiently access large numbers of diverse scaffolds and thus achieve better structural diversity (Figure 1.26).[138,139] Synthetic planning is performed in forward pathways rather than retrosynthetically and may help to increase coverage of chemical space including unexplored regions that could potentially allow for the identification of novel binding motifs.[109]

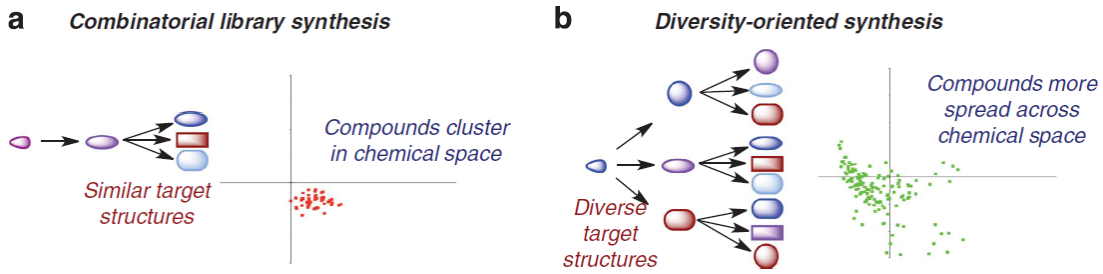

Figure 1.26. A comparison between the overall synthetic strategies used in combinatorial library synthesis (**a**) and diversity-oriented synthesis (DOS) (**b**), respectively. The branching pathways of DOS enable synthesis of more diverse compounds as illustrated by the increased coverage of chemical space. Reprinted with permission from reference.[109] Copyright (2010) of Springer Nature.

Overall, there exists two approaches for generating scaffold diversity in DOS – the reagent-based and the substrate-based approach (Figure 1.27).[109] In the reagent-based approach, a common starting material is subjected to different divergent and complexity-generating reactions in a branching fashion. This is accomplished in one of two ways: **1**) by using a densely functionalized molecule with different functional groups that can be transformed by different reagents[140] or **2**) by exploiting a pluripotent functional group that can participate in a number of different reactions.[141] In contrast, the substrate-based approach is based on pre-encoded substrates that are folded into distinct scaffolds under common reaction conditions.[142]

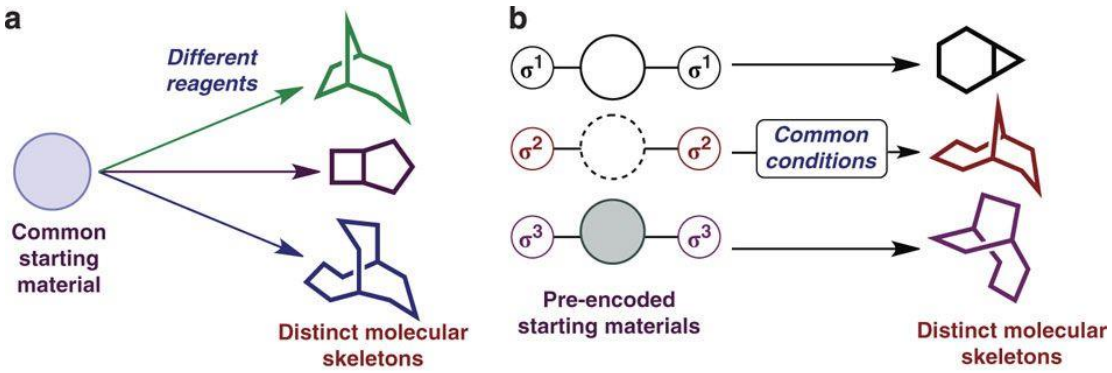

Figure 1.27. Two overall DOS strategies to create scaffold diversity. (**a**) The reagent-based approach is based on common starting materials, which are subjected to different reaction conditions. (**b**) In the substrate-based approach, a set of different, pre-encoded substrates are transformed into distinct scaffolds under common reaction conditions. Reprinted with permission from reference.[109] Copyright (2010) of Springer Nature.

A common feature for many DOS campaigns was identified by Nielsen and Schreiber and termed the build/couple/pair (B/C/P) three-phase strategy (Figure 1.28).[143] Central building blocks are initially synthesized (build phase) and subsequently combined to form one or several densely functionalized intermediates (couple phase). Finally, scaffold diversity is generated through a series of folding-type processes in which different parts of an intermediate is connected (pair phase). This B/C/P approach can serve as a useful tool for planning target compounds in a DOS campaign.

Within the DOS philosophy, complementary approaches has since emerged that prioritize certain areas of chemical space. Biology-oriented synthesis (BIOS) targets compounds based on natural product-like scaffolds in order to increase the biological relevance of compounds synthesized.[144,145] The closely related privileged-substructure-based DOS (pDOS) concentrate on privileged structures, typically derived from bioactive compounds, that are capable of binding multiple targets, *e.g.* the benzopyran scaffold.[146] Another example includes lead-oriented synthesis (LOS) that focuses on delivering compounds with specific molecular properties favorable for lead optimization.[147,148]


benzopyran

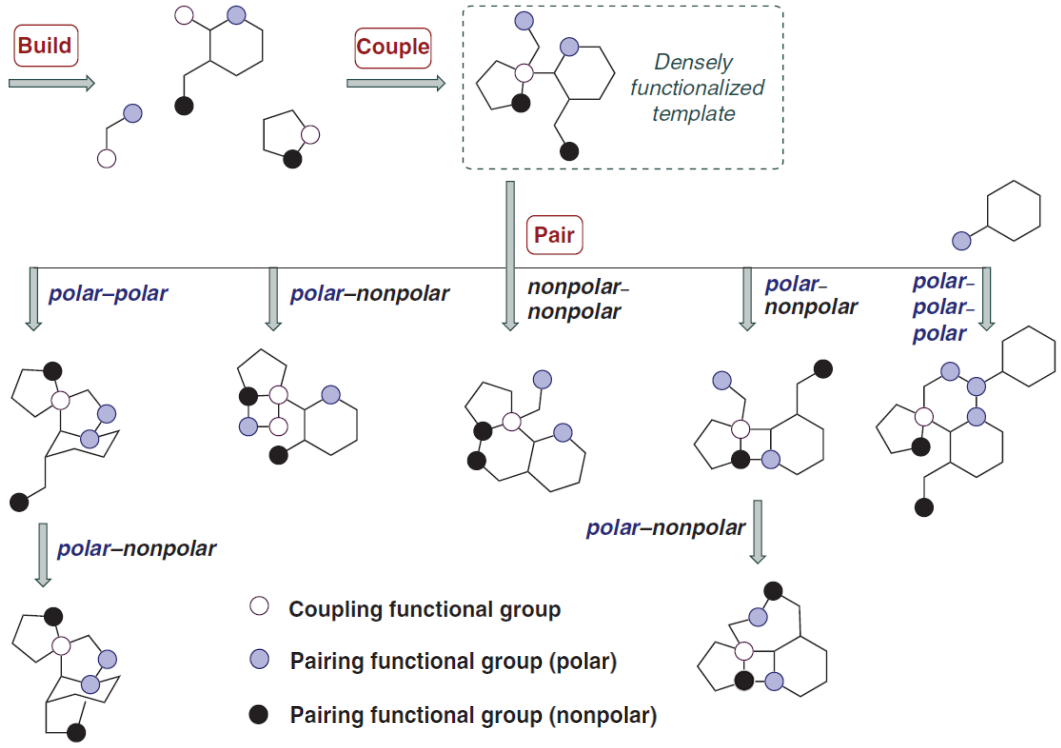

Figure 1.28. The build/couple/pair strategy in DOS. A set of building blocks is initially synthesized (build phase) and is followed by a series of intermolecular coupling reactions (couple phase). Finally, intramolecular couplings in pairwise combinations (polar-polar, polar-nonpolar *etc*.) generate scaffold diversity (pair phase). Adapted with permission from reference.[143] Copyright (2007) of John Wiley and Sons.

1.5.1. Applications in FBDD

DOS was originally developed for the construction of diverse HTS compounds but over the past decade the methodology has also been successfully employed for the synthesis of novel fragment collections.[149–158] The first example from 2011 was a substrate-based approach using the B/C/P methodology to synthesize 3D fragments from three proline-based building blocks (Scheme 1.1). Functionalization of these building blocks followed by intramolecular pairing using either ring-closing metathesis (RCM) or oxo-Michael reactions afforded a series of fused and spiro bicyclic fragments.[149]

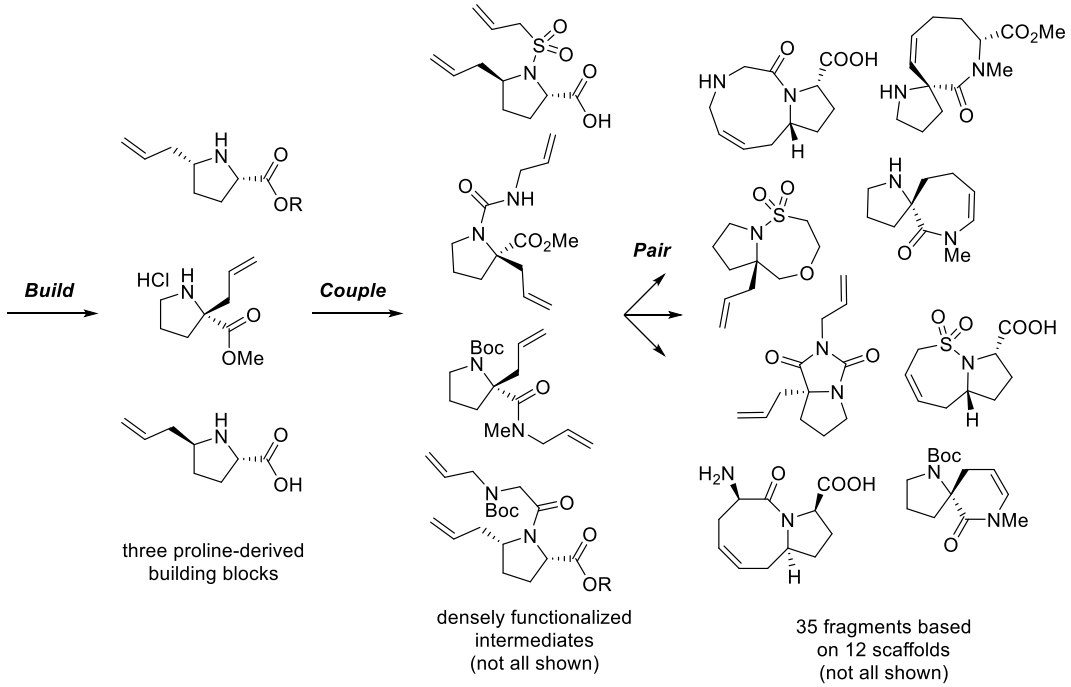

Scheme 1.1. Synthesis of highly shape diverse fragments using the build/couple/pair approach from three proline-derived building blocks.[149]

A recent example by Spring and co-workers involved the use of a reagent-based strategy starting from a single α,α-disubstituted propargyl amino ester (Scheme 1.2). By exploiting the three reactive handles with a broad range of chemistry, the building block was transformed into a series of highly functionalized intermediates that were subsequently ring closed to afford a small collection of *N*-substituted quaternary carbon-containing fragments.[156]

In 2017, Nelson and co-workers applied DOS for the construction of a natural product-inspired fragment collection (Scheme 1.3).[151] An intramolecular [5+2] cycloaddition strategy was employed to construct four bridged core scaffolds. Subsequent ring distortion reactions (expansion, cleavage, annulation, or substitution) afforded a small library of polycyclic fragments with natural product-like substructures. Interestingly, the biological relevance of the library was demonstrated by identification of novel hits against three epigenetic targets *via* X-ray crystallographic screening.

However, in spite of these excellent examples of DOS, the number of reported fragment library syntheses are relative low, especially given the popularity of FBDD. Thus, continued effort into the synthesis of diverse fragments is still highly desired.[104]

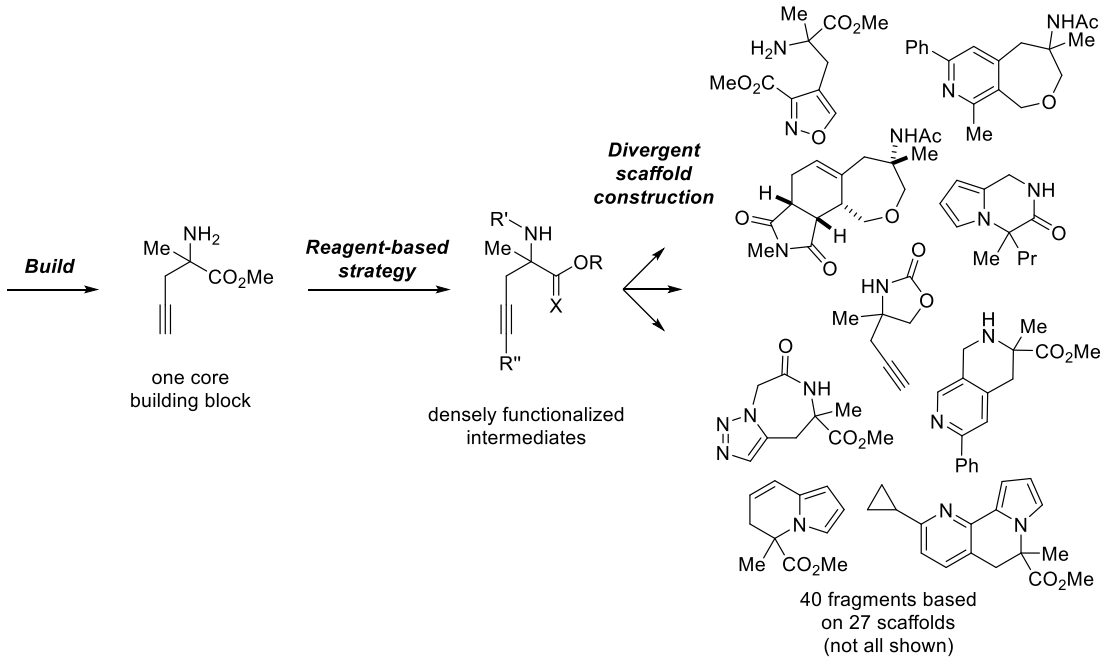

Scheme 1.2. Synthesis of diverse *N*-substituted quaternary carbon-containing fragments using a reagent-based approach from an α,α-disubstituted propargyl amino ester.[156]

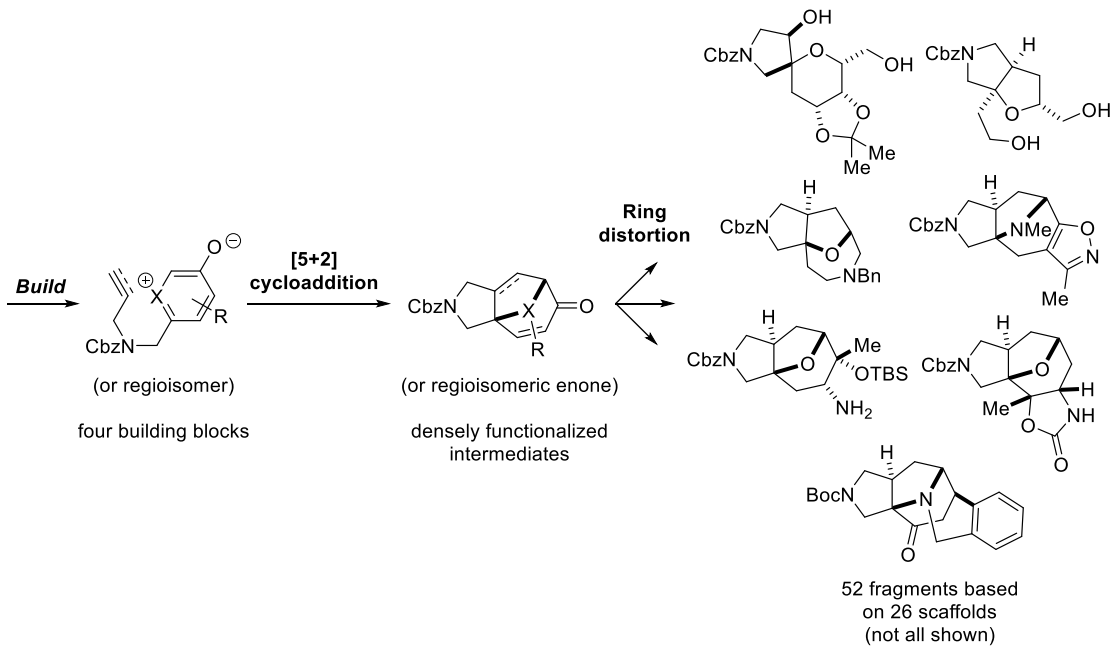

Scheme 1.3. Diversity-oriented synthesis of 52 natural product-like fragments *via* four bridged core scaffolds that were based on an intramolecular [5+2] cycloaddition. X-ray crystallographic screening against three epigenetic proteins afforded hit rates of 4–15%

1.6. Fluorine

Fluorine is the 9th element of the periodic table and is the 13th most abundant element in the Earth's crust. By itself, the element exists as F_2 – a pale yellow, poisonous gas with a stinging odor. However, due to the highly oxidative nature of diatomic fluorine, the element does not occur freely in nature. The element was first isolated in 1886 by the French chemist Henri Moissan, an accomplishment that afforded him the Nobel prize in chemistry in 1906.[159] The name fluorine originates from the Latin fluere, which means to flow, and is a reference to the main fluorine-containing ore, fluorite (CaF_2), used as a metallurgical flux.[160]

Fluorine has been widely integrated in a number of materials and chemicals including refrigerants, aerosol propellants, agrochemicals, lubricants, surfactants, and pharmaceuticals. However, in spite of its high abundance in the Earth's crust, only about a dozen fluorine-containing natural products have been identified (Figure 1.29).[161]

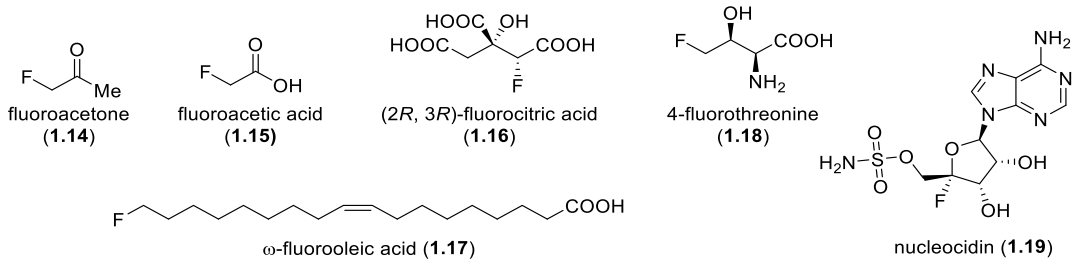

Figure 1.29. Examples of a very limited number of fluorinated natural products. Compounds **1.14**–**1.17** have been isolated from plants and **1.14**, **1.16**, and **1.19** from bacteria.

1.6.1. Properties of Fluorine

Fluorine exists 100% as a single isotope, ^{19}F, with the electronic configuration [$1s^2 2s^2 2p^5$]. It is the most electronegative element of the periodic table with a Pauling electronegativity value of 3.98 (Figure 1.30).[160] Table 1.2 compares a list of key properties of the C–F bond with similar bonds.

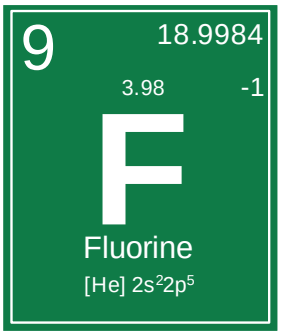

Figure 1.30. The element of fluorine.

Trifluoromethyl is an often encountered group in medicinal chemistry. While it is almost five times heavier than the methyl group (molecular weights of 69 Da and 15 Da, respectively), the CF_3-group is only about 1.8 times larger (van der Waals volumes of 39.8 Å^3 and 21.6 Å^3, respectively). The steric bulk of the CF_3-group has been much debated but is generally accepted to be similar or slightly larger than the ethyl group, although clearly of a different shape.[134,162] However, while the introduction of fluorine results in an increase of molecular weight, fluorinated compounds (< 6 fluorine atoms) generally behave similarly to their non-fluorinated analogues in a variety of *in vitro* assays including P-glycoprotein (P-gp) recognition, metabolic stability, and membrane permeability. Thus, it has been suggested that the added molecular weight can typically be ignored in efficiency metric calculations.[134,163]

The strong electron withdrawing effect of fluorine can significantly reduce the pK_a of adjacent functional groups such as carboxylic acids, amines, and alcohols by several orders of magnitude (Table 1.3).[164,165] Thus, fluorine can heavily influence the lipophilicity of a molecule depending on its environment. While the introduction of fluorine is often expected to increase lipophilicity, aliphatic fluorine can in many cases lead to a decrease of logP.[166,167] This is in particular true when fluorine if positioned adjacent to oxygen or another fluorine atom to stabilize a more polar conformation (*e.g.* by the *gauche* effect).[167–169]

Table 1.2. Key properties of the C–F and C–CF_3 moieties.[133,134,170–172]

Bond	Bond length (Å)	vdW radius[a] (Å)	vdW volume[a] (Å^3)	Electro-negativity	Dipole moment μ (D)	BDE (kJ/mol)
C–H	1.09	1.20	7.24	2.20	-0.4	413
C–F	1.35	1.47	13.3	3.98	1.41	441
C–Cl	1.77	1.75	22.5	3.16	1.87	328
C=O	1.23	1.52	14.7	3.44	2.33	355
C–OH	1.48	1.52	14.7	3.44	1.66	351
C–Me	1.53	1.73	21.6	2.55	0	-
C–CF_3	~1.50	2.11	39.8	~3.4[b]	~2.34	-
C–Et	1.53	-	38.9	2.55	0	-

[a] of atom/group (not bond). [b] variable depending on the method of determination.[173,174] vdW = van der Waals; BDE: bond dissociation energy.

Table 1.3. pK_a values of selected compounds.[164,165]

Compound	pK_a	Compound	pK_a
CH_3COOH	4.8	CH_3CH_2OH	15.9
CH_2FCOOH	2.6	CF_3CH_2OH	12.4
CHF_2COOH	1.3	$CH_3CH_2NH_3^+$	10.7
CF_3COOH	0.5	$CH_2FCH_2NH_3^+$	9.0
CF_3CH_2COOH	3.1	$CHF_2CH_2NH_3^+$	7.3
$CF_3CH_2CH_2COOH$	4.2	$CF_3CH_2NH_3^+$	5.8

Fluorine can in certain cases participate in hydrogen-bonding as a HBA, although such interactions are rare and the bonding is weak.[134,175–178] Unlike other halogens, fluorine can generally not participate in halogen bonding due to its near-spherical electron distribution (no electron-deficient σ-hole).[179] However, the CF_3-moiety may engage in a weak, but nevertheless interesting tetrel bonding (–CF_3···O/N) through a similar σ-hole interaction on the sp^3-carbon (Figure 1.31). Like the halogen bond, this binding interaction is optimal at an angle of 180° to the C-CF_3 bond.[180]

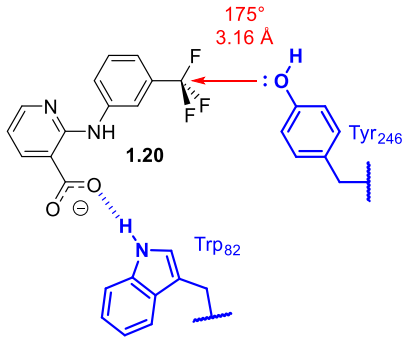

Figure 1.31. Key binding interactions between niflumic acid (**1.20**) and NMRAL1 in a co-crystal complex illustrates an example of CF_3-mediated tetrel bonding.[181]

1.6.2. Fluorine in Medicinal Chemistry

Fluorine has played an significant role in medicinal chemistry since approval of the first fluorinated drug, fludrocortisone, in 1955 (Figure 1.32).[182] The electronic properties and relative small size of fluorine has made it a valuable isostere in drug design and fluorine has been used to influence numerous properties including potency, conformation, clearance, pK_a, and permeability. Today, approximately 25% of all marketed drugs contain fluorine (Figure 1.32).[134,168,183–185]

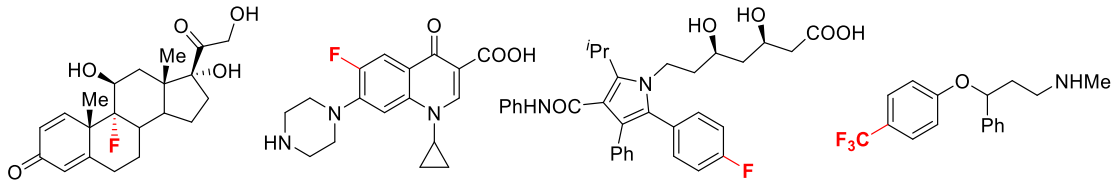

Figure 1.32. Structures of selected fluorinated FDA-approved drugs – the first fluorinated drug, fludrocortisone, and three fluorine-containing blockbuster drugs.[182]

The use of fluorine as a bioisostere in drug molecules has predominantly been achieved through simple replacement of hydrogen atoms. However, over the years numerous other fluorine-containing isosteres have been deployed with a few examples shown in Figure 1.34. Most often, fluorine is introduced as a metabolic blocker to alter the rate or route of metabolism. Metabolic labile sites, both aromatic and aliphatic, can in many cases be protected through fluorination partly due to the increased bond strength of the C–F bond. Metabolic deflourination can, however, also readily occur during biotransformation and release highly toxic metabolites. Thus, thorough metabolic studies should always be carried out.[168,186]

Fluorine has also been used to enhance membrane permeability of drugs. One strategy involves the use of intramolecular hydrogen-bonding to shield a nearby HBD and thus enhance passive permeability (Figure 1.33). This has typically been performed by introduction of fluorine in the *ortho*-position of *N*-phenylamides or benzamide derivatives.[134] A similar approach involves the use of fluorine to modulate the basicity of proximal amines and thereby decreasing the population of protonated species for improved membrane permeability.

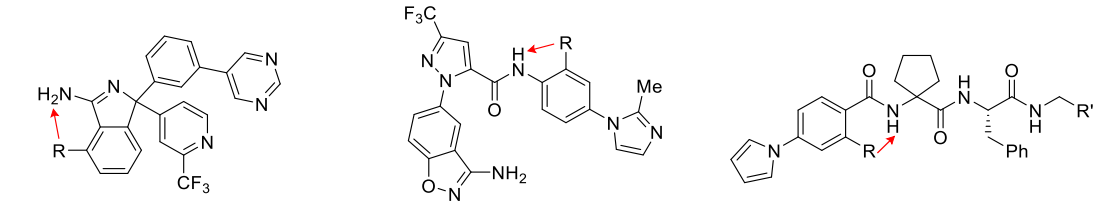

1.21, R = H, P_{app} = 0.13 × 10^{-6} cm/s
1.22, R = F, P_{app} = 39 × 10^{-6} cm/s

1.23, R = H, P_{app} = 0.82 × 10^{-6} cm/s
1.24, R = F, P_{app} = 7.41 × 10^{-6} cm/s

1.25, R = H, P_{app} = <1 × 10^{-6} cm/s
1.26, R = F, P_{app} = 13.8 × 10^{-6} cm/s

Figure 1.33. Examples of fluorine participating in intramolecular hydrogen-bonding to shield a proximal hydrogen bond donor and increase cell permeability – BACE1 inhibitors **1.21** and **1.22**, coagulation enzyme factor Xa inhibitors **1.23** and **1.24**, and human NK2 receptor inhibitors **1.25** and **1.26**. The effects were not due to a decrease of either pK_a or hydrophobicity. P_{app} refers to Caco-2 permeability.[134,168]

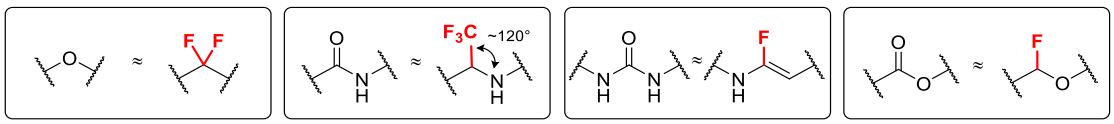

Figure 1.34. A few examples of fluorine-containing isosteres. Difluoroalkanes can be used as isosteres of oxygen with the two fluorine atoms mimicking the lone pairs of oxygen. The CF_2-moiety also exhibits similar electronegativity to that of oxygen. The trifluoroethylamine moiety is comparable to that of an amide with similar bond angles but increased enzymatic stability. The C–F dipole and electron density mimics that of the oxygen while significantly reducing the basicity of the amine such that it more resembles an amide. Other examples include fluoroenamines as isosteres of urea due to similar topologies and the ester isostere α-fluoro ether, which can be used to increase chemical and metabolic stability of esters.[134]

Finally, fluorine can also be useful as a conformational control element. Due to the highly polarized C–F bond with a low lying σ^* orbital, there is a strong preference for vicinal functionalities to align *gauche* with aliphatic fluorine. This phenomenon has been exploited in both drug design and organocatalysis and an example is shown in Figure 1.35.[167,168]

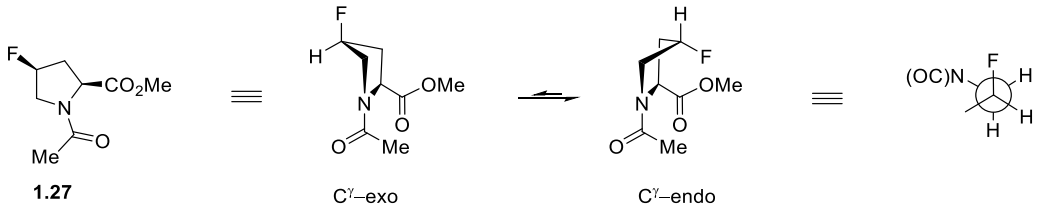

Figure 1.35. Fluorine can stabilize more sterically demanding conformations due to the *gauche* effect. *N*-Acetyl proline methyl ester normally adopts the Cγ-exo conformation, however, introduction of fluorine in the 4-(*S*) position shifts the equilibrium towards the normally less favorable Cγ-endo conformation.

1.6.3. ^{19}F NMR Spectroscopy

Aside from ^{1}H and ^{13}C, ^{19}F is one the most studied nuclei in NMR spectroscopy (Figure 1.36). ^{19}F is 100% abundant and exhibits a high magnetogyric ratio (γ) at 0.94 times that of ^{1}H. Fluorine NMR has a comparable intrinsic sensitivity (83%) to that of proton NMR making it the second most sensitive nucleus for NMR spectroscopy. With a spin quantum number of ½, fluorine couples to both proton and carbon (^{13}C) similar to what is observed for ^{1}H.[187–189]

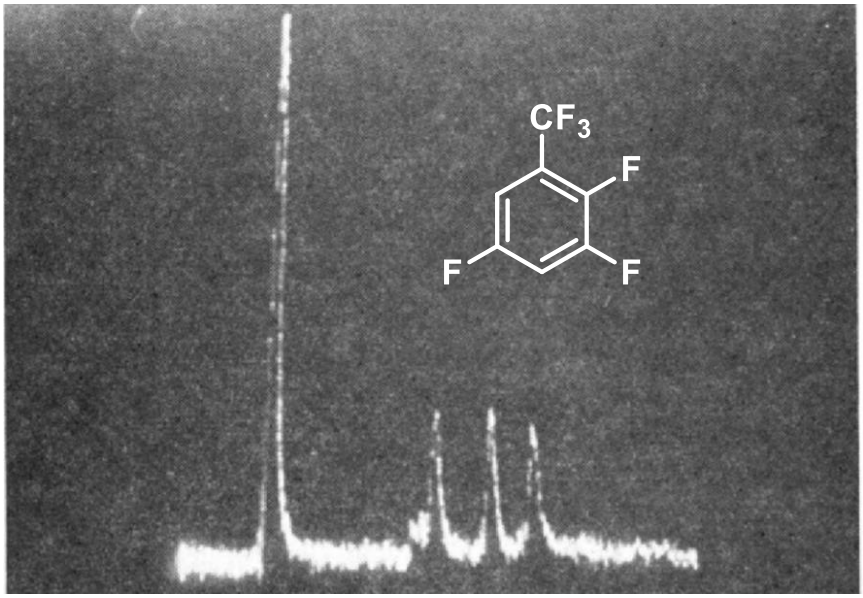

Figure 1.36. The first recorded ^{19}F NMR spectra from 1952: 2,3,5-trifluorobenzotrifluoride recorded at 26 MHz field strength. The strong signal is assigned to the CF_3-group and the three weak lines, from left to right, to the 5-, 3- and 2-fluorines. Figure adapted from reference.[187]

In contrast to proton, fluorine is characterized by a large chemical shift anisotropy (CSA) resulting in a chemical shift range spanning over 350 ppm for organofluorine compounds. The most relevant C–^{19}F resonances are found in the range from -50 to -250 ppm (Figure 1.37).[50,188,190]

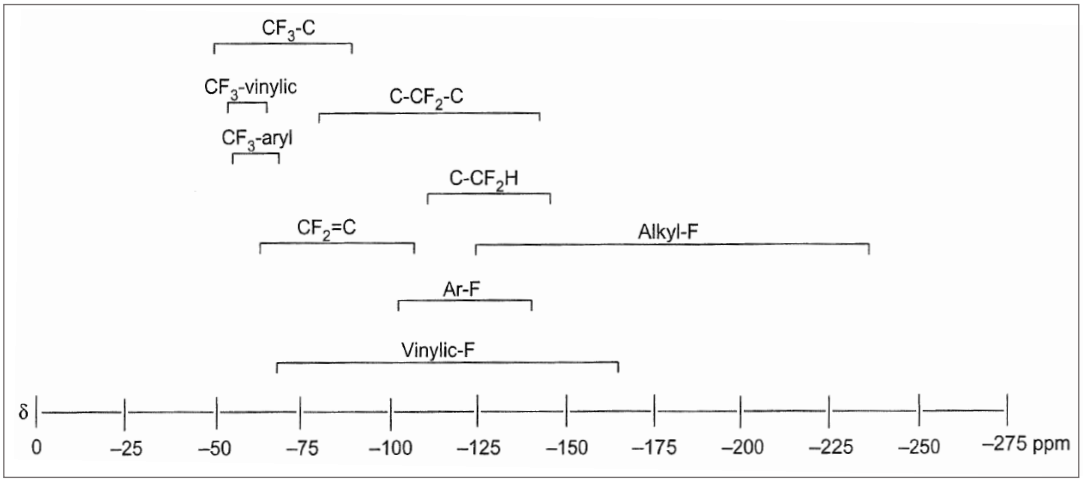

Figure 1.37. An overview of the chemical shift range of the most useful C–^{19}F signals (relative to the signal of $CFCl_3$ at 0 ppm). Figure adapted from reference.[188]

1.6.4. ^{19}F NMR-Based Screening

^{19}F NMR-based screening is predominantly performed using T_2-relxation based experiments, often based on a CPMG scheme (see section: Ligand-Observed NMR Spectroscopy, p. 8). The use of ^{19}F NMR for screening of compounds was first reported by Kihlberg and co-workers in 1994,[191] and has since been further improved primarily by Dalvit and co-workers.[50,52,190,192,193] Compared to ^{1}H NMR-based methods, the use of ^{19}F NMR offers a series of key advantages including increased sensitivity, simplicity, and sample throughput. Because of the prevalence of protons, overlap of signals from fragments, water, additives, and proteins is a major limitation of using ^{1}H NMR. Consequently, screening cocktails for ^{1}H NMR-based methods are typically limited to only a handful of fragments (Figure 1.38).[41,194]

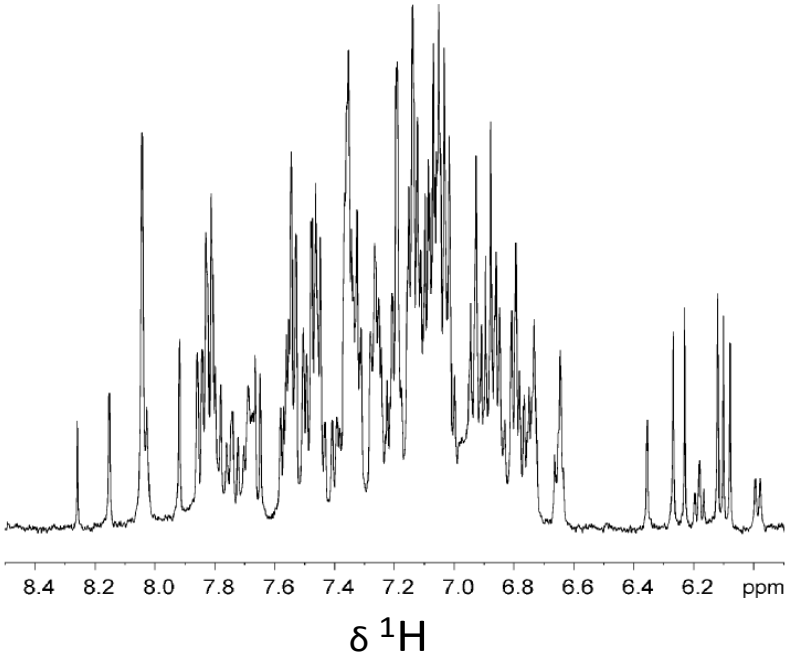

Figure 1.38. Partial ^{1}H NMR spectrum of a screening cocktail with 11 fragments. Significant overlap of signals can make it difficult to identify a potential binder. Figure adapted from reference.[191]

In contrast, the larger CSA of fluorine and the presence of only one fluorine moiety per screening compound significantly reduces the risk of spectral overlap in ^{19}F NMR (Figure 1.39). Furthermore, buffers and additives can be completely ignored due to the absence of fluorine in these. This facilitate screening of cocktails containing ≥30 fragments and at both ligand and protein concentrations significantly lower than for ^{1}H NMR.[193,194] Finally, the large CSA of fluorine makes the nucleus highly sensitivity to changes in its chemical environment including protein binding. ^{19}F NMR-based screening is therefore among the most sensitive

techniques for detection of binding.[195] Indeed, the method has even been used to detect binding of one enantiomer over the other when screening of racemates.[192]

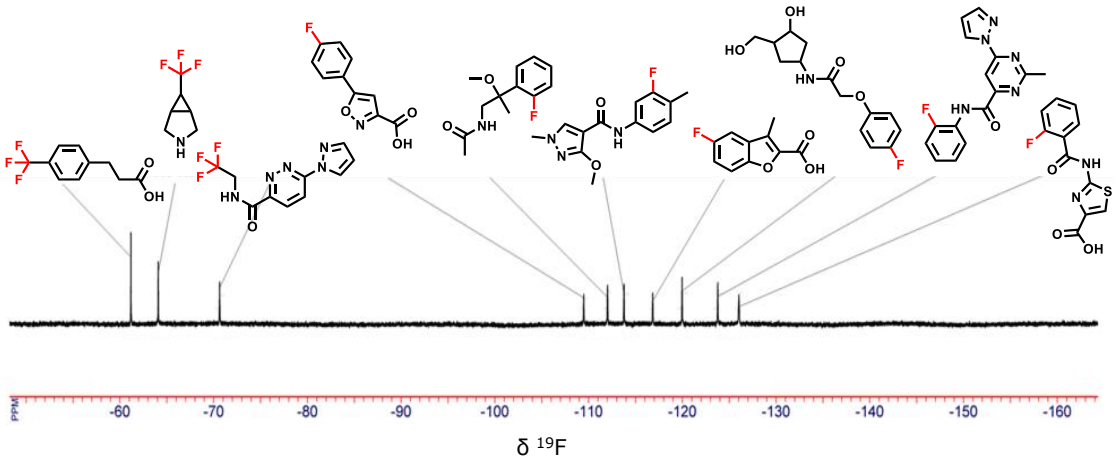

Figure 1.39. Example of a screening cocktail containing 10 fluorinated fragments (^{1}H decoupled ^{19}F NMR). Figure adapted from reference.[196]

In addition to ligand-observed experiments, protein-observed ^{19}F NMR using fluorinated amino acids has also become increasingly popular. This approach generally make use of chemical shift perturbations to identify binding sites and determine affinities. While the high CSA of fluorine is a major concern in regards to peak broadening in large molecules, the method has shown amenable with a 180 kDa protein.[197]

1.6.5. Fluorine Moieties for ^{19}F NMR

The main drawback of using ^{19}F NMR-based screening is the need of fluorinated molecules. The most relevant organofluorine moieties include CF, CF_2, CF_3, and SF_5 – each with their inherent advantages. CF is the simplest fluorine moiety and has the largest chemical shift dispersion (Figure 1.37). Ar–F represents the vast majority of CF-moieties in screening compounds due to its greater stability compared to C(sp^3)–F and its higher prevalence in available building blocks.[198–204]

The aliphatic CF_2-group is more stable and offers higher sensitivity due to the added fluorine. However, the presence of stereocenters renders the two fluorine atoms diastereotopic and results in subsequent loss of sensitivity with doubling of signals.[188]

The CF_3-group offers the highest sensitivity and screening can be performed at lower concentrations. Even though the CF_3-moiety has a smaller ^{19}F chemical shift dispersion (~35 ppm), screening cocktails of up 40 CF_3-containing fragments have been reported.[50,190,195,205]

Finally, the more uncommon pentafluorosulfanyl (SF_5) has received increasing attention for use in medicinal chemistry and ^{19}F NMR screening.[134,205–207] With an octahedral geometry, the bulky SF_5 has two ^{19}F NMR signals arising from the axial (1F, pentet) and equatorial (4F, doublet) fluorine, respectively. Interestingly, these chemical shifts appear downfield from the internal standard $CFCl_3$ and generally appear in the range of 55–90 ppm.[188]

Part II

The 3F Library: Fluorinated Fsp^3-rich Fragments for Expeditious ^{19}F NMR-based Screening

2.1. Project Outline

Ligand-based ^{1}H NMR methods are among the most widely applied screening techniques used in FBDD.[10] However, due to the abundance of protons in compounds, solvents, additives, and biomolecules, overlap of signals is a major challenge. Design of screening cocktails requires careful planning and such cocktails are typically limited to only a handful of fragments at a time. Furthermore, these experiments rely on a relatively high protein consumption to obtain reliable results.[41] In contrast, ^{19}F NMR offers increased sensitivity and simplicity and enables screening of ≥ 30 fragments simultaneously at lower protein concentrations.[193]

Unfortunately, ^{19}F NMR screening is currently limited by a low availability and poor diversity of fluorinated fragments. Similar to most drug-like small molecules, available fluorinated fragment are dominated by rather flat topologies (exemplified by a high degree of sp^2-hybridized carbon atoms) and similar structural features.[119,121] In contrast, natural products tend to have greater saturation (Fsp^3) and more chiral centers, which results in more three-dimensional structures.[116–118] Importantly, higher degrees of Fsp^3 have also been correlated with better outcomes in drug development due to improved solubility and less off-target binding.[118,121,122]

In an effort to increase the usefulness of ^{19}F NMR in FBDD, a fluorinated Fsp^3-rich fragment (3F) library with excellent shape diversity was targeted. To ensure sufficient aqueous solubility of the fragments, a low average AlogP of the library was also highly desirable. Finally, as a proof of concept for the application of the 3F library, ^{19}F NMR screening of the 3F library against a range of disease-related targets was conducted followed by subsequent validation of potential hits using secondary screening assays.

2.2. Library Design

While organofluorine chemistry has become increasingly versatile,[208–210] it was decided to use fluorinated starting materials for the construction of the 3F library in order to save synthetic steps. Among the readily available and practical fluorine moieties, CF, CF_2, CF_3, and SF_5, the CF_3-group was selected for its sensitivity and chemical stability. The use of CF_2 was omitted to avoid issues with diastereotopic signals. Likewise, the SF_5-group was discarded for its two ^{19}F NMR signals and in particular for its bulkiness and large molecular weight (127 Da). The simplest C(sp^3)–F moiety was considered, however, its lower chemical stability could be a concern with certain transformations.[198] Although the Ar–F moiety is typically used instead, its high molecular weight (95 Da), lipophilicity, and flatness made this moiety less suited for the 3F library.

Ultimately, it was decided to build the 3F library from a small group of similar and readily available trifluoromethylated α,β-unsaturated starting materials (**2.1**–**2.6**). Exploiting the synthetic versatility of such unsaturated systems would enable easy access to large structural diversity (Figure 2.1). Importantly, having the CF_3-group situated directly on the unsaturated system would also facilitate a larger dispersion of resulting ^{19}F chemical shifts compared to a more distal CF_3-group.

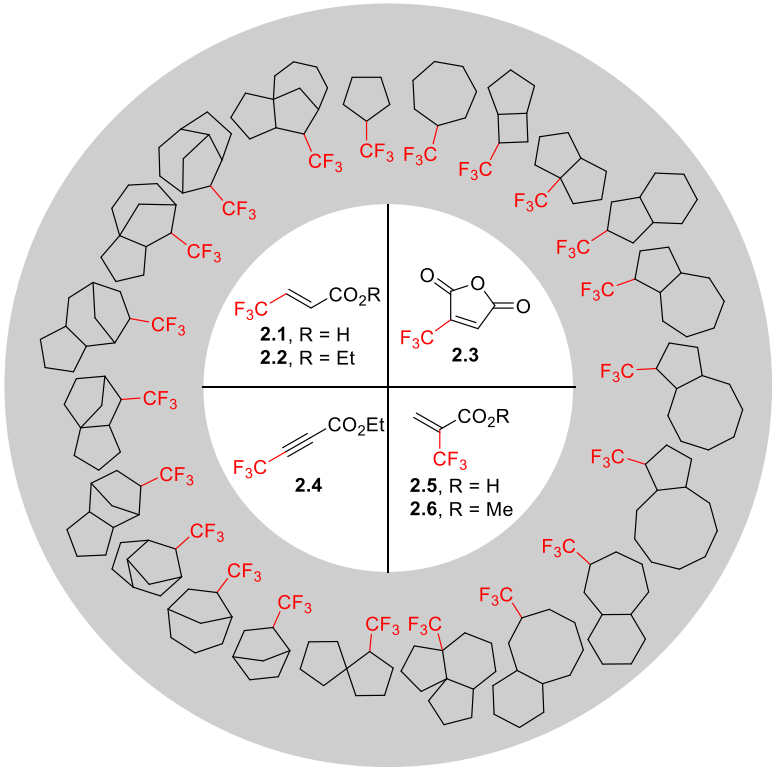

Figure 2.1. Diverse ring systems accessed from this (trifluoromethylated) α,β-unsaturated system. Adapted with permission from reference.[1] Copyright (2020) John Wiley and Sons.

Fragments were generally designed accordingly to a slightly modified Ro3.[35] While the Ro3 guidelines suggest molecular weights below 300 Da, the increased mass of fluorine over hydrogen can typically be ignored for efficiency metric calculations and ^{19}F NMR screening.[134,193] For this reason, an increased molecular weight limit of 354 Da was chosen to compensate for the presence of the CF_3-group. As a strategy to achieve a high degree of 'three-dimensionality' and good shape diversity, installation of multiple stereocenters and increasing saturation (Fsp^3) were targeted. In order to synthesize the 3F library in an efficient manner, fragments were to be synthesized using DOS in no more than five steps from the chosen starting materials. Finally, all chiral fragments were prepared as racemates to enable screening of all enantiomers.

2.3. Library Synthesis

Starting from the six trifluoromethylated compounds **2.1**–**2.6**, nine core scaffolds were initially synthesized. Each contained 3–5 synthetic handles that were further functionalized or modified to afford a novel library of structurally diverse fluorinated fragments in a maximum of five steps from **2.1**–**2.6**. The following chapters are dedicated to each of these nine core scaffolds and the sub-libraries synthesized thereof. Chapters are titled accordingly to the chemistry used to synthesize the respective core scaffolds and begins with a short comparison to similar natural products or bioactive compounds. Reaction overviews of each sub-library can be found in the Supporting Information (Schemes S1–S9).

2.3.1. Furan Diels-Alder

The oxabicyclo[2.2.1]heptane scaffold is well-represented among natural products and in several bioactive molecules (Figure 2.2).[211–214] The small bridged bicyclic scaffold can be accessed *via* a Diels-Alder (DA) reaction[215] with furan and contains a high degree of saturation and a reasonably 3D character.

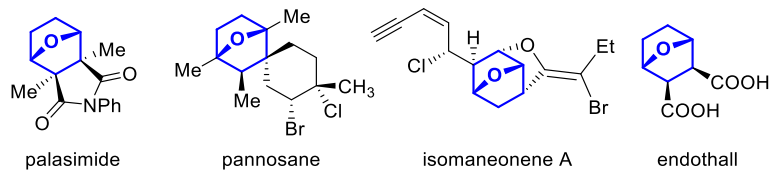

Figure 2.2. Examples of compounds containing an oxabicyclo[2.2.1]heptane moiety - the natural products palasimide,[211] pannosane,[212] and isomaneonene A,[213] and the herbicide endothall.[214]

In 1956, McBee *et al*. reported a Diels-Alder reaction between **2.1** and furan in which one diastereomer crystallized directly from the solution in high yields.[216] However, attempts to reproduce these results failed, affording an inseparable 3:2 mixture of crystalline diastereomers instead (Scheme 2.1).

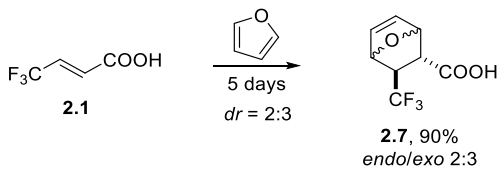

Scheme 2.1. Diels-Alder reaction between **2.1** and furan.

Inspired by the simple procedure reported by McBee *et al.*, a screen with various substituted furans was set up (Table 2.1). Gratifyingly, the reaction between **2.1** and 2-methylfuran afforded a diastereomerically pure crystalline product in 90% yield (entry 3). Interestingly, NMR analysis of the remaining filtrate revealed a similar 3:2 mixture of diastereomers as observed for entry 1, but with the crystallized product as the minor product. Reaction with other monosubstituted furans proceeded with poor regioselectivity and resulted in mixtures of 4 diastereomers (entries 5–8). Furan with strong electron withdrawing groups (EWGs) did not undergo Diels-Alder reaction with **2.1**, even at elevated temperatures (entries 9 and 10). A hetero Diels-Alder reaction with oxazole was also attempted but failed to react with **2.1** (entry 11). Finally, subjecting acrylate **2.2** to the same Diels-Alder conditions with either furan or 2-methylfuran afforded mixtures of diastereomers without crystallization (entries 2 and 4).

Based on the encouraging results from the reaction with 2-methylfuran (Table 2.1, entry 3), it was decided to base this sub-library on **2.8**. While the regiochemistry **2.8** was as expected, in accordance with HOMO/LUMO pairing, the relative stereochemistry could not be accurately assigned with NMR spectroscopy alone. Thus, an intramolecular iodolactonization was performed to elucidate whether the *endo* or *exo* product had been formed. Satisfyingly, this reaction afforded lactone **2.9** in 80% yield and **2.8** was therefore assigned as the *endo* product (Scheme 2.2). The stereochemistry of **2.8** was later unequivocally confirmed by X-ray crystallography (Figure 2.3).

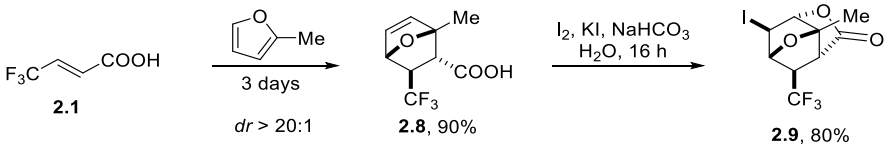

Scheme 2.2. A highly regio- and diastereoselective Diels-Alder reaction between **2.1** and neat 2-methylfuran to install four consecutive stereocenters. The *endo* stereochemistry (in respect to the carboxylic acid) of DA product **2.8** was confirmed by an intramolecular iodolactonization.

Table 2.1. Diels-Alder reaction of **2.1** and **2.2** with various dienes. The reactions were performed neat.

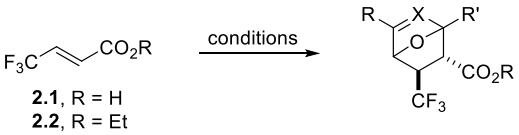

2.1, R = H
2.2, R = Et

Entry	Dienophile	Diene	Temp. (°C)	Time (h)	Result	*dr*
1	**2.1**		22	120	two diastereomers 90% yield	3:2
2	**2.2**		22	120	two diastereomers	58:42
3	**2.1**	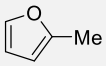	22	72	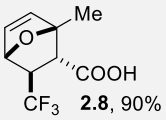 **2.8**, 90%	>20:1
4	**2.2**	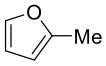	22	72	two diastereomers	56:44
5	**2.1**	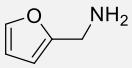	22	72	four diastereomers	ND
6	**2.1**	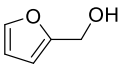	22	72	four diastereomers	ND
7	**2.1**	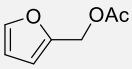	22	120	four diastereomers	ND
8	**2.1**		22	120	four diastereomers	ND
9	**2.1**	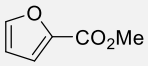	140[a]	4	no reaction	NA
10	**2.1**	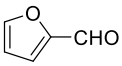	140[a]	4	no reaction	NA
11	**2.1**		22	120	no reaction	NA

[a] μW heating; *dr* = diastereomeric ratio; NA = not applicable; ND = not determined

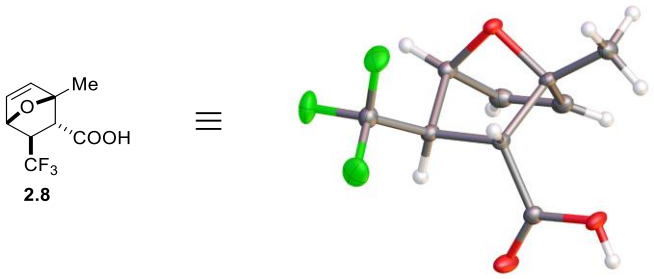

Figure 2.3. X-ray single crystal structure of **2.8**.

With core scaffold **2.8** in hand, derivatization of the carboxylic acid was identified as a key step in achieving further diversity. Amidation with *N*-allylmethylamine using HATU as coupling reagent proceeded in excellent yield and without any epimerization observed (Scheme 2.3). Next, a tandem ring-opening metathesis (ROM) of the strained endocyclic olefin followed by ring-closing metathesis (RCM)[217] to form a more thermodynamically stable alkene was envisioned. Satisfyingly, using Hoveyda-Grubbs 2nd generation catalyst[218] (HG II) under an ethylene atmosphere afforded the natural product-like bicyclic fragment **2.11** in 60% yield (Scheme 2.3). In the absence of ethylene gas, only ROM was observed and resulted in a complex mixture.

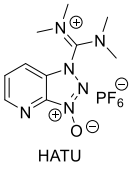

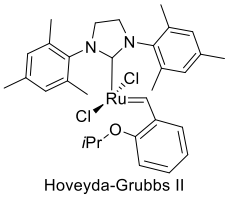

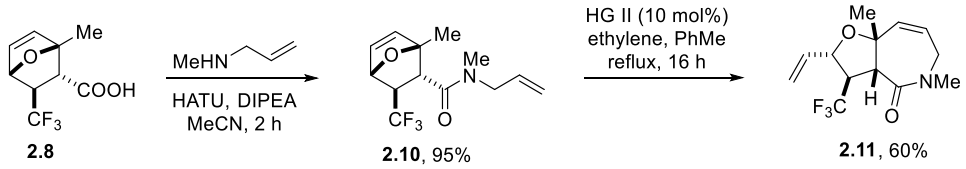

Scheme 2.3. Amidation of **2.8** with an olefin-containing secondary amine followed by tandem ROM/RCM afforded a bicyclic scaffold.

Employing the same strategy with different olefin-containing amines (synthesized *via* reductive amination), a series of *cis*-fused [5,7], [5,8], and [5,9] bicyclic fragments (**2.16**–**2.18**) were synthesized (Scheme 2.4). Surprisingly, carboxylic acid-containing amide **2.15** did not undergo ROM/RCM but instead underwent a retro-Diels-Alder reaction to afford **2.19**.

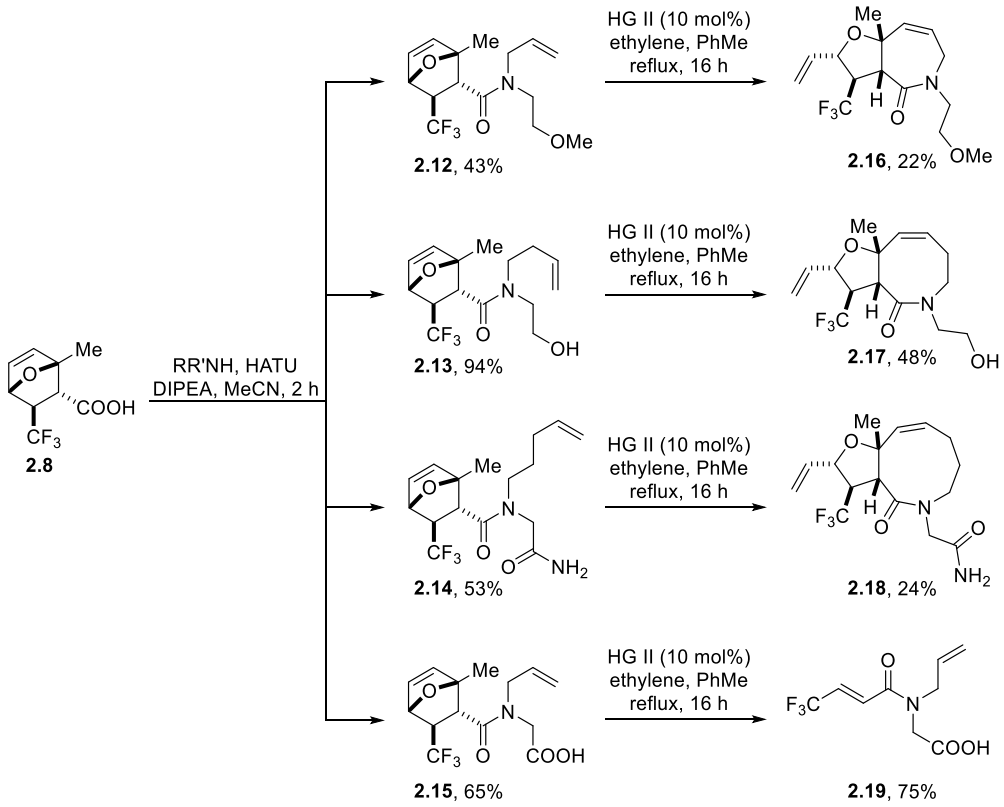

Scheme 2.4. Amidation of **2.8** followed by RCM/ROM afforded a series of *cis*-fused [5,7], [5,8], and [5,9] bicyclic fragments. Amide **2.15** underwent a retro-Diels-Alder reaction to give **2.19** instead of the expected ROM/RCM product.

Inspired by the successful iodolactonization of **2.8** (Scheme 2.2), epoxidation followed by intramolecular *N*-epoxide-opening with an amide was attempted on the core scaffold. Benzyl and ^{t}Bu amides **2.20** and **2.21** were synthesized in high yields and then subjected to standard epoxidation conditions with *m*CPBA (Scheme 2.5). Subsequent treatment with ^{t}BuOK facilitated base-mediated *N*-epoxide-opening to afford tricyclic fragments **2.22** and **2.23** in good yields over two steps.

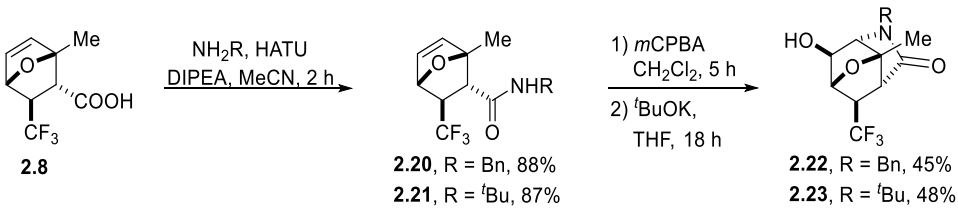

Scheme 2.5. Amidation followed by epoxidation and base-mediated intramolecular *N*-epoxide-opening to form tricyclic fragments.

Aiming to use the same approach for construction of an eight-membered ring, alcohol-containing amide **2.24** was synthesized in 85% yield (Scheme 2.6). However, the subsequent epoxidation of **2.24** proceeded slowly and upon increasing the temperature spontaneous amide-*O*-epoxide-opening and hydrolysis occurred to afford lactone **2.26**. While this fragment was not initially targeted, it was included in the library.

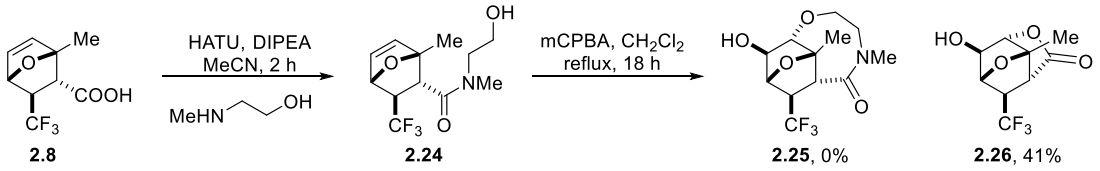

Scheme 2.6. Amidation of **2.8** followed by epoxidation and intramolecular epoxide-opening.

In a similar approach to synthesize an eight-membered ring containing tricyclic scaffold, amidation with 2-(methylamino)phenol was attempted. However, this weaker and bulky amine failed to undergo amidation using either HATU, PyBroP, or BTFFH as coupling reagents and the synthesis of this scaffold type was abandoned (Scheme 2.7).

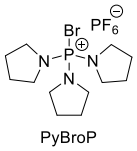

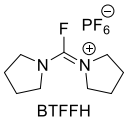

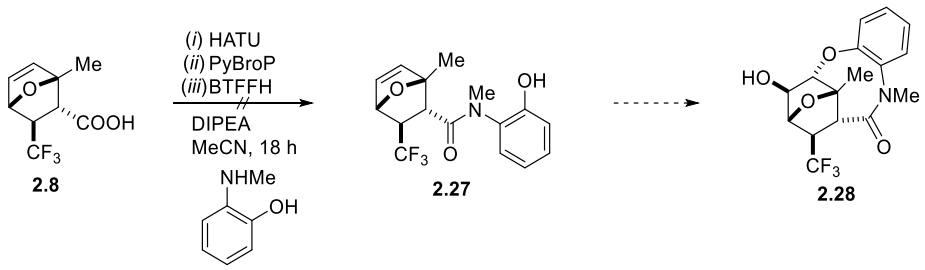

Scheme 2.7. Attempted amidation of **2.8** with 2-(methylamino)phenol failed.

Next, oxidative cleavage of the endocyclic olefin of core scaffold **2.8** was investigated. Amides **2.20** and **2.29** (the latter was synthesized in 83% yield from **2.8**) were subjected to an Upjohn dihydroxylation (Scheme 2.8).[219] Using catalytic K_2OsO_4 with NMO as oxidant afforded *syn*-diol fragments **2.30** and **2.31** in a highly diastereoselective manner. Oxidative cleavage of **2.30** using $NaIO_4$ followed by reductive conditions gave ring-opened diol **2.32** in 39% yield. From diol **2.31**, acetal formation was performed to give the tricyclic fragment **2.34** in a moderate yield. Attempts to perform oxidative cleavage followed by reductive cyclization with amines failed to afford the desired ring-expanded fragments **2.33** and **2.35**.

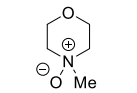

N-Methylmorpholine *N*-oxide (NMO)

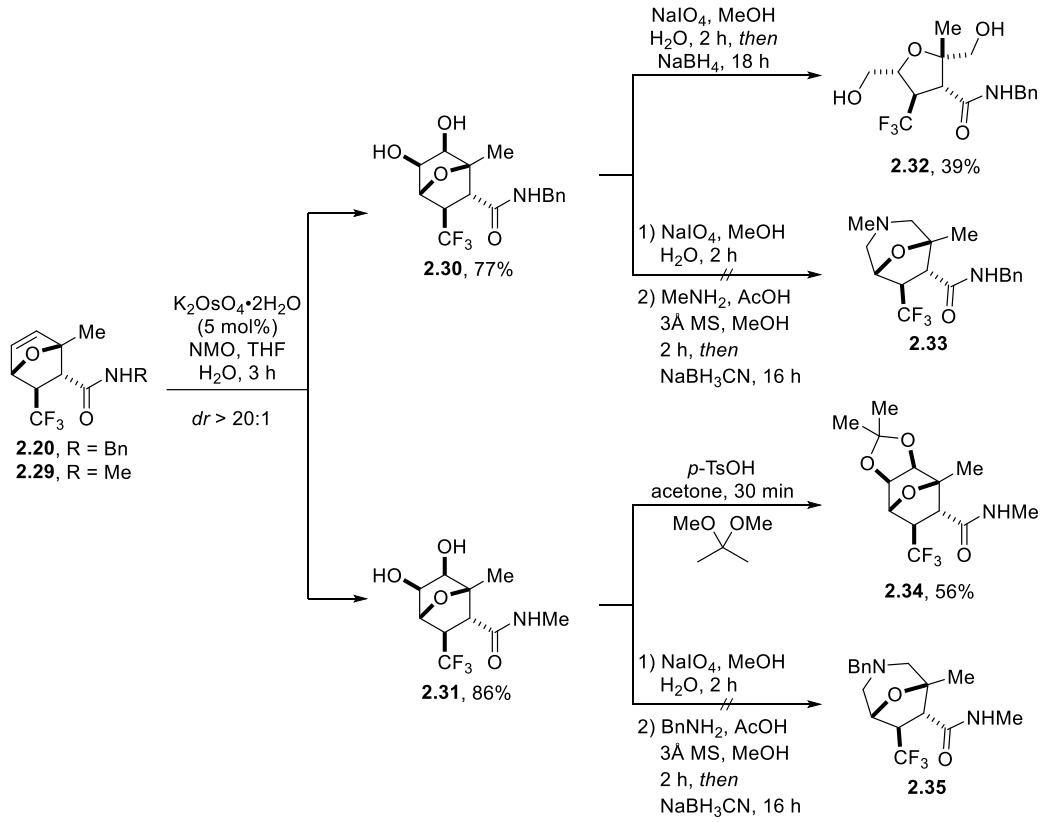

Scheme 2.8. Dihydroxylation of amides **2.20** and **2.29** afforded diols **2.30** and **2.31**. Oxidative cleavage of diol **2.30** under reductive conditions formed ring-opened diol **2.33** while acetal formation of **2.31** formed **2.34**. Attempts to perform reductive cyclizations failed. Amide **2.29** was synthesized from **2.8** in 83% yield.

In a similar approach, dihydroxylation of **2.8** afforded diol **2.36** in 58% yield (Scheme 2.9). Targeting lactone **2.37**, a subsequent oxidative cleavage and reduction by $NaBH_4$ was performed but failed to produce the desired lactone and yielded a complex mixture instead.

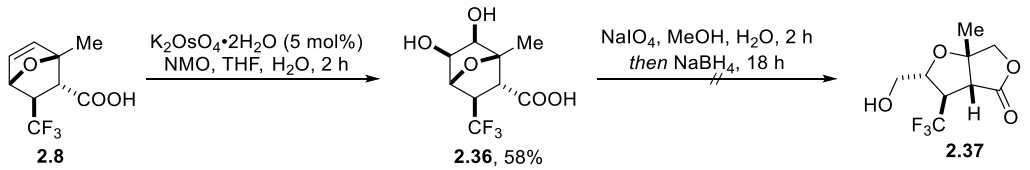

Scheme 2.9. Dihydroxylation of **2.8** and subsequent attempted oxidative cleavage and reduction.

To show that other derivatizations than amidation of the carboxylic acid were possible, **2.8** was set up for a Mitsunobu reaction.[220] As the endocyclic olefin proved unstable towards $LiAlH_4$, catalytic hydrogenation was performed prior to reduction and afforded alcohol **2.38** in 80% yield over two steps (Scheme 2.10). A Mitsunobu reaction was then performed with pyridine-3-ol as the nucleophile to give fragment **2.39** in 55% yield.

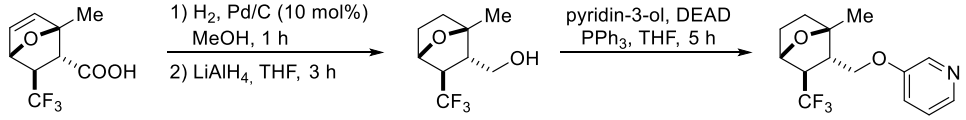

2.8 **2.38**, 80% **2.39**, 55%

Scheme 2.10. Catalytic hydrogenation, reduction, and Mitsunobu reaction of **2.8**.

Finally, to include additional fragments in the library, a series of amidations of **2.8** were performed. To increase the stability and Fsp^3 of the fragments, catalytic hydrogenation was carried out prior to amidation (Scheme 2.11).

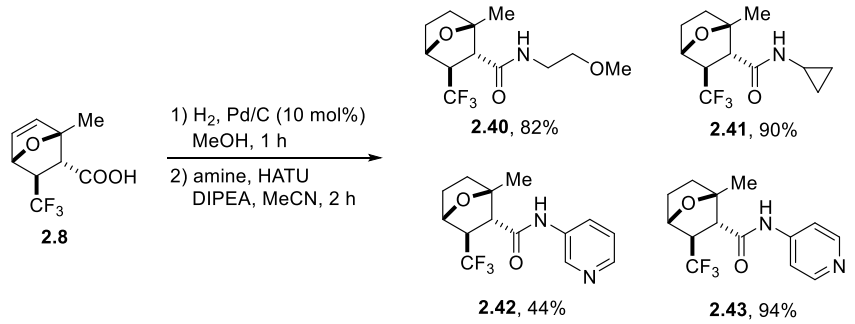

2.8 **2.40**, 82% **2.41**, 90% **2.42**, 44% **2.43**, 94%

Scheme 2.11. Catalytic hydrogenation followed by amidation of core scaffold **2.8** to afford additional fragments.

2.3.2. Intramolecular Diels-Alder

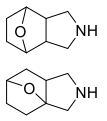

epoxy-indoles

Inspired by the successful Diels-Alder reaction, a similar bridged epoxy-isoindole scaffold was synthesized *via* amidation and a subsequent intramolecular Diels-Alder (IMDA) reaction of **2.1**. Interestingly, no natural products or bioactive molecules contains this exact tricyclic scaffold, although clearly similar to natural products such as palasimide (Figure 2.2).

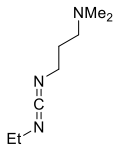

EDC

Initial amidations of **2.1** using HOAt- or HOBt-containing coupling reagents including HATU, PyBoP, or EDC/HOBt, gave only 50–80% yields due to partial 1,4-addition of HOAt or HOBt to **2.1**. Instead, *in situ* formation of an acid bromide using PyBroP was found to be highly effective (>90% yield). Using a series of furfurylamines, amidation with PyBroP followed by a highly diastereoselective IMDA reaction was accomplished and afforded epoxy-isoindole-based fragments **2.44**–**2.47** in 60–95% yield (Scheme 2.12). Attempts to perform the IMDA reaction on a secondary amide and form **2.48** failed – likely due to the large free energy difference between the amide *cis* and *trans* forms.[221]

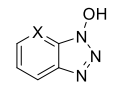

HOBt, X = CH
HOAt, X = N

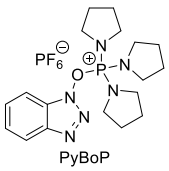

PyBoP

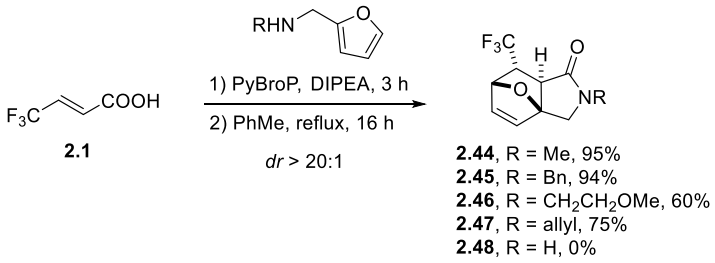

Scheme 2.12. Amidation of **2.1** followed by intramolecular Diels-Alder reaction to form a tricyclic scaffold.

Looking to derivatize the epoxy-isoindole scaffold, Upjohn dihydroxylations of the olefin in **2.44**–**2.46** were accomplished with excellent diastereoselectivity to afford diols **2.49**–**2.51** in high yields (Scheme 2.13).

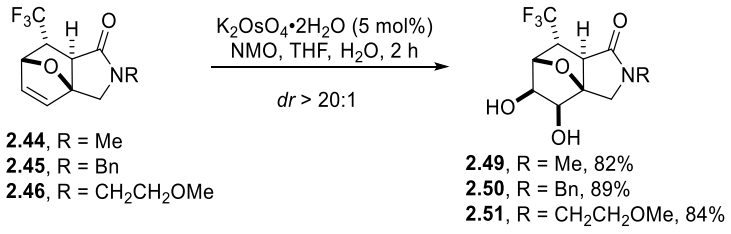

Scheme 2.13. Upjohn dihydroxylations.

With the diols in hand, ring expansion by oxidative bond cleavage and reductive cyclization was performed. While this reaction sequence had been unsuccessful for the furan Diels-Alder scaffold (Scheme 2.8), diols **2.49**–**2.51** turned out to be better substrates. Oxidative bond scissoring with $NaIO_4$ followed by addition of various amines and $NaBH_3CN$ under anhydrous conditions afforded ring-expanded fragments **2.52**–**2.56** in 55–64% yield (Scheme 2.14). Attempts to improve the yields by addition of either AcOH or using the corresponding HCl salts did not afford better results. Satisfyingly, this procedure also worked with two examples of dinucleophiles to afford **2.57** and **2.58** with a new seven- and nine-membered ring, respectively. Reaction with ethylenediamine failed to produce the desired **2.59**.

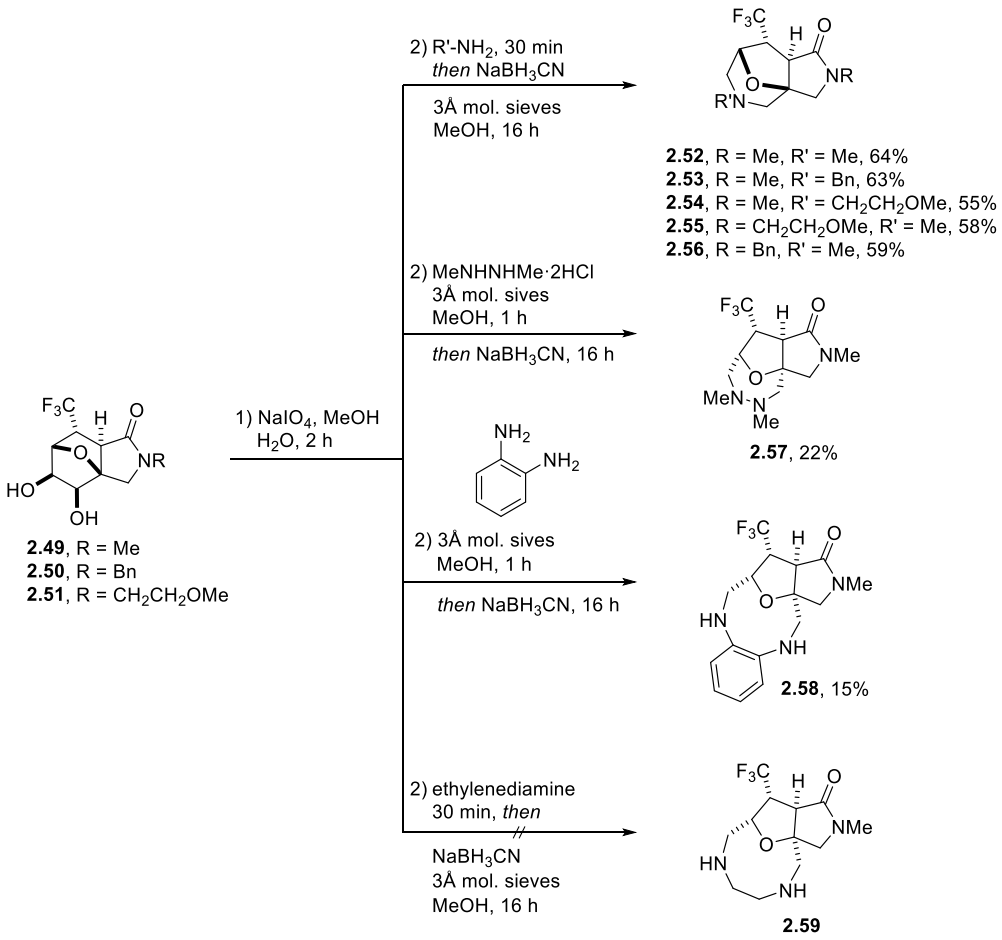

Scheme 2.14. Oxidative bond scissoring followed by reductive cyclization.

In addition to reductive cyclization, a double reductive amination after oxidative cleavage of **2.49** was also attempted. However, even with a large excess of methylamine and the use of a stronger reducing agent only cyclized product **2.52** was isolated (Scheme 2.15). Reduction

with $NaBH_4$ afforded ring-opened diols **2.61** and **2.62** in high yields. Finally, acetal formation of **2.49** afforded the tetracyclic fragment **2.63** in excellent yield.

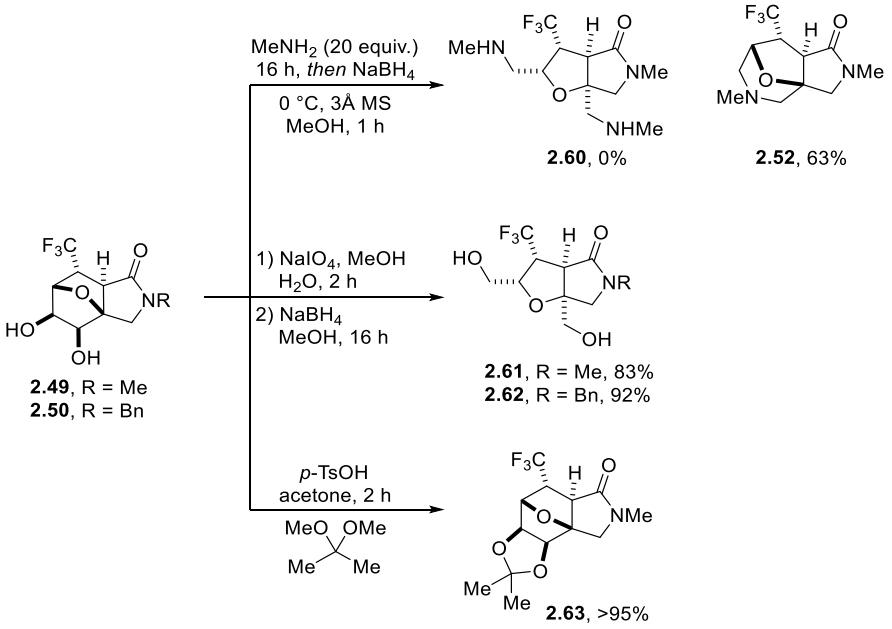

Scheme 2.15. Additional derivatizations of diol **2.49** and **2.50**: oxidative cleavage and acetal formation.

From allyl **2.47**, a ROM/RCM cascade reaction was attempted but failed to form the target fragment **2.64**, likely due to the strained nature of the resulting amide (Scheme 2.16).

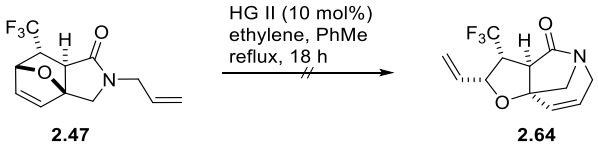

Scheme 2.16. Attempted ROM/RCM of **2.47**.

As an approach to easily access new derivatives, debenzylation of **2.45** was attempted. Disappointingly, the attempted hydrogenolysis only caused olefin reduction while heating in acid primarily resulted in a complex mixture partly due to cleavage of the ether bridge (Scheme 2.17).

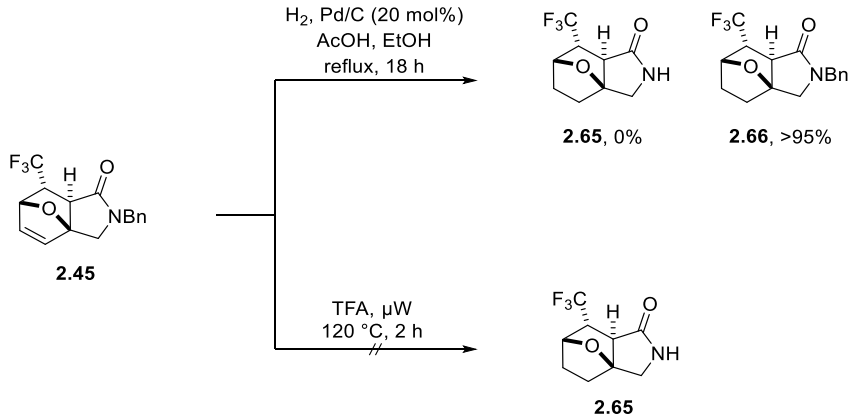

Scheme 2.17. Attempted debenzylation of **2.45**.

Several approaches to ring-open the ether bridge in **2.45** were also attempted (Scheme 2.18). While **2.45** remained stable towards $NaBH_4$, $LiAlH_4$ yielded a complex mixture where pyrrole **2.68** was the only product isolated. However, with an AlogP > 3, this fragment was not kept for screening. Subjecting methylated **2.44** to $LiAlH_4$ also produced a complex mixture but no products were isolated. Attempts to perform the ring-opening with a nucleophile in the presence of a Lewis acid also failed. Heating in the presence of NaOMe resulted in a complex mixture while the softer nucleophile NaSEt failed to react with **2.45**.

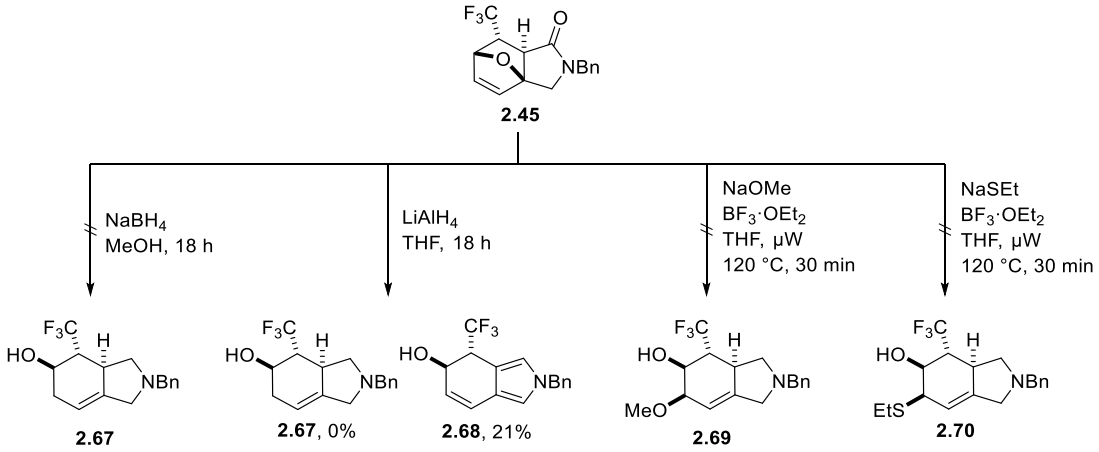

Scheme 2.18. Attempts to ring-open the ether bridge in **2.45**.

Using the same IMDA strategy, anhydride **2.3** was reacted with *N*-methylfurfurylamine to form a similar core scaffold containing a CF_3-substituted quaternary carbon center (Scheme

2.19). While anhydride-opening by the amine proceeded smoothly at ambient temperature with excellent regioselectivity at the least sterically hindered carbonyl, the reaction afforded a 1:4 mixture of **2.71** and IMDA product **2.72**. Attempts to push the conversion towards the IMDA product by heating failed. Instead, catalytic hydrogenation of the crude mixture over Pd/C led to exclusive formation of the tricyclic IMDA product **2.73** in excellent yield and diastereoselectivity.

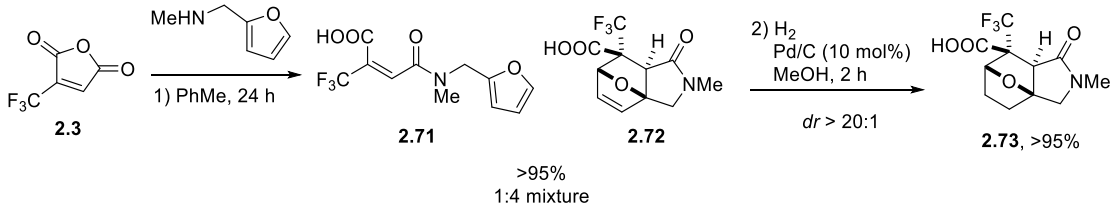

Scheme 2.19. IMDA reaction between anhydride **2.3** and *N*-methylfurfurylamine followed by catalytic hydrogenation to push the equilibrium towards the IMDA form.

Two derivatives based on **2.73** were prepared. Reduction with $LiAlH_4$ afforded amino alcohol **2.74** in 30% yield while amidation with dimethylamine gave fragment **2.75** in 70% yield (Scheme 2.20).

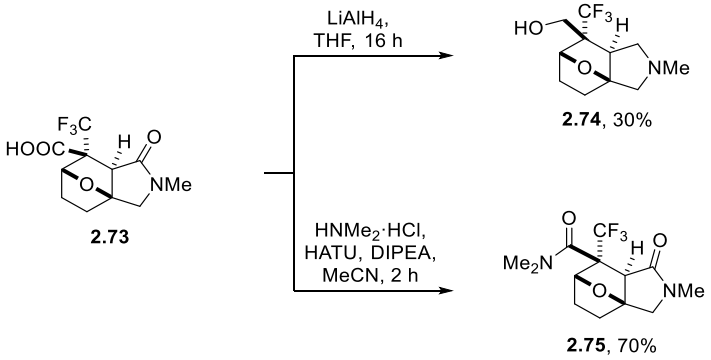

Scheme 2.20. Two derivatives of **2.73** were prepared by reduction and amidation, respectively.

2.3.3. Pyrrole Diels-Alder

In a similar effort, it was envisioned that the electron-deficient starting materials could undergo a Diels-Alder reaction with pyrrole to form a bridged azabicycle and thus gaining an extra handle for derivatization. Such nitrogen-bridged scaffolds are commonly found among natural products and bioactive compounds (Figure 2.4).[222–225]

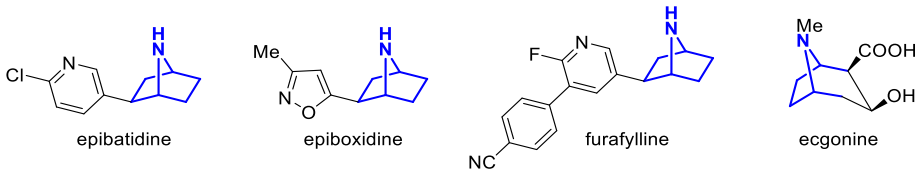

Figure 2.4: Examples of bioactive compounds containing a bridged nitrogen – the potent non-opioid analgesic epibatidine[222] isolated from an Ecuadoran poison frog and its less toxic analogue epiboxidine.[223] Furafylline is a selective cytochrome P450IA1 inhibitor used in the treatment of asthma[224] while the tropane ecgonine is found in coca leaves.[225]

While pyrrole has a higher degree of aromaticity than furan and thus less easily undergoes Diels-Alder reactions,[226] several examples of Diels-Alder reactions using electron-deficient pyrroles can be found in the literature.[227,228] Thus, commercially available *N*-Boc-pyrrole was subjected to different conditions in order to facilitate a Diels-Alder reaction (Table 2.2). Repeating the same conditions used for the furan-based Diels-Alder with **2.1** did not result in any product formation (entry 1). Switching to acrylate **2.2** and using microwave (μW) heating at 120 °C in neat *N*-Boc-pyrrole also failed to undergo a Diels-Alder reaction and increasing the temperature further only resulted in Boc-deprotection (entry 2). Gratifyingly, when using alkyne **2.4** instead the desired Diels-Alder reaction proceeded with quantitative yield at 120 °C (entry 3). Not surprisingly, reacting alkyne **2.3** with unprotected pyrrole at 160 °C did not yield any Diels-Alder product (entry 4).

Table 2.2. Diels-Alder reaction with pyrrole. Reactions were performed neat.

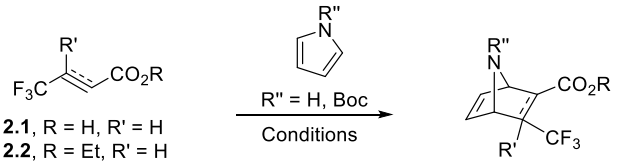

Entry	Dienophile	Diene	Temp. (°C)	Time (h)	Yield (%)
1	**2.1**	*N*-Boc-pyrrole	22	120	0
2	**2.2**	*N*-Boc-pyrrole	120[a]	8	0[b]
3	**2.4**	*N*-Boc-pyrrole	120[a]	2	>95 (**2.76**)
4	**2.4**	Pyrrole	160[a]	2	0

[a] μW heating. [b] temperatures above 120 °C caused Boc-deprotection.

Aiming to synthesize a small sub-library based on the pyrrole Diels-Alder core scaffold **2.76** with different amine and carbonyl substituents, olefin reduction by catalytic hydrogenation was performed next (Scheme 2.21). Unfortunately, using 10% Pd/C in EtOH resulted in an inseparable 1:1 mixture of *endo*/*exo* diastereomers.

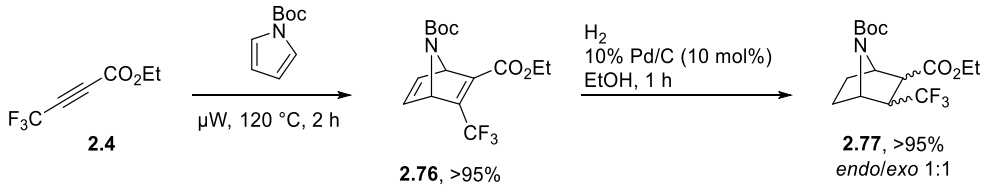

Scheme 2.21. Diels-Alder reaction between alkyne **2.4** and *N*-Boc-pyrrole followed by hydrogenation.

To improve the stereoselectivity of the catalytic hydrogenation, a small screen of different conditions was set up (Table 2.3). Performing the hydrogenation in an H-Cube flow reactor in MeOH only slightly improved the *endo*/*exo*-stereoselectivity to 1:1.4 (entry 2). Changing the catalyst to $Pd(OH)_2$ in the H-Cube reactor further improved the stereoselectivity to 1:4 (entry 3). Interestingly, addition of 2-methylpyridine, which is known to affect the properties of palladium,[229] effectively reversed the stereoselectivity to favor *exo*-face attack and afforded a 3:1 mixture of *endo*/*exo* diastereomers (entry 4). Repeating the initial conditions from entry 1 with the aprotic solvent THF gave an excellent *dr* of 1:19 (entry 5). However, full stereocontrol was finally achieved (*dr* = 1:100) when simply reducing the palladium on carbon loading from 10% to 5% in EtOH (entry 6).

Table 2.3. Catalytic hydrogenation of **2.76**.

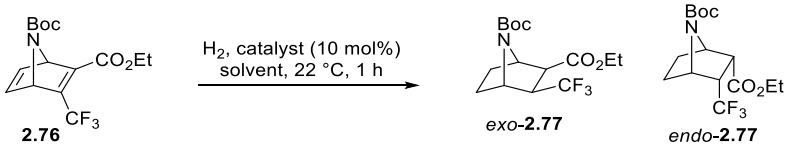

Entry	Catalyst	Additive	Solvent	*dr* (*endo*/*exo*)[a]
1	10% Pd/C	-	EtOH	1:1
2[b]	10% Pd/C	-	MeOH	1:1.4
3[b]	10% $Pd(OH)_2$	-	MeOH	1:4
4[b]	10% Pd/C	2-methylpyridine	MeOH	3:1
5	10% Pd/C	-	THF	1:19
6	5% Pd/C	-	EtOH	1:100

[a] determined by crude NMR. [b] performed in H-Cube flow hydrogenation reactor. *dr* = diastereomeric ratio.

With *exo*-**2.77** produced in excellent stereoselectivity, hydrolysis of the ester was accomplished with LiOH in 85% yield (Scheme 2.22). Subsequent HATU-mediated amidation and Boc-deprotection with TFA afforded amides **2.79**, **2.80**, and **2.81** in 56–73% yield.

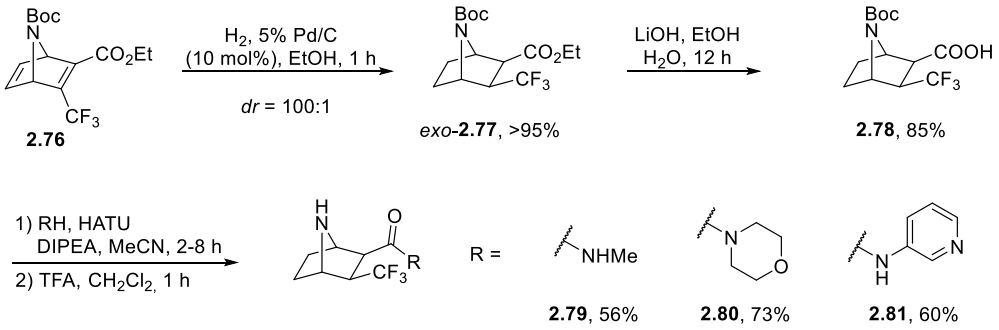

Scheme 2.22. Stereoselective catalytic hydrogenation of **2.76** afforded *exo*-**2.77**. Subsequent hydrolysis, amidation, and Boc-deprotection gave three amide-containing fragments.

From methylamide **2.79**, three additional fragments were synthesized *via N*-derivatizations (Scheme 2.23). Reductive alkylation with 3-hydroxybenzaldehyde afforded **2.82** in 43% yield, sulfonylation with MsCl gave **2.83** in 79% yield, and urea formation with cyclopentyl isocyanate produced fragment **2.84** in 87% yield (Scheme 2.23).

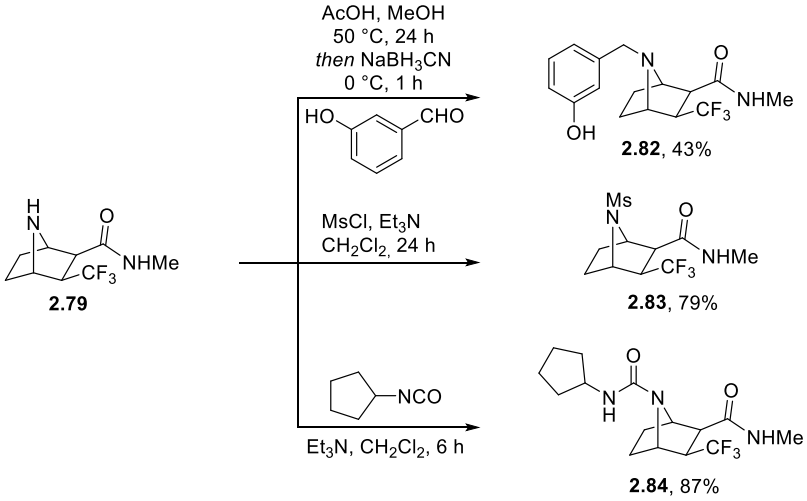

Scheme 2.23. *N*-Derivatizations of **2.79**.

Acylation of amides **2.80** and **2.81** afforded another two fragments for the 3F library (Scheme 2.24).

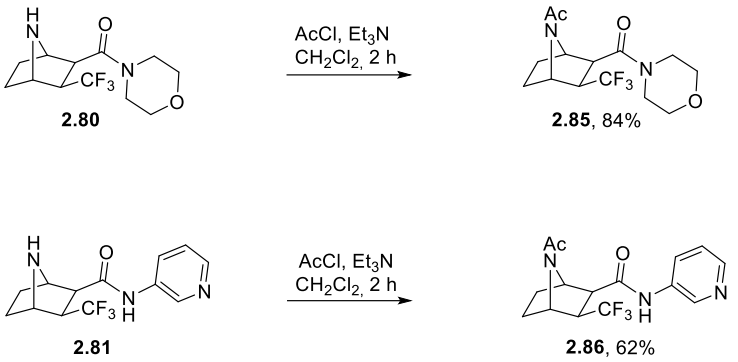

Scheme 2.24. Acylation of amide-containing fragments **2.80** and **2.81**.

To access additional derivatives of the pyrrole Diels-Alder core scaffold, a Michael addition to **2.76** was accomplished using methylamine in good diastereoselectivity (Scheme 2.25). In contrast to the hydrogenation, Michael addition occurred primarily from the *exo*-face. From **2.87**, catalytic hydrogenation and Boc-deprotection afforded **2.88** in 80% yield. Finally *N*-derivatization with ethyl isocyanate was performed in 74% yield to afford **2.89**.

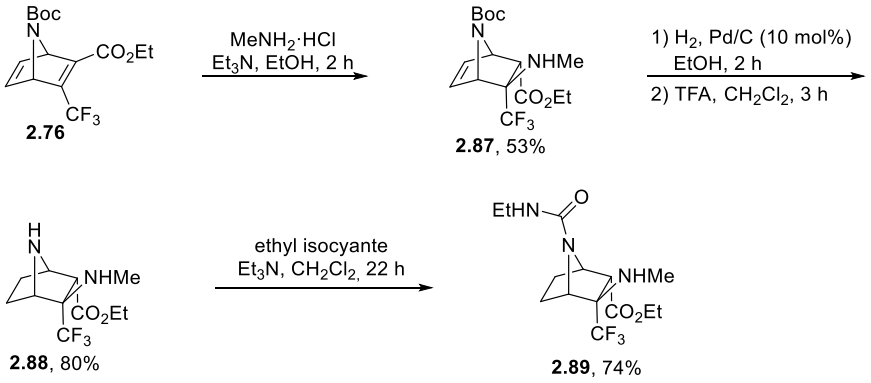

Scheme 2.25. Michael addition on **2.76** followed by hydrogenation, Boc-deprotection, and *N*-derivatization.

A Michael addition using allylamine was also performed to afford **2.90** with the same stereochemistry (Scheme 2.26). A subsequent tandem ROM/RCM was attempted in order to synthesize *trans*-fused [5,6] bicyclic **2.91**. However, no ring-closed products were isolated.

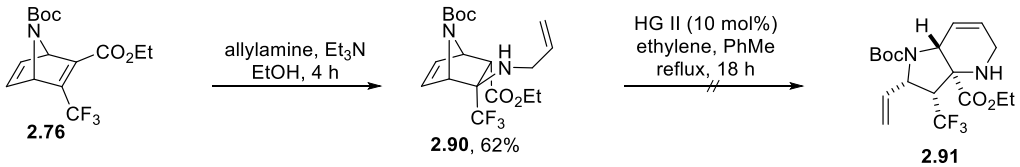

Scheme 2.26. Michael additions followed by an attempted ROM/RCM.

In a different approach, a chemoselective azomethine ylide-mediated [3+2] cycloaddition on the activated alkene of **2.76** was performed. Using azomethine ylide precursor **2.92** with catalytic TFA afforded **2.93** in 53% *via exo*-face attack (Scheme 2.27). Subsequent reduction and global deprotection gave tricyclic fragment **2.94** in excellent yield.

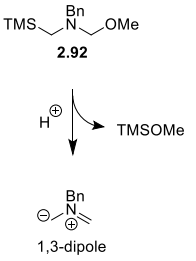

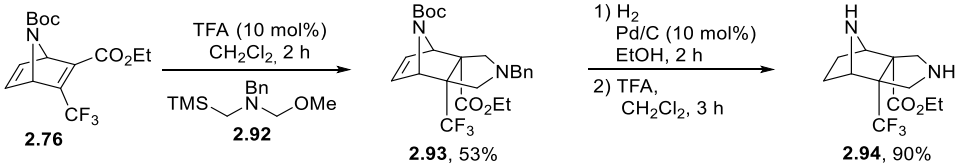

Scheme 2.27. [3+2] Cycloaddition with **2.76** followed by global deprotection afforded tricyclic **2.93**.

Finally, oxidative bond scissoring and reductive cyclization was also attempted on this Diels-Alder scaffold. While K_2OsO_4 reacts more readily with electron-rich alkenes, the previously described conditions (Scheme 2.8 and Scheme 2.13) resulted in a complex mixture that included doubly dihydroxylated products. Changing the solvent system from THF/H_2O to acetone/*n*-BuOH/H_2O and reducing the catalyst loading to 2 mol% enabled more selective mono-dihydroxylation. Subsequent hydrogenation to stop the reaction afforded crude **2.95** as a mixture of *endo*/*exo syn*-diols (Scheme 2.28).

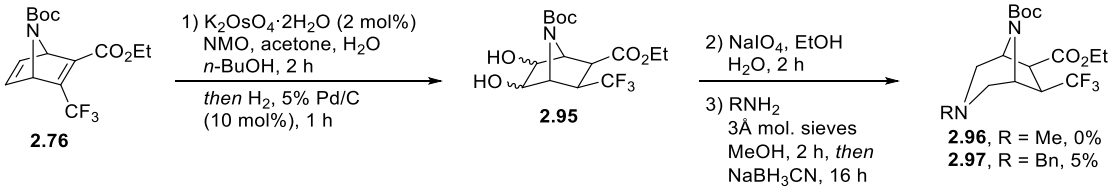

Scheme 2.28. Oxidative bond scissoring and reductive cyclization of core scaffold **2.76**.

Attempts to work-up or purify the diol resulted in partial degradation and instead crude **2.95** was subjected directly to oxidative cleavage with $NaIO_4$ and then reductive amination conditions using either methyl- or benzylamine. Both amines resulted in complex mixtures but with benzylamine the reductive cyclized product **2.97** was isolated in 5% yield over three steps (Scheme 2.28). Attempts to improve the yield were unsuccessful and the scaffold was ultimately abandoned as deprotection still had to be performed in order to reduce the molecular weight below 354 Da.

2.3.4. [5+2] Cycloaddition

In a continued effort to exploit the complexity generating-powers of cycloadditions, attention was directed towards [5+2] cycloaddition. This cycloaddition would allow for the construction of larger bridged bicyclic scaffolds such as the natural product-like oxabicyclo[3.2.1]octane scaffold (Figure 2.5).[230–233]

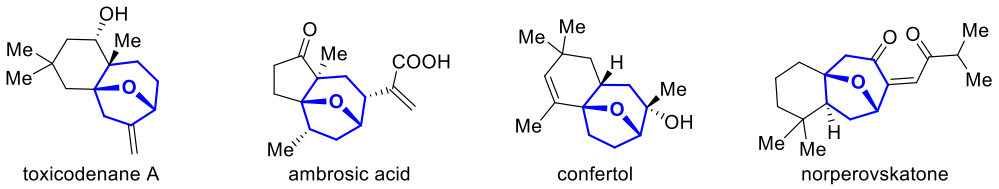

Figure 2.5: Examples of natural products containing an oxabicyclo[3.2.1]octane moiety – toxicodenane A,[230] ambrosic acid,[231] confertol,[232] and norperovskatone.[233]

While [5+2] cycloadditions are typically encountered in intramolecular pathways,[234] several examples of intermolecular reactions have been reported.[235–237] The majority of the intermolecular cycloadditions rely on the oxidopyrylium ylide salt **2.100** – a reactive intermediate that is synthesized in three steps from commercially available kojic acid (Scheme 2.29).[238]

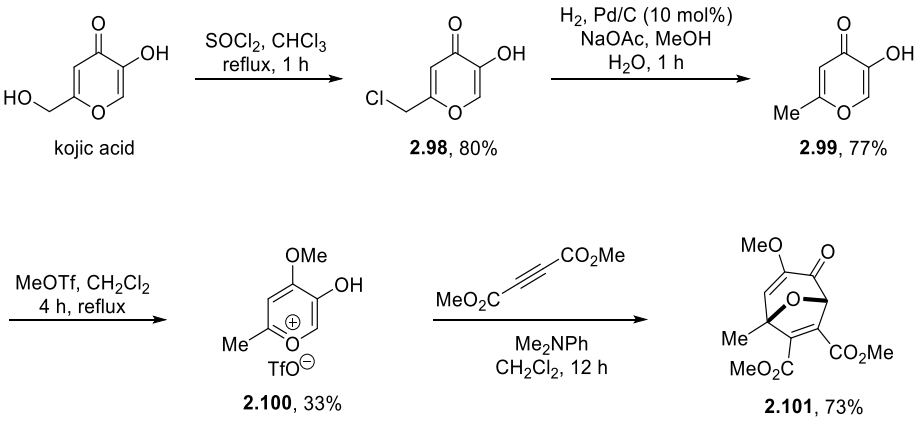

Scheme 2.29. Synthesis of α-deoxykojic acid (**2.99**)[239] and its subsequent conversion into oxopyrrylium ylide **2.100** for use in intermolecular [5+2] cycloadditions.[238]

In a more straight-forward approach, it was envisioned that commercially available maltol, a structural isomer of α-deoxykojic acid (**2.99**),[240] would undergo the same reaction sequence.

Pleasingly, repeating the oxidopyrylium ylide formation with MeOTf, maltol was easily converted into the corresponding oxopyrrylium ylide **2.102** in excellent yield – significantly higher than reported for α-deoxykojic acid (Scheme 2.30).[iv]

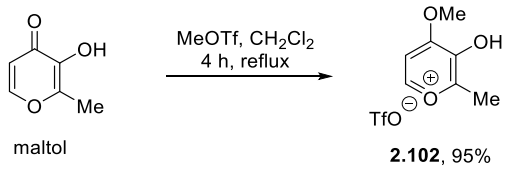

Scheme 2.30. Oxopyrrylium ylide formation from commercially available maltol.

Inspired by a microwave assisted [5+2] cycloaddition,[235] oxopyrrylium ylide **2.102** was activated by base and reacted with an excess of alkyne **2.4** to afford bridged bicyclic core scaffold **2.103** in 77% yield (Scheme 2.31). The use of a weak and sterically hindered base, $^{i}Pr_2NPh$, ensured slow deprotonation of **2.102** to minimize dimerization of the reactive ylide species. The reaction proceeded highly regioselectively with **2.103** as the only observed product in addition to some dimerization of **2.102**.

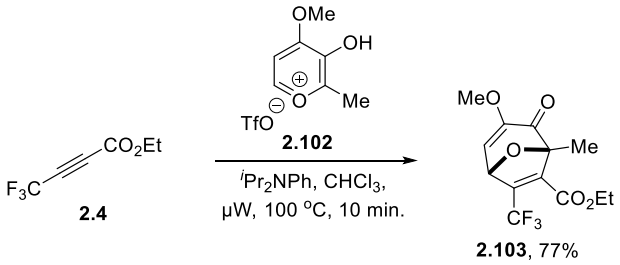

Scheme 2.31. Synthesis of core scaffold **2.103** using a [5+2] cycloaddition.

To access fragments without α,β-unsaturation, **2.103** was subjected to a diastereoselective catalytic hydrogenation to provide saturated **2.104** in 84% yield (Scheme 2.32). Subsequent global reduction with $LiAlH_4$ successfully afforded diol **2.105** in excellent yield. Attempts to perform reductive amination of **2.104** failed as no imine formation occurred. Ester hydrolysis was also attempted but resulted in complex mixtures (Scheme 2.32).

[iv] During preparation of the manuscript based on this work, a similar approach was also demonstrated by Murelli and co-workers.[363]

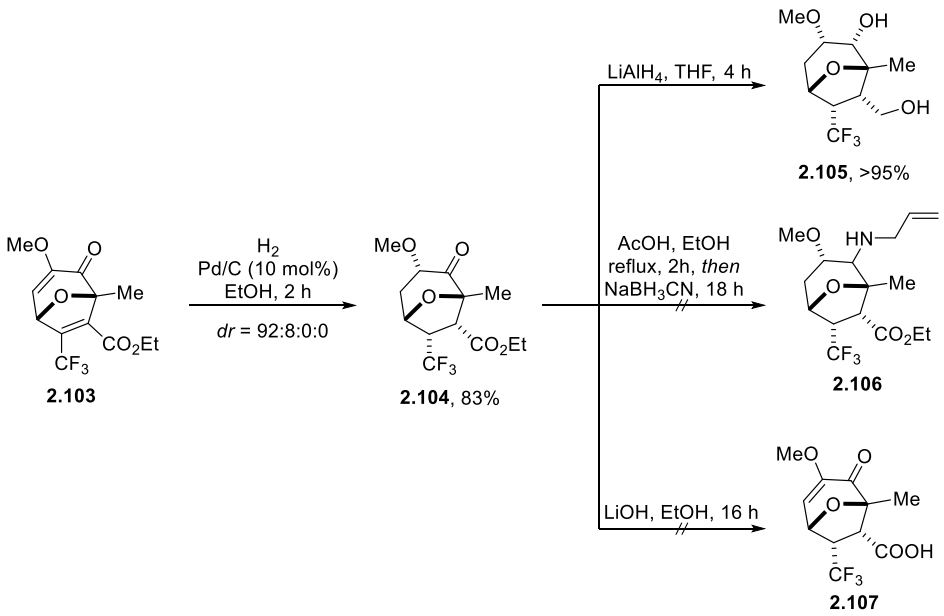

Scheme 2.32. Derivatization of **2.103**.

Core scaffold **2.103** was also subjected to two Michael additions (Scheme 2.33). 1,4-Addition by amine nucleophiles proceeded with excellent regio- and diastereoselectivity with only *exo*-face attack of the most electron deficient α,β-unsaturated system observed. However, the reactions yielded two diastereomers as at the stereochemistry of the α-position could not be controlled. In order to remove the other α,β-unsaturated alkene, the Michael addition adducts were subsequently diastereoselectively reduced with $NaBH_4$. Using methylamine, fragments **2.108** and **2.109** were obtained in 56% and 30% yield, respectively. Interestingly, a lactone had spontaneously formed in **2.109** where the ethyl ester had ended up in the *endo* position.

Using but-3-en-1-amine, the reaction cascade gave an inseparable mixture of **2.110** and lactone **2.111** in 80% yield (Scheme 2.33). A subsequent attempt to perform a tandem ROM/RCM reaction failed to ring open the enol ether and instead afforded dealkylated fragments **2.112** and **2.113** in 53% and 15% yield, respectively.

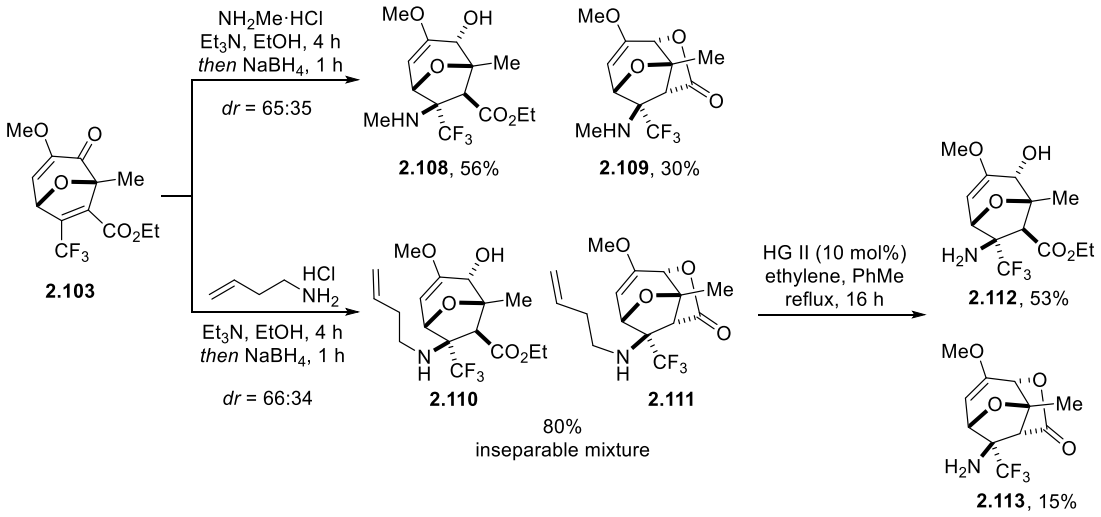

Scheme 2.33. Michael additions to **2.103**.

In order to access examples of tropolone-based fragments, cleavage of the ether bridge was carried out using a Lewis acid. While reaction with BBr_3 yielded a complex mixture, the use of BCl_3 facilitated a slightly more controlled ring opening and allowed for the isolation of two ring-opening products, tropolones **2.114** and **2.115** in 32% and 14% yield, respectively (Scheme 2.34).

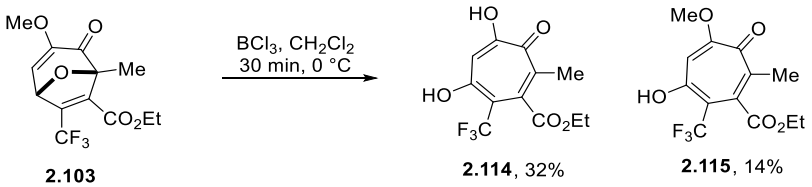

Scheme 2.34. Ether bridge cleavage of **2.103** using BCl_3.

Although tropolones are highly unsaturated and structurally flat, the moiety is often encountered in nature and in bioactive molecules for which reason the fragments were included in the library (Figure 2.6).[241]

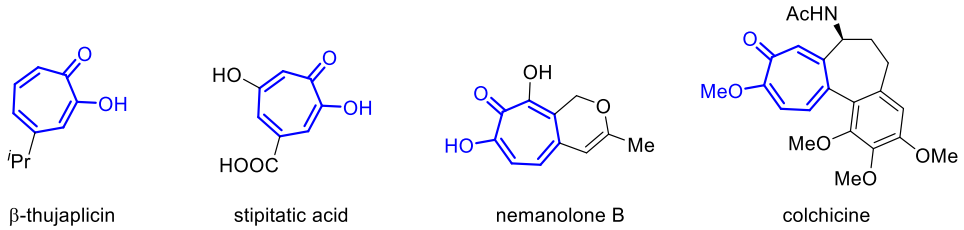

Figure 2.6: Examples of tropolone-containing natural products – β-thujaplicin, stipitatic acid, nemanolone B, and colchicine.[241]

Finally, **2.103** was subjected to the previously described azomethine ylide [3+2] cycloaddition. However, poor chemoselectivity was observed and resulted in a mixture of products (Scheme 2.35).

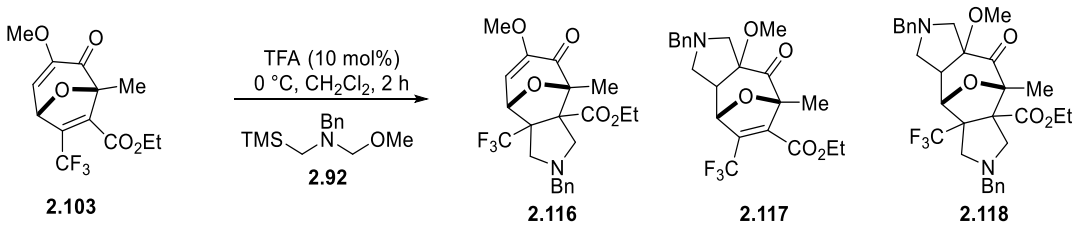

Scheme 2.35. Attempted azomethine ylide-mediated [3+2] cycloaddition of **2.103** resulted in a mixture of products.

Because of the poor chemoselectivity of the [3+2] cycloaddition, it was decided to repeat the [5+2] cycloaddition with acrylate **2.2**. Again, this reaction proceeded with excellent regio- stereoselectivity but also good diastereoselectivity to afford **2.119** in 57% yield (Scheme 2.36).

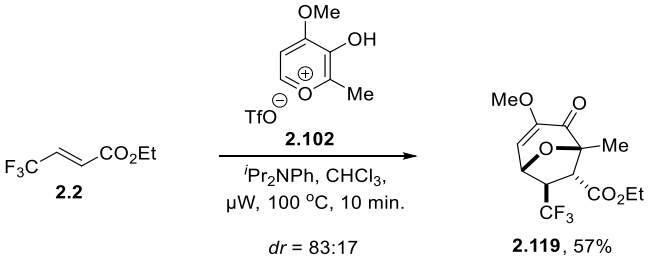

Scheme 2.36. [5+2] Cycloaddition with **2.2** afforded **2.119** as the major product. The other diastereomer was not isolated as a pure compound.

An azomethine ylide-mediated [3+2] cycloaddition of scaffold **2.119** could now be performed diastereoselectively at the only alkene present. Subsequent debenzylation by catalytic hydrogenolysis afforded fragment **2.120** in 88% yield over two steps (Scheme 2.37).

Scaffold **2.119** was also subjected to a ketone reduction with $NaBH_4$ to afford lactone **2.121** in 46% yield. Looking to further modify lactone **2.121** *via* the enol ether, a β-lactam formation using ethyl isocyanate was attempted. Unfortunately, no conversion of **2.121** was observed even at elevated temperatures (Scheme 2.37). Oxidative cleavage of the enol ether was also attempted. However, both a two-step Upjohn dihydroxylation and then $NaIO_4$-mediated cleavage cascade as well as ozonolysis under reductive conditions resulted in complex mixtures (Scheme 2.37). Finally, **2.119** was subjected to a Grignard reaction[242] with allylmagnesium bromide but also yielded a complex mixture (Scheme 2.37).

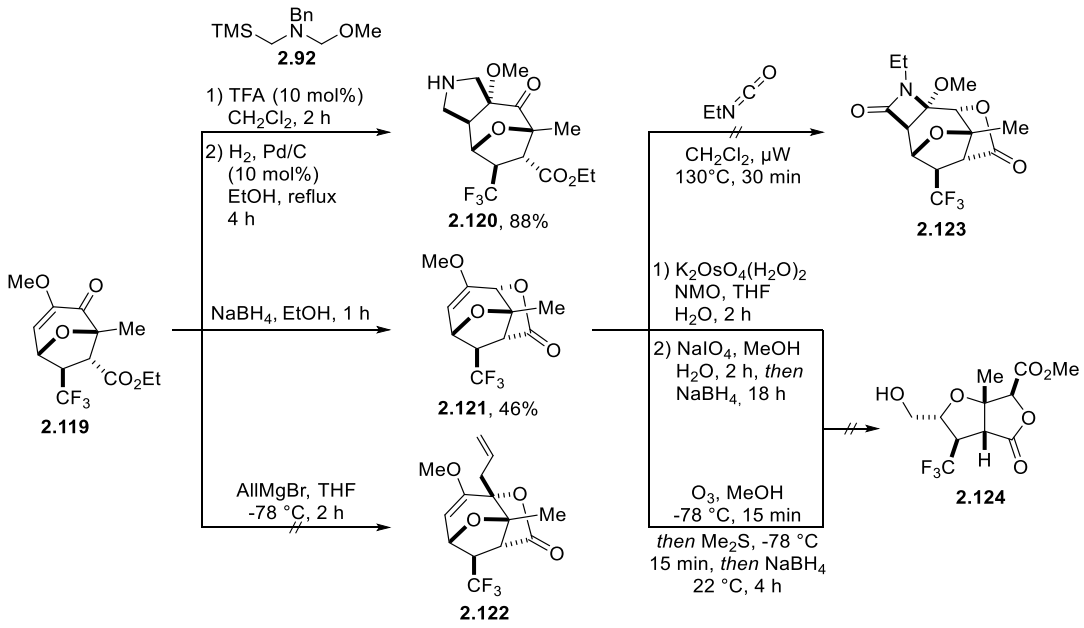

Scheme 2.37. Derivatization of **2.119**.

2.3.5. [2+2] Cycloaddition

Another cycloaddition that was investigated was the [2+2] cycloaddition. While thermal [2+2] cycloadditions are disallowed, unsaturated systems are known to undergo stepwise Michael-aldol-like [2+2] cycloadditions.[243] Examples of structures that can be accessed by this approach include *cis*-fused [5,4] bicycles which are commonly encountered in nature (Figure 2.7).[244–247]

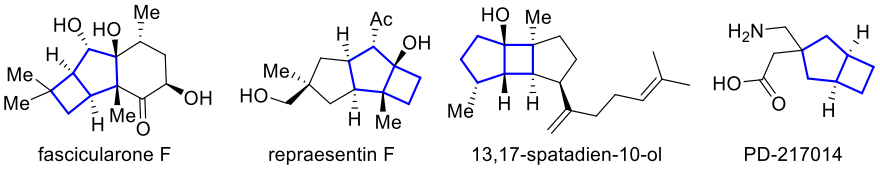

Figure 2.7: Examples of bioactive compounds containing a *cis*-fused [5,4] bicyclic moiety – the natural products fascicularone F,[245] repraesentin F,[244] and 13,17-spatadien-10-ol[246] and the GABA analogue PD-217014 that underwent clinical trials for treatment of visceral hypersensitivity.[247]

Inspired by the work of Franck-Neumann *et al.*,[248] an initial [2+2] cycloaddition was performed between alkyne **2.4** and silyl enol ether **2.125** promoted by $ZrCl_4$. Satisfyingly, the reaction proceeded smoothly with excellent regio- and stereoselectivity to form the *cis*-fused [5,4] bicyclic fragment **2.126** in 93% yield (Scheme 2.38).

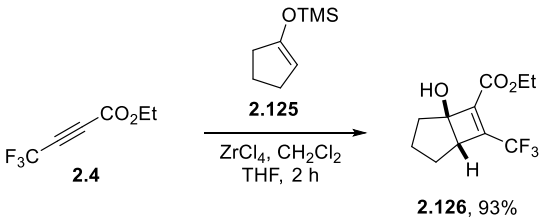

Scheme 2.38. [2+2] Cycloaddition.

Encouraged by the excellent result, the cycloaddition was repeated with oxopiperidine silyl enol ether **2.128** in an attempt to install another handle in the scaffold (Table 2.4). However, using the same conditions no reaction was observed (entry 1) and applying heat resulted in a complex mixture (entry 2). Changing the promoter to either $BF_3{\cdot}OEt_2$ or catalytic amounts of Tf_2NH did not work either (entries 3 and 4). Finally, the reaction was repeated using the fluoride-based initiators TBAF and AgF. While the use of TBAF resulted in a complex mixture (entry 5), AgF showed partial conversion of **2.4** to a new product. Unfortunately, this turned out to be the Michael addition product **2.130** (entry 6).

Table 2.4. Attempted conditions to facilitate a [2+2] cycloaddition between **2.4** and silyl enol ether **2.128**.

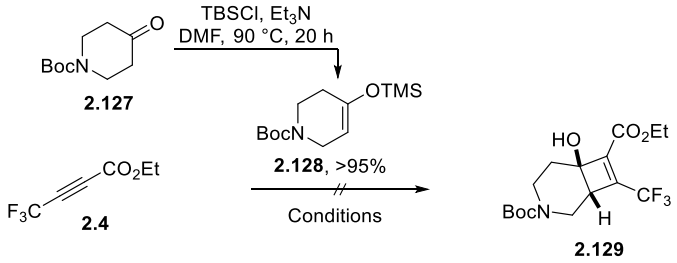

Entry	Promoter	Solvent	Temp.	Time (h)	Product
1	$ZrCl_4$	CH_2Cl_2/THF	22 °C	24	NR
2	$ZrCl_4$	CH_2Cl_2/THF	reflux	18	complex mixture
3	$BF_3{\cdot}OEt_2$	THF	22 °C	24	NR
4	Tf_2NH	CH_2Cl_2	22 °C	16	NR
5	TBAF	THF	0 °C	1	complex mixture
6	AgF	THF	22 °C	24	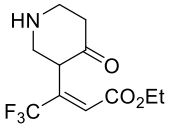 **2.130**, 39%

NR: no reaction

In an attempt to find another suitable silyl enol ether for the [2+2] cycloaddition, a screen of different silyl enol ethers was set up (Table 2.5). Switching the *N*-protecting group from Boc to benzyl did not change the outcome neither did a 2-methyl substituent (entries 2 and 3). Surprisingly, repeating the initial cycloaddition (entry 1) with the corresponding six-membered silyl enol ether **2.133** gave no conversion of **2.4** either (entry 4). Thus, issues related to this reaction could be originating from ring size rather than the presence of a nitrogen atom. Like observed for **2.128**, using AgF instead of $ZrCl_4$ with **2.133** gave only partial conversion to the Michael addition product (entry 5). Regrettably, attempting the [2+2] cycloaddition with other five-membered silyl enol ethers did not yield any products (entries 6 and 7). Finally, a four-membered silyl enol ether was synthesized but also failed to react with alkyne **2.4** (entry 8).

Table 2.5. Screen of silyl enol ethers for [2+2] cycloaddition with alkyne **2.4**.

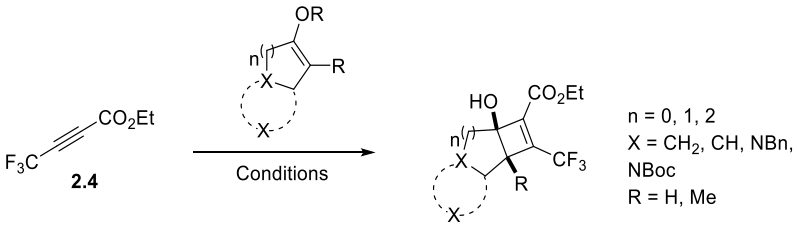

Entry	Silyl enol ether	Promoter	Solvent	Temp. (°C)	Time (h)	Result
1	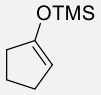 **2.125**	$ZrCl_4$	CH_2Cl_2/THF	22	2	**2.126**, 93%
2[a]	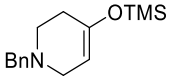 **2.131**	$ZrCl_4$	CH_2Cl_2/THF	22	24	NR
3[b]	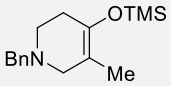 **2.132**	$ZrCl_4$	CH_2Cl_2/THF	22	24	NR
4	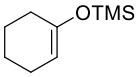 **2.133**	$ZrCl_4$	CH_2Cl_2/THF	22	24	NR
5	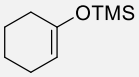 **2.133**	AgF	THF	22	24	partial Michael addition
6[c],[f]	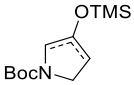 **2.134**	$ZrCl_4$	CH_2Cl_2/THF	22	24	NR
7[g]	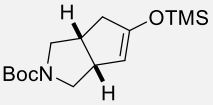 **2.135**	$ZrCl_4$	CH_2Cl_2/THF	22	24	NR
8[h]	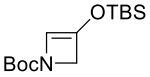 **2.136**	$ZrCl_4$	CH_2Cl_2/THF	22	4	NR

[a] Silyl enol ether synthesized from ketone using TBSCl, Et_3N, DMF, 21 h (>95%). [b] Synthesized from ketone using TBSCl, Et_3N, DMF, 21 h (>95%). [c] Mixture of silyl enol ether isomers and ketone used. [d] Synthesized from ketone using TBSCl, Et_3N, DMF, 21 h (70%). [e] Silyl enol ether synthesized from ketone using TBSCl, Et_3N, DMF, 21 h (57%). [h] Synthesized from ketone using TBSOTf, LiHMDS, THF, -78 °C, 1 h (22%). NR: no reaction

As a final approach to synthesize a cyclobutene-containing scaffold with an additional handle, a [2+2] photocycloaddition with a non-activated alkene was attempted. Unfortunately, alkyne **2.4** failed to react with *N*-Boc-3-pyrroline under UV light irradiation around 350 nm in the presence of acetophenone as sensitizer (Scheme 2.39).

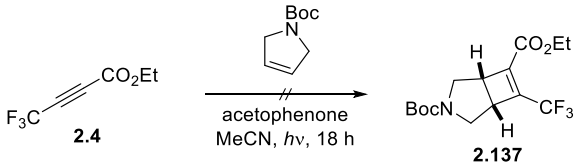

Scheme 2.39. Attempted [2+2] photocycloaddition under UV light irradiation at 350 nm.

With only one [2+2] cycloaddition working, it was decided to continue with **2.126** as the core scaffold for this sub-library. In an attempt to derivatize **2.126**, a Michael addition with methylamine was attempted. However, degradation of **2.126** was observed instead of 1,4-addition (Scheme 2.40). Serendipitously, the degradation turned out to be a remarkably efficient base-mediated rearrangement that proceeded with excellent stereoselectivity to form the α,β-unsaturated ketone **2.138** in quantitative yield.

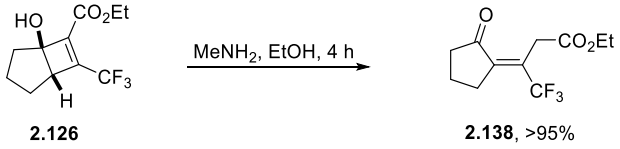

Scheme 2.40. Attempted Michael addition resulted in a ring-rearrangement.

Exploiting this newly formed α,β-unsaturated system, **2.138** was subjected to a [3+2] cycloaddition with azomethine ylide precursor **2.92** to afford spirocyclic **2.139** (Scheme 2.41). Without purification, **2.139** was further modified to reduce the molecular weight below 354 Da – hydrogenolysis afforded fragment **2.142** in 78% yield over three steps, reduction with $LiBH_4$ gave diol **2.141** in 76% yields over three steps, and finally hydrogenolysis followed by $NaBH_4$-mediated reduction formed tricyclic lactone **2.140** in 44% yield over four steps.

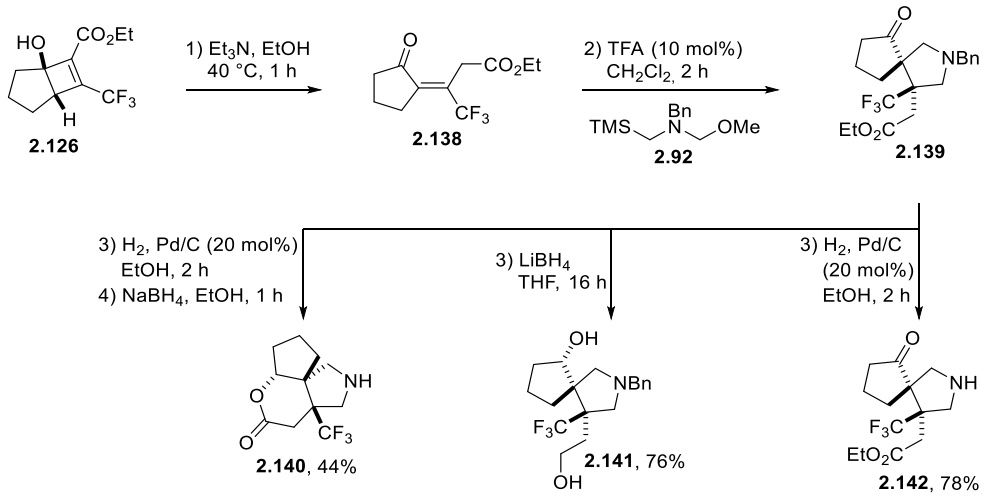

Scheme 2.41. Base-mediated ring-rearrangement of **2.126** followed by [3+2] cycloaddition and further modifications to reach spirocyclic fragments **2.140**, **2.141**, and **2.142**.

From **2.138** a few additional reactions were attempted but both a [3+2] cycloaddition with ethyl diazoacetate and a Diels-Alder reaction failed (Scheme 2.42). Likewise, Michael addition with an amine was unsuccessful.

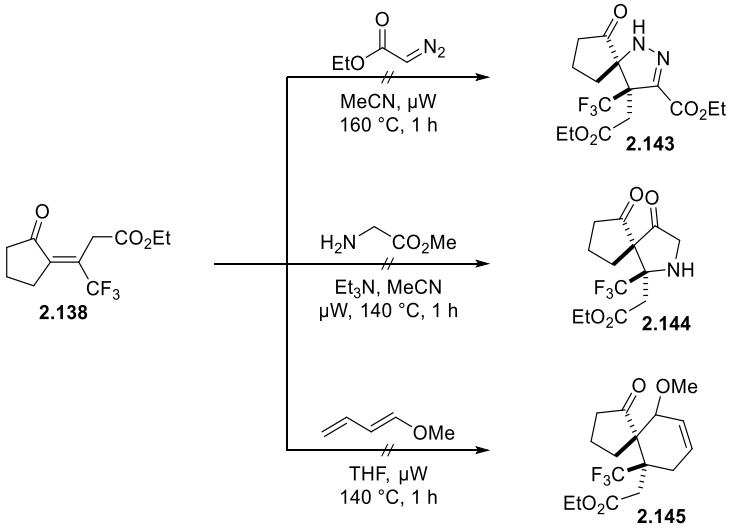

Scheme 2.42. Other attempted reactions with α,β-unsaturated ketone **2.138**.

To access more scaffold diversity, an acid-mediated ring-expansion was envisioned. However, while **2.126** proved to be highly base-sensitive the scaffold remained surprisingly stable towards acidic conditions and survived being subjected to μW heating at 120 °C in neat TFA (Scheme 2.43).

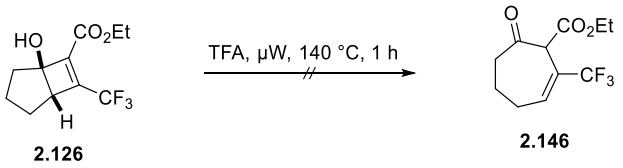

2.126 **2.146**

Scheme 2.43. Attempted acid-mediated ring-expansion of **2.126**.

To include an example of a [5,4] bicyclic scaffold in the library without the α,β-unsaturated system, catalytic hydrogenation of **2.126** afforded fragment **2.147** in 93% yield (Scheme 2.44). The hydrogenation occurred exclusively from the convex face and was performed under acidic conditions to avoid degradation of **2.126**. Reduction of **2.126** with $LiBH_4$ was also attempted but resulted in a complex mixture. Instead, performing the reduction after hydrogenation allowed for the isolation of one product, ring-opened diol **2.148** in 28% yield (Scheme 2.44). Finally, **2.126** was subjected to another [3+2] cycloaddition with **2.92** to give tricyclic **2.149**. Disappointingly, subsequent hydrogenolysis or $LiBH_4$-reduction failed to afford desired fragments **2.150** and **2.151,** respectively (Scheme 2.44).

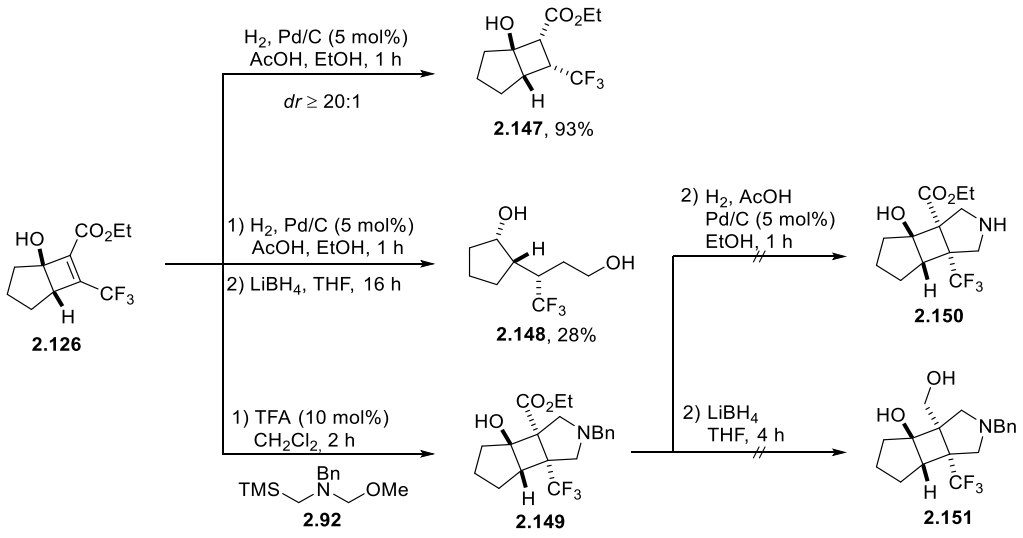

Scheme 2.44. Derivatizations performed on core scaffold **2.126**.

2.3.6. Double [3+2] cycloaddition – Pyrrolidine

Relying on the ease of the azomethine ylide-mediated [3+2] cycloaddition, a highly three-dimensional double-pyrrolidine core scaffold was targeted next. While multiple nitrogen-containing *cis*-fused [5,5] bicyclic scaffolds exists among natural products and bioactive compounds, only a few and complex natural products contain a double pyrrolidine moiety (Figure 2.8).[249–252]

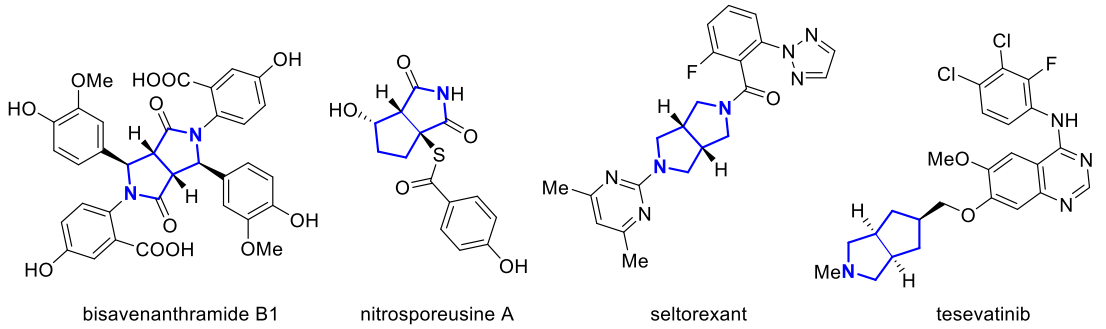

Figure 2.8: Examples of compounds containing a nitrogen-containing [5,5] *cis*-fused scaffold – the natural products bisavenanthramide B1[249] and nitrosporeusine A[250], the drug candidate seltorexant[251] for treatment of insomnia, and the multi-kinase inhibitor tesevatinib.[252]

Reaction between alkyne **2.4** and azomethine ylide precursor **2.92** proceeded smoothly to afford a new core scaffold **2.152** in 89% yield (Scheme 2.45).

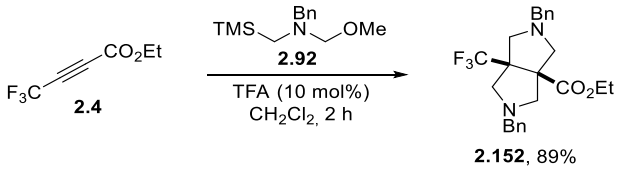

Scheme 2.45. A double [3+2] cycloaddition to form core scaffold **2.152**.

Bicycle **2.152** was subjected to a series of *N*-derivatizations to create a small sub-library based on the pyrrolidine scaffold (Scheme 2.46). To reduce the molecular weight, the ester was first reduced to the corresponding alcohol using $LiAlH_4$. Then, debenzylation was achieved using catalytic hydrogenolysis to afford **2.153** in quantitative yield. Alternatively, addition of formaldehyde during the hydrogenolysis formed the dimethylated fragment **2.154** in 48% yield over two steps. From **2.153**, subsequent acylation with propanoyl chloride afforded fragment **2.155** in 88% while desymmetrization was achieved by performing mono reductive alkylation followed by acylation to afford fragment **2.156** in 35% yield.

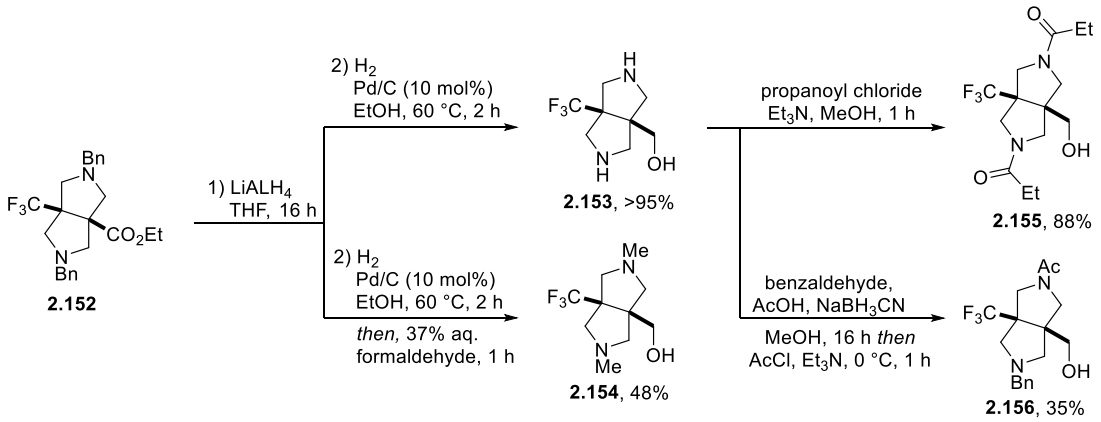

Scheme 2.46. *N*-Derivatizations of core scaffold **2.152**.

Another small fragment (**2.156**) was obtained by direct debenzylation of **2.152** in quantitative yield (Scheme 2.47). Finally, one example of an ester derivatization was achieved by hydrolysis followed by HATU-mediated amidation of the corresponding carboxylic acid. Subsequent debenzylation by catalytic hydrogenolysis provided fragment **2.158** in 54% yield over three steps (Scheme 2.47).

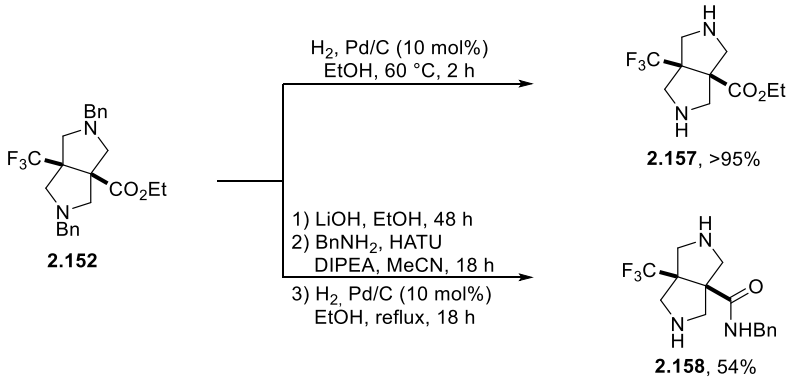

Scheme 2.47. Additional fragments synthesized from **2.152**.

2.3.7. [3+2] Cycloaddition – Dihydropyrazole

The final cycloaddition-based core scaffold to be synthesized was a dihydropyrazole scaffold accessed *via* a [3+2] cycloaddition. Dihydropyrazole moieties are rare in nature and among drugs but a few examples do exist (Figure 2.9).[253,254]

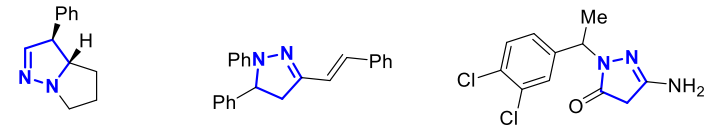

newbouldine 1,5-diphenyl-3-styryl-pyrazoline muzolimine

Figure 2.9: Examples of compounds containing a dihydropyrazole moiety or similar – the natural products newbouldine and 1,5-diphenyl-3-styryl-pyrazoline[253] and the saluretic compound muzolimine.[254]

Highly activated alkenes are known to undergo catalyst-free cyclopropanation with diazoacetates.[255] In the hope that acrylate **2.2** would be sufficiently electron deficient, the starting material was reacted with ethyl diazoacetate. However, instead of cyclopropanation acrylate **2.2** underwent an efficient [3+2] cycloaddition to form dihydropyrazole **2.159** in quantitative yield (Scheme 2.48).

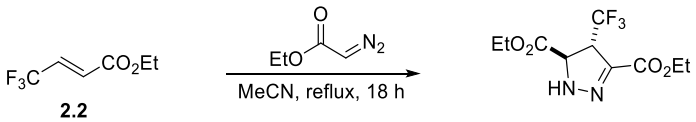

Scheme 2.48. Attempted cyclopropanation of **2.2** afforded dihydropyrazole **2.159**.

Because of the excellent yield and highly substituted nature of the formed dihydropyrazole, it was decided to investigate this scaffold further. However, due to potential difficulties of differentiating the two ethyl esters, the reaction was repeated using carboxylic acid **2.1**. Disappointingly, this reaction led to decarboxylation and yielded a mixture of compounds (Scheme 2.49). As an alternative approach, amidation of the carboxylic acid was performed prior to the diazoacetate-mediated [3+2] cycloaddition. Because of the lower electrophilic nature of the resulting unsaturated amide, the cycloaddition required microwave heating at 140 °C. Surprisingly, this reaction sequence afforded two regioisomers, **2.161** and **2.162**, in 43% and 15% yield, respectively (Scheme 2.49).

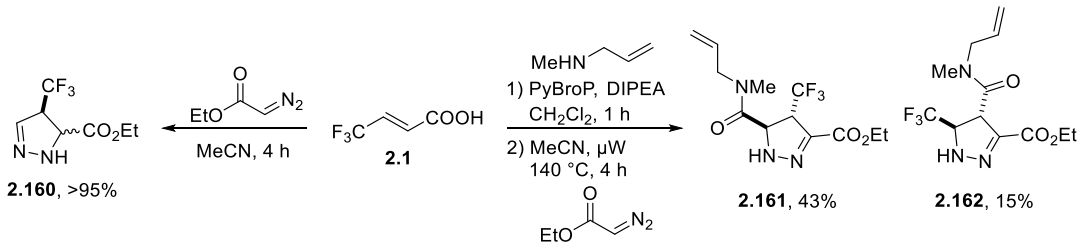

Scheme 2.49. Subjecting carboxylic acid **2.1** to a [3+2] cycloaddition with ethyl diazoacetate resulted in decarboxylation and a mixture of diastereomers. Instead, amidation of **2.1** was performed prior to the cycloaddition.

Aiming to form a bicyclic system by cyclization between the olefin and dihydropyrazole ring, *N*-derivatization of **2.161** followed by RCM was attempted (Scheme 2.50). Regrettably, all attempts to ring close with Hoveyda-Grubbs 2nd generation catalyst failed to form the targeted eight-membered rings.

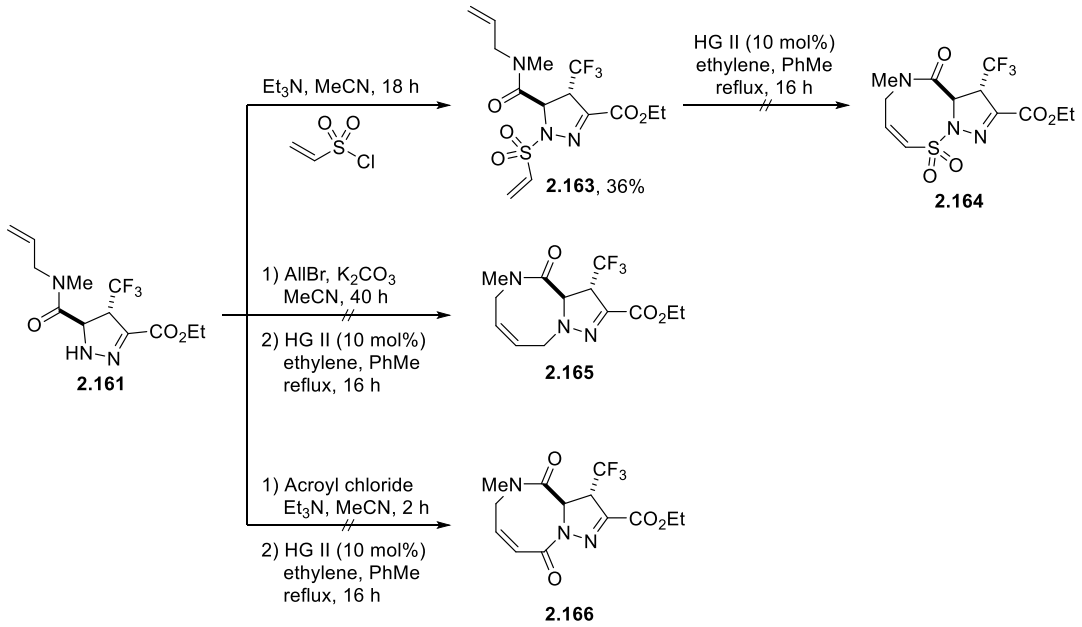

Scheme 2.50. *N*-derivatization with olefin-containing electrophiles of **2.161** followed by attempted RCM.

Inspired by the efficient decarboxylation observed with carboxylic acid **2.1**, the [3+2] cycloaddition was repeated with carboxylic acid **2.5** as an approach to access additional dihydropyrazole derivatives. Theoretically, this approach would afford a single product with a lower molecular weight and thus allow for greater possibilities of derivatizing the scaffold.

Satisfyingly, carboxylic acid **2.5** underwent the expected [3+2] cycloaddition and decarboxylation cascade to afford dihydropyrazole **2.168** in quantitative yield (Scheme 2.51).

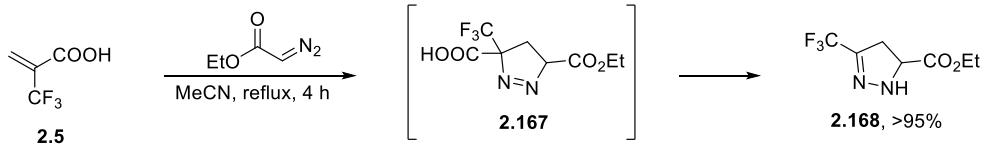

Scheme 2.51. [3+2] Cycloaddition and decarboxylation of **2.5**.

A few derivatives of **2.168** were synthesized *via N*-derivatization (Scheme 2.52). Sulfonylation was accomplished in 76% yield to give **2.169** while acylation afforded **2.170** in 53% yield. Surprisingly, PyBroP-mediated coupling with 2-hydroxyacetic failed to produce the desired acylated product. Instead, partial isomerization of the dihydropyrazole double bond occurred to give the more stable **2.171**.

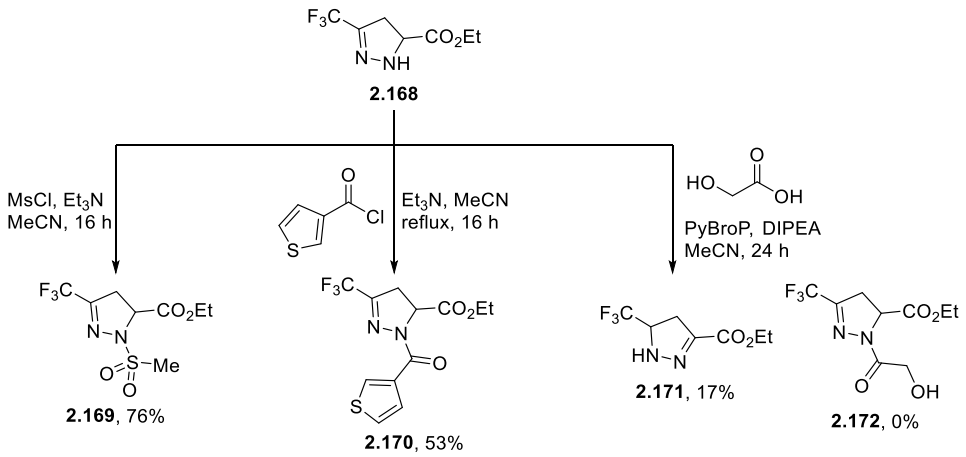

Scheme 2.52. *N*-Derivatization of **2.168**.

As an alternative approach, the targeted **2.172** was synthesized by acylation with 2-(benzyloxy)acetyl chloride followed by catalytic hydrogenolysis (Scheme 2.53). Unfortunately, attempts to perform a subsequent lactonization between the unprotected alcohol and the ethyl ester were unsuccessful.

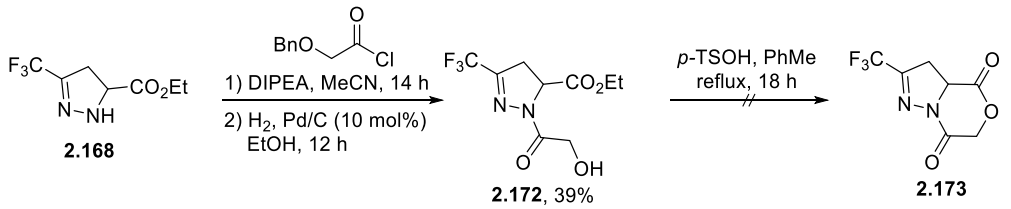

Scheme 2.53. Acylation of **2.168** followed debenzylation to afford **2.172**. Subsequent attempts to perform lactonization failed.

In an effort to further decorate the dihydropyrazole scaffold and install a CF_3-substituted quaternary carbon center, carboxylic acid **2.5** was subjected to amidation prior to cycloaddition. Amidation of **2.5** proved more challenging than with **2.1** and afforded morpholine amide **2.174** in only moderate yield. The subsequent [3+2] cycloaddition also proceeded sluggishly to form quaternary center-containing **2.175** in a poor yield of 33%. Unfortunately, purification of **2.175** was difficult and a purity higher than 80% could not be achieved.

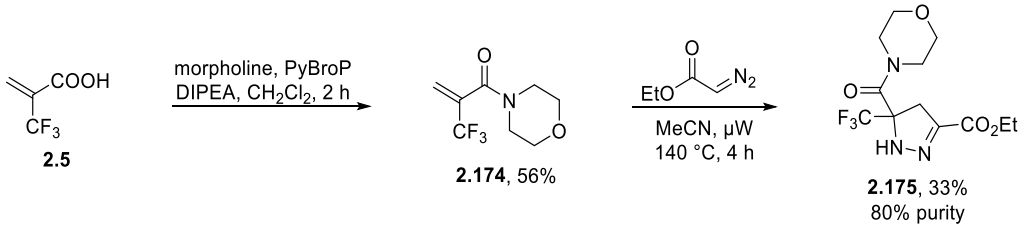

Scheme 2.54. Amidation and diazoacetate-mediated [3+2] cycloaddition of carboxylic acid **2.5** afforded **2.175** with a CF_3-substituted quaternary carbon center.

As an alternative strategy to install a quaternary center, the reaction was repeated using *t*-butyl ester **2.176** as starting material. Gratifyingly, this reaction afforded dihydropyrazole **2.177** in 78% yield (Scheme 2.55). With two distinguishable esters, **2.177** would likely be a better starting point for a potential SAR study in the event of a potential hit.

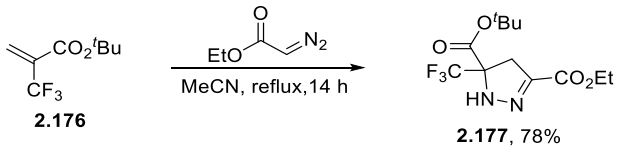

Scheme 2.55. Synthesis of **2.178** with a CF_3-substituted quaternary carbon center.

2.3.8. Dinucleophile Cyclization

In addition to the array of cycloadditions employed to create structural diversity, a series of small- to medium-sized rings were synthesized *via* a Michael addition and intramolecular amidation sequence. Numerous examples of such heterocyclic ring systems are found throughout nature and in various drugs (Figure 2.10).[256–258]

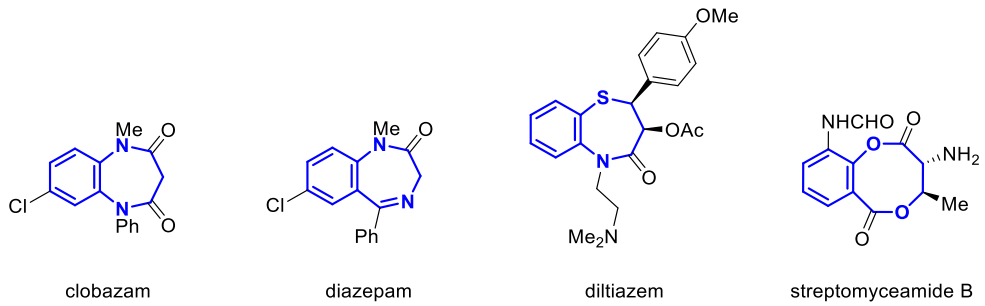

Figure 2.10: Examples of heteroatom-containing medium-sized rings – the central nervous system drugs clobazam and diazepam,[256] the calcium-channel blocker diltiazem used against high blood pressure,[257] and the natural product streptomyceamide B.[258]

To test the feasibility of the proposed Michael addition and intramolecular amidation sequence, two dinucleophiles, *o*-phenylenediamine and 2-aminobenzylamine, were initially selected for reaction with carboxylic acid **2.1**. Michael addition was accomplished upon heating while intramolecular amidation was facilitated by HATU. This afforded seven-membered **2.178** in 65% yield using a one-pot sequence while eight-membered **2.180** was synthesized over two steps via **2.179** (Scheme 2.56).

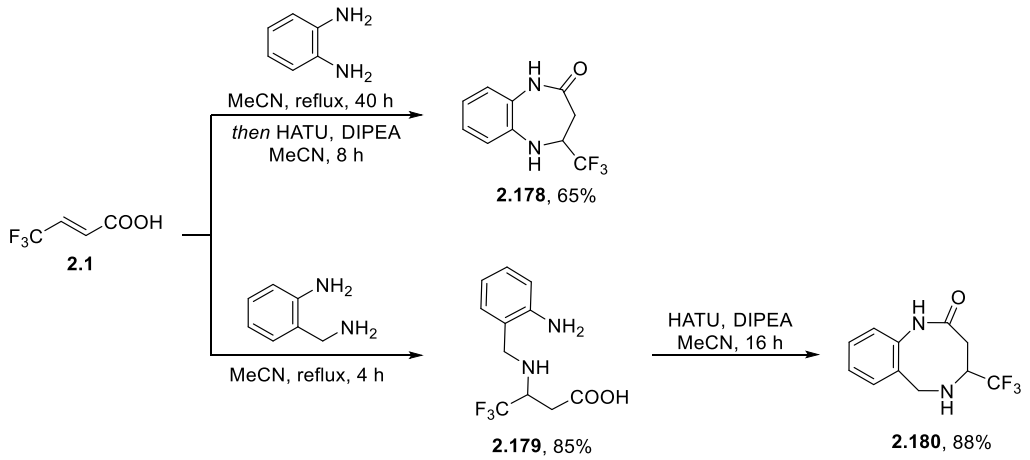

Scheme 2.56. A Michael addition and intramolecular amidation sequence to form seven- and eight-membered rings.

With two examples of medium-sized rings successfully synthesized, carboxylic acid **2.1** was reacted with a series of other dinucleophiles in an attempt to access additional scaffolds (Table 2.6). Similar to the initial cyclizations, reaction with 4,5-dimethoxybenzene-1,2-diamine and 2-amino-5-chlorobenzylamine afforded new derivatives of the original scaffolds, **2.181** (entry 1) and **2.184** (entry 4), respectively. Michael addition with ethylenediamine yielded the highly polar **2.182** that was insoluble in organic solvents (entry 2). Attempting to perform the intramolecular amidation in the presence of water (MeCN/H_2O 4:1) with either HATU or using microwave heating at 140 °C failed to produce the desired cyclized product. The same microwave procedure was also attempted with the acrylate **2.2** but also failed to produce the ring-closed product. Similarly, reacting *N*-acyl ethylenediamine with carboxylic acid **2.1** only resulted in Michael addition (entry 3). Interestingly, reacting **2.1** with thiophene-3,4-diamine using only heating afforded the six-membered **2.185** in 20% yield (entry 5). Reaction with dinucleophiles of lower nucleophilicity failed to produce any useful products (entries 6–8). Attempts to form nine-membered rings using the two step sequence failed due to lack of intramolecular amidation (entries 9 and 10).

To add a few derivatives to the library, a handful of derivatizations were performed on two of the products – the seven-membered **2.179** and the eight-membered **2.180**. From **2.179**, reduction of the amide was accomplished with $LiAlH_4$ to afford **2.188** in 85% yield (Scheme 2.57). Subsequent sulfonylation and amidation yielded fragments **2.189** and **2.190**, respectively.

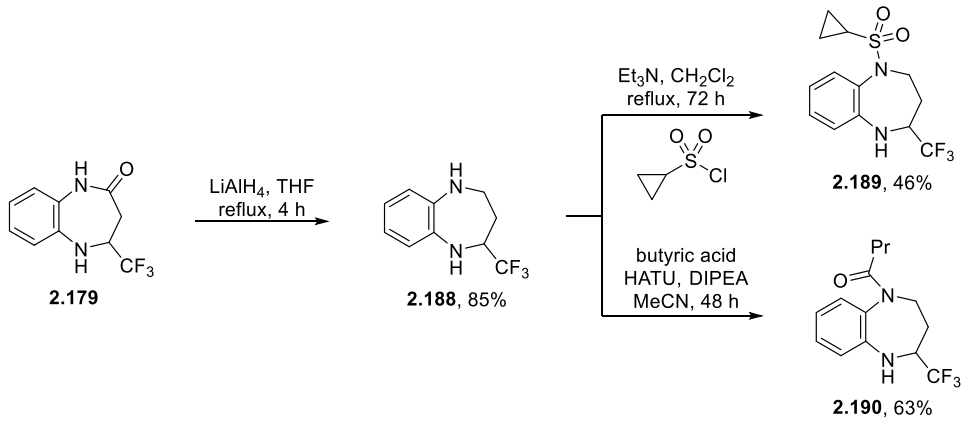

Scheme 2.57. Reduction of **2.179** followed two examples of *N*-derivatization.

Table 2.6. Attempted Michael addition and intramolecular amidations on **2.1**.

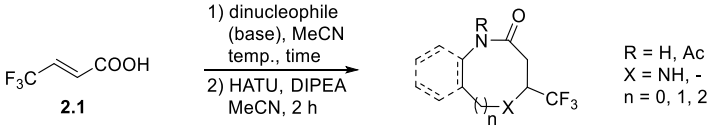

Entry	Dinucleophile	Temp.	Time (h)	Product	Yield (%)
1[a]	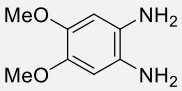	reflux	48	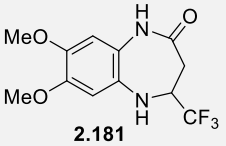 **2.181**	33
2[b]	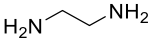	reflux	3	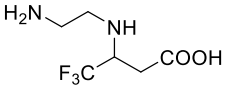 **2.182**	63
3[c]	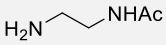	reflux	3	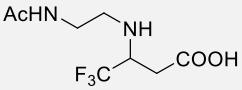 **2.183**	70
4	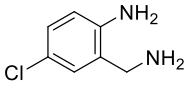	reflux	4	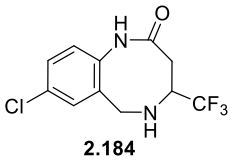 **2.184**	54
5[d]	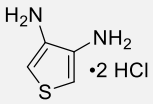	140 °C[e]	4	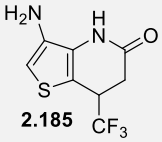 **2.185**	21
6	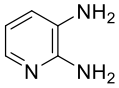	140 °C[e]	4	no reaction	0
7[d]	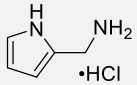	140 °C[e]	4	complex mixture	0
8	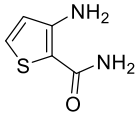	140 °C[e]	4	no reaction	0
9	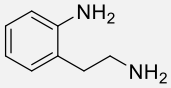	reflux	3	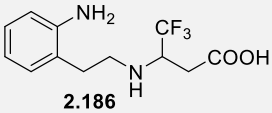 **2.186**	34
10[d]	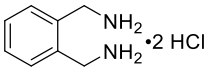	reflux	3	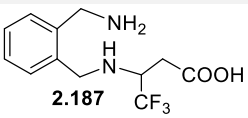 **2.187**	ND

[a] HATU was not added. [b] Amidation was attempted in MeCN/H_2O 4:1 using either HATU or µW heating at 160 °C. [c] Same result with PyBroP. [d] Et_3N was added to neutralize HCl. [e] µW heating.

From the eight-membered **2.180**, three examples of *N*-derivatizations were performed (Scheme 2.58). Acylation of the amide was achieved with acetic anhydride to afford **2.191** in 40% yield while alkylations afforded **2.192** and **2.193** in high yields.

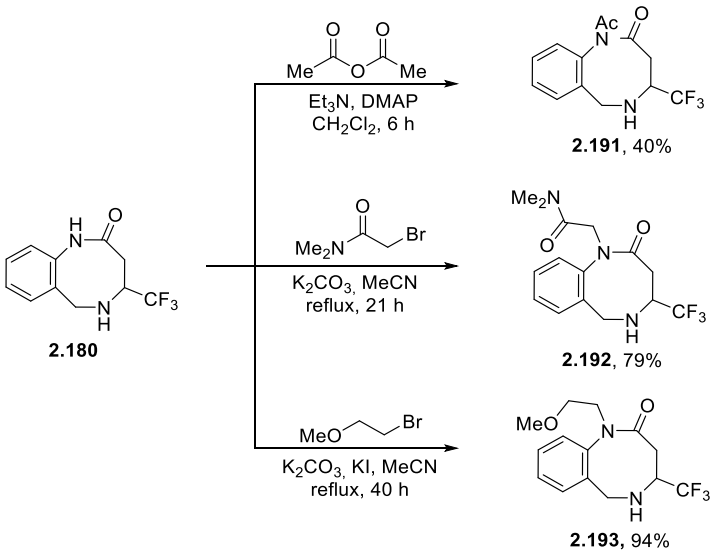

Scheme 2.58. *N*-Derivatizations of eight-membered **2.180**.

Surprisingly, no alkylation nor acylation was observed on the nitrogen atom adjacent to the CF_3-group on either scaffold. Thus, in an attempt to selectively derivatize this position in **2.180**, alkylation of 2-aminobenzylamine was performed prior to Michael addition (Scheme 2.59). Unfortunately, this alkylated amine failed to undergo a Michael addition with carboxylic acid **2.1**.

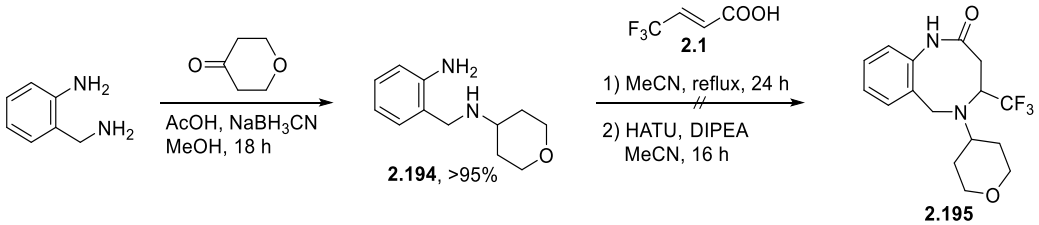

Scheme 2.59. Attempted Michael addition and intramolecular amidation with alkylated diamine **2.194**.

2.3.9. Hydrazine Cyclization – Pyrazolidinone

Employing the same Michael addition and intramolecular amidation strategy as described in the previous chapter, a set of five-membered rings were targeted *via* reaction with different hydrazines. Figure 2.11 shows examples of natural products and bioactive compounds containing nitrogen-nitrogen single bonds.[253,259–261]

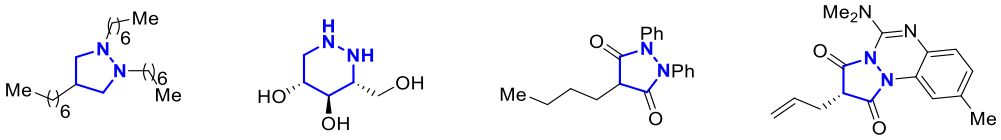

Figure 2.11: Examples of small rings with a nitrogen-nitrogen single bond – the natural product garceine,[253] the α-/β-glucosidase inhibitor azafagomine,[259] and the NSAIDs phenylbutazone[260] and azapropazone.[261]

Starting from acrylate **2.2**, cyclization was accomplished with hydrazine hydrate in refluxing EtOH to afford β-CF_3 pyrazolidinone **2.196** in quantitative yield (Scheme 2.60).

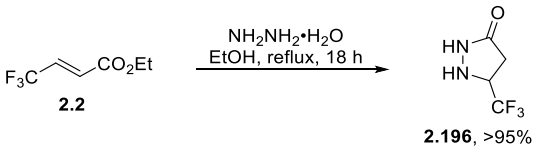

Scheme 2.60. Synthesis of pyrazolidinone **2.196** from acrylate **2.2** and hydrazine hydrate.

While synthesis of the pyrazolidinone scaffold proceeded smoothly, attempts to derivatize **2.196** proved more challenging. Most reaction conditions caused oxidation of the ring to form an aromatic pyrazole scaffold. Out of several reaction conditions tested, only two reactions were found to produce non-aromatic products (Scheme 2.61). Dialkylation with allyl bromide afforded **2.197** in 68% yield and cyclization with acroyl chloride gave **2.198** in only 6% yield.

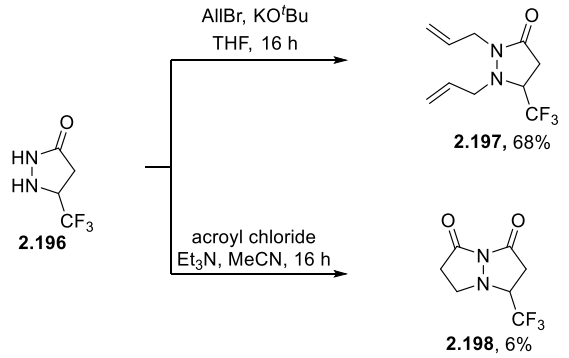

Scheme 2.61. Derivatization of β-CF_3 pyrazolidinone **2.196**.

In the light of the poor reactivity of **2.196**, derivatives of the pyrazolidinone fragment was instead targeted by the use of differently substituted hydrazines (Scheme 2.62). Unfortunately, only Michael addition adducts were observed in refluxing EtOH and increasing the temperature in a microwave reactor resulted in complex mixtures.

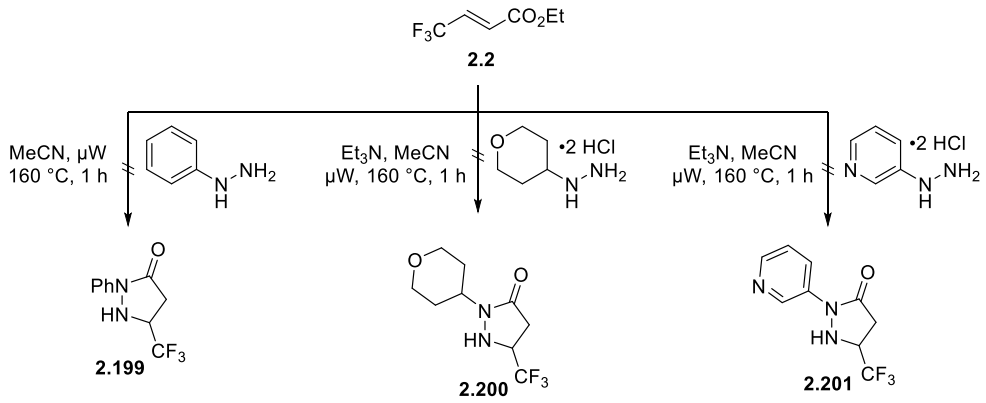

Scheme 2.62. Attempted syntheses of substituted β-CF_3 pyrazolidinones.

As an alternative, the reactions were repeated using the starting material **2.6**. Gratifyingly, two of the three reaction successfully formed the desired α-CF_3 pyrazolidinone products (Scheme 2.63). Using microwave heating, reaction with phenylhydrazine afforded the expected regioisomer **2.202** in 75% yield. Reaction with 4-tetrahydropyran hydrazine resulted in formation of several products from which pyrazolidinone **2.203** was isolated in 17% yield. 3-Pyridinehydrazine failed to react with **2.6**. Surprisingly, the use of hydrazine afforded a complex mixture

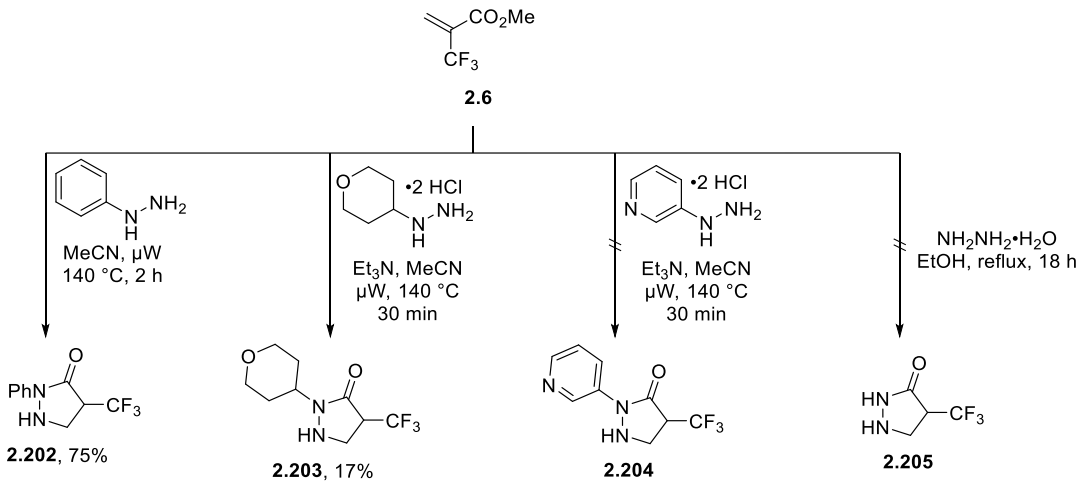

Scheme 2.63. Syntheses of α-CF_3 pyrazolidinone derivatives from **2.6**.

As an alternative approach, α-CF_3 pyrazolidinone **2.205** was synthesized from carboxylic acid **2.5** instead, which proceeded smoothly (Scheme 2.64).

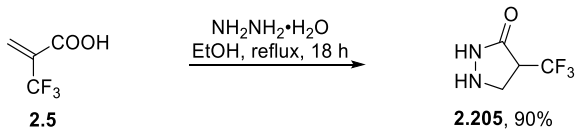

Scheme 2.64. Synthesis of α-CF_3 pyrazolidinone **2.205** from carboxylic acid **2.5**.

With the trifluoromethyl group now situated farther away from the nitrogen atoms, derivatization of α-CF_3 pyrazolidinone **2.205** was predicted to be more facile. However, in addition to continued issues of aromatization, **2.205** was also found be base sensitive. Thus, attempts to *N*-alkylate or *N*-sulfonylate were unsuccessful. Interestingly, crude ^{19}F NMR indicated release of fluoride ($\delta\ ^{19}F \approx -125$ ppm) to form the difluoromethylene species **2.206** (Scheme 2.65).

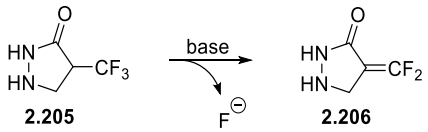

Scheme 2.65. Suspected loss of fluoride from α-CF_3 pyrazolidinone **2.205** under basic conditions.

As an alternative approach, *N*-alkylation was accomplished by reductive alkylation to afford benzylated **2.207**, albeit in poor yield (Scheme 2.66). The successful imine formation was also exploited to perform a subsequent azomethine ylide-mediated [3+3] cycloaddition to form a 1,2,4-triazinane scaffold. Following *N*-debenzylation by catalytic hydrogenolysis, triazinane diastereomers **2.209** and **2.210** were isolated in 11% and 5% yield, respectively, over three steps (Scheme 2.66).

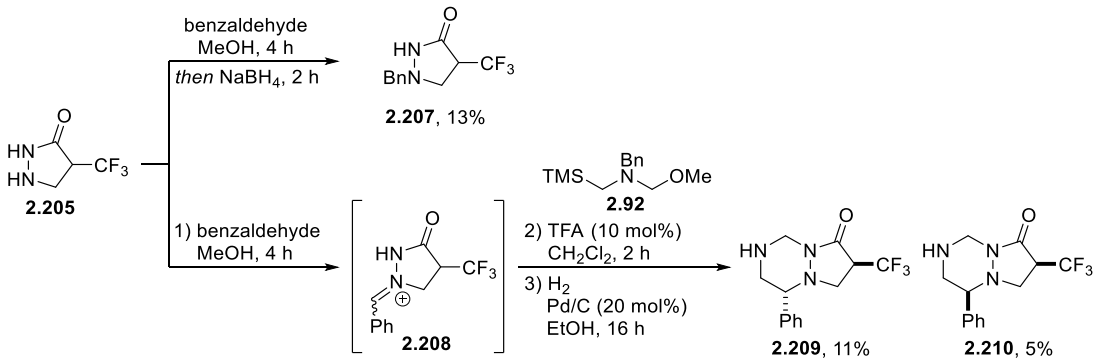

Scheme 2.66. Derivatization of pyrazolidinone **2.205**.

2.3.10. Other Scaffolds

[3+2] Cycloadditions

In addition to the two successful [3+2] cycloadditions used in the construction of the 3F library, two additional [3+2] cycloadditions had also been attempted. Targeting scaffold **2.211**, acrylate **2.2** was reacted with commercially available 1-aminopyridinium iodide under basic conditions (Scheme 2.67). Unfortunately, the reaction yielded a mixture compounds that were difficult to purify. However, it became apparent that the major product was a diastereomer of **2.212**. Thus, **2.211** had underwent a subsequent Diels-Alder with another molecule of **2.2** reaction to form a bridged tricyclic scaffold.

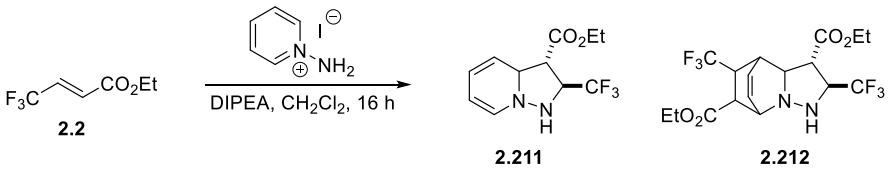

Scheme 2.67. A tandem [3+2] cycloaddition and Diels-Alder reaction afforded **2.212** (stereochemistry unknown).

The rate of the Diels-Alder reaction was found to be significantly faster than the initial [3+2] reaction and even in a large excess of 1-aminopyridinium iodide, **2.212** was the predominant product. Due to a high molecular weight of 430 Da, this compound was not included in the library. A possible approach to prevent the subsequent Diels-Alder reaction and avoid diastereomers could be to use alkyne **2.4** instead to form a more stable pyrazolo[1,5-a]pyridine scaffold. However, due to the flat structure of this scaffold it was not pursued.


pyrazolo[1,5-*a*]pyridine

In a similar approach, a pyridazinium ylide-mediated [3+2] cycloaddition was attempted (Scheme 2.68). Acrylate **2.2** was reacted with cycloimmonium salt **2.213**, which was easily prepared from pyridazine and 2-bromoacetamide, to afford the desired bicyclic **2.214** as an inseparable 1:1 mixture of diastereomers and in poor yield. Attempts to optimize the diastereoselectivity including the use of methyl ester **2.6** as dipolarophile were unsuccessful and this route was also abandoned.

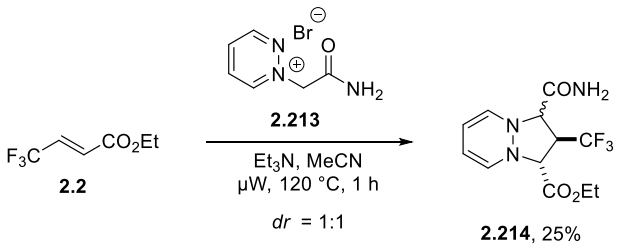

Scheme 2.68. [3+2] Cycloaddition between **2.2** and **2.213** afforded a mixture of diastereomers in a poor yield.

β-(Thio)lactam formation

Synthesis of a β-lactam or β-thiolactam scaffold for the 3F library was attempted by a reaction between acrylate **2.2** and a (thio)cyanate salt. Although this reaction had no precedence in the literature, it was hypothesized that **2.2** could be electrophilic enough to facilitate *N*-attack from a cyanate salt. Using KNCO in the presence of 18-crown-6 to bind potassium and thus increase the nucleophicity of the cyanate ion, the reaction was carried out using microwave heating (Scheme 2.69). However, in spite of temperatures at 180 °C, no conjugate addition was observed. Similarly, attempts using the potentially more nucleophilic KNCS were also unsuccessful.

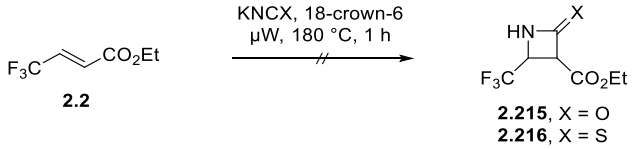

Scheme 2.69. Attempted β-(thio)lactam formation with potassium (thio)cyanate.

Cyclopropanation

A few attempts to perform cyclopropanation was also undertaken. As previously described, ethyl diazoacetate has been used as a cyclopropanation reagent of highly activated alkenes. Thus, it was hypothesized that the most electron deficient starting material, anhydride **2.3**, would be able to undergo cyclopropanation. However, the reaction only yielded a complex mixture and this route was not pursued further (Scheme 2.70).

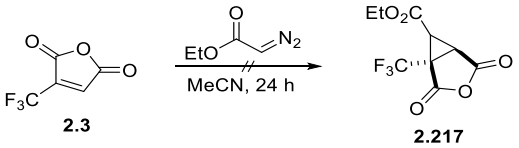

Scheme 2.70. Attempted cyclopropanation of anhydride **2.3** with ethyl diazoacetate.

Inspired by Zhang and coworkers,[262] a $PhI(OAc)_2$-mediated cyclopropanation of acrylate **2.2** was also investigated. While this reaction has successfully been employed in the cyclopropanation of activated alkenes in the literature using malononitrile as nucleophile, these conditions failed to afford the target cyclopropane **2.218** (Scheme 2.71).

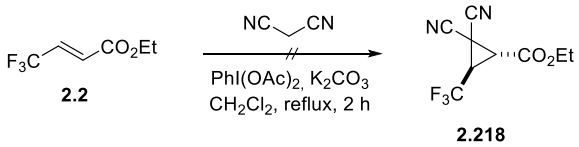

Scheme 2.71. Attempted $PhI(OAc)_2$-mediated cyclopropanation.

Finally, a base-mediated cyclocondensation between diethyl 2-chloromalonate and ethyl ester **2.2** was attempted (Scheme 2.72). Unfortunately, no cyclized products were observed in this reaction either.

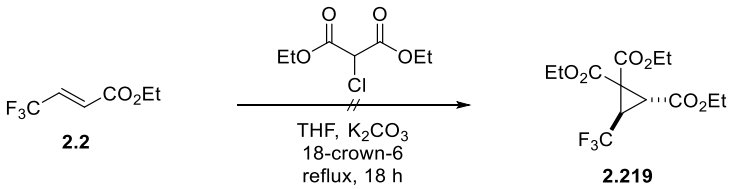

Scheme 2.72. Attempted cyclocondensation of acrylate **2.2**.

Intramolecular Epoxide-Opening

A six-membered scaffold (**2.221**) was targeted *via* an intramolecular epoxide-opening (Scheme 2.73). An initial PyBroP-mediated amidation with *N*-methyl-*N*'-Boc-ethylenediamine afforded **2.220** in 66% yield.

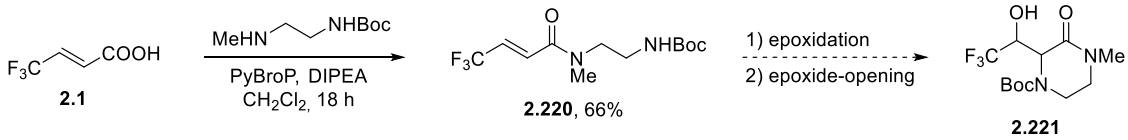

Scheme 2.73. Aiming to perform an intramolecular epoxide-opening, amidation of **2.1** was carried out first.

Subsequent attempts to perform a nucleophilic epoxidation on **2.220** proved more difficult (Table 2.7). Reaction with either mCPBA or mCPBA/KOH failed to epoxidize the α,β-unsaturated system (entries 1 and 2). Instead, epoxidation was achieved with H_2O_2/LiOH at ambient temperature (entry 3). Unfortunately, several other products were also formed which hampered purification and increasing the temperature only yielded a more complex mixture (entry 4). Finally, epoxidation was attempted with ^{t}BuOOH and Sm(O^{i}Pr)$_3$ but this combination also failed to produce the desired epoxide (entry 5).

Table 2.7. Attempted conditions for nucleophilic epoxidation of **2.220**.

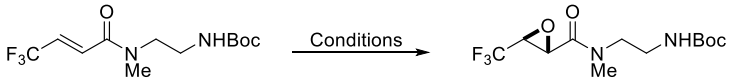

2.221 **2.222**

Entry	Epoxidation agent	Catalyst/base	Solvent	Temp.	Time (h)	Result
1	mCPBA	-	CH_2Cl_2	reflux	24	no reaction
2	mCPBA	KOH	CH_2Cl_2	reflux	18	no reaction
3	H_2O_2	LiOH	THF/H_2O	22 °C	72	impure epoxide
4	H_2O_2	LiOH	THF/H_2O	reflux	16	complex mixture
5	*t*BuOOH	Sm(O^{i}Pr)$_3$	THF	reflux	4	complex mixture

With the impure epoxide at hand (from entry 3), an intramolecular epoxide-opening was attempted under basic conditions (Scheme 2.74). Unsatisfyingly, no ring-closed products were observed and the synthesis of **2.221** was abandoned. Attempts to perform the reaction under acidic conditions to facilitate both Boc-deprotection and epoxide-opening were not carried out.

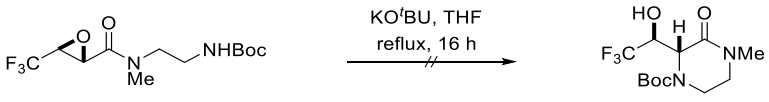

2.222 **2.221**

Scheme 2.74. Attempted intramolecular base-mediated epoxide-opening.

2.4. Chemoinformatic Library Analysis

A total of 115 fluorinated fragments based on 67 distinct atomic frameworks[263] were successfully synthesized during this campaign. A summary of the synthetic pathways used in the construction of the 3F library is provided in Figure 2.13.

2.4.1. Physicochemical Properties

An overview of calculated physicochemical properties of the 3F library and two commercial fluorinated fragment libraries, Key Organics (461 fragments) and Maybridge (5295 fragments), is given in Table 2.8. Comparative plots of molecular weight vs. AlogP and distribution of Fsp^3 are shown in Figure 2.12 and Figure 2.14, respectively. In the latter, the Fsp3 distribution of natural products and FDA-approved drugs showed practically identical with a close-to uniform distribution across all bins. Interestingly, the 3F library exhibited a similar trend, although with a slightly higher degree of Fsp^3.

Table 2.8. Average physicochemical properties of the 3F, Key Organics, and Maybridge fluorinated fragment libraries. Adapted with permission from reference.[1] Copyright (2020) John Wiley and Sons.

	Ideal range	3F library	Key Organics ^{19}F library	Maybridge ^{19}F library
MW	<300[a]	284 ± 41	187 ± 29	285 ± 55
AlogP	0–3[a]	0.8 ± 0.9	1.9 ± 0.6	3.2 ± 1.2
HBA	≤3[a]	2.7 ± 1.2	1.4 ± 0.9	2.2 ± 1.3
HBD	≤3[a]	0.8 ± 0.8	0.6 ± 0.6	0.8 ± 0.8
PSA	≤60 Å^2[a]	52 ± 16	37 ± 12	58 ± 24
Chiral centers	-	3.3 ± 1.8	0.1 ± 0.3	0.2 ± 0.5
Fsp^3	≥0.47[121]	0.7 ± 0.2	0.2 ± 0.2	0.2 ± 0.2
NP-likeness score[b]	>0[264]	0.0 ± 0.5	-1.0 ± 0.5	-1.1 ± 0.4

[a] Based on the Ro3.[35] [b] compared to a score of 1.1 ± 0.6 for a collection of 2712 natural products (*vide infra*). MW = molecular weight; AlogP = atomic partition coefficient; HBA = hydrogen bond acceptors, HBD = hydrogen bond donors; PSA = polar surface area; Fsp^3 = fraction sp^3-hybridized carbon; NP = natural product; green: inside ideal range; yellow: extreme of ideal range; red: outside ideal range.

Prominently, the 3F library exhibited a low average AlogP, which was considerably lower than the commercial collection. As most fragment-based screening is performed in aqueous media and with relative high fragment concentrations, aqueous solubility is an important parameter. Furthermore, the 3F library was significantly more complex with more stereocenters and a high Fsp^3 of 0.7 compared to 0.2 for both Key Organics and Maybridge libraries (drug candidates have an average value of 0.47[121]). Finally, the 3F library also showed a higher degree of natural product-likeness (*vide infra*).

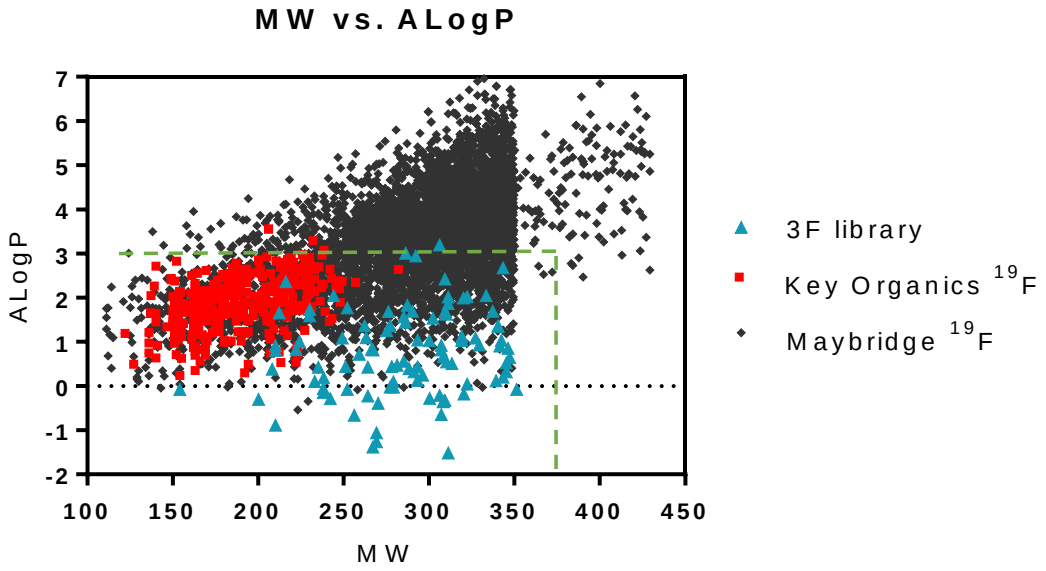

Figure 2.12. Comparison of MW vs. AlogP distributions of the 3F, Key Organics, and Maybridge fluorinated libraries. The green dashed line represents CF_3-fragment space. Compared to Key Organics, the 3F library is distributed over a larger area in the plot with an average higher MW but lower AlogP. Interestingly, over half of the fluorinated fragments from Maybridge violate the 'Rule of Three' parameter AlogP < 3. Reprinted with permission from reference.[1] Copyright (2020) John Wiley and Sons.

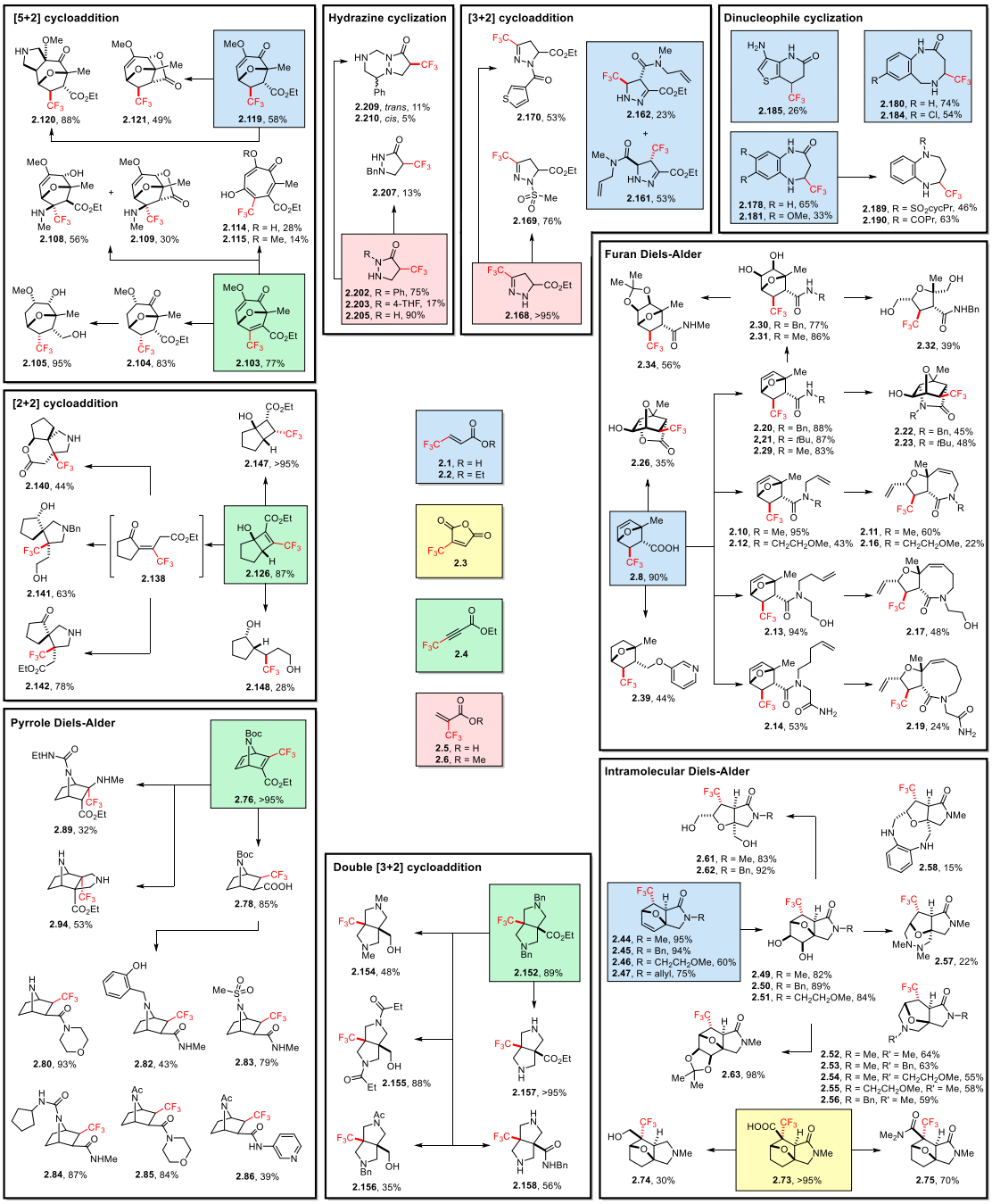

Figure 2.13. Synthesis of the 3F library containing 115 fluorinated fragments based on 67 distinct atomic frameworks (not all shown). Starting from six similar and readily available fluorinated compounds **2.1**–**2.6**, nine core scaffolds were synthesized (color-coding indicates starting material used). The main reaction types used to form each of the core scaffolds are listed in the top left hand corner of each box. Adapted with permission from reference.[1] Copyright (2020) John Wiley and Sons.

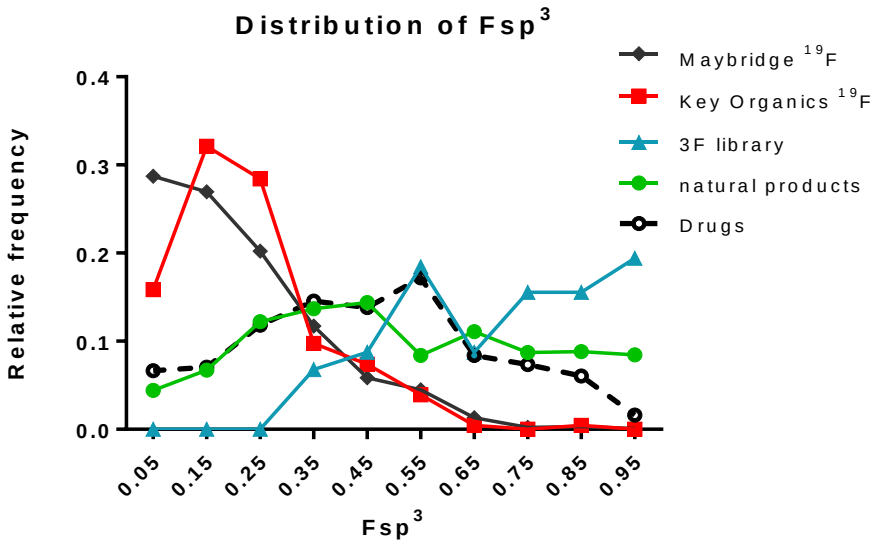

Figure 2.14. Distribution of Fsp^3 shows a significantly higher proportion of Fsp^3 among the 3F library compared to the two fluorinated commercial collections (Key Organics and Maybridge). Both natural products and FDA-approved drugs show a more equal distribution across Fsp^3 bins. Values are binned in sections of 0.1. X-axis show mean value of each bin. Adapted with permission from reference.[1] Copyright (2020) John Wiley and Sons.

2.4.2. PMI Analysis

To evaluate the shape diversity of the 3F library, PMI analysis of the library was carried out and compared to the Key Organics fluorinated fragments and a collection of natural products (Figure 2.15). The 3F library (average $Fsp^3 = 0.7$) exhibited a close-to uniform distribution in the PMI plot indicating a high degree of shape diversity. Compared to the library from Key Organics (average $Fsp^3 = 0.2$), the 3F library demonstrated a significantly higher degree of both shape diversity and three-dimensionality. While the commercial fragments were largely two-dimensional and predominantly situated in the so-called "flatland", [118,121] only 5% of the 3F library was found here. Interestingly, when compared to the collection of natural products (average $Fsp^3 = 0.5$), a more similar distribution were observed further pointing towards good natural product-likeness of the 3F library.

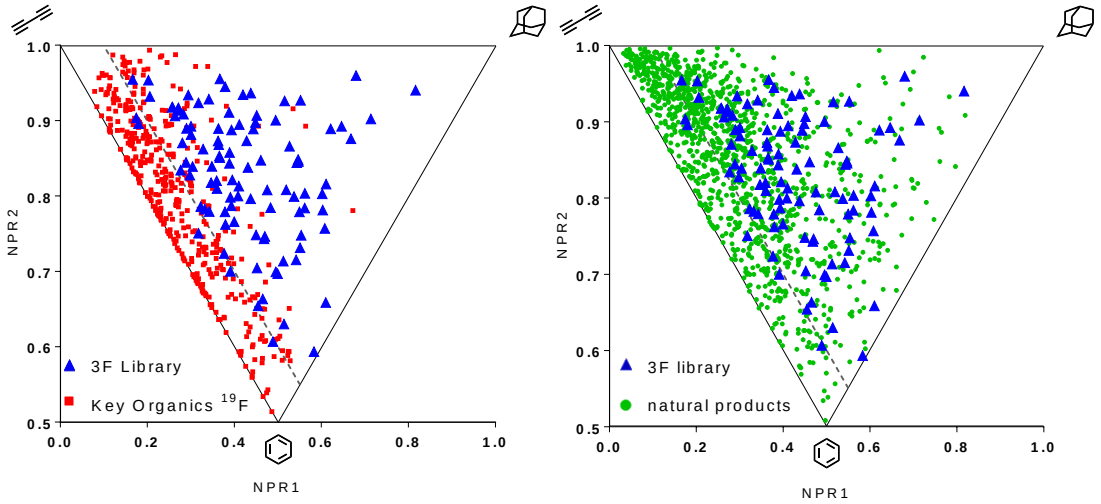

Figure 2.15. Principal moment of inertia (PMI) analysis of the 3F library (blue), a commercial fluorinated fragment library (Key Organics, red), and a collection of 1356 natural products (NuBBE database,[135] green). "Flatland" is situated below the dashed line (NPR1 + NPR2 < 1.1).[118] The three corners of the plot represent three geometrical extremes - rod-like, disc-like, and spherical shapes, respectively. NPR: normalized PMI ratios.[136] Adopted with permission from reference.[1] Copyright (2020) John Wiley and Sons.

To show the shape diversity of each of the nine sub-libraries that constitute the 3F library, separate PMI analyses are provided in Figure 2.16. Interestingly, the three Diels-Alder-based scaffolds all show good distributions around the center of the PMI plot (top row). Although fewer fragments were synthesized from the [5+2] and [2+2] cycloadditions, they seem to exhibit slightly higher shape diversity but are still distributed around the center of the plot (middle row). The most three-dimensional fragments are found among the *cis*-fused [5,5] pyrrolidine fragments from the double [3+2] cycloaddition (middle row, right). Not surprisingly, the small monocyclic fragments and fragments based on the dinucleophile cyclization show the lowest degree of three-dimensionality (bottom row).

2.4.3. Natural Product-Likeness

The natural product-likeness (NP-likeness) of the 3F library was analyzed using a "Natural-Product-Likeness Scorer".[264,265] The analysis is performed by dividing each compound into smaller substructures and then comparing them to two reference sets – synthetic molecules from the ZINC database[266] and a collection of representative natural products. On a logarithmic scale, each compound is assigned a score, typically in the range of -3 to 3, based on its resemblance to either reference set. Positive values indicate higher resemblance to natural products and negative values indicate a more synthetic character.

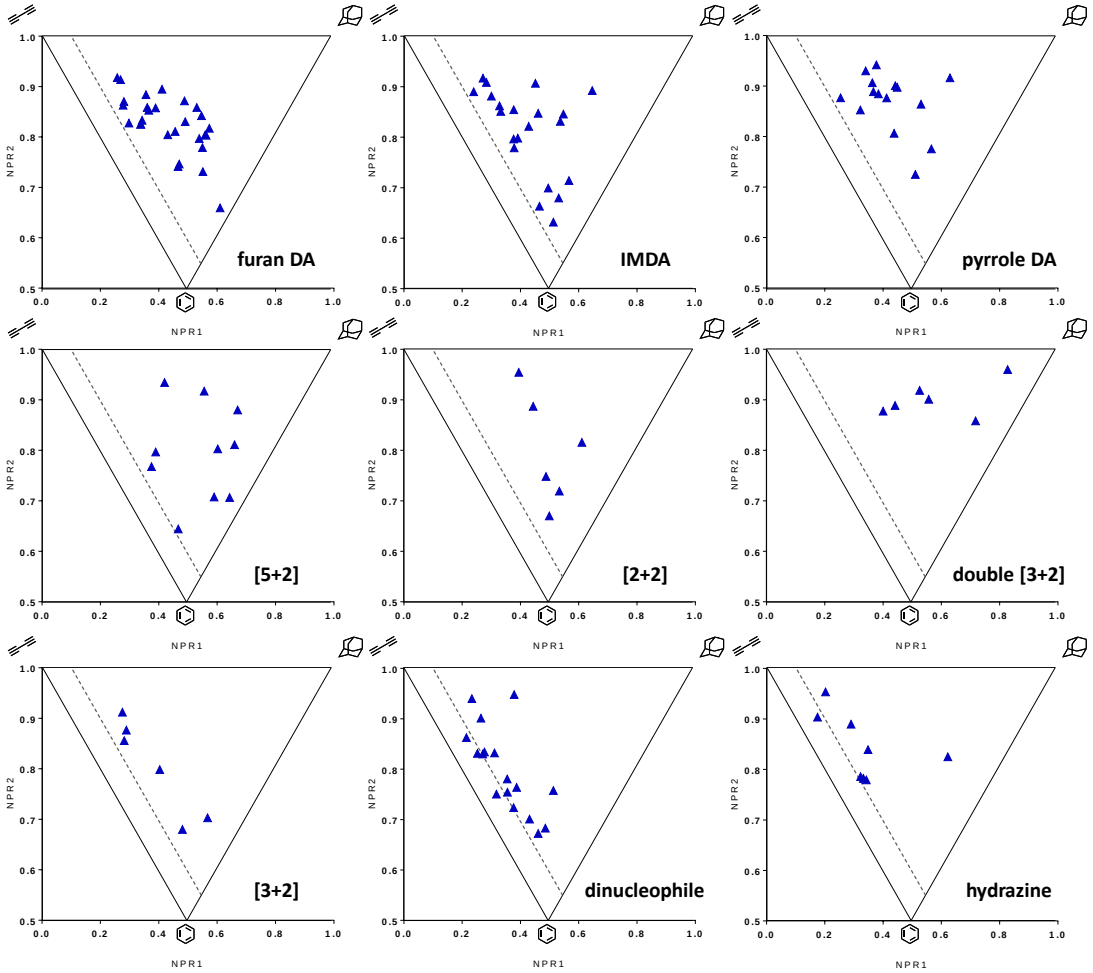

Figure 2.16. PMI analyses of the individual sub-libraries of the 3F library. Reprinted with permission from reference.[1] Copyright (2020) John Wiley and Sons.

Using this algorithm, the NP-likeness score was calculated for 3F, Key Organics and Maybridge fluorinated fragment libraries, and compared to a collection of 2712 natural products (Figure 2.17). Not surprisingly, the collection of natural products scored the highest. Interestingly, the 3F library showed significantly more natural product-like than the two commercial libraries. With an average score of 0.0, the 3F library did, however, still show an equal resemblance (or dissemblance) to synthetic compounds and natural products. Compared to FDA-approved drugs, the 3F library showed a similar average score although the score distribution of the drugs was wider.

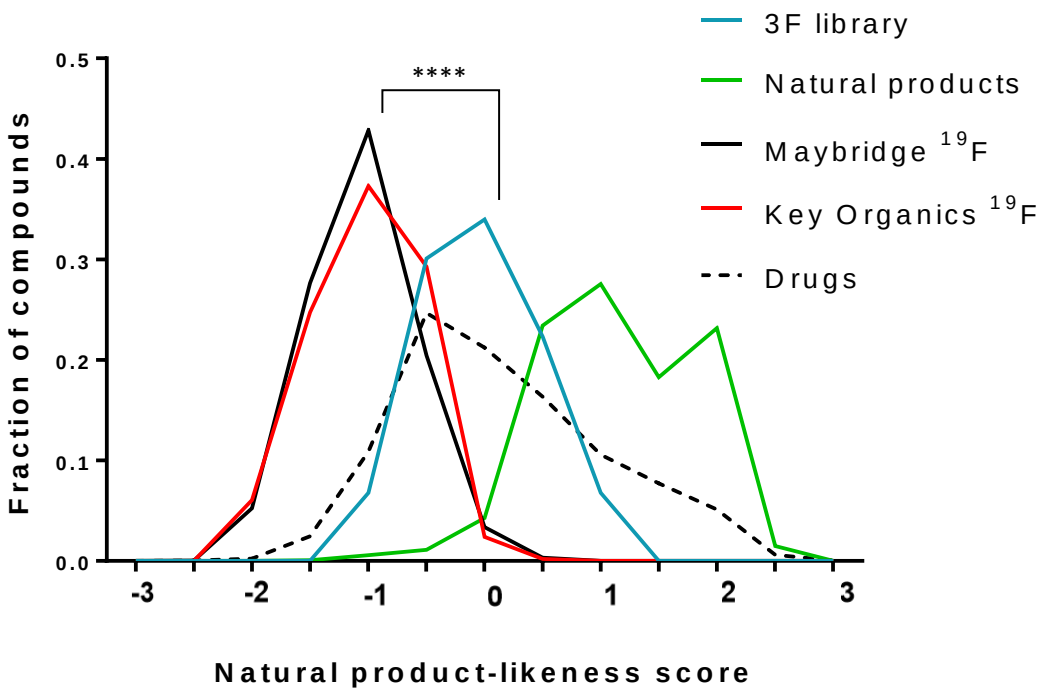

Figure 2.17. Natural product-likeness analysis[265] of the 3F library, two commercial fluorinated libraries, and a collection of 2712 natural products (NuBBE database[135]). Logarithmic scale. Statistics were calculated using a one-tailed nonparametric Mann-Whitney test. ****$p < 0.0001$. Adapted with permission from reference.[1] Copyright (2020) John Wiley and Sons.

When comparing the NP-likeness score of fluorinated compounds to drugs and natural products, it should be noted that the presence of fluorine effectively decreases the NP-likeness score as fluorine is practically nonexistent in nature.[161] For example, calculating the NP-likeness of the 3F library without fluorine (substituted with H), the average NP-likeness score increased from 0.0 to 0.3.

2.5. NMR-Based Screening

To demonstrate the utility of the synthesized 3F library, NMR-based screening of multiple disease-relevant protein targets was performed. Fragments were screened using a primary ^{19}F NMR assay and hits were subsequently validated using secondary NMR experiments.

2.5.1. Quality Control

Prior to screening, NMR-based quality control of the 115 synthesized fragments was carried out by individual fragment analyses in phosphate buffered saline (PBS).[267] In total, 13 fragments were removed from the library due to either ^{19}F NMR peak broadening (possible aggregation), unwanted functionalities, or chemical instability (Figure 2.18). Tropone **2.115** passed the quality control but was later found to be unstable during screening.

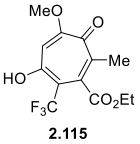

2.115

In addition to quality control, this exercise also provided $\delta^{19}F$ of each fragment in PBS for later design of screening cocktails.

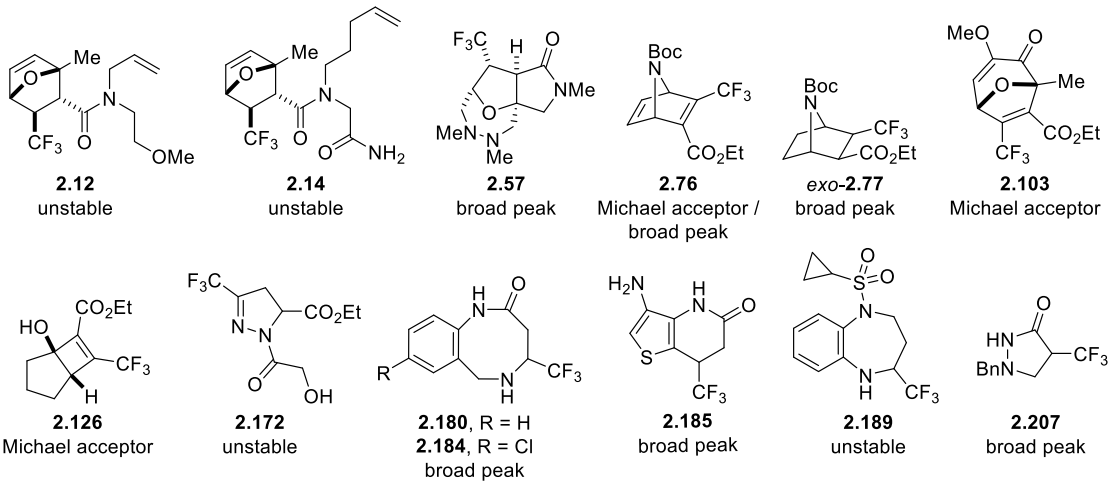

Figure 2.18. Fragments that failed quality control. "Broad peak" refers to a significant broadening or disappearance of ^{19}F NMR signals in the aqueous buffer making hit identification difficult.

During quality control, it also became apparent that approximately 20% of the fragments exhibited a significant or complete loss of their ^{19}F signal intensities (fast T_2-relaxation rate) during the CPMG experiment (Figure 2.19). Thus, disappearance of signal intensity for these fragments did not correspond to protein binding. While such behavior is normally attributed to aggregation, the majority of these 'CPMG-sensitive' compounds were reasonably polar with

most containing a basic nitrogen atom. However, this effect has been reported for molecules existing in different states with large differences in $\delta^{19}F$ caused by either tautomerization, protonation, conformational exchange (*e.g. cis*/*trans* of an amide bond), and/or transient hydrogen bonding.[190] Thus, amine protonation and amide bond rotation were plausible explanations for these observations and screening of these compounds was still possible if applying a shorter CPMG scheme (*e.g.* 20 ms relaxation delay instead of 200 ms).

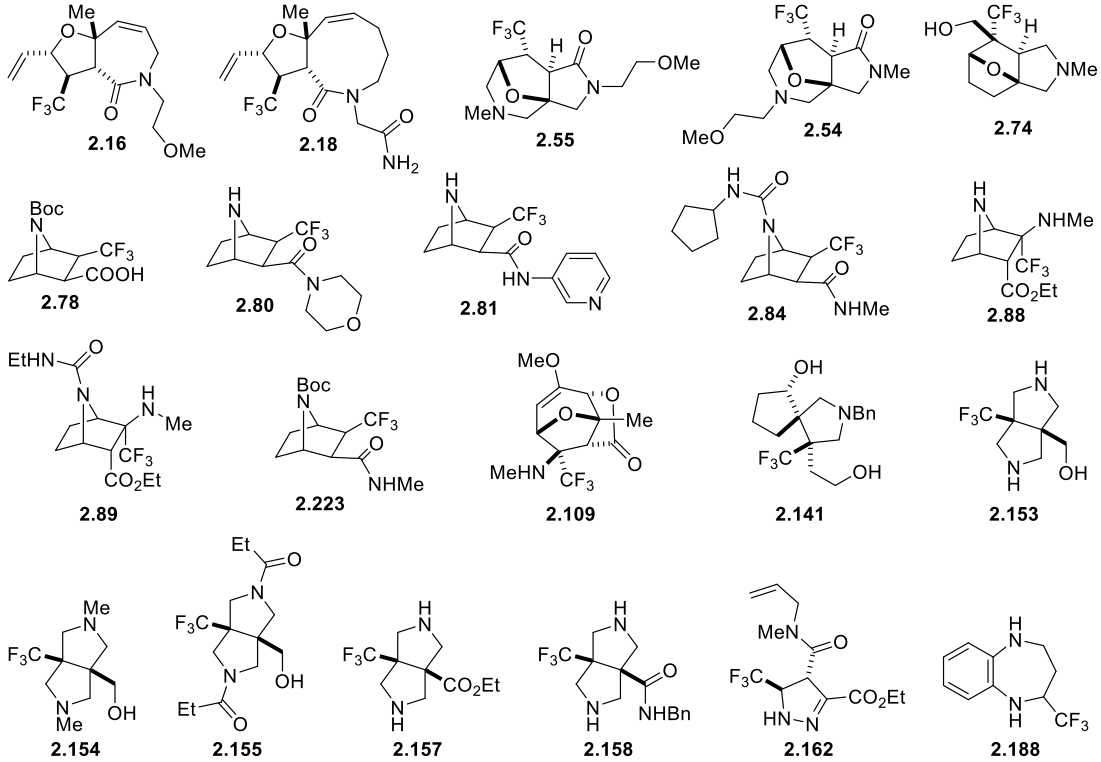

Figure 2.19. Structures of 'CPMG-sensitive' fragments exhibiting a significant or complete loss of ^{19}F NMR signal intensities upon application of a 200 ms CPMG scheme.

The 102 fragments, including 'CPMG-sensitive' fragments, that passed quality control were pooled in cocktails containing 17–25 fragments based on the distribution of chemical shifts (see the Supporting Information for cocktail compositions, Tables S2–S10). This also ensured excellent structural diversity with each cocktail containing fragments from at least six of the nine core scaffold groups.

2.5.2. Protein Targets

For set-up and optimization of the ^{19}F NMR assay, readily available human serum albumin (HSA) was selected as a test target. HSA is the most abundant blood plasma protein and primarily functions as a transport protein for both endo- and exogenous molecules.[268] Protein binding generally increases plasma solubility, reduces toxicity, and protects against oxidation of the bound molecules. Thus, HSA binding is of interest in drug discovery as it may significantly impact pharmacokinetic properties of bioactive molecules. In addition, HSA holds enzymatic properties, most notably esterase activity.[268]

For additional screening of the 3F library, four disease-relevant targets were selected – the two oncology-related kinases p70S6K1 and p38γ, the Alzheimer's disease target BACE1, and C-type lectin receptor DC-SIGN, which is associated with viral infections and autoimmunity.

The serine/threonine kinase ribosomal protein S6 kinase beta-1 (p70S6K1) is involved in signaling pathways regulating cell proliferation and survival.[269,270] Deregulation or overexpression of p70S6K1 has been associated with several types of aggressive cancers including lung and ovarian cancers.[271,272] Evidence also indicates that p70S6K1 is involved in chemotherapy resistance for various tumors.[271] Targeting this enzyme may serve as a novel therapeutic strategy or as a strategy to enhance the efficacy of other anti-cancer drugs. To date, no inhibitors have been approved for clinical use.[272–274]

p38γ is also a serine/threonine kinase and has been associated with various inflammation-related diseases including diabetes, neurodegeneration, and cancer.[275] The kinase is part of the p38 mitogen-activated protein kinase (MAPK) family, which comprise the four isoforms p38α, p38β, p38γ, and p38δ. These isoforms are further divided into two subsets (p38α/β and p38γ/δ) based on sequence homology and substrate specificity. Thus, to evaluate the selectivity of hits, screening against p38α and p38δ was also performed.

β-secretase 1 or β-site amyloid precursor protein cleaving enzyme 1 (BACE1) has been linked to Alzheimer's disease (AD) – a progressive neurodegenerative disorder that is the most common cause of dementia.[276,277] The disease is characterized by extracellular accumulation of amyloid β (Aβ) peptide plaques in cerebral tissues and BACE1 has been identified as a major driver of Aβ production and deposition by cleaving of the Aβ precursor protein.[278] The aspartic protease has therefore been proposed as a promising therapeutic target for treatment of AD and numerous developed inhibitors are undergoing clinical trials.[279]

Finally, the dendritic cell-specific intercellular adhesion molecules-3-grabbing non-integrin (DC-SIGN) is a Ca^{2+}-dependent dendritic cell surface receptor responsible for mediating transient adhesion to T-cells.[280] Dendritic cells are antigen-presenting cells that are responsible for activating the adaptive immune system (B- and T-cells). Thus, DC-SIGN help facilitate important immunological roles and has been linked to both autoimmunity,[281,282] transplantation tolerance,[283] and viral infections including HIV *trans*-infection of T-cells.[284]

2.5.3. Primary ^{19}F NMR-Based Screening

^{19}F NMR screening was performed using a CPMG scheme (both 20 ms and 200 ms relaxation delays) and binding was determined as a significant reduction (>50%) of ^{19}F signal intensities upon addition of the protein (Figure 2.20). Screening was performed on a 600 MHz spectrometer with an acquisitions time of 2 h per cocktail, which enabled screening of the entire library (five cocktails) against one target per day.

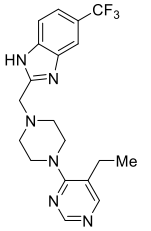

PF-4708671
K_d(p70S6K1) = 20 nM

A total of seven protein targets were screened and screening results are shown in Table 2.9 (see the Supporting Information for NMR data, Figures S10–S50). For screening against p70S6K1 and DC-SIGN a known ligand was subsequently added to determine if binding was associated with a known binding site. For p70S6K1, the inhibitor PF-4708671[272] was selected, while Ca^{2+} was used for DC-SIGN. Hits that were successfully displaced are highlighted with a black frame in Table 2.9. Fragments highlighted with a blue background were subsequently validated by a secondary NMR assay while an asterix (*) indicates *in vitro* activity. K_i- and K_d-values were measured using ^{19}F NMR (*vide infra*).

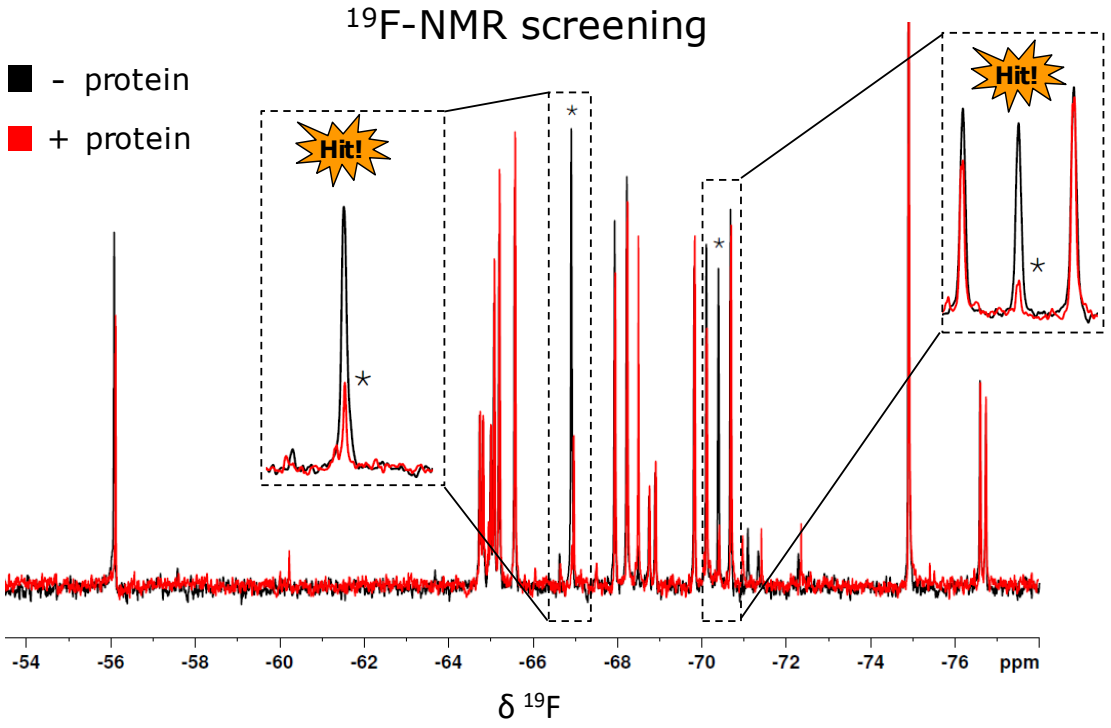

Figure 2.20. Example of ^{19}F NMR screening results against BACE1 that shows two binders. Both spectra were recorded using a CPMG scheme (200 ms). Reprinted with permission from reference.[1] Copyright (2020) John Wiley and Sons.

Table 2.9. NMR screening results. Fragments highlighted with a blue background were validated with a secondary assay (^{1}H or ^{19}F NMR). A black frame indicates specific binding as determined by displacement with a known ligand. An asterix indicates >25% *in vitro* enzyme inhibition at 10 mM. LE

Target	Hits	Hit rate[a]
HSA[b]	**2.42**, **2.147**, **2.53**, **2.58**, **2.161**, **2.168**, **2.170**, **2.179**, **2.181**, **2.186**, **2.190**, **2.191**, **2.114**, **2.202**, **2.209**	15%
p70S6K1[c]	**2.114**, **2.120**, **2.191**	3%
p38γ/δ[d],[e]	**2.42** (K_d ND), **2.43** (K_d = 750 µM, LE = 0.19), **2.209**, **2.39**, **2.49**, **2.114** (K_d = 400 µM, LE = 0.23), **2.191** (K_d = 250 µM, LE = 0.25), **2.170**, **2.190**, **2.120**, **2.198**	11%
p38α[b]	**2.39**, **2.42**, **2.43**, **2.49**, **2.114**, **2.170**, **2.190**, **2.191**, **2.198**, **2.203**, **2.209**, **2.210**	12%
BACE1	**2.26**, **2.105**, **2.120**, **2.121**, **2.147**, **2.168**, **2.198**	7%
DC-SIGN [f],[g]	**2.53** (K_i = 4.1 mM, LE = 0.14), **2.43** (K_i = 2.7 mM, LE = 0.17), **2.114** (K_d = 150 µM, LE = 0.26), **2.42**, **2.66** (K_i = 3.3 mM, LE = 0.15), **2.170** (K_i = 12.9 mM, LE = 0.13), **2.188** (K_i = 3.2 mM, LE = 0.23), **2.45**, **2.81**	9%

[a] For primary ^{19}F NMR screen. [b] Validation by ^{1}H NMR was not performed. [c] Inhibitor PF-4708671 was used as competitive ligand. [d] Hits and validation were identical for p38γ and p38δ. [e] K_d-values were performed on p38γ only. [f] Ca^{2+} was used as competitive ligand. [g] K_d for **2.114** was determined using ^{1}H–^{15}N HSQC. LE = ligand efficiency.

2.5.4. Validation by ^{1}H NMR

In an effort to validate the identified hits against p70S6K1, p38γ, and BACE1, binding was subsequently evaluated by WaterLOGSY and STD ^{1}H NMR experiments (Figure 2.21). Based on dispersion of ^{1}H signals, hits against each target were pooled into small cocktails of up to four compounds each. The ^{1}H NMR experiments were performed on an 800 MHz spectrometer and hits validated by at least one of the experiments are highlighted with a blue background in Table 2.9.

As an illustration of the efficiency of screening by ^{19}F NMR, the screening conditions applied for the primary ^{19}F NMR assay and the subsequent ^{1}H NMR validation assay are compared in Table 2.10. Noticeably, the ^{1}H NMR assay required extended acquisition time (even at a higher field strength) with increased concentrations of both ligands and protein. Moreover, due to ^{1}H signal overlap screening was only performed with up to four fragments at a time.

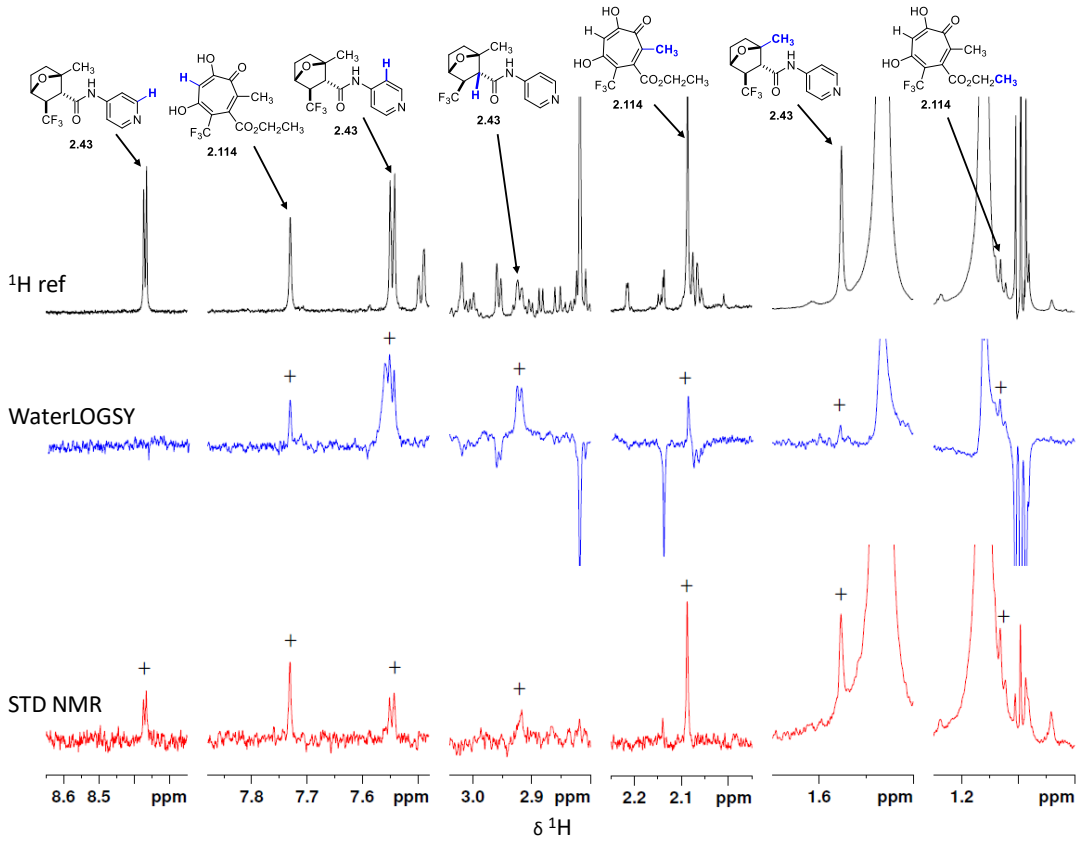

Figure 2.21. Example of ^{1}H NMR validation results from STD and WaterLOGSY experiments. These results show validation of p38γ hits **2.43** and **2.114** while **2.49** and **2.191** were not validated in this cocktail. Positive signals in the WaterLOGSY and STD spectra indicate protein binding. STD spectrum was recorded using protein irradiation at 0.339 ppm.

Table 2.10. Conditions used for the primary ^{19}F NMR screening assay and the secondary ^{1}H NMR validation assay (both STD and WaterLOGSY experiments) against p38γ.

	N	Time	Field strength (MHz)	[Ligands] (µM)	[p38γ] (µM)	Background nuisance
^{19}F NMR CPMG screen	≤25	2 h	600	25	5.7	no
^{1}H NMR (STD & WaterLOGSY)	≤4	14 h[a]	800	200	11.4	yes[b]

[a] Performing irradiation of three protein-associated signals in the STD experiment. [b] Water, buffer (*e.g.* HEPES or Tris·HCl), and additives (*e.g.* glycerol or DTT). N = number of fragments pr. cocktail.

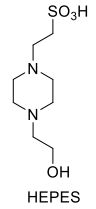

HEPES

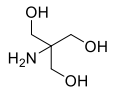

Tris base

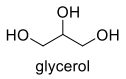

glycerol

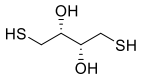

1,4-dithiothreitol (DTT)

2.5.5. Further Studies

Hits against p38γ were further evaluated using an enzymatic assay that measures phosphorylation of a peptide substrate (Figure 2.22).[v] At 10 mM, fragments **2.42**, **2.43**, **2.114** and **2.191** demonstrated >25% inhibition of the kinase. Notably, tropolone **2.114** exhibited almost complete inhibition of p38γ, similar to the pan-p38 kinase inhibitor BIRB-796.[285] Only minor inhibition was observed for the remaining hits.

Continuing with the four hits exhibiting the highest *in vitro* activity, binding affinities were measured using ^{19}F NMR-based differential chemical shift perturbation (dCSP).[286] This ligand-observed ^{19}F NMR experiment provides a quick estimation of K_d (<1 mM) by comparing $\Delta\delta^{19}$F at different protein–ligand ratios. Alternatively, if only subtle changes in chemical shift are observed, determination can instead be based on changes in peak width at half height maximum ($\Delta\nu_{1/2}$).

Using this approach, K_d-values for **2.43** and **2.114** were estimated from $\Delta\delta^{19}$F to be 750 µM and 400 µM, respectively. Due to smaller changes in $\Delta\delta^{19}$F for **2.191**, the K_d-value for this hit was based on $\Delta\nu_{1/2}$ and estimated at 250 µM. Unfortunately, data measured for **2.42** was inconclusive although both peak broadening and changes in chemical shift were observed (Table 2.9). These results indicate that **2.191** is the strongest binder although it exhibited the lowest *in vitro* activity of the four hits. However, this K_d-value is likely less accurate as it is based on far smaller changes in $\nu_{1/2}$ rather than larger chemical shift perturbations.

Hits against DC-SIGN[vi] were subsequently validated using a FAXS-type reporter assay by displacement of a known fluorinated reporter molecule, *N*-acetylmannosamine-based **2.224**.[287] Six of the nine hits were validated using this approach. Based on changes in observed relaxation rates of **2.224**, K_i-values could also be determined (Table 2.9). All hits exhibited low millimolar K_i-values similar to the K_i-value determined for mannose (2.34 mM).

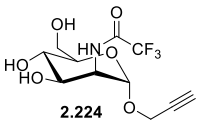

2.224

[v] Enzymatic studies with p38γ were performed by the Cuenda group at CNB/CSIC
[vi] Screening against DC-SIGN was performed by the Rademacher group at MPI

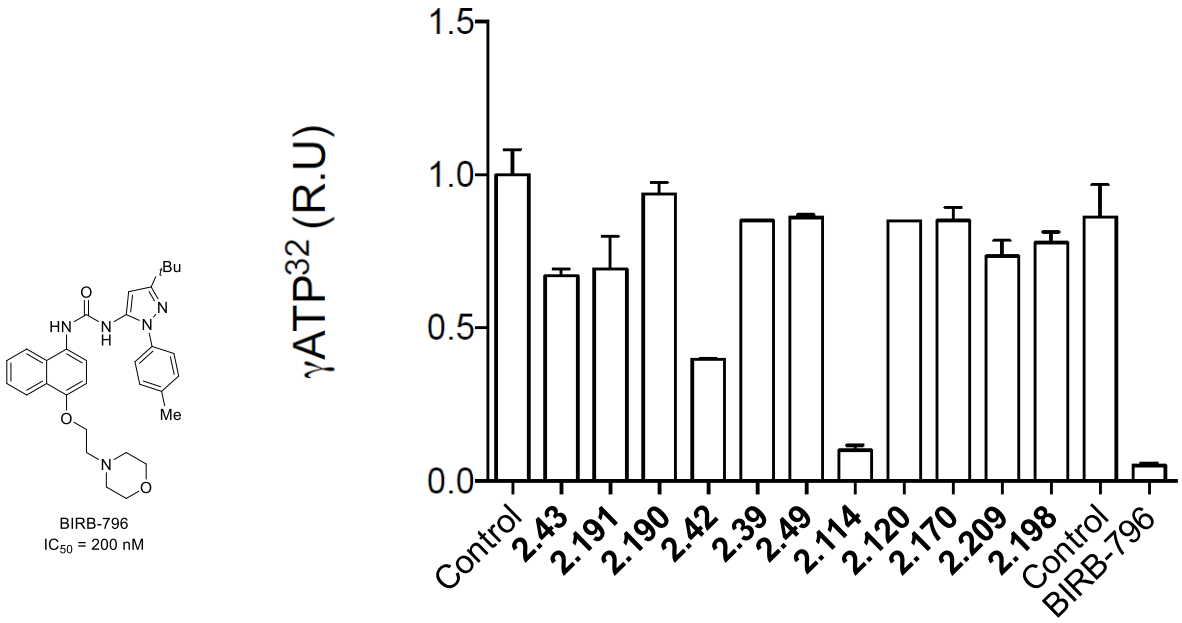

Figure 2.22. Radioactive p38γ assay with myelin basic protein (MBP)[vii] as substrate. Shown results are at 10 mM compound concentrations. BIRB-796[285] (pan-p38 kinase inhibitor) was used as a positive control.

For the most potent hit, tropolone **2.114**, further binding studies were performed by ^{1}H–^{15}N HSQC NMR using ^{15}N-labeled DC-SIGN (Figure 2.23). Titration with **2.114** resulted in significant chemical shift perturbations and reduced resonance intensities of several amino acids. These amino acids consisted of four non-associated allosteric residues and three residues (270Met, 310Ser, and 374Phe) situated in binding site III of DC SIGN (Figure 2.24).[288] Quantification of chemical shift perturbations from these three residues resulted in a calculated K_d-value of 150 ± 50 µM.

[vii] MBP: Ala-Pro-Arg-Thr-Pro-Gly-Gly-Arg-Arg

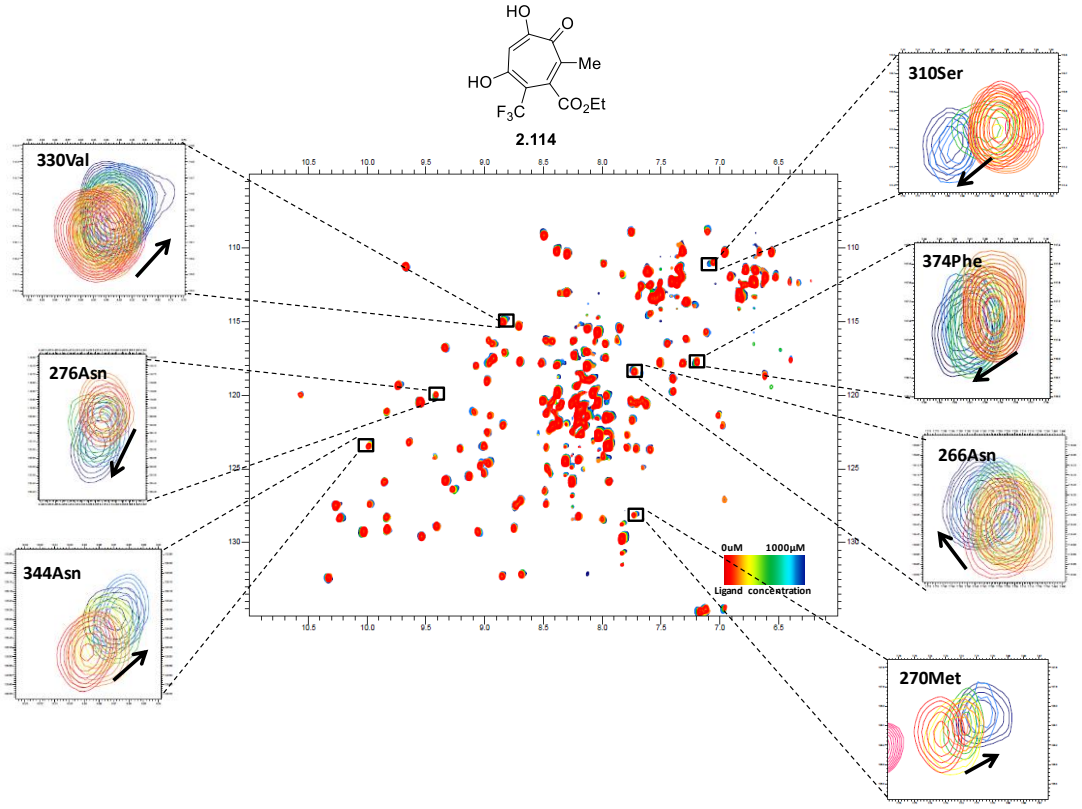

Figure 2.23. ^{1}H-^{15}N-HSQC NMR of DC-SIGN showing titration data with **2.114**. Based on chemical shift perturbations a K_d-value of 150 ± 50 µM was calculated.

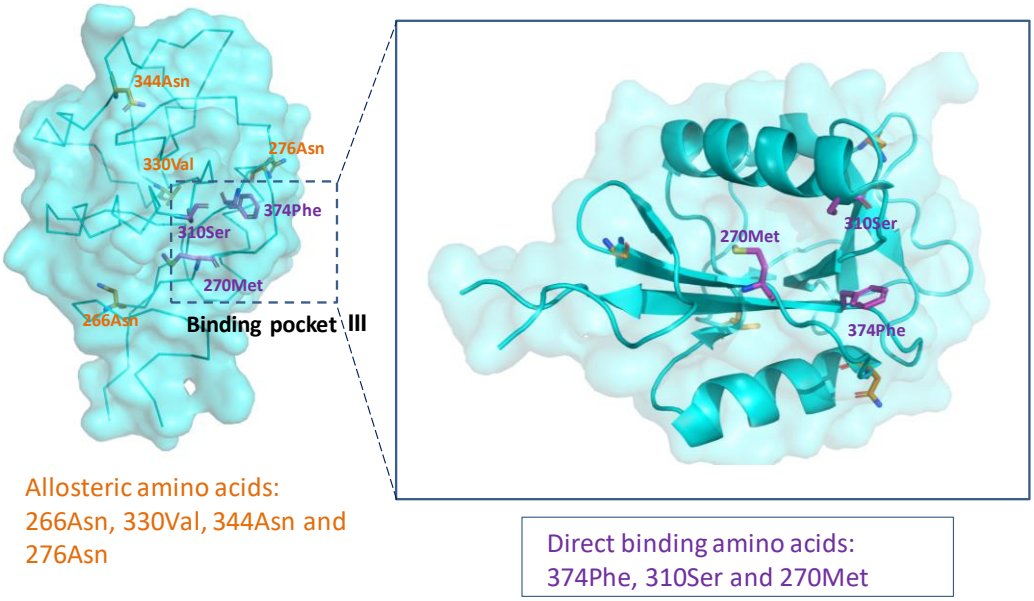

Figure 2.24. Binding site hypothesis for **2.114** based on site III amino acids 270Met, 310Ser, and 374Phe (highlighted in purple). Chemical shifts of four allosteric amino acids were also affected by binding of **2.114** (orange).

2.5.6. Analysis and Discussion

Generally, the ^{19}F NMR-based screening of the 3F library afforded relative high hit rates between 3–15%. Although hit rates in the 5–10% range is commonly encountered in fragment screens,[10,286] a lower hit rate was expected for these complex and three-dimensional fragments in the 3F library.[289] Nevertheless, it has been argued that hit rates for three-dimensional structures are not necessarily lower than for more two-dimensional structures, in spite of what may be intuitively reasoned.[118] Indeed, similar reports of high hit rates (>10%) for complex fragments have previously been reported (see for example Scheme 1.3).[151] However, a high hit rate against HSA was expected as the transport protein is known to accommodate a broad range of small molecules and drugs (typical K_d = 1–100 µM).[268]

The high hit rate may also be a result of the higher sensitivity of ^{19}F NMR compared to other methods such as ^{1}H NMR and SPR, leading to detection of otherwise overlooked hits. Moreover, the use of ligand-observed NMR methods are also more prone to false positives than for instance protein-observed NMR spectroscopy or X-ray crystallography.[10]

To analyze the fragment hits, PMI analysis and natural product-likeness scoring were performed (Figure 2.25). Overall, hits showed a fairly broad distribution in the PMI plot with BACE1 hits exhibiting the highest degree of three-dimensionality and DC-SIGN hits the lowest. Looking at the natural product-likeness of the hits, a wide distribution across the NP-likeness range of the 3F library was observed. While average scores were positive for hits against p70S6K1 and BACE1 and negative for hits against p38γ/δ and DC-SIGN, there is no evidence to support the advantage of natural product-like fragments. However, these datasets are small and no statistically significant conclusions can be drawn from these analyses. For this, screening of larger fragment collections against additional targets should be performed for a more accurate chemoinformatic evaluation.

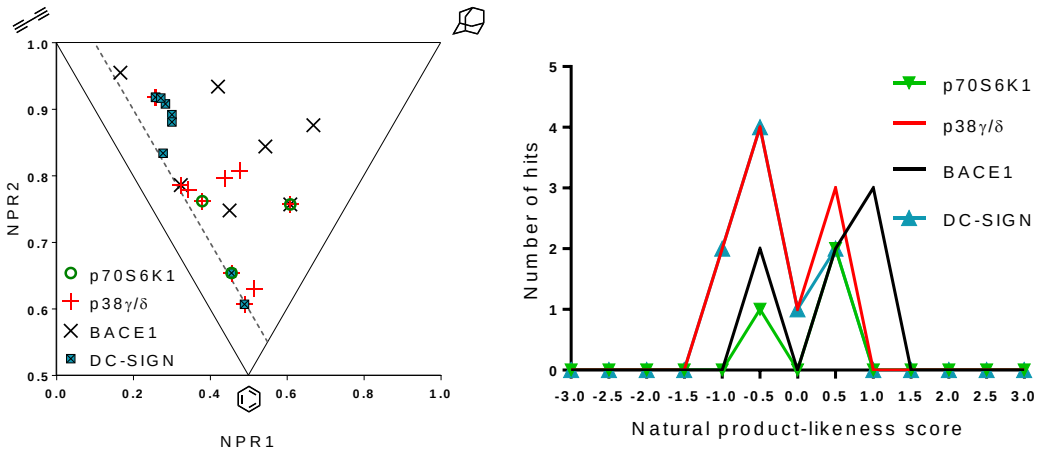

Figure 2.25. PMI and natural product-likeness analyses of the fragment hits. Natural product-likeness scores are binned sections of 0.5.

Looking at the hits against p38γ, no selectivity towards this isoform was observed (Table 2.9). All p38γ hits were also identified against the closely related isoform p38δ with an identical ^{1}H NMR validation rate. Similarly, 10 of the 11 hits were also identified as binders of p38α in the ^{19}F NMR assay. While **2.120** was not identified as a p38α binder, this fragment could not be validated against p38γ and showed only little-to-no activity at 10 mM *in vitro*. This lack of selectivity across the isoforms was later further validated by enzymatic studies of all p38γ hits against the four isoforms (see the Supporting Information Figure S30). Furthermore, the hits **2.114**, **2.120**, and **2.191** were also identified as binders to p70S6K1.

It was envisioned that some selectivity could be achieved at this early stage for such relatively complex fragments. However, kinases are structurally similar and selectivity is often achieved during hit-to-lead optimization. This has also been demonstrated against other kinases where selective inhibitors have been developed from non-selective hits.[93] In regards to the relatively hit rates of 11–12% against the p38 kinases, this not unusual. Indeed, hit rates as high as 34% with non-focused libraries have been reported against p38α using SPR-based screening.[290]

Interestingly, while most of the hits identified contained an aromatic moiety, all hits against BACE1 were non-aromatic and generally more three-dimensional. This trend fits well with many BACE1 inhibitors containing a quaternary carbon center and thus higher 3D character (Figure 2.26).[291,292] However, with a hit rate of 7% this is surprisingly high compared to the ~1% hit rate typically reported from other screens.[286]

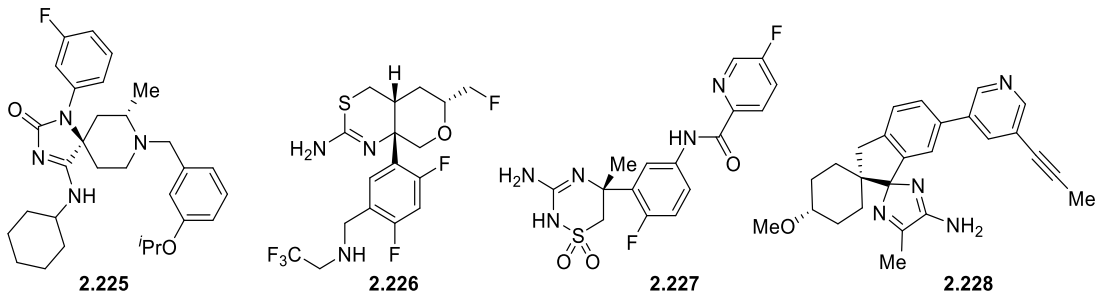

Figure 2.26. Developed BACE1 inhibitors containing a quaternary center.[292]

Finally, screening against DC-SIGN afforded a 9% hit rate, which is similar to previous reports of 5–16% fragment hit rates against this target.[288,293] Actually, two of the screens had also utilized ligand-observed ^{19}F NMR, which resulted in the highest hit rates of 14% and 16%, respectively. While most of the 3F library hits contained new chemotypes compared to previously reported hits, a few structural similarities was observed for two of the hits (Figure 2.27).

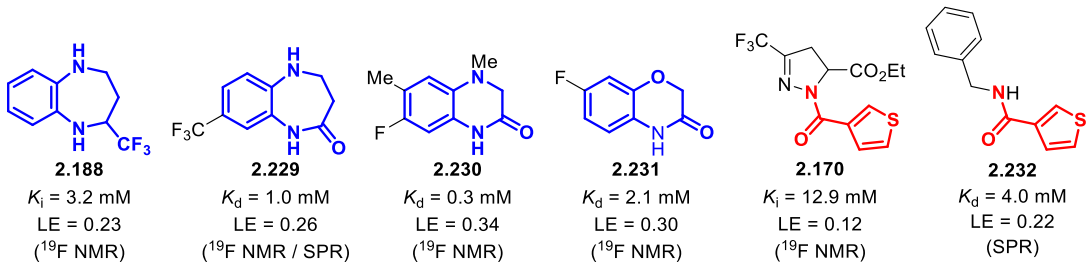

Figure 2.27. Similar DC-SIGN hits obtained from the 3F library (**2.188** and **2.170**) and previously reported screens (similarities highlighted in blue and red). Screening methods applied are listed under each structure. K_d-values were determined using SPR.[288]

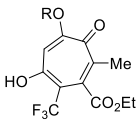

2.114, R = H
2.115, R = Me

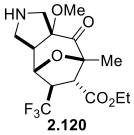

2.120

Of the 30 hits obtained against the four central targets, five hits were identified against two targets (**2.42**, **2.43**, **2.170**, **2.191**, and **2.198**) and two hits were found to bind three of the targets (**2.114** and **2.120**). Thus, some caution should be taken with these potentially promiscuous binders. In particularly, tropolone **2.114** could be potentially reactive, *e.g.* as a Michael acceptor, and does not seem unlikely given the observed instability of **2.115** during screening. However, displacement of **2.114** was achieved during screening against p70S6K1 and many examples of stable tropolones exist.[241]

While ligand-observed ^{19}F NMR does not provide any binding information (unless displacement with a known binder is performed), it is a fast, simple, and sensitive assay ideally suited as a primary screening method. The major limitation is the need for labeled fragments, but once such a library has been assembled, screening is easily performed. Binding affinities can be determined using ^{19}F NMR but it is not the most accurate approach. Therefore, ^{19}F NMR screening should ideally be combined with other screening methods such as X-ray crystallography, SPR, or ITC to obtain information on binding mode and affinity. However, it is a particularly useful method for screening targets that are either difficult to crystallize or immobilize.

Overall, these screening results demonstrate the applicability of the 3F library. Hits were obtained against all seven protein targets screened with hit rates of 3–15%. Screening of a relatively small fragment library may therefore be sufficient in obtaining useful hits. Importantly, hits originated from eight of the nine central scaffold groups, which underlines the importance of library and scaffold diversity. However, whether the 3F library will be able to produce truly high impact hits that can be optimized into promising lead compounds, only time will tell.

2.6. Conclusion

To address the need of more diverse fragments and easier screening workflows, a novel library of three-dimensional fluorinated fragments was synthesized in an efficient manner (Figure 2.28). Starting from six readily available and fluorinated starting materials, 115 structurally diverse fluorinated Fsp^3-rich fragments (3F) were synthesized using diversity-oriented synthesis. The fragments exhibited highly desirable physicochemical properties, most noteworthy a low average AlogP of 0.8 and a high Fsp^3 of 0.7, which are significant improvements over typical commercial fragment collections. Importantly, the 3F library showed an excellent shape diversity as demonstrated by principal moment of inertia analysis.

To demonstrate the utility of the 3F library, ^{19}F NMR-based screening of the fluorinated fragments was performed. Following quality control, 102 of the synthesized fragments were screening against seven protein targets resulting in hit rates ranging from 3–15% (Figure 2.28). Hits against four disease-relevant proteins (p70S6K1, p38γ, BACE1, and DC-SIGN) were subsequently validated by secondary NMR assays resulting in a validation rate of 2/3.

The diverse 3F library presents the first example of a synthetic fragment library tailor-made for ^{19}F-NMR screening. Combined with the ease of performing ^{19}F NMR-based screening, our results underscore that this approach should find broad application within fragment-based drug discovery.

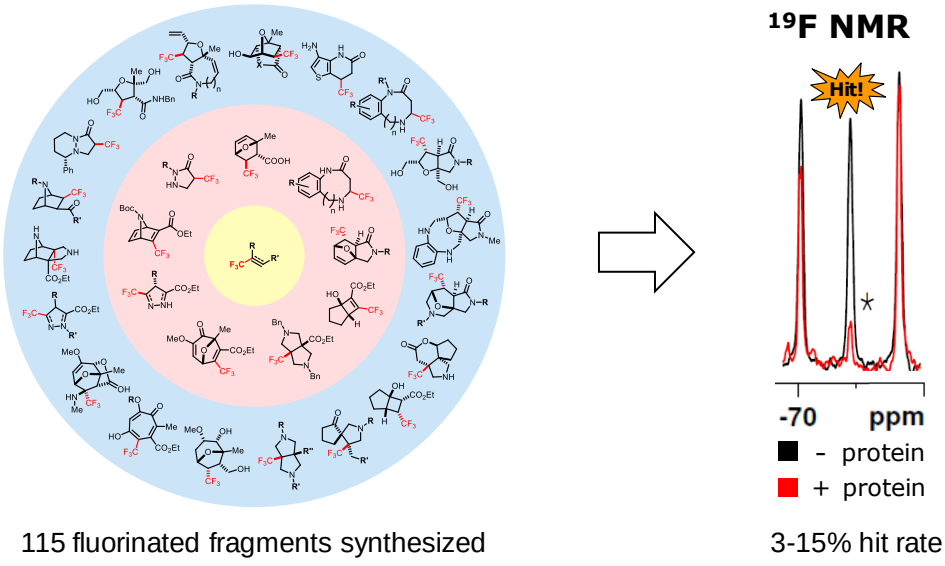

Figure 2.28. Synthesis of the fluorinated Fsp^3-rich fragment (3F) library (from inside out, representative structures shown). Biological evaluation using ^{19}F NMR against seven protein targets afforded a range of different hits in 3–15% hit rates. Adapted with permission from reference.[1] Copyright (2020) John Wiley and Sons.

2.7. Future Perspectives

Having demonstrated the usefulness of the 3F library in obtaining new hit compounds, continued screening is currently ongoing. After publication of the herein described results, a series of additional protein targets have been screened and more are planned in the near future. While the 3F library can be used on its own, it would be advantageous to combine it with additional fluorinated fragments, *e.g.* from commercial sources, to expand the number and diversity of one's library. Furthermore, it would be highly interesting to compare properties and hit rates of hits obtained from different fragment collections under identical screening conditions.

Another interesting approach involves the use of fluorinated hits as spy molecules in subsequent FAXS experiments. These spy screens enable screening of non-labeled molecules in search of additional hits (see Figure 1.7). At the time of writing, this approach has been successfully adopted to p38γ using **2.170** as spy molecule. The screening is currently ongoing but almost 100 non-fluorinated fragments have been screened with new fragment hits already identified.

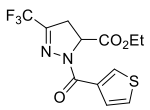

2.170

Hit-to-lead progression of the fragment hits is a natural next step in this project and efforts towards obtaining crystal structures for some of the proteins is currently ongoing. Such information will enable structure-guided design of new ligands and will be a tremendous aid for future medicinal chemistry.

The most important and labor intensive part of hit-to-lead optimization is often synthesis of new analogues. Thus, while waiting for crystal structures it may be advantageous to begin exploring further synthesis of new analogues – either by exploiting available handles or *via* synthesis using other starting materials or building blocks. In particular, synthesis of non-fluorinated analogues are desirable in order to evaluate whether or not fluorine participates in any binding interactions or simply behaves as a reporter tag. If the latter is the case, this position can then be used as a point for further derivatization. However, due to the strong electron withdrawing effect of the CF_3-group, synthesis of non-fluorinated analogues is expected to be more difficult as the starting materials will be less electrophilic.

At the time of writing, initial steps towards synthesis of non-fluorinated analogues of p38γ hits have been initiated (Scheme 2.75). Starting from crotonic acid (**2.233**), Michael addition with 2-aminobenzylamine followed by a HATU-mediated intramolecular amidation and Boc-protection afforded the eight-membered **2.234** in 76% yield over two steps. The [5+2] cycloaddition-based core scaffold has also been synthesized without fluorine. Reacting alkyne **2.236** with oxopyrrylium ylide **2.102** as previously described afforded **2.237** in 29% yield. As expected, a lower yield was observed when using a less activated alkyne. Finally, attempts to synthesize the furan-based Diels-Alder scaffold has been done with both acid **2.233** and acrylate **2.239**. Regrettably, even in the presence of different Lewis acids at elevated temperatures no reaction between 2-methylfuran and either starting material was observed. However, other Lewis acids such as $AlCl_3$ or $SnCl_4$ are still to be tested.

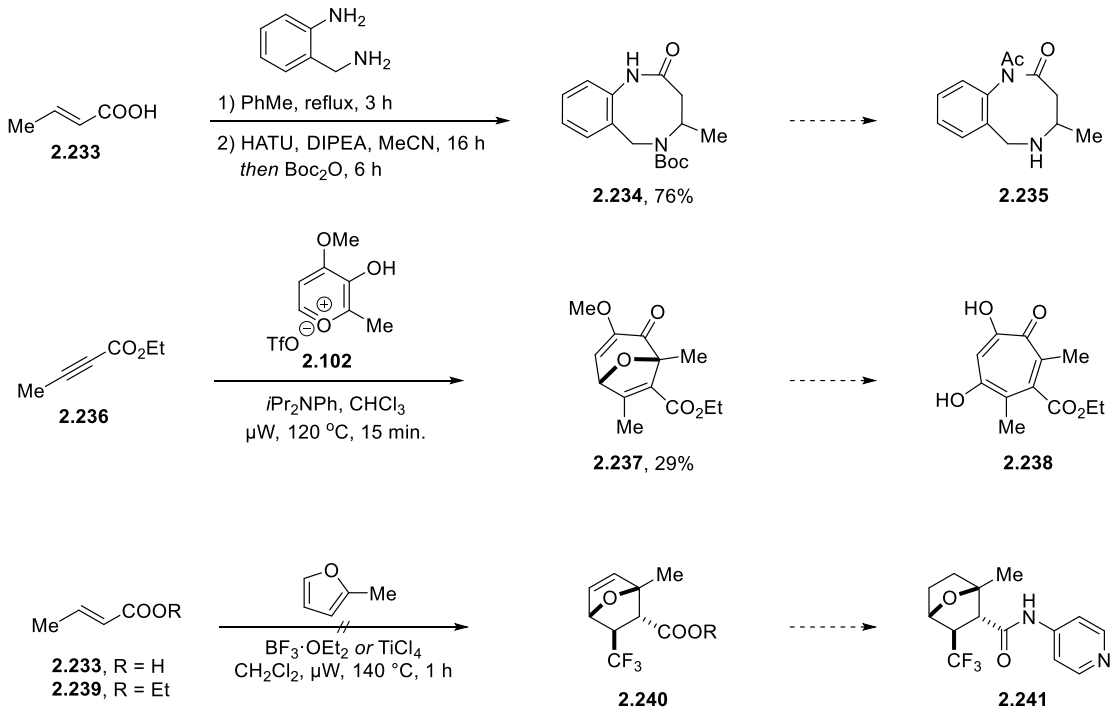

Scheme 2.75. Initial steps towards synthesis of non-fluorinated p38γ hits.

Finally, as part of future hit-to-lead campaigns, enantioselective synthesis of the fragment hits should also be investigated so individual enantiomers may be tested. Although much progress in asymmetric reactions has been accomplished including Diels-Alder reactions,[294,295] various cycloadditions including [5+2] and [3+2],[296,297] and aza-Michael additions,[298] this will likely be a challenging task that will require significant optimization. The use of chiral HPLC may be used as an alternative approach for the separation of enantiomers.

Part III

Fsp^3-rich and Diverse Fragments Inspired by Natural Products as a Collection to Enhance Fragment-Based Drug Discovery

3.1. Project Outline

The experimental work carried out for Part III of this thesis was conducted at the University of Cambridge under supervision of Professor David R. Spring. The project was part of an ongoing campaign to synthesize structurally diverse, Fsp^3-rich, and natural product-like fragments for FBDD.

An efficient strategy to install complexity and three-dimensionality into small molecules is the incorporation of quaternary centers. In particular all-carbon quaternary stereocenters are of significant interest for their metabolic stability[299,300] and ubiquitous presence in natural products (Figure 3.1).[301] Unfortunately, such entities are heavily underrepresented in most screening collections and their synthesis remains a challenge due to their conformational restrictions and congested nature.[302,303]

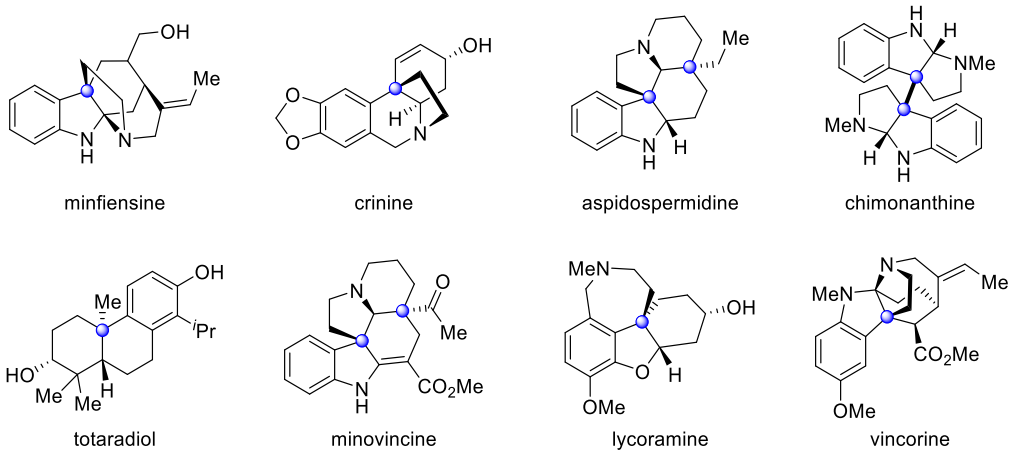

Figure 3.1. A selection of natural products with all-carbon quaternary stereocenters.[301]

Relying on the incorporation of an all-carbon quaternary stereocenter to enhance three-dimensionality and natural product-likeness of fragments, a DOS strategy was designed around the building block **3.1**. (Figure 3.2). The stereochemical-rich and densely functionalized nature of this building block would serve as an excellent starting point for a divergent synthetic scheme. Furthermore, the synthetic importance of such 3-hydroxy-2,2-disubstituted-cyclopentan-1-ones has previously been demonstrated in the total synthesis of several natural products including many terpenoids (Figure 3.2).[304–306]

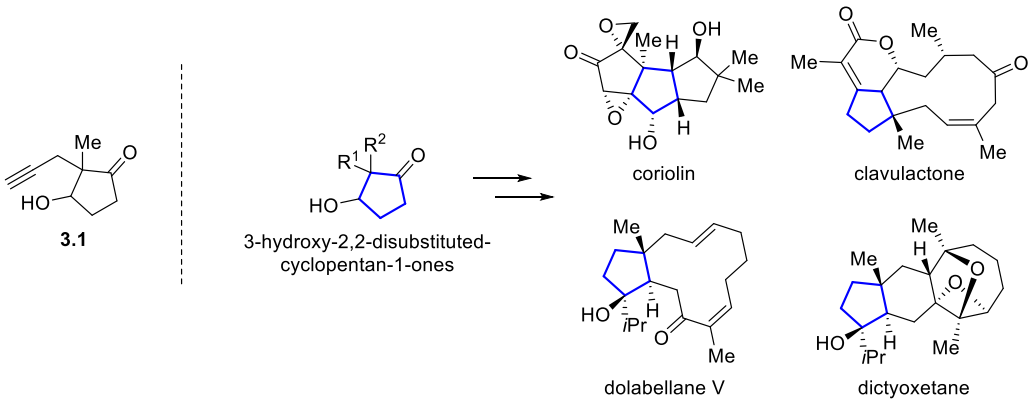

Figure 3.2. The densely functionalized **3.1** was selected as the central building block for this DOS campaign. Numerous natural products have been synthesized from such 3-hydroxy-2,2-disubstituted-cyclopentan-1-one building blocks.[304–306]

Initial work on this project had focused on the synthesis of building block **3.1** as its two diastereomers, *syn*-**3.1** and *anti*-**3.1**,[viii] and had been accomplished in two steps from **3.2** (Scheme 3.1). A diastereomeric ratio of 62:38 in favor of *syn* had been observed during reductive desymmetrization of **3.3**.

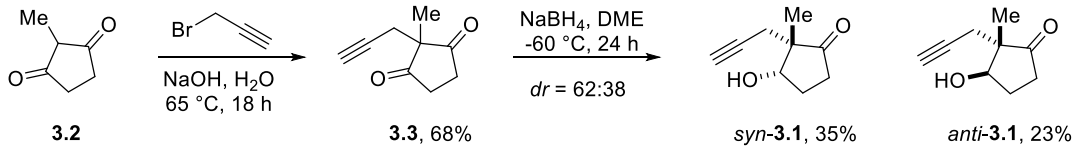

Scheme 3.1. Synthesis of the central building blocks.

Based on *syn*-**3.1** and *anti*-**3.1**, early progress had afforded a number of new fragments (Scheme 3.2). Work had primarily been centered around the alcohol and alkyne handles of the *syn* building block aiming to perform various cyclizations. Investigation into several promising fragment intermediates had also been undertaken with synthesis of α,β-unsaturated **3.4** and amide **3.19**. Unfortunately, attempts to perform Diels-Alder reactions on **3.4** had failed. Amide **3.19** had been transformed into bicyclic **3.20** but its subsequent deprotection had proven difficult.

To exemplify the versatility of the targeted approach, six-membered versions of the building blocks, *syn*- and *anti*-**3.23**, had also been prepared in a similar fashion (Scheme 3.2). Building block *syn*-**3.23** had then been subjected to a series of similar reactions to demonstrate its

[viii] *syn*/*anti* refers to the stereochemical relationship between the alkyne and hydroxyl groups

compatibility with the library methodology. This afforded fragments **3.24**, **3.25**, and **3.26** in similar yields to what had been observed for the corresponding five-membered derivatives.

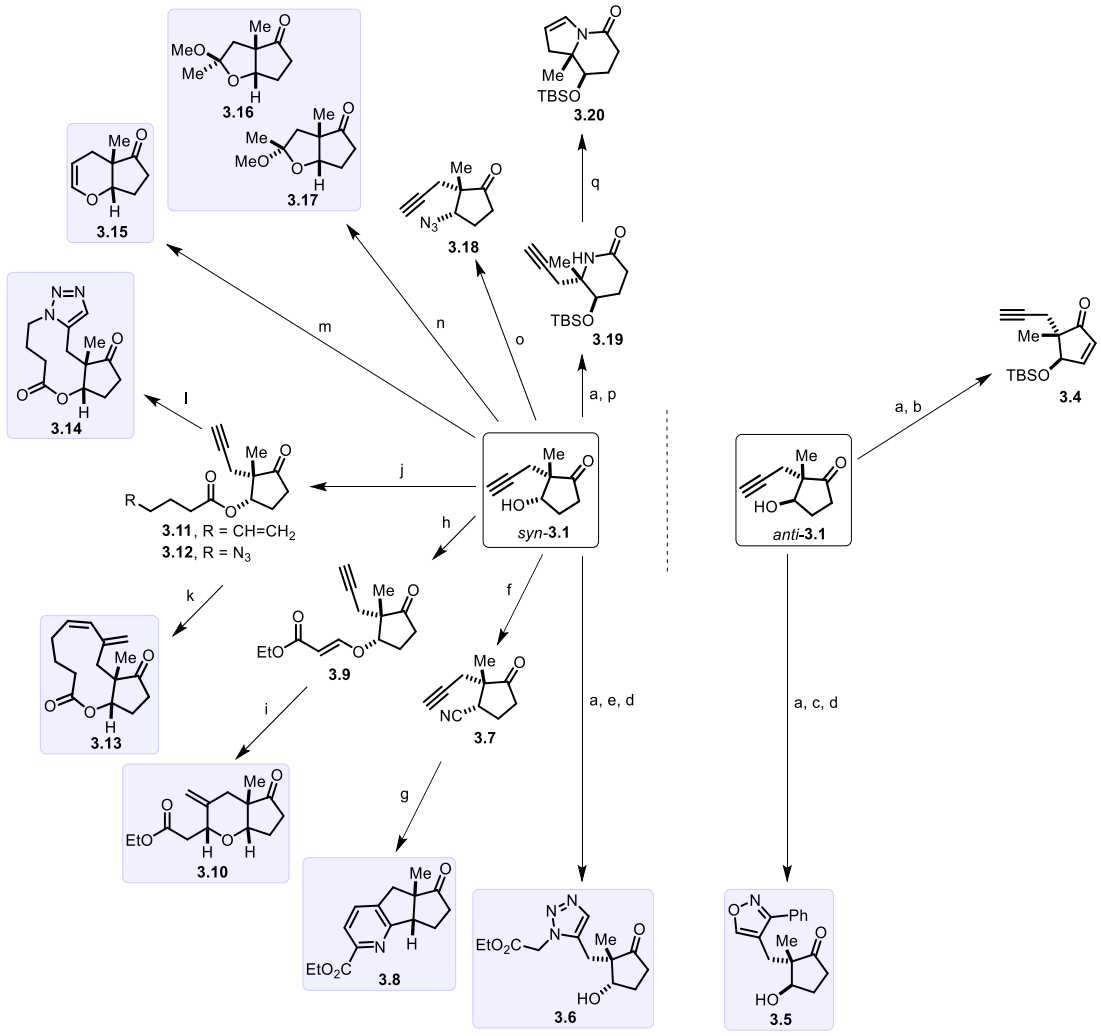

Scheme 3.2. Library overview at the beginning of this project. Final fragments highlighted with blue. Reagents and conditions: (**a**) TBSCl, DMF, 16 h, 95–98%; (**b**) IBX, PhF, DMSO, 65 °C, 24 h, 45%; (**c**) α-chlorobenzaldoxime, Et_3N, DCE, 80 °C, 24 h, 77%; (**d**) TBAF, AcOH, THF, 5 days, 76–80%; (**e**) ethyl azidoacetate, $[Cp^*RuCl]_4$, PhMe, 18 h, 86%; (**f**) MsCl, pyridine, 24 h, *then* KCN, DMSO, 5 days, 60%; (**g**) $CpCo(CO)_2$, ethyl propiolate, PhMe, reflux, 18 h, 10%; (**h**) ethyl propiolate, NMM, CH_2Cl_2, 2 h, 93%; (**i**) Bu_3SnH, AIBN, PhMe, 80 °C, 12 h, *then* *p*-TsOH, CH_2Cl_2, 2 h, 59%; (**j**) RCOOH, DCC, DMAP, CH_2Cl_2, 16 h, **3.11** (91%), **3.12** (84%); (**k**) Grubbs II, ethylene, PhMe, reflux, 16 h, 83%; (**l**) Cp*RuCl(cod), PhMe, reflux, 24 h, 88%; (**m**) NHS, $^tBu_4NPF_6$, $NaHCO_3$, PPh_3, $CpRu(PPh_3)_2Cl$, DMF, 80 °C, 56 h, 65%; (**n**) $[Ir(cod)Cl]_2$, MeOH, 4 h, **3.16** (18%), **3.17** (58%); (**o**) *i*. MsCl, pyridine, 2 h *ii*. NaN_3, DMSO, 85 °C, 24 h, 63%; (**p**) *o*-(mesitylenesulfonyl)hydroxylamine, CH_2Cl_2, 18 h, *then* $BF_3{\cdot}OEt_2$, 1 h, 66%; (**q**) *i*. $InCl_3$, DIBALH, Et_3B, I_2, THF, -78 °C, 5 h *ii*. Cs_2CO_3, CuI, *N*,*N*'-dimethylethyl-1,2-diamine, PhMe, 85 °C, 3 h, 64%. Adapted from reference[307] with permission from The Royal Society of Chemistry.

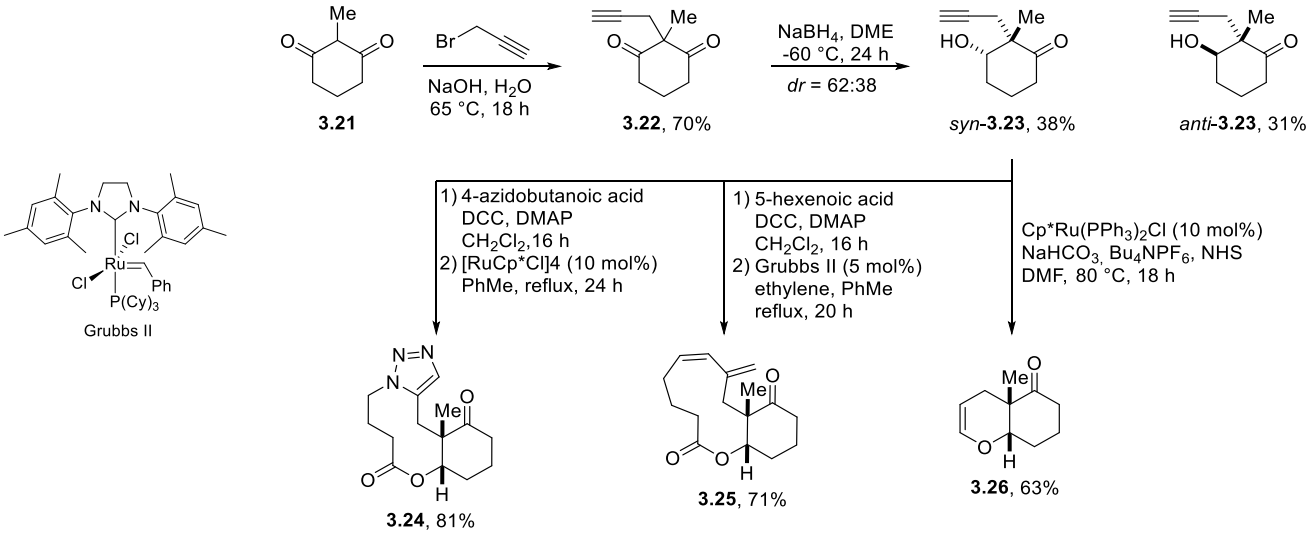

Scheme 3.3. To demonstrate the utility of the synthetic approach, the six-membered building blocks *syn*- and *anti*-**3.23** had been synthesized. The former had been subjected to a series of reactions to show its compatibility with the chemistry used on the five-membered building block.

The aim of this project was to finish the initiated library through investigation of the remaining building block handles. In particular, modification of the ketone and the non-substituted 'right-hand side' of the building blocks was targeted (Figure 3.3). Further work on both the α,β-unsaturated **3.4** and amide **3.19** was also to be carried out. Ideally, the synthesized fragments should contain multiple handles for potential hit optimization, exhibit high degrees of Fsp^3 and 3D character, and be of high natural product-likeness. Introduction of additional nitrogen atoms was also desired to further increase the diversity of the library. To further underline the versatility of the methodology, building blocks carrying a different substituent than a methyl group were to be synthesized. Finally, all fragments should be synthesized in a maximum of five steps from the building blocks and generally cohere to the Ro3 guidelines.

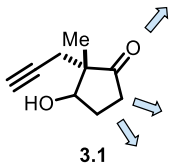

Figure 3.3. Library expansion was planned primarily *via* manipulation of three main handles (blue arrows).

3.2. Library Synthesis

The following chapter has been divided into four sub-chapters dealing with the building block synthesis, synthesis of fragments from the *syn*-**3.1** and from *anti*-**3.1**, respectively, and finally synthesis of a new set of building block derivatives.

3.2.1. Building Block Synthesis

Following the developed procedure, *syn*-**3.1** and *anti*-**3.1** were synthesized in two steps from commercially available cyclopentanedione **3.3** (Scheme 3.4). Alkylation of **3.3** with propargyl bromide proceeded smoothly to give **3.3** in an improved yield of 88%. Reductive desymmetrization was then accomplished with subequimolar amounts of $NaBH_4$ (0.6 equiv.) at -60 °C to minimize diol formation. Not surprisingly, hydride attack proceeded predominantly from the least sterically hindered face (*dr* = 62:38) to afford *syn*-**3.1** and *anti*-**3.1** in 38% and 27% yield, respectively. To enable a wider range of reactions, TBS protection of the two building block hydroxyl groups was accomplished with TBSCl in quantitative yields (Scheme 3.4).

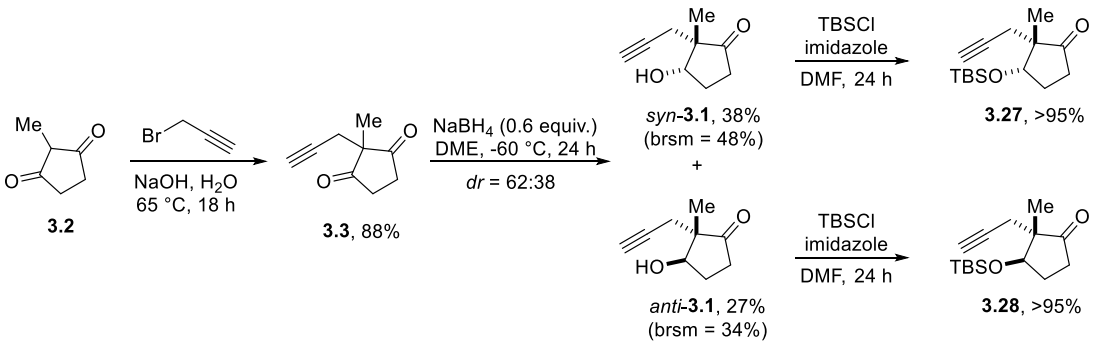

Scheme 3.4. Synthesis of the *syn* and *anti* building blocks in slightly improved yields.

3.2.2. *Anti* Building Block Chemistry

Fragments based on the *anti* building block were all synthesized from the TBS protected building block **3.28** as the alcohol was not used for cyclizations.

Grignard Reaction

With little chemistry performed on the ketone, a Grignard reaction[242] was initially investigated. Gratifyingly, reacting **3.28** with allylmagnesium bromide afforded the desired diastereomer **3.29** as the major product in 62% yield (Scheme 3.5).

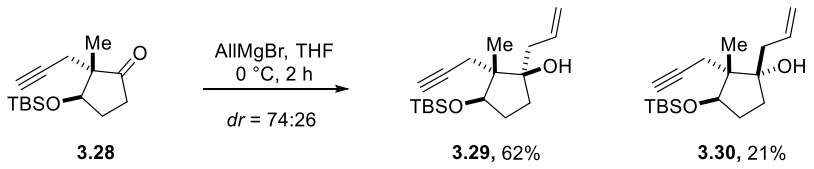

3.28 **3.29**, 62% **3.30**, 21%

Scheme 3.5. Diastereoselective Grignard reaction with allylmagnesium bromide.

With **3.29** in hand, two ring-closing reactions were carried out (Scheme 3.6). Ring-closing enyne metathesis (RCEYM) using Grubbs II catalyst under an ethylene atmosphere successfully formed a [5,6]-bicyclic scaffold. Subsequent TBS deprotection with TBAF afforded **3.31** in 66% yield over two steps. Alternatively, performing an intramolecular Pauson-Khand reaction[308,309] with NMO as a promoter led to formation of a tricyclic scaffold. Following TBS deprotection, the tricyclic diastereomers **3.32** and **3.33** were isolated in 42% and 17% yield, respectively, over two steps. Direct TBS deprotection of **3.29** afforded diol **3.34** in 87% yield. In an effort to access spirocyclic fragments, derivatization of the tertiary alcohol of **3.29** was also attempted. However, both acylation and alkylation reactions failed due to lack of conversion (Scheme 3.6).

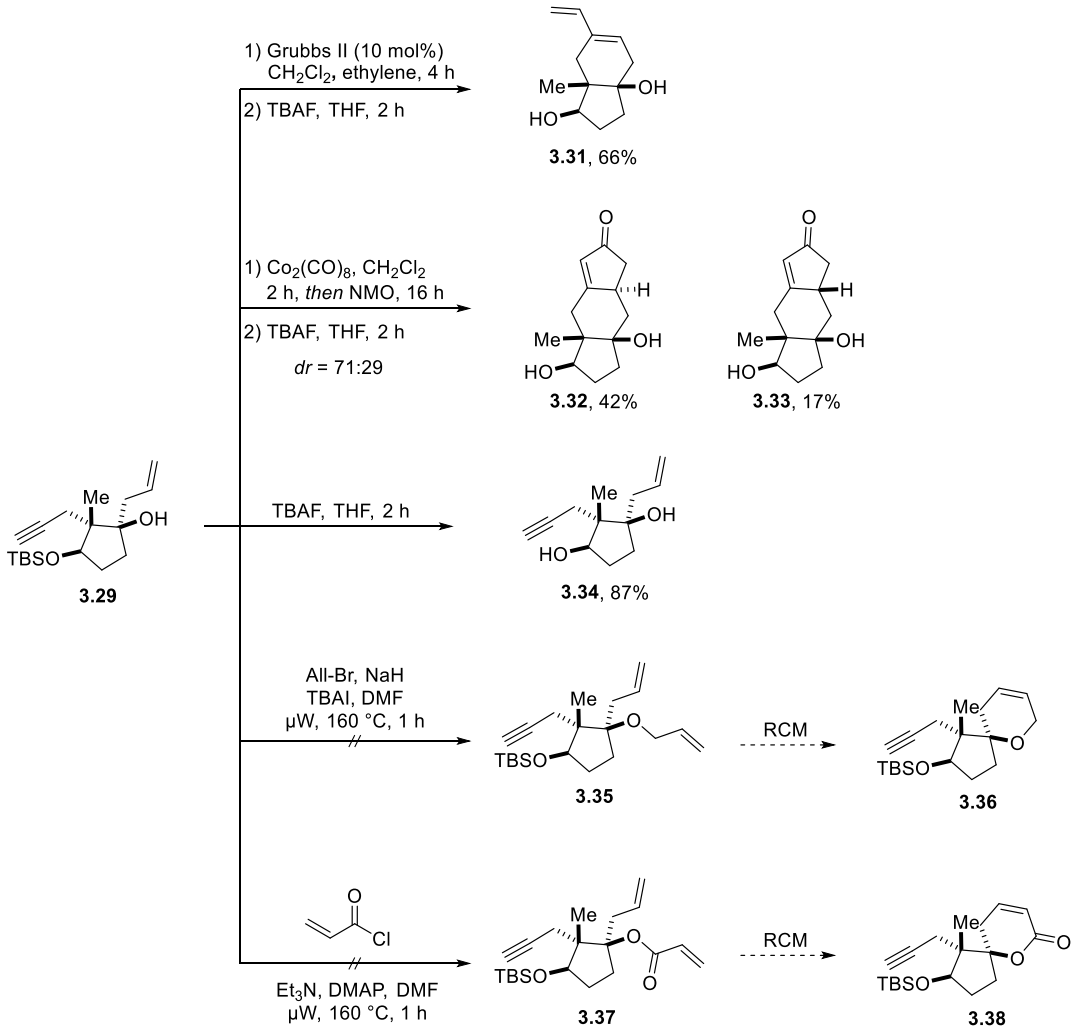

Scheme 3.6. Reactions carried out on Grignard reaction product **3.29**.

In an attempt to synthesize larger bi- and tricyclic ring systems, the Grignard reaction was repeated using 3-butenylmagnesium bromide (Scheme 3.7). However, even in the presence of the Lewis acid $CeCl_3$ the reaction turned into a complex mixture – likely a result of various side reactions arising from the significantly lower reactivity of this non-allylic Grignard reagent.[310]

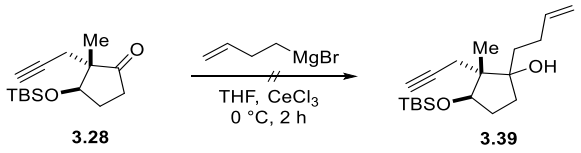

Scheme 3.7. Attempted Grignard reaction using 3-butenylmagnesium bromide.

α,β–Unsaturation

Looking to functionalize the 'right-hand side' of the building block, approaches to afford an α,β-unsaturated system were investigated. α-Methylenation was successfully performed *via* a microwave-assisted one-pot Mannich reaction–deamination cascade.[311,312] Reacting **3.28** with excess Et_2NH (12 equiv.) and CH_2Br_2 (6 equiv.) using microwave heating afforded α,β-unsaturated **3.40** in 68% yield (Scheme 3.8).

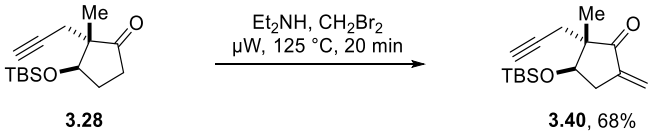

3.28 **3.40**, 68%

Scheme 3.8. α-Methylenation of the ketone using a microwave-assisted one-pot Mannich reaction–deamination cascade.

Exploiting the reactivity of the formed α,β-unsaturated system, several [3+2] cycloadditions were carried out to form spirocyclic compounds (Scheme 3.9). Reacting **3.40** with chloro-oxime **3.41** afforded **3.42** in 70% yield with excellent diastereo-, chemo-, and regioselectivity. Similar to the Grignard reaction, the reaction occurred primarily on the 'bottom-face' of the ring to give the stereochemistry shown. No cycloaddition with the alkyne or formation of regioisomers were observed. Removal of the TBS ether with TBAF gave **3.43** in a modest 44% yield and was attributed to degradation of the dihydroisoxazole moiety.

5,5-dimethyl-1-pyrroline *N*-oxide (DMPO)

In a similar fashion, the commercially available nitrone DMPO was reacted with **3.40** to afford **3.44** as the major product (unknown stereochemistry) in 53% yield (Scheme 3.9). However, as TBS deprotection with TBAF yielded an impure product, this route was abandoned.

Instead, **3.40** was set up to undergo another [3+2] cycloaddition with azomethine ylide precursor **2.92**. This reaction proceeded with lower diastereoselectivity than observed for the chloro-oxime reaction but allowed for the isolation of both diastereomers in 61% and 32% yield, respectively (**3.46** and **3.47**). Subsequent TBS deprotection afforded **3.48** and **3.49** in high yields. Aiming to increase the Fsp^3 of the library, debenzylation and alkyne reduction was then accomplished by catalytic hydrogenation to give **3.50** and **3.51**, both in quantitative yields (Scheme 3.9).

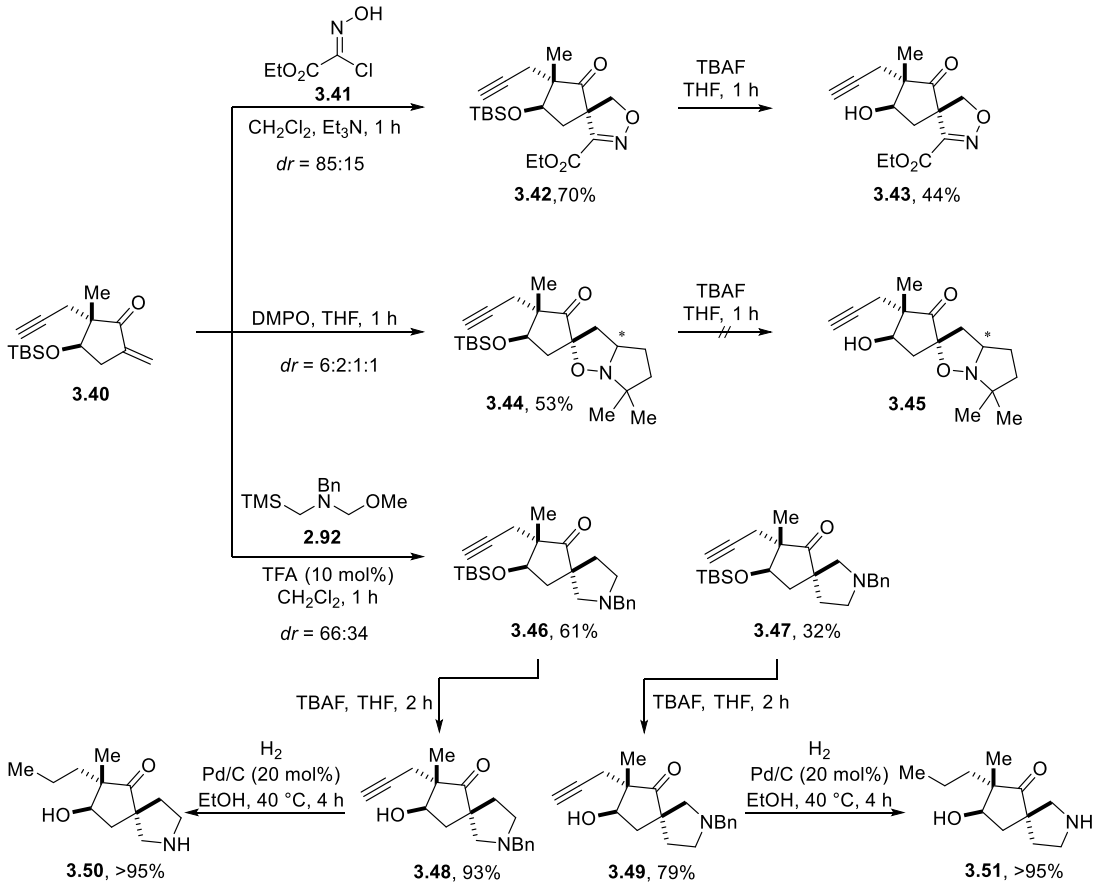

Scheme 3.9. Synthesis of spirocyclic fragments.

Three other cycloadditions were also attempted on **3.40** (Scheme 3.10). Reaction with ethyl diazoacetate resulted in a complex mixture, while **3.40** failed to undergo Diels-Alder reactions with either Danishefsky's diene[313] or furan.

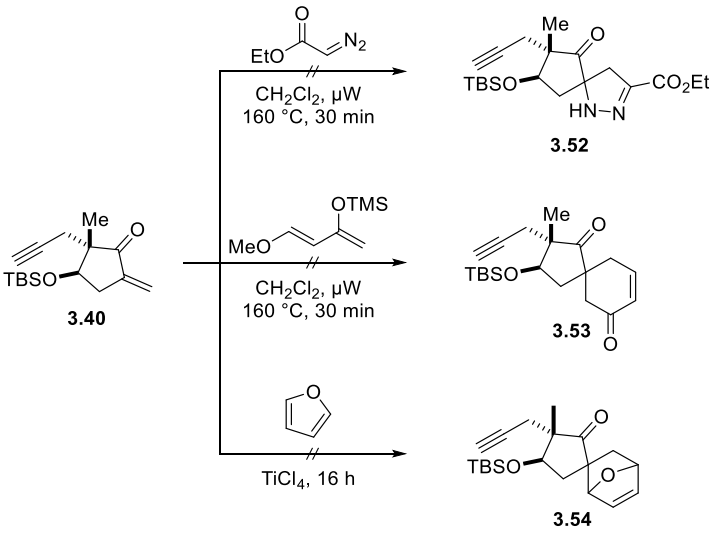

Scheme 3.10. Failed cycloadditions.

In addition to the described cycloadditions, a series of Michael addition–condensation cascade reactions were attempted (Scheme 3.11). While the reaction between **3.40** and hydrazine afforded a complex mixture, reactions with thiourea or benzene-1,2-diamine both led to cyclized products (**3.56** and **3.58**, respectively) in moderate yields, albeit as ~1:1 diastereomeric mixtures. Unfortunately, TBS deprotection of both **3.56** and **3.58** failed to produce any isolatable products, possibly due to instability of the C=N bonds. Finally, a Michael addition with sodium azide was attempted with the intention of performing a subsequent intramolecular ruthenium-catalyzed azide alkyne cycloaddition (RuAAC).[314] However, no Michael addition products were observed and instead intermolecular cycloaddition with the alkyne occurred at elevated temperatures (Scheme 3.11).

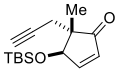

3.4

Another approach to obtain derivatization of the 'right-hand side' of the building block involved the introduction of an *endo*-cyclic α,β-unsaturated alkene. This approach had previously been investigated by synthesis of **3.4** (Scheme 3.2). However, this intermediate had failed to undergo subsequent Diels-Alder reactions.

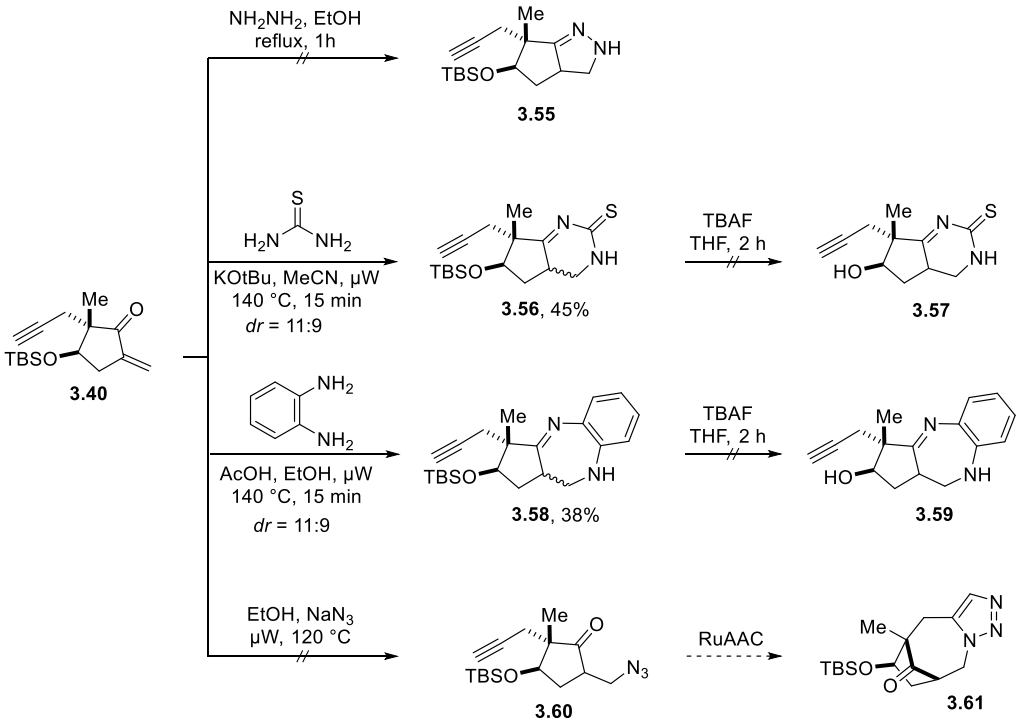

Scheme 3.11. Michael addition–cyclization reactions.

Thus, in an effort to synthesize fragments from **3.4**, this intermediate was resynthesized using IBX in a two solvent system (Scheme 3.12).[315] Similar to previous experience, only partial conversion of **3.28** was achieved even with a large excess of IBX. Increasing the temperature further than 70 °C led to formation of several byproducts. Furthermore, as separation of **3.4** from unreacted **3.28** was challenging, crude **3.4** was reacted directly with azomethine ylide precursor **2.92**. Gratifyingly, the two resulting diastereomers were easily separable and afforded **3.62** and **3.63** in 12% and 10% yield, respectively, over two steps. Subsequent TBS deprotections with TBAF afforded **3.64** and **3.65** in high yields. One attempt to hydrogenate each of the two bicyclic fragments was performed but both resulted in formation of impure products.

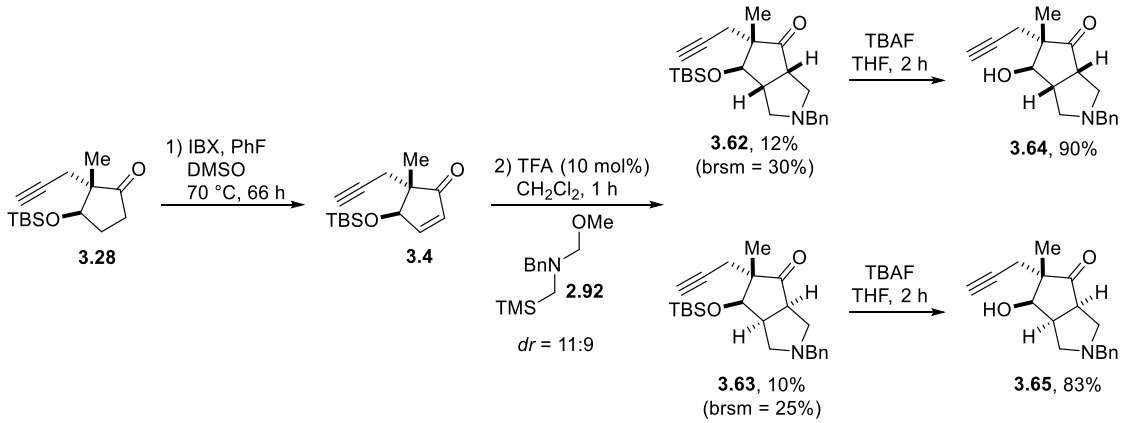

Scheme 3.12. IBX-mediated α,β-unsaturation followed by a [3+2] cycloaddition.

α–Allylation

Next, a bridged bicyclic fragment was targeted *via* α-allylation of **3.28** and subsequent RCEYM. Unexpectedly, alkylation using LDA and allyl bromide occurred primarily on the 'top-face' of **3.28** and afforded the undesired '*anti*' diastereomer as the major product in an inseparable mixture of diastereomers (Table 3.1, entry 1). Furthermore, full conversion of **3.28** was not achieved as diallylated product was also formed. Thus, different bases and conditions were screened to improve the yield and selectivity. While the use of NaH, NaHMDS, and KHMDS predominantly led to formation of dialkylated **3.67** (Table 3.1, entries 2, 4, and 5), LiHMDS successfully produced the desired *syn*-**3.66** as the major product in a decent yield (Table 3.1, entry 3).

Table 3.1. α-Allylation of **3.28**.

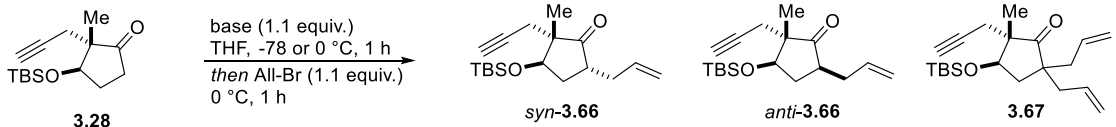

Entry	Base	Temp. (°C)	Major product	*dr* (*syn*/*anti*)[a]	Yield (%)[b]
1	LDA	-78	*anti*-**3.66**	33:67	30
2	NaH	0	**3.67**[c]	ND	38
3	LiHMDS	-78	*syn*-**3.66**	72:28	62
4	NaHMDS	-78	**3.67**[c]	ND	ND
5	KHMDS	-78	**3.67**[c]	ND	ND

[a] alkyne–alkene stereochemical relationship; [b] diastereomers were inseparable; [c] estimation by TLC/ LC-MS

In a final attempt to improve the synthesis of *syn*-**3.66**, α-methylene **3.40** was subjected to conjugate addition conditions using organocopper chemistry. The organocopper reagent was generated *in situ* from vinylmagnesium bromide and CuI and then reacted with **3.40** to form **3.66** in 89% yield (Scheme 3.13). However, with a *dr* of 3:1 in favor of the undesired *anti* diastereomer, this route was abandoned.

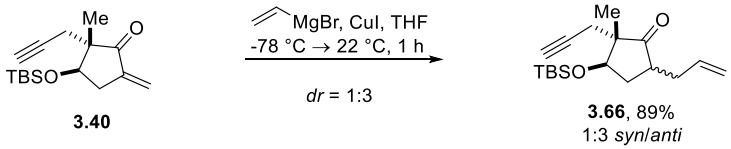

Scheme 3.13. Organocopper-mediated conjugate addition to **3.40**.

Continuing with the LiHMDS procedure (Table 3.1, entry 3), subsequent RCEYM successfully ring-closed *syn*-**3.66** to form a bridged bicyclic scaffold. Following TBS deprotection, fragment **3.68** was isolated from the non-cyclized byproducts in 33% yield over two steps (Scheme 3.14). The low yield was in part due to incomplete conversion of the ethylene-enyne cross metathesis intermediate **3.69**, however, attempts to remove excess ethylene gas and push the reaction to completion led to formation of several byproducts.

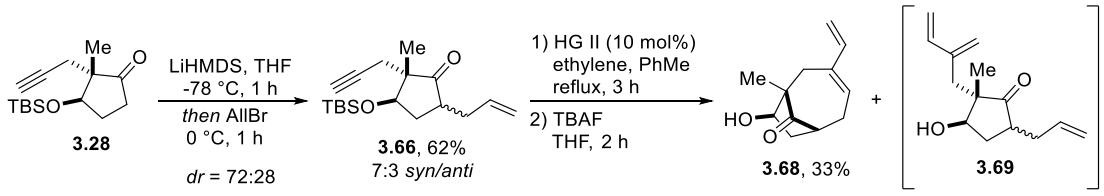

Scheme 3.14. Synthesis of bridged bicyclic fragment **3.68** *via* α-allylation and RCEYM of **3.28**. While full conversion of *syn*/*anti*-**3.66** to the corresponding intermediate *syn*/*anti*-**3.69** was achieved, *syn*-**3.69** did not fully ring-close to **3.68**.

With diallylated product **3.67** synthesized, spirocycle formation *via* RCM was attempted (Scheme 3.15). However, no conversion of **3.67** was observed with Hoveyda-Grubbs II in either refluxing CH_2Cl_2 or PhMe. The reaction was not attempted with ethylene gas.

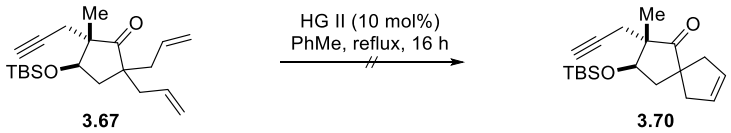

Scheme 3.15. Attempted spirocycle formation by RCM of **3.67**.

Other Reactions

In an effort to access a *cis*-fused [5,4] ring system, a [2+2] cycloaddition was also attempted. TBS-protected **3.28** was transformed into the corresponding silyl enol ether **3.71** with TBSOTf and then reacted with methyl propiolate and a Lewis acid. Unfortunately, neither use of $ZrCl_4$ or $TiCl_4$ facilitated the [2+2] cycloaddition (Scheme 3.16). While $ZrCl_4$ simply returned **3.28**, $TiCl_4$ caused deprotection of both TBS groups.

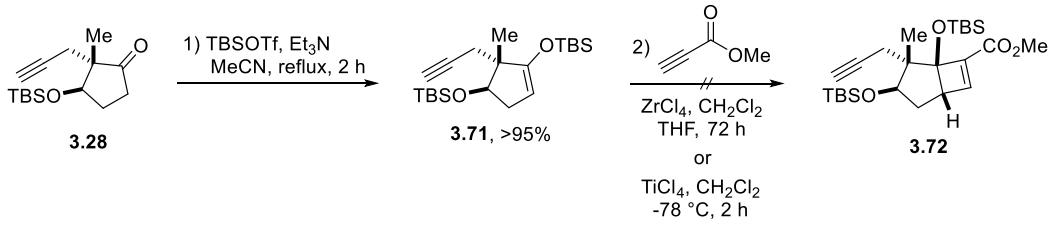

Scheme 3.16. Attempted route to a *cis*-fused [5,4] ring system.

3.2.3. *Syn* Building Block Chemistry

Ring-expansions

Beckmann rearrangement[316,317] and Baeyer-Villiger oxidation[318] (BVO) were envisioned as tools to perform ring-expansions of the building block. Following a previously developed procedure for the Beckmann rearrangement, the bulky aminating reagent *o*-mesitylsulfonylhydroxylamine (**3.74**)[319] was synthesized in 27% yield over two steps from 2-mesitylenesulfonyl chloride. Then, **3.27** underwent a Lewis acid-promoted Beckmann rearrangement with **3.74** to afford lactam **3.19** in 84% yield as an inseparable 4:1 mixture of regioisomers (Scheme 3.17). Fortunately, the isomers were easily separable at later stages.

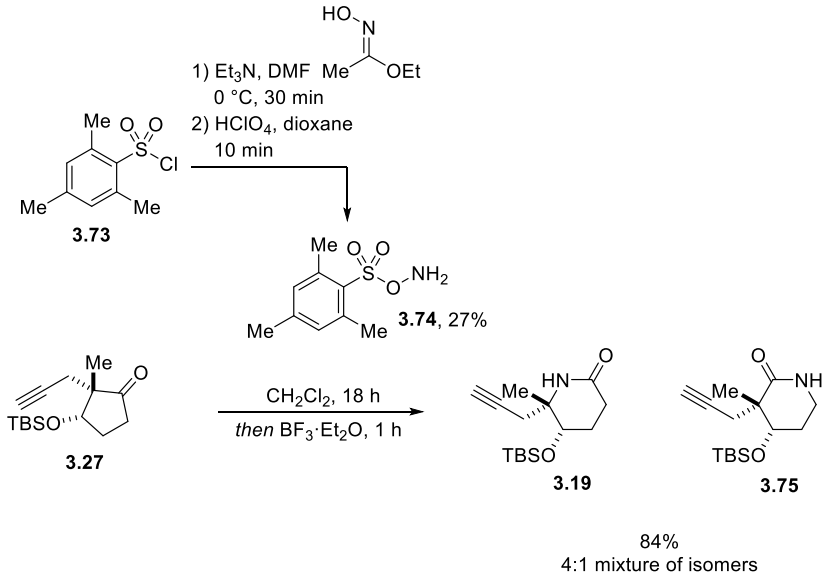

Scheme 3.17. One-pot Beckmann rearrangement.

In a similar fashion, subjecting **3.27** to standard BVO conditions with mCPBA afforded the expected lactone **3.76** in 29% yield after TBS deprotection (Scheme 3.18). Only one isomer was observed in agreement with the superior migratory aptitude of a tertiary substituted carbon atom. The low yield of this reaction was the result of incomplete conversion of **3.27**, however, increasing the temperature by microwave heating resulted in formation of multiple byproducts.

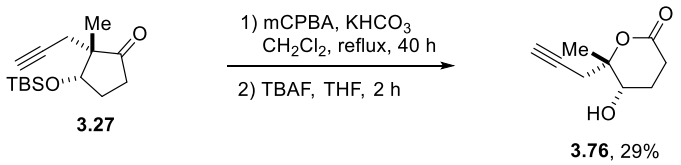

Scheme 3.18. Baeyer-Villiger oxidation.

Looking to exploit the lactam nitrogen for cyclization reactions, two approaches were undertaken. First, a previously performed intramolecular *N*-alkylation was repeated using a two-step procedure *via* a vinyl iodide intermediate.[320] Hydroindiation of the alkyne by *in situ* generated $HInCl_2$ followed by iodine quenching afforded vinyl iodide **3.77**, which was used directly in the next step without purification.[321] Conditions described by Buchwald and co-workers were then employed to facilitate intramolecular vinylation of the lactam to form indolizidinone **3.20** in 73% yield over two steps (Scheme 3.19).[322] Subsequent TBS deprotection afforded fragment **3.78** in excellent yield.

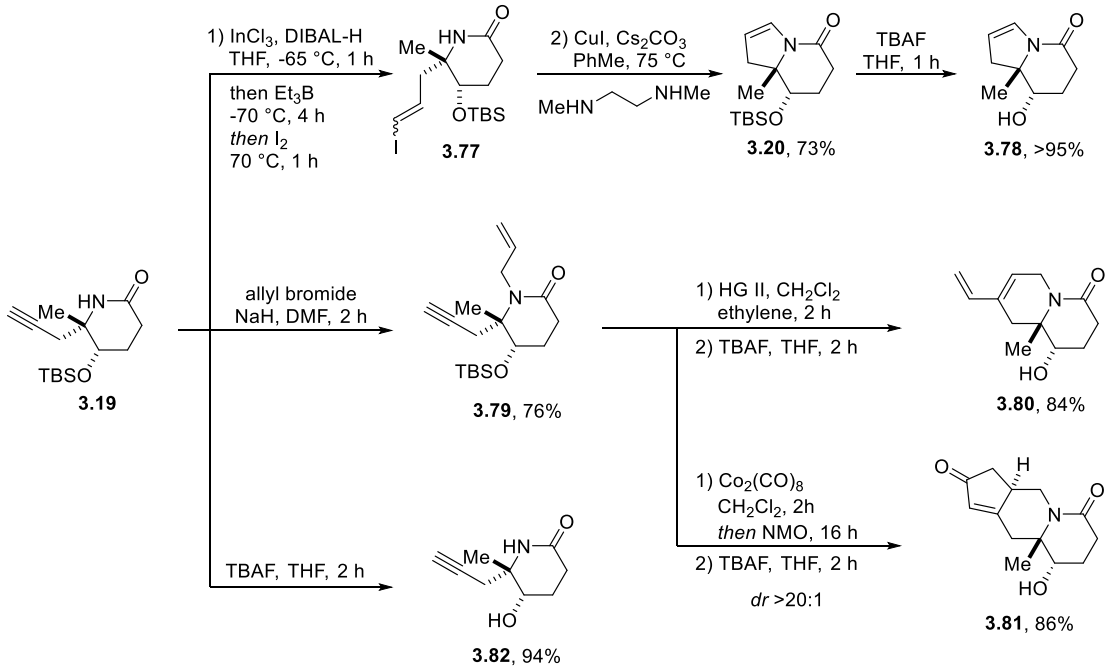

Scheme 3.19. Reactions with lactam **3.19**.

In the second approach, **3.19** was allylated and set up for pairing with the alkyne as previously performed on the Grignard product **3.29**. Allylation with NaH and allyl bromide afforded **3.79** in 76% yield (Scheme 3.19). Then, RCEYM and TBS deprotection formed [6,6]-bicyclic fragment **3.80** in 84% yield over two steps. Compound **3.79** was also subjected to a highly

diastereoselective intramolecular Pauson-Khand reaction which afforded tricyclic fragment **3.81** after TBS deprotection in 86% yield. Finally, to include the simple lactam scaffold in the fragment library as well, TBS deprotection was performed directly on **3.19** to give fragment **3.82** in excellent yield. Regrettably, other attempts to functionalize (*via* acylation or alkylation) the lactam nitrogen of **3.19** failed due to lack of conversion (Scheme 3.20).

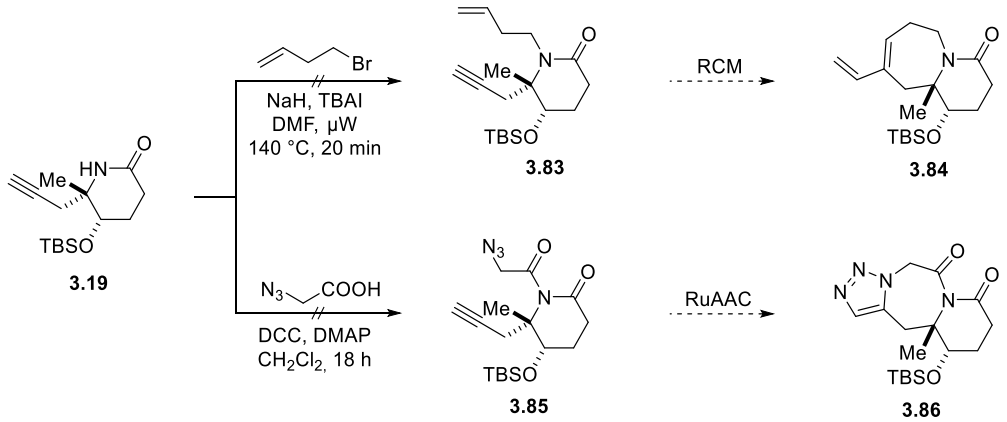

Scheme 3.20. Unsuccessful attempts to functionalize amide **3.19**.

Ketone Chemistry

With one Grignard reaction and different ring-expanding reactions successfully performed on the ketone, additional transformations of the carbonyl were investigated. Reductive amination was considered a natural next step for further derivatization but proved a significant challenge. Using allylamine, imine formation of the sterically hindered ketone was only achieved with microwave heating at 140 °C (Scheme 3.21). Disappointingly, subjecting the imine to reductive conditions resulted in complex mixtures. Several reducing agents were attempted including $NaBH_4$, $NaBH_3CN$, $NaBH(OAc)_3$, and MeMgBr, with the latter two performed in aprotic solvents. Using $NaBH_4$, one byproduct was successfully isolated – bicyclic **3.89** in 15% yield. Thus, side reactions involving the alkyne seemed a likely culprit for the failed approach.

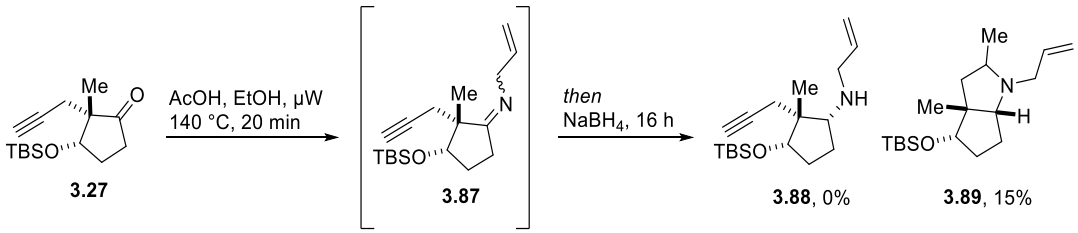

Scheme 3.21. Attempted reductive amination of **3.27**.

Aiming to synthesize additional spirocyclic fragments, **3.27** was subjected to a series of other ketone transforming reactions (Scheme 3.22). Acid-catalyzed acetal formation with ethylene glycol failed without any signs of product formation. Likewise, the ketone remained unreactive towards both Wittig[323–325] and Horner-Wadsworth-Emmons[326–328] reactions even at elevated temperatures. Finally, a reductive cross-coupling with methyl acrylate under SmI_2–^{t}BuOH conditions[329] was attempted but also failed to achieve any conversion.

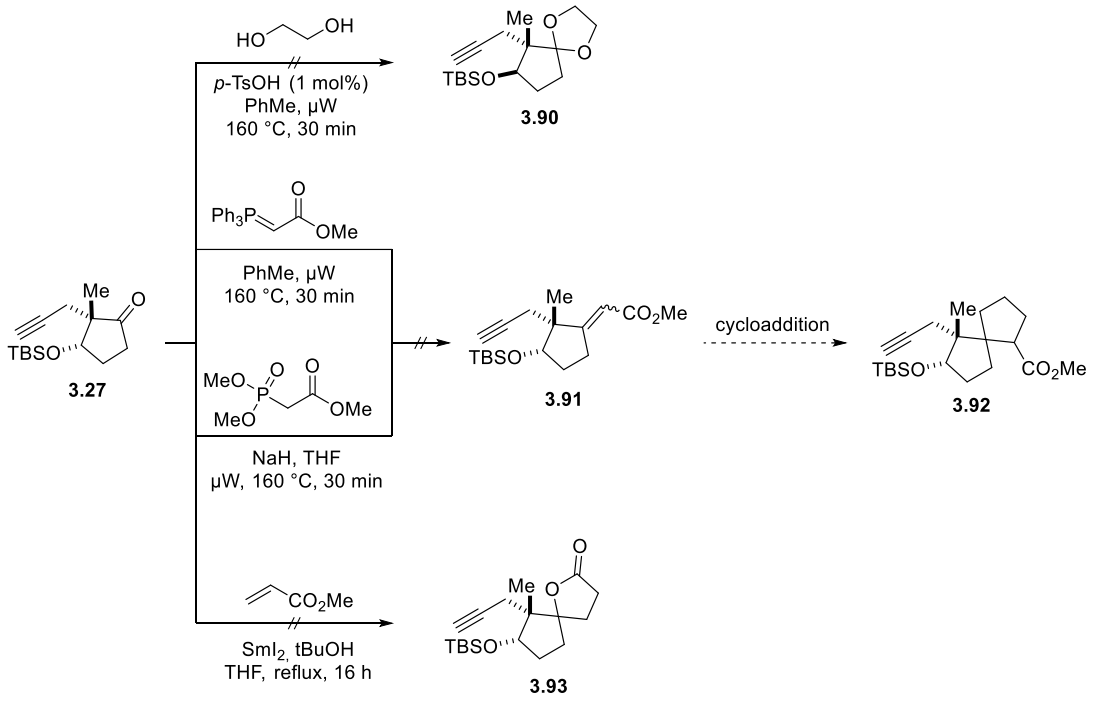

Scheme 3.22. Attempted chemistry to transform the ketone of the *syn* building block.

Alcohol Functionalization

Attention was then directed to the alcohol of unprotected *syn*-**3.1**. While most of the previously synthesized fragments had been prepared *via* derivatization of the alcohol (Scheme 3.2), a few additional experiments were performed. A palladium-catalyzed 5-*exo*-*dig* cyclization was accomplished under a CO atmosphere to give β-alkoxyacrylate **3.94** in 33% yield (Scheme 3.23). The used procedure was designed to minimize formation of acetal byproducts,[330] however, the products **3.94**, **3.16**, and **3.17** were formed in a roughly 1:1:1 ratio. As acetals **3.16** and **3.17** had been previously synthesize they were not isolated. In an attempt to synthesize another spirocyclic fragment, **3.94** was subjected to an azomethine ylide-mediated [3+2] cycloaddition. However, even at elevated temperatures the β-alkoxyacrylate moiety failed to react with the normally very reactive azomethine ylide species.

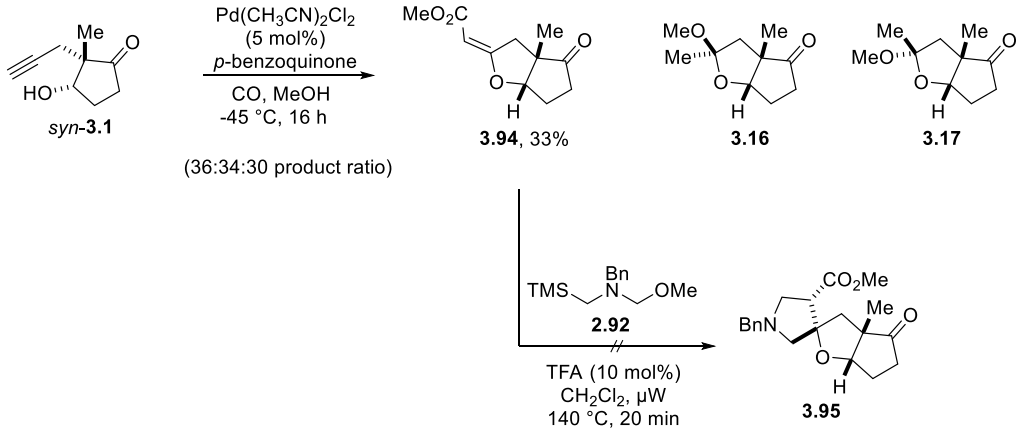

Scheme 3.23. Palladium-catalyzed 5-*exo-dig* cyclization.

Alkylation of the alcohol had previously proven challenging and derivatizations had instead been performed by acylation. Thus, three additional acylations of *syn*-**3.1** were performed using DCC/DMAP coupling conditions (Scheme 3.24). Coupling with acrylic acid afforded **3.96** in 51% while coupling with azide-containing carboxylic acids afforded **3.98** and **3.12** in excellent yields. From **3.96**, RCEYM was envisioned to provide an eight-membered derivative of the previously synthesized 11-membered RCEYM product **3.13**. Unexpectedly, **3.96** underwent a highly diastereoselective tandem enyne cross-metathesis (EYCM)–IMDA reaction to form bridged tricyclic **3.97** in 87% yield. At first glance, the structure of this strained anti-Bredt[331,332] molecule looked unlikely. However, bridgehead double bonds are possible in larger ring systems and are indeed found in many natural products.[333] Furthermore, syntheses of similar bicyclo[5.3.1]undec-7-ene scaffolds *via* EYCM-IMDA sequences have previously been reported.[334,335]

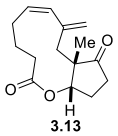

Azide **3.12** had previously been synthesized and subjected to a RuAAC to form the 10-membered ring in **3.14**. Using the same conditions with Cp*RuCl(cod) as catalyst, **3.98** also underwent RuAAC to afford the eight-membered derivative **3.99** in 88% yield (Scheme 3.24). Attempts to form more strained bridged nine- and 11-membered rings (**3.100** and **3.101**, respectively) *via* a copper(I)-catalyzed alkyne azide cycloaddition[336,337] (CuAAC) failed.

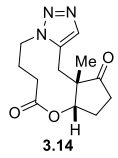

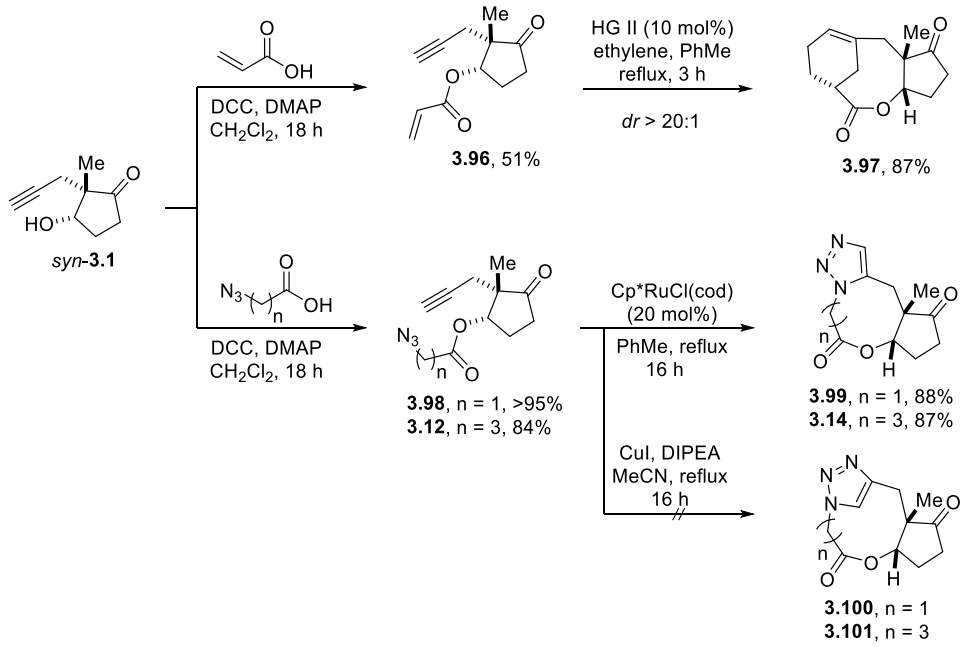

Scheme 3.24. Acylation of *syn*-**3.1** followed by cyclization. Compounds **3.12** and **3.14** were synthesized previously and only shown here for comparison.

Alcohol Substitution

As reductive amination of the ketone had failed, substitution of the alcohol oxygen for a nitrogen-atom was investigated. Previous work on the project had successfully substituted the hydroxyl group with an azide group to form **3.18** *via* a mesylate intermediate (Scheme 3.25). Interestingly, this sequence had proceeded with an overall retention of configuration, which was attributed to a bridged oxetane intermediate (**3.102**) formed *via* reversible azide addition to the ketone.[338]

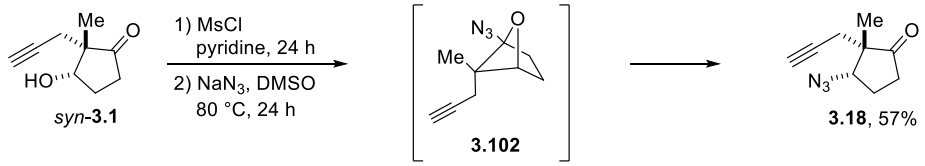

Scheme 3.25. Previous work. Substitution had occurred *via* the proposed oxetane intermediate **3.102** resulting in overall retention of configuration.[338]

With this in mind, mesylation of *syn*-**3.1** was accomplished with MsCl and pyridine followed by attempted substitution with allylamine. Unfortunately, the substitution failed to produce the desired amine **3.103** and instead imine **3.104** (stereochemistry unknown) was formed in 59% yield over two steps (Scheme 3.26). Based on the poor results from earlier attempts to perform reductive amination, this pathway was abandoned. As an alternative approach, resynthesis of **3.18** with NaN_3 was performed in 63% yield. In addition to the substitution reactions, an elimination reaction with DBU was also attempted but resulted in demesylation and an inversion of stereochemistry (Scheme 3.26).

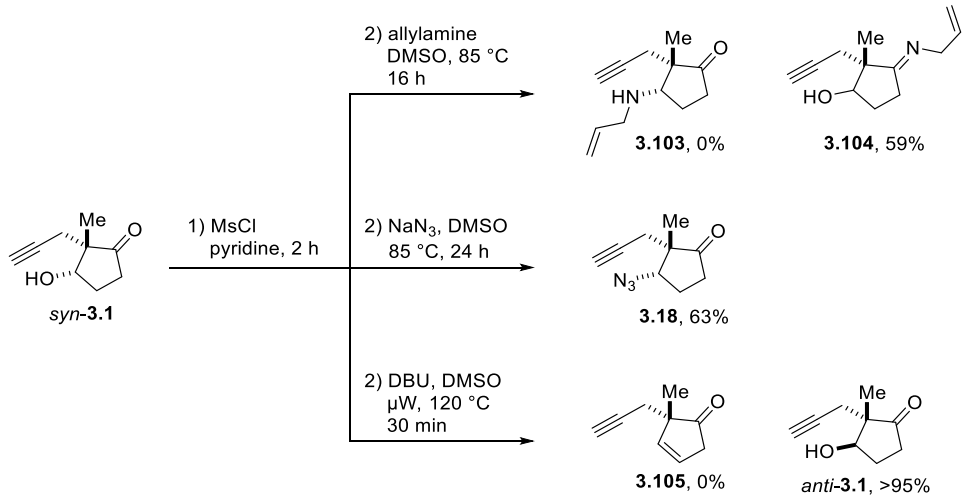

Scheme 3.26. Introduction of an azide *via* mesylation and substitution.

Azide **3.18** was then transformed into the corresponding amine by a Staudinger reaction[339] and then Boc-protected to afford **3.106** in 59% yield (Scheme 3.27). Aiming to create nitrogen-containing ring systems, alkylation of the Boc-protected amine was attempted. Unfortunately, alkylation using NaH failed to produce the desired **3.107** and instead alkylation occurred exclusively alpha to the ketone forming **3.108**. Instead, a gold-catalyzed intramolecular hydroamination was carried out. Inspired by the work of Catalán and co-workers,[340] a 6-*exo*-*dig* cyclization was accomplished using the rather exotic gold catalyst SPhosAu(MeCN)SbF_6 to give **3.109**, although in poor yield. The major product was the hydration product **3.110** (Scheme 3.27).

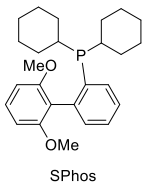

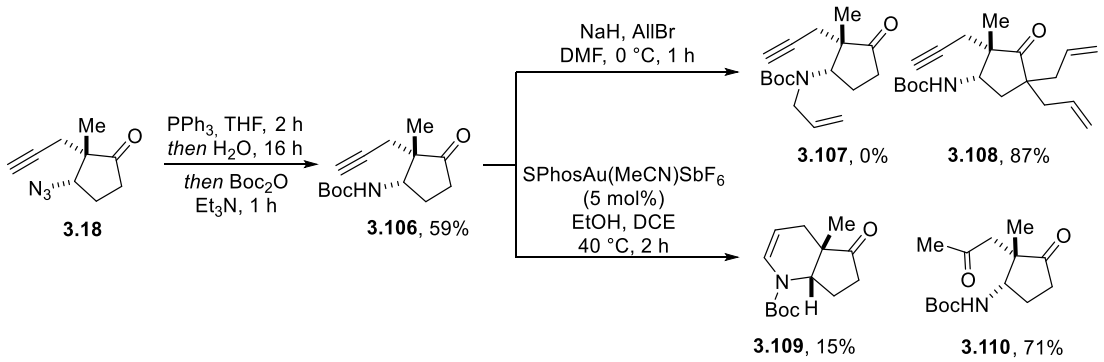

Scheme 3.27. Synthesis of Boc-protected amine **3.106** *via* a Staudinger reaction.

In an attempt to cyclize **3.110**, the amine was Boc deprotected with TFA and subjected to reductive conditions to facilitate intramolecular reductive alkylation (Scheme 3.27). However, no cyclized products were observed.

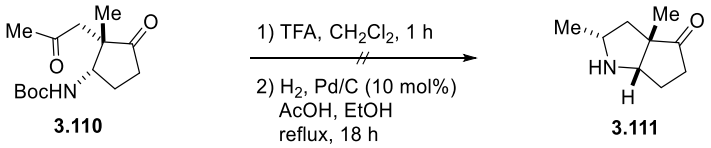

Scheme 3.28. Attempted intramolecular reductive alkylation of **3.110**.

Other reactions

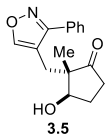

Similar to fragments **3.5** and **3.6** synthesized prior to this project, **3.27** was subjected to a ruthenium-catalyzed [3+2] cycloaddition with chloro-oxime **3.41**. However, the reaction afforded an inseparable mixture of regioisomers and no further attempts to optimize the conditions were carried out.

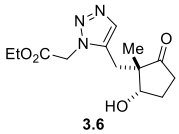

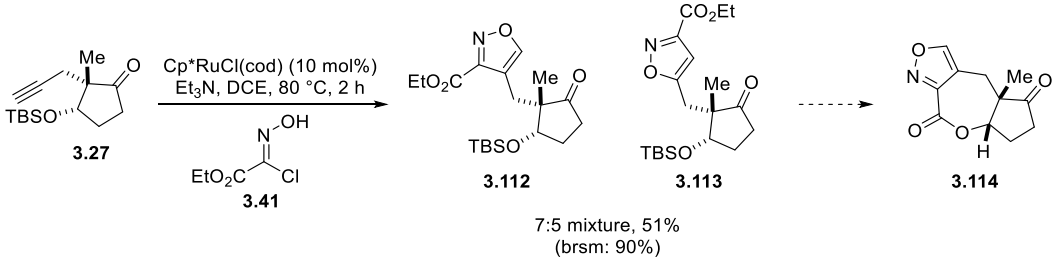

Scheme 3.29. [3+2] cycloaddition on the alkyne of **3.27**.

3.2.4. Building Block Derivatives

To further demonstrate the versatility of this DOS approach, a pair of building block analogues bearing a cyclopropylmethyl group instead of the methyl group were synthesized (Scheme 3.30). From cyclopentane-1,3-dione (**3.115**), the cyclopropylmethyl group was installed using an amino acid-catalyzed olefination–hydrogenation cascade[341] to afford **3.116** in 91% yield. Subsequent alkylation was performed as previously described to give **3.117** in 65% yield. With the increased bulkiness of the methylcyclopropyl group, reductive desymmetrization proceeded with reversed diastereoselectivity and afforded *syn*-**3.118** and *anti*-**3.118** in 19% and 54% yield, respectively.

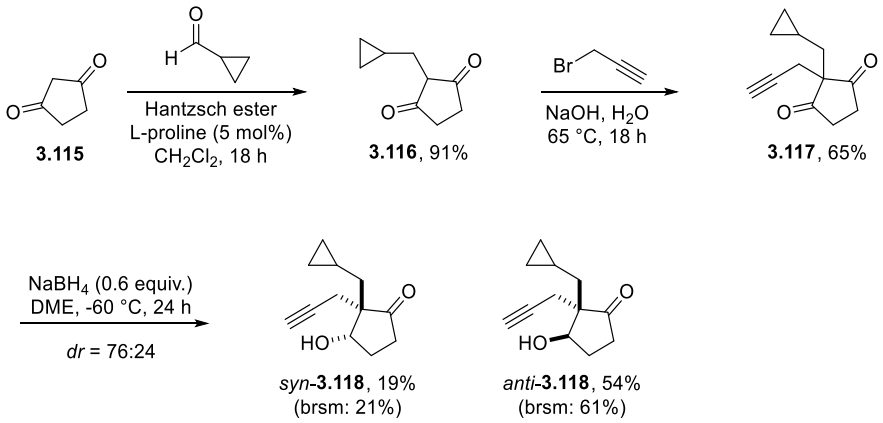

Scheme 3.30. Synthesis of *syn* and *anti* cyclopropylmethyl building block derivatives.

To demonstrate the compatibility of the new building blocks with the developed library strategy, *syn*-**3.118** was subjected to a ruthenium-catalyzed 6-*endo*-*dig* cycloisomerization.[342] This reaction had previously been successfully performed on both *syn*-**3.1** and the six-membered *syn*-**3.23**. Using 10% catalyst loading, dihydropyran **3.119** was obtained in 70% yield, and thus underlining the possibility for further library expansion on this position (Scheme 3.31).

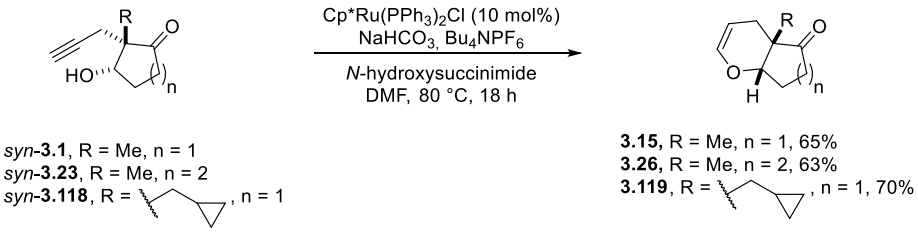

Scheme 3.31. To prove the compatibility of the cyclopropylmethyl building block with the developed synthetic strategy, *syn*-**3.118** was subjected to a 6-*endo*-*dig* cyclization. This reaction had previously been performed on both *syn*-**3.1** and the six-membered *syn*-**3.23** with similar yields.

3.3. Chemoinformatic Library Analysis

A total of 42 fragments (including building block derivatives) were synthesized for this library with 24 new fragments synthesized during this project. In order to create better balance between fragments synthesized from the *syn* and *anti* building blocks, ring-expanded amide fragments **3.19**, **3.78**, **3.80**, **3.81**, and **3.82** were later resynthesized from *anti*-**3.1** by other members of the Spring group (**3.120–3.124**). An overview of the final fragment library, henceforth the "quaternary fragment (QF) library", is depicted in Scheme 3.32.

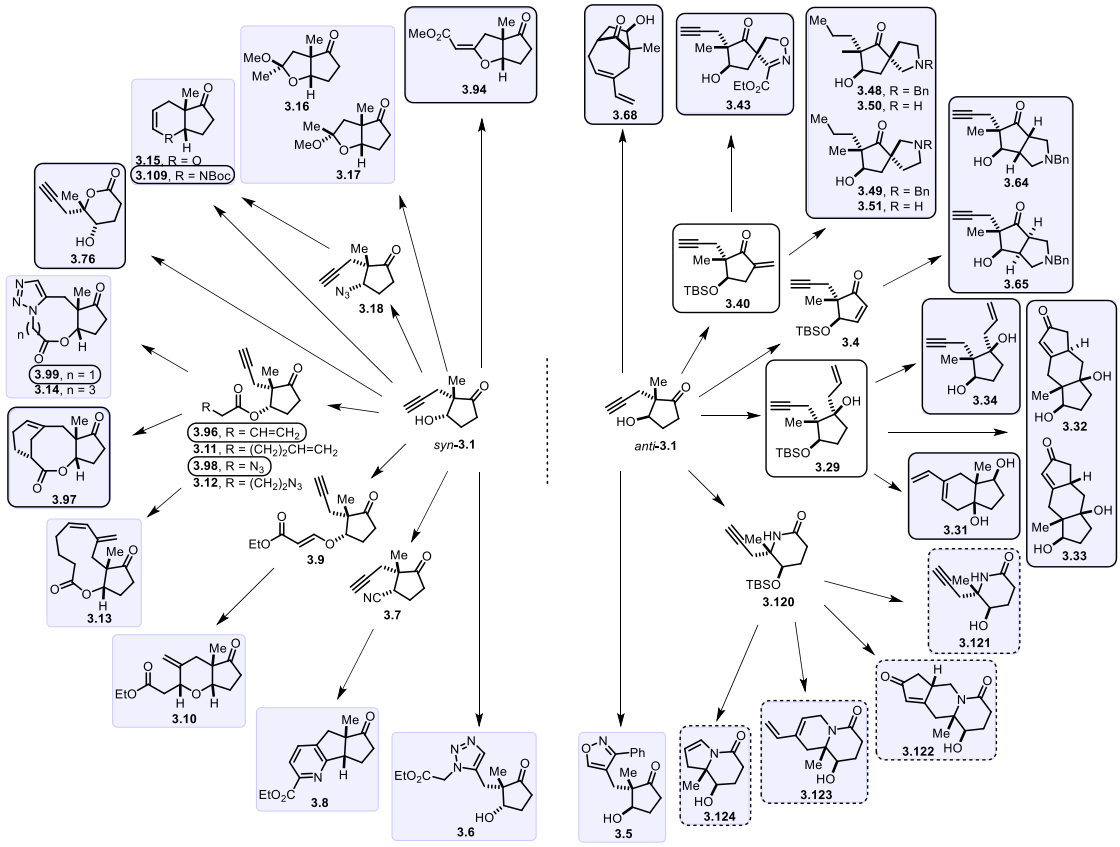

Scheme 3.32. Overview of the quaternary fragment (QF) library. Fragments highlighted by a frame were synthesized during this project. Fragments highlighted by a dashed frame were synthesized as the *syn* diastereomer but were later synthesized in the shown *anti* configuration by other members in the Spring group. Adapted from reference[307] with permission from The Royal Society of Chemistry.

3.3.1. Physicochemical Properties

An overview of calculated physicochemical properties of the QF library and two commercial collections, Maybridge diversity set (2736 fragments) and Life Chemicals 3D fragment library (1376 fragments), is given in Table 3.2. Comparative plots of molecular weight vs. AlogP and distribution of Fsp^3 are provided in Figure 3.4 and Figure 3.5, respectively.

Table 3.2. Average physicochemical properties of the QF library, Maybridge diversity set, and Life Chemicals 3D fragments.

	Ideal range	QF library	Maybridge diversity set	Life Chemicals 3D fragments
MW	<300[a]	215 ± 45	180 ± 39	250 ± 54
AlogP	0–3[a]	1.4 ± 0.9	1.7 ± 0.9	1.1 ± 1.2
HBA	≤3[a]	2.6 ± 0.9	1.4 ± 0.9	2.6 ± 1.1
HBD	≤3[a]	1.1 ± 0.9	0.6 ± 0.7	1.1 ± 1.0
PSA	≤60 $Å^2$[a]	47 ± 15	45 ± 18	62 ± 21
Chiral centers	-	2.6 ± 0.7	0.2 ± 0.6	1.3 ± 0.6
Fsp^3	≥0.47[121]	0.7 ± 0.1	0.3 ± 0.3	0.6 ± 0.2
NP-likeness score[b]	>0[264]	1.2 ± 0.6	-0.6 ± 0.7	-0.4 ± 0.6

[a] Based on the Ro3.[35] [b] compared to a score of 1.1 ± 0.6 for a collection of 2712 natural products. MW = molecular weight; AlogP = atomic partition coefficient; HBA = hydrogen bond acceptors, HBD = hydrogen bond donors; PSA = polar surface area; Fsp^3 = fraction sp^3-hybridized carbon; NP = natural product; green: inside ideal range; yellow: extreme of ideal range; red: outside ideal range.

All three fragment libraries exhibited desirable properties in regards to the Ro3 except for PSA of Life Chemicals' 3D fragments. The QF library showed high Fsp^3 comparable to the Life Chemicals' 3D fragments but significantly higher than the Maybridge diversity set. Importantly, the QF library scored high in natural product-likeness, while both commercial collections were of predominantly synthetic character (*vide infra*).

3.3.2. PMI Analysis

The shape diversity of the synthesized library was evaluated using PMI analysis (Figure 3.6). Similar to the 3F library, the QF library exhibited a good distribution in the plot with a larger degree of three-dimensionality than the commercial collections. While the 3D fragment library from Life Chemicals appeared more three-dimensional than the Maybridge diversity set, these '3D fragments' were still predominantly clustered in the left hand side of the plot. Compared to natural products, the QF library showed a more similar distribution.

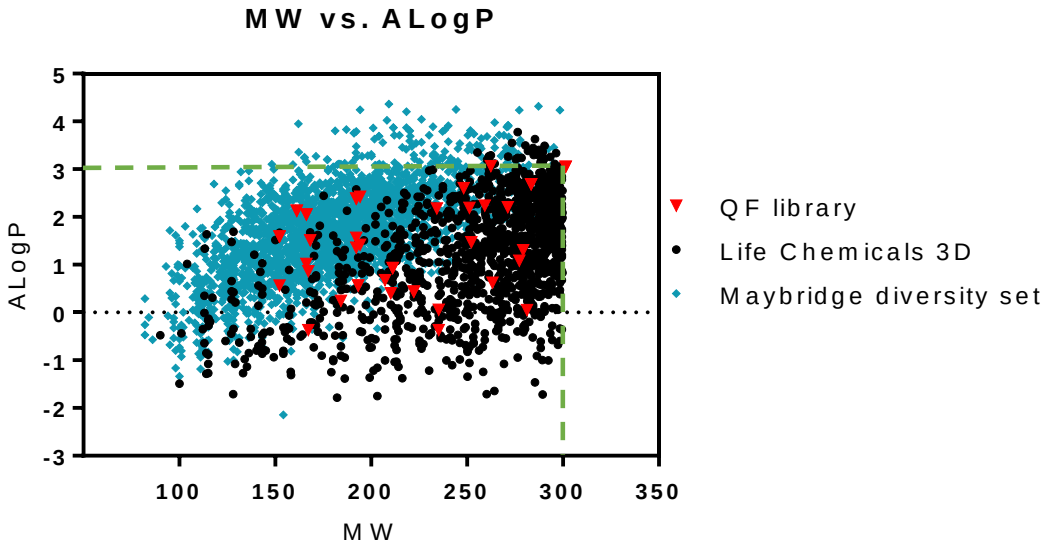

Figure 3.4. Comparison of MW vs. AlogP distributions of the QF library and two collections of commercial fragments (Maybridge diversity set and Life Chemicals 3D fragments). Despite of its small size, the QF library exhibited an excellent distribution in the plot. The green dashed line represents Ro3 space.

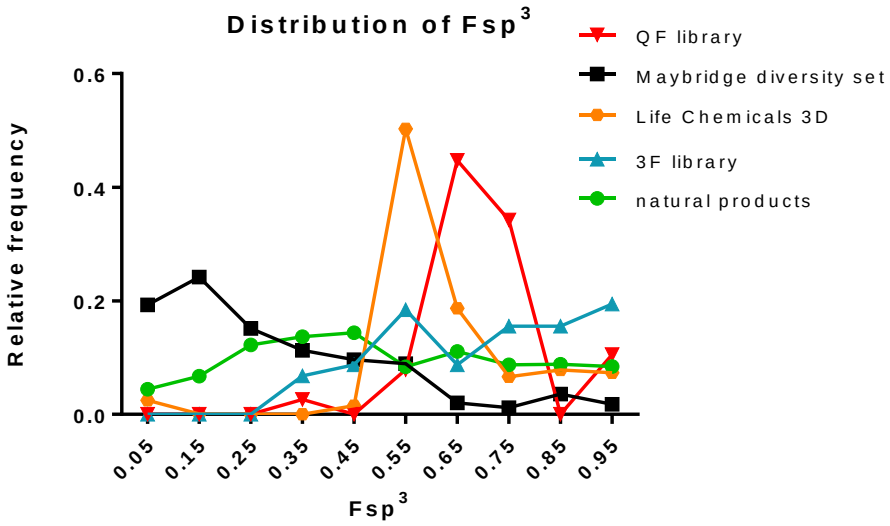

Figure 3.5. Distribution of Fsp^3. The QF library shows a narrow distribution around a high fractions of Fsp^3, similar to the 3D fragments from Life Chemicals. Values are binned in sections of 0.1.

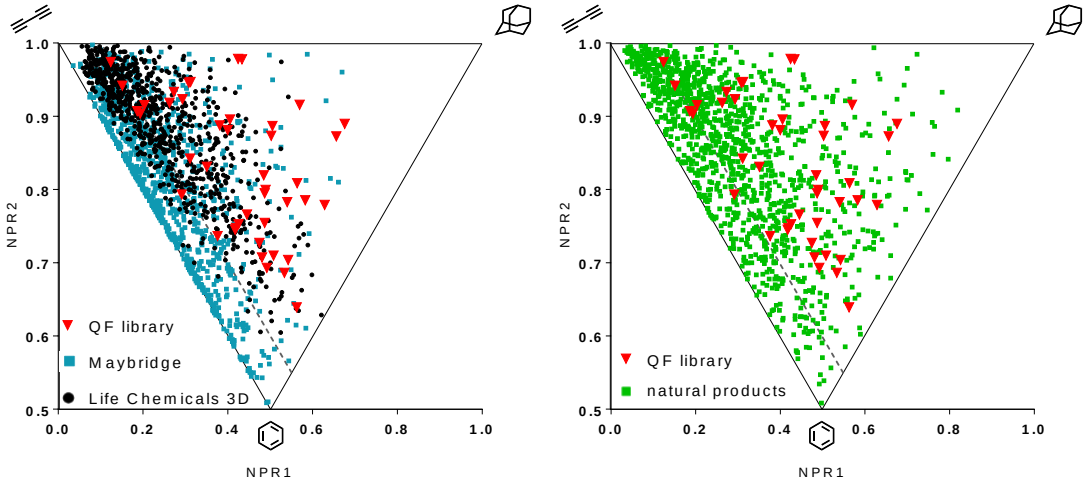

Figure 3.6. PMI analysis of the QF library compared to two commercial fragment libraries (*left*) and a collection of 1356 natural products (NuBBE database,[135] *right*). "Flatland" is situated below the dashed line (NPR1 + NPR2 < 1.1).[118] The three corners of the plot represent three geometrical extremes - rod-like, disc-like, and spherical shapes, respectively. NPR: normalized PMI ratios.[136]

3.3.3. Natural Product-Likeness

The natural product-likeness of the QF library was analyzed using the previously described natural product-likeness scoring system (Section 2.4.2). Satisfyingly, the QF library showed a high degree of natural product-likeness similar to the scoring of a collection of 2712 natural products (Figure 3.7). In contrast to the 3F library and the two commercial collections, the QF library demonstrated significantly higher natural product-likeness.

Interestingly, while the QF library achieved a high NP-likeness score, only few of the synthesized scaffolds were actually found in known natural products. As the core scaffold is an important parameter for biological activity,[108–111] it could be argued that the QF library is actually less natural product-like than the performed analysis indicates. Thus, the fragments could also be classified as belonging to the family of "pseudo-natural products".[343]

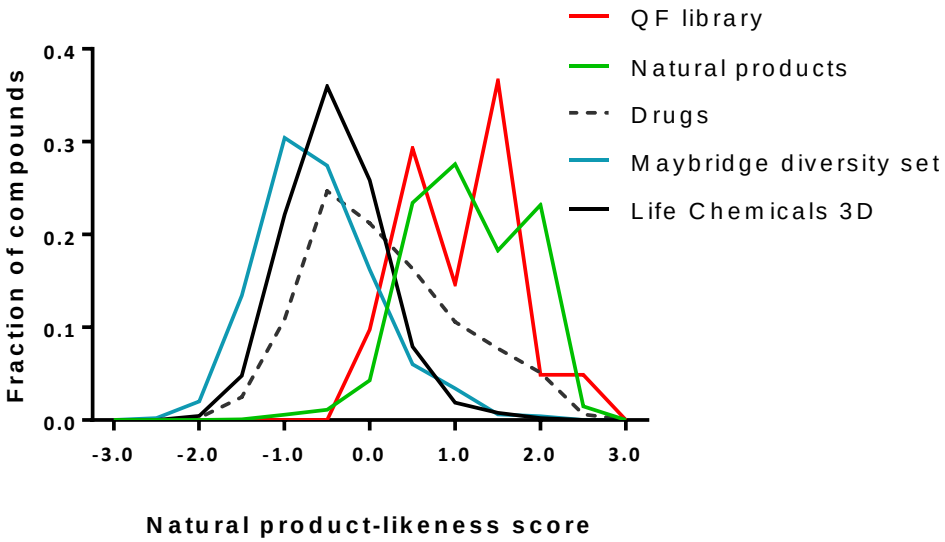

Figure 3.7. Natural product-likeness analysis of the quaternary fragment (QF) library and comparison to other libraries.[265] The NuBBE database of 2712 natural products was used as source for natural products.[135] Logarithmic scale.

3.4. Conclusion

In an effort to further expand the available fragment-like space, a library of diverse fragments inspired by natural products were constructed. Aiming to finalize the initiated quaternary fragment (QF) library, 24 new fragments were synthesized including a pair of new building blocks bearing a cyclopropylmethyl substituent. The majority of the work was based on the *anti* building block to achieve a more even distribution of stereochemistry in the library. To increase the diversity of the collection, 11 new nitrogen-containing fragments had been prepared.

Combined with previous work, an efficient approach to the synthesis of novel fragments bearing all-carbon quaternary centers was developed. In total, 42 structurally diverse and complex fragments based on 22 unique frameworks were synthesized in a maximum of five steps from the central building blocks (Figure 3.8). Fragments were Ro3-compliant and exhibited a high degree of both Fsp^3 and natural product-likeness to address the need of more diverse fragments for screening. Moreover, all fragments contained multiple handles for easier hit-to-lead chemistry. Finally, the versatility of the approach was demonstrated by variation to both ring size and substituent of the building blocks.

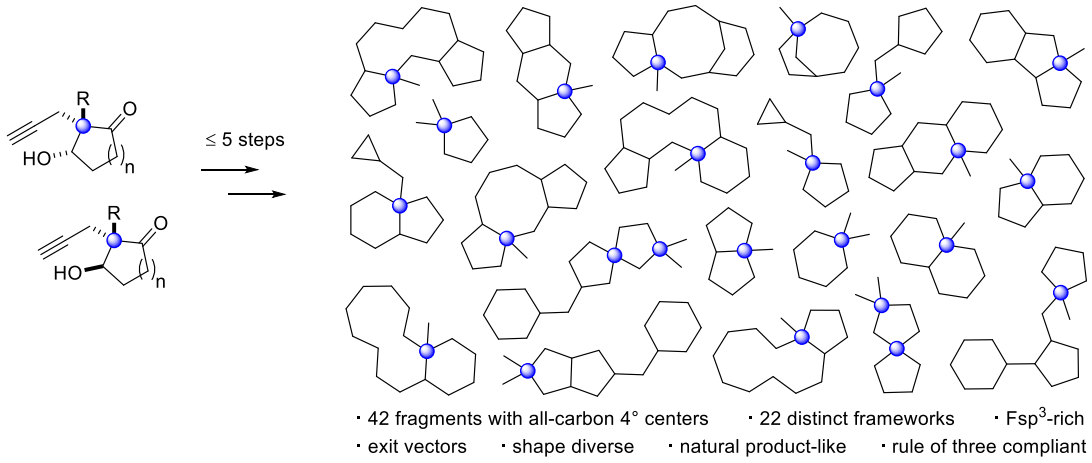

Figure 3.8. Diversity-oriented synthesis of 42 structurally diverse fragments with all-carbon quaternary centers based on 22 distinct frameworks.

3.5. Future Perspectives

Screening of the fragment library is planned in the near future by X-ray crystallography. In the event of finding a hit, it will be important to determine which of the enantiomers are the most potent. Thus, enantioselective reductive desymmetrization of diketone **3.3** should be investigated. Fortunately, asymmetric reduction of ketones has been the focus of much research over the years and a selection of strategies have been developed including enzyme catalyzed reduction, metal-catalyzed transfer hydrogenation, and oxazaborolidine-based reductions (Scheme 3.33).[344–346]

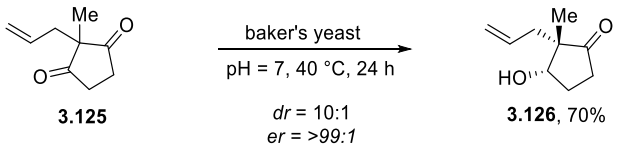

Scheme 3.33. Asymmetric enzyme catalyzed reduction of a 1,3-diketone substrate using baker's yeast.[347]

Although it was considered outside the scope of this library approach, altering the building block substituent to include a functional group (amine, alkene, carbonyl group etc.) could allow for further library expansion. In principle, additional spirocyclic fragments could be obtained by reactions between this substituent and the alkyne. Scheme 3.34 shows a selection of fragments that could potentially be accessed *via* reactions involving an amine-containing substituent.

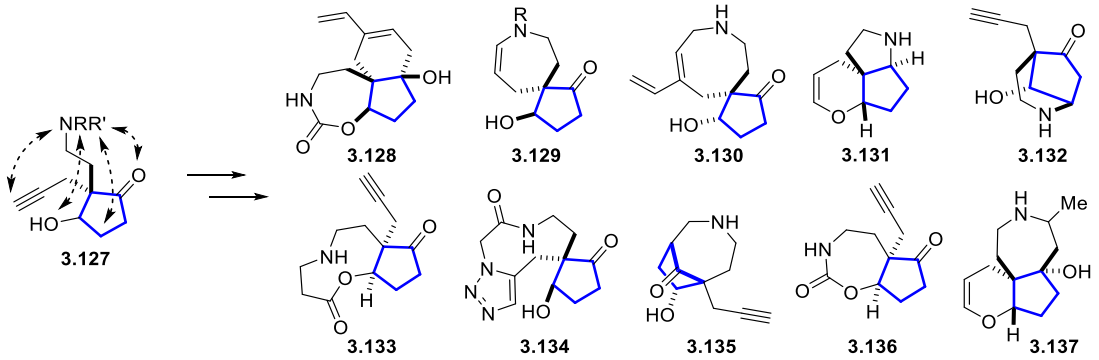

Scheme 3.34. Incorporation of a reactive functionality (*e.g.* an amine) into the substituent position of the building block would potentially allow for further library expansion. The five-membered ring from the building block is highlighted in blue.

Furthermore, it could also be of interest to prepare a set of six-membered nitrogen-containing building blocks, *e.g. syn*- and *anti*-**3.139** (Scheme 3.35). These building blocks would contain another handle for further derivatizations and potentially for additional intramolecular pairing reactions. Synthesis of such building blocks could likely be performed using the same route as described for the methylcyclopropyl substituted *syn*- and *anti*-**3.118**.

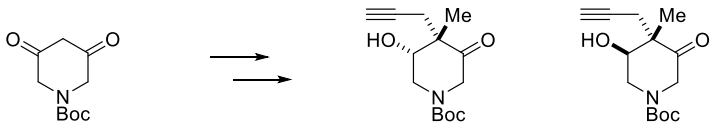

3.138 *syn*-**3.139** *anti*-**3.139**

Scheme 3.35. Six-membered nitrogen-containing building blocks.

Experimentals

4.1. Part II

General (synthesis)

Commercially available reagents were used without further purification and all solvents were of HPLC quality. All fluorinated starting materials were purchased from Fluorochem Ltd. Unless otherwise stated, reactions were carried out as open-system reactions and were monitored by thin layer chromatography (TLC), reversed-phase ultra-performance liquid chromatography mass spectrometry (RP-UPLC-MS), and/or ^{19}F NMR spectroscopy. Analytical TLC was conducted on Merck aluminum sheets covered with silica (C60). The plates were either visualized under UV-light or stained by dipping in a developing agent followed by heating. $KMnO_4$ [3 g in water (300 mL) along with K_2CO_3 (20 g) and 5% aq. NaOH (5 mL)] or ninhydrin [0.1 g in AcOH (0.5 mL) and acetone (100 mL)] were used as developing agents. Flash column chromatography was performed using Merck Geduran® Si 60 (40-63 µm) silica gel. Analytical RP-UPLC-MS (ESI) analysis was performed on a S2 Waters AQUITY RP-UPLC system equipped with a diode array detector using an Thermo Accucore C18 column (d 2.6 µm, 2.1 x 50 mm; column temp: 50 °C; flow: 1.0 mL/min). Eluents A (10 mM NH_4OAc in H_2O) and B (10 mM NH_4OAc in MeCN) were used in a linear gradient (5% B to 100% B) in 2.4 min and then held for 0.1 min at 100% B (total run time: 2.6 min). The LC system was coupled to a SQD mass spectrometer. All new compounds were characterized by ^{1}H NMR, ^{13}C NMR, ^{19}F NMR, IR, HRMS (ESI), and melting point (byproducts were not fully characterized). Preparative RP-HPLC was performed using REVELERIS® Prep Purification System by GRACE equipped with a diode array detector using a C18 column (5 µM; flow: 20 mL/min). Eluents A (H_2O) and B (MeCN) were used in a linear gradient (5% B to 100% B) in 21 min. H-Cube hydrogenation was performed in an H-Cube® Pro by ThalesNano Inc.

NMR data were acquired at 298 K using either a 400 MHz Bruker AVANCE III HD spectrometer equipped with a Prodigy CryoProbe, a 400 MHz Bruker AVANCE II spectrometer equipped with BBFO SmartProbe, a 600 MHz Bruker AVANCE III spectrometer equipped with a Bruker BBFO SmartProbe, or a 800 MHz Bruker AVANCE III HD spectrometer equipped with a TCI CryoProbe. The chemical shifts (δ) are reported in parts per million (ppm) and the coupling constants (*J*) in Hz. For spectra recorded in DMSO-d_6, chemical shifts are reported relative to the signal for DMSO-d_5 (δ 2.50 ppm for ^{1}H NMR and δ 39.52 ppm for ^{13}C NMR). For spectra recorded in $CDCl_3$, chemical shifts are reported relative to the signal for $CHCl_3$ (δ 7.26 ppm for ^{1}H NMR and δ 77.16 ppm for ^{13}C NMR). For spectra recorded in CD_3OD, chemical shifts are reported relative to the signal for CHD_2O(D/H) (δ 3.31 ppm for ^{1}H NMR and δ 49.00 ppm for ^{13}C NMR). For spectra recorded in D_2O, ^{1}H chemical shifts are reported relative to the signal for HDO (δ 4.79 ppm for ^{1}H NMR) and ^{13}C chemical shifts are referenced using the deuterium lock-signal from solvent with δ (TMS) = 0 ppm. ^{19}F chemical

shifts are referenced using the deuterium lock-signal with $\delta(CFCl_3)$ = 0 ppm. Spectrometers were calibrated using $PhCF_3$ as ^{19}F NMR standard with $\delta(CDCl_3)$ = -63.73 ppm. NMR data was analyzed using MestReNova (v11.0.0-17609) by Mestrelab Research S.L.

IR analysis was performed on a Bruker Alpha FT-IR spectrometer. In the reporting of IR, s = strong signal, m = medium signal, w = weak signal, and br. = broad signal. Melting points were obtained using a Stuart SMP30 melting point apparatus and are uncorrected. Analytical LC-HRMS (ESI) analysis was performed on an Agilent 1100 RP-LC system or a Waters Alliance 2695. The Agilent 1100 was equipped with a diode array detector using a Phenomenex Luna C18 column (d 3 µm, 2.1 x 50 mm; column temp: 40 °C; flow: 0.4 mL/min). Eluents A (0.1% HCO_2H in H_2O) and B (0.1% HCO_2H in MeCN) were used in a linear gradient (20% B to 100% B) in a total run time of 15 min. The LC system was coupled to a Micromass LCT orthogonal time-of-flight mass spectrometer equipped with a Lock Mass probe operating in positive electrospray mode. The Waters Alliance 2695 was equipped with a diode array detector without a column. Eluents A (0.1% HCO_2H in H_2O) and B (0.1% HCO_2H in MeCN) were used as a 1:1 mixture in a linear gradient with a total run time of 3 min. The LC system was coupled to a Micromass LCT Premier XE operating in positive electrospray mode.

Data collection for single crystal X-ray crystallography was performed on an Agilent Supernova Diffractometer using CuKα radiation. All crystals were mounted on a glass rod and cooled using an Oxford CryoSystem cooling device. Data were processed and scaled using the *CrysAlisPro* software (Agilent Technologies). The SHELXL-97 programs were used for the solving and refinement of all structures.[348] Hydrogen atoms were kept at ideal positions (at distances 0.96 and 0.86 Å for CH and NH, respectively). Data collection and refinement details may be found in the Supporting Information.

General procedure A – PyBroP amidation

To an ice-cooled solution of carboxylic acid (1 mmol) in anhydrous CH_2Cl_2 (10 mL, 0.1 M), was added PyBroP (559 mg, 1.2 mmol) and DIPEA (0.523 mL, 3 mmol) and the solution was stirred under a N_2 atmosphere for 10 min. Then, amine (1.05 mmol) was added and the reaction was stirred for another 2 h at 22 °C. Sat. aq. $NaHCO_3$ (15 mL) was added and the layers were separated. The aqueous phase was extracted with CH_2Cl_2 (1 × 15 mL) and the combined organic layers were dried over $MgSO_4$, filtered, and concentrated *in vacuo* to give the crude amide product.

General procedure B – HATU amidation

To a solution of carboxylic acid (1 mmol), amine (1.2 mmol), and DIPEA (0.523 mL, 3 mmol) in MeCN (10 mL) was added HATU (475 mg, 1.25 mmol) and the solution was stirred at 22 °C for 2 h. The mixture was concentrated *in vacuo* to give the crude amide.

General procedure C – Reductive amination

To a solution of furfural (911 µL, 1.1 mmol) in ethanol (2.5 mL, 0.4 M) was added amine (1 mmol) and stirred at 22 °C for 1 h. The solution was cooled to 0 °C and added $NaBH_4$ (94.6 mg, 2.50 mmol) portion wise. After stirring 1 h at 0 °C, cooling was removed and the solution was stirred at 22 °C for 16 h. The reaction was concentrated *in vacuo* and 10% aq. K_2CO_3 (2.5 mL) was added. The aqueous phase was extracted with CH_2Cl_2 (3x 3 mL) The combined organic layers were dried over Na_2SO_4 and concentrated *in vacuo*. The crude product was purified by flash column chromatography to give the desired product.

General procedure D – Oxidative cleavage and reductive cyclization

To a solution of diol (1 mmol) in MeOH/H_2O (9:1, 1 mL, 0.1 M), was added $NaIO_4$ (428 mg, 2 mmol) and the suspension was stirred 2 h at 21 °C. Then, dimethyl sulfide (3 mmol, 222 µL) was added and the suspension was stirred another 5 min. Precipitate was removed by filtration and the filtrate was concentrated *in vacuo*. The crude dialdehyde was dissolved in anhydrous MeOH (2 mL, 0.05 M), added amine (1.1 mmol) and 3Å molecular sieves, and stirred under a N_2 atmosphere for 1 h at 21 °C. The mixture was then cooled to 0 °C and $NaBH_3CN$ (251 mg, 4 mmol) was added portion wise. After stirring 1 h at 0 °C, cooling was removed and the mixture was stirred 16 h at 21 °C. Molecular sieves were removed by filtration through celite and the filtrate was concentrated *in vacuo*. The crude was purified by flash column chromatography to give the desired product.

General procedure E – Boc deprotection using TFA

To a solution of Boc-protected amine (1 mmol) in CH_2Cl_2 (7.5 mL) was added TFA (2.5 mL) and the reaction mixture was stirred at 22 °C for 1 h. MeCN (10 mL) was added and the mixture was concentrated *in vacuo* (repeated 4 times to remove residual TFA) to afford the crude deprotected amine.

Furan Diels Alder

Compounds **2.12**, **2.15**, **2.16**, **2.19**, **2.21**, **2.24**, **2.26**, **2.34**, and **2.247** were synthesized by MSc student Katarzyna J. Śniady. Compounds **2.13**, **2.14**, **2.17**, **2.18**, **2.22**, **2.34**, **2.242**, **2.243**, and **2.244** were synthesized by BSc student Anastasia E. Richter. Compounds **2.36**, **2.38**, **2.39**, and **2.40** were synthesized by BSc student Joakim M. Svensson. Compounds **2.41** and **2.42** were synthesized by BSc student Pernille V. Christensen.

(1*R**,2*R**,3*R**,4*S**)-1-Methyl-3-(trifluoromethyl)-7-oxabicyclo[2.2.1]hept-5-ene-2-carboxylic acid (2.8)

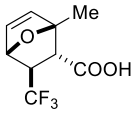

(*E*)-4,4,4-Trifluorocrotonic acid **2.1** (2.14 g, 15.3 mmol) was suspended in 2-methylfuran (2.76 ml, 30.6 mmol) and left for 3 days without stirring at 22 °C. After 3 days, crystals were collected by filtration and washed with ice-cold PhMe (3 × 3 mL) to give the title compound as a white crystalline solid (3.05 g, 90%).

m.p.: 117–119 °C; **^{1}H NMR** (400 MHz, DMSO-*d6*) δ 12.83 (broad s, 1H), 6.57 (dd, *J* = 5.7, 1.9 Hz, 1H), 6.29 (d, *J* = 5.7 Hz, 1H), 5.01 (d, *J* = 1.9 Hz, 1H), 2.83 – 2.68 (m, 2H), 1.70 (s, 3H); **^{13}C NMR** (101 MHz, DMSO-d_6) δ 171.1, 138.2, 137.1, 127.2 (q, $^1J_{CF}$ = 276.0 Hz), 87.3, 77.7 (q, $^3J_{CF}$ = 2.5 Hz), 50.2, 48.8 (q, $^2J_{CF}$ = 26.6 Hz), 17.8; **^{19}F NMR** (377 MHz, DMSO-*d6*) δ -66.65; **IR** (neat) cm^{-1}: 3209 (br. O–H), 1740 (s, C=O), 1640 (m, C=C); **HRMS** (ESI) calcd for $[C_9H_{10}F_3O_3]$ $[M+H]^+$ 223.0577, found 223.0583.

(2*R**,3*R**,3a*R**,6*R**,6a*S**,7*R**)-3-iodo-6a-methyl-7-(trifluoromethyl)tetrahydro-2,6-methanofuro[3,2-*b*]furan-5(2*H*)-one (2.9)

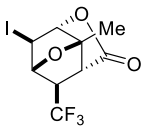

To a solution of $NaHCO_3$ (784 mg, 9.22 mmol) in H_2O (15 mL) was added **2.8** (512 mg, 2.30 mmol) and a solution of I_2 (643 mg, 2.54 mmol) and KI (2.30 g, 13.8 mmol) in H_2O (15 mL) and the reaction mixture was stirred at 22 °C for 16 h. The aqueous phase was extracted with CH_2Cl_2 (3 × 30 mL) and the combined organic layers were washed with 10% aq. $Na_2S_2O_3$ (1 × 40 mL), sat. aq. $NaHCO_3$ (1 × 40 mL), and sat. aq. NaCl (1 × 40 mL). The organic layers were dried over $MgSO_4$, filtered, and concentrated *in vacuo* to give the title compound as a white solid (640 mg, 80%).

R_f = 0.68 (EtOAc/heptane 2:3); **^{1}H NMR** (400 MHz, $CDCl_3$) δ 4.90 (s, 1H), 4.82 (s, 1H), 3.98 (s, 1H), 2.95 (qd, *J* = 8.6, 2.4 Hz, 1H), 2.62 (d, *J* = 2.4 Hz, 1H), 1.80 (s, 3H); **^{13}C NMR** (101 MHz, $CDCl_3$) δ 172.54, 123.85 (q, $^1J_{CF}$ = 279.5 Hz), 91.47, 90.88, 83.61 (q, $^3J_{CF}$ = 2.4 Hz), 52.79 (q, $^2J_{CF}$ = 29.5 Hz), 45.62 (d, $^3J_{CF}$ = 1.3 Hz), 23.78, 15.89; **^{19}F NMR** (377 MHz, $CDCl_3$) δ -69.91; **IR** (neat) cm^{-1}: 1776 (s, C=O); **HRMS** (ESI) calcd for $[C_9H_9F_3IO_3]$ $[M+H]^+$ 348.9543, found 348.9585.

(1*R,2*R**,3*R**,4*S**)-*N*-allyl-*N*,1-dimethyl-3-(trifluoromethyl)-7-oxabicyclo[2.2.1]hept-5-ene-2-carboxamide (2.10)**

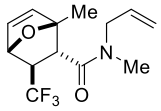

Following *general procedure B* using **2.8** (856 mg, 3.85 mmol) and *N*-allylmethylamine (0.462 mL, 4.82 mmol) afforded the title compound as a light yellow oil (891 mg, 84%) after purification by flash column chromatography (EtOAc/heptane 2:1).

***R*f** = 0.24 (EtOAc/heptane 2:1); **^{1}H NMR** (400 MHz, $CDCl_3$) δ 6.52 (dd, *J* = 5.7, 1.9 Hz, 1H), 6.17 (dd, *J* = 5.7, 4.0 Hz, 1H), 5.86 – 5.65 (m, 1H), 5.32 – 5.07 (m, 2H), 5.04 – 4.96 (m, 1H), 4.27 – 3.93 (m, 2H), 3.16 (d, *J* = 5.1 Hz, 0.6H, major rotamer), 3.13 (s, 1.6H, major rotamer), 3.06 (d, *J* = 5.1 Hz, 0.4H, minor rotamer), 2.94 (s, 1.4H, minor rotamer), 2.74 (qd, *J* = 9.5, 5.1 Hz, 1H), 1.68 (s, 1.6H, major rotamer), 1.66 (s, 1.4H, minor rotamer); **^{13}C NMR** (101 MHz, $CDCl_3$) δ 169.8 (minor rotamer), 169.3 (major rotamer), 138.1 (minor rotamer), 137.9 (major rotamer), 135.3 (major rotamer), 135.2 (minor rotamer), 132.5 (major rotamer), 132.2 (minor rotamer), 127.2 (q, $^{1}J_{CF}$ = 277.9 Hz, major rotamer), 127.1 (q, $^{1}J_{CF}$ = 278.0 Hz, minor rotamer), 117.9 (minor rotamer), 117.4 (major rotamer), 88.83 (major rotamer), 88.79 (minor rotamer), 79.3, 53.2 – 52.4 (m, 2 rotamers), 52.8 (minor rotamer), 51.0 (major rotamer), 46.0 (major rotamer), 45.8 (minor rotamer), 35.8 (major rotamer), 34.6 (minor rotamer), 18.4 (minor rotamer), 18.3 (major rotamer); **^{19}F NMR** (377 MHz, $CDCl_3$) δ -67.53 (minor rotamer), -67.85 (major rotamer); **IR** (neat) cm^{-1}: 3087 (m, C=C–H), 1639 (s, C=O); **HRMS** (ESI) calcd for $[C_{13}H_{17}F_3NO_2]$ $[M+H]^+$ 276.1206, found 276.1215.

(2*S,3*R**,3a*R**,8a*R**)-5,8a-Dimethyl-3-(trifluoromethyl)-2-vinyl-2,3,3a,5,6,8a-hexahydro-4*H*-furo[3,2-*c*]azepin-4-one (2.11)**

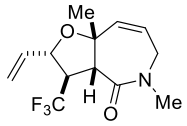

To a solution of **2.10** (145 mg, 0.500 mmol) in PhMe (10 mL) was added Hoveyda-Grubbs 2nd generation catalyst (15.7 mg, 25.0 µmol) and the mixture was refluxed under an ethylene atmosphere for 16 h. The mixture was concentrated *in vacuo* and purified directly by flash column chromatography (EtOAc/heptane 1:5) to give the title compound as an off-white amorphous solid (82.0 mg, 60%).

***R*f** = 0.33 (EtOAc/heptane 1:5); **^{1}H NMR** (400 MHz, $CDCl_3$) δ 6.12 – 5.98 (m, 2H), 5.91 (ddd, *J* = 17.1, 10.2, 7.0 Hz, 1H), 5.40 (dt, *J* = 17.1, 1.1 Hz, 1H), 5.26 (dt, *J* = 10.2, 1.1 Hz, 1H), 4.48 (t, *J* = 7.7 Hz, 1H), 4.24 – 4.13 (m, 1H), 4.10 – 3.99 (m, 1H), 3.35 – 3.25 (m, 2H), 3.03 (s, 3H), 1.48 (s, 3H); **^{13}C NMR** (101 MHz, $CDCl_3$) δ 168.6, 139.4, 136.1, 126.9 (q, $^{1}J_{CF}$ = 277.4 Hz), 125.0, 118.7, 82.0, 76.2 (q, $^{3}J_{CF}$ = 2.3 Hz), 55.4 (d, $^{3}J_{CF}$ = 1.5 Hz), 50.8 (q, $^{2}J_{CF}$ = 26.6 Hz), 45.2, 36.5, 25.9 (q, $^{3}J_{CF}$ = 1.4 Hz); **^{19}F NMR** (377 MHz, $CDCl_3$) δ -67.31; **IR** (neat) cm^{-1}: 1644 (s, C=O); **HRMS** (ESI) calcd for $[C_{13}H_{17}F_3NO_2]$ $[M+H]^+$ 276.1206, found 276.1206.

_N_-(2-Methoxyethyl)prop-2-en-1-amine (2.242)

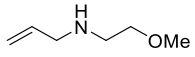

To a solution of 1-bromo-2-methoxyethane (1.35 ml, 14.4 mmol) in MeOH (60 mL) was added allylamine (4.32 mL, 57.6 mmol) and NaI (539 mg, 3.60 mmol) and the mixture was stirred at reflux for 3 h. The solution was concentrated *in vacuo*, dissolved in sat. aq. NH_4Cl (60 mL), and washed with EtOAc (2 × 60 mL). The aqueous phase was basified to pH 12 with 40% aq. NaOH and extracted with EtOAc (4 × 50 mL). The combined organic layers were combined, dried over Na_2SO_4, and concentrated *in vacuo* to give a title compound as a colorless oil (151 mg, 9%) that was used directly in the next step without further purification.

(1*R,2*R**,3*R**,4*S**)-*N*-Allyl-*N*-(2-methoxyethyl)-1-methyl-3-(trifluoromethyl)-7-oxabicyclo [2.2.1]hept-5-ene-2-carboxamide (2.12)**

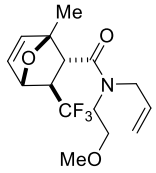

Following *general procedure B* using **2.8** (185 mg, 0.833 mmol) and amine **2.242** (151 mg, 1.30 mmol) afforded the title compound as a yellow oil (103 mg, 39%) after purification by flash column chromatography (EtOAc/heptane 2:3).

***R*f** = 0.49 (acetone/heptane 4:7); **^{1}H NMR** (400 MHz, $CDCl_3$) δ 6.56 – 6.48 (m, 1H), 6.17 (d, *J* = 5.6 Hz, 0.4H, minor rotamer), 6.14 (d, *J* = 5.6 Hz, 0.6H, major rotamer), 5.85 – 5.67 (m, 1H), 5.28 – 5.07 (m, 2H), 5.01 (s, 1H), 4.32 (d, *J* = 17.7 Hz, 0.6H, major rotamer), 4.19 (dd, *J* = 15.3, 5.6 Hz, 0.4H, minor rotamer), 4.07 (dd, *J* = 17.7, 5.6 Hz, 0.6H, major rotamer), 3.90 – 3.82 (m, 0.4H, minor rotamer), 3.81 – 3.67 (m, 1H), 3.51 – 3.46 (m, 2H), 3.33 (d, *J* = 2.7 Hz, 3H), 3.31 – 3.23 (m, 1H), 3.08 (d, *J* = 5.0 Hz, 1H), 2.73 (qd, *J* = 9.4, 5.0 Hz, 1H), 1.68 – 1.67 (m, 3H, rotamers); **^{13}C NMR** (101 MHz, $CDCl_3$) δ 169.9 (major rotamer), 169.8 (minor rotamer), 138.2 (minor rotamer), 138.0 (major rotamer), 135.3 (major rotamer), 135.1 (minor rotamer), 133.2 (minor rotamer), 132.9 (major rotamer), 126.9 (d, $^1J_{CF}$ = 278.3 Hz), 117.6 (major rotamer), 117.0 (minor rotamer), 88.92 (minor rotamer), 88.90 (major rotamer), 79.3 (m, rotamers), 71.0 (major rotamer), 70.4 (minor rotamer), 59.1 (minor rotamer), 59.0 (major rotamer), 52.9 (m, rotamers), 52.1 (major rotamer), 49.4 (minor rotamer), 47.6 (minor rotamer), 46.7 (major rotamer), 45.8 (major rotamer), 45.7 (minor rotamer), 18.3; **^{19}F NMR** (377 MHz, $CDCl_3$) δ -67.41, -67.49; **IR** (neat) cm^{-1}: 3040 (m, C=C–H), 1640 (s, C=O); **HRMS** (ESI) calcd for $[C_{15}H_{21}F_3NO_3]$ $[M+H]^+$ 320.1468, found 320.1468.

2-(But-3-en-1-ylamino)ethan-1-ol (2.243)

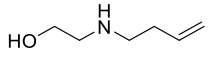

To a solution of 4-bromo-but-1-ene (1.20 mL, 11.9 mmol) in MeOH (48 mL) was added aminoethanol (2.15 mL, 35.5 mmol) and NaI (463 mg, 3.09 mmol) and the mixture was stirred at reflux for 3 h. The solution was concentrated *in vacuo*,

dissolved in sat. aq. NH_4Cl (50 mL), and washed with EtOAc (2 × 50 mL). The aqueous phase was basified to pH 12 with 40% aq. NaOH and extracted with EtOAc (4 × 50 mL). The combined organic layers were combined, dried over Na_2SO_4, and concentrated *in vacuo* to give a title compound as a brown oil (548 mg, 40%) that was used directly in the next step without further purification.

(1*R,2*R**,3*R**,4*S**)-*N*-(But-3-en-1-yl)-*N*-(2-hydroxyethyl)-1-methyl-(trifluoromethyl)-7-oxabicyclo[2.2.1]hept-5-ene-2-carboxamide (2.13)**

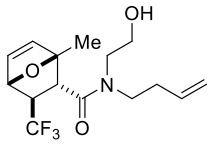

Following *general procedure B* using **2.8** (250 mg, 1.13 mmol) and amine **2.243** (259 mg, 2.25 mmol) afforded the title compound as a colorless oil (129 mg, 37%) after purification by flash column chromatography (EtOAc/heptane 3:2).

***R*f** = 0.27 (EtOAc/heptane 3:2); **^{1}H NMR** (400 MHz, DMSO-d_6) δ 6.54 – 6.50 (m, 1H), 6.00 (t, *J* = 5.8 Hz, 1H), 5.85 – 5.67 (m, 1H), 5.11 – 5.04 (m, 1H), 5.03 – 5.00 (m, 1H), 4.98 (d, *J* = 1.8 Hz, 1H), 4.81 (t, *J* = 5.4 Hz, 0.7H, major rotamer), 4.65 (t, *J* = 5.4 Hz, 0.3H, minor rotamer), 3.90 – 3.62 (m, 2H), 3.49 (q, *J* = 5.8 Hz, 1.4H, major rotamer), 3.43 (q, *J* = 5.8 Hz, 0.6H, minor rotamer), 3.22 (d, *J* = 4.8 Hz, 1H), 3.12 – 2.95 (m, 2H), 2.72 (pd, *J* = 10.0, 4.8 Hz, 1H), 37 – 2.14 (m, 2H), 1.63 (s, 1H, minor rotamer), 1.60 (s, 2H, major rotamer); **^{13}C NMR** (101 MHz, DMSO-d_6) δ 168.7 (major rotamer), 168.4 (minor rotamer), 138.0 (major rotamer), 137.8 (minor rotamer), 136.5 (major rotamer), 135.8 (minor rotamer), 135.7 (major rotamer), 135.4 (minor rotamer), 127.9 (q, $^1J_{CF}$ = 278.1 Hz, minor rotamer), 127.8 (q, $^1J_{CF}$ = 278.1 Hz, major rotamer), 117.9 (minor rotamer), 116.9 (major rotamer), 89.1 (minor rotamer), 88.8 (major rotamer), 78.8 (d, $^3J_{CF}$ = 2.4 Hz, minor rotamer), 78.7 (d, $^3J_{CF}$ = 2.4 Hz, major rotamer), 59.2 (major rotamer), 59.1 (minor rotamer), 51.6 (q, $^2J_{CF}$ = 26.3 Hz, major rotamer), 51.4 (q, $^2J_{CF}$ = 26.6 Hz, minor rotamer), 50.2 (major rotamer), 48.7 (major rotamer), 48.6 (minor rotamer) 45.7 (minor rotamer), 45.54 (major rotamer), 45.50 (minor rotamer), 33.7 (minor rotamer), 32.3 (major rotamer), 18.3 (major rotamer), 18.2 (minor rotamer); **^{19}F NMR** (377 MHz, DMSO-d_6) δ -65.82 (major rotamer), -65.90 (minor rotamer); **IR** (neat) cm^{-1}: 3438 (br., O–H), 3041 (m, C=C–H), 1737 (s, C=O), 1624 (s, C=C); **HRMS** (ESI) calcd for $[C_{15}H_{20}F_3NO_3]$ $[M+H]^+$ 320.1468, found 320.1469.

2-(Pent-4-en-1-ylamino)acetamide (2.244)

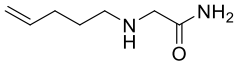

To a solution of glycinamide hydrochloride (3.34 g, 30.2 mmol) in MeOH (40 mL) was added NaOMe (1.58 g, 29.2 mmol) and the solution was stirred at 22 °C for 5 min. 5-Bromo-1-pentene (1.20 mL, 10.1 mmol) and NaI (377 mg, 2.52 mmol) were added and the reaction mixture was stirred at reflux for 16 h. Sat. aq. NH_4Cl

(40 mL) was added and the mixture was washed with EtOAc (2 × 40 mL). The aqueous phase was basified to pH 12 with 40% aq. NaOH and then extracted with EtOAc (4 × 40 mL). The combined organic layers were dried over Na_2SO_4, filtered, and concentrated *in vacuo*. The crude product was filtered through a short plug of silica to give the title compound as an impure colorless oil (1.50 g, 105%) that was used directly in the next step without further purification.

(1*R,2*R**,3*R**,4*S**)-*N*-(2-Amino-2-oxoethyl)-1-methyl-*N*-(pent-4-en-1-yl)-3-(trifluoromethyl)-7-oxabicyclo[2.2.1]hept-5-ene-2-carboxamide (2.14)**

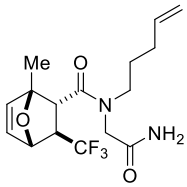

Following *general procedure B* using **2.8** (250 mg, 1.13 mmol) and amine **2.244** (320 mg, 2.25 mmol) afforded the title compound as a brown oil (184 mg, 53%) after purification by flash column chromatography (EtOAc/heptane/AcOH 80:20:2).

***R*f** = 0.18 (EtOAc/heptane/AcOH 80:20:2); **^{1}H NMR** (400 MHz, CD_3OD) δ 6.54 – 6.46 (m, 1H), 6.13 (d, *J* = 5.6 Hz, 0.25H, minor rotamer), 6.07 (d, *J* = 5.6 Hz, 0.75H, major rotamer), 5.91 – 5.76 (m, 1H), 5.15 – 4.92 (m, 3H), 4.39 – 4.25 (m, 1H), 3.97 – 3.85 (m, 1H), 3.71 (d, *J* = 16.2 Hz, 1H), 3.29 – 3.18 (m, 2H), 2.73 (qd, *J* = 9.6, 4.9 Hz, 1H), 2.18 – 1.98 (m, 2H), 1.76 (s, 3H), 1.68 – 1.56 (m, 2H); **^{13}C NMR** (101 MHz, CD_3OD) δ 172.9, 172.0 (minor rotamer), 171.5 (major rotamer), 139.0 (minor rotamer), 138.9 (minor rotamer), 138.8 (major rotamer), 138.6 (major rotamer), 136.5 (major rotamer), 136.4 (minor rotamer), 128.6 (d, $^1J_{CF}$ = 277.5 Hz), 116.2 (major rotamer), 115.5 (minor rotamer), 90.6 (major rotamer), 90.3 (minor rotamer), 80.3 (d, $^3J_{CF}$ = 2.5 Hz), 53.4 (q, $^2J_{CF}$ = 27.0 Hz), 51.6 (minor rotamer), 50.4 (major rotamer), 50.1 (major rotamer), 49.1 (minor rotamer), 47.2 (minor rotamer), 46.8 (major rotamer), 32.1 (minor rotamer), 31.5 (major rotamer), 29.0 (major rotamer), 27.5 (minor rotamer), 18.4 (major rotamer), 18.2 (minor rotamer); **^{19}F NMR** (377 MHz, CD_3OD) δ -68.90 (minor rotamer), -68.92 (major rotamer); **IR** (neat) cm^{-1}: 3466 (br., N–H), 1713 (s, C=O), 1626 (s, C=O), 1615 (s, C=C).

***N*-Allyl-*N*-((1*R**,2*R**,3*R**,4*S**)-1-methyl-3-(trifluoromethyl)-7-oxabicyclo[2.2.1]hept-5-ene-2-carbonyl)glycine (2.15)**

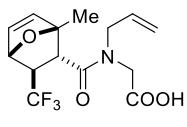

To a solution of **2.8** (56.0 mg, 0.252 mmol) in MeCN (2 ml) was added HATU (105 mg, 0.277 mmol) and DIPEA (0.176 ml, 1.01 mmol) and the mixture was stirred at 22 °C for 10 min. Then, allylglycine (43.5 mg, 0.378 mmol) was added and the reaction mixture was stirred for another 1 h. The reaction mixture was concentrated *in vacuo* and purified by flash column chromatography (EtOAc/heptane/AcOH 65:33:2) to give the title compound as a brown oil (52.0 mg, 65%).

R*f* = 0.62 (EtOAc/AcOH 98:2); **^{1}H NMR** (400 MHz, CD_3OD) δ 6.49 (dd, *J* = 5.5, 1.9 Hz, 1H), 6.04 (d, *J* = 5.5 Hz, 1H), 5.88 (dddd, *J* = 17.2, 10.4, 5.5, 4.8 Hz, 1H), 5.28 – 5.16 (m, 2H), 4.98

(d, *J* = 2.0 Hz, 1H), 4.53 (ddq, J = 17.4, 4.8, 1.6 Hz, 1H), 4.33 (dd, J = 17.2, 1.1 Hz, 1H), 4.01 (ddt, J = 17.4, 5.6, 1.6 Hz, 1H), 3.71 (d, J = 17.2 Hz, 1H), 3.22 (d, J = 4.9 Hz, 1H), 2.72 (qd, J = 9.7, 4.9 Hz, 1H), 1.74 (s, 3H); **^{13}C NMR** (101 MHz, CD_3OD) δ 172.1, 172.0, 138.8, 136.6, 134.0, 128.4 (q, $^1J_{CF}$ = 277.4 Hz), 118.0, 90.5, 80.3 (d, $^3J_{CF}$ = 2.4 Hz), 53.5 (q, $^2J_{CF}$ = 27.1 Hz), 53.1, 49.3, 46.7, 18.4; **IR** (neat) cm^{-1}: 3492 (br., O–H), 3004 (m, C=C–H), 1769 (s, C=O); **HRMS** (ESI) calcd. for $[C_{14}H_{17}F_3NO_4]$ $[M+H–C_5H_6O]^+$ 238.0686, found 238.0691 (only retro Diels-Alder product observed)

(2*S,3*R**,3a*R**,8a*R**)-5-(2-Methoxyethyl)-8a-methyl-3-(trifluoromethyl)-2-vinyl-2,3,3a,5, 6,8a-hexahydro-4*H*-furo[3,2-c]azepin-4-one (2.16)**

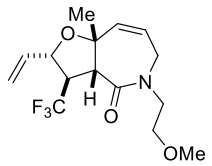

To a solution of **2.12** (50.0 mg, 0.157 mmol) in PhMe (16 mL) was added Hoveyda-Grubbs 2nd generation catalyst (4.9 mg, 7.8 µmol) and the mixture was refluxed under an ethylene atmosphere for 6 h. The mixture was concentrated *in vacuo* and purified directly by flash column chromatography (EtOAc/heptane 1:3) to give the title compound as a brown oil (11.0 mg, 22%).

***R*$_f$** = 0.50 (EtOAc/heptane 1:1); **^{1}H NMR** (400 MHz, $CDCl_3$) δ 6.03 – 5.92 (m, 1H), 5.91 – 5.78 (m, 2H), 5.34 (d, *J* = 17.1 Hz, 1H), 5.20 (d, *J* = 10.3 Hz, 1H), 4.41 (t, *J* = 7.8 Hz, 1H), 4.14 – 4.01 (m, 1H), 3.99 – 3.89 (m, 1H), 3.68 – 3.56 (m, 1H), 3.52 – 3.38 (m, 4H), 3.26 (s, 3H), 3.20 (d, *J* = 5.1 Hz, 1H), 1.41 (s, 3H); **^{13}C NMR** (101 MHz, $CDCl_3$) δ 168.2, 138.1, 136.1, 126.9 (d, $^1J_{CF}$ = 277.5 Hz), 126.1, 118.8, 82.1, 76.2 (d, $^3J_{CF}$ = 2.4 Hz), 71.8, 59.0, 55.5 (d, $^3J_{CF}$ = 1.3 Hz), 50.7 (q, $^2J_{CF}$ = 26.6 Hz), 49.2, 44.6, 26.1; **^{19}F NMR** (377 MHz, $CDCl_3$) δ -67.30; **IR** (neat) cm^{-1}: 1650 (s, C=O); **HRMS** (ESI) calcd for $[C_{15}H_{21}F_3NO_3]$ $[M+H]^+$ 320.1468, found 320.1468.

(2*S,3*R**,3a*R**,9a*R**,*Z*)-5-(2-Hydroxyethyl)-9a-methyl-3-(trifluoromethyl)-2-vinyl-3,3a,5, 6,7,9a-hexahydrofuro[3,2-*c*]azocin-4(*2H*)-one (2.17)**

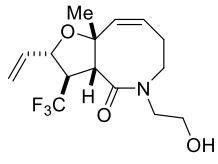

To a solution of **2.13** (60.0 mg, 0.188 mmol) in PhMe (10 mL) was added Hoveyda-Grubbs 2nd generation catalyst (6.0 mg, 9.4 µmol) and the mixture was refluxed under an ethylene atmosphere for 16 h. The mixture was concentrated *in vacuo* and purified directly by flash column chromatography (EtOAc/heptane 3:2) to give the title compound as a brown oil (29.0 mg, 48%).

***R*$_f$** = 0.22 (EtOAc/heptane 3:2); **^{1}H NMR** (400 MHz, DMSO-d_6) δ 5.93 – 5.81 (m, 1H), 5.58 (dd, *J* = 12.9, 2.9 Hz, 1H), 5.42 (ddd, *J* = 17.1, 1.6, 0.9 Hz, 1H), 5.34 (m, 1H), 5.28 (ddd, *J* = 10.3, 1.6, 0.9 Hz, 1H), 4.67 (t, *J* = 5.4 Hz, 1H), 4.44 (dd, *J* = 9.5, 7.2 Hz, 1H), 4.11 – 3.95 (m, 1H), 3.77 – 3.67 (m, 1H), 3.64 (d, *J* = 7.3 Hz, 1H), 3.58 (dd, *J* = 13.0, 6.0 Hz, 1H), 3.49 – 3.41

(m, 2H), 3.28 (d, *J* = 6.9 Hz, 1H), 2.97 (dt, *J* = 13.0, 6.5 Hz, 1H), 2.58 – 2.43 (m, 1H), 2.39 – 2.28 (m, 1H), 1.52 (s, 3H); **^{13}C NMR** (101 MHz, DMSO-d_6) δ 169.6, 136.2, 136.0, 126.2 (q, $^1J_{CF}$ = 277.8 Hz), 124.2, 119.2, 85.1, 75.6 (d, $^3J_{CF}$ = 2.4 Hz), 58.9, 52.8, 51.4 (q, $^2J_{CF}$ = 25.1 Hz), 47.9, 43.7, 25.7, 25.6; **^{19}F NMR** (377 MHz, DMSO-d_6) δ -66.23; **IR** (neat) cm^{-1}: 3445 (br., O–H), 3020 (w, C=C–H), 1633 (s, C=O); **HRMS** (ESI) calcd for $[C_{15}H_{21}F_3NO_3]$ $[M+H]^+$ 320.1468, found 320.1466.

2-((2*S,3*R**,3a*R**,10a*R**,*E*)-10a-Methyl-4-oxo-3-(trifluoromethyl)-2-vinyl-2,3,3a,4,6,7,8,10a-octahydro-5*H*-furo[3,2-*c*]azonin-5-yl)acetamide (2.18)**

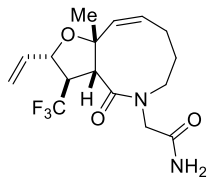

To a solution of **2.14** (29.0 mg, 0.0837 mmol) in PhMe (9 mL) was added Hoveyda-Grubbs 2nd generation catalyst (2.6 mg, 4.2 µmol) and the mixture was refluxed under an ethylene atmosphere for 6 h. The mixture was concentrated *in vacuo* and purified directly by flash column chromatography (EtOAc) to give the title compound as an off-white amorphous solid (7.0 mg, 24%).

***R*$_f$** = 0.59 (EtOAc/MeOH 9:1); **^{1}H NMR** (400 MHz, CD_3OD) δ 6.11 – 6.01 (m, 1H), 5.61 – 5.47 (m, 2H), 5.39 (dt, *J* = 17.2, 1.1 Hz, 1H), 5.25 (dd, *J* = 10.3, 1.1 Hz, 1H), 4.58 – 4.49 (m, 1H), 4.25 – 4.17 (m, 1H), 4.06 – 3.93 (m, 1H), 3.88 (d, *J* = 3.3 Hz, 1H), 3.66 – 3.61 (m, 1H), 3.48 – 3.35 (m, 2H), 2.57 – 2.40 (m, 1H), 2.33 – 2.21 (m, 1H), 1.86 – 1.68 (m, 2H), 1.66 (s, 3H); **^{13}C NMR** (101 MHz, CD_3OD) δ 174.8, 173.7, 137.9, 135.8, 131.4, 125.1 (d, $^1J_{CF}$ = 277.7 Hz), 119.0, 88.2, 78.9 (d, $^3J_{CF}$ = 2.1 Hz), 55.1 (d, $^2J_{CF}$ = 26.5 Hz), 53.6, 52.9, 50.5, 29.5, 27.0, 25.5; **^{19}F NMR** (377 MHz, CD_3OD) δ -68.18; **IR** (neat) cm^{-1}: 3376 (br., N–H) , 1690 (s, C=O), 1616 (s, C=O); **HRMS** (ESI) calcd for $[C_{16}H_{22}F_3N_2O_3]$ $[M+H]^+$ 347.1577, found 347.1589.

(*E*)-*N*-Allyl-*N*-(4,4,4-trifluorobut-2-enoyl)glycine (2.19)

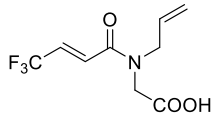

To a solution of **2.15** (108 mg, 92.9 µmol) in PhMe (16 mL) was added Hoveyda-Grubbs 2nd generation catalyst (21.2 mg, 21.2 µmol) and the mixture was refluxed under an ethylene atmosphere for 16 h. The mixture was concentrated *in vacuo* and purified directly by flash column chromatography (EtOAc/heptane/AcOH 60:40:2) to give the title compound as a brown oil (60.0 mg, 75%).

***R*$_f$** = 0.38 (EtOAc/heptane/AcOH 67:33:2), **^{1}H NMR** (400 MHz, CD_3OD) δ 7.17 (dq, *J* = 15.4, 2.0 Hz, 0.6H), 7.08 (ddd, *J* = 15.3, 2.6, 1.5 Hz, 0.4H), 6.88 – 6.67 (m, 1H), 5.95 (ddt, *J* = 17.1, 10.4, 5.2 Hz, 0.6H), 5.88 – 5.70 (m, 0.4H), 5.33 – 5.18 (m, 2H), 4.25 (d, *J* = 7.4 Hz, 0.8H), 4.19 (dt, *J* = 5.2, 2.0 Hz, 1.2H), 4.17 (s, 1.2H), 4.13 (dt, *J* = 6.1, 1.5 Hz, 0.8H).

(1*R,2*R**,3*R**,4*S**)-*N*-Benzyl-1-methyl-3-(trifluoromethyl)-7-oxabicyclo[2.2.1]hept-5-ene-2-carboxamide (2.20)**

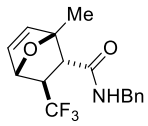

Following *general procedure B* using **2.8** (1.00 g, 4.50 mmol) and benzylamine (737 mL, 0.675 mmol) afforded the title compound as a white solid (1.20 g, 85%) after purification by flash column chromatography (EtOAc/heptane 1:2).

***R*f** = 0.25 (EtOAc/heptane 1:2); **m.p.**: 98–100 ºC; **^{1}H NMR** (400 MHz, DMSO-*d*$_6$) δ 8.70 (t, *J* = 5.9 Hz, 1H), 7.34 (m, 2H), 7.28 – 7.21 (m, 3H), 6.55 (dd, *J* = 5.6, 1.9 Hz, 1H), 6.10 (d, *J* = 5.6 Hz, 1H), 5.00 (d, *J* = 1.9 Hz, 1H), 4.30 (qd, *J* = 15.2, 5.9 Hz, 2H), 2.80 – 2.68 (m, 2H), 1.60 (s, 3H); **^{13}C NMR** (101 MHz, DMSO-*d*$_6$) δ 168.6, 139.8, 137.9, 136.3, 128.8 (2C), 127.9 (q, $^{1}J_{CF}$ = 278.2 Hz), 127.5 (2C), 127.3, 88.3 78.55 (d, $^{3}J_{CF}$ = 2.1 Hz), 50.4, 50.2 (q, $^{2}J_{CF}$ = 26.3 Hz), 42.9, 18.0; **^{19}F NMR** (377 MHz, DMSO-*d*$_6$) δ - 66.43; **IR** (neat) cm^{-1}: 3295 (s, N–H), 1642 (s, C=O), 1546 (s, C=C); **HRMS** (ESI) calcd for [$C_{16}H_{17}F_3NO_2$] [M+H]$^+$ 312.1206, found 312.1200.

(1*R,2*R**,3*R**,4*S**)-*N*-(*tert*-Butyl)-1-methyl-3-(trifluoromethyl)-7-oxabicyclo[2.2.1]hept-5-ene-2-carboxamide (2.21)**

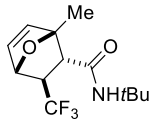

Following *general procedure B* using **2.8** (534 mg, 2.40 mmol) and *tert*-butylamine (760 µL, 7.21 mmol) afforded the title compound as a white solid (578 mg, 87%) after purification by flash column chromatography (EtOAc/heptane 2:7).

***R*f** = 0.54 (EtOAc/heptane 2:3); **m.p.**: 129–130 °C; **^{1}H NMR** (400 MHz, DMSO-*d6*) δ 7.71 (broad s, 1H), 6.48 (dd, J = 5.6, 1.9 Hz, 1H), 6.01 (d, J = 5.6 Hz, 1H), 4.94 (d, J = 1.9 Hz, 1H), 2.74 (d, J = 5.0 Hz, 1H), 2.61 (qd, J = 10.1, 5.0 Hz, 1H), 1.57 (s, 3H), 1.23 (s, 9H); **^{13}C NMR** (101 MHz, DMSO-*d6*) δ 167.4, 137.4, 135.5, 127.5 (observed by HMBC), 87.7, 78.1, 50.3, 50.0, 49.0 (d, $^{2}J_{CF}$ = 32.0 Hz), 28.4 (3C), 17.3; **^{19}F NMR** (377 MHz, DMSO-*d6*) δ -66.26; **IR** (neat) cm^{-1}: 3348 (s, N–H), 1677 (s, C=O), 1530 (s, C=C); **HRMS** (ESI) calcd for [$C_{13}H_{19}F_3NO_2$] [M+H]$^+$ 278.1362, found 278.1365

(1*R,2*R**,4*R**,5*S**,6*R**,7*R**)-*N*-Benzyl-5-methyl-7-(trifluoromethyl)-3,8-dioxatricyclo [3.2.1.0^{2,4}]octane-6-carboxamide (2.245)**

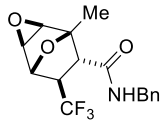

To an ice-cooled solution of **2.20** (150 mg, 0.482 mmol) in CH_2Cl_2 (5 mL) was added mCPBA (415 mg, 2.41 mmol) and the solution was stirred at 22 °C for 5 h. The mixture was quenched with sat. aq. Na_2SO_3 (5 mL) and the layers were separated. The organic layer was washed with sat. aq. $NaHCO_3$ (1 × 5 mL). The organic layer was dried over $MgSO_4$, filtered, and concentrated *in vacuo*. The crude product

was purified by flash column chromatography (EtOAc/heptane/AcOH 30:70:2) to give a title compound as white solid (108 mg, 68%).

***R*$_f$** = 0.33 (EtOAc/heptane/AcOH 30:70:2); **m.p.**: 129–131 ºC; **^{1}H NMR** (400 MHz, $CDCl_3$) δ 7.39 – 7.32 (m, 2H), 7.32 – 7.28 (m, 1H), 7.27 – 7.23 (m, 2H), 6.07 (t, *J* = 5.7 Hz, 1H), 4.59 (s, 1H), 4.53 – 4.40 (m, 2H), 3.54 (d, *J* = 3.3 Hz, 1H), 3.49 (d, *J* = 3.3 Hz, 1H), 3.02 (qd, *J* = 9.4, 5.7 Hz, 1H), 2.58 (d, *J* = 5.7 Hz, 1H), 1.60 (s, 3H); **^{13}C NMR** (101 MHz, $CDCl_3$) δ 167.3, 137.3, 128.8 (2C), 127.8, 127.4 (2C), 127.3 (q, $^1J_{CF}$ = 278.8 Hz), 83.3, 74.4 (d, $^3J_{CF}$ = 2.5 Hz), 55.7, 50.9, 50.5, 49.7 (q, $^2J_{CF}$ = 28.4 Hz), 44.0, 15.6; **^{19}F NMR** (377 MHz, $CDCl_3$) δ -68.93; **IR** (neat) cm^{-1}: 3388 (s, N–H), 1679 (s, C=O), 1539 (s, C=C); **HRMS** (ESI) calcd for $[C_{16}H_{17}F_3NO_3]$ $[M+H]^+$ 328.1155, found 328.1160.

(2*R,3*S**,6*R**,6a*S**,7*R**)-4-Benzyl-3-hydroxy-6a-methyl-7-(trifluoromethyl)hexahydro-5*H*-2,6-methanofuro[3,2-*b*]pyrrol-5-one (2.22)**

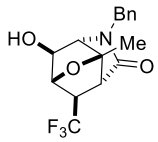

To a solution of **2.245** (96. mg, 0.293 mmol) in anhydrous THF (3 mL) was added a solution of *t*BuOK (34.0 mg, 0.293 mmol) in anhydrous THF (3 mL) and the solution was stirred under an atmosphere of N_2 at 22 ℃ for 18 h. The mixture was quenched with sat. aq. NH_4Cl (6 mL) and the mixture was extracted with CH_2Cl_2 (3 × 6 mL). The combined organic layers were dried over $MgSO_4$, filtered, and concentrated *in vacuo*. The crude product was purified by flash column chromatography (EtOAc/heptane 1:1) to give a title compound as a white amorphous solid (55 mg, 58%).

***R*$_f$** = 0.17 (EtOAc/heptane 1:1); **^{1}H NMR** (400 MHz, DMSO-d_6) δ 7.44 – 7.21 (m, 5H), 5.31 (d, *J* = 4.5 Hz, 1H), 4.74 (d, *J* = 15.1 Hz, 1H), 4.45 (s, 1H), 4.02 (d, *J* = 15.1 Hz, 1H), 3.76 (d, *J* = 4.5 Hz, 1H), 3.17 (qd, *J* = 10.1, 2.0 Hz, 1H), 2.91 (s, 1H), 2.33 – 2.32 (m, 1H), 1.46 (s, 3H); **^{13}C NMR** (101 MHz, DMSO-d_6) δ 171.5, 136.2, 128.7 (2C), 127.8 (2C), 127.5, 125.8 (q, $^1J_{CF}$ = 278.5 Hz), 87.2, 82.4 (d, $^3J_{CF}$ = 2.4 Hz), 75.8, 70.8, 49.1 (q, $^2J_{CF}$ = 27.4 Hz), 49.0, 45.0, 15.4; **^{19}F NMR** (377 MHz, DMSO-d_6) δ -68.35; **IR** (neat) cm^{-1}: 3391 (br., O–H), 1677 (s, C=O); **HRMS** (ESI) calcd for $[C_{16}H_{17}F_3NO_3]$ $[M+H]^+$ 328.1155, found 328.1156.

(2*R,3*S**,3a*S**,6*R**,6a*S**,7*R**)-4-(*tert*-Butyl)-3-hydroxy-6a-methyl-7-(trifluoromethyl)hexahydro-5*H*-2,6-methanofuro[3,2-*b*]pyrrol-5-one (2.23)**

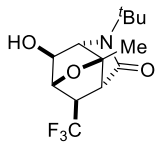

To an ice-cooled solution of **2.21** (108 mg, 0.389 mmol) in CH_2Cl_2 (5 mL) was added mCPBA (450 mg, 1.83 mmol) and the solution was stirred at 22 °C for 16 h. The mixture was quenched with sat. aq. Na_2SO_3 (5 mL) and the layers were separated. The organic layer was washed with sat. aq. $NaHCO_3$ (3 × 5 mL). The organic layer was dried over $MgSO_4$, filtered, and concentrated *in vacuo*. The crude epoxide dissolved in anhydrous THF (5 mL) and added a solution of ^{t}BuOK (43.7 mg,

0.389 mmol) in anhydrous THF (5 mL) and the reaction mixture was stirred under an atmosphere of N_2 at reflux for 40 h. The mixture concentrated *in vacuo* and purified directly by flash column chromatography (EtOAc/heptane 2:3) to give a title compound as a white solid (57 mg, 48%).

***R*f** = 0.54 (EtOAc/heptane 1:2); **m.p.**: 135–137°C; **^{1}H NMR** (400 MHz, $CDCl_3$) δ 4.63 (s, 1H), 3.78 (s, 1H), 3.30 (t, *J* = 1.5 Hz, 1H), 2.61 (qd, *J* = 9.2, 2.4 Hz, 1H), 2.34 (s, 1H), 1.65 (s, 3H), 1.59 (s, 1H), 1.44 (s, 9H); **^{13}C NMR** (101 MHz, $CDCl_3$) δ 172.3, 125.0 (d, $^1J_{CF}$ = 278.8 Hz), 87.2, 82.8 (d, $^3J_{CF}$ = 2.4 Hz), 78.9, 72.0, 54.8, 51.1 (d, $^3J_{CF}$ = 1.1 Hz), 51.0 (d, $^2J_{CF}$ = 29.0 Hz), 28.6, 15.9; **^{19}F NMR** (377 MHz, $CDCl_3$) δ -69.85; **IR** (neat) cm^{-1}: 3367 (br., O–H), 1675 (s, C=O); **HRMS** (ESI) calcd for $[C_{13}H_{19}F_3NO_3]$ $[M+H]^+$ 294.1312, found 294.1317.

(1*R,2*R**,3*R**,4*S**)-*N*-(2-Hydroxyethyl)-*N*,1-dimethyl-3-(trifluoromethyl)-7-oxabicyclo [2.2.1]hept-5-ene-2-carboxamide (2.24)**

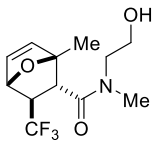

To a solution of **2.8** (104 mg, 0.468 mmol) in MeCN (5 ml) was added PyBroP (273 mg, 0.585 mmol) and DIPEA (327 µL, 1.91 mmol) and the solution was stirred at 22 °C for 10 min. Then, 2-(methylamino)ethanol (187 µL, 2.29 mmol) was added and the reaction mixture was stirred at 22 °C for 2 h. The mixture was concentrated *in vacuo* and purified directly by flash column chromatography (EtOAc) to give the title compound as yellow oil (123 mg, 94%, 90% purity).

***R*f** = 0.35 (EtOAc); **^{1}H NMR** (400 MHz, CD_3OD) δ 6.55 – 6.50 (m, 1H), 6.12 – 6.10 (m, 1H), 5.00 – 4.99 (m, 1H), 3.91 (dt, J = 14.9, 6.0 Hz, 0.5H), 3.76 – 3.68 (m, 1.5H), 3.68 – 3.64 (m, 1.5H), 3.48 (dt, *J* = 14.9, 5.3 Hz, 0.5H), 3.38 – 3.35 (m, 0.5H), 3.31 (s, 2H), 3.27 (d, *J* = 5.0 Hz, 0.5H), 2.98 (s, 1H), 2.75 (qd, *J* = 9.7, 5.3 Hz, 1H), 1.69 (s, 1.5H), 1.68 (s, 1.5H); ^{13}C NMR (101 MHz, CD_3OD) δ 162.3 (minor rotamer), 161.9 (major rotamer), 129.3 (minor rotamer), 129.1 (major rotamer), 127.2 (minor rotamer), 127.0 (major rotamer), 120.4 (q, $^1J_{CF}$ = 277.0 Hz), 80.8 (major rotamer), 80.7 (minor rotamer), 70.9 – 70.6 (m, rotamers), 51.0 (major rotamer), 50.6 (minor rotamer), 44.2 (major rotamer), 44.0 (q, $^2J_{CF}$ = 27.1 Hz, minor rotamer), 43.8 (q, $^2J_{CF}$ = 27.1 Hz, major rotamer), 42.7 (minor rotamer), 37.6 (major rotamer), 37.3 (minor rotamer), 28.9 (major rotamer), 25.8 (minor rotamer), 8.9; **^{19}F NMR** (377 MHz, CD_3OD) δ -68.79 (minor rotamer), -69.26 (major rotamer); **IR** (neat) cm^{-1}: 3419 (br., O–H), 1624 (s, C=O); **HRMS** (ESI) calcd for $[C_{12}H_{17}F_3NO_3]$ $[M+H–C_5H_6O]^+$ 198.0736, found 198.0744 (only reverse Diels-Alder product observed).

(2*R,3*R**,3a*S**,6*R**,6a*S**,7*R**)-3-Hydroxy-6a-methyl-7-(trifluoromethyl)tetrahydro-2,6-methanofuro[3,2-*b*]furan-5(2*H*)-one (2.26)**

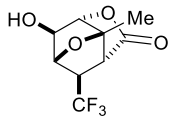

To an ice-cooled solution of **2.24** (103 mg, 0.369 mmol) in anhydrous CH_2Cl_2 (4 ml) was added mCPBA (455 mg, 1.84 mmol) and the reaction mixture was stirred at reflux under an atmosphere of N_2 for 18 h. The mixture was concentrated *in vacuo* and purified directly by flash column chromatography (EtOAc/heptane/AcOH 28:70:2) to give the title compound as yellow oil (32.2 mg, 41%).
***R*f** = 0.46 (EtOAc/heptane 1:1); **^{1}H NMR** (400 MHz, DMSO-d_6) δ 5.69 (broad s, 1H), 4.52 (s, 1H), 4.16 (t, *J* = 1.3 Hz, 1H), 3.97 (s, 1H), 3.56 (qd, *J* = 10.0, 2.3 Hz, 1H), 2.69 (d, *J* = 2.3 Hz, 1H), 1.60 (s, 3H); **^{13}C NMR** (101 MHz, DMSO-d_6) δ 173.6, 124.2 (q, $^1J_{CF}$ = 278.7 Hz), 88.8 (2C), 81.8 (d, $^3J_{CF}$ = 2.3 Hz), 76.7, 48.1 (q, $^2J_{CF}$ = 28.1 Hz), 45.5 (d, $^3J_{CF}$ = 1.1 Hz), 15.1; **^{19}F NMR** (377 MHz, DMSO-d_6) δ -68.36; **IR** (neat) cm^{-1}: 3492 (br., O–H), 1769 (s, C=O); **HRMS** (ESI) calcd for $[C_9H_{10}F_3O_4]$ $[M+H]^+$ 239.0526, found 239.0525.

(1*R,2*R**,3*R**,4*S**)-*N*,1-Dimethyl-3(trifluoromethyl)-7-oxabicyclo[2.2.1]hept-5-ene-2-carboxamide (2.29)**

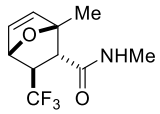

Following *general procedure B* using **2.8** (2.00 g, 9.00 mmol) and methylamine hydrochloride (1.80 g, 27.0 mmol) afforded the title compound as a white solid (1.77 g, 83%) after purification by flash column chromatography (EtOAc/heptane 1:1).
***R*f** = 0.26 (EtOAc/heptane 1:1); **m.p.**: 119–121 ºC; **^{1}H NMR** (400 MHz, DMSO-d_6) δ 8.07 (broad s, 1H), 6.51 (dd, *J* = 5.6, 1.9 Hz, 1H), 6.08 (d, *J* = 5.6 Hz, 1H), 4.97 (d, *J* = 1.9 Hz, 1H), 2.74 – 2.61 (m, 2H), 2.59 (d, *J* = 4.6 Hz, 3H), 1.57 (s, 3H); **^{13}C NMR** (101 MHz, DMSO-d_6) δ 168.4, 137.6, 135.7, 127.4 (q, $^1J_{CF}$ = 278.1 Hz), 87.7, 78.0 (d, $^3J_{CF}$ = 2.3 Hz), 50.0, 49.4 (q, $^2J_{CF}$ = 26.2 Hz), 25.9, 17.5; **^{19}F NMR** (377 MHz, DMSO-d_6) δ -66.44; **IR** (neat) cm^{-1}: 3318 (s, N–H), 1644 (s, C=O), 1566 (s, N–H); **HRMS** (ESI) calcd for $[C_{10}H_{13}F_3NO_2]$ $[M+H]^+$ 236.0893, found 236.0891.

(1*S,2*R**,3*R**,4*R**,5*S**,6*R**)-*N*-Benzyl-5,6-dihydroxy-1-methyl-3-(trifluoromethyl)-7-oxabicyclo[2.2.1]heptane-2-carboxamide (2.30)**

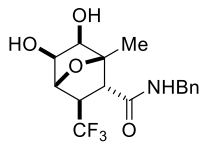

To a solution of **2.20** (299 mg, 0.960 mmol) in THF/H_2O (5:1, 10 mL) was added *N*-methylmorpholine oxide (236 mg, 2.02 mmol) and $K_2OsO_4{\cdot}(H_2O)_2$ (17.7 mg, 48.0 µmol) and the turbid reaction mixture was stirred at 22 °C 3 h. THF was removed *in vacuo* and sat. aq. $NaHCO_3$ (5 mL) and sat. aq. Na_2SO_3 (5 mL) were added. The solution was extracted with CH_2Cl_2 (3 × 10 mL) and the combined organic layers were dried over $MgSO_4$, filtered, and concentrated *in*

vacuo. The crude product was purified by flash column chromatography (EtOAc/heptane 3:2) to give the title compound as white solid (254 mg, 77%).
R_f = 0.45 (EtOAc/heptane 2:1); **m.p.**: 168–170 °C; **^{1}H NMR** (400 MHz, CD_3OD) δ 7.35 – 7.29 (m, 2H), 7.29 – 7.22 (m, 3H), 4.46 (d, *J* = 14.9 Hz, 1H), 4.40 – 4.28 (m, 2H), 4.13 – 4.05 (m, 1H), 4.02 (d, *J* = 6.0 Hz, 1H), 2.98 (qd, *J* = 9.7, 6.0 Hz, 1H), 2.73 (d, *J* = 6.0 Hz, 1H), 1.49 (s, 3H); **^{13}C NMR** (101 MHz, CD_3OD) δ 170.3, 139.7, 129.6 (2C), 128.5 (2C), 128.4, 125.7 (observed by HMBC), 89.4, 83.3 (d, $^3J_{CF}$ = 1.9 Hz), 75.4, 71.8, 54.1, 44.5, 15.5; **^{19}F NMR** (377 MHz, CD_3OD) δ -71.60; **IR** (neat) cm^{-1}: 3406 (br., O–H), 1642 (s, C=O); **HRMS** (ESI) calcd for $[C_{16}H_{19}F_3NO_4]$ $[M+H]^+$ 346.1261, found 346.1261.

(1*R,2*R**,4*R**)-5,6-Dihydroxy-*N*,1-dimethyl-3-(trifluoro)-7-oxabicyclo[2.2.1]heptane-2-carboxamide (2.31)**

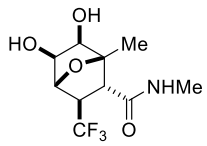

To a solution of **2.29** (400 mg, 41.7 mmol) in THF/H_2O (5:1, 16 mL) was added *N*-methylmorpholine oxide (319 mg, 2.72 mmol) and $K_2OsO_4{\cdot}(H_2O)_2$ (31.0 mg, 0.0850 mmol) and the turbid reaction mixture was stirred at 22 °C for 18 h. The reaction mixture was concentrated *in vacuo* and purified directly by flash column chromatography (CH_2Cl_2/MeOH 9:1) to give a title compound as yellow solid (397 mg, 87%).
R_f = 0.28 (CH_2Cl_2/MeOH 9:1); **m.p.**: > 230 ºC (decomp.); **^{1}H NMR** (400 MHz, DMSO-d_6) δ 8.23 (q, *J* = 4.6 Hz, 1H), 4.87 (d, *J* = 5.2 Hz, 1H), 4.75 (d, *J* = 6.7 Hz, 1H), 4.16 (s, 1H), 3.86 (m, 2H), 2.93 (qd, *J* = 10.1, 6.1 Hz, 1H), 2.63 (d, *J* = 4.6 Hz, 3H), 2.59 (d, *J* = 6.1 Hz, 1H), 1.37 (s, 3H); **^{13}C NMR** (101 MHz, DMSO-d_6) δ 168.1, 127.1 (q, $^1J_{CF}$ = 277.4 Hz), 87.4, 81.2 (d, $^3J_{CF}$ = 1.6 Hz), 73.6, 69.8, 52.0, 46.6 (q, $^2J_{CF}$ = 27.2 Hz), 25.9, 15.2; **^{19}F NMR** (377 MHz, DMSO-d_6) δ -68.55; **IR** (neat) cm^{-1}: 3392 (s, N–H), 3296 (br., O–H), 1656 (s, C=O), 1568 (s, N–H); **HRMS** (ESI) calcd for $[C_{10}H_{15}F_3NO_4]$ $[M+H]^+$ 270.0948, found 270.0945.

(2*S,3*S**,4*R**,5*R**)-*N*-Benzyl-2,5-bis(hydroxymethyl)-2-methyl-4-(trifluoromethyl)tetrahydrofuran-3-carboxamide (2.32)**

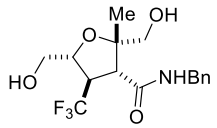

To a solution of **2.31** (100 mg, 0.290 mmol) in MeOH/H_2O (9:1, 3 mL) was added $NaIO_4$ (186 mg, 0.869 mmol) and the reaction mixture was stirred at 22 °C for 2 h. Precipitate was removed by filtration and the filtrate was placed on ice and added $NaBH_4$ (110 mg, 2.90 mmol). The reaction mixture was stirred at 22 °C for 18 h. The mixture was concentrated *in vacuo* and purified directly by flash column chromatography (EtOAc/heptane 2:1) to give the title compound as a colorless oil (39.0 mg, 39%).
R_f = 0.31 (EtOAc/heptane 2:1); **^{1}H NMR** (400 MHz, $CDCl_3$) δ 7.39 – 7.30 (m, 3H), 7.28 – 7.24 (m, 2H), 6.46 (broad s, 1H), 4.57 – 4.43 (m, 2H), 4.31 (dt, *J* = 9.4, 2.2 Hz, 1H), 4.05 –

3.95 (m, 2H), 3.68 (dd, *J* = 12.3, 2.2 Hz, 1H), 3.53 – 3.42 (m, 2H), 2.93 (d, *J* = 11.6 Hz, 1H), 1.26 (s, 3H); **^{13}C NMR** (101 MHz, $CDCl_3$) δ 170.1, 137.2, 129.1 (2C), 128.2, 127.9 (2C), 125.9 (d, $^1J_{CF}$ = 278.1 Hz), 85.8, 78.7 (d, $^3J_{CF}$ = 2.2 Hz), 69.3, 63.0, 57.2, 47.5 (q, $^2J_{CF}$ = 27.2 Hz), 44.5, 25.0; **^{19}F NMR** (377 MHz, $CDCl_3$) δ -69.24; **IR** (neat) cm^{-1}: 3377 (br., N/O–H), 1638 (s, C=O); **HRMS** (ESI) calcd for $[C_{16}H_{21}F_3NO_4]$ $[M+H]^+$ 348.1417, found 348.1433.

(3a*R,4*S**,5*R**,6*R**,7*R**,7a*R**)-*N*-2,2,4-Tetramethyl-6-(triflurormethyl)hexahydro-4,7-epoxybenzo[*d*][1,3]dioxole-5-carboxamide (2.34)**

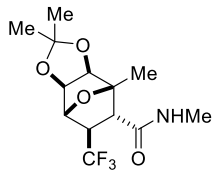

To a solution **2.18** (83.0 mg, 0.308 mmol) in acetone (3 mL) was added 2,2-dimethoxypropane (0.755 mL, 6.17 mmol) and *p*-TsOH (1.0 mg, 5.26 µmol) and the solution was stirred at 22 °C for 30 min. Sat. aq. $NaHCO_3$ (3 mL) was added and the solution was extracted with CH_2Cl_2 (3 × 3 mL). The combined organic layers were dried over $MgSO_4$, filtered, and concentrated *in vacuo* to give the title compound as a white solid (56.0 mg, 55%).
m.p.: 121–123 ºC; **^{1}H NMR** (400 MHz, $CDCl_3$) δ 5.72 (br. s, 1H), 4.47 (s, 1H), 4.45 (s, 2H), 2.96 (qd, *J* = 9.5, 5.7 Hz, 1H), 2.87 (d, *J* = 4.8 Hz, 3H), 2.39 (d, *J* = 5.7 Hz 1H) 1.56 (s, 3H), 1.45 (s, 3H), 1.28 (s, 3H); **^{13}C NMR** (101 MHz, $CDCl_3$) δ 168.8, 126.9 (q, $^1J_{CF}$ = 277.3 Hz), 112.4, 86.7, 83.1, 80.4, 79.7 (q, $^3J_{CF}$ = 2.0 Hz), 53.5, 47.7 (q, $^2J_{CF}$ = 28.7 Hz), 27.4, 26.3, 25.8, 15.6; **^{19}F NMR** (377 MHz, $CDCl_3$) δ -68.23; **IR** (neat) cm^{-1}: 3394 (s, N–H), 1683 (s, C=O), 1567 (s, N–H); **HRMS** (ESI) calcd for $[C_{13}H_{19}F_3NO_4]$ $[M+H]^+$ 310.1261, found 310.1261.

(1*S,2*R**,3*R**,4*R**,5*S**,6*R**)-5,6-Dihydroxy-1-methyl-3-(trifluoromethyl)-7-oxabicyclo [2.2.1]heptane-2-carboxylic acid (2.36)**

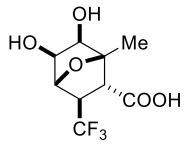

To a solution of **2.8** (2.00 g, 9.00 mmol) in THF/H_2O (9:1, 15 mL) was added *N*-methylmorpholine oxide (1.58 g, 13.5 mmol) and $K_2OsO_4 \cdot (H_2O)_2$ (166 mg, 0.450 mmol) and the turbid reaction mixture was stirred at 22 °C for 2 h. THF (5 mL) was added and the mixture was dried over $MgSO_4$, filtered, and concentrated *in vacuo*. The crude product was purified by flash column chromatography (EtOAc/AcOH 98:2) to give the title compound as a green solid (1.34 g, 58%).
***R*$_f$** = 0.23 (EtOAc/AcOH 98:2) **m.p.**: 147–149 °C; **^{1}H NMR** (400 MHz, DMSO-d_6) δ 4.14 (s, 1H), 3.87 (d, *J* = 6.1 Hz, 1H), 3.65 (d, *J* = 6.1 Hz, 1H), 3.00 (qd, *J* = 10.1, 5.7 Hz, 1H), 2.58 (d, *J* = 5.7 Hz, 1H), 1.46 (s, 3H); **^{13}C NMR** (101 MHz, DMSO-d_6) δ 170.9, 127.0 (q, $^1J_{CF}$ = 277.6 Hz), 87.2, 80.9 (d, $^3J_{CF}$ = 1.5 Hz), 73.4, 70.5, 51.9, 46.6 (q, $^2J_{CF}$ = 27.2 Hz), 15.5; **^{19}F NMR**: (377 MHz, DMSO-d_6) δ -71.78; **IR** (neat) cm^{-1}: 3232 (s, O–H), 1702 (s, C=O) ; **HRMS** (ESI) calcd for $[C_9H_{12}F_3O_5]$ $[M+H]^+$ 257.0631, found 257.0638.

(1*R,2*R**,3*R**,4*S**)-1-Methyl-3-(trifluoromethyl)-7-oxabicyclo[2.2.1]heptane-2-carboxylic acid (2.246)**

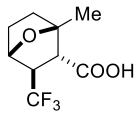

To a solution of **2.8** (253 mg, 1.14 mmol) in MeOH (10 mL) was added 10% Pd/C (125 mg, 0.118 mmol) and the resulting suspension was stirred under an atmosphere of H_2 for 1 h. The suspension was filtered through a pad of celite and concentrated *in vacuo* to give the title compound as a white solid (253 mg, 99%). **m.p.**: 134–136 °C; **^{1}H NMR** (400 MHz, CD_3OD) δ 4.61 (d, *J* = 5.5 Hz, 1H), 3.08 (qd, *J* = 9.9, 5.5 Hz, 1H), 2.73 (dd, *J* = 5.5, 2.2 Hz, 1H), 1.93 (tt, *J* = 12.0, 5.0 Hz, 1H), 1.83 (ddd, *J* = 12.4, 9.0, 4.5 Hz, 1H), 1.69 (ddd, *J* = 12.0, 9.0, 4.5 Hz, 1H), 1.64 (s, 3H), 1.44 (tdd, *J* = 12.4, 4.5, 2.3 Hz, 1H); **^{13}C NMR** (101 MHz, CD_3OD) δ 173.1, 128.1 (q, $^1J_{CF}$ = 276.9 Hz), 87.3, 77.8 (q, $^3J_{CF}$ = 2.5 Hz), 55.8 (d, $^3J_{CF}$ = 1.8 Hz), 52.9 (q, $^2J_{CF}$ = 27.6 Hz), 32.1, 31.9, 20.6; **^{19}F NMR** (377 MHz, CD_3OD) δ -72.35; **IR** (neat) cm-1: 3100 (br., O–H), 1730 (s, C=O); **HRMS** (ESI) calcd for [$C_9H_{12}F_3O_3$] [M+H]+ 225.0733, found 225.0740.

((1*R,2*S**,3*R**,4*S**)-1-Methyl-3-(trifluoromethyl)-7-oxabicyclo[2.2.1]heptan-2-yl) methanol (2.38)**

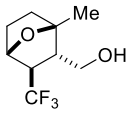

To an ice-cooled solution of **2.246** (2.04 g, 9.08 mmol) in anhydrous THF (16 mL) was added $LiAlH_4$ (2M in THF, 14.0 mL, 28.1 mmol) and the solution was stirred under an atmosphere of N_2 at 22 °C for 3 h. The solution was placed on ice and added water (2.0 mL), 15% aqueous NaOH (2.0 mL), and then water (6.0 mL). Precipitate was removed by filtration and the filtrate was added water (10 mL) and extracted with CH_2Cl_2 (4 × 10 mL). The crude product was purified *in vacuo* in a glass oven B-585 Kugelrohr set at 70 °C to give the title compound as a colorless oil (1.53 g, 80%).
^{1}H NMR (400 MHz, CD_3OD) δ 4.52 (d, *J* = 5.6 Hz, 1H), 3.76 (dd, *J* = 11.6, 5.6 Hz, 1H), 3.60 (dd, *J* = 11.6, 8.5 Hz, 1H), 2.27 (qd, *J* = 9.8, 6.0 Hz, 1H), 2.12 – 1.96 (m, 2H), 1.96 – 1.83 (m, 1H), 1.60 (ddd, *J* = 12.4, 9.2, 4.9 Hz, 1H), 1.52 (s, 3H), 1.39 (tdd, *J* = 12.4, 4.9, 2.1 Hz, 1H); **^{13}C NMR** (101 MHz, CD_3OD) δ 128.5 (d, $^1J_{CF}$ = 275.1 Hz), 87.6, 77.3 (q, $^3J_{CF}$ = 2.7 Hz), 62.6, 52.9 (q, $^2J_{CF}$ = 27.0 Hz), 51.9 (d, $^3J_{CF}$ = 0.7 Hz), 32.1, 30.8, 21.2; **^{19}F NMR** (377 MHz, CD_3OD) δ -71.97; **IR** (neat) cm^{-1}: 3425 (br., O–H); **HRMS** (ESI) calcd for [$C_9H_{14}F_3O_2$] $[M+H]^+$ 211.0940, found 211.0937.

3-(((1*R,2*S**,3*R**,4*S**)-1-Methyl-3-(trifluoromethyl)-7-oxabicyclo[2.2.1]heptan-2-yl) methoxy)pyridine (2.39)**

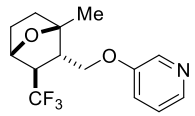

To an ice-cooled solution of **2.38** (100 mg, 0.476 mmol), pyridin-3-ol (91.0 mg, 0.951 mmol), and PPh_3 (250 mg, 0.951 mmol) in anhydrous THF (5 mL) was added DEAD (40% in PhMe, 0.431 mL, 0.859 mmol) dropwise and the reaction mixture was stirred under an atmosphere of N_2 at 22 °C for

5 h. The solution was concentrated *in vacuo* and purified directly by flash column chromatography (EtOAc/heptane 3:2) to give the title compound as a yellow oil (75.0 mg, 55%).
R_f = 0.33 (EtOAc/heptane 3:2); **^{1}H NMR** (400 MHz, CD_3OD) δ 8.27 (dd, *J* = 2.9, 0.7 Hz, 1H), 8.17 (dd, *J* = 4.7, 1.3 Hz, 1H), 7.47 (ddd, *J* = 8.5, 2.9, 1.4 Hz, 1H), 7.40 (ddd, *J* = 8.5, 4.7, 0.7 Hz, 1H), 4.60 (d, *J* = 5.4 Hz, 1H), 4.25 (dd, *J* = 10.1, 5.8 Hz, 1H), 4.16 (dd, *J* = 10.1, 8.3 Hz, 1H), 2.53 (qd, *J* = 9.6, 5.9 Hz, 1H), 2.33 (dtd, *J* = 8.0, 5.8, 2.0 Hz, 1H), 2.05 – 1.84 (m, 2H), 1.71 (ddd, *J* = 12.2, 9.7, 5.1 Hz, 1H), 1.60 (s, 3H), 1.53 – 1.37 (m, 1H); **^{13}C NMR** (101 MHz, $CDCl_3$) δ 154.6, 142.3, 137.2, 129.5 (d, $^1J_{CF}$ = 278.1 Hz), 124.1, 121.6, 85.9, 75.9 (q, $^3J_{CF}$ = 2.4 Hz), 67.4, 51.9 (q, $^2J_{CF}$ = 27.5 Hz), 47.9 (d, $^3J_{CF}$ = 1.4 Hz), 31.5, 30.1, 21.9; **^{19}F NMR** (377 MHz, D_2O) δ -70.27; **IR** (neat) cm^{-1}: 1575 (s, C=C); **HRMS** (ESI) calcd for $[C_{14}H_{17}F_3NO_2]$ $[M+H]^+$ 288.1206, found 288.1210.

(1*R,2*R**,3*R**,4*S**)-*N*-(2-Methoxyethyl)-1-methyl-3-(trifluoromethyl)-7-oxabicyclo[2.2.1] heptane-2-carboxamide (2.40)**

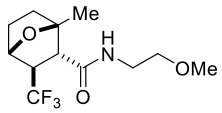

Following *general procedure B* using **2.246** (202 mg, 0.902 mmol) and 2-ethoxyethylamine (120 µL, 1.35 mmol) afforded the title compound as a white solid (207 mg, 82%) after purification by flash column chromatography (EtOAc/heptane 1:1, R_f = 0.26).
m.p.: 68–70 °C; R_f = 0.26 (EtOAc/heptane 1:1); **^{1}H NMR** (400 MHz, CD_3OD) δ 4.61 (d, *J* = 5.3 Hz, 1H), 3.56 – 3.44 (m, 3H), 3.36 (s, 3H), 3.32 – 3.26 (m, 1H), 3.06 (qd, *J* = 10.0, 5.8 Hz, 1H), 2.73 (dd, *J* = 5.8, 2.0 Hz, 1H), 2.02 (ddd, *J* = 12.2, 9.2, 4.6 Hz, 1H), 1.91 (tt, *J* = 12.1, 5.3 Hz, 1H), 1.74 (ddd, *J* = 12.1, 9.2, 4.6 Hz, 1H), 1.57 (s, 3H), 1.34 (tdd, *J* = 12.2, 4.6, 2.1 Hz, 1H); **^{13}C NMR** (101 MHz, CD_3OD) δ 171.3, 128.2 (q, $^1J_{CF}$ = 276.9 Hz), 87.7, 78.2 (q, $^3J_{CF}$ = 2.3 Hz), 71.9, 58.9, 56.4 (d, $^3J_{CF}$ = 1.6 Hz), 52.7 (q, $^2J_{CF}$ = 27.4 Hz), 40.5, 32.2, 31.7, 20.2; **^{19}F NMR** (377 MHz, CD_3OD) δ -72.11; **IR** (neat) cm^{-1}: 3313 (s, N–H), 1644 (s, C=O), 1557 (s, N–H); **HRMS** (ESI) calcd for $[C_{12}H_{18}F_3NO_3]$ $[M+H]^+$ 282.1312, found 282.1316.

(1*R,2*R**,3*R**,4*S**)-*N*-Cyclopropyl-1-methyl-3-(trifluoromethyl)-7-oxabicyclo[2.2.1] heptane-2-carboxamide (2.41)**

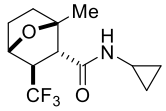

Following *general procedure B* using **2.246** (112 mg, 0.500 mmol) and cyclopropylamine (52 µL, 0.750 mmol) afforded the title compound as a white solid (119 mg, 90%) after purification by flash column chromatography (EtOAc/heptane 2:3).
m.p.: 115–117 °C; R_f = 0.48 (EtOAc/heptane 2:3); **^{1}H NMR** (400 MHz, DMSO-d_6) δ 8.23 (d, *J* = 4.1 Hz, 1H), 4.55 (d, *J* = 5.4 Hz, 1H), 2.99 (qd, *J* = 10.4, 5.8 Hz, 1H), 2.67 (ddt, *J* = 11.3, 7.2, 4.1 Hz, 1H), 2.54 (dd, *J* = 5.8, 2.0 Hz, 1H), 1.88 (ddd, *J* = 12.0, 9.2, 4.6 Hz, 1H), 1.83 –

1.68 (m, 1H), 1.62 (ddd, *J* = 11.8, 9.2, 4.6 Hz, 1H), 1.42 (s, 3H), 1.21 (tdd, *J* = 12.0, 4.6, 2.0 Hz, 1H), 0.71 – 0.59 (m, 2H), 0.46 – 0.31 (m, 2H); **^{13}C NMR** (101 MHz, DMSO-d_6) δ 169.3, 127.0 (d, $^{1}J_{CF}$ = 277.8 Hz), 85.7, 75.9 (d, $^{3}J_{CF}$ = 2.4 Hz), 54.3, 50.6 (q, $^{2}J_{CF}$ = 26.4 Hz), 31.0, 30.2, 22.5, 19.9, 6.1, 5.7; **^{19}F NMR** (377 MHz, D_2O) δ -70.64; **IR** (neat) cm^{-1}: 3310 (s, N–H), 1661 (s, C=O), 1531 (s, N–H); **HRMS** (ESI) calcd for [$C_{12}H_{17}F_3NO_2$] [M+H]+ 264.1206, found.264.1217.

(1*R,2*R**,3*R**,4*S**)-1-Methyl-*N*-(pyridin-3-yl)-3-(trifluoromethyl)-7-oxabicyclo[2.2.1] heptane-2-carboxamide (2.42)**

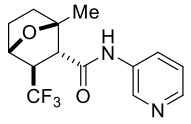

Following *general procedure B* using **2.246** (117 mg, 0.522 mmol) and 3-aminopyridine (100 µL, 0.574 mmol) with a reaction time of 18 h afforded the title compound as a beige solid (68.0 mg, 44%) after purification by flash column chromatography (EtOAc/heptane/Et_3N 60:40:1).

m.p.: 124–125 °C; ***R*$_f$** = 0.20 (EtOAc/heptane/Et_3N 60:40:1); **^{1}H NMR** (400 MHz, DMSO-d_6) δ 10.80 (s, 1H), 8.34 (ddd, *J* = 4.8, 2.0, 1.0 Hz, 1H), 8.09 (dt, *J* = 8.4, 1.0 Hz, 1H), 7.80 (ddd, *J* = 8.4, 7.4, 2.0 Hz, 1H), 7.14 (ddd, *J* = 7.4, 4.8, 1.0 Hz, 1H), 4.62 (d, *J* = 5.3 Hz, 1H), 3.19 (dd, *J* = 6.1, 1.6 Hz, 1H), 3.07 (qd, *J* = 10.4, 6.0 Hz, 1H), 1.94 (ddd, *J* = 12.1, 9.2, 4.6 Hz, 1H), 1.90 – 1.76 (m, 1H), 1.71 (ddd, *J* = 11.9, 9.2, 4.6 Hz, 1H), 1.55 (s, 3H), 1.28 (tdd, *J* = 12.1, 4.6, 1.8 Hz, 1H); **^{13}C NMR** (101 MHz, DMSO-d_6) δ 168.4, 151.6, 148.1, 138.3, 125.4 (observed by HMBC), 119.9, 113.8, 86.3, 76.1, 54.7, 50.8 (d, $^{2}J_{CF}$ = 25.6 Hz), 31.0, 30.3, 19.7; **^{19}F NMR** (377 MHz, D_2O) δ -70.59; **IR** (neat) cm^{-1}: 3239 (s, N–H), 1697 (s, C=O), 1594 (s, N–H), 1528 (s, C=C); **HRMS** (ESI) calcd for [$C_{14}H_{16}F_3N_2O_2$] $[M+H]^+$ 301.1158, found. 301.1144.

(1*R,2*R**,3*R**,4*S**)-1-Methyl-*N*-(pyridin-3-yl)-3-(trifluoromethyl)-7-oxabicyclo [2.2.1] heptane-2-carboxamide (2.43)**

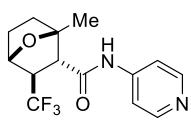

Following *general procedure B* using **2.246** (112 mg, 0.500 mmol) and 4-aminopyridine (96 µL, 0.550 mmol) with a reaction time of 18 h afforded the title compound as a white amorphous solid (141 mg, 94%) after purification by flash column chromatography (EtOAc/Et_3N 99:1).

***R*$_f$** = 0.38 (EtOAc/Et_3N 99:1); **^{1}H NMR** (400 MHz, DMSO-d_6) δ 10.60 (s, 1H), 8.53 – 8.37 (m, 2H), 7.69 – 7.49 (m, 2H), 4.65 (d, *J* = 5.3 Hz, 1H), 3.09 (qd, *J* = 10.0, 5.8 Hz, 1H), 2.93 (dd, *J* = 5.8, 1.8 Hz, 1H), 2.69 (s, 4H), 1.94 (ddd, *J* = 12.0, 9.2, 4.6 Hz, 1H), 1.84 (tq, *J* = 10.0, 5.0 Hz, 1H), 1.72 (ddd, *J* = 12.0, 9.2, 4.6 Hz, 1H), 1.55 (s, 3H), 1.30 (tdd, *J* = 12.0, 4.6, 1.8 Hz, 1H); **^{13}C NMR** (101 MHz, DMSO-d_6) δ 168.6, 150.5 (2C), 145.1, 126.8 (q, $^{1}J_{CF}$ = 277.8 Hz), 113.5 (2C), 86.2, 76.2 (d, $^{3}J_{CF}$ = 2.1 Hz), 55.5, 50.9 (q, $^{2}J_{CF}$ = 26.6 Hz), 30.9, 30.2, 19.9; **^{19}F NMR** (377 MHz, DMSO-d_6) δ -69.10; **IR** (neat) cm^{-1}: 3239 (s, N–H), 1697 (s, C=O), 1594 (s,

N–H), 1528 (s, C=C); **HRMS** (ESI) calcd for [$C_{14}H_{16}F_3N_2O_2$] [M+H]+ 301.1158, found 301.1143.

((1*R,2*R**,3*R**,4*S**)-1-Methyl-3-(trifluoromethyl)-7-oxabicyclo[2.2.1]heptan-2-yl) (morpholino)methanone (2.247)**

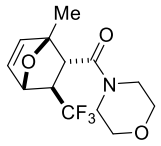

Following *general procedure B* using **2.8** (208 mg, 0.900 mmol) and morpholine (120 µL, 1.35 mmol) afforded the title compound as a brown oil (150 mg, 58%) after purification by flash column chromatography (EtOAc/heptane 2:3).

***R*f** = 0.48 (EtOAc/heptane 3:2); **m.p.**: 99–101 °C; **^{1}H NMR** (400 MHz, DMSO-d_6) δ 6.54 (dd, *J* = 5.6, 1.9 Hz, 1H), 6.06 (d, *J* = 5.6 Hz, 1H), 5.00 (d, *J* = 1.9 Hz, 1H), 3.78 – 3.35 (m, 8H), 3.20 (d, *J* = 4.9 Hz,1H), 2.78 (qd, *J* = 10.2, 4.9 Hz, 1H), 1.62 (s, 3H); **^{13}C NMR** (101 MHz, DMSO-d_6) δ 167.0, 137.4, 135.6, 127.3 (d, $^1J_{CF}$ = 283.3 Hz), 88.4, 78.2 (q, $^3J_{CF}$ = 2.3 Hz), 66.5, 66.2, 51.1 (q, $^2J_{CF}$ = 26.3 Hz), 46.5, 44.6, 42.6, 17.5; **^{19}F NMR** (377 MHz, DMSO-d_6) δ -66.19; **IR** (neat) cm^{-1}: 1625 (s, C=O); **HRMS** (ESI) calcd for [$C_{13}H_{17}F_3NO_3$] $[M+H]^+$ 292.1155, found 292.1159.

Intramolecular Diels Alder

(3a*S**,6*R**,7*R**,7a*R**)-2-Methyl-7-(trifluoromethyl)-2,3,7,7a-tetrahydro-3a,6-epoxy-isoindol-1(6*H*)-one (2.44)

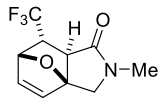

Following *general procedure A* using (*E*)-4,4,4-trifluorocrotonic acid **2.1** (925 mg, 6.41 mmol) and *N*-methylfurfurylamine (748 mg, 6.73 mmol) afforded the crude amide, which was suspended in PhMe (320 mL) and refluxed for 16 h. The reaction mixture was concentrated *in vacuo* and the crude product was purified by flash column chromatography (EtOAc/heptane 2:1) to give the title compound as an off-white solid (1.60 g, 95%).

R_f = 0.29 (EtOAc/heptane 2:1); **m.p.:** 120–122 °C; **^{1}H NMR** (400 MHz, DMSO-d_6) δ 6.73 (d, J = 5.7 Hz, 1H), 6.44 – 6.36 (m, 1H), 5.21 (dd, J = 4.3, 1.6 Hz, 1H), 4.10 (d, J = 11.8 Hz, 1H), 3.56 (d, J = 11.8 Hz, 1H), 3.11 (qt, J = 9.9, 4.3 Hz, 1H), 2.78 (s, 3H), 2.59 (d, J = 4.4 Hz, 1H); **^{13}C NMR** (101 MHz, DMSO-d_6) δ 170.6, 136.2, 133.5, 125.4 (q, $^1J_{CF}$ = 277.2 Hz), 90.6, 78.0 (q, $^3J_{CF}$ = 2.8 Hz), 50.5, 49.4 (q, $^3J_{CF}$ = 1.8 Hz), 44.8 (q, $^2J_{CF}$ = 27.1 Hz), 29.4; **^{19}F NMR** (377 MHz, DMSO-d_6) δ -64.18; **IR** (neat) cm^{-1}: 3073 (s, C=C–H), 1687 (s, C=O), 1634 (s, C=C); **HRMS** (ESI) calcd for $C_{10}H_{11}F_3NO_2$ $[M+H]^+$ 234.0736, found 234.0736.

N-Benzylfurfurylamine (2.248)

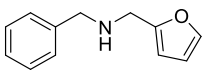

Following *general procedure C* using benzylamine (3.12 mL, 28.6 mmol) afforded the title compound as a colorless oil (4.85 g, 91%) after purification by flash column chromatography (EtOAc/heptane/Et_3N 20:80:1).

R_f = 0.21 (EtOAc/heptane/Et_3N 20:80:1); **^{1}H NMR** (400 MHz, $CDCl_3$) δ 7.38 (dd, J = 1.9, 0.8 Hz, 1H), 7.36 – 7.30 (m, 4H), 7.29 – 7.23 (m, 1H), 6.33 (dd, J = 3.2, 1.8 Hz, 1H), 6.22 – 6.12 (m, 1H), 3.80 (s, 4H); **^{13}C NMR** (101 MHz, $CDCl_3$) δ 153.8, 141.9, 139.8, 128.4 (2C), 128.3 (2C), 127.1, 110.1, 107.1, 52.8, 45.4. All spectroscopic data were consistent with those in the literature.[349]

(3a*S**,6*R**,7*R**,7*aR**)-2-Benzyl-7-(trifluoromethyl)-2,3,7,7a-tetrahydro-3a,6-epoxyiso-indol-1(6*H*)-one (2.45)

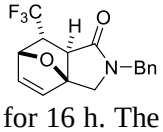

Following *general procedure A* using (*E*)-4,4,4-trifluorocrotonic acid **2.1** (2.66 g, 18.4 mmol) and *N*-benzylfurfurylamine **2.248** (3.55 g, 19.0 mmol) afforded the crude amide, which was suspended in PhMe (95 mL) and refluxed for 16 h. The reaction mixture was concentrated *in vacuo* and the crude product was purified

by flash column chromatography (EtOAc/heptane 3:7) to give the title compound as an off-white solid (1.60 g, 95%).

R_f = 0.27 (EtOAc/heptane 3:7); **m.p.**: 126–128 °C; **^{1}H NMR** (400 MHz, DMSO-d_6) δ 7.38 – 7.31 (m, 2H), 7.31 – 7.21 (m, 3H), 6.72 (d, J = 5.7 Hz, 1H), 6.41 (dp, J = 5.1, 1.7 Hz, 1H), 5.24 (dd, J = 4.3, 1.6 Hz, 1H), 4.48 (d, J = 15.3 Hz, 1H), 4.42 (d, J = 15.2 Hz, 1H), 4.02 (d, J = 11.9 Hz, 1H), 3.50 (d, J = 11.9 Hz, 1H), 3.21 (qt, J = 10.0, 4.3 Hz, 1H), 2.77 (d, J = 4.3 Hz, 1H); **^{13}C NMR** (101 MHz, DMSO-d_6) δ 171.5, 136.9, 136.7, 134.1, 129.0 (2C), 127.9 (2C), 127.7, 124.6 (q, $^1J_{CF}$ = 277.5 Hz), 91.1, 78.6 (q, $^3J_{CF}$ = 2.7 Hz), 50.0 (d, $^3J_{CF}$ = 1.9 Hz), 48.8, 46.0, 45.4 (q, $^2J_{CF}$ = 27.0 Hz); **^{19}F NMR** (377 MHz, DMSO-d_6) δ -64.13; **IR** (neat) cm^{-1}: 3030 (m, C=C–H), 1667 (s, C=O); **HRMS** (ESI) calcd for $C_{16}H_{15}F_3NO_2$ $[M+H]^+$ 310.1049, found 310.1048.

N-2-Methoxyethylfurfurylamine (2.249)

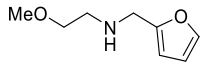

Following *general procedure C* using 2-methoxyethylamine (4.05 mL, 46.6 mmol) afforded the title compound as a yellow oil (6.60 g, 91%) after purification by flash column chromatography (EtOAc/heptane/Et_3N 50:50:1).

R_f = 0.26 (EtOAc/heptane/Et_3N 50:50:1); **^{1}H NMR** (400 MHz, $CDCl_3$) δ 7.33 (dd, J = 1.9, 0.8 Hz, 1H), 6.28 (dd, J = 3.2, 1.9 Hz, 1H), 6.16 (dd, J = 3.2, 0.8 Hz, 1H), 3.78 (d, J = 0.7 Hz, 2H), 3.54 – 3.44 (m, 2H), 3.33 (s, 3H), 2.81 – 2.74 (m, 2H); **^{13}C NMR** (101 MHz, $CDCl_3$) δ 153.9, 141.9, 110.2, 107.0, 72.0, 58.9, 48.5, 46.3; **IR** (neat) cm^{-1}: 3333 (br., N–H), 1530 (m, C=C); **HRMS** (ESI) calcd for $[C_8H_{14}NO_2]$ $[M+H]^+$ 156.1019, found 156.0992.

(3a*S**,6*R**,7*R**,7a*R**)-2-(2-Methoxyethyl)-7-(trifluoromethyl)-2,3,7,7a-tetrahydro-3a,6-epoxyisoindol-1(6*H*)-one (2.46)

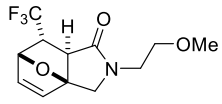

Following *general procedure A* using (*E*)-4,4,4-trifluorocrotonic acid **2.1** (2.02 g, 14.0 mmol) and *N*-2-methoxyethylfurfurylamine **2.249** (2.28 g, 14.7 mmol) afforded the crude amide, which was suspended in PhMe (700 mL) and refluxed for 16 h. The reaction mixture was concentrated *in vacuo* and the crude product was purified by flash column chromatography (EtOAc/heptane 2:1) to give the title compound as a yellow oil (2.34 g, 60%).

R_f = 0.30 (EtOAc/heptane 2:1); **^{1}H NMR** (400 MHz, DMSO-d_6) δ 6.74 (d, J = 5.8 Hz, 1H), 6.41 (dp, J = 5.2, 1.7 Hz, 1H), 5.21 (dd, J = 4.3, 1.7 Hz, 1H), 4.14 (d, J = 12.0 Hz, 1H), 3.65 (d, J = 12.0 Hz, 1H), 3.57 – 3.48 (m, 1H), 3.44 (p, J = 5.2 Hz, 2H), 3.28 – 3.26 (m, 1H), 3.27 – 3.2 (m, 4H), 2.62 (d, J = 4.3 Hz, 1H); **^{13}C NMR** (101 MHz, DMSO-d_6) δ 170.7, 136.2, 133.6, 125.4 (q, $^1J_{CF}$ = 277.1 Hz), 90.7, 78.0 (q, $^3J_{CF}$ = 2.8 Hz), 69.5, 57.9, 49.5 (d, $^3J_{CF}$ = 1.9 Hz), 49.4, 44.8 (q, $^2J_{CF}$ = 27.1 Hz), 41.8; **^{19}F NMR** (377 MHz, DMSO-d_6) δ -64.16; **IR** (neat) cm^{-1}: 1675 (s, C=O); **HRMS** (ESI) calcd for $C_{12}H_{14}F_3NO_3$ $[M+H]^+$ 278.0999, found 278.0999.

***N*-Allylfurfurylamine (2.250)**

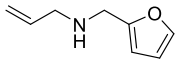

Following *general procedure C* using allylamine (1.83 mL, 24.5 mmol) afforded the title compound as a yellow oil (2.69 g, 80%) after purification by flash column chromatography (EtOAc/heptane/Et_3N 40:60:1).

$\boldsymbol{R_f}$ = 0.26 (EtOAc/heptane/Et_3N 40:60:1); **^{1}H NMR** (400 MHz, $CDCl_3$) δ 7.34 (dd, *J* = 1.9, 0.8 Hz, 1H), 6.29 (dd, *J* = 3.2, 1.8 Hz, 1H), 6.16 (dd, *J* = 3.2, 0.8 Hz, 1H), 5.89 (ddt, *J* = 17.2, 10.3, 6.0 Hz, 1H), 5.18 (dq, *J* = 17.2, 1.6 Hz, 1H), 5.10 (dq, *J* = 10.2, 1.4 Hz, 1H), 3.77 (s, 2H), 3.24 (dt, *J* = 6.0, 1.5 Hz, 2H); **^{13}C NMR** (101 MHz, $CDCl_3$) δ 153.9, 141.9, 136.5, 116.4, 110.2, 107.1, 51.5, 45.4. All spectroscopic data were consistent with those in the literature.[350]

(3a*S,6*R**,7*R**,7a*R**)-2-Allyl-7-(trifluoromethyl)-2,3,7,7a-tetrahydro-3a,6-epoxyisoindol-1(6*H*)-one (2.47)**

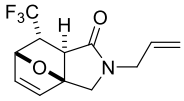

Following *general procedure A* using (*E*)-4,4,4-trifluorocrotonic acid **2.1** (1.47 g, 10.2 mmol) and *N*-allylfurfurylamine **2.250** (1.47 g, 10.7 mmol) afforded the crude amide, which was suspended in PhMe (500 mL) and refluxed for 16 h. The reaction mixture was concentrated *in vacuo* and the crude product was purified by flash column chromatography (EtOAc/heptane 1:1) to give the title compound as an off-white solid (1.98 g, 75%).

$\boldsymbol{R_f}$ = 0.35 (EtOAc/heptane 1:1); **m.p.**: 126–128 °C; **^{1}H NMR** (400 MHz, $CDCl_3$) δ 6.58 (d, *J* = 5.8 Hz, 1H), 6.41 (dp, *J* = 5.2, 1.7 Hz, 1H), 5.74 (ddt, *J* = 17.3, 9.9, 5.9 Hz, 1H), 5.27 – 5.18 (m, 2H), 5.16 (dd, *J* = 4.3, 1.7 Hz, 1H), 4.05 – 3.88 (m, 3H), 3.64 (d, *J* = 12.0 Hz, 1H), 3.23 (qt, *J* = 9.2, 4.3 Hz, 1H), 2.58 (d, *J* = 4.2 Hz, 1H); **^{13}C NMR** (101 MHz, $CDCl_3$) δ 170.9, 135.0, 134.7, 131.7, 124.9 (q, $^1J_{CF}$ = 277.1 Hz), 118.3, 90.5, 78.8 (q, $^3J_{CF}$ = 2.8 Hz), 50.2 (d, $^3J_{CF}$ = 1.8 Hz), 48.8, 45.7 (q, $^2J_{CF}$ = 28.3 Hz), 45.4; **^{19}F NMR** (377 MHz, $CDCl_3$) δ -65.58; **IR** (neat) cm^{-1}: 3024 (m, C=C–H), 1673 (s, C=O), 1646 (s, C=C); **HRMS** (ESI) calcd for $C_{12}H_{13}F_3NO_2$ $[M+H]^+$ 260.0893, found 260.0894.

(3a*S,4*S**,5*R**,6*S**,7*R**,7a*R**)-4,5-Dihydroxy-2-methyl-7-(trifluoromethyl)hexahydro-3a,6-epoxyisoindol-1(4*H*)-one (2.49)**

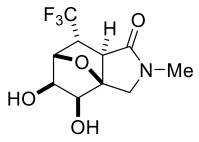

To a solution of **2.44** (794 mg, 3.06 mmol, 90% purity) in THF/H_2O (4:1, 35 mL), was added *N*-methylmorpholine oxide (538 mg, 4.60 mmol) and $K_2OsO_4 \cdot (H_2O)_2$ (56.5 mg, 0.153 mmol) and the reaction mixture was stirred 2 h at 21 °C. The reaction was dried over $MgSO_4$ and concentrated *in vacuo*. The crude product was purified by flash column chromatography (EtOAc) to give the title compound as a beige solid (668 mg, 82%).

R_f = 0.30 (EtOAc); **m.p.**: 195–197 °C; **^{1}H NMR** (400 MHz, DMSO-d_6) δ 5.12 (d, J = 6.0 Hz, 1H), 4.97 (d, J = 6.3 Hz, 1H), 4.32 (d, J = 5.0 Hz, 1H), 4.11 (t, J = 6.0 Hz, 1H), 3.97 (t, J = 6.3 Hz, 1H), 3.72 (d, J = 12.0 Hz, 1H), 3.42 (d, J = 12.0 Hz, 1H), 2.90 (qt, J = 10.4, 5.0 Hz, 1H), 2.79 (d, J = 5.5 Hz, 1H), 2.76 (s, 3H); **^{13}C NMR** (101 MHz, DMSO-d_6) δ 170.9, 125.8 (q, $^1J_{CF}$ = 277.5 Hz), 90.6, 82.1 (d, $^3J_{CF}$ = 2.4 Hz), 71.0, 70.7 (q, $^3J_{CF}$ = 2.7 Hz), 49.2, 47.1 (d, $^3J_{CF}$ = 2.6 Hz), 45.7 (q, $^2J_{CF}$ = 27.6 Hz), 29.5; **^{19}F NMR** (377 MHz, DMSO-d_6) δ -68.54; **IR** (neat) cm^{-1}: 3481 (s, O–H), 3317 (br., O–H), 1683 (s, C=O); **HRMS** (ESI) calcd for $C_{10}H_{12}F_3NO_4$ $[M+H]^+$ 268.0791, found 268.0792.

(3a*S,4*S**,5*R**,6*S**,7*R**,7a*R**)-2-Benzyl-4,5-dihydroxy-7-(trifluoromethyl)hexahydro-3a,6-epoxyisoindol-1(4*H*)-one (2.50)**

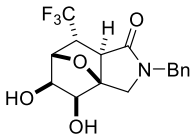

To a solution of **2.45** (2.13 g, 6.89 mmol) in THF/H_2O (5:1, 60 mL), was added *N*-methylmorpholine oxide (1.29 g, 11.0 mmol) and $K_2OsO_4{\cdot}(H_2O)_2$ (127 mg, 344 µmol) and the reaction mixture was stirred 2 h at 21 °C. THF was removed *in vacuo* and then added sat. aq. $NaHCO_3$ (30 mL). The aqueous phase was extracted with CH_2Cl_2 (3x 60 mL) and the combined organic layers were dried over $MgSO_4$ and concentrated *in vacuo*. The crude product was purified by flash column chromatography (EtOAc/heptane 1:1) to give the title compound as a beige amorphous solid (2.10 g, 89%).

R_f = 0.22 (EtOAc/heptane 1:1); **^{1}H NMR** (400 MHz, $CDCl_3$) δ 7.37 – 7.26 (m, 3H), 7.24 – 7.18 (m, 2H), 4.56 – 4.38 (m, 4H), 4.01 (d, J = 5.8 Hz, 1H), 3.64 (d, J = 12.3 Hz, 1H), 3.49 (d, J = 12.4 Hz, 1H), 3.13 (br. s, 2H), 3.05 (tt, J = 9.9, 5.1 Hz, 1H), 2.65 (d, J = 5.0 Hz, 1H); **^{13}C NMR** (101 MHz, $CDCl_3$) δ 171.1, 135.5, 129.1 (2C), 128.2 (2C), 128.1, 125.2 (d, $^1J_{CF}$ = 277.5 Hz), 90.9, 82.6 (q, $^3J_{CF}$ = 2.1 Hz), 72.4, 72.0 (q, J = 2.8 Hz), 48.2 (q, $^3J_{CF}$ = 1.9 Hz) 47.2 (2C), 46.8 (q, $^2J_{CF}$ = 29.0 Hz); **^{19}F NMR** (377 MHz, $CDCl_3$) δ -64.89; **IR** (neat) cm^{-1}: 3389 (br., O–H), 3032 (m, C=C–H), 1670 (s, C=O), 1532 (m, C=C); **HRMS** (ESI) calcd for $[C_{16}H_{17}F_3NO_4]$ $[M+H]^+$ 344.1104, found 344.1100.

(3a*S,4*S**,5*R**,6*S**,7*R**,7a*R**)-4,5-Dihydroxy-2-(2-methoxyethyl)-7-(trifluoromethyl)hexahydro-3a,6-epoxyisoindol-1(4*H*)-one (2.51)**

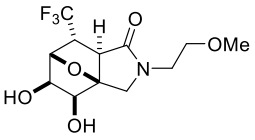

To a solution of **2.46** (460 mg, 1.66 mmol) in THF/H_2O (4:1, 15 mL), was added *N*-methylmorpholine oxide (311 mg, 2.65 mmol) and $K_2OsO_4{\cdot}(H_2O)_2$ (30.6 mg, 83.0 µmol) and the reaction mixture was stirred 2 h at 21 °C. The reaction was dried over $MgSO_4$ and concentrated *in vacuo*. The crude product was purified by flash column chromatography (CH_2Cl_2/MeOH 9:1) to give the title compound as a light-yellow solid (436 mg, 84%).

R_f = 0.48 (CH_2Cl_2/MeOH 9:1); **m.p.**: 109–111 °C; **^{1}H NMR** (400 MHz, DMSO-d_6) δ 5.06 (d, J = 5.9 Hz, 1H), 4.94 (d, J = 6.1 Hz, 1H), 4.33 (d, J = 5.0 Hz, 1H), 4.12 (t, J = 5.9 Hz, 1H), 3.99 (t, J = 6.1 Hz, 1H), 3.76 (d, J = 12.0 Hz, 1H), 3.53 (d, J = 12.1 Hz, 1H), 3.50 – 3.39 (m, 3H), 3.31 – 3.28 (m, 1H), 3.25 (s, 3H), 2.90 (qt, J = 10.2, 5.0 Hz, 1H), 2.83 (d, J = 5.4 Hz, 1H); **^{13}C NMR** (101 MHz, DMSO-d_6) δ 170.9, 125.7 (q, $^1J_{CF}$ = 277.8 Hz), 90.7, 82.0 (d, $^3J_{CF}$ = 2.4 Hz), 71.0, 70.6 (d, $^3J_{CF}$ = 3.0 Hz), 69.6, 57.9, 48.07, 47.1 (d $^3J_{CF}$ = 2.6 Hz), 45.7 (q, $^2J_{CF}$ = 27.6 Hz), 41.9; **^{19}F NMR** (377 MHz, DMSO-d_6) δ -63.23; **IR** (neat) cm^{-1}: 3471 (s, O–H), 3306 (br., O–H), 1667 (s, C=O); **HRMS** (ESI) calcd for $C_{12}H_{17}F_3NO_5$ $[M+H]^+$ 312.1053, found 312.1053.

(3a*R**,7*S**,8*R**,8a*R**)-2,5-Dimethyl-8-(trifluoromethyl)octahydro-1*H*-3a,7-epoxypyrrolo[3,4-*c*]azepin-1-one (2.52)

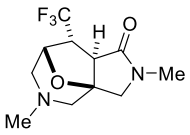

Following *general procedure D* using **2.49** (105 mg, 393 µmol) and methylamine (33% in EtOH, 1.95 mL, 15.7 mmol) afforded title compound as a white solid (66.0 mg, 64%) after purification by flash column chromatography (EtOAc/heptane/Et_3N 70:30:2).

R_f = 0.25 (EtOAc/heptane 7:3); **m.p.**: 96–98 °C; **^{1}H NMR** (400 MHz, DMSO-d_6) δ 4.49 (d, J = 6.4 Hz, 1H), 3.40 (d, J = 11.4 Hz, 1H), 3.29 (d, J = 11.4 Hz, 1H), 3.15 (d, J = 6.1 Hz, 1H), 3.02 (qt, J = 10.4, 6.2 Hz, 1H), 2.81 (d, J = 10.8 Hz, 1H), 2.72 (d, J = 0.7 Hz, 3H), 2.67 (d, J = 12.2 Hz, 1H), 2.29 – 2.23 (m, 2H), 2.18 (s, 3H); **^{13}C NMR** (101 MHz, DMSO-d_6) δ 171.9, 126.3 (q, $^1J_{CF}$ = 278.3 Hz), 83.9, 75.8 (d, $^3J_{CF}$ = 2.3 Hz), 58.9, 54.6, 54.3, 49.7 (q, $^3J_{CF}$ = 1.8 Hz), 49.1 (q, $^2J_{CF}$ = 28.4 Hz), 45.0, 29.7; **^{19}F NMR** (377 MHz, DMSO-d_6) δ -63.73; **IR** (neat) cm^{-1}: 1687 (s, C=O); **HRMS** (ESI) calcd for $C_{11}H_{16}F_3N_2O_2$ $[M+H]^+$ 265.1158, found 265.1158.

(3a*R**,7*S**,8*R**,8a*R**)-5-Benzyl-2-methyl-8-(trifluoromethyl)octahydro-1*H*-3a,7-epoxypyrrolo[3,4-*c*]azepin-1-one (2.53)

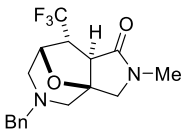

Following *general procedure D* using **2.49** (108 mg, 393 µmol) and benzylamine (52.9 µL, 484 µmol) afforded title compound as a white solid (85.5 mg, 63%) after purification by flash column chromatography (EtOAc/heptane 3:2).

R_f = 0.29 (EtOAc/heptane 3:2); **m.p.**: 119–121 °C; **^{1}H NMR** (400 MHz, $CDCl_3$) δ 7.35 – 7.25 (m, 5H), 4.48 (d, J = 6.4 Hz, 1H), 3.71 (d, J = 12.9 Hz, 1H), 3.52 – 3.27 (m, 3H), 3.25 (d, J = 11.3 Hz, 1H), 3.10 (qt, J = 9.7, 6.1 Hz, 1H), 2.95 (d, J = 12.2 Hz, 1H), 2.82 (s, 3H), 2.76 – 2.56 (m, 2H), 2.39 (d, J = 11.0 Hz, 1H); **^{13}C NMR** (101 MHz, $CDCl_3$) δ 170.1, 135.1, 127.2 (2C), 126.6 (2C), 125.7, 123.6 (q, $^1J_{CF}$ = 278.2 Hz), 81.7, 74.5, 60.0, 54.5, 53.0, 51.1, 47.9 (q, $^2J_{CF}$ = 29.4 Hz), 47.8, 28.0; **^{19}F NMR** (377 MHz, $CDCl_3$) δ -64.99; **IR** (neat) cm^{-1}: 1681 (s, C=O); **HRMS** (ESI) calcd for $C_{17}H_{20}F_3N_2O_2$ $[M+H]^+$ 341.1471, found 341.1471.

3a*R*,7*S**,8*R**,8a*R**)-5-(2-Methoxyethyl)-2-methyl-8-(trifluoromethyl)octahydro-1*H*-3a,7-epoxypyrrolo[3,4-*c*]azepin-1-one (2.54)**

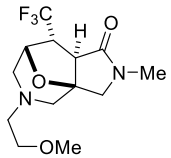

Following *general procedure D* using **2.49** (102 mg, 382 µmol) and methylamine (33% in EtOH, 1.95 mL, 15.7 mmol) afforded title compound as a light yellow oil (72.0 mg, 61%) after purification by flash column chromatography (EtOAc/heptane/Et_3N 60:10:1).

***R*f** = 0.26 (EtOAc/heptane 6:1); **^{1}H NMR** (400 MHz, CD_3OD) δ 4.57 (d, *J* = 6.3 Hz, 1H), 3.60 (td, *J* = 5.6, 1.3 Hz, 2H), 3.56 (d, *J* = 11.6 Hz, 1H), 3.48 (d, *J* = 9.5 Hz, 1H), 3.46 (d, *J* = 4.3 Hz, 1H), 3.42 (s, 3 H), 3.20 – 3.07 (m, 1H), 3.04 – 2.97 (m, 2H), 2.94 (s, 3H), 2.70 (td, *J* = 5.6, 1.5 Hz, 2H), 2.64 (d, *J* = 10.9 Hz, 1H), 2.59 (dd, *J* = 12.2, 2.8 Hz, 1H); **^{13}C NMR** (101 MHz, CD_3OD) δ 174.7, 127.1 (q, $^1J_{CF}$ = 277.6 Hz), 85.1, 77.8 (q, $^3J_{CF}$ = 2.2 Hz), 71.6, 58.8, 58.6, 57.4, 56.0, 53.8, 51.2 (q, $^3J_{CF}$ = 1.9 Hz), 51.0 (q, $^2J_{CF}$ = 29.3 Hz), 30.1; **^{19}F NMR** (377 MHz, CD_3OD) δ -66.24; **IR** (neat) cm^{-1}: 1690 (s, C=O); **HRMS** (ESI) calcd for $C_{13}H_{20}F_3N_2O_3$ $[M+H]^+$ 309.1421, found 309.1422.

(3a*R,7*S**,8*R**,8a*R**)-2-(2-Methoxyethyl)-5-methyl-8-(trifluoromethyl)octahydro-1*H*-3a,7-epoxypyrrolo[3,4-*c*]azepin-1-one (2.55)**

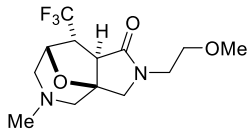

Following *general procedure D* using **2.51** (144 mg, 463 µmol) and methylamine (85.8 µL, 689 µmol) afforded title compound as a colorless oil (84.0 mg, 59%) after purification by flash column chromatography (EtOAc/heptane/Et_3N 70:30:2).

***R*f** = 0.24 (EtOAc/heptane 7:3); **^{1}H NMR** (400 MHz, CD_3OD) δ 4.38 (d, *J* = 6.6 Hz, 1H), 3.45 – 3.39 (m, 5H), 3.32 – 3.25 (m, 1H), 3.25 – 3.22 (m, 4H), 2.94 (qt, *J* = 9.9, 6.2 Hz, 1H), 2.75 – 2.66 (m, 2H), 2.31 – 2.21 (m, 2H), 2.16 (s, 3H); **^{13}C NMR** (101 MHz, CD_3OD) δ 174.9, 128.5 (q, $^1J_{CF}$ = 277.3 Hz), 85.2, 77.6 (q, $^3J_{CF}$ = 1.9 Hz), 71.0, 60.0, 58.9, 55.4, 55.0, 51.4 (q, $^3J_{CF}$ = 1.9 Hz), 51.1 (q, $^2J_{CF}$ = 29.2 Hz), 44.9, 43.8; **^{19}F NMR** (377 MHz, CD_3OD) δ -66.51; **IR** (neat) cm^{-1}: 1689 (s, C=O); **HRMS** (ESI) calcd for $C_{13}H_{20}F_3N_2O_3$ $[M+H]^+$ 309.1421, found 309.1421.

(3a*R,7*S**,8*R**,8a*R**)-2-Benzyl-5-methyl-8-(trifluoromethyl)octahydro-1*H*-3a,7-epoxypyrrolo[3,4-*c*]azepin-1-one (2.56)**

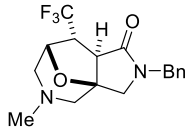

To a solution of **2.50** (110 mg, 320 µmol) in MeOH/H_2O (9:1, 4 mL), was added $NaIO_4$ (137 mg, 641 µmol) and the suspension was stirred 2 h at 21 °C. Then, MeOH was removed *in vacuo* and the crude was suspended in sat. aq. $NaHCO_3$ (4 mL) and extracted with CH_2Cl_2 (3x 4 mL). The combined organic layers were dried over Na_2SO_4, filtered, and concentrated *in vacuo*. The crude dialdehyde was dissolved in anhydrous MeOH (7 mL), added methylamine (33% in EtOH,

44.0 µL, 354 µmol) and 3Å molecular sieves, and stirred under a N_2 atmosphere for 30 min at 21 °C. The mixture was then cooled to 0 °C and $NaBH_3CN$ (80.8 mg, 1.29 mmol) was added portion wise. After stirring 1 h at 0 °C, cooling was removed and the mixture was stirred 16 h at 21 °C. Molecular sieves were removed by filtration through celite and the filtrate was concentrated *in vacuo*. The crude was purified by flash column chromatography (EtOAc/heptane/Et_3N 33:67:2) to give the title compound as an off-white solid (64.0 mg, 58%). R_f = 0.27 (EtOAc/heptane 1:2); **m.p.**: 78–80 °C; **^{1}H NMR** (400 MHz, CD_3OD) δ 7.54 – 7.16 (m, 5H), 4.64 (d, *J* = 14.9 Hz, 1H), 4.59 (ddd, *J* = 6.4, 2.7, 1.4 Hz, 1H), 4.48 (d, *J* = 14.9 Hz, 1H), 3.51 (d, *J* = 6.0 Hz, 1H), 3.46 – 3.37 (m, 3H), 3.21 (qt, *J* = 9.9, 6.2 Hz, 1H), 2.93 – 2.85 (m, 2H), 2.46 – 2.40 (m, 2H), 2.34 (s, 3H); **^{13}C NMR** (101 MHz, CD_3OD) δ 174.8, 137.1, 129.8 (2C), 129.0 (2C), 128.8, 127.1 (q, $^1J_{CF}$ = 277.5 Hz), 85.0, 77.7 (d, $^3J_{CF}$ = 2.2 Hz), 59.9, 55.4, 53.4, 51.5 (q, $^3J_{CF}$ = 2.0 Hz), 51.1 (q, $^2J_{CF}$ = 29.2 Hz), 47.5, 44.9; **^{19}F NMR** (377 MHz, CD_3OD) δ -66.50; **IR** (neat) cm^{-1}: 1682 (s, C=O); **HRMS** (ESI) calcd for $C_{17}H_{20}F_3N_2O_2$ $[M+H]^+$ 341.1471, found 341.1471.

(5*S,6*R**,6a*R**,9a*S**)-2,3,8-Trimethyl-6-(trifluoromethyl)octahydro-5,9a-epoxypyrrolo[3,4-*d*][1,2]diazocin-7(1*H*)-one (2.57)**

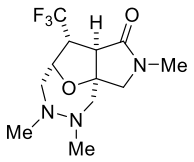

Following *general procedure D* using **2.49** (95.0 mg, 356 µmol) and *N,N'*-dimethylhydrazine dihydrochloride (52.1 mg, 392 µmol) afforded title compound as a colorless oil (23.0 mg, 22%) after purification by flash column chromatography (EtOAc/MeOH/NH_3 380:20:1).

R_f = 0.25 (EtOAc/MeOH/NH_3 380:20:1); **^{1}H NMR** (400 MHz, a) δ 4.51 (dd, *J* = 7.7, 4.0 Hz, 1H), 3.48 (d, *J* = 11.6 Hz, 1H), 3.42 (d, *J* = 8.0 Hz, 1H), 3.38 – 3.31 (m, 2H), 3.25 (dd, *J* = 14.9, 4.0 Hz, 1H), 3.15 – 3.01 (m, 1H), 2.87 – 2.76 (m, 4H), 2.70 – 2.58 (m, 1H), 2.56 (s, 3H), 2.46 (s, 3H); **^{13}C NMR** (101 MHz, CD_3OD) δ 174.9, 127.1 (q, $^1J_{CF}$ = 277.7 Hz), 89.2, 80.5 (q, $^3J_{CF}$ = 1.8 Hz), 63.6, 59.6, 56.6, 52.6 (q, $^2J_{CF}$ = 28.4 Hz), 51.7, 40.9, 34.7, 29.7; **^{19}F NMR** (377 MHz, CD_3OD) δ -65.24; **IR** (neat) cm^{-1}: 1689 (s, C=O); **HRMS** (ESI) calcd for $C_{12}H_{19}F_3N_3O_2$ $[M+H]^+$ 294.1424, found 294.1424.

(3a*R,4*R**,5*S**,13a*R**)-2-Methyl-4-(trifluoromethyl)-1,2,4,5,6,7,12,13-octahydro-5,13a-epoxybenzo[*b*]pyrrolo[3,4-*f*][1,4]diazecin-3(3a*H*)-one (2.58)**

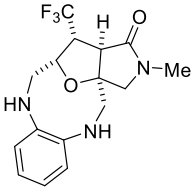

Following *general procedure D* using **2.49** (52.0 mg, 195 µmol) and *o*-phenylenediamine (23.2 mg, 214 µmol) afforded title compound as a light brown amorphous solid (10 mg, 15%) after purification by preparative RP-HPLC using eluents A (H_2O) and B (MeCN) in a linear gradient (5% B to 100% B) in 21 min.

^{1}H NMR (400 MHz, $CDCl_3$) δ 7.11 (dd, *J* = 8.3, 1.5 Hz, 1H), 6.99 (td, *J* = 7.6, 1.4 Hz, 1H), 6.81 – 6.74 (m, 2H), 4.65 – 4.60 (m, 1H), 3.47 – 3.33 (m, 4H), 3.29 – 3.19 (m, 1H), 3.16 (d, *J* = 11.3 Hz, 1H), 3.02 (d, *J* = 12.2 Hz, 1H), 2.94 – 2.89 (m, 1H), 2.89 (s, 3H); **^{13}C NMR** (101 MHz, $CDCl_3$) δ 171.8, 140.6, 137.3, 126.2, 122.7, 121.8, 120.1, 117.0, 83.9, 77.2, 56.0, 54.9, 50.1, 49.6, 49.4 (d, $^{2}J_{CF}$ = 29.0 Hz), 30.0; **^{19}F NMR** (377 MHz, $CDCl_3$) δ -64.88; **IR** (neat) cm^{-1}: 3448 (br., N–H), 3359 (br., N–H), 1680 (s, C=O), 1500 (m, C=C); **HRMS** (ESI) calcd for $C_{16}H_{19}F_3N_3O_2$ $[M+H]^+$ 342.1424, found 342.1425.

(2*S,3*R**,3a*R**,6a*S**)-2,6a-Bis(hydroxymethyl)-5-methyl-3-(trifluoromethyl)hexahydro-4H-furo[2,3-*c*]pyrrol-4-one (2.61)**

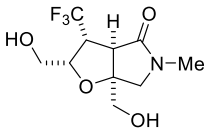

To a solution of **2.49** (127 mg, 0.475 mmol) in MeOH/H_2O (1:1, 6 mL) was added $NaIO_4$ (203 mg, 0.951 mmol) and the reaction mixture was stirred at 22 °C for 2 h. Precipitate was removed by filtration and the filtrate was cooled to 0 °C. $NaBH_4$ (90 mg, 2.38 mmol) was added and the mixture was stirred at 22 °C for 1 h. The mixture was concentrated *in vacuo* and purified directly by flash column chromatography (EtOAc/MeOH 9:1) to give the title compounds as a light-yellow oil (106 mg, 83%)

***R*$_f$** = 0.30 (CH_2Cl_2/MeOH 9:1); **^{1}H NMR** (400 MHz, CD_3OD) δ 4.20 (dddq, *J* = 7.4, 5.6, 3.6, 1.7 Hz, 1H), 3.97 – 3.79 (m, 3H), 3.77 – 3.65 (m, 2H), 3.55 (d, *J* = 11.4 Hz, 1H), 3.29 (s, 1H), 3.22 (tdd, *J* = 12.0, 6.6, 3.1 Hz, 1H), 2.98 (s, 3H); **^{13}C NMR** (101 MHz, CD_3OD) δ 173.3, 127.6 (q, $^{1}J_{CF}$ = 279.6 Hz), 85.5, 80.9, 65.1, 61.5 (q, $^{3}J_{CF}$ = 2.3 Hz), 59.1, 51.7 (d, $^{3}J_{CF}$ = 2.0 Hz), 49.6 (q, $^{3}J_{CF}$ = 27.9 Hz), 29.9; **^{19}F NMR** (377 MHz, CD_3OD) δ -66.52; **IR** (neat) cm^{-1}: 3433 (s, O–H), 3204 (br., O–H), 1667 (s, C=O); **HRMS** (ESI) calcd for $C_{10}H_{15}F_3NO_4$ $[M+H]^+$ 270.0948, found 270.0948.

(2*S,3*R**,3a*R**,6a*S**)-5-Benzyl-2,6a-bis(hydroxymethyl)-3-(trifluoromethyl)hexahydro-4*H*-furo[2,3-*c*]pyrrol-4-one (2.62)**

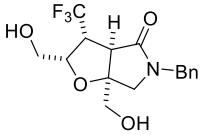

To a solution of **2.50** (144 mg, 0.419 mmol) in MeOH/H_2O (9:1, 10 mL) was added $NaIO_4$ (179 mg, 0.839 mmol) and the reaction mixture was stirred at 22 °C for 2 h. Precipitate was removed by filtration and the filtrate was added sat. aq. $NaHCO_3$ (10 mL) and CH_2Cl_2 (20 mL). The layers were separated and the aqueous phase was extracted with CH_2Cl_2 (2 × 20 mL). The combined organic layers were dried over $MgSO_4$, filtered, and concentrated *in vacuo*. The crude di-aldehyde was dissolved in MeOH (5 mL) and cooled to 0 °C. $NaBH_4$ (80 mg, 2.10 mmol) was added and the mixture was stirred at 22 °C for 1 h. Sat. aq. $NaHCO_3$ (10 mL) was added and the suspension was extracted with CH_2Cl_2 (5 × 10 mL). The combined organic layers were dried over $MgSO_4$, filtered, and concentrated *in vacuo*. The crude product was purified by flash

column chromatography (EtOAc/heptane 3:1) to give the title compounds as a colorless oil (134 mg, 93%)

***R*f** = 0.32 (EtOAc/heptane 3:1); **^{1}H NMR** (400 MHz, DMSO-d_6) δ 7.41 – 7.18 (m, 5H), 5.24 (t, *J* = 5.7 Hz, 1H), 4.93 (t, *J* = 5.4 Hz, 1H), 4.53 – 4.36 (m, 2H), 3.95 (dtt, *J* = 7.9, 4.1, 1.7 Hz, 1H), 3.71 – 3.63 (m, 1H), 3.61 (d, *J* = 11.1 Hz, 1H), 3.57 – 3.47 (m, 1H), 3.41 (d, *J* = 5.2 Hz, 2H), 3.27 – 3.15 (m, 4H); **^{13}C NMR** (101 MHz, DMSO-d_6) δ 170.7, 136.2, 128.7 (2C), 127.6 (2C), 127.5, 126.5 (q, $^{1}J_{CF}$ = 280.5 Hz), 83.8, 79.6, 63.2, 59.4, 54.7, 49.7, 47.5 (q, $^{2}J_{CF}$ = 26.8 Hz), 45.6; **^{19}F NMR** (377 MHz, DMSO-d_6) δ -63.98; **IR** (neat) cm^{-1}: 3393 (br., O–H), 1672 (s, C=O); **HRMS** (ESI) calcd for $C_{16}H_{19}F_3NO_4$ $[M+H]^+$ 346.1261, found 346.1262.

(3a*S,4*S**,5*R**,5a*R**,8a*S**,8b*S**)-2,2,7-Trimethyl-5-(trifluoromethyl)hexahydro-4,8a-epoxy[1,3]dioxolo[4,5-*e*]isoindol-6(4*H*)-one (2.63)**

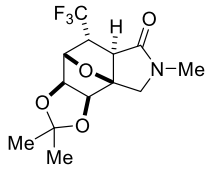

To a suspension of **2.49** (80.0 mg, 93% purity, 278 µmol) in acetone (3 mL) was added 2,2-dimethoxypropane (0.685 mL, 5.57 mmol) and *p*-TsOH (0.5 mg, 2.8 µmol) and the solution was stirred under a N_2 atmosphere for 2 h at 21 °C. Then, sat. aq. $NaHCO_3$ (5 mL) was added and the mixture was extracted with CH_2Cl_2 (3x 5 mL). The combined organic layers were dried over $MgSO_4$, filtered, and concentrated *in vacuo* to give the title compound as an off-white solid (84.2 mg, 98%).

m.p.: 121–123 °C; **^{1}H NMR** (400 MHz, $CDCl_3$) δ 4.76 (dd, *J* = 5.2, 1.1 Hz, 1H), 4.51 (d, *J* = 5.0 Hz, 1H), 4.42 (d, *J* = 5.2 Hz, 1H), 3.79 (d, *J* = 12.0 Hz, 1H), 3.59 (d, *J* = 12.0 Hz, 1H), 3.03 (qt, *J* = 10.0, 5.0 Hz, 1H), 2.90 (s, 3H), 2.53 (d, *J* = 5.0 Hz, 1H), 1.47 (s, 3H), 1.32 (s, 3H); **^{13}C NMR** (101 MHz, $CDCl_3$) δ 170.7, 125.3 (q, $^{1}J_{CF}$ = 277.8 Hz), 112.8, 89.2, 80.5 (q, $^{3}J_{CF}$ = 3.0 Hz), 80.3, 79.5 (q, $^{3}J_{CF}$ = 2.3 Hz), 49.6, 47.1 (q, $^{3}J_{CF}$ = 2.2 Hz), 46.3 (q, $^{2}J_{CF}$ = 29.2 Hz), 30.3, 26.0, 25.4; **^{19}F NMR** (377 MHz, $CDCl_3$) δ -64.49; **IR** (neat) cm^{-1}: 1690 (s, C=O); **HRMS** (ESI) calcd for $C_{13}H_{17}F_3NO_4$ $[M+H]^+$ 308.1104, found 308.1105.

(3a*S,6*R**,7*R**,7a*R**)-2-Benzyl-7-(trifluoromethyl)hexahydro-3a,6-epoxyisoindol-1(4*H*)-one (2.66)**

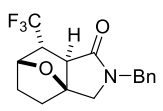

To a solution of **2.45** (100 mg, 0.323 mmol) in EtOH (4 mL) was added 10% Pd/C (34.4 mg, 32.3 mmol) and the resulting suspension was stirred under an atmosphere of H_2 for 2 h. The reaction was filtered through a pad of celite and the filtrate was concentrated *in vacuo* to give the title compound as an off-white solid (99.2 mg, >95%).

m.p.: 103–105 °C; **^{1}H NMR** (400 MHz, DMSO-d_6) δ7.39 – 7.32 (m, 2H), 7.32 – 7.25 (m, 1H), 7.26 – 7.21 (m, 2H), 4.75 (t, *J* = 4.7 Hz, 1H), 4.43 (d, *J* = 3.0 Hz, 2H), 3.63 (d, *J* = 11.7 Hz, 1H), 3.44 (d, *J* = 11.7 Hz, 1H), 3.07 (ttd, *J* = 10.1, 5.2, 1.2 Hz, 1H), 2.97 (d, *J* = 5.2 Hz, 1H),

1.92 – 1.66 (m, 4H); **^{13}C NMR** (101 MHz, DMSO-d_6) δ 172.4, 136.9, 129.0 (2C), 127.9 (2C), 127.7, 126.5 (q, $^1J_{CF}$ = 277.6 Hz), 89.0, 76.6 (q, $^3J_{CF}$ = 2.6 Hz), 51.0 (d, $^3J_{CF}$ = 2.3 Hz), 49.5 (q, $^2J_{CF}$ = 26.8 Hz), 49.1, 45.9, 28.1, 25.9; **^{19}F NMR** (377 MHz, D_2O) δ -65.12; **IR** (neat) cm^{-1}: 3040 (w, C=C–H), 1674 (s, C=O)

(4R,5R)-2-benzyl-4-(trifluoromethyl)-4,5-dihydro-2H-isoindol-5-ol (2.68)

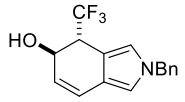

To an ice-cooled solution of **2.45** (88.8 mg, 0.287 mmol) in anhydrous THF (3 mL) was added $LiAlH_4$ (2.0 M in THF, 0.431 mL, 0.861 mmol). After stirring under an atmosphere of N_2 for 1 h at 0 °C, cooling was removed and the mixture was stirred another 17 h. Then, $Na_2SO_4(H_2O)_{10}$ was added portion wise until bubbling ceased and precipitate was removed by filtration. The filtrate was concentrated *in vacuo* and purified by flash column chromatography (EtOAc/heptane 1:3) to give the title compound as a colorless oil (18.0 mg, 21%).

***R*$_f$** = 0.60 (EtOAc/heptane 1:1); **^{1}H NMR** (400 MHz, $CDCl_3$) δ 7.39 – 7.27 (m, 3H), 7.21 – 7.06 (m, 2H), 6.66 (dd, *J* = 2.0, 1.1 Hz, 1H), 6.57 (d, *J* = 2.0 Hz, 1H), 6.51 (dt, *J* = 9.7, 1.0 Hz, 1H), 5.72 (dd, *J* = 9.7, 4.4 Hz, 1H), 5.00 (s, 2H), 4.65 (d, *J* = 5.1 Hz, 1H), 3.68 (qdd, *J* = 9.7, 4.4, 1.0 Hz, 1H), 1.86 (s, 1H); **^{13}C NMR** (101 MHz, $CDCl_3$) δ 136.4, 127.9 (2C), 127.0, 126.3 (2C), 125.6 (q, $^1J_{CF}$ = 280.0 Hz), 121.8, 121.6, 120.0, 117.8, 116.6, 108.5 (q, $^3J_{CF}$ = 1.9 Hz), 63.9 (q, $^3J_{CF}$ = 2.8 Hz), 52.7, 44.9 (q, $^2J_{CF}$ = 26.1 Hz).

(3a*S,6*R**,7*R**,7a*R**)-2-Methyl-1-oxo-7-(trifluoromethyl)octahydro-3a,6-epoxyisoindole-7-carboxylic acid (2.73)**

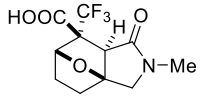

To an ice-cooled solution of trifluoromethylmaleic anhydride **2.3** (140 mg, 843 mmol) in PhMe (5.0 mL) was added *N*-methylfurfurylamine (94.0 mg, 844 mmol). After stirring 5 min. at 0 °C, cooling was removed and the turbid reaction mixture was stirred another 24 h. Then, precipitate was collected by filtration and washed with PhMe (3 × 5 ml). The crude IMDA-product was dissolved in MeOH (16 mL), added 10% Pd/C (86.0 mg, 80.8 mmol), and stirred under an atmosphere of H_2 for 2 h. The reaction was filtered through a pad of celite and the filtrate was concentrated *in vacuo* to give the title compound as an off-white solid (226 mg, >95%).

m.p.: 222–224 °C; **^{1}H NMR** (400 MHz, DMSO-d_6) δ 4.76 (d, *J* = 4.7 Hz, 1H), 3.66 – 3.54 (m, 2H), 2.96 (s, 1H), 2.74 (s, 3H), 2.03 – 1.90 (m, 1H), 1.90 – 1.79 (m, 2H), 1.74 (td, *J* = 11.7, 4.4 Hz, 1H); **^{13}C NMR** (101 MHz, DMSO-d_6) δ 169.4, 166.4, 125.0 (d, $^1J_{CF}$ = 280.7 Hz), 87.7, 82.0, 63.4 (q, $^2J_{CF}$ = 23.8 Hz), 54.1 (d, $^3J_{CF}$ = 1.8 Hz), 50.6, 29.4, 29.0, 26.5 (d, $^3J_{CF}$ = 2.8 Hz); **^{19}F NMR** (377 MHz, DMSO-d_6) δ -63.21; **IR** (neat) cm^{-1}: 1741 (s, C=O), 1629 (s, C=O); **HRMS** (ESI) calcd for $[C_{11}H_{13}F_3NO_4]$ $[M+H]^+$ 280.0791, found 280.0775.

((3a*S,6*R**,7*S**,7a*S**)-2-Methyl-7-(trifluoromethyl)octahydro-3a,6-epoxyisoindol-7-yl) methanol (2.74)**

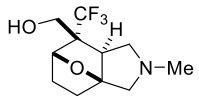

To an ice-cooled solution of **2.73** (87.0 mg, 312 µmol) in anhydrous THF (10 mL) was added $LiAlH_4$ (2.0 M in THF, 950 µL, 1.87 mmol). After stirring 1 h at 0 °C, cooling was removed and the solution was stirred another 15 h under a nitrogen atmosphere. Then, $Na_2SO_4(H_2O)_{10}$ was added portion wise until bubbling ceased and precipitate was removed by filtration. The filtrate was concentrated *in vacuo* and purified by flash column chromatography (CH_2Cl_2/MeOH/NH_3 380:20:1) to give the title compound as an off-white amorphous solid (23.5 mg, 30%).

***R*f** = 0.14 (CH_2Cl_2/MeOH/NH_3 380:20:1); **^{1}H NMR** (400 MHz, CD_3OD) δ 4.51 (d, *J* = 5.0 Hz, 1H), 3.87 (dq, *J* = 11.6, 1.9 Hz, 1H), 3.69 (d, *J* = 11.6 Hz, 1H), 2.94 (d, *J* = 11.4 Hz, 1H), 2.77 (d, *J* = 11.4 Hz, 1H), 2.71 (dd, *J* = 8.7, 6.9 Hz, 1H), 2.57 – 2.41 (m, 2H), 2.38 (s, 3H), 2.13 – 2.01 (m, 1H), 1.95 – 1.73 (m, 3H); **^{13}C NMR** (101 MHz, CD_3OD) δ 128.9 (q, $^1J_{CF}$ = 281.9 Hz), 97.6, 80.7 (d, $^3J_{CF}$ = 1.9 Hz), 62.1 (q, $^3J_{CF}$ = 2.4 Hz), 59.2 (q, $^2J_{CF}$ = 21.7 Hz), 58.8, 55.5, 52.1 (q, $^3J_{CF}$ = 2.8 Hz), 42.3, 30.9, 27.6 (q, $^3J_{CF}$ = 2.4 Hz); **^{19}F NMR** (377 MHz, CD_3OD) δ -66.89; **IR** (neat) cm^{-1}: 3144 (br., O–H); **HRMS** (ESI) calcd for [$C_{11}H_{17}F_3NO_2$] $[M+H]^+$ 252.1206, found 252.218.

(3a*S,6*R**,7*R**,7a*R**)-*N*,*N*,2-trimethyl-1-oxo-7-(trifluoromethyl)octahydro-3a,6-epoxy-isoindole-7-carboxamide (2.75)**

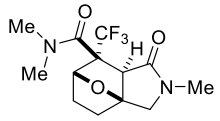

To a solution of **2.73** (77 mg, 278 µmol) in MeCN (3.0 mL), was added dimethylamine hydrochloride (45.3 mg, 556 µmol), DIPEA (200 µL, 1.11 mmol), and HATU (132 mg, 347 µmol) and the mixture was stirred 16 h. The reaction mixture was concentrated *in vacuo* and purified directly by flash column chromatography (CH_2Cl_2/MeOH 19:1) to give the title compound as a white solid (64.0 mg, 75%).

***R*f** = 0.19 (CH_2Cl_2/MeOH 19:1); **m.p.**: 137–139 °C; **^{1}H NMR** (400 MHz, CD_3OD) δ 5.31 (d, *J* = 5.3 Hz, 1H), 3.73 (d, *J* = 11.8 Hz, 1H), 3.66 (d, *J* = 11.8 Hz, 1H), 3.31 (s, 1H), 3.12 – 3.07 (m, 6H), 2.90 (d, *J* = 0.7 Hz, 3H), 2.22 – 2.02 (m, 2H), 1.98 (ddd, *J* = 11.7, 8.5, 4.4 Hz, 1H), 1.87 (td, *J* = 11.7, 5.0 Hz, 1H); **^{13}C NMR** (101 MHz, CD_3OD) δ 172.8, 165.6, 126.5 (q, $^1J_{CF}$ = 282.1 Hz), 89.9, 83.6 (q, $^3J_{CF}$ = 2.2 Hz), 69.0 (q, $^2J_{CF}$ = 24.7 Hz), 57.3 (q, $^3J_{CF}$ = 3.1 Hz), 52.0, 39.9 (d, $^3J_{CF}$ = 3.5 Hz, 2C), 30.8, 30.3, 27.8 (q, $^3J_{CF}$ = 2.7 Hz); **^{19}F NMR** (377 MHz, CD_3OD) δ -59.77; **IR** (neat) cm^{-1}: 1699 (s, C=O), 1631 (s, C=O); **HRMS** (ESI) calcd for [$C_{13}H_{18}F_3N_2O_3$] $[M+H]^+$ 307.1264, found 307.1268.

Pyrrole Diels-Alder

Compounds **2.86** and **2.89** were synthesized by BSc student Sanne L. Møller. The remaining compounds, except **2.76, 2.77**, and **2.93**, were synthesized by MSc student Daniela Danková.

7-(*tert*-Butyl) 2-ethyl (1*S**,4*R**)-3-(trifluoromethyl)-7-azabicyclo[2.2.1]hepta-2,5-diene-2,7-dicarboxylate (2.76)

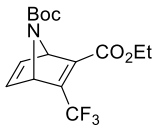

A mixture of ethyl (*E*)-4,4,4-trifluoro-2-butynoate **2.4** (0.430 mL, 3.00 mmol) and *N*-Boc-pyrrole (2.00 mL, 12.0 mmol) was subjected to microwave heating at 120 °C for 2 h. The crude was purified directly by flash column chromatography (EtOAc/heptane 1:20 to 1:5) to afford the title compound as a yellow oil (1.01 g, >95%).

R_f = 0.50 (EtOAc/heptane 1:5); **^{1}H NMR** (400 MHz, $CDCl_3$) δ 7.23 – 6.99 (m, 2H), 5.56 – 5.30 (m, 2H), 4.39 – 4.15 (m, 2H), 1.41 (s, 9H), 1.31 (t, *J* = 7.1 Hz, 3H); **^{13}C NMR** (101 MHz, $CDCl_3$) δ 162.0, 154.1, 143.4, 142.0, 131.6, 120.3, 82.0, 69.5, 68.3, 62.0, 28.1 (3C), 14.0. CF_3 carbon not observed; **^{19}F NMR** (377 MHz, $CDCl_3$) δ -62.14; **IR** (neat) cm^{-1}: 1715 (s, C=O), 1630 (s, C=O); **HRMS** (ESI) calcd. for $[C_{15}H_{18}F_3NO_4Na]$ $[M+Na]^+$ 356.1080, found 356.1090.

7-(*tert*-Butyl) 2-ethyl (1*S**,2*R**,3*S**,4*R**)-3-(trifluoromethyl)-7-azabicyclo[2.2.1]heptane-2,7-dicarboxylate (*exo*-2.77)

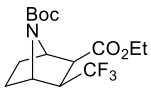

To a solution of **2.76** (1.50 g, 4.50 mmol) in EtOH (45 mL) was added 5% Pd/C (0.958 g, 0.450 mmol) and the resulting suspension was stirred under an atmosphere of H_2 at 22 °C for 1 h. The suspension was filtered through a pad of celite and concentrated *in vacuo* to give the title compound as a transparent oil (1.46 g, 96%).

^{1}H NMR (400 MHz, $CDCl_3$) δ 4.47 – 4.30 (m, 2H), 4.25 – 4.07 (m, 2H), 3.22 – 3.05 (m, 2H), 2.30 – 2.17 (m, 1H), 1.96 – 1.78 (m, 2H), 1.78 – 1.67 (m, 1H), 1.45 (s, 9H), 1.25 (t, *J* = 7.2 Hz, 3H); **^{13}C NMR** (101 MHz, $CDCl_3$) δ 169.2, 154.8, 125.7 (q, $^1J_{CF}$ =279.1 Hz), 80.9, 61.1, 59.1, 58.6, 46.1, 45.6, 28.3 (3C), 24.9, 23.8, 14.0; **^{19}F NMR** (377 MHz, DMSO-d_6) δ -59.43; **IR** (neat) cm^{-1}: 1724 (s, C=O), 1703 (s, C=O).

(1*S**,2*R**,3*S**,4*R**)-7-(*tert*-Butoxycarbonyl)-3-(trifluoromethyl)-7-azabicyclo[2.2.1] heptane-2-carboxylic acid (2.78)

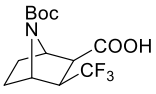

To a solution of *exo*-**2.77** (0.750 g, 2.20 mmol) in EtOH (22 mL) was added 2M aq. LiOH (4.45 mL) and the reaction mixture was stirred at 22 °C for 12 h. The mixture was concentrated *in vacuo*, redissolved in water (30 mL), neutralized with sat. aq. NH_4Cl to pH 7, and extracted with EtOAc (5 × 60 mL). The combined organic

layers were washed with brine (1 × 30 mL), dried over Na_2SO_4, filtered, and concentrated *in vacuo* to afford the title compound as a white solid (0.580 g, 85%).
m.p.: 116–118 °C; **^{1}H NMR** (400 MHz, $CDCl_3$) δ 4.70 – 4.57 (m, 1H), 4.53 – 4.39 (m, 1H), 3.51 – 3.32 (m, 1H), 2.71 (d, *J* = 5.6 Hz, 1H), 2.07 – 1.84 (m, 2H), 1.82 – 1.66 (m, 1H), 1.61 – 1.51 (m, 1H), 1.42 (s, 9H); **^{13}C NMR** (101 MHz, $CDCl_3$) δ 166.7, 154.5, 126.0 (q, $^1J_{CF}$ = 277.8 Hz), 81.3, 60.9, 57.2, 49.1, 47.2 (q, $^2J_{CF}$ = 29.7 Hz), 29.3, 28.2 (3C), 24.3; **^{19}F NMR** (377 MHz, $CDCl_3$) δ -65.46; **IR** (neat) cm^{-1}: 3301 (br., O–H), 1653 (s, C=O), 1624 (s, C=O); **HRMS** (ESI) calcd. for $[C_{13}H_{19}F_3NO_4]$ $[M+H]^+$ 332.1080, found 332.1087.

tert-Butyl (1*S**,2*R**,3*S**,4*R**)-2-(methylcarbamoyl)-3-(trifluoromethyl)-7-azabicyclo[2.2.1]heptane-7-carboxylate (2.223)

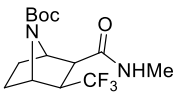

To a suspension of *exo*-**2.77** (0.500 g, 1.62 mmol) in MeCN (16 mL) was added HATU (0.736 g, 1.94 mmol) and DIPEA (1.13 mL, 6.48 mmol) and the solution was stirred at 22 °C for 10 min. Then, methylamine hydrochloride (0.218 g, 3.24 mmol) was added and the solution was stirred at 22 °C for 2 h. EtOAc (40 mL) was added and the solution was washed with sat. aq. NH_4Cl (40 mL). The aqueous phase was extracted with EtOAc (3×30 mL). The combined organic layers were washed with deionized water (40 mL), brine (2×40 mL) and dried over Na_2SO_4, filtered and concentrated *in vacuo* to afford the crude as yellow solid. The crude was purified by flash column chromatography on silica gel (EtOAc/heptane 1:3 to 1:2) to give the title compound as an amorphous solid (0.421 g, 81%).
R_f = 0.47 (EtOAc/heptane/AcOH 1:1); **^{1}H NMR** (400 MHz, $CDCl_3$) δ 5.91 (br. s, 1H), 4.57 – 4.22 (m, 2H), 3.46 – 3.24 (m, 1H), 2.82 (d, *J* = 4.7 Hz, 3H), 2.49 (d, *J* = 5.7 Hz, 1H), 2.03 – 1.81 (m, 2H), 1.78 – 1.68 (m, 1H), 1.56 – 1.44 (m, 10H); **^{13}C NMR** (101 MHz, $CDCl_3$) δ 171.1, 154.7, 126.2 (d, $^1J_{CF}$ =277.5 Hz), 81.0, 61.0, 56.9, 50.3, 48.2, 29.1, 28.3 (3C), 26.8, 24.4; **^{19}F NMR** (377 MHz, $CDCl_3$) δ -65.19; **IR** (neat) cm^{-1}: 3340 (s, N–H), 1669 (s, C=O), 1645 (s, C=O), 1575 (s, N–H); **HRMS** (ESI) calcd. for $[C_{14}H_{22}F_3N_2O_3]$ $[M+H]^+$ 323.1577, found 323.1581.

(1*S**,2*R**,3*S**,4*R**)-*N*-Methyl-3-(trifluoromethyl)-7-azabicyclo[2.2.1]heptane-2-carboxamide (2.79)

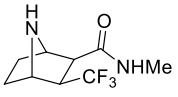

Following *general procedure E* using **2.223** (363 mg, 1.13 mmol) afforded the title compound as a sticky off-white solid (173 mg, 69%) after purification by flash column chromatography (CH_2Cl_2/MeOH/Et_3N 100:0:0.5 to 98:2:0.5).
R_f = 0.29 (CH_2Cl_2/MeOH/ Et_3N 90:10:2); **^{1}H NMR** (400 MHz, $CDCl_3$) δ 6.47 – 6.25 (br. s, 1H), 3.81 (td, *J* = 4.5, 0.9 Hz, 1H), 3.71 (dt, *J* = 5.2, 1.2 Hz, 1H), 2.93 (qtd, *J* = 10.1, 5.2, 1.9

Hz, 1H), 2.78 (d, *J* = 4.8 Hz, 3H), 2.52 (s, 1H), 2.38 (d, *J* = 5.1 Hz, 1H), 1.90 – 1.65 (m, 2H), 1.65 – 1.47 (m, 1H), 1.32 (ddd, *J* = 12.1, 8.9, 5.1 Hz, 1H); **^{13}C NMR** (101 MHz, $CDCl_3$) δ 174.3, 126.6 (q, $^1J_{CF}$ = 278.0 Hz), 62.7, 56.9 (q, $^3J_{CF}$ = 1.8 Hz) 50.7 (q, $^2J_{CF}$ = 26.6 Hz), 50.2 (q, $^3J_{CF}$ = 1.7 Hz), 28.7, 26.5, 24.6 (q, $^3J_{CF}$ = 2.1 Hz); **^{19}F NMR** (377 MHz, $CDCl_3$) δ -64.79; **IR** (neat) cm^{-1}: 3266, 2964, 1638, 1561, 1410, 1358, 1255, 1217, 1148, 1104; **HRMS** (ESI) calcd. for $[C_9H_{14}F_3N_2O]$ $[M+H]^+$ 223.1053, found 223.1060.

tert-Butyl (1*S,2*R**,3*S**,4*R**)-2-(morpholine-4-carbonyl)-3-(trifluoromethyl)-7-azabicyclo [2.2.1]heptane-7-carboxylate (2.251)**

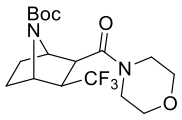

To a solution of *exo*-**2.77** (0.472 g, 1.62 mmol) was suspended in MeCN (15 mL) was added HATU (0.695 g, 1.84 mmol) and DIPEA (1.00 mL, 6.12 mmol) and the solution was stirred at 22 °C for 10 min. Then, morpholine (161 µL, 1.84 mmol) was added and the mixture was stirred at 22 °C for 1 h. EtOAc (40 mL) was added and the solution was washed with sat. aq. NH_4Cl (40 mL). The aqueous phase was extracted with EtOAc (3 × 30 mL) and the combined organic layers were washed with water (1 × 40 mL), brine (2 × 40 mL), dried over Na_2SO_4, filtered, and concentrated *in vacuo*. The crude product was purified by flash column chromatography (EtOAc/heptane 1:4 to 1:2) to give the title compound as a sticky off-white solid (0.452 g, 78%).

***R*$_f$** = 0.45 (EtOAc/heptane 1:1); **^{1}H NMR** (400 MHz, $CDCl_3$) δ 4.64 – 4.10 (m, 2H), 4.03 – 3.83 (m, 1H), 3.60 (m, 8H), 2.76 – 2.58 (m, 1H), 2.04 – 1.84 (m, 2H), 1.84 – 1.62 (m, 1H), 1.53 (m, 1H), 1.48 – 1.31 (m, 9H); **^{13}C NMR** (101 MHz, $CDCl_3$) δ 174.7, 154.5 (d), 126.4 (d, $^1J_{CF}$ = 277.6 Hz), 80.7, 67.0, 66.6, 60.6, 57.1, 56.3, 47.5, 46.3 (d), 42.9, 29.9, 28.3 (3C), 24.4; **^{19}F NMR** (377 MHz, , $CDCl_3$) δ -64.81 (minor rotamer), -65.17 (major rotamer); **IR** (neat) cm^{-1}: 1700 (s, C=O), 1648 (s, C=O).

Morpholino((1*S,2*R**,3*S**,4*R**)-3-(trifluoromethyl)-7-azabicyclo[2.2.1]heptan-2-yl) methanone (2.80)**

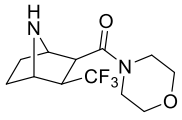

Following *general procedure E* using **2.251** (435 mg, 1.15 mmol) afforded the title compound as a sticky off-white solid (297 mg, 93%) after purification by flash column chromatography (CH_2Cl_2/MeOH/Et_3N 100:0:0.5 to 98:2:0.5).

***R*$_f$** = 0.45 (CH_2Cl_2/MeOH/ Et_3N 90:10:2); **^{1}H NMR** (400 MHz, $CDCl_3$) δ 3.87 (t, *J* = 4.7 Hz, 1H), 3.72 – 3.46 (m, 9H), 3.35 – 3.21 (m, 1H), 2.81 (d, *J* = 5.3 Hz, 1H), 2.50 (br. s, 1H), 1.90 – 1.75 (m, 2H), 1.74 – 1.57 (m, 1H), 1.45 – 1.31 (m, 1H); **^{13}C NMR** (101 MHz, $CDCl_3$) δ 171.6, 126.8 (q, $^1J_{CF}$ = 278.4 Hz), 67.0, 66.7, 62.8, 57.2, 51.02 – 49.76 (m), 46.3, 45.8, 42.8, 28.8, 24.1; **^{19}F NMR** (377 MHz, $CDCl_3$) δ -64.33; **IR** (neat) cm^{-1}: 1632 (s, C=O).

(1*S,2*R**,3*S**,4*R**)-*N*-(Pyridin-3-yl)-3-(trifluoromethyl)-7-azabicyclo[2.2.1]heptane-2-carboxamide (2.81**)

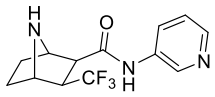

To a suspension of *exo*-**2.77** (0.400 g, 1.29 mmol) in MeCN (12.9 mL) was added HATU (1.13 g, 2.96 mmol) and DIPEA (0.902 mL, 5.16 mmol) and the solution was stirred at 22 °C for 10 min. Then, 3-aminopyridine (243 mg, 2.58 mmol) was added and the reaction mixture was stirred at 50 °C for 8 h. EtOAc (40 mL) was added and the solution was washed with 3M aq. NaOH (1 × 10 mL). The aqueous phase was extracted with EtOAc (5 × 30 mL) and the combined organic layers were washed with brine (2 × 40 mL), dried over Na_2SO_4, filtered, concentrated *in vacuo*, and filtered through a short silica plug.

The crude amide was dissolved in CH_2Cl_2 (5 mL) and TFA (1.6 mL) was added. The reaction mixture was stirred at 22 °C for 1 h and then was diluted with MeCN (5 mL). The mixture was concentrated *in vacuo* and then co-evaporated *in vacuo* with MeCN (5 × 50mL) to remove the residual TFA. The crude product was purified by flash column chromatography (CH_2Cl_2/MeOH/ Et_3N 100:0:0.5 to 98:2:0.5) to afford the title compound as a sticky off-white solid (189 mg, 60%).

R_f = 0.70 (CH_2Cl_2/MeOH/Et_3N 90:10:2); **^{1}H NMR** (400 MHz, $CDCl_3$) δ 9.26 (br. s, 1H), 8.56 (dd, *J* = 2.7, 0.7 Hz, 1H), 8.33 (dd, *J* = 4.8, 1.5 Hz, 1H), 8.18 (ddd, *J* = 8.3, 2.7, 1.5 Hz, 1H), 7.30 – 7.24 (m, 1H), 3.99 – 3.88 (m, 2H), 3.02 (m, 1H), 2.81 (br. s, 1H), 2.62 (d, *J* = 5.0 Hz, 1H), 2.05 – 1.91 (m, 1H), 1.86 – 1.72 (m, 1H), 1.67 – 1.41 (m, 2H); **^{13}C NMR** (101 MHz, $CDCl_3$) δ 172.2, 145.3, 141.2, 135.1, 127.1, 125.5 (q, $^1J_{CF}$ = 277.8 Hz), 123.8, 62.2, 56.9, 50.8, 50.0 (d, $^2J_{CF}$ = 27.5 Hz), 29.1, 25.7; **^{19}F NMR** (377 MHz, $CDCl_3$) δ -65.18; **IR** (neat) cm^{-1}: 3224 (br., N–H), 1731 (s, C=O); **HRMS** (ESI) calcd. for $[C_{13}H_{15}F_3N_3O]$ $[M+H]^+$ 286.1162, found 286.1170.

(2*S,4*S**)-7-(3-Hydroxybenzyl)-*N*-methyl-3-(trifluoromethyl)-7-azabicyclo[2.2.1] heptane-2-carboxamide (2.82)**

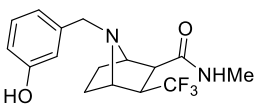

To a solution of **2.79** (50.0 mg, 0.225 mmol) in MeOH (2.5 mL) was added 3-hydroxybenzaldehyde (41.2 mg, 0.338 mmol) and AcOH (250 µL) and the reaction mixture was stirred at 50 °C for 4 h. The reaction was cooled on ice and $NaCNBH_3$ (28.3 mg, 0.450 mmol) was added. After 5 min. cooling was removed and the mixture was stirred at 22 °C for another 4 h. Additional 3-hydroxybenzaldehyde (25.0 mg, 0.205 mmol) was added and the reaction was stirred for 22 °C for 10 h when additional $NaCNBH_3$ (25.0 mg, 0.397 mmol) was added. After stirring another 4 h, water (5 mL) was added and the mixture was extracted with EtOAc (5 × 10 mL). The combined organic layers were washed with brine (1 × 30 mL), filtered, and concentrated *in*

vacuo. The crude product was purified by flash column chromatography on (EtOAc/heptane 1:2 to 3:1) to give the title compound as a sticky off-white solid (31.7 mg, 43%).
R_f = 0.51 (EtOAc/heptane/Et_3N 20:60:2); **^{1}H NMR** (400 MHz, $CDCl_3$) δ 7.49 (q, *J* = 4.9 Hz, 1H), 7.16 (t, *J* = 7.8 Hz, 1H), 6.90 – 6.84 (m, 1H), 6.84 – 6.78 (m, 1H), 6.77 – 6.70 (m, 1H), 3.62 – 3.53 (m, 2H), 3.43 – 3.33 (m, 2H), 2.95 – 2.78 (m, 1H), 2.66 (d, *J* = 4.9 Hz, 3H), 2.38 (d, *J* = 5.2 Hz, 1H), 2.07 – 1.78 (m, 3H), 1.48 – 1.33 (m, 1H); **^{13}C NMR** (101 MHz, $CDCl_3$) δ 175.1, 157.3, 140.1, 129.8, 126.0 (q, $^1J_{CF}$ = 277.8 Hz), 120.0, 115.7, 115.0, 63.6, 60.5, 51.0, 50.4, 50.1, 26.1, 25.4, 21.6; **^{19}F NMR** (377 MHz, $CDCl_3$) δ -65.27; **IR** (neat) cm^{-1}: 3273 (s, O–H), 1650 (s, C=O), 1588 (s, N–H), 1533 (s, C=C); **HRMS** (ESI) calcd. for [$C_{16}H_{20}F_3N_2O_2$] $[M+H]^+$ 329.1471, found 329.1489.

(1*S**,2*R**,3*S**,4*R**)-*N*-Methyl-7-(methylsulfonyl)-3-(trifluoromethyl)-7-azabicyclo[2.2.1] heptane-2-carboxamide (2.83)

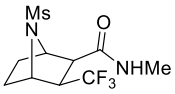

To a solution of **2.79** (50.0 mg, 0.225 mmol) in CH_2Cl_2 (2.5 mL) was added Et_3N (122 µL, 0.900 mmol) and methanesulfonyl chloride (33.0 µL, 0.430 mmol) and the reaction mixture was stirred at 22 °C for 24 h. Water (2 mL) was added and the mixture was then extracted with EtOAc (3 × 10 mL), dried over Na_2SO_4, filtered, and concentrated *in* vacuo. The crude product was purified by flash column chromatography (CH_2Cl_2/MeOH/Et_3N (100:0:0.5 to 98:2:0.5) to give the title compound as a white solid (53.2 mg, 79%).
R_f = 0.79 (CH_2Cl_2/MeOH/Et_3N 90:10:2); **m.p.**: 192–194 °C; **^{1}H NMR** (400 MHz, DMSO-d_6) δ 8.04 (q, *J* = 4.7 Hz, 1H), 4.48 (td, *J* = 4.4, 1.1 Hz, 1H), 4.34 (d, *J* = 4.7 Hz, 1H), 3.64 – 3.48 (m, 1H), 3.04 (s, 3H), 2.63 (d, *J* = 4.7 Hz, 3H), 2.53 (d, *J* = 5.7 Hz, 1H), 2.05 – 1.71 (m, 3H), 1.70 – 1.52 (m, 1H); **^{13}C NMR** (101 MHz, DMSO-d_6) δ 169.4, 126.3, 64.1, 58.7, 48.5, 46.0 (d, $^2J_{CF}$ = 26.7 Hz), 41.6, 29.3, 26.1, 24.3; **^{19}F NMR** (377 MHz, $CDCl_3$) δ -65.30; **IR** (neat) cm^{-1}: 1644 (s, C=O), 1394 (s, S=O); **HRMS** (ESI) calcd. for [$C_{10}H_{16}F_3N_2O_3S$] $[M+H]^+$ 301.0828, found 301.0841.

(1*S**,2*R**,3*S**,4*R**)-*N*^{7}-Cyclopentyl-*N*^{2}-methyl-3-(trifluoromethyl)-7-azabicyclo[2.2.1] heptane-2,7-dicarboxamide (2.84)

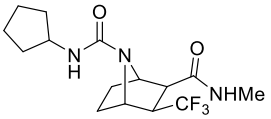

To a solution of **2.79** (37.9 mg, 0.170 mmol) in CH_2Cl_2 (2 mL) was added Et_3N (37.6 µL, 0.255 mmol) and cyclopentyl isocyanate (22.3 µL, 0.187 mmol) and the reaction mixture was stirred at 22 °C for 6 h. The mixture was concentrated *in vacuo* and purified directly by flash column chromatography (CH_2Cl_2/MeOH/EtOAc (99:1:1 to 97:3:0) to give the title compound as a white solid (49.3 mg, 87%).

***R*f** = 0.60 (CH_2Cl_2/MeOH/Et_3N 90:10:2); **m.p.**: 155–157 °C; **^{1}H NMR** (400 MHz, $CDCl_3$) δ 5.95 (br. s, 1H), 4.51 (d, *J* = 5.0 Hz, 1H), 4.46 (td, *J* = 4.5, 1.2 Hz, 1H), 4.02 (p, *J* = 6.9 Hz, 1H), 3.22 – 3.03 (m, 1H), 2.81 (s, 3H), 2.56 (d, *J* = 5.8 Hz, 1H), 2.07 – 1.83 (m, 4H), 1.83 – 1.28 (m, 8H); **^{13}C NMR** (101 MHz, $CDCl_3$) δ 171.6, 157.1, 126.2 (d, $^1J_{CF}$ = 274.4 Hz), 60.4, 57.6, 52.6, 50.3, 49.5 (d, $^2J_{CF}$ = 27.3 Hz), 33.4, 33.3, 28.9, 23.9, 23.8; **^{19}F NMR** (377 MHz, $CDCl_3$) δ -64.88; **IR** (neat) cm^{-1}: 3358 (s, N–H), 1734 (s, C=O), 1625 (s, C=O), 1535 (s, N–H); **HRMS** (ESI) calcd. for $[C_{15}H_{23}F_3N_3O_2]$ $[M+H]^+$ 334.1737, found 334.1754.

1-((1*S,2*R**,3*S**,4*R**)-2-(Morpholine-4-carbonyl)-3-(trifluoromethyl)-7-azabicyclo[2.2.1] heptan-7-yl)ethan-1-one (2.85)**

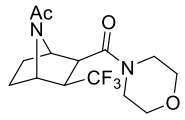

To a solution of **2.80** (60.0 mg, 0.216 mmol) in CH_2Cl_2 (2.5 mL) was added Et_3N (30.0 µL, 0.432 mmol) and acetyl chloride (30.0 µL, 0.432 mmol) and the reaction mixture was stirred at 22 °C for 2 h. Water (2 mL) was added and the mixture was extracted with EtOAc (5 × 5 mL). The combined organic layers were washed with brine (1 × 10 mL), dried over Na_2SO_4, filtered, and concentrated *in vacuo*. The crude product was purified by flash column chromatography (EtOAc/MeOH/Et_3N (200:0:1 to 180:20:1) to give the title compound as a white solid (65.0 mg, 84%).
***R*f** = 0.54 (CH_2Cl_2/MeOH/Et_3N 90:10:2); **m.p.**: 133–135 °C; **^{1}H NMR** (400 MHz, $CDCl_3$) δ 4.92 (td, *J* = 4.7, 1.2 Hz, 0.4H, minor rotamer), 4.69 (d, *J* = 5.2 Hz, 0.6H, major rotamer), 4.39 (td, *J* = 4.7, 1.2 Hz, 0.6H, major rotamer), 4.15 (d, *J* = 4.6 Hz, 0.4H, minor rotamer), 3.99 (qtd, *J* = 10.1, 5.2, 1.8 Hz, 0.6H, major rotamer), 3.85 – 3.39 (m, 8.4H), 2.87 (d, *J* = 5.9 Hz, 0.4H, minor rotamer), 2.71 (d, *J* = 5.1 Hz, 0.6H, major rotamer), 2.15 – 1.87 (m, 5H), 1.86 – 1.70 (m, 1H), 1.69 – 1.48 (m, 1H); **^{13}C NMR** (101 MHz, $CDCl_3$) δ 169.5 (minor rotamer), 168.1 (major rotamer), 167.93 (major rotamer), 167.89 (minor rotamer), 125.9 (m), 67.01 (minor rotamer), 66.95 (major rotamer), 66.7 (major rotamer), 66.5 (minor rotamer), 61.4 (minor rotamer), 57.8 (major rotamer), 57.2 (major rotamer), 53.7 (minor rotamer), 47.9 (d, $^2J_{CF}$ = 27.1 Hz, minor rotamer) 47.1 (d, $^2J_{CF}$ = 27.4 Hz, major rotamer), 46.4, 46.2 (major rotamer), 45.9 (minor rotamer), 43.1 (minor rotamer), 42.8 (major rotamer), 30.6 (minor rotamer), 28.1 (major rotamer), 26.0 (major rotamer), 23.5 (minor rotamer), 21.7 (minor rotamer), 21.3 (major rotamer); **^{19}F NMR** (377 MHz, $CDCl_3$) δ -64.50 (minor rotamer), -65.14 (major rotamer); **IR** (neat) cm^{-1}: 1644 (s, C=O); **HRMS** (ESI) calcd. for $[C_{14}H_{20}F_3N_2O_3]$ $[M+H]^+$ 321.1421, found 321.1425.

(1*R,2*R**,3*S**,4*S**)-7-Acetyl-*N*-(pyridin-3-yl)-3-(trifluoromethyl)-7-azabicyclo [2.2.1] heptane-2-carboxamide (2.86)**

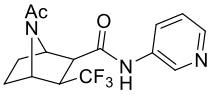

To a solution of **2.81** (80.0 mg, 0.280 mmol) in CH_2Cl_2 (6 mL) was added Et_3N (46.9 µL, 0.340 mmol) and acetyl chloride (27.9 µL, 0.320 mmol) and the solution was stirred at 22 °C for 2 h. The solution was concentrated *in vacuo* and purified directly by flash column chromatography (acetone/heptane/Et_3N 100:100:1) to give the title compound as a red/orange oil (56.6 mg, 62%).

***R*f** = 0.33 (acetone/heptane/Et_3N 100:100:1); **^{1}H NMR** (400 MHz, DMSO-d_6) δ 10.58 (s, 0.6H, major rotamer), 10.47 (s, 0.4H, minor rotamer), 8.70 (dd, *J* = 6.4, 2.5 Hz, 1H), 8.28 (ddd, *J* = 7.3, 4.7, 1.5 Hz, 1H), 8.01 (dddd, *J* = 17.2, 8.3, 2.5, 1.5 Hz, 1H), 7.36 (td, *J* = 7.6, 4.7 Hz, 1H), 4.76 – 4.68 (m, 1H), 4.68 – 4.59 (m, 1H), 3.68 (qd, *J* = 9.9, 8.0, 3.7 Hz, 0.4H, minor rotamer), 3.47 – 3.36 (m, 0.6H, major rotamer), 2.96 (d, *J* = 5.8 Hz, 0.6H, major rotamer), 2.85 (d, *J* = 5.5 Hz, 0.4H, minor rotamer), 2.03 – 1.93 (m, 2H), 1.86 – 1.72 (m, 3.5H), 1.70 – 1.47 (m, 1.5H); **^{13}C NMR** (101 MHz, DMSO-d_6) δ 169.7 (major rotamer), 168.8 (minor rotamer), 167.5 (major rotamer), 167.2 (minor rotamer), 144.6, 140.8, 135.6 (minor rotamer), 135.4 (major rotamer), 126.31 (q, $^1J_{CF}$ = 278.0 Hz), 126.29 (major rotamer), 126.2 (minor rotamer), 123.8 (major rotamer), 123.7 (minor rotamer), 61.7 (major rotamer), 58.8 (minor rotamer), 56.5 (minor rotamer), 53.4 (d, $^3J_{CF}$ = 1.6 Hz, major rotamer), 49.9 (major rotamer), 49.0 (minor rotamer), 45.3 (q, $^2J_{CF}$ = 26.7 Hz, major rotamer), 45.2 (q, $^2J_{CF}$ = 26.5 Hz, minor rotamer), 30.0 (major rotamer), 28.1 (major rotamer), 24.9 (d, $^3J_{CF}$ = 2.0 Hz, minor rotamer), 23.0 (minor rotamer), 21.4 (major rotamer), 21.1 (minor rotamer); **^{19}F NMR** (377 MHz, DMSO-d_6) δ -63.64 (major rotamer), -63.86 (minor rotamer); **IR** (neat) cm^{-1}: 3412 (br., N–H), 3060 (s, C=C–H), 1690 (s, C=O), 1627 (s, C=O) 1587 (s, N–H), 1545 (s, C=C); **HRMS** (ESI) calcd for $[C_{15}H_{17}F_3N_3O_2]$ $[M+H]^+$ 328.1273, found 328.1377.

7-(*tert*-Butyl) 2-ethyl (1*S,2*R**,3*S**,4*R**)-3-(methylamino)-3-(trifluoromethyl)-7-aza-bicyclo[2.2.1]hept-5-ene-2,7-dicarboxylate (2.87)**

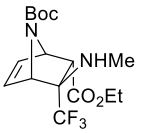

To a solution of **2.76** (500 mg, 1.50 mmol) in EtOH (15 mL) was added methylamine hydrochloride (111 mg, 1.65 mmol) and Et_3N (270 µL, 1.95 mmol) and the reaction mixture was stirred at 22 °C for 3 h. The mixture was concentrated *in vacuo* purified directly by flash column chromatography (EtOAc/heptane 1:15 to 1:5) to give the title compound as a colorless oil (288 mg, 53%).

***R*f** = 0.45 (EtOAc/heptane 2:5); **^{1}H NMR** (400 MHz, CCl_3) δ 6.94 – 6.63 (m, 1H), 6.42 – 6.13 (m, 1H), 4.96 – 4.58 (m, 2H), 4.28 – 3.97 (m, 2H), 3.26 – 3.04 (m, 1H), 2.57 (s, 3H), 1.85 (s, 1H), 1.43 (s, 9H), 1.22 (t, *J* = 7.2 Hz, 3H); **^{13}C NMR** (101 MHz, $CDCl_3$) δ 168.3, 153.3, 138.1 (major rotamer), 137.6 (minor rotamer), 131.9 (minor rotamer), 130.5 (major rotamer), 124.4 (q, $^1J_{CF}$ = 287.6 Hz), 79.6, 64.4 (minor rotamer), 63.6 (major rotamer), 61.0 (minor rotamer),

60.1, 59.8 (major rotamer), 54.4, 30.4, 27.1 (3C), 12.8; **^{19}F NMR** (377 MHz, $CDCl_3$) δ -63.04 (major rotamer), -64.07 (minor rotamer); **IR** (neat) cm^{-1}: 3367 (s, N–H), 1744 (s, C=O), 1694 (s, C=O), 1594 (s, C=C); **HRMS** (ESI) calcd. for $[C_{16}H_{24}F_3N_2O_4]$ $[M+H]^+$ 365.1683, found 365.1684.

7-(*tert*-Butyl) 2-ethyl (1*S,2*R**,3*S**,4*R**)-3-(methylamino)-3-(trifluoromethyl)-7-aza-bicyclo[2.2.1]heptane-2,7-dicarboxylate (2.252)**

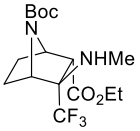

To a solution of **2.87** (250 mg, 0.686 mmol) in EtOH (7 mL) was added 5% Pd/C (0.146 mg, 69.0 µmol) and the resulting suspension was stirred under an atmosphere of H_2 for at 22 °C for 2 h. The mixture was filtered through a pad of celite and concentrated *in vacuo* to give the title compound as a colorless oil (251 mg, >95%).

^{1}H NMR (400 MHz, $CDCl_3$) δ 4.51 – 4.06 (m, 4H), 2.93 – 2.82 (m, 1H), 2.49 (s, 3H), 2.22 – 2.04 (m, 1H), 1.81 (s, 4H), 1.46 (s, 9H), 1.25 (t, *J* = 7.1 Hz, 3H); **^{13}C NMR** (101 MHz, $CDCl_3$) δ 169.0, 155.6, 125.8 (d, $^1J_{CF}$ = 289.3 Hz), 80.4, 72.1, 62.0, 61.0, 58.1, 54.9, 30.7, 28.3 (3C), 24.8, 22.8, 14.0; **^{19}F NMR** (377 MHz, $CDCl_3$) δ -63.39 (major rotamer), -64.67 (minor rotamer); **IR** (neat) cm^{-1}: 1711 (s, C=O), 1698 (s, C=O); **HRMS** (ESI) calcd. for $[C_{16}H_{26}F_3N_2O_4]$ $[M+H]^+$ 367.1839, found 367.1843.

Ethyl (1*S,2*R**,3*S**,4*R**)-3-(methylamino)-3-(trifluoromethyl)-7-azabicyclo[2.2.1]heptane-2-carboxylate (2.88)**

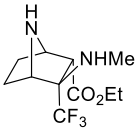

Flowing *general procedure E* using **2.252** (210 mg, 0.587 mmol) afforded the title compound as a white solid (126 mg, 80%) after purification by flash column chromatography (CH_2Cl_2/MeOH/Et_3N 200:0:1 to 196:4:1).

***R*$_f$** = 0.56 (CH_2Cl_2/MeOH/ Et_3N 90:10:2); **m.p.**: 82–84 °C; **^{1}H NMR** (400 MHz, $CDCl_3$) δ 4.15 (qq, *J* = 10.8, 7.1 Hz, 2H), 3.93 – 3.78 (m, 1H), 3.66 – 3.53 (m, 1H), 2.63 – 2.54 (m, 1H), 2.49 (q, *J* = 1.7 Hz, 3H), 2.23 – 2.05 (m, 1H), 1.85 – 1.58 (m, 3H), 1.25 (t, *J* = 7.1 Hz, 3H); **^{13}C NMR** (101 MHz, , $CDCl_3$) δ 169.4, 126.7 (q, $^1J_{CF}$ = 289.8 Hz), 71.1 (q), 63.1, 60.9, 59.4, 57.3, 30.5, 23.8, 22.7, 14.0; **^{19}F NMR** (377 MHz, $CDCl_3$) δ -62.94, **IR** (neat) cm^{-1}: 3367 (br., N–H), 1701 (s, C=O); **HRMS** (ESI) calcd. for $[C_{11}H_{18}F_3N_2O_2]$ $[M+H]^+$ 267.1315, found 267.1317.

Ethyl (1*S,2*R**,3*S**,4*R**)-7-(ethylcarbamoyl)-3-(methylamino)-3-(trifluoromethyl)-7-azabicyclo[2.2.1]heptane-2-carboxylate (2.89)**

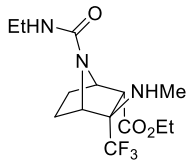

To a solution of **2.88** (60.0 mg, 0.225 mmol) in CH_2Cl_2 (2.5 mL) was added Et_3N (47.0 µL, 0.338 mmol) and ethyl isocyanate (23.2 µL, 0.293 mmol) and the reaction mixture was stirred at 22 °C for 22 h. The mixture was concentrated *in vacuo* and purified directly by flash column chromatography (EtOAc/heptane (3:1 to 97:3) to give the title compound as a sticky off-white solid (56.2 mg, 74%).

***R*$_f$** = 0.58 (CH_2Cl_2/MeOH/Et_3N 90:10:2); **m.p.**: 76–78 °C; **^{1}H NMR** (400 MHz, $CDCl_3$) δ 4.59 (s, 1H), 4.36 (d, *J* = 4.5 Hz, 1H), 4.25 – 4.21 (m, 1H), 4.16 (dtt, *J* = 13.8, 7.1, 3.6 Hz, 2H), 3.33 – 3.16 (m, 2H), 2.99 (d, *J* = 4.4 Hz, 1H), 2.51 (t, *J* = 1.4 Hz, 3H), 2.20 – 2.10 (m, 1H), 2.03 (br. s, 1H), 1.90 – 1.72 (m, 3H), 1.25 (t, *J* = 7.1 Hz, 3H), 1.13 (t, *J* = 7.2 Hz, 3H); **^{13}C NMR** (101 MHz, $CDCl_3$) δ 168.9, 158.0, 125.8 (q, $^1J_{CF}$ = 288.3 Hz), 71.7 (q, $^2J_{CF}$ = 25.8 Hz), 63.7, 61.1, 59.2, 54.3, 35.6, 30.6, 24.5, 23.1, 15.5, 14.0; **^{19}F NMR** (377 MHz, $CDCl_3$) δ -64.57; **IR** (neat) cm^{-1}: 3303 (br., N–H), 1698 (s, C=O), 1677 (s, C=O), 1603 (s, N–H); **HRMS** (ESI) calcd. for $[C_{14}H_{23}F_3N_3O_3]$ $[M+H]^+$ 338.1686, found 338.1685.

7-(*tert*-Butyl) 2-ethyl (1*S,2*R**,3*S**,4*R**)-3-(allylamino)-3-(trifluoromethyl)-7-azabicyclo [2.2.1]hept-5-ene-2,7-dicarboxylate (2.90)**

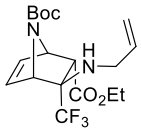

To a solution of **2.76** (300 mg, 0.900 mmol) in EtOH (9 mL) was added allylamine (0.101 mL, 1.355 mmol) and Et_3N (270 µL, 1.95 mmol) and the reaction mixture was stirred at 22 °C for 4 h. The mixture was concentrated *in vacuo* purified directly by flash column chromatography (EtOAc/heptane 1:5 to 2:5) to give the title compound as a yellow oil (216 mg, 62%).

***R*$_f$** = 0.55 (EtOAc/heptane 1:5); **^{1}H NMR** (400 MHz, $CDCl_3$) δ 6.78 (d, *J* = 17.1 Hz, 1H), 6.28 (d, *J* = 17.1 Hz, 1H), 6.00 – 5.81 (m, 1H), 5.32 – 5.01 (m, 2H), 4.93 – 4.58 (m, 2H), 4.20 – 4.02 (m, 2H), 3.64 – 3.34 (m, 2H), 3.20 (s, 1H), 1.89 (s, 1H), 1.43 (s, 9H), 1.26 – 1.19 (m, 3H); 13C NMR (101 MHz, $CDCl_3$) δ 169.40 (minor rotamer), 169.35 (major rotamer), 154.1, 139.7 (major rotamer), 138.8 (minor rotamer), 136.3 (major rotamer), 134.1 (minor rotamer), 132.8 (minor rotamer), 131.8 (major rotamer), 125.5 (q, $^1J_{CF}$ = 287.2 Hz), 116.5 (major rotamer), 116.3 (minor rotamer), 85.2 (q, $^3J_{CF}$ = 5.8 Hz), 81.0 (major rotamer), 77.5 (minor rotamer), 66.1 (major rotamer), 65.6 (minor rotamer), 62.0 (minor rotamer), 61.3, 61.2 (major rotamer), 56.1 (minor rotamer), 55.2 (major rotamer), 47.7, 28.4 (3C), 14.0; **^{19}F NMR** (377 MHz, $CDCl_3$) δ -64.06 (major rotamer), -64.39 (minor rotamer); **IR** (neat) cm^{-1}: 3322 (s, N–H), 1702 (s, C=O), 1623 (m, C=C); **HRMS** (ESI) calcd. for $[C_{18}H_{26}F_3N_2O_4]$ $[M+H]^+$ 391.1839, found 391.1986.

8-(*tert*-Butyl) 3a-ethyl (3a*R,4*S**,7*R**,7a*S**)-2-benzyl-7a-(trifluoromethyl)-1,2,3,4,7,7a-hexahydro-3a*H*-4,7-epiminoisoindole-3a,8-dicarboxylate (2.93)**

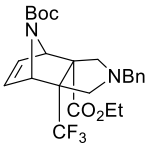

To an ice-cooled solution of **2.76** (100 mg, 0.300 mmol) and *N*-(methoxymethyl)-*N*-(trimethylsilylmethyl)benzylamine (84.0 µL, 0.330 mmol) in CH_2Cl_2 (6 mL) was added trifluoroacetic acid (0.1 M in CH_2Cl_2, 0.300 mL, 30.0 µmol) dropwise and the reaction mixture was stirred at 22 °C for 2 h. The mixture was concentrated *in vacuo* and purified directly by flash column chromatography (EtOAc/heptane /Et_3N 95:5:1 to 90:10:1) to give the title compound as a yellow oil (82.0 mg, 59%).

R_f = 0.58 (EtOAc/heptane 2:5); **^{1}H NMR** (400 MHz, $CDCl_3$) δ 7.57 – 7.08 (m, 5H), 6.86 – 6.62 (m, 1H), 6.48 – 6.25 (m, 1H), 4.79 – 4.39 (m, 2H), 4.38 – 4.20 (m, 1H), 4.20 – 4.03 (m, 1H), 4.01 – 3.54 (m, 2H), 3.54 – 3.14 (m, 2H), 2.66 – 2.35 (m, 2H), 1.42 (m, 9H), 1.28 (m, 3H); **^{13}C NMR** (101 MHz, $CDCl_3$) δ 167.0, 155.2, 140.1 (minor rotamer), 138.6, 138.2 (major rotamer), 135.0 (major rotamer), 133.2 (minor rotamer), 128.4 (2C), 128.3 (2C), 127.2, 81.1, 66.5, 65.8 (minor rotamer), 65.6 (major rotamer), 65.1, 62.7, 62.0, 61.3, 59.7 (minor rotamer), 59.4 (major rotamer), 58.5, 28.4 (major rotamer, 3C), 28.2 (minor rotamer, 3C), 13.9. CF_3 was not observed; **^{19}F NMR** (377 MHz, $CDCl_3$) δ -62.13 (minor rotamer), -64.32 (major rotamer); **IR** (neat) cm^{-1}: 1717 (s, C=O); **HRMS** (ESI) calcd. for $[C_{24}H_{30}F_3N_2O_4]$ $[M+H]^+$ 467.2152, found 467.2161.

Ethyl (3a*R,4*S**,7*R**,7a*S**)-7a-(trifluoromethyl)octahydro-3a*H*-4,7-epiminoisoindole-3a-carboxylate (2.94)**

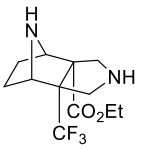

To a solution of **2.93** (50.0 mg, 0.107 mmol) in EtOH (2.5 mL) was added 10% Pd/C (11.4 mg, 10.7 µmol) and the resulting suspension was stirred under an atmosphere of H_2 at 22 °C for 2 h. The mixture was filtered through a pad of celite and concentrated *in vacuo*. The crude debenzylated product was subjected to *general procedure E* to give to give the title compound as a yellow oil (26.7 mg, 90%).

^{1}H NMR (400 MHz, CD_3OD) δ 4.30 (q, *J* = 7.1 Hz, 2H), 3.93 (d, *J* = 5.3 Hz, 1H), 3.89 (d, *J* = 4.6 Hz, 1H), 3.85 (d, *J* = 12.3 Hz, 1H), 3.76 – 3.61 (m, 3H), 2.15 (ddd, *J* = 18.6, 9.8, 5.7 Hz, 2H), 1.80 (tdd, *J* = 12.3, 5.3, 2.7 Hz, 1H), 1.71 – 1.60 (m, 1H), 1.34 (t, *J* = 7.1 Hz, 3H); **^{13}C NMR** (101 MHz, CD_3OD) δ 167.8, 127.8 (q), 66.9, 66.5, 62.9, 62.8, 61.6, 58.2, 53.4, 26.1, 25.3, 14.1; **^{19}F NMR** (377 MHz, CD_3OD) δ -76.89; **IR** (neat) cm^{-1}: 3300 (br., N–H), 1734 (s, C=O); **HRMS** (ESI) calcd for $[C_{12}H_{18}F_3N_2O_2]$ $[M+H]^+$ 278.1241, found 278.1248

8-(*tert*-Butyl) 6-ethyl (1*S,5*R**,6*R**)-3-benzyl-7-(trifluoromethyl)-3,8-diazabicyclo [3.2.1] octane-6,8-dicarboxylate (2.98)**

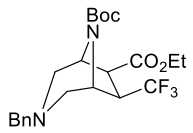

To an ice-cooled solution of **2.76** (1.00 g, 3.00 mmol) in acetone/H_2O/*n*-BuOH (19:1:1, 30 mL) was added *N*-methylmorpholine oxide (369 mg, 3.45 mmol) and $K_2OsO_4 \cdot (H_2O)_2$ (22.0 mg, 0.0600 mmol) and the turbid reaction mixture was stirred on ice for 2 h and then at 22 °C for 1 h. 5% Pd/C (639 mg, 0.300 mmol) was added to the mixture and the resulting suspension was stirred under an atmosphere of H_2 at 22 °C for 1 h. The reaction was quenched with 10% aq. Na_2SO_3 (0.50 mL) and stirred for 30 min, then filtered through a pad of celite and concentrated *in vacuo*. The crude diol was dissolved in EtOH/ H_2O (9:1, 30 mL) and added $NaIO_4$ (1.95 g, 9.17 mmol) and the reaction mixture was stirred at 22 °C for 17 h. Precipitate was filtered off and washed with sat. aq. $NaHCO_3$ (60 mL). The filtrate was extracted with CH_2Cl_2 (5 × 100 mL) and the combined organic layers were washed with brine (1 × 200 mL), dried over Na_2SO_4, filtered, and concentrated *in vacuo* to give the crude, impure dialdehyde (1.13 g) that was used directly in the next step without further purification.

To a solution of crude aldehyde (250 mg, 0.681 mmol) in anhydrous MeOH (13 mL) was added 3Å MS and benzylamine (88.8 µL, 0.817 mmol) and the reaction mixture was stirred at 22 °C for 2 h. The mixture was cooled to 0 °C and added $NaBH_3CN$ (170 mg, 2.72 mmol). After 10 min., cooling was removed and the mixture was stirred at 22 °C for 16 h. Sat. aq. $NaHCO_3$ (10 mL) was added and the mixture was filtered. The filtrate was extracted with PhMe (3 × 30 mL) and the combined organic layers were washed with brine (1 × 60 mL), dried over Na_2SO_4, filtered, and concentrated *in vacuo*. The crude product was purified by flash column chromatography (PhMe/EtOAc/Et_3N 99:1:1 to 96:4:1, to give the title compound as an off-white amorphous solid (14.4 mg, 5%).

R_f = 0.59 (PhMe/EtOAc 2:1); **^{1}H NMR** (400 MHz, $CDCl_3$) δ 7.43 – 7.20 (m, 5H), 4.69 – 4.42 (m, 2H), 4.22 – 4.07 (m, 2H), 3.59 – 3.43 (m, 2H), 3.43 – 3.23 (m, 2H), 2.75 – 2.61 (m, 2H), 2.41 – 2.20 (m, 2H), 1.47 (d, 9H, rotamers), 1.24 (dt, *J* = 9.9, 7.2 Hz, 3H); **^{13}C NMR** (101 MHz, $CDCl_3$) δ 170.79 (minor rotamer), 170.77 (major rotamer), 152.3 (minor rotamer), 151.8 (major rotamer), 137.8, 128.9, 128.6, 127.6, 126.4 (d, $^1J_{CF}$ = 279.7 Hz), 80.3 (minor rotamer), 80.2 (major rotamer), 61.8 (minor rotamer), 61.7 (major rotamer), 61.4 (major rotamer), 61.3 (minor rotamer), 57.8 (major rotamer), 57.4 (minor rotamer), 57.00 (minor rotamer), 56.97 (major rotamer), 56.8 (minor rotamer), 56.7 (major rotamer), 55.7 (d, $^3J_{CF}$ = 2.7 Hz, major rotamer), 54.7 (d, $^3J_{CF}$ = 2.7 Hz, minor rotamer), 50.7 (d, $^2J_{CF}$ = 27.8 Hz, major rotamer), 50.1 (d, $^2J_{CF}$ = 27.9 Hz, minor rotamer), 48.62 (minor rotamer), 48.59 (major rotamer). 28.5 (3C, rotamers), 14.0 (minor rotamer), 13.9 (major rotamer); **^{19}F NMR** (377 MHz, $CDCl_3$) δ -65.25 (major rotamer), -65.42 (minor rotamer); **IR** (neat) cm^{-1}: 1740 (s, C=O), 1700 (s, C=O); **HRMS** (ESI) calcd. for $[C_{22}H_{30}F_3N_2O_4]$ $[M+H]^+$ 443.2152, found 443.2162.

[5+2] Cycloaddition

3-Hydroxy-4-methoxy-2-methylpyrylium trifluoromethanesulfonate (2.102)

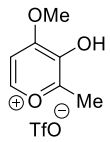

To a suspension of 3-hydroxy-2-methyl-4*H*-pyran-4-one (1.33 g, 10.6 mmol) in anhydrous CH_2Cl_2 (6 mL) was added methyl trifluoromethanesulfonate (1.79 mL, 15.8 mmol) and the reaction mixture was refluxed under an atmosphere of N_2 for 4 h. Then, the solution was concentrated *in vacuo* to give the title compound as a light pink solid (2.91 g, 95%).

m.p.: 94–96 °C; **^{1}H NMR** (400 MHz, D_2O) δ 8.92 (d, *J* = 5.2 Hz, 1H), 7.73 (d, *J* = 5.2 Hz, 1H), 4.38 (s, 3H), 2.77 (s, 3H); **^{13}C NMR** (101 MHz, D_2O) δ 168.4, 166.1, 160.1, 141.8, 119.6 (d, *J* = 317.2 Hz), 107.3, 59.7, 15.6; **^{19}F NMR** (377 MHz, D_2O) δ -78.79; **IR** (neat) cm^{-1}: 3083 (br., O–H), 1631 (s, C=C).

Ethyl (1*S**,5*S**-3-methoxy-5-methyl-4-oxo-7-(trifluoromethyl)-8-oxabicyclo[3.2.1]octa-2,6-diene-6-carboxylate (2.103)

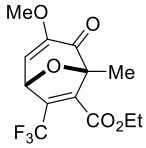

To a suspension of **2.102** (86.0 mg, 0.296 mmol) in $CHCl_3$ (0.5 mL) was added ethyl 4,4,4-trifluorobut-2-ynoate **2.4** (332 mg, 2.96 mmol) and *N*,*N*-diisopropylaniline (69.0 µL, 0.356 mmol) and the solution was subjected to microwave heating at 100 °C for 10 min. The reaction mixture was concentrated *in vacuo* and purified directly by flash column chromatography (EtOAc/heptane 2:7) to give the title compound as a yellow oil (70.0 mg, 77%).

***R*$_f$** = 0.27 (EtOAc/heptane 2:7); **^{1}H NMR** (400 MHz, $CDCl_3$) δ 6.08 (d, *J* = 4.8 Hz, 1H), 5.36 (d, *J* = 4.8 Hz, 1H), 4.38 – 4.15 (m, 2H), 3.61 (s, 3H), 1.66 (s, 3H), 1.30 (t, *J* = 7.1 Hz, 3H); **^{13}C NMR** (101 MHz, $CDCl_3$) δ 187.7, 161.3, 146.8, 146.0 (q, *J* = 36.5 Hz), 140.5 (q, *J* = 4.0 Hz), 120.9 (q, *J* = 271.0 Hz), 113.3, 94.1, 77.3 (q, *J* = 2.1 Hz), 62.4, 55.3, 16.3, 14.0; **^{19}F NMR** (377 MHz, $CDCl_3$) δ -61.51; **IR** (neat) cm^{-1}: 1718 (s, C=O), 1659 (s, C=O), 1613 (s, C=C); **HRMS** (ESI) calcd for $[C_{13}H_{14}F_3O_5]$ $[M+H]^+$ 307.0788, found 307.0794.

Ethyl (1*S**,3*S**,5*S**,6*R**,7*S**)-3-methoxy-5-methyl-4-oxo-7-(trifluoromethyl)-8-oxabicyclo [3.2.1]octane-6-carboxylate (2.104)

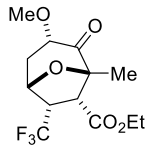

To a solution of **2.103** (353 mg, 1.15 mmol) in EtOH (23 mL) was added 5% Pd/C (245 mg, 0.115 mmol) and the resulting suspension was stirred under an atmosphere of H_2 at 21 °C for 4 h. Then, the mixture was filtered through a pad of celite, concentrated *in vacuo*, and purified directly by flash column chromatography (EtOAc/heptane 2:7) to give the title compound as a white crystalline solid (295 mg, 83%).

***R*f** = 0.20 (EtOAc/heptane 2:7); **m.p.**: 92–94 °C; **^{1}H NMR** (400 MHz, CD_3OD) δ 4.91 (ddd, *J* = 9.8, 5.7, 2.9 Hz, 1H), 4.26 (t, *J* = 10.0 Hz, 1H), 4.11 (qq, *J* = 11.0, 7.1 Hz, 2H), 3.56 – 3.43 (m, 4H), 3.37 (d, *J* = 11.0 Hz, 1H), 2.74 (dt, *J* = 13.7, 10.0 Hz, 1H), 2.25 (ddd, *J* = 13.7, 10.0, 2.9 Hz, 1H), 1.50 (s, 3H), 1.26 (t, *J* = 7.1 Hz, 3H); **^{13}C NMR** (101 MHz, CD_3OD) δ 211.4, 170.0, 126.1 (q, $^{1}J_{CF}$ = 277.6 Hz), 91.2, 77.4, 74.3 (q, $^{3}J_{CF}$ = 1.9 Hz), 62.8, 58.9, 55.5 (q, $^{3}J_{CF}$ = 1.5 Hz), 51.4 (q, $^{2}J_{CF}$ = 28.3 Hz), 25.8 (q, $^{4}J_{CF}$ = 2.2 Hz), 21.12, 14.2; **^{19}F NMR** (377 MHz, CD_3OD) δ -60.40; **IR** (neat) cm^{-1}: 1744 (s, C=O), 1729 (s, C=O).

(1*S,2*S**,3*S**,5*S**,6*S**,7*S**)-7-(Hydroxymethyl)-3-methoxy-1-methyl-6-(trifluoromethyl)-8-oxabicyclo[3.2.1]octan-2-ol (2.105)**

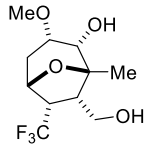

To an ice-cooled solution of **2.104** (36.0 mg, 0.116 mmol) in anhydrous THF (2.5 mL) was added $LiAlH_4$ (2.0 M in THF, 290 µL, 0.580 mmol) and the reaction mixture was stirred at 21 °C under an atmosphere of N_2 for 4 h. The mixture was cooled to 0 °C and was added $Na_2SO_4(H_2O)_{10}$ portion wise until bubbling ceased. The suspension was filtered and the filtrate was added sat. aq. $NaHCO_3$ (5 mL) and extracted with CH_2Cl_2 (5 × 5 mL). The combined organic layers were dried over $MgSO_4$, filtered, and concentrated *in vacuo*. The crude was purified by flash column chromatography (EtOAc/heptane 1:1) to give the title compound as an off-white solid (30.0 mg, 96%).
***R*f** = 0.21 (EtOAc/heptane 1:1); **m.p.**: 101–103 °C; **^{1}H NMR** (400 MHz, DMSO-d_6) δ 4.79 (d, *J* = 7.0 Hz, 1H), 4.39 – 4.26 (m, 2H), 4.23 (t, *J* = 6.0 Hz, 1H), 3.71 (dt, *J* = 11.2, 6.6 Hz, 1H), 3.60 (t, *J* = 7.0 Hz, 1H), 3.51 – 3.32 (m, 2H), 3.23 (s, 3H), 2.49 – 2.38 (m, 1H), 2.09 – 1.93 (m, 2H), 1.36 (s, 3H); **^{13}C NMR** (101 MHz, DMSO-d_6) δ 126.5 (d, $^{3}J_{CF}$ = 278.8 Hz), 84.5, 76.2, 74.5, 72.5 (q, $^{1}J_{CF}$ = 2.9 Hz), 58.2, 57.4, 49.3, 47.8 (q, $^{2}J_{CF}$ = 27.5 Hz), 30.6, 27.3; **^{19}F NMR** (377 MHz, DMSO-d_6) δ -58.37; **IR** (neat) cm^{-1}: 3145 (br., O–H); **HRMS** (ESI) calcd for $[C_{11}H_{18}F_3O_4]$ $[M+H]^+$ 271.1152, found 271.1136.

Ethyl (1*S,4*S**,5*S**,6*S**,7*R**)-4-hydroxy-3-methoxy-5-methyl-7-(methylamino)-7-(trifluoromethyl)-8-oxabicyclo[3.2.1]oct-2-ene-6-carboxylate (2.108) and (3*R**,3a*S**,5*S**,7a*S**,8*R**)-7-methoxy-3a-methyl-8-(methylamino)-8-(trifluoromethyl)-3,3a,5,7a-tetrahydro-2*H*-3,5-methanofuro[3,2-*b*]pyran-2-one (2.109)**

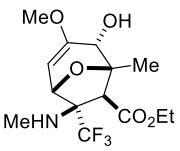

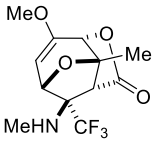

To suspension of **2.103** (120 mg, 0.392 mmol) in EtOH (4 mL) was added methylamine hydrochloride (30.4 mg, 0.451 mmol) and Et_3N (105 µL, 0.784 mmol) and the reaction mixture was stirred at 21 °C for 4 h. The solution was cooled to 0 °C and added $NaBH_4$ (59.3mg, 1.57 mmol). After 15 min., cooling was removed and the reaction mixture was stirred at 21 °C for 1 h. Then, SiO_2 (875 mg) was added and the mixture was concentrated *in vacuo* and purified by flash column chromatography (EtOAc/heptane 1:2) to give the title compounds **2.108** as a yellow amorphous solid (74.5 mg, 56%) and **2.109** as a colorless amorphous solid (33.0 mg, 30%).

Data for **2.108**: $\boldsymbol{R_f}$ = 0.28 (EtOAc/heptane 1:2); **^{1}H NMR** (400 MHz, DMSO-d_6) δ 5.78 (d, *J* = 5.1 Hz, 1H), 4.80 (dd, *J* = 5.0, 1.6 Hz, 1H), 4.69 (d, *J* = 5.0 Hz, 1H), 4.16 – 3.98 (m, 3H), 3.80 (s, 1H), 3.47 (s, 3H), 2.44 (q, *J* = 5.9 Hz, 1H), 2.34 (d, *J* = 5.9 Hz, 3H), 1.37 (s, 3H), 1.16 (t, *J* = 7.1 Hz, 3H); **^{13}C NMR** (101 MHz, DMSO-d_6) δ 169.5, 155.3, 125.9 (d, $^1J_{CF}$ = 286.5 Hz), 94.2, 83.4, 74.0 (q, $^2J_{CF}$ = 23.0 Hz), 73.3, 71.8, 60.3, 54.4, 47.9, 29.6, 20.9, 13.9; **^{19}F NMR** (377 MHz, DMSO-d_6) δ -66.43; **IR** (neat) cm^{-1}: 3516 (s, N–H), 3350 (br., O–H), 1725 (s, C=O), 1662 (m, C=C); **HRMS** (ESI) calcd for $[C_{14}H_{21}F_3NO_5]$ $[M+H]^+$ 340.1372, found 340.1362.

Data for **2.109**: $\boldsymbol{R_f}$ = 0.14 (EtOAc/heptane 1:2); **^{1}H NMR** (400 MHz, DMSO-d_6) δ 5.32 (d, *J* = 5.8 Hz, 1H), 4.84 (d, *J* = 1.3 Hz, 1H), 4.68 (d, *J* = 5.9 Hz, 1H), 3.51 (s, 3H), 2.89 – 2.79 (m, 2H), 2.34 (dd, *J* = 5.8, 1.5 Hz, 3H), 1.56 (s, 3H); **^{13}C NMR** (101 MHz, DMSO-d_6) δ 172.3, 153.8, 125.0 (q, $^1J_{CF}$ = 286.8 Hz), 99.5, 86.1, 80.7, 76.5 (q, $^2J_{CF}$ = 23.4 Hz), 76.1, 55.0, 53.1, 30.0, 21.2; **^{19}F NMR** (377 MHz, DMSO-d_6) δ -63.74; **IR** (neat) cm^{-1}: 3358 (s, N–H), 1776 (s, C=O), 1666 (m, C=C); **HRMS** (ESI) calcd for $[C_{12}H_{15}F_3NO_4]$ $[M+H]^+$ 294.0948, found 294.0945.

Ethyl (1*S,4*S**,5*S**,6*S**,7*R**)-7-(but-3-en-1-ylamino)-4-hydroxy-3-methoxy-5-methyl-7-(trifluoromethyl)-8-oxabicyclo[3.2.1]oct-2-ene-6-carboxylate (2.110) and (3*R**,3a*S**,5*S**,7a*S**,8*R**)-8-(but-3-en-1-ylamino)-7-methoxy-3a-methyl-8-(trifluoromethyl)-3,3a,5,7a-tetrahydro-2H-3,5-methanofuro[3,2-*b*]pyran-2-one (2.111)**

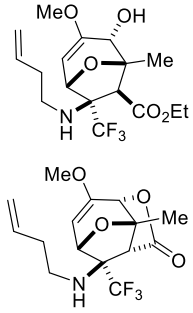

To suspension of **2.103** (114 mg, 0.372 mmol) in EtOH (7 mL) was added but-3-en-1-amine hydrochloride (50.1 mg, 0.465 mmol) and Et_3N (98.9 µL, 0.745 mmol) and the reaction mixture was stirred at 21 °C for 4 h. The solution was cooled to 0 °C and added $NaBH_4$ (42.3 mg, 1.12 mmol). After 15 min., cooling was removed and the reaction mixture was stirred at 21 °C for 1 h. Then, SiO_2 (1 g) was added and the mixture was concentrated *in vacuo* and purified by flash column chromatography (EtOAc/heptane 3:8) to give a mixture of the title compounds as a yellow oil (100 mg, 80%). $\boldsymbol{R_f}$ = 0.44 (EtOAc/heptane 2:3).

Ethyl (1*S,4*S**,5*S**,6*S**,7*R**)-7-amino-4-hydroxy-3-methoxy-5-methyl-7-(trifluoromethyl)-8-oxabicyclo[3.2.1]oct-2-ene-6-carboxylate (2.112) and (3*R**,3a*S**,5*S**,7a*S**,8*R**)-8-amino-7-methoxy-3a-methyl-8-(trifluoromethyl)-3,3a,5,7a-tetrahydro-2*H*-3,5-methanofuro[3,2-*b*]pyran-2-one (2.113)**

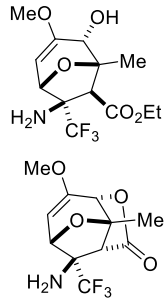

To a solution of **2.110** and **2.111** (3:2 mixture, 98.0 mg, 0.258 mmol) in PhMe (26 mL) was added Hoveyda-Grubbs 2nd generation catalyst (8.1 mg, 12.9 µmol) and the mixture was refluxed under an ethylene atmosphere for 16 h. The mixture was concentrated *in vacuo* and purified directly by flash column chromatography (EtOAc/heptane 2:3) to give **2.112** (51.0 mg, 53%) and **2.113** (14.0 mg, 15%) both as off-white amorphous solids.

Data for **2.112**: $\boldsymbol{R_f}$ = 0.52 (EtOAc/heptane 3:2); **^{1}H NMR** (400 MHz, $CDCl_3$) δ 4.82 (dd, *J* = 4.7, 1.8 Hz, 1H), 4.29 (d, *J* = 4.5 Hz, 2H), 4.27 – 4.13 (m, 2H), 3.83 (s, 1H), 3.60 (s, 3H), 2.43 (dtd, *J* = 18.7, 7.1, 1.7 Hz, 3H), 2.48 – 2.24 (m, 3H), 1.47 (s, 3H), 1.27 (t, *J* = 7.1 Hz, 3H); **^{13}C NMR** (101 MHz, $CDCl_3$) δ 170.5, 154.5, 125.3 (d, $^1J_{CF}$ = 281.8 Hz), 93.9, 84.2, 79.5, 74.5, 71.9 (q, $^2J_{CF}$ = 25.2 Hz), 61.2, 55.2, 47.4, 21.2, 14.3; **^{19}F NMR** (377 MHz, $CDCl_3$) δ -73.21.

Data for **2.113**: $\boldsymbol{R_f}$ = 0.28 (EtOAc/heptane 3:2); **^{1}H NMR** (400 MHz, $CDCl_3$) δ 5.17 (d, *J* = 5.8 Hz, 1H), 4.69 (d, *J* = 0.8 Hz, 1H), 4.44 (d, *J* = 5.8 Hz, 1H), 3.60 (s, 3H), 2.58 (s, 1H), 1.87 (s, 2H), 1.71 (s, 3H); **^{13}C NMR** (101 MHz, $CDCl_3$) δ 171.1, 154.5, 124.4 (q, $^1J_{CF}$ = 282.4 Hz), 98.0, 86.9, 81.4, 80.4, 72.9 (q, $^2J_{CF}$ = 26.5 Hz), 58.2, 55.3, 22.4; **^{19}F NMR** (377 MHz, $CDCl_3$) δ -69.90.

Ethyl 4,6-dihydroxy-2-methyl-3-oxo-7-(trifluoromethyl)cyclohepta-1,4,6-triene-1-carboxylate (2.114) and ethyl 6-hydroxy-4-methoxy-2-methyl-3-oxo-7-(trifluoromethyl)cyclohepta-1,4,6-triene-1-carboxylate (2.115)

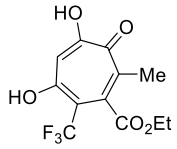

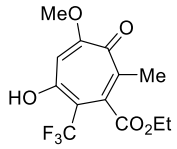

To an ice-cooled solution of BCl_3 (1.0 M in CH_2Cl_2, 3.27 mL, 3.27 mmol) in anhydrous CH_2Cl_2 (9 mL) under an atmosphere of N_2 was added an ice-cooled solution of **2.103** (84.0 mg, 0.274 mmol) in anhydrous CH_2Cl_2 (12 mL) and the reaction mixture was stirred at 0 °C for 1 h. Then, water (25 mL) was added and the mixture was stirred at 21 °C for 1 h. The layers were separated and the aqueous phase was extracted with CH_2Cl_2 (1 × 25 mL). The combined organic layers were dried over $MgSO_4$, filtered, and concentrated *in vacuo*. The crude was purified by flash column chromatography (EtOAc/heptane 1:5 to EtOAc) to give the title compounds **2.114** as a yellow oil (22.2 mg, 28%) and **2.115** as a colorless oil (12.2 mg, 14%).

Data for **2.114**: $\boldsymbol{R_f}$ = 0.30 (EtOAc); **^{1}H NMR** (400 MHz, $CDCl_3$) δ 7.97 (s, 1H), 4.43 (q, *J* = 7.1 Hz, 2H), 2.53 (s, 3H), 2.38 – 2.11 (m, 1H), 1.39 (t, *J* = 7.1 Hz, 3H); **^{13}C NMR** (101 MHz, $CDCl_3$) δ 181.6, 171.4, 170.1, 167.1, 141.5, 137.1, 135.8, 131.1, 123.6 (d, $^1J_{CF}$ = 267.4 Hz), 62.7, 20.4, 13.9; **^{19}F NMR** (377 MHz, $CDCl_3$) δ -57.48; **IR** (neat) cm^{-1}: 3320 (br., O–H), 1737 (s, C=O), 1516 (s, C=C); **HRMS** (ESI) calcd for $[C_{12}H_{12}F_3O_5]$ $[M+H]^+$ 293.0631, found 293.0631.

Data for **2.115**: $\boldsymbol{R_f}$ = 0.30 (EtOAc/heptane 1:5); **^{1}H NMR** (400 MHz, $CDCl_3$) δ 7.52 (s, 1H), 4.38 (q, *J* = 7.1 Hz, 2H), 3.96 (s, 3H), 2.29 (s, 3H), 1.37 (t, *J* = 7.1 Hz, 3H); **^{13}C NMR** (101 MHz, $CDCl_3$) δ 182.3, 166.1, 157.9, 142.8, 132.9, 132.5 (q, $^3J_{CF}$ = 6.8 Hz), 127.2, 124.0 (q, $^2J_{CF}$ = 35.5 Hz), 122.8 (q, $^1J_{CF}$ = 270.5 Hz), 62.6, 59.7, 19.2, 13.8; **^{19}F NMR** (377 MHz, $CDCl_3$) δ -59.88; **IR** (neat) cm^{-1}: 1734 (s, C=O), 1629 (s, C=C); **HRMS** (ESI) calcd for $[C_{13}H_{14}F_3O_5]$ $[M+H]^+$ 307.0788, found 307.0786.

Ethyl (1*S,5*S**,6*R**,7*R**)-3-methoxy-5-methyl-4-oxo-7-(trifluoromethyl)-8-oxabicyclo [3.2.1]oct-2-ene-6-carboxylate (2.119)**

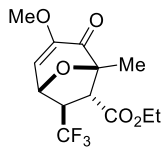

To a suspension of **2.102** (2.00 g, 6.89 mmol) in $CHCl_3$ (2.0 mL) was added ethyl (*E*)-4,4,4-trifluorobut-2-enoate **2.2** (15.2 mL, 82.7 mmol) and *N*,*N*-diisopropylaniline (69.0 µL, 0.356 mmol) and the solution was subjected to microwave heating at 100 °C for 10 min. The reaction mixture was concentrated *in vacuo* and purified directly by flash column chromatography (EtOAc/heptane/Et_3N 30:80:2) to give the title compound as an off-white solid (1.21 g, 57%).

$\boldsymbol{R_f}$ = 0.22 (EtOAc/heptane 3:8); **m.p.**: 75–77 °C; **^{1}H NMR** (400 MHz, $CDCl_3$) δ 6.12 (d, *J* = 5.4 Hz, 1H), 4.99 (d, *J* = 5.4 Hz, 1H), 4.25 – 4.01 (m, 2H), 3.64 (s, 3H), 3.52 – 3.35 (m, 1H), 3.16 (d, *J* = 4.7 Hz, 1H), 1.70 (s, 3H), 1.25 (t, *J* = 7.1 Hz, 3H); **^{13}C NMR** (101 MHz, $CDCl_3$) δ

190.2, 168.5, 151.1, 126.1 (q, $^{1}J_{CF}$ = 278.8 Hz), 115.6, 89.60, 73.3 (q, $^{3}J_{CF}$ = 2.8 Hz), 62.4, 55.4, 52.1 (q, $^{2}J_{CF}$ = 26.2 Hz), 52.0, 20.1, 14.0; **^{19}F NMR** (377 MHz, $CDCl_3$) δ -70.27; **IR** (neat) cm^{-1}: 1743 (s, C=O), 1705 (s, C=O), 1626 (s, C=C); **HRMS** (ESI) calcd for $[C_{13}H_{16}F_3O_5]$ $[M+H]^+$ 309.0944, found 309.0943.

Ethyl (3a*R,4*S**,5*R**,6*R**,7*S**,8a*R**)-8a-methoxy-7-methyl-8-oxo-5-(trifluoromethyl) decahydro-4,7-epoxycyclohepta[*c*]pyrrole-6-carboxylate (2.120)**

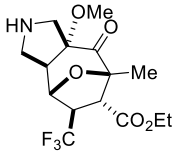

To an ice-cooled solution of **2.119** (241 mg, 0.783 mmol) and *N*-(methoxymethyl)-*N*-(trimethylsilylmethyl)benzylamine (315 µL, 1.17 mmol) in anhydrous CH_2Cl_2 (5.0 mL) was added trifluoroacetic acid (0.5 M in CH_2Cl_2, 150 µL, 78.3 µmol) dropwise and the reaction mixture was stirred under an atmosphere of N_2 at 21 °C for 2 h. The mixture was concentrated *in vacuo* and filtered through a short plug of silica. The residue was dissolved in EtOH (12 mL), added 10% Pd/C (167 mg, 0.157 mmol), and stirred at reflux under an atmosphere of H_2 for 4 h. The suspension was filtered through a plug of celite, concentrated *in vacuo*, and purified by flash column chromatography (EtOAc/MeOH/Et_3N 95:3:2) to give the title compound as a colorless oil (242 mg, 88%).

***R*$_f$** = 0.23 (EtOAc/MeOH/Et_3N 95:3:2); **^{1}H NMR** (400 MHz, CD_3OD) δ 4.53 (d, *J* = 2.2 Hz, 1H), 4.33 (dq, *J* = 10.8, 7.1 Hz, 1H), 4.22 (dq, *J* = 10.8, 7.1 Hz, 1H), 3.66 – 3.52 (m, 2H), 3.27 (s, 3H), 3.19 – 3.10 (m, 2H), 3.08 (d, *J* = 12.4 Hz, 1H), 2.96 (dd, *J* = 12.4, 0.9 Hz, 1H), 2.69 (dd, *J* = 7.8, 5.3 Hz, 1H), 1.64 (s, 3H), 1.38 (t, *J* = 7.1 Hz, 3H); **^{13}C NMR** (101 MHz, CD_3OD) δ 207.7, 168.0, 127.1 (d, $^{1}J_{CF}$ = 277.3 Hz), 90.8, 88.9, 78.4 (d, $^{3}J_{CF}$ = 2.7 Hz), 62.1, 59.1, 55.2 (d, $^{3}J_{CF}$ = 1.7 Hz), 54.2, 52.7, 51.8 (q, $^{2}J_{CF}$ = 28.1 Hz), 48.8, 19.4, 13.4; **^{19}F NMR** (377 MHz, CD_3OD) δ -72.64; **IR** (neat) cm^{-1}: 3328 (m, N–H), 1725 (s, C=O); **HRMS** (ESI) calcd for $[C_{15}H_{21}F_3NO_5]$ $[M+H]^+$ 352.1366, found 352.1344.

(3*R,3a*S**,5*S**,7a*S**,8*R**)-7-Methoxy-3a-methyl-8-(trifluoromethyl)-3,3a,5,7a-tetrahydro-2*H*-3,5-methanofuro[3,2-*b*]pyran-2-one (2.121)**

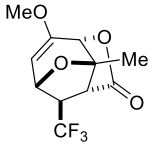

To an ice-cooled solution of **2.119** (750 mg, 2.43 mmol) in EtOH (24 mL) was added $NaBH_4$ (96.7 mg, 2.55 mmol). After 5 min. of stirring, cooling was removed and the reaction mixture was stirred at 22 °C for 1 h. Then, SiO_2 (4.25 g) was added and the mixture was concentrated *in vacuo* and purified by flash column chromatography (EtOAc/heptane 1:2) to give the title compound as a white solid (296 mg, 46%).

***R*$_f$** = 0.29 (EtOAc/heptane 1:2); **m.p.**: 80–82 °C; **^{1}H NMR** (400 MHz, $CDCl_3$) δ 5.32 (dd, *J* = 6.0, 1.6 Hz, 1H), 4.90 (d, *J* = 6.0 Hz, 1H), 4.71 (d, *J* = 1.6 Hz, 1H), 3.56 (s, 3H), 3.00 (qd, *J* = 9.3, 2.6 Hz, 1H), 2.81 (d, *J* = 2.6 Hz, 1H), 1.69 (s, 3H); **^{13}C NMR** (101 MHz, $CDCl_3$) δ 174.0,

155.8, 125.3 (q, $^{1}J_{CF}$ = 279.8 Hz), 102.0, 85.8, 81.9, 73.6, 55.4, 55.0 (q, $^{2}J_{CF}$ = 27.9 Hz), 48.5, 21.3; **^{19}F NMR** (377 MHz, $CDCl_3$) δ -71.24; **IR** (neat) cm^{-1}: 1775 (s, C=O), 1665 (s, C=C); **HRMS** (ESI) calcd for $[C_{11}H_{12}F_3O_4]$ $[M+H]^+$ 265.0682, found 265.0678.

[2+2] Cycloaddition

Ethyl (1*S**,5*R**)-5-hydroxy-7-(trifluoromethyl)bicyclo[3.2.0]hept-6-ene-6-carboxylate (2.126)

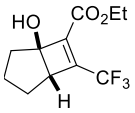

To an ice-cooled solution of ethyl 4,4,4-trifluorobut-2-ynoate **2.4** (2.90 g, 17.5 mmol) and 1-(trimethylsiloxy)cyclopentene (3.42 mL, 19.2 mmol) in CH_2Cl_2 (60 mL) was added $ZrCl_4$ (4.48 g, 19.2 mmol) and then THF (30 mL) and the reaction mixture was stirred at 22 °C for 2 h. Sat. aq. NH_4Cl (90 mL) was added and the layers were separated. The aqueous phase was extracted with CH_2Cl_2 (1 x 90 mL) and the combined organic layers were dried over $MgSO_4$, filtered, and concentrated *in vacuo*. The crude product was purified by flash column chromatography (EtOAc/heptane 1:3) to give the title compound as a yellow oil (4.00 g, 93%).

R_f = 0.22 (EtOAc/heptane 1:3); **^{1}H NMR** (400 MHz, $CDCl_3$) δ 4.27 (qd, *J* = 7.1, 1.6 Hz, 2H), 3.05 (dp, *J* = 6.8, 1.4 Hz, 1H), 2.71 (br. s, 1H), 2.20 – 2.10 (m, 1H), 1.95 – 1.82 (m, 1H), 1.76 – 1.42 (m, 4H), 1.32 (t, *J* = 7.1 Hz, 3H); **^{13}C NMR** (101 MHz, $CDCl_3$) δ 159.7, 140.6 (q, $^2J_{CF}$ = 37.7 Hz), 139.5 (q, $^3J_{CF}$ = 5.2 Hz), 119.3 (q, $^1J_{CF}$ = 272.5 Hz), 84.8, 61.5, 53.4 (q, $^3J_{CF}$ = 1.7 Hz), 32.8, 24.4, 23.9, 14.1; **^{19}F NMR** (377 MHz, $CDCl_3$) δ -63.73; **IR** (neat) cm^{-1}: 3414 (br., O–H), 1723 (s, C=O), 1666 (s, C=C); **HRMS** (ESI) calcd. for [$C_{11}H_{14}F_3O_3$] [M+H]+ 251.0889, found 251.0884.

tert-Butyl 4-((trimethylsilyl)oxy)-3,6-dihydropyridine-1(2*H*)-carboxylate (2.128)

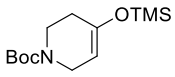

Following a reported procedure.[351] To a solution of *tert*-butyl 4-oxopiperidine-1-carboxylate (1.28 g, 6.42 mmol) in anhydrous DMF (7 mL) was added TMSCl (1.63 mL, 12.9 mmol) and Et_3N (3.58 mL, 25.7 mmol) and the reaction mixture was stirred under an atmosphere of N_2 at 90 °C for 21 h. Pentane (30 mL) was added and the mixture was washed with 5% aq. $NaHCO_3$ (1 × 30 mL), H_2O (1 × 30 mL), and brine (1 × 30 mL). The organic layer was dried over $MgSO_4$ and concentrated *in vacuo* to give the title compound as an orange oil (1.70 g, >95%).

R_f = 0.45 (EtOAc/heptane 1:4); **^{1}H NMR** (400 MHz, $CDCl_3$) δ 4.79 (s, 1H), 3.87 (s, 2H), 3.52 (t, *J* = 5.8 Hz, 2H), 2.11 (s, 2H), 1.46 (s, 9H), 0.19 (s, 9H); **^{13}C NMR** (101 MHz, $CDCl_3$) δ 155.0, 148.9, 101.0, 79.7, 42.2, 40.3, 30.2, 28.6 (3C), 0.4 (3C). Spectroscopic data were consistent with those reported in the literature.[351]

Ethyl (*E*)-4,4,4-trifluoro-3-(4-oxopiperidin-3-yl)but-2-enoate (2.130)

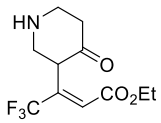

To a solution of **2.4** (68.8 mg, 0.409 mmol) in anhydrous THF (4 mL) was added **2.128** (1.75 mg, 0.614 mmol) and AgF (62.3 mg, 0.491 mmol) and the reaction mixture was stirred under an atmosphere of N_2 at 22 °C for 24 h. Precipitate was removed by filtration and the filtrate was concentrated *in vacuo*. The crude product was purified by flash column chromatography (EtOAc/heptane 1:9) to give the title compound as a yellow oil (42.0 mg, 39%).

R_f = 0.25 (EtOAc/heptane; **^{1}H NMR** (400 MHz, $CDCl_3$) δ 6.36 (p, *J* = 1.4 Hz, 1H), 5.18 (td, *J* = 7.9, 7.3, 1.4 Hz, 1H), 4.22 (qd, *J* = 7.1, 1.9 Hz, 2H), 3.98 – 3.80 (m, 2H), 2.38 (qd, *J* = 7.3, 3.8 Hz, 1H), 2.11 – 1.80 (m, 3H), 1.31 (t, *J* = 7.1 Hz, 3H); **^{13}C NMR** (101 MHz, $CDCl_3$) δ 164.8, 144.2 (q, *J* = 27.4 Hz), 123.0 (q, *J* = 6.3 Hz), 122.8 (q, *J* = 276.1 Hz), 75.0, 69.2, 61.2, 32.6, 26.2, 14.1.

1-Benzyl-4-((trimethylsilyl)oxy)-1,2,3,6-tetrahydropyridine (2.131)

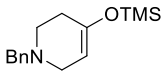

To a solution of 1-benzylpiperidin-4-one (1.60 g, 8.45 mmol) in anhydrous DMF (8 mL) was added TMSCl (2.15 mL, 16.9 mmol) and Et_3N (4.71 mL, 33.8 mmol) and the reaction mixture was stirred under an atmosphere of N_2 at 90 °C for 21 h. Pentane (35 mL) was added and the mixture was washed with 5% aq. $NaHCO_3$ (1 × 35 mL), H_2O (1 × 35 mL), and brine (1 × 35 mL). The organic layer was dried over Na_2SO_4 and concentrated *in vacuo* to give the title compound as an orange oil (2.16 g, >95%).

^{1}H NMR (400 MHz, $CDCl_3$) δ 7.29 – 7.14 (m, 5H), 4.70 (tt, *J* = 3.5, 1.2 Hz, 1H), 3.51 (s, 2H), 2.91 (dt, *J* = 3.5, 2.7 Hz, 2H), 2.52 (t, *J* = 5.9 Hz, 2H), 2.06 (tdd, *J* = 5.9, 2.7, 1.2 Hz, 2H), 0.12 (s, 9H); **^{13}C NMR** (101 MHz, $CDCl_3$) δ 149.1, 138.6, 129.2 (2C), 128.3 (2C), 127.1, 101.5, 62.3, 51.6, 50.0, 30.5, 0.5 (3C).

1-Benzyl-5-methyl-4-((trimethylsilyl)oxy)-1,2,3,6-tetrahydropyridine (2.132)

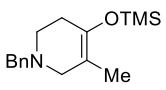

To a solution of 1-benzylpiperidin-4-one (126 mg, 0.620mmol) in anhydrous DMF (6 mL) was added TMSCl (0.158 mL, 1.24 mmol) and Et_3N (0.330 mL, 2.48 mmol) and the reaction mixture was stirred under an atmosphere of N_2 at 90 °C for 21 h. Pentane (20 mL) was added and the mixture was washed with 5% aq. $NaHCO_3$ (1 × 20 mL), H_2O (1 × 20 mL), and brine (1 × 20 mL). The organic layer was dried over Na_2SO_4 and concentrated *in vacuo* to give the title compound as an orange oil (157 mg, 92%, 3:1 mixture of silyl enol ether isomers).

tert-Butyl 3-((trimethylsilyl)oxy)-2,5-dihydro-1*H*-pyrrole-1-carboxylate and _tert_-butyl 4-((trimethylsilyl)oxy)-2,3-dihydro-1*H*-pyrrole-1-carboxylate (2.134)

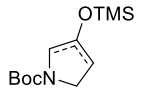

To a solution of 1-benzylpiperidin-4-one (1.00 g, 5.40 mmol) in anhydrous DMF (6 mL) was added TMSCl (1.16 mL, 9.18 mmol) and Et_3N (2.44 mL, 18.4 mmol) and the reaction mixture was stirred under an atmosphere of N_2 at 90 °C for 21 h. Pentane (20 mL) was added and the mixture was washed with 5% aq. $NaHCO_3$ (1 × 20 mL), H_2O (1 × 20 mL), and brine (1 × 20 mL). The organic layer was dried over Na_2SO_4 and concentrated *in vacuo* to give the title compound as an orange oil (1.13 g, 70%).

tert-Butyl (3a*R,6a*R**)-5-((trimethylsilyl)oxy)-3,3a,4,6a-tetrahydrocyclopenta[*c*]pyrrole-2(1*H*)-carboxylate (2.135)**

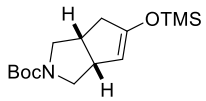

To a solution of *tert*-butyl 5-oxohexahydrocyclopenta[*c*]pyrrole-2(1*H*)-carboxylate (277 mg, 1.23 mmol) in anhydrous DMF (4 mL) was added TMSCl (0.234 mL, 1.84 mmol) and Et_3N (0.514 mL, 3.69 mmol) and the reaction mixture was stirred under an atmosphere of N_2 at 90 °C for 21 h. Pentane (25 mL) was added and the mixture was washed with 5% aq. $NaHCO_3$ (1 × 25 mL), H_2O (1 × 25 mL), and brine (1 × 25 mL). The organic layer was dried over Na_2SO_4 and concentrated *in vacuo* to give the title compound as an orange oil (209 mg, 57%)

R_f = 0.65 (EtOAc/heptane 1:2); **^{1}H NMR** (400 MHz, $CDCl_3$) δ 4.52 (s, 1H), 3.62 (s, 1H), 3.50 – 3.35 (m, 1H), 3.24 (ddt, *J* = 7.9, 5.8, 2.4 Hz, 2H), 3.14 – 2.95 (m, 1H), 2.73 (p, *J* = 7.9, 7.4 Hz, 1H), 2.55 (ddt, *J* = 16.0, 7.9, 2.1 Hz, 1H), 2.01 (d, *J* = 16.0 Hz, 1H), 1.44 (d, *J* = 5.8 Hz, 9H), 0.19 (s, 9H); **^{13}C NMR** (101 MHz, $CDCl_3$) δ 154.6 (minor rotamer), 154.5 (major rotamer), 154.2 (minor rotamer), 154.1 (major rotamer), 105.3, 79.7 (minor rotamer), 79.1 (major rotamer), 52.9 (minor rotamer), 52.6 (major rotamer), 51.6 (minor rotamer), 51.2 (major rotamer), 46.2 (minor rotamer), 45.4 (major rotamer), 39.5, 38.7 (major rotamer), 37.8 (minor rotamer), 28.7 (3C), 0.1 (3C).

tert-Butyl 3-((_tert_-butyldimethylsilyl)oxy)azete-1(2*H*)-carboxylate (2.136)

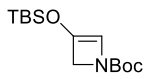

To a solution of *tert*-butyl 3-oxoazetidine-1-carboxylate (206 mg, 1.20 mmol) in anhydrous THF (6 mL) at -78 °C was added TBSOTf (0.332 mL, 1.44 mmol) and LiHMDS (1.32 mL, 1.32 mmol) and the reaction mixture was stirred under an atmosphere of N_2 at -78 °C for 1 h. Then, sat. aq. NH_4Cl (6 mL) was added and the mixture was slowly warmed to 22 °C. The mixture was extracted with CH_2Cl_2 (2 × 6 mL) and the combined organic layers were dried over Na_2SO_4, filtered, and concentrated *in vacuo*. The crude product was purified by flash column chromatography (EtOAc/heptane 1:12) to give the title compound as a colorless oil (76.0 mg, 22%).

R_f = 0.60 (EtOAc/heptane 1:2); **^{1}H NMR** (400 MHz, $CDCl_3$) δ 5.70 (s, 1H), 4.30 (s, 2H), 1.45 (s, 9H), 0.93 (s, 12H), 0.18 (s, 6H); **^{13}C NMR** (101 MHz, $CDCl_3$) δ 155.6, 139.4, 114.7, 79.8, 60.0, 28.3 (3C), 25.4 (3C), 18.1, -5.0 (2C).

Ethyl (*E*)-4,4,4-trifluoro-3-(2-oxocyclopentylidene)butanoate (2.138)

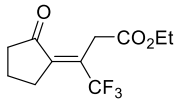

To a solution of **2.126** (668 mg, 2.67 mmol) in EtOH (13 mL) was added Et_3N (1.12 mL, 8.01 mmol) and the reaction mixture was stirred at 40 °C for 1 h. The mixture was concentrated *in vacuo* to give the title compound as a colorless oil (668 mg, >95%).

R_f = 0.50 (EtOAc/heptane 2:3); **^{1}H NMR** (400 MHz, $CDCl_3$) δ 4.15 (q, *J* = 7.2 Hz, 2H), 3.85 (t, *J* = 1.3 Hz, 2H), 2.96 (tddd, *J* = 5.2, 4.3, 2.9, 1.3 Hz, 2H), 2.41 (t, *J* = 7.8 Hz, 2H), 1.98 (p, *J* = 7.8 Hz, 2H), 1.25 (t, *J* = 7.2 Hz, 3H); **^{13}C NMR** (101 MHz, $CDCl_3$) δ 207.9, 169.3, 141.2 (q, $^3J_{CF}$ = 3.2 Hz), 128.8 (q, $^2J_{CF}$ = 31.1 Hz), 123.7 (q, $^1J_{CF}$ = 276.3 Hz), 61.3, 39.5, 31.5 (q, $^3J_{CF}$ = 2.4 Hz), 29.8 (q, $^3J_{CF}$ = 1.8 Hz), 19.3, 14.2; **^{19}F NMR** (377 MHz, $CDCl_3$) δ -64.54.

Ethyl 2-((4*S,5*S**)-2-benzyl-6-oxo-4-(trifluoromethyl)-2-azaspiro[4.4]nonan-4-yl)acetate (2.139)**

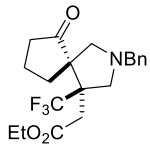

To a solution of **2.138** (668 mg, 2.67 mmol) in CH_2Cl_2 (13 mL) was added *N*-(methoxymethyl)-*N*-(trimethylsilylmethyl)benzylamine (0.969 mL, 4.00 mmol) and TFA (0.5 M in CH_2Cl_2, 0.535 mL, 0.267 mmol). The solution was stirred at 22 °C for 2 h and the concentrated *in vacuo*. The crude product was filtered through a short plug of silica to give the title compound as an impure yellow oil (1.27 g) that was used directly in the next step without further purification.

(3a*S,6a*R**,9a*S**)-3a-(trifluoromethyl)octahydrocyclopenta[2,3]pyrano[3,4-*c*]pyrrol-5(1*H*)-one (2.140)**

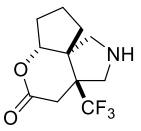

To a solution of **2.139** (192 mg, 0.501 mmol) in EtOH (10 mL) was added 10% Pd/C (107 mg, 0.100 mmol) and the resulting suspension was stirred under an atmosphere of H_2 at 22 °C for 2 h. The suspension was filtered through a plug of celite and the filtrate was cooled to 0 °C. $NaBH_4$ (28.4 mg, 0.751 mmol) was added and the solution was stirred at 22 °C for 1 h. Sat. aqueous $NaHCO_3$ (10 mL) was added and the mixture was extracted with CH_2Cl_2 (3 × 10 mL). The combined organic layers were dried over Na_2SO_4, concentrated *in vacuo*, and purified by flash column chromatography (EtOAc/heptane 3:1) to give the title compound as a white amorphous solid (44.0 mg, 44%)

R_f = 0.26 (EtOAc/heptane 3:1); **^{1}H NMR** (400 MHz, $CDCl_3$) δ 4.45 (dd, *J* = 9.7, 8.4 Hz, 1H), 3.37 (d, *J* = 11.4 Hz, 1H), 3.30 (d, *J* = 11.2 Hz, 1H), 3.01 (d, *J* = 11.4 Hz, 1H), 2.87 (d, *J* = 15.2

Hz, 1H), 2.75 (d, *J* = 11.2 Hz, 1H), 2.56 (d, *J* = 15.2 Hz, 1H), 2.19 – 2.08 (m, 1H), 1.90 – 1.63 (m, 6H); **^{13}C NMR** (101 MHz, $CDCl_3$) δ 171.4, 127.5 (q, $^1J_{CF}$ = 280.9 Hz), 81.9, 56.7 (q, $^3J_{CF}$ = 2.1 Hz), 55.1, 53.5, 52.0 (q, $^2J_{CF}$ = 25.3 Hz), 36.6 (q, $^3J_{CF}$ = 2.6 Hz), 29.4 (q, $^3J_{CF}$ = 2.4 Hz), 25.0, 19.0; **^{19}F NMR** (377 MHz, $CDCl_3$) δ -71.85; **IR** (neat) cm^{-1}: 3326 (br., N–H), 1751 (s, C=O); **HRMS** (ESI) calcd for $[C_{11}H_{15}F_3NO_2]$ $[M+H]^+$ 250.1049, found 250.1049.

(4*S,5*S**,6*S**)-2-Benzyl-4-(2-hydroxyethyl)-4-(trifluoromethyl)-2-azaspiro[4.4]nonan-6-ol (2.141)**

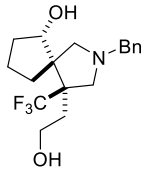

To an ice-cooled solution of **2.139** (118 mg, 0.308 mmol) in THF (6 mL) was added $LiBH_4$ (40.2 mg, 1.85 mmol) and the mixture was stirred at 22 °C for 16 h. SiO_2 (750 mg) was added and the suspension was concentrated *in vacuo* and purified by flash column chromatography (EtOAc/heptane/Et_3N 50:50:2) to give the title compound as a colorless oil (64.0 mg, 76%).

***R*$_f$** = 0.26 (EtOAc/heptane 1:1); **^{1}H NMR** (400 MHz, $CDCl_3$) δ 7.42 – 7.26 (m, 5H), 4.15 – 4.05 (m, 1H), 3.82 – 3.56 (m, 4H), 3.25 – 3.14 (m, 2H), 2.69 (d, *J* = 11.1 Hz, 1H), 2.54 – 2.39 (m, 1H), 2.25 – 2.02 (m, 3H), 1.89 – 1.72 (m, 1H), 1.69 – 1.46 (m, 4H); **^{13}C NMR** (101 MHz, $CDCl_3$) δ 137.0, 129.2 (d, $^1J_{CF}$ = 284.9 Hz), 128.9 (2C), 128.7 (2C), 127.9, 75.9, 59.8, 59.82 (2C), 58.75, 55.7, 52.0 (q, $^2J_{CF}$ = 22.6 Hz), 34.7, 30.5, 28.4 (d, $^3J_{CF}$ = 2.4 Hz), 19.2; **^{19}F NMR** (377 MHz, $CDCl_3$) δ -66.11; **IR** (neat) cm^{-1}: 3358 (br., O–H); **HRMS** (ESI) calcd for $[C_{18}H_{25}F_3NO_2]$ $[M+H]^+$ 344.1832, found 344.1850.

Ethyl 2-((4*S,5*S**)-6-oxo-4-(trifluoromethyl)-2-azaspiro[4.4]nonan-4-yl)acetate (2.142)**

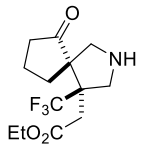

To a solution of **2.139** (336 mg, 0.876 mmol) in EtOH (18 mL) was added 10% Pd/C (187 mg, 0.175 mmol) and the resulting suspension was stirred under an atmosphere of H_2 at 22 °C for 2 h. The suspension was filtered through a plug of celite and the filtrate was concentrated *in vacuo*. The crude product was purified by flash column chromatography (EtOAc/heptane/Et_3N 55:45:2) to give the title compound as a colorless oil (160 mg, 78%).

***R*$_f$** = 0.35 (EtOAc/heptane 3:2); **^{1}H NMR** (400 MHz, $CDCl_3$) δ 4.07 (qq, *J* = 10.8, 7.2 Hz, 2H), 3.34 (d, *J* = 13.4 Hz, 1H), 3.24 (d, *J* = 16.0 Hz, 1H), 3.13 (d, *J* = 12.7 Hz, 1H), 3.08 (d, *J* = 13.4 Hz, 1H), 2.79 (d, *J* = 12.8 Hz, 1H), 2.72 (d, *J* = 16.0 Hz, 1H), 2.68 – 2.56 (m, 2H), 2.45 – 2.26 (m, 2H), 2.19 – 2.04 (m, 1H), 1.93 (dd, *J* = 12.8, 6.8 Hz, 1H), 1.72 (qdd, *J* = 12.7, 8.2, 6.8 Hz, 1H), 1.22 (t, *J* = 7.2 Hz, 3H); **^{13}C NMR** (101 MHz, $CDCl_3$) δ 218.7, 171.0, 128.4 (q, $^1J_{CF}$ = 284.6 Hz), 60.9, 60.5, 58.1, 57.7 (q, $^3J_{CF}$ = 3.0 Hz), 54.5 (q, $^2J_{CF}$ = 22.6 Hz), 36.8, 34.5 (q, $^3J_{CF}$ = 2.7 Hz), 31.3 (q, $^3J_{CF}$ = 2.6 Hz), 20.7, 14.2; **^{19}F NMR** (377 MHz, $CDCl_3$) δ -69.59; **IR** (neat) cm^{-1}: 3325 (br., N–H), 1720 (s, C=O); **HRMS** (ESI) calcd for $[C_{13}H_{19}F_3NO_3]$ $[M+H]^+$ 294.1312, found 294.1308.

Ethyl (1*S,5*R**,6*R**,7*R**)-5-hydroxy-7-(trifluoromethyl)bicyclo[3.2.0]heptane-6-carboxylate (2.147)**

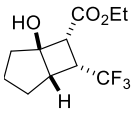

To a solution of **2.126** (800 mg, 3.20 mmol) in EtOH/AcOH (4:1, 50 mL) was added 5% Pd/C (681 mg, 0.320 mmol) and the resulting suspension was stirred under an atmosphere of H_2 at 22 °C for 1 h. The suspension was filtered through a plug of celite and the filtrate was concentrated *in vacuo* to give the title compound as a colorless oil (807 mg, >95%).

^{1}H NMR (400 MHz, $CDCl_3$) δ 4.25 – 4.06 (m, 2H), 3.54 (d, *J* = 11.9 Hz, 1H), 3.38 (pd, *J* = 11.8, 10.4 Hz, 1H), 2.86 (s, 1H), 2.75 – 2.66 (m, 1H), 2.40 – 2.27 (m, 1H), 2.02 – 1.91 (m, 1H), 1.91 – 1.80 (m, 2H), 1.80 – 1.67 (m, 2H), 1.26 (t, *J* = 7.1 Hz, 3H); **^{13}C NMR** (101 MHz, $CDCl_3$) δ 169.3, 126.5 (q, $^1J_{CF}$ = 278.3 Hz), 84.3, 60.9, 48.3 (q, $^3J_{CF}$ = 2.4 Hz), 45.1 (q, $^3J_{CF}$ = 2.0 Hz), 38.0, 35.9 (q, $^2J_{CF}$ = 29.2 Hz), 27.2, 25.9, 14.2; **^{19}F NMR** (377 MHz, $CDCl_3$) δ -60.90; **IR** (neat) cm^{-1}: 3428 (br., O–H), 1724 (s, C=O); **HRMS** (ESI) calcd for [$C_{11}H_{16}F_3O_3$] $[M+H]^+$ 253.1046, found 253.1037.

(1*S,2*S**)-2-((*S**)-1,1,1-Trifluoro-4-hydroxybutan-2-yl)cyclopentan-1-ol (2.148)**

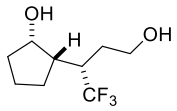

To an ice-cooled solution of **2.147** (274 mg, 1.09 mmol) in THF (15 mL) was added $LiBH_4$ (95.0 mg, 4.35 mmol) and the reaction mixture was stirred at 22 °C for 16 h. Then, SiO_2 (1.85 g) was added and the suspension was concentrated *in vacuo* and purified directly by flash column chromatography (EtOAc/heptane 1:1) to give the title compound as a colorless oil (63.0 mg, 28%)

***R*$_f$** = 0.29 (EtOAc/heptane 1:1); **^{1}H NMR** (400 MHz, DMSO-d_6) δ 4.56 (t, *J* = 5.2 Hz, 1H), 4.43 (d, *J* = 4.0 Hz, 1H), 4.05 – 3.96 (m, 1H), 3.46 (dtd, *J* = 13.7, 8.9, 7.9, 4.9 Hz, 2H), 2.57 (dtt, *J* = 16.1, 6.3, 3.5 Hz, 1H), 1.82 – 1.38 (m, 9H); **^{13}C NMR** (101 MHz, DMSO-d_6) δ 129.1 (q, $^1J_{CF}$ = 281.3 Hz), 71.6 (d, $^3J_{CF}$ = 1.3 Hz), 58.8 (d, $^4J_{CF}$ = 1.0 Hz), 43.9 (q, $^3J_{CF}$ = 1.6 Hz), 37.8 (q, $^2J_{CF}$ = 24.0 Hz), 34.7, 30.4 (q, $^3J_{CF}$ = 2.1 Hz), 26.4, 20.5; **^{19}F NMR** (377 MHz, DMSO-d_6) δ -67.17; **IR** (neat) cm^{-1}: 3329 (br., O–H); **HRMS** (ESI) calcd for [$C_9H_{16}F_3O_2$] $[M+H]^+$ 213.1097, found 213.1102.

Double [3+2] Cycloaddition

Ethyl (3as,6as)-2,5-dibenzyl-6a-(trifluoromethyl)hexahydropyrrolo[3,4-*c*]pyrrole-3a (1*H*) -carboxylate (2.152)

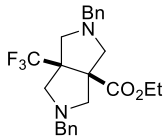

To an ice-cooled solution of ethyl (*E*)-4,4,4-trifluorobut-2-ynoate **2.4** (1.58 g, 9.04 mmol, 95% purity) and *N*-(methoxymethyl)-*N*-(trimethylsilylmethyl)benzylamine (6.89 mL, 27.1 mmol) in anhydrous CH_2Cl_2 (18 mL) was added trifluoroacetic acid (1.0 M in CH_2Cl_2, 0.904 mL, 0.904 mmol) dropwise and the reaction mixture was stirred under an atmosphere of N_2 at 21 °C for 2 h. Sat. aq. $NaHCO_3$ (25 mL) was added and the layers were separated. The organic layer was washed with brine (1 × 25 mL), dried over Na_2SO_4, filtered, and concentrated *in vacuo*. The crude was purified by flash column chromatography (heptane/Et_3N 98:2) to give the title compound as a colorless oil (3.48 g, 89%).

***R*$_f$** = 0.13 (heptane/Et_3N 98:2); **^{1}H NMR** (400 MHz, $CDCl_3$) δ 7.34 – 7.14 (m, 10H), 4.11 (q, *J* = 7.1 Hz, 2H), 3.66 (d, *J* = 13.4 Hz, 2H), 3.56 (d, *J* = 13.4 Hz, 2H), 3.12 (d, *J* = 9.2 Hz, 2H), 2.88 (d, *J* = 9.4 Hz, 2H), 2.61 (d, *J* = 9.4 Hz, 2H), 2.55 (d, *J* = 9.2 Hz, 2H), 1.24 (t, *J* = 7.1 Hz, 3H); **^{13}C NMR** (101 MHz, $CDCl_3$) δ 171.9, 138.6 (2C), 128.3 (8C), 127.03 (2C), 126.98 (q, $^1J_{CF}$ = 280.7 Hz), 62.8 (q, $^2J_{CF}$ = 25.8 Hz), 62.7 (2C), 61.3, 60.4 (q, $^3J_{CF}$ = 2.1 Hz, 2C), 59.9, 58.5 (2C), 13.8; **^{19}F NMR** (377 MHz, $CDCl_3$) δ -68.88; **IR** (neat) cm^{-1}: 3028 (m, C=C–H), 1722 (s, C=O); **HRMS** (ESI) calcd for $C_{24}H_{28}F_3N_2O_2$ $[M+H]^+$ 433.2097, found 433.2099.

((3as,6as)-2,5-Dibenzyl-6a-(trifluoromethyl)hexahydropyrrolo[3,4-*c*]pyrrol-3a(1*H*)-yl) methanol (2.253)

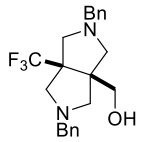

To an ice-cooled solution of **2.152** (674 mg, 1.56 mmol) in anhydrous THF (12 mL) was added $LiAlH_4$ (2.0 M in THF, 3.12 mL, 6.23 mmol) and the reaction mixture was stirred at under an atmosphere of N_2 21 °C for 16 h. The mixture was cooled to 0 °C and added sequentially water (0.25 mL), 15% aq. NaOH (0.25 mL), and water (0.75 mL). Precipitate was removed by filtration and washed with CH_2Cl_2 (3 × 15 mL). The filtrate was dried over Na_2SO_4, filtered, and concentrated *in vacuo* to give the crude product as an impure yellow oil (605 mg). The crude product was used directly in the next step without further purification.

((3as,6as)-6a-(Trifluoromethyl)hexahydropyrrolo[3,4-*c*]pyrrol-3a(1*H*)-yl)methanol (2.153)

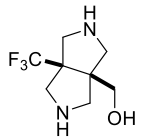

To a solution of **2.253** (284 mg, 0.727 mmol) in EtOH (10 mL) was added 10% Pd/C (77.4 mg, 72.7 µmol) and the resulting suspension was stirred under an H_2-atmosphere at 60 °C for 2 h. The mixture was filtered through a pad of celite and concentrated *in vacuo* to give the crude product as a white amorphous solid (150 mg, 98%). The crude product was used directly in the next step without further purification.

^{1}H NMR (400 MHz, CD_3OD) δ 3.77 (d, *J* = 1.3 Hz, 1H), 3.30 (d, *J* = 12.4 Hz, 1H), 3.12 (d, *J* = 12.0 Hz, 1H), 2.99 (d, *J* = 12.4 Hz, 1H), 2.94 (d, *J* = 12.0 Hz, 1H); **^{13}C NMR** (101 MHz, CD_3OD) δ 129.8 (q, $^1J_{CF}$ = 280.5 Hz), 64.3 (q, $^3J_{CF}$ = 3.8 Hz), 63.6 (q, $^2J_{CF}$ = 23.9 Hz), 63.2, 58.3 (2C), 56.5 (q, *J* = 2.7 Hz, 2C); **^{19}F NMR** (377 MHz, CD_3OD) δ -68.41; **IR** (neat) cm^{-1}: 3278 (s, N–H), 3213 (s, N–H, 3156 (br., O–H); **HRMS** (ESI) calcd for $[C_8H_{14}F_3N_2O]$ $[M+H]^+$ 211.1053, found 211.1033.

((3as,6as)-2,5-Dimethyl-6a-(trifluoromethyl)hexahydropyrrolo[3,4-*c*]pyrrol-3a(1*H*)-yl) methanol (2.154)

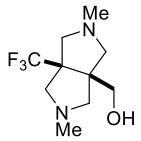

To a solution of **2.253** (100 mg, 0.256 mmol) in EtOH (3 mL) was added 10% Pd/C (54.5 mg, 51.2 µmol) and the resulting suspension was stirred under an H_2-atmosphere at 60 °C for 2 h. The mixture was cooled to 21 °C and formaldehyde (37% in water, 41.6 µL, 0.563 mmol) was added. After stirring 2 h at 21 °C, the mixture was filtered through a pad of celite and the filtrate was concentrated *in vacuo*. The crude was purified by flash column chromatography (EtOAc/MeOH/NH_3 380:20:1) to give the title compound as a white amorphous solid (29.0 mg, 48%).

***R*$_f$** = 0.20 (EtOAc/MeOH/NH_3 380:20:1); **^{1}H NMR** (400 MHz, DMSO-d_6) δ 4.83 (t, *J* = 5.1 Hz, 1H), 3.48 (d, *J* = 4.2 Hz, 2H), 2.70 (d, *J* = 9.5 Hz, 2H), 2.58 (d, *J* = 9.0 Hz, 2H), 2.53 – 2.50 (m, 2H), 2.42 (d, *J* = 9.0 Hz, 2H), 2.21 (s, 6H); **^{13}C NMR** (101 MHz, DMSO-d_6) δ 128.2 (q, $^1J_{CF}$ = 281.2 Hz), 65.1 (2C), 63.0 (q, $^3J_{CF}$ = 2.6 Hz, 2C), 62.5 (q, $^3J_{CF}$ = 3.6 Hz), 58.6 (q, $^2J_{CF}$ = 24.3 Hz), 58.5, 41.0 (2C); **^{19}F NMR** (377 MHz, DMSO-d_6) δ -65.93; **IR** (neat) cm^{-1}: 3166 (br., O–H); **HRMS** (ESI) calcd for $C_{10}H_{18}F_3N_2O$ $[M+H]^+$ 239.1366, found 239.1366.

1,1'-((3as,6as)-3a-(Hydroxymethyl)-6a-(trifluoromethyl)tetrahydropyrrolo[3,4-*c*]pyrrole-2,5(1*H*,3*H*)-diyl)bis(propan-1-one) (2.155)

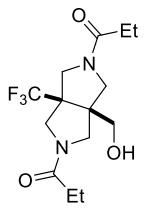

To a solution of **2.153** (79.0 mg, 0.376 mmol) in CH_2Cl_2/MeOH (3:1, 4 mL) was added Et_3N (0.150 mL, 1.13 mmol) and propionyl chloride (72.0 µL, 0.827 mmol) and the reaction mixture was stirred 30 min. The mixture was concentrated *in vacuo* and concentrated directly by flash column chromatography (EtOAc/MeOH 19:1) to give the title compound as a white solid (106 mg, 88%).
***R*f** = 0.33 (EtOAc/MeOH 19:1); **m.p.**: 47–49 °C; **^{1}H NMR** (400 MHz, CD_3OD) δ 4.11 – 3.89 (m, 2H), 3.90 – 3.38 (m, 8H), 2.46 – 2.18 (m, 4H), 1.28 – 0.89 (m, 6H) (rotamers); **^{13}C NMR** (101 MHz, CD_3OD) δ 175.9 – 174.8 (m, 2C), 128.2 (d, $^1J_{CF}$ = 281.8 Hz), 63.1 – 62.5 (m), 58.1 – 57.5 (m), 56.6 – 55.6 (m), 54.9 – 53.4 (m, 2C), 52.8 – 51.1 (m, 2C), 28.2 (2C), 9.1 (2C) (four rotamers); **^{19}F NMR** (377 MHz, CD_3OD) δ -70.54 – -70.64 (m) (rotamers); **IR** (neat) cm^{-1}: 3381 (br., O–H), 1622 (s, C=O); **HRMS** (ESI) calcd for $C_{14}H_{22}F_3N_2O_3$ $[M+H]^+$ 323.1577, found 323.1577.

1-((3a*R,6a*S**)-5-Benzyl-3a-(hydroxymethyl)-6a-(trifluoromethyl)hexahydropyrrolo[3,4-*c*]pyrrol-2(1*H*)-yl)ethan-1-one (2.156)**

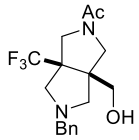

To a solution of **2.153** (66.0 mg, 0.314 mmol) in MeOH (7 mL) was added AcOH (200 µL, 0.691 mmol) and benzaldehyde (32.0 µL, 0.314 mmol) and the reaction mixture was stirred at 21 °C for 1 h. Then, the mixture was cooled to 0 °C and $NaBH_4$ (30.0 mg, 0.785 mmol) was added. After 15 min., cooling was removed and the reaction mixture was stirred at 21 °C for 16 h. The solution was cooled to 0 °C and added 4 M HCl (4 drops) to quench excess $NaBH_4$. Et_3N (0.850 mL, 6.28 mmol) and acetyl chloride (41.0 µL, 0.628 mmol) were added and the reaction mixture was stirred at 0 °C for 1 h. The mixture was then concentrated *in vacuo* and purified directly by flash column chromatography (EtOAc/Et_3N 98:2) to give the title compound as a colorless amorphous solid (35.0 mg, 35%).
***R*f** = 0.19 (EtOAc/Et_3N 98:2); **^{1}H NMR** (400 MHz, CD_3OD) δ 7.39 – 7.23 (m, 5H), 4.02 (dd, *J* = 12.6, 5.9 Hz, 1H), 3.90 – 3.62 (m, 7H), 2.92 – 2.80 (m, 3H), 2.74 (d, *J* = 9.6 Hz, 1H), 2.15 – 2.07 (m, 3H) (two rotamers); **^{13}C NMR** (101 MHz, CD_3OD) δ 171.4 (major rotamer), 171.3 (minor rotamer), 139.6, 129.6 (2C), 129.4 (2C), 128.9 (d, $^1J_{CF}$ = 280.0 Hz, major rotamer), 128.8 (d, $^1J_{CF}$ = 280.9 Hz, minor rotamer), 128.3, 64.5 (d, $^3J_{CF}$ = 3.8 Hz, minor rotamer), 64.43 (minor rotamer), 64.40 (d, $^3J_{CF}$ = 4.1 Hz, major rotamer), 64.1 (major rotamer), 61.6 (d, $^3J_{CF}$ = 2.2 Hz, major rotamer), 61.4 (d, $^3J_{CF}$ = 2.1 Hz, minor rotamer), 59.92 (minor rotamer), 59.89 (major rotamer), 58.9 (major rotamer), 58.8 (minor rotamer), 57.7 (major rotamer), 57.5 (minor rotamer), 56.1 (q, $^3J_{CF}$ = 3.2 Hz, minor rotamer), 55.7, 54.2 (q, $^3J_{CF}$ = 2.5 Hz, major rotamer), 21.81 (minor rotamer), 21.79 (major rotamer); **^{19}F NMR** (377 MHz, CD_3OD) δ -69.27 (minor

rotamer), -69.40 (major rotamer); **IR** (neat) cm^{-1}: 3362 (br., O–H), 1624 (s, C=O); **HRMS** (ESI) calcd for $[C_{17}H_{22}F_3N_2O_2]$ $[M+H]^+$ 343.1628, found 343.1620.

Ethyl (3as,6as)-6a-(trifluoromethyl)hexahydropyrrolo[3,4-*c*]pyrrole-3a(1*H*)-carboxylate (2.157)

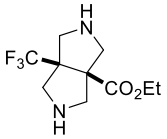

To a solution of **2.152** (35.0 mg, 80.9 µmol) in EtOH (2 mL) was added 10% Pd/C (17.2 mg, 16.2 µmol) and the resulting suspension was stirred at under an H_2-atmosphere at 60 °C for 2 h. The mixture was filtered through a pad of celite and concentrated *in vacuo* to give the title compound as a white amorphous solid (19.0 mg, 93%).

^{1}H NMR (400 MHz, CD_3OD) δ 4.24 (q, *J* = 7.2 Hz, 2H), 3.58 (d, *J* = 12.3 Hz, 2H), 3.38 (d, *J* = 8.2 Hz, 3H), 3.00 (d, *J* = 12.6 Hz, 2H), 2.91 (d, *J* = 12.3 Hz, 2H), 1.32 (t, *J* = 7.2 Hz, 3H); **^{13}C NMR** (101 MHz, CD_3OD) δ 173.3, 128.9 (q, $^1J_{CF}$ = 280.4 Hz), 69.6 (q, $^2J_{CF}$ = 24.3 Hz), 66.4, 62.7, 57.9, 56.2 (2C), (q, $^3J_{CF}$ = 2.6 Hz, 2C), 14.1; **^{19}F NMR** (377 MHz, CD_3OD) δ -69.65; **IR** (neat) cm^{-1}: 3205 (s, N–H), 1716 (s, C=O); **HRMS** (ESI) calcd for $[C_{10}H_{16}F_3N_2O_2]$ $[M+H]^+$ 253.1158, found 253.1091.

2,5-Dibenzyl-6a-(trifluoromethyl)hexahydropyrrolo[3,4-*c*]pyrrole-3a(1*H*)-carboxylic acid (2.254)

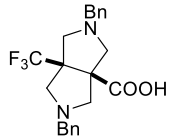

To a solution of ester **2.152** (793 mg, 1.83 mmol) in EtOH (37 ml) was added LiOH (2 M in water, 3.67 mL) and the reaction mixture was stirred at 22 °C for 2 days. Two-thirds of the solvent was removed *in vacuo*, added sat. aq. $NaHCO_3$ (40 mL), and extracted with CH_2Cl_2 (3 × 40 mL). The combined organic layers were dried over $MgSO_4$, filtered, and concentrated *in vacuo* to give the title compound as an off white solid (735 mg, 99%).

m.p.: 45–47 °C; **^{1}H NMR** (400 MHz, $CDCl_3$) δ 7.36 – 7.20 (m, 10H), 3.73 – 3.62 (m, 2H), 3.50 (d, *J* = 13.0 Hz, 2H), 3.16 (d, *J* = 9.2 Hz, 2H), 2.82 (d, *J* = 9.6 Hz, 2H), 2.57 – 2.45 (m, 4H); **^{13}C NMR** (101 MHz, $CDCl_3$) δ 176.9, 137.8 (2C), 129.1 (2C), 128.5 (4C), 127.5 (m), 127.3 (4C), 63.7 (2C), 61.4 (d, $^2J_{CF}$ = 25.0 Hz), 61.0, 60.3 (2C), 58.8 (2C); **^{19}F NMR** (377 MHz, $CDCl_3$) δ -69.01; **IR** (neat) cm^{-1}: 3350 (br., O–H), 1597 (s, C=O); **HRMS** (ESI) calcd for $[C_{22}H_{23}F_3N_2O_2]$ $[M+H]^+$ 405.1784, found 405.1789.

_N_,2,5-Tribenzyl-6a-(trifluoromethyl)hexahydropyrrolo[3,4-_c_]pyrrole-3a(1_H_)-carboxamide (2.255)

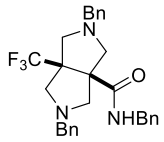

To a solution of carboxylic acid **2.254** (144 mg, 0.519 mmol) in MeCN (6 mL) was added benzylamine (142 µl, 1.30 mmol), DIPEA (271 µl, 1.56 mmol), and HATU (341 mg, 953 µmol) and the reaction mixture was stirred at 22 °C for 18 h. The mixture was concentrated *in vacuo* and purified directly by flash column chromatography (EtOAc/heptane/Et_3N 20:70:2) to give the title compound coreless oil (168 mg, 96%).

***R*$_f$** = 0.29 (EtOAc/heptane 2:7); **^{1}H NMR** (400 MHz, $CDCl_3$) δ 7.63 (t, *J* = 5.1 Hz, 1H), 7.43 – 7.12 (m, 15H), 4.37 (d, *J* = 5.1 Hz, 2H), 3.72 (d, *J* = 12.8 Hz, 2H), 3.57 (d, *J* = 12.8 Hz, 2H), 3.09 (d, *J* = 9.4 Hz, 2H), 2.98 (d, *J* = 9.4 Hz, 2H), 2.64 (t, *J* = 9.4 Hz, 4H); **^{13}C NMR** (101 MHz, $CDCl_3$) δ 171.2, 138.2 (2C), 138.1 (4C), 128.8 (4C), 128.6 (2C), 128.6, 128.3, 127.7 (CF_3 observed by HMBC), 127.5, 127.4 (2C), 61.7 (d, $^2J_{CF}$ = 25.2 Hz), 61.3, 60.9 (d, $^3J_{CF}$ = 2.1 Hz, 2C), 60.0 (2C), 59.0 (2C), 44.2; **^{19}F NMR** (377 MHz, $CDCl_3$) δ -69.64; **IR** (neat) cm^{-1}: 3325, , 2920, 2822, 1673, 1529; **HRMS** (ESI) calcd for $[C_{29}H_{31}F_3N_3O]$ $[M+H]^+$ 494.2414, found 494.2419.

_N_-Benzyl-6a-(trifluoromethyl)hexahydropyrrolo[3,4-_c_]pyrrole-3a(1_H_)-carboxamide (2.158)

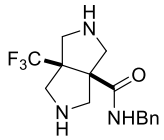

To a solution of amide **2.255** (70.0 mg, 0.142 mmol) in EtOH (3 ml) was added 10% Pd/C (38.0 mg, 35.5 µmol) and the resulting suspension was stirred at reflux under an atmosphere of H_2 for 18 h. The mixture was filtered through a pad of celite, concentrated *in vacuo*, and purified by flash column chromatography (CH_2Cl_2/MeOH/NH_3 380:19:1) to give the title compound as a colorless oil (25.0 mg, 56%)

***R*$_f$** = 0.26 (EtOAc/heptane/Et_3N 70:28:2); **^{1}H NMR** (400 MHz, CD_3OD) δ 7.37 – 7.20 (m, 5H), 4.38 (s, 2H), 3.48 (d, *J* = 11.8 Hz, 2H), 3.40 – 3.27 (m, 3H), 2.95 (d, *J* = 11.8 Hz, 2H), 2.85 (d, *J* = 11.8 Hz, 2H); **^{13}C NMR** (101 MHz, CD_3OD) δ 173.5, 139.7, 129.5 (2C), 129.4 (2C), 129.1 (q, $^1J_{CF}$ = 280.3 Hz), 128.8, 128.2, 67.6 (q, $^2J_{CF}$ = 24.2 Hz), 65.8, 57.2 (2C), 56.0 (q, $^3J_{CF}$ = 2.6 Hz, 2C), 44.7; **^{19}F NMR** (377 MHz, CD_3OD) δ -69.55; **IR** (neat) cm^{-1}: 3305 (br., N–H), 1650 (s, C=O), 1534 (m, C=C); **HRMS** (ESI) calcd for $[C_{15}H_{19}F_3N_3O]$ $[M+H]^+$ 314.1475, found 314.1475.

[3+2] Cycloaddition – Dihydropyrazole

Compounds **2.170** was synthesized by Thomas P. Klevin. Compounds **2.169**, **2.171**, **2.172**, and **2.177** were synthesized by BSc student Mie A. Larsen.

Diethyl (4*S**,5*R**)-4-(trifluoromethyl)-4,5-dihydro-1*H*-pyrazole-3,5-dicarboxylate (2.159)

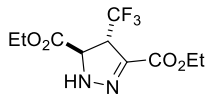

To a solution of 2-(trifluoromethyl)propenoic acid **2.5** (413 mg, 295 mmol) in MeCN (20 mL) was added ethyl diazoacetate (85% purity, 360 µL, 2.95 mmol) and the solution was stirred at 22 °C for 2 h. The solution was concentrated *in vacuo* to give the title compound as a yellow oil (587 mg, 95%).

R_f = 0.49 (EtOAc/heptane 1:1); **^{1}H NMR** (400 MHz, $CDCl_3$) δ 7.02 (br. s, 1H), 4.60 (d, *J* = 3.7 Hz, 1H), 4.37 – 4.29 (m, 3H), 4.26 (q, *J* = 7.3 Hz, 2H), 1.34 (t, *J* = 7.0 Hz, 3H), 1.31 (t, *J* = 7.3 Hz, 3H); **^{13}C NMR** (101 MHz, $CDCl_3$) δ 169.0, 160.8, 136.1, 124.4 (q, *J* = 280.7 Hz), 63.7 (q, *J* = 2.1 Hz), 63.2, 61.9, 51.6 (q, *J* = 31.0 Hz), 14.2, 14.1; **^{19}F NMR** (377 MHz, $CDCl_3$) δ -69.50.

Ethyl (4*S**,5*R**)-5-(allyl(methyl)carbamoyl)-4-(trifluoromethyl)-4,5-dihydro-1*H*-pyrazole-3-carboxylate (2.161) and ethyl (4*S**,5*R**)-4-(allyl(methyl)carbamoyl)-5-(trifluoromethyl)-4,5-dihydro-1*H*-pyrazole-3-carboxylate (2.162)

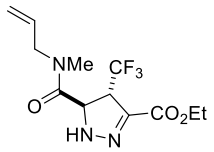

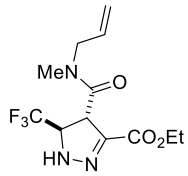

Following *general procedure A* using (*E*)-4,4,4-trifluorocrotonic acid **2.1** (682 mg, 4.72 mmol) and *N*-allylmethylamine (0.545 mL, 5.68 mmol) afforded the crude amide. The crude amide was dissolved in MeCN (20 mL) and ethyl diazoacetate (85 wt. %, 0.872 mL, 7.10 mmol) was added. The solution was then subjected to microwave heating at 140 °C for 4 h. The mixture was concentrated *in vacuo* and purified directly by flash column chromatography (EtOAc/heptane 2:3) to give the title compounds **2.161** (625 mg, 43%) and **17** (224 mg, 15%) both as viscous yellow oils.

Data for **2.161**: R_f = 0.18 (EtOAc/heptane 2:3); **^{1}H NMR** (400 MHz, $CDCl_3$) δ 6.89 (br. s, 1H), 5.91 – 5.62 (m, 1H), 5.42 – 5.11 (m, 2H), 4.81 (dd, *J* = 20.4, 3.5 Hz, 1H), 4.45 – 3.83 (m, 5H), 3.04 (s, 1.6H, major rotamer), 2.98 (s, 1.4H, minor rotamer), 1.35 (td, *J* = 7.1, 1.9 Hz, 3H); **^{13}C NMR** (101 MHz, $CDCl_3$) δ 167.9 (minor rotamer), 167.4 (major rotamer), 160.94 (minor rotamer), 160.88 (major rotamer), 136.8 (minor rotamer), 131.7 (major rotamer), 124.8 (d, $^1J_{CF}$ = 281.5 Hz), 119.0, 117.9, 62.9 (major rotamer), 62.8 (minor rotamer), 61.92 (major rotamer), 61.86 (minor rotamer), 52.6 (d, $^2J_{CF}$ = 30.1 Hz, minor rotamer), 52.5 (d, $^2J_{CF}$ = 30.2 Hz, major rotamer), 51.5 (major rotamer), 51.3 (minor rotamer), 35.1 (major rotamer), 34.1 (minor rotamer), 14.3; **^{19}F NMR** (377 MHz, $CDCl_3$) δ -68.43 (major rotamer), -68.45 (minor rotamer); **IR** (neat) cm^{-1}: 3296 (br., N–H), 1709 (s, C=O), 1650 (s, C=O); **HRMS** (ESI) calcd for $[C_{12}H_{17}F_3N_3O_3]$ $[M+H]^+$ 308.1217, found 308.1220.

Data for **2.162**: R_f = 0.27 (EtOAc/heptane 2:3); **^{1}H NMR** (400 MHz, $CDCl_3$) δ 6.65 (br. s, 1H), 5.92 – 5.64 (m, 1H), 5.32 – 5.15 (m, 2H), 4.80 (dpd, *J* = 16.2, 6.9, 2.6 Hz, 1H), 4.59 – 4.37 (m, 1.5H), 4.28 (qd, *J* = 7.1, 3.9 Hz, 2H), 4.17 – 3.83 (m, 1.5H), 3.19 (s, 1.7H, major rotamer), 3.01 (s, 1.3H, minor rotamer), 1.33 (td, *J* = 7.2, 0.9 Hz, 3H); **^{13}C NMR** (101 MHz, $CDCl_3$) δ 168.6, 161.5 (minor rotamer), 161.4 (major rotamer), 141.3 (major rotamer), 140.7 (minor rotamer), 132.2 (minor rotamer), 132.1 (major rotamer), 124.4 (major rotamer, d, $^1J_{CF}$ = 278.1 Hz), 124.3 (minor rotamer, d, $^1J_{CF}$ = 278.1 Hz) 117.8 (minor rotamer), 117.7 (major rotamer), 67.4 (minor rotamer, q, $^2J_{CF}$ = 31.6 Hz), 67.3 (major rotamer, q, $^2J_{CF}$ = 31.6 Hz), 61.94 (major rotamer), 61.90 (minor rotamer), 53.2 (minor rotamer), 51.1 (major rotamer), 47.93 (major rotamer), 47.85 (minor rotamer), 35.8 (major rotamer), 34.9 (minor rotamer), 14.30 (minor rotamer), 14.28 (major rotamer); **^{19}F NMR** (377 MHz, $CDCl_3$) δ -74.99 (minor rotamer), -75.23 (major rotamer); **IR** (neat) cm^{-1}: 3293 (br., N–H), 1740 (s, C=O), 1636 (s, C=O); **HRMS** (ESI) calcd for $[C_{12}H_{17}F_3N_3O_3]$ $[M+H]^+$ 308.1217, found 308.1219.

Ethyl (4*S,5*R**)-5-(allyl(methyl)carbamoyl)-4-(trifluoromethyl)-1-(vinylsulfonyl)-4,5-dihydro-1*H*-pyrazole-3-carboxylate (2.163)**

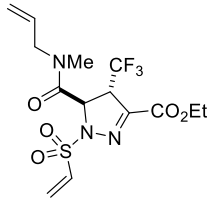

To a solution of **2.161** (341 mg, 1.11 mmol) in CH_2Cl_2 (12 mL) was added ethenesulfonyl chloride (154 mg, 1.22 mmol) and Et_3N (309 µL, 2.22 mmol) and the solution was stirred at 22 °C for 16 h. Sat. aq. $NaHCO_3$ (12 mL) was added and the layers were separated. The organic layer was dried over $MgSO_4$, filtered, and concentrated *in vacuo*. The crude product was purified by flash column chromatography (EtOAc/heptane 2:3, R_f = 0.23) to give the title compound as a colorless oil (157 mg, 36%).

^{1}H NMR (400 MHz, $CDCl_3$) δ 6.83 – 6.65 (m, 1H), 6.49 (d, *J* = 4.0 Hz, 0.6H, major rotamer), 6.45 (d, *J* = 4.0 Hz, 0.4H, minor rotamer), 6.15 (d, *J* = 9.9 Hz, 1H), 5.94 – 5.62 (m, 1H), 5.45 (d, *J* = 4.9 Hz, 0.6H, major rotamer), 5.38 (d, *J* = 4.0 Hz, 0.4H, minor rotamer), 5.35 – 5.19 (m, 2H), 4.34 (qd, *J* = 7.2, 2.3 Hz, 2H), 4.29 – 4.22 (m, 1H), 4.22 – 4.09 (m, 1H), 3.97 (ddt, *J* = 17.5, 5.1, 1.8 Hz, 0.4H), 3.89 (ddt, *J* = 15.2, 5.9, 1.4 Hz, 0.6H, major rotamer), 3.13 (s, 2H, major rotamer), 2.97 (s, 1H, minor rotamer), 1.34 (t, *J* = 7.1 Hz, 3H); **^{13}C NMR** (101 MHz, $CDCl_3$) δ 166.40 (minor rotamer), 166.38 (major rotamer), 159.6, 140.7 (q, $^3J_{CF}$ = 1.3 Hz, minor rotamer), 140.4 (q, $^3J_{CF}$ = 1.3 Hz, major rotamer), 134.3, 131.5 (minor rotamer), 131.4 (major rotamer), 131.1 (minor rotamer), 130.9 (major rotamer), 123.8 (q, $^1J_{CF}$ = 280.6 Hz, major rotamer), 123.7 (q, $^1J_{CF}$ = 281.2 Hz, minor rotamer), 118.5 (minor rotamer), 118.4 (major rotamer), 62.7, 61.3 (q, $^3J_{CF}$ = 2.0 Hz, minor rotamer), 61.2 (q, $^3J_{CF}$ = 2.0 Hz, major rotamer), 55.52 (q, $^2J_{CF}$ = 30.8 Hz, major rotamer), 55.37 (q, $^2J_{CF}$ = 30.6 Hz, minor rotamer), 52.5 (minor rotamer), 51.2 (major rotamer), 35.2 (minor rotamer), 34.7 (major rotamer), 14.2; **^{19}F NMR** (377 MHz, $CDCl_3$) δ -67.90, -68.01; **IR** (neat) cm^{-1}: 1723 (s, C=O), 1658 (s, C=O), 1364 (s, S=O); **HRMS** (ESI) calcd for $[C_{14}H_{19}F_3N_3O_5S]$ $[M+H]^+$ 398.0992, found 398.0931.

Ethyl 3-(trifluoromethyl)-4,5-dihydro-1*H*-pyrazole-5-carboxylate (2.168)

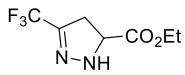

To a solution of 2-(trifluoromethyl)propenoic acid **2.5** (413 mg, 295 mmol) in MeCN (20 mL) was added ethyl diazoacetate (85% purity, 360 µL, 2.95 mmol) and the solution was stirred at 22 °C for 2 h. The solution was concentrated *in vacuo* to give the title compound as a yellow oil (587 mg, 95%).

^{1}H NMR (400 MHz, $CDCl_3$) δ 4.44 (dd, *J* = 11.9, 5.2 Hz, 1H), 4.24 (q, *J* = 7.2 Hz, 2H), 3.25 (ddq, *J* = 17.4, 5.3, 1.3 Hz, 1H), 3.20 – 3.06 (m, 1H), 1.30 (t, *J* = 7.2 Hz, 3H). **^{13}C NMR** (101 MHz, $CDCl_3$) δ 171.31, 141.36 (q, $^2J_{CF}$ = 37.8 Hz), 120.43 (q, $^1J_{CF}$ = 269.6 Hz), 62.44, 61.36, 33.78, 14.21. **^{19}F NMR** (377 MHz, $CDCl_3$) δ -66.99; **IR** (neat) cm^{-1}: 3349 (br., N–H), 1734 (s, C=O); **HRMS** (ESI) calcd. for $C_7H_{10}N_2F_3O_2$ $[M+H]^+$ 211.0689, found 211.0810

Ethyl 1-(methylsulfonyl)-3-(trifluoromethyl)-4,5-dihydro-1*H*-pyrazole-5-carboxylate (2.169)

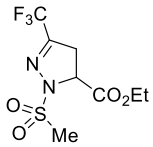

To a solution of **2.168** (100 mg, 0.476 mmol) in CH_2Cl_2 (10 mL) was added methanesulfonyl chloride (44.2 µL, 0.571 mmol) and Et_3N (133 µL, 0.952 mmol) and the reaction mixture was stirred at 22 °C for 16 h. Water (10 mL) was added and the phases were separated. The aqueous phase was extracted with CH_2Cl_2 (3 × 5 mL) and the combined organic layers were dried over $MgSO_4$, filtered, and concentrated *in vacuo*. The crude product was purified by flash column chromatography (EtOAc/heptane 1:2) to give the title compound as an off-white solid (104 mg, 76%).

***R*$_f$** = 0.26 (EtOAc/heptane 1:2); **m.p.**: 105–107 °C; **^{1}H NMR** (400 MHz, $CDCl_3$) δ 5.07 (dd, *J* = 12.7, 7.6 Hz, 1H), 4.29 (qd, *J* = 7.1, 2.6 Hz, 2H), 3.49 (ddd, *J* = 18.1, 7.6, 1.3 Hz, 1H), 3.19 (ddd, *J* = 18.1, 7.6, 1.3 Hz, 1H), 1.33 (t, *J* = 7.1 Hz, 3H); **^{13}C NMR** (101 MHz, $CDCl_3$) δ 168.7, 144.6 (q, $^2J_{CF}$ = 39.4 Hz), 118.9 (q, $^1J_{CF}$ = 271.4 Hz), 62.6, 61.1, 40.1, 36.1, 13.8; **^{19}F NMR** (377 MHz, $CDCl_3$) δ -67.29; **IR** (neat) cm^{-1}: 1739 (s, C=O), 1396 (m, S=O); **HRMS** (ESI) calcd. for $C_8H_{12}F_3N_2O_4S$ $[M+H]^+$ 289.0464, found 289.0464.

Ethyl 1-(thiophene-3-carbonyl)-3-(trifluoromethyl)-4,5-dihydro-1*H*-pyrazole-5-carboxylate (2.170)

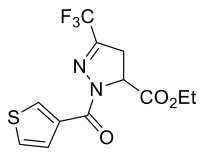

To a solution of **2.168** (100.0 mg, 0.476 mmol) in MeCN (5 mL) was added thiophene-3-carbonyl chloride (76.0 mg, 0.523 mmol) and Et_3N (73.0 µL, 0.523 mmol) and the solution was stirred at reflux for 24 h. The solution was concentrated *in vacuo* and purified directly by flash column chromatography (EtOAc/heptane 1:3, R_f = 0.34) to give the title compound as a white solid (80.0 mg, 53%).

***R*f** = 0.34 (EtOAc/heptane 1:3); **m.p.**: 87–88 °C; **^{1}H NMR** (400 MHz, $CDCl_3$) δ 8.41 (dd, *J* = 3.0, 1.2 Hz, 1H), 7.73 (dd, *J* = 5.1, 1.2 Hz, 1H), 7.30 (dd, *J* = 5.1, 3.0 Hz, 1H), 5.19 (dd, *J* = 12.8, 6.6 Hz, 1H), 4.28 (qd, *J* = 7.1, 1.5 Hz, 2H), 3.43 (ddq, *J* = 18.6, 12.8, 1.5 Hz, 1H), 3.13 (ddq, *J* = 18.6, 6.6, 1.3 Hz, 1H), 1.31 (t, *J* = 7.1 Hz, 3H); **^{13}C NMR** (101 MHz, $CDCl_3$) δ 168.7, 161.1, 144.21 (q, $^{2}J_{CF}$ = 39.0 Hz), 134.1, 133.2, 129.5, 124.9, 119.5 (d, $^{1}J_{CF}$ = 270.9 Hz), 62.3, 59.7, 34.2, 14.0; **^{19}F NMR** (377 MHz, $CDCl_3$) δ -67.31; IR (neat) cm^{-1}: 1732 (s, C=O), 1649 (s, C=O), 1506 (m, C=C); **HRMS** (ESI) calcd. for $[C_{12}H_{12}F_3N_2O_3S]$ $[M+H]^+$ 321.0515, found 321.0703

Ethyl 5-(trifluoromethyl)-4,5-dihydro-1*H*-pyrazole-3-carboxylate (2.171)

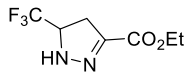

To a solution of **2.168** (95.0 mg, 0.452 mmol) in MeCN (5 mL) was added HATU (206 mg, 0.542 mmol), DIPEA (0.315 mL, 1.81 mmol), and (51.3 mg, 0.542 mmol) and the reaction mixture was stirred 22 °C for 42 h. The mixture was concentrated *in vacuo* and purified directly by flash column chromatography (EtOAc/heptane 1:2) to give the title compound as a yellow oil (16.0 mg, 17%)

^{1}H NMR (400 MHz, DMSO-d_6) δ 8.94 (s, 1H), 4.68 (dddd, *J* = 15.9, 10.1, 5.0, 3.3 Hz, 1H), 4.18 (q, *J* = 7.1 Hz, 2H), 3.23 (dd, *J* = 17.7, 13.2 Hz, 1H), 2.88 (dd, *J* = 17.7, 8.6 Hz, 1H), 1.23 (t, *J* = 7.1 Hz, 3H); **^{13}C NMR** (101 MHz, DMSO-d_6) δ 161.4, 139.6, 125.1 (q, $^{1}J_{CF}$ = 279.2 Hz), 60.4, 60.1 (q, $^{2}J_{CF}$ = 30.2 Hz), 31.7, 14.1; **^{19}F NMR** (377 MHz, DMSO-d_6) δ -75.61; **IR** (neat) cm^{-1}: 3302 (br., N–H), 1747 (s, C=O); **HRMS** (ESI) calcd. for $C_7H_{10}N_2F_3O_2$ $[M+H]^+$ 211.0689, found 211.0810.

Ethyl 1-(3-(hydroxymethoxy)-2-oxopropyl)-3-(trifluoromethyl)-4,5-dihydro-1*H*-pyrazole-5-carboxylate (2.172)

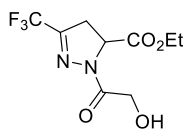

To a solution of **2.168** (205 mg, 0.975 mmol) in MeCN (10 mL) was added 2-(benzyloxy)acetyl chloride (216 mg, 1.17 mmol) and DIPEA (0.340 mL, 1.95 mmol) and the reaction mixture was stirred at 22 °C for 14 h. The mixture was concentrated *in vacuo* and dissolved in EtOH (6 mL). 10% Pd/C (10.4 mg, 97.6 µmol) was added and the resulting suspension was stirred under an atmosphere of H_2 at 22 °C for 12 h. The mixture filtered through a pad of celite and concentrated *in vacuo*. The crude product was purified by flash column chromatography (EtOAc/heptane 5:6) to give the title compound as a colorless oil (103 mg, 39%).

***R*f** = 0.23 (EtOAc/heptane 5:6); **^{1}H NMR** (400 MHz, DMSO-d_6) δ 5.24 (t, *J* = 6.5 Hz, 1H), 5.05 (dd, *J* = 13.0, 6.1 Hz, 1H), 4.33 (d, *J* = 6.5 Hz, 2H), 4.15 (qd, *J* = 7.1, 1.8 Hz, 2H), 3.67 – 3.53 (qq, *J* = 4 Hz, 1H), 3.34 – 3.24 (qq, *J* = 4 Hz, 1H), 1.21 (t, *J* = 7.1 Hz, 3H); **^{13}C NMR** (101 MHz, DMSO-d_6) δ 170.7, 168.6, 144.8 (q, $^{2}J_{CF}$ = 37.9 Hz), 119.5 (q, $^{1}J_{CF}$ = 270.8 Hz), 61.6,

59.9, 58.6, 34.4, 13.9; **^{19}F NMR** (377 MHz, CD_3OD) δ -69.00; **IR** (neat) cm^{-1}: 1747 (s, C=O), 1701 (s, C=O), 1604 (m, C=N).

1-morpholino-2-(trifluoromethyl)prop-2-en-1-one (2.174)

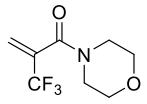

Following *general procedure A* using 2-(trifluoromethyl)acrylic acid **2.5** (86.0 mg, 0.614 mmol) and morpholine (56.0 µL, 0.644 mmol) afforded the crude amide as a colorless oil after filtration through a short plug of silica. The crude product was used directly in the next step without further purification.

***R*$_f$** = 0.38 (EtOAc/heptane 7:3); **^{1}H NMR** (400 MHz, $CDCl_3$) δ 6.07 (s, 1H), 5.68 (s, 1H), 3.68 (d, *J* = 16.8 Hz, 6H), 3.51 (s, 2H); ^{13}C NMR (101 MHz, $CDCl_3$) δ 162.7, 134.4 (q, $^2J_{CF}$ = 32.4 Hz), 122.9 (q, $^3J_{CF}$ = 5.5 Hz), 121.3 (q, $^1J_{CF}$ = 273.7 Hz), 66.6 (2C), 47.6, 42.5; **^{19}F NMR** (377 MHz, $CDCl_3$) δ -65.55.

Ethyl 5-(morpholine-4-carbonyl)-5-(trifluoromethyl)-4,5-dihydro-1*H*-pyrazole-3-carboxylate (2.175)

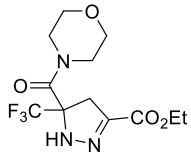

To a solution of **2.174** (70.0 mg, 0.335 mmol) in MeCN (3 mL) was added ethyl diazoacetate (43.0 µL, 0.368 mmol) and the reaction mixture was subjected to microwave heating at 140 °C for 4 h. The mixture was concentrated *in vacuo* and purified directly by flash column chromatography (EtOAc/heptane 5:6) to give the title compound as a colorless oil (36.0 mg, 33%).

***R*$_f$** = 0.31 (EtOAc/heptane 1:1); **^{1}H NMR** (400 MHz, $CDCl_3$) δ 7.79 – 7.48 (m, 1H), 4.31 (q, *J* = 7.1 Hz, 2H), 3.82 – 3.63 (m, 6H), 3.54 (d, *J* = 7.5 Hz, 2H), 3.48 (dd, *J* = 18.1, 1.8 Hz, 1H), 3.32 (d, *J* = 18.1 Hz, 1H), 1.35 (t, *J* = 7.1 Hz, 3H); ^{13}C NMR (101 MHz, $CDCl_3$) δ 163.9, 161.3, 141.4, 123.8 (q, $^1J_{CF}$ = 282.1 Hz), 72.4 (q, $^2J_{CF}$ = 28.8 Hz), 66.6, 66.5 (3C), 61.8, 37.6 (d, $^3J_{CF}$ = 1.2 Hz), 14.2; **^{19}F NMR** (377 MHz, $CDCl_3$) δ -75.78.

5-(*tert*-Butyl) 3-ethyl 5-(trifluoromethyl)-4,5-dihydro-1*H*-pyrazole-3,5-dicarboxylate (2.177)

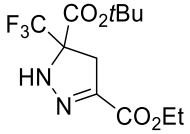

To a solution of *tert*-butyl 2-(trifluoromethyl)acrylate **2.176** (196 mg, 0.998 mmol) in MeCN (10 mL) was added ethyl diazoacetate (1.02 mL, 1.20 mmol, 15% in PhMe) and the solution was stirred at reflux for 14 h. The solution was concentrated *in vacuo* to give the title compound as a yellow oil (240 mg, 78%).

^{1}H NMR (400 MHz, $CDCl_3$) δ 6.93 (s, 1H), 4.32 (q, *J* = 7.2 Hz, 2H), 3.57 (d, *J* = 18.6 Hz, 1H), 3.33 (d, *J* = 18.6 Hz, 1H), 1.50 (s, 9H), 1.36 (t, *J* = 7.2 Hz, 3H); **^{13}C NMR** (101 MHz, $CDCl_3$)

δ 165.3, 160.9, 142.2, 123.2 (q, $^{1}J_{CF}$ = 282.1 Hz), 85.6, 73.8 (q, $^{2}J_{CF}$ = 29.4 Hz), 61.6, 37.0 (d, $^{3}J_{CF}$ = 1.4 Hz), 27.5 (3C), 13.9; **^{19}F NMR** (377 MHz, $CDCl_3$) δ -75.01; **IR** (neat) cm^{-1}: 3338 (br., N–H), 1738 (s, C=O), 1702 (s, C=O). **HRMS** (ESI) calcd for $[C_8H_{10}F_3N_3O_4]$ $[M+H–C_4H_8]^+$ 255.0587, found 255.0583 (loss of ^{t}Bu ester).

Dinucleophile Cyclizations

Compounds was **2.182**, **2.188**, **2.189**, **2.190**, **2.191**, **2.193** and **2.194** were synthesized by MSc student Ida S. A. Jensen. Compounds **2.181**, **2.184**, and **2.192** were synthesized by BSc student Julie Forchhammer. Compounds **2.183** and **2.256** were synthesized by Thomas P. Klevin. Compound **2.185** was synthesized by BSc student Mie A. Larsen. Compound **2.186** was synthesized by MSc student Katarzyna J. Śniady.

4-(Trifluoromethyl)-1,3,4,5-tetrahydro-2*H*-benzo[*b*][1,4]diazepin-2-one (2.178)

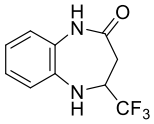

To a solution of (*E*)-4,4,4-trifluorocrotonic acid **2.1** (155 mg, 1.11 mmol) in MeCN (20 mL) was added *o*-phenylenediamine (251 mg, 2.32 mmol) and the reaction mixture was stirred at reflux for 40 h. Then, HATU (421 mg, 1.11 mmol) and DIPEA (0.394 mL, 2.21 mmol) was added and the solution was stirred at 22 °C for 8 h. The mixture was concentrated *in vacuo* and purified directly by flash column chromatography (EtOAc/heptane 2:3) to give the title compound as a white solid (166 mg, 65%).

***R*f** = 0.21 (EtOAc/heptane 2:3); **m.p.**: 186–188 °C; **^{1}H NMR** (400 MHz, DMSO-d_6) δ 9.69 (s, 1H), 7.01 (dd, *J* = 7.9, 1.6 Hz, 1H), 6.96 (ddd, 7.9, 6.7, 1.9 Hz, 1H), 6.90 (dd, 7.9, 1.9 Hz, 1H), 6.86 (ddd, 7.9, 6.7, 1.6 Hz, 1H), 5.89 (d, *J* = 4.2 Hz, 1H), 4.46 (m, 1H), 2.63 (dd, *J* = 13.9, 5.1 Hz, 1H), 2.48 (dd, *J* = 13.9, 7.1 Hz, 1H); **^{13}C NMR** (101 MHz, DMSO-d_6) δ 169.0, 137.4, 129.1, 125.6 (q, $^{1}J_{CF}$ = 282 Hz), 124.8, 122.0, 121.7, 121.3, 59.3 (q, $^{2}J_{CF}$ = 28.5 Hz), 32.7; **^{19}F NMR** (377 MHz, DMSO-d_6) δ -75.43; **HRMS** (ESI) calcd for $[C_{10}H_{10}F_3N_2O]$ $[M+H]^+$ 231.0742, found 231.0740; **IR** (neat) cm^{-1}: 3307 (s, N–H), 3200 (br., N–H), 3048 (s, C=C–H), 1666 (s, C=O), 1497 (s, C=C).

3-((2-Aminobenzyl)amino)-4,4,4-trifluorobutanoic acid (2.179)

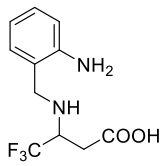

To a solution of (*E*)-4,4,4-trifluorocrotonic acid **2.1** (109 mg, 755 µmol) in MeCN (8 mL) was added 2-aminobenylamine (203 mg, 1.66 mmol) and the reaction mixture was stirred at reflux for 4 h. The solution was concentrated *in vacuo* and the crude product was purified directly by flash column chromatography (EtOAc/heptane/AcOH 50:50:1) to give the title compound as a white solid (168 mg, 85%).

***R*f** = 0.30 (EtOAc/heptane/AcOH 50:50:1); **m.p.**: 106–108 °C; **^{1}H NMR** (400 MHz, DMSO-d_6) δ 7.04 – 6.87 (m, 2H), 6.63 (dd, *J* = 8.4, 1.3 Hz, 1H), 6.49 (td, *J* = 7.3, 1.2 Hz, 1H), 3.73 (s, 2H), 3.56 (pd, *J* = 7.8, 5.5 Hz, 1H), 2.62 – 2.50 (m, 2H); **^{13}C NMR** (101 MHz, DMSO-d_6) δ 171.6, 147.5, 129.5, 128.0, 126.9 (q, $^{1}J_{CF}$ = 284.3 Hz), 122.6, 115.8, 114.8, 55.4 (q, $^{2}J_{CF}$ = 27.6 Hz), 49.7, 34.0; **^{19}F NMR** (377 MHz, DMSO-d_6) δ -73.44; **IR** (neat) cm^{-1}: 3423 (m, N–H),

3325 (s, N–H), 3084 (br., O–H), 1745 (s, C=O), 1591 (s, C=C); **HRMS** (ESI) calcd for $[C_{11}H_{14}F_3N_2O_2]$ $[M+H]^+$ 263.1002, found 263.1003.

4-(Trifluoromethyl)-3,4,5,6-tetrahydrobenzo[*b*][1,5]diazocin-2(1*H*)-one (2.180)

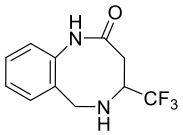

To a solution of **2.179** (101 mg, 0.385 mmol) and DIPEA (0.20 mL, 1.2 mmol) in MeCN (50 mL) was added HATU (220 mg, 0.577 mmol) and stirred at 21 °C for 2 h. Then, the reaction mixture was concentrated *in vacuo*, dissolved in CH_2Cl_2 (15 mL), and washed with sat. aq. $NaHCO_3$ (2 × 10 mL). The organic layer was dried over $MgSO_4$, filtered, and concentrated *in vacuo*. The crude was purified by flash column chromatography (EtOAc/heptane 1:1) to give the title compound as a light yellow solid (830 mg, 88%).

***R*f** = 0.25 (EtOAc/heptane 1:1); **m.p.**: 157–159 °C; **^{1}H NMR** (400 MHz, DMSO-*d*$_6$) δ 9.97 (s, 1H), 7.41 (dd, *J* = 7.4, 1.9 Hz, 1H), 7.31 (td, *J* = 7.4, 2.0 Hz, 1H), 7.27 (td, *J* = 7.3, 1.6 Hz, 1H), 7.02 (dd, *J* = 7.4, 1.8 Hz, 1H), 3.87 (dd, *J* = 14.1, 6.3 Hz, 1H), 3.54 (m, 1H), 3.38 (dd, *J* = 14.1, 3.0 Hz, 1H), 3.22 (td, *J* = 6.2, 3.0 Hz, 1H), 2.27 (d, *J* = 12.5, 1H), 2.10 (dd, *J* = 12.6, 9.4, 1H); **^{13}C NMR** (101 MHz, DMSO-*d*$_6$) δ 170.5, 136.7, 136.0, 131.9, 128.1, 126.7, 125.9 (q, $^1J_{CF}$ = 280 Hz), 124.2, 55.8 (q, $^2J_{CF}$ = 28.0 Hz), 46.5, 34.5; **^{19}F NMR** (377 MHz, DMSO-*d*$_6$) δ -75.26; **IR** (neat) cm^{-1}: 3348 (m, N–H), 3172 (br., N–H), 3050 (m, C=C–H), 1661 (s, C=O), 1493 (m, C=C); **HRMS** (ESI) calcd for $[C_{11}H_{12}F_3N_2O]$ $[M+H]^+$ 245.0896, found 245.0900.

7,8-Dimethoxy-4-(trifluoromethyl)-1,3,4,5-tetrahydro-2*H*-benzo[*b*][1,4]diazepin-2-one (2.181)

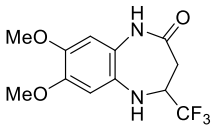

To a solution of 4,5-dimethoxybenzene-1,2-diamine (50.0 mg, 0.297 mmol) in MeCN (20 mL) was added (*E*)-4,4,4-trifluorocrotonic acid **2.1** (41.0 mg, 0.297 mmol) and the reaction mixture was stirred at reflux for 44 h. The mixture was concentrated *in vacuo* and purified directly flash column chromatography (EtOAc/heptane 1:1) to give the title compound as a brown oil (28.0 mg, 33%).

***R*f** = 0.33 (EtOAc/heptane 1:1); **^{1}H NMR** (400 MHz, $CDCl_3$) δ 8.41 (s, 1H), 6.51 (s, 1H), 6.48 (s, 1H), 4.34 (dddd, *J* = 12.3, 11.0, 6.9, 5.4 Hz, 1H), 3.86 (s, 3H), 3.84 (s, 3H), 2.72 (dd, *J* = 13.0, 11.0 Hz, 1H), 2.62 (ddd, *J* = 13.0, 5.4, 1.3 Hz, 1H); **^{13}C NMR** (101 MHz, $CDCl_3$) δ 171.6, 147.7, 146.0, 129.4, 128.0 (d, $^1J_{CF}$ = 285.7 Hz), 122.9, 107.3, 106.4, 61.8 (d, $^2J_{CF}$ = 29.0 Hz), 56.5, 56.4, 31.9; **^{19}F NMR** (377 MHz, $CDCl_3$) δ -78.15; **IR** (neat) cm^{-1}: 3323 (s, N–H), 3297 (br., N–H), 1648 (s, C=O), 1518 (s, C=C); **HRMS** (ESI) calcd for $[C_{12}H_{14}F_3N_2O_3]$ $[M+H]^+$ 291.0951, found 291.0982.

3-((2-Aminoethyl)amino)-4,4,4-trifluorobutanoic acid (2.182)

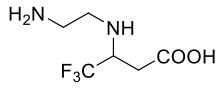

To a solution of (*E*)-4,4,4-trifluorocrotonic acid **2.1** (155 mg, 1.11 mmol) in MeCN (15 mL) was added ethylenediamine (0.739 mL, 1.11 mmol) and the reaction mixture was stirred at reflux for 3 h. Precipitate was collected by filtration and washed with MeCN (2 × 5 mL) to give the title compound as a white solid (0.136 mg, 63%).

m.p.: 200–202 °C; **^{1}H NMR** (400 MHz, D_2O) δ 3.57 (dqd, *J* = 14.8, 7.5, 4.2 Hz, 1H), 3.18 – 2.97 (m, 4H), 2.62 (dd, *J* = 15.4, 4.2 Hz, 1H), 2.35 (dd, *J* = 15.4, 9.8 Hz, 1H); **^{13}C NMR** (101 MHz, D_2O) δ 178.4, 126.5 (q, $^{1}J_{CF}$ = 289 Hz), 56.5 (q, $^{2}J_{CF}$ = 28 Hz), 43.8, 38.9, 37.90; **^{19}F NMR** (377 MHz, D_2O) δ -75.03; **IR** (neat) cm^{-1}: 3330 (s, N–H), 3001 (br., O–H), 1636 (s, C=O); **HRMS** (ESI) calcd. for $[C_6H_{12}F_3N_2O_2]$ $[M+H]^+$ 201.0845, found 201.0870.

3-((2-Acetamidoethyl)amino)-4,4,4-trifluorobutanoic acid (2.183)

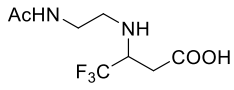

To a solution of (*E*)-4,4,4-trifluorocrotonic acid **2.1** (200.0 mg, 1.43 mmol) in MeCN (10 mL) was added *N*-(2-aminoethyl)acetamide (357 mg, 3.49 mmol) and the solution stirred at reflux for 24 h. The solution was concentrated *in* vacuo and purified directly by flash column chromatography (EtOAc/MeOH/AcOH 90:9:1) to give the title compound as a yellow amorphous solid (240 mg, 70%).

***R*$_f$** = 0.27 (EtOAc/MeOH/AcOH 90:9:1); **^{1}H NMR** (400 MHz, CD_3OD) δ 3.65 – 3.51 (m, 1H), 3.23 (td, *J* = 6.7, 6.0, 2.5 Hz, 2H), 2.91 (dt, *J* = 11.9, 5.8 Hz, 1H), 2.80 (dt, *J* = 12.4, 6.3 Hz, 1H), 2.63 (dd, *J* = 16.1, 3.8 Hz, 1H), 2.43 (dd, *J* = 16.1, 9.7 Hz, 1H), 1.94 (s, 3H); **^{13}C NMR** (101 MHz, CD_3OD) δ 173.0, 172.1, 126.62 (q, $^{1}J_{CF}$ = 283.1 Hz), 56.5 (q, $^{2}J_{CF}$ = 28.4 Hz), 46.8, 39.2, 34.2 (d, $^{3}J_{CF}$ = 2.2 Hz), 21.2; **^{19}F NMR** (377 MHz, CD_3OD) δ -76.73; **IR** (neat) cm^{-1}: 3411 (M, N–H), 3350 (m, N–H), 3010 (br., O–H), 1718 (S, C=O), 1680 (S, C=O); **HRMS** (ESI) calcd. for $[C_8H_{14}F_3N_2O_3]$ $[M+H]^+$ 243.0951, found 243.0938.

8-Chloro-4-(trifluoromethyl)-3,4,5,6-tetrahydrobenzo[*b*][1,5]diazocin-2(1*H*)-one (2.184)

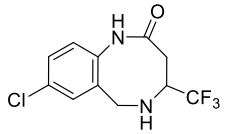

To a solution of 2-aminomethyl)-4-chloroaniline (175 mg, 1.12 mmol) in MeCN (6 mL) was added (*E*)-4,4,4-trifluorocrotonic acid **2.1** (75.0 mg, 0.536 mmol) and the reaction mixture was stirred at reflux for 4 h. The mixture was concentrated *in vacuo* and filtered through a short plug of silica. The crude Michael adduct was dissolved in MeCN (5 mL) and added HATU (192 mg, 0.505 mmol) and DIPEA (117 μL, 0.674 mmol). The reaction mixture was stirred at 22 °C for 2 h and then concentrated *in vacuo*. The residue was dissolved in CH_2Cl_2 (10 mL) and washed with sat. aq. $NaHCO_3$ (2 × 10 mL), dried over $MgSO_4$, filtered, and concentrated *in vacuo*. The

crude product was purified by flash column chromatography (EtOAc/heptane 1:1) to give the title compound as a white amorphous solid (86.0 mg, 54%).
R_f = 0.30 (EtOAc/heptane 1:1); **^{1}H NMR** (400 MHz, DMSO-d_6) δ 9.98 (s, 1H), 7.48 (d, J = 2.5 Hz, 1H), 7.36 (dd, J = 8.4, 2.5 Hz, 1H), 7.09 (d, J = 8.4 Hz, 1H), 3.86 (dd, J = 14.2, 6.2 Hz, 1H), 3.54 (h, J = 7.9 Hz, 1H), 3.36 (dd, J = 14.2, 3.5 Hz, 1H), 3.23 (td, J = 6.2, 3.5 Hz, 1H), 2.28 (d, J = 12.9 Hz, 1H), 2.11 (dd, J = 12.9, 9.3 Hz, 1H); **^{13}C NMR** (101 MHz, DMSO-d_6) δ 170.4, 137.9, 135.7, 131.4, 130.6, 128.0, 126.3, 126.0, 55.8, 46.1, 34.7; **^{19}F NMR** (377 MHz, DMSO-d_6) δ -74.99; **IR** (neat) cm^{-1}: 3333 (m, N–H), 3166 (br., N–H), 1664 (s, C=O), 1488 (m, C=C); **HRMS** (ESI) calcd for $[C_{11}H_{11}ClF_3N_2O]$ $[M+H]^+$ 279.0507, found 279.0494.

3-Amino-7-(trifluoromethyl)-6,7-dihydrothieno[3,2-*b*]pyridin-5(4*H*)-one (2.185)

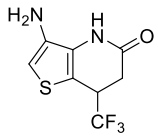

To a suspension of thiophene-3,4-diamine dihydrochloride (201 mg, 1.07 mmol) in MeCN (4 mL) was added Et_3N (600 µL, 4.29 mmol) and (*E*)-4,4,4-trifluorocrotonic acid **2.1** (100 mg, 0.714 mmol) and the suspension was subjected to µW heating at 140 °C for 2 h. The suspension was filtered and the filtrate was concentrated *in* vacuo. The crude product was purified by flash column chromatography (EtOAc/heptane 3:2) to give the title compound as a brown solid (34.6 mg, 21%).
R_f = 0.23 (EtOAc/heptane 3:2); **m.p.**: 122–123 °C; **^{1}H NMR** (400 MHz, $CDCl_3$) δ 10.31 (s, 1H), 6.20 (s, 1H), 3.76 (br. s, 2H), 3.70 (pd, J = 8.4, 4.9 Hz, 2H), 3.24 – 2.53 (q, J = 16 Hz, 1H), 3.03 – 2.85 (m, 2H); **^{13}C NMR** (101 MHz, $CDCl_3$) δ 169.8, 134.8, 130.8, 126.0 (q, $^1J_{CF}$ = 280.8 Hz), 107.71 (q, $^3J_{CF}$ = 1.9 Hz), 102.5, 38.8 (q, $^2J_{CF}$ = 30.4 Hz), 31.1; **^{19}F NMR** (377 MHz, $CDCl_3$) δ -72.92; **IR** (neat) cm^{-1}: 3407 (m, N–H), 3212 (br., N–H), 1670 (s, C=O), 1495 (m, C=C).

3-((2-Aminophenethyl)amino)-4,4,4-trifluorobutanoic acid (2.186)

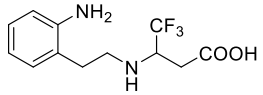

To a solution of (*E*)-4,4,4-trifluorocrotonic acid **2.1** (263 mg, 1.88 mmol) in MeCN (13 ml) was added 2-(2-aminoethyl)aniline (320 mg, 2.35 mmol) and DIPEA (258 µl, 1.48 mmol) and the mixture was refluxed for 3 h. The reaction mixture was concentrated *in vacuo* and purified directly by flash column chromatography (EtOAc/heptane/AcOH 65:33:2) to give the title compound as an off-white solid (175 mg, 34%).
R_f = 0.45 (EtOAc/heptane/AcOH 73:25:2); **m.p.:** 157–158 °C; **^{1}H NMR** (400 MHz, CD_3OD) δ 7.05 – 6.93 (m, 2H), 6.75 (dd, J = 7.8, 1.2 Hz, 1H), 6.68 (td, J = 7.8, 1.2 Hz, 1H), 3.74 – 3.61 (m, 1H), 3.05 – 2.89 (m, 2H), 2.73 – 2.66 (m, 3H), 2.49 (dd, J = 16.2, 8.8 Hz, 1H); **^{13}C NMR** (101 MHz, CD_3OD) δ 173.9, 145.7, 131.0, 128.3, 127.8 (d, $^1J_{CF}$ = 282.5 Hz), 126.2, 120.2, 117.6, 58.1 (q, $^2J_{CF}$ = 28.5 Hz), 48.9, 35.1, 33.0; **^{19}F NMR** (377 MHz, CD_3OD) δ -76.40; **IR**

(neat) cm^{-1}: 3403 (br., N–H), 3369 (br., N–H), 1578 (s, C=O), 1458 (m, C=C); **HRMS** (ESI) calcd for $[C_{12}H_{15}F_3N_2O_2]$ $[M+H]^+$ 277.1158, found 277.1158.

2-(Trifluoromethyl)-2,3,4,5-tetrahydro-1*H*-benzo[*b*][1,4]diazepine (2.188)

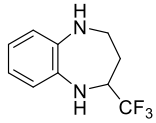

To an ice-cooled solution of **2.178** (288 mg, 1.25 mmol) in anhydrous THF under an atmosphere of N_2 was added $LiAlH_4$ (2 M in THF, 2.0 mL, 3.80 mmol). After 5 min., cooling was removed and the reaction mixture was stirred at reflux for 4 h. The reaction mixture was then cooled to 0 °C and excess reagent was quenched by addition of water (4 mL) and 1 M NaOH (1 mL). Precipitate was removed by filtration and the filtrate was concentrated *in vacuo*. The crude was purified by flash column chromatography (EtOAc:heptane 2:7) to give the title compound as a light brown solid (230 mg, 85%).

***R*f** = 0.21 (EtOAc/heptane 2:7); **m.p.**: 47–48 °C ; **^{1}H NMR** (400 MHz, DMSO-d_6) δ 6.84 (d, *J* = 7.5 Hz, 1H), 6.68 – 6.59 (m, 2H), 6.54 (ddd, *J* = 7.7, 5.2, 3.6 Hz, 1H), 5.28 (t, *J* = 3.7 Hz, 1H), 5.11 (d, *J* = 3.3 Hz, 1H), 3.76 (pdd, *J* = 8.4, 4.6, 3.3 Hz, 1H), 3.18 (ddt, *J* = 12.2, 8.1, 3.1 Hz, 1H), 3.02 (ddt, *J* = 13.4, 7.3, 3.7 Hz, 1H), 2.01 (ddt, *J* = 13.0, 8.4, 4.0 Hz, 1H), 1.82 (dddd, *J* = 13.5, 8.4, 7.2, 3.1 Hz, 1H); **^{13}C NMR** (101 MHz, DMSO-d_6) δ 141.7, 135.7, 126.6 (q, $^1J_{CF}$ = 283.0 Hz) 121.4, 121.4, 118.9, 118.2, 56.2 (q, $^2J_{CF}$ = 26.4 Hz), 42.2, 29.9; **^{19}F NMR** (377 MHz, DMSO-d_6) δ -72.45; **IR** (neat) cm^{-1}: 3330 (s, N–H), 1602 (s, C=O), 1485 (s, C=C); **HRMS** (ESI) calcd for $[C_{10}H_{12}F_3N_2]$ $[M+H]^+$ 217.0954, found 217.0947.

1-(Cyclopropylsulfonyl)-4-(trifluoromethyl)-2,3,4,5-tetrahydro-1*H*-benzo[*b*][1,4] diazepine (2.189)

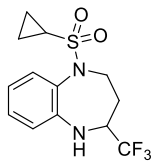

To a solution of **2.188** (70.0 mg, 0.324 mmol) in anhydrous CH_2Cl_2 (6 mL) under an atmosphere of N_2 was added cyclopropane sulfonyl chloride (99.0 µL, 971 µmol) and Et_3N (100 µL, 712 µmol) and the reaction mixture was stirred at reflux for 3 days. The reaction mixture was then concentrated *in vacuo* and purified directly by flash column chromatography (EtOAc/heptane 1:5) to give the title compound as a colorless oil (48.0 mg, 46%).

***R*f** = 0.19 (EtOAc/heptane 1:5); **^{1}H NMR** (800 MHz, DMSO-d_6) δ 7.11 (dd, *J* = 7.8, 1.6 Hz, 1H), 7.07 (td, *J* = 7.8, 1.6 Hz, 1H), 7.03 (dd, *J* = 7.8, 1.6 Hz, 1H), 6.86 (td, *J* = 7.8, 1.6 Hz, 1H), 5.80 (d, *J* = 2.8 Hz, 1H), 4.16 – 4.05 (m, 1H), 3.88 (ddd, *J* = 14.1, 6.6, 4.9 Hz, 1H), 3.55 (ddd, *J* = 13.3, 8.4, 4.4 Hz, 1H), 2.20 (ddt, *J* = 13.3, 8.7, 4.4 Hz, 1H), 1.97 – 1.88 (m, 2H), 1.47 (ddd, *J* = 10.7, 8.1, 6.2 Hz, 1H), 1.35 (ddd, *J* = 10.7, 8.1, 6.2 Hz, 1H), 1.18 (ddd, *J* = 11.4, 8.1, 6.2 Hz, 1H), (CH_2)-C<u>H</u>-S(O)$_2$- was not observed ^{1}H NMR; **^{13}C NMR** (101 MHz, DMSO-d_6) δ 142.7, 133.0, 127.2, 127.0, 126.2 (q, $^1J_{CF}$ = 285.0 Hz), 121.1, 121.0, 55.0 (q, $^2J_{CF}$ = 27.3 Hz), 52.0, 42.4, 27.5, 12.1, 10.2; **^{19}F NMR** (377 MHz, DMSO-d_6) δ -73.22; **IR** (neat) cm^{-1}: 3330

(br., N–H), 1492 (s, C=C), 1252 (s, S=O); **HRMS** (ESI) calcd for $[C_{13}H_{16}F_3N_2O_2S]$ $[M+H]^+$ 221.0879, found 221.0892.

1-(4-(Trifluoromethyl)-2,3,4,5-tetrahydro-1*H*-benzo[*b*][1,4]diazepin-1-yl)butan-1-one (2.190)

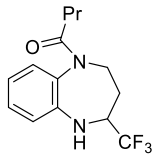

To a solution of **2.188** (72.0 mg, 0.333 mmol) in DMF (10 mL) was added butyric acid (62.0 µL, 67.0 µmol), DIPEA (0.290 mL, 1.67 mmol), and HATU (253 mg, 0.666 mmol) and the solution was stirred at 22 °C for 48 h. The reaction mixture was concentrated *in vacuo*, dissolved in CH_2Cl_2 (10 mL), and washed with brine (3 × 10 mL). The organic layer was dried over Na_2SO_4, filtered, and concentrated *in vacuo*. The crude product was purified by flash column chromatography (EtOAc:heptane 1:3) to give the title compound as an off-white solid (60.0 mg, 63%). R_f = 0.23 (EtOAc/heptane 1:3); **m.p.**: 76–77 °C; **^{1}H NMR** (400 MHz, DMSO-d_6) δ 7.26 – 6.99 (m, 3H), 6.99 – 6.87 (m, 1H), 5.87 (d, *J* = 4.1 Hz, 0.6H, major rotamer), 5.56 (br. s., 0.4H, minor rotamer) 4.52 (dt, *J* = 13.5, 4.9 Hz, 1H), 3.97 (tq, *J* = 9.1, 4.4 Hz, 0.6H, major rotamer), 3.72 (br. s., 0.4H, minor rotamer), 2.99 – 2.70 (m, 1H), 2.16 – 1.63 (m, 4H), 1.41 (ddt, *J* = 14.2, 11.0, 6.9 Hz, 2H), 0.81 – 0.65 (m, 3H); **^{13}C NMR** (101 MHz, DMSO-d_6) δ 171.4 (major rotamer), 171.3 (minor rotamer), 143.7 (minor rotamer), 142.9 (major rotamer), 132.6 (major rotamer), 132.2 (minor rotamer), 128.9 (minor rotamer), 128.5 (major rotamer), 128.3 (minor rotamer), 128.2 (major rotamer), 126.4 (q, $^1J_{CF}$ = 287.4 Hz, major rotamer), 125.7 (d, $^1J_{CF}$ = 281.0 Hz, minor rotamer), 121.7 (major rotamer), 121.6 (minor rotamers, 2C), 121.3 (major rotamer), 55.4 (q, $^2J_{CF}$ = 28.1 Hz, minor rotamer), 53.1 (q, $^2J_{CF}$ = 26.6 Hz, major rotamer), 41.5 (major rotamer), 41.3 (minor rotamer), 35.3 (minor rotamer), 35.1 (major rotamer), 25.8 (minor rotamer), 25.7 (major rotamer), 18.0, 13.6 (major rotamer), 13.5 (minor rotamer); **^{19}F NMR** (377 MHz, DMSO-d_6) δ -71.02 (major rotamer), -73.93 (minor rotamer); **IR** (neat) cm^{-1}: 3311 (s, N–H, 1639 (s, C=O), 1498 (s, C=C); **HRMS** (ESI) calcd for $[C_{14}H_{18}F_3N_2O]$ $[M+H]^+$ 287.1366, found 287.1358.

1-Acetyl-4-(trifluoromethyl)-3,4,5,6-tetrahydrobenzo[*b*][1,5]diazocin-2(1*H*)-one (2.191)

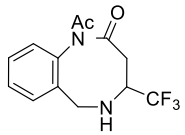

To an ice-cooled solution of **2.180** (150 mg, 0.614 mmol) in CH_2Cl_2 (15 mL) was added Et_3N (100 mL, 0.921 mmol), acetic anhydride (0.100 mL, 1.05 mmol), and DMAP (3.0 mg, 26 µmol) and the reaction mixture was stirred for 6 h at 21 °C. Then, the reaction mixture was washed with a sat. aq. $NaHCO_3$ (2 × 15 mL) and 0.1 M HCl (1 × 15 mL). The organic layer was dried over Na_2SO_4, filtered, and concentrated *in vacuo*. The crude was purified by flash column chromatography (EtOAc/heptane 1:2) to give the title compound as a white solid (71.0 mg, 40%).

***R*f** = 0.31 (EtOAc/heptane 1:2); **m.p.**: 94–95 °C; **^{1}H NMR** (400 MHz, DMSO-d_6) δ 7.47 (dd, *J* = 7.6, 1.8 Hz, 1H), 7.41 (td, *J* = 7.4, 1.5 Hz, 1H), 7.36 (td, *J* = 7.5, 1.9 Hz, 1H), 7.18 (dd, *J* = 7.7, 1.5 Hz, 1H), 3.86 (dd, *J* = 14.2, 4.9 Hz, 1H), 3.77 (q, *J* = 7.4 Hz, 1H), 3.46 (d, *J* = 14.2, 1H), 3.31 (m, 1H), 2.58 (s, 3H), 2.47 (d, *J* = 12.9, 1H), 2.23 (t, *J* = 11.6, 1H); **^{13}C NMR** (101 MHz, DMSO-d_6) δ 173.4, 172.2, 138.9, 137.1, 131.7, 129.1, 128.4, 128.1, 125.5 (q, $^1J_{CF}$ = 281 Hz), 57.6 (q, *J* = 29.0 Hz), 45.6, 36.7, 27.2; **^{19}F NMR** (377 MHz, DMSO-d_6) δ -75.76; **IR** (neat) cm^{-1}: 3298 (s, N–H), 1698 (s, C=O); **HRMS** (ESI) calcd for [$C_{13}H_{14}F_3N_2O_2$] $[M+H]^+$ 287.1015, found 287.1002.

(1-(2-(Dimethylamino)-2-oxoethyl)-4-(trifluoromethyl)-3,4,5,6-tetrahydrobenzo[*b*][1,5] diazocin-2(1*H*)-ylidene)oxonium (2.192)

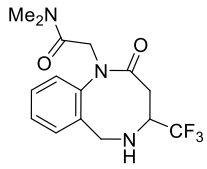

To a solution of **2.180** (101 mg, 0.414 mmol) in MeCN (25 mL) was added K_2CO_3 (174 mg, 1.26 mmol) and 2-bromo-*N*,*N*-dimethylacetamide (89.0 µL, 0.827 mmol) and the suspension was stirred at reflux for 21 h. The reaction mixture was concentrated *in vacuo*, dissolved in CH_2Cl_2 (25 mL), and washed with water (3 × 25 mL). The organic layer was dried over $MgSO_4$, filtered, and concentrated *in vacuo*. The crude product was purified by flash column chromatography (EtOAc/heptane 4:1) to give the title compound as a white amorphous solid (108 mg, 79%).

***R*f** = 0.30 (EtOAc/heptane 4:1); **^{1}H NMR** (400 MHz, DMSO-d_6) δ 7.42 (dd, *J* = 6.7, 2.3 Hz, 1H), 7.40 – 7.26 (m, 4H), 4.76 – 4.46 (m, 2H), 3.95 (dd, *J* = 14.2, 2.3 Hz, 1H), 3.82 (dd, *J* = 14.2, 4.9 Hz, 1H), 3.54 (q, *J* = 7.8 Hz, 1H), 3.20 (br. s, 1H), 2.98 (s, 3H), 2.80 (s, 4H), 2.31 (d, *J* = 12.7 Hz, 1H), 2.12 (dd, *J* = 12.7, 10.2 Hz, 1H); **^{13}C NMR** (101 MHz, DMSO-d_6) δ 169.3, 167.1, 141.2, 137.8, 131.9, 128.4, 127.6, 125.7 (CF_3, observed by HMBC), 124.3, 51.4, 50.5, 46.1, 35.9, 35.1, 34.3; **^{19}F NMR** (377 MHz, DMSO-d_6) δ -75.24; **IR** (neat) cm^{-1}: 3490 (br., N–H), 3308 (br., N–H), 1644 (s, C=O), 1456 (m, C=C); **HRMS** (ESI) calcd for [$C_{15}H_{19}F_3N_3O_2$] $[M+H]^+$ 330.1424, found 330.1440.

1-(2-Methoxyethyl)-4-(trifluoromethyl)-3,4,5,6-tetrahydrobenzo[*b*][1,5]diazocin-2(1*H*)-one (2.193)

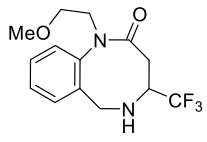

To a solution of **2.180** (0.120 g, 0.491 mmol) in anhydrous MeCN (20 mL) was added KI (100 mg, 0.604 mmol), K_2CO_3 (200 mg, 1.45 mmol), and 2-bromoethyl methyl ether (0.10 mL, 1.07mmol) and the mixture was stirred at reflux for 40 h. The reaction mixture was concentrated *in vacuo*, dissolved in CH_2Cl_2 (20 mL), and washed with water (3 × 20 mL). The organic

layer was dried over $MgSO_4$, filtered, and concentrated *in vacuo*. The crude product was purified by flash column chromatography (EtOAc/heptane 1:1) to give the title compound as a light yellow solid (140 mg, 94%).

R_f = 0.29 (EtOAc/heptane 1:1); **m.p.**: 84–86 °C; **^{1}H NMR** (400 MHz, $CDCl_3$) δ 7.43 (dd, *J* = 6.9, 2.1 Hz, 1H), 7.40-7.30 (m, 3H), 4.42 (ddd, *J* = 14.0, 7.6, 4.4 Hz, 1H), 3.97 (d, *J* = 14.2 Hz, 1H), 3.74-3.60 (m, 3H), 3.58-3.44 (m, 2H), 3.25 (s, 3H), 2.54 (d, 12.6, 1H), 2.24 (dd, *J* = 12.7, 10.3 Hz, 1H), 1.93 (br. s, 1H); **^{13}C NMR** (101 MHz, $CDCl_3$) δ 170.5, 140.8, 138.1, 131.5, 129.3, 128.7, 125.5, 125.4 (q, $^1J_{CF}$ = 278 Hz), 69.6, 58.6, 58.1 (q, $^2J_{CF}$ = 28.5 Hz), 49.1, 46.9, 35.6; **^{19}F NMR** (377 MHz, $CDCl_3$) δ -76.10; **IR** (neat) cm^{-1}: 3323 (s, N–H), 1643 (s, C=O); **HRMS** (ESI) calcd for $[C_{14}H_{18}F_3N_2O_2]$ $[M+H]^+$ 303.1319, found 303.1315.

N-(2-Aminobenzyl)tetrahydro-2*H*-pyran-4-amine (2.194)

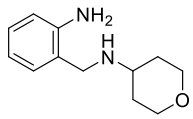

To a solution of tetrahydro-4*H*-pyran-4-one (207 mg, 2.07 mmol) in MeOH (20 mL) was added 2-aminobenzylamine (379 mg, 3.10 mmol) and AcOH (0.177 mL, 3.10 mmol) and the reaction mixture was stirred ta 22 °C for 3 h. The solution was cooled to 0 °C and added $NaBH_3CN$ (390 mg, 6.20 mmol) and the mixture was stirred at 0 °C for 1 h. Then, cooling was removed and the solution was stirred at 22 °C for 16 h. SiO_2 (4.8 g) was added and the suspension was concentrated *in vacuo* and purified directly by flash column chromatography (EtOAc/Et_3N 50:1) to give the title compound as a light yellow solid (421 mg, 99%).

R_f = 0.19 (EtOAc/Et_3N 50:1); **m.p.:** 72–74 °C; **^{1}H NMR** (400 MHz, DMSO-d_6) δ 6.98 (dd, *J* = 7.6, 1.6 Hz, 1H), 6.94 (td, *J* = 7.6, 1.6 Hz, 1H), 6.60 (dd, *J* = 7.6, 1.2 Hz, 1H), 6.48 (td, *J* = 7.6, 1.2 Hz, 1H), 5.22 (s, 2H), 3.81 (dt, *J* = 11.5, 3.8 Hz, 2H), 3.64 (s, 2H), 3.33 (s, 1H), 3.26 (td, *J* = 11.5, 2.3 Hz, 2H), 2.56 (tt, *J* = 10.2, 3.8 Hz, 1H), 1.83 – 1.74 (m, 2H), 1.33 – 1.21 (m, 2H); **^{13}C NMR** (101 MHz, DMSO-d_6) δ 147.5, 127.4, 123.8, 115.8, 114.6, 65.9, 52.7, 48.3, 33.1; **IR** (neat) cm^{-1}: 3384 (s, N–H), 3322 (s, N–H), 3300 (s, N–H), 3034 (m, C=C–H), 1631 (s, C=C); **HRMS** (ESI) calcd. for $[C_{12}H_{19}N_2O]$ [M+H]+ 207.1492, found 207.1492.

4,4,4-Trifluoro-1,3-dimorpholinobutan-1-one (2.256)

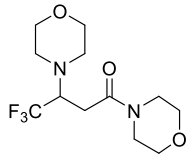

To an ice-cooled solution of (*E*)-4,4,4-trifluorocrotonic acid **2.1** (140 mg, 1.00 mmol) in CH_2Cl_2 (10 mL) was added PyBroP (560 mg, 1.20 mmol), DIPEA (522 µL, 2.99 mmol) and then morpholine (90.1 µL, 1.04 mmol) and the solution was stirred at 22 °C for 72 h. Saturated aqueous $NaHCO_3$ (10 mL) was added and the phases were separated. The aqueous phase was extracted with CH_2Cl_2 (1 × 15 mL) and the combined organic layers were dried over $MgSO_4$, filtered, and concentrated *in vacuo*. The crude product was purified by flash column chromatography (EtOAc/heptane 1:1) to give the title compound as colorless oil (80.0 mg, 52%).

***R*$_f$** = 0.33 (EtOAc/heptane 1:1); **^{1}H NMR** (400 MHz, CD_3OD) δ 3.84 (pd, *J* = 8.8, 4.3 Hz, 1H), 3.73 – 3.65 (m, 4H), 3.65 – 3.57 (m, 8H), 2.93 (dd, *J* = 16.0, 8.8 Hz, 1H), 2.89 – 2.82 (m, 2H), 2.78 – 2.65 (m, 2H), 2.58 (dd, *J* = 16.0, 4.3 Hz, 1H); **^{13}C NMR** (101 MHz, CD_3OD) δ 168.9, 126.94 (q, $^1J_{CF}$ = 287.9 Hz), 67.3 (2C), 66.4, 66.3, 62.2 (q, $^2J_{CF}$ = 26.2 Hz), 49.8 (2C), 46.0, 42.3, 28.7 (d, $^3J_{CF}$ = 1.6 Hz); **^{19}F NMR** (377 MHz, CD_3OD) δ -71.01; **IR** (neat) cm^{-1}: 1634 (s, C=O); **HRMS** (ESI) calcd. for $[C_{12}H_{20}F_3N_2O_3]$ $[M+H]^+$ 297.1421, found 297.1434.

Hydrazine Cyclization – Pyrazolidinone

Compound was **2.207** synthesized by MSc student Ana Laura da Silva.

5-(Trifluoromethyl)pyrazolidin-3-one (**2.196**)

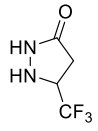

To a solution of ethyl (*E*)-4,4,4-trifluorobut-2-enoate **2.2** (8.87 g, 52.8 mmol) in EtOH (525 mL) was added hydrazine hydrate (50-60% in water, 3.28 mL, 52.8 mmol) and the solution was stirred at reflux for 18 h. The solution was concentrated in vacuo to give the title compound as a light pink solid (7.97 g, 98%).

m.p.: 116–118 °C; **^{1}H NMR** (400 MHz, CD_3OD) δ 5.83 – 5.64 (m, 1H), 4.58 (dd, *J* = 17.4, 10.0 Hz, 1H), 3.98 (dd, *J* = 17.5, 2.6 Hz, 1H); **^{13}C NMR** (101 MHz, CD_3OD) δ 175.6, 124.0 (d, *J* = 288.5 Hz), 57.6 (q, *J* = 31.5 Hz), 32.3 (d, *J* = 1.6 Hz); **^{19}F NMR** (377 MHz, CD_3OD) δ -80.46; **IR** (neat) cm^{-1}: 3246 (s, N–H), 1643 (s, C=O); **HRMS** (ESI) calcd for $[C_4H_6F_3N_2O]$ $[M+H]^+$ 155.0427, found 155.0434.

1,2-Diallyl-5-(trifluoromethyl)pyrazolidin-3-one (2.197)

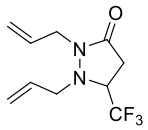

To a solution of **2.196** (1.14 g, 7.40 mmol) in anhydrous THF (50 mL) was added allyl bromide (1.76 mL, 20.3 mmol) and a solution of ^{t}BuOK (2.28 g, 20.3 mmol) in THF (25 mL) and the reaction mixture was stirred under an atmosphere of N_2 at 22 °C for 16 h. Precipitate was removed by filtration and the filtrate was concentrated *in vacuo*. CH_2Cl_2 (50 mL) and sat. aq. $NaHCO_3$ (50 mL) were added and the layers were separated. The organic layer was dried over $MgSO_4$, filtered, and concentrated *in vacuo* to give the title compound as a brown oil.

^{1}H NMR (400 MHz, $CDCl_3$) δ 5.95 – 5.71 (m, 2H), 5.41 – 5.16 (m, 4H), 4.31 – 4.16 (m, 1H), 3.92 – 3.78 (m, 1H), 3.67 (dqd, *J* = 9.8, 7.5, 2.0 Hz, 1H), 3.54 (ddt, *J* = 13.9, 6.1, 1.4 Hz, 1H), 3.42 (dd, *J* = 13.9, 7.5 Hz, 1H), 3.08 – 2.91 (m, 1H), 2.49 (dd, *J* = 17.6, 2.0 Hz, 1H); **^{13}C NMR** (101 MHz, $CDCl_3$) δ 168.7, 132.1, 131.3, 124.7 (q, *J* = 279.5 Hz), 121.8, 118.8, 59.2, 58.5 (q, *J* = 31.5 Hz), 46.4, 29.8 (d, *J* = 1.3 Hz); **^{19}F NMR** (377 MHz, $CDCl_3$) δ -78.41; **IR** (neat) cm^{-1}: 1690 (s, C=O); **HRMS** (ESI) calcd for $[C_{10}H_{14}F_3N_2O]$ $[M+H]^+$ 235.1053, found 235.1013.

3-(Trifluoromethyl)tetrahydro-1*H*,7*H*-pyrazolo[1,2-*a*]pyrazole-1,7-dione (2.198)

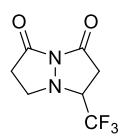

To an ice-cooled solution of **2.196** (487 mg, 3.16 mmol) in MeCN (30 mL) was added acryloyl chloride (300 mg, 3.32 mmol) and Et_3N (881 µL, 6.32 mmol) and the reaction mixture was stirred at 22 °C for 16 h. The mixture was concentrated *in vacuo* and purified directly by flash column chromatography (EtOAc/heptane 1:1) to give the title compound as a white amorphous solid (37.0 mg, 6%).

***R*f** = 0.24 (EtOAc/heptane 1:1); **^{1}H NMR** (400 MHz, CD_3OD) δ 4.05 (tq, *J* = 9.8, 6.1 Hz, 1H), 3.77 (tt, *J* = 8.5, 0.9 Hz, 1H), 3.27 (ddd, *J* = 13.4, 8.7, 7.3 Hz, 1H), 3.16 (d, *J* = 9.7 Hz, 2H), 3.14 – 3.05 (m, 1H), 2.82 (ddd, *J* = 17.1, 7.3, 0.9 Hz, 1H); **^{13}C NMR** (101 MHz, CD_3OD) δ 167.28, 164.41, 125.61 (q, *J* = 276.3 Hz), 65.22 (q, *J* = 31.9 Hz), 55.27, 36.81, 36.27 (q, *J* = 2.2 Hz); **^{19}F NMR** (377 MHz, CD_3OD) δ -76.75; **IR** (neat) cm^{-1}: 1774 (s, C=O), 1714 (s, C=O); **HRMS** (ESI) calcd for $[C_{17}H_8F_3N_2O_2]$ $[M+H]^+$ 209.0532, found 209.0532.

2-Phenyl-4-(trifluoromethyl)pyrazolidin-3-one (2.202)

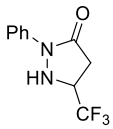

To a solution of 2-(trifluoromethyl)acrylic acid **2.6** (25.0 mg, 0.178 mmol) in MeCN (5 mL) was added phenylhydrazine (20.0 mg, 0.192 mmol) and Et_3N (22.5 µL 0.179 mmol) and the solution was subjected to microwave heating at 140 °C for 2 h. The solution was concentrated *in vacuo* and purified directly by flash column chromatography (EtOAc/heptane 1:4) to give the title compound as a dark red solid (30.0 mg, 75%).

***R*f** = 0.45 (EtOAc/heptane 2:1); **^{1}H NMR** (400 MHz, $CDCl_3$) δ 7.89 – 7.80 (m, 2H), 7.43 – 7.33 (m, 2H), 7.23 – 7.13 (m, 1H), 3.81 (dd, *J* = 12.7, 8.4 Hz, 1H), 3.70 (dd, *J* = 12.7, 6.3 Hz, 1H), 3.62 – 3.40 (m, 1H); **^{13}C NMR** (101 MHz, $CDCl_3$) δ 163.6, 137.9, 128.9 (2C), 125.3, 121.6 (d, *J* = 288.5 Hz), 118.7 (2C), 49.3 (d, *J* = 28.5 Hz), 43.8 (d, *J* = 2.7 Hz); **^{19}F NMR** (377 MHz, $CDCl_3$) δ -68.31; **IR** (near) cm^{-1}: 3244 (s, N–H), 1685 (s, C=O), 1595 (m, C=C); **HRMS** (ESI) calcd. for $[C_{10}H_{10}F_3N_2O]$ $[M+H]^+$ 231.0740, found 231.0745.

2-(Tetrahydro-2*H*-pyran-4-yl)-4-(trifluoromethyl)pyrazolidin-3-one (2.203)

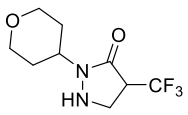

To a solution of 2-(trifluoromethyl)acrylic acid **2.6** (146 mg, 1.04 mmol) in MeCN (10 mL) was added (tetrahydro-2*H*-pyran-4-yl)hydrazine dihydrochloride (201 mg, 1.06 mmol) and Et_3N (580 µL 4.17 mmol) and the solution was subjected to microwave heating at 140 °C for 30 min. The solution was concentrated *in vacuo* and purified directly by flash column chromatography (CH_2Cl_2/MeOH/NH_3 380:20:1) to give the title compound as an off-white amorphous solid (41.0 mg, 17%).

***R*f** = 0.27 (CH_2Cl_2/MeOH/NH_3 380:20:1); **^{1}H NMR** (400 MHz, CD_3OD) δ 4.21 (tt, *J* = 11.8, 4.3 Hz, 1H), 4.04 (ddq, *J* = 11.7, 4.6, 1.6 Hz, 2H), 3.77 – 3.60 (m, 2H), 3.53 (tdd, *J* = 12.0, 4.8, 2.2 Hz, 2H), 3.47 – 3.37 (m, 1H), 1.99 (dqd, *J* = 33.7, 12.4, 4.7 Hz, 2H), 1.65 (tdq, *J* = 12.8, 4.3, 2.2 Hz, 2H); **^{13}C NMR** (101 MHz, CD_3OD) δ 166.7 (q, *J* = 2.4 Hz), 126.2 (q, *J* = 277.2 Hz), 67.9, 67.9, 51.7, 49.1 (q, *J* = 28.5), 45.3 (q, *J* = 2.8 Hz), 30.7, 30.6; **^{19}F NMR** (377 MHz, CD_3OD) δ -70.13; **IR** (neat) cm^{-1}: 3235 (s, N–H), 1678 (s, C=O); **HRMS** (ESI) calcd for $[C_9H_{14}F_3N_2O_2]$ $[M+H]^+$ 239.1002, found 239.1004.

4-(Trifluoromethyl)pyrazolidin-3-one (2.205)

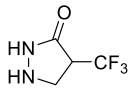

To a solution of methyl 2-(trifluoromethyl)acrylate **2.5** (2.40 g, 15.6 mmol) in EtOH (310 mL) was added hydrazine hydrate (50–60% in water, 881 mL, 15.6 mmol) and the solution was stirred at reflux for 2 h. The solution was concentrated *in vacuo* to give the title compound as a yellow oil (2.16 g, 90%).

^{1}H NMR (400 MHz, CD_3OD) δ 3.69 (dd, *J* = 11.3, 8.3 Hz, 1H), 3.59 (tt, *J* = 17.2, 8.3 Hz, 1H), 3.49 (dd, *J* = 11.3, 8.3 Hz, 1H); **^{13}C NMR** (101 MHz, CD_3OD) δ 170.8, 126.2 (q, *J* = 277.0 Hz), 47.7 (q, *J* = 28.4 Hz), 47.2 (q, *J* = 2.6 Hz); **^{19}F NMR** (377 MHz, CD_3OD) δ -69.88; **HRMS** (ESI) calcd for $[C_4H_6F_3N_2O]$ $[M+H]^+$ 155.0427, found 155.0433.

1-Benzyl-4-(trifluoromethyl)pyrazolidin-3-one (2.207)

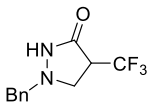

To a solution of **2.205** (99.0 mg, 0.642 mmol) in MeOH (7 mL) was added benzaldehyde (80.0 µL, 0.779 mmol) and the reaction mixture was stirred at 22 °C for 4 h. Then, $NaBH_4$ (48.6 mg, 1.28 mmol) was added and the mixture was stirred for another 2 h. SiO_2 (750 mg) was added and the suspension was concentrated *in vacuo* and purified directly by flash column chromatography (EtOAc/heptane 2:5) to give the title compound as a yellow oil (20.0 mg, 13%).

R_f = 0.28 (EtOAc/heptane 2:5); **^{1}H NMR** (400 MHz, CD_3OD) δ 7.45 – 7.34 (m, 5H), 4.02 – 3.91 (m, 2H), 3.77 (dq, *J* = 10.6, 9.1 Hz, 1H), 3.61 (dd, *J* = 11.9, 8.9 Hz, 1H), 3.49 – 3.41 (m, 1H); **^{13}C NMR** (101 MHz, CD_3OD) δ 183.8, 136.9, 130.6, 129.7, 129.1, 125.0 (d, *J* = 281.4 Hz), 64.5, 52.0 (d, *J* = 2.4 Hz), 45.9; **^{19}F NMR** (377 MHz, CD_3OD) δ 69.53; **IR** (neat) cm^{-1}: 3220 (br., N–H), 1684 (s, C=O); **HRMS** (ESI) calcd for $[C_{11}H_{12}F_3N_2O]$ $[M+H]^+$ 245.0896, found 245.0885.

(4*R,7*S**)-4-Phenyl-7-(trifluoromethyl)hexahydro-8*H*-pyrazolo[1,2-*a*][1,2,4]triazin-8-one (2.209) and (4*S**,7*S**)-4-Phenyl-7-(trifluoromethyl)hexahydro-8*H*-pyrazolo[1,2-*a*][1,2,4] triazin-8-one (2.210)**

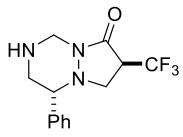

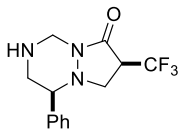

To a solution of **2.205** (100 mg, 0.649 mmol) in MeOH (2 mL) was added benzaldehyde (80.0 µL, 0.779 mmol) and the reaction mixture was stirred at 22 °C for 4 h. The mixture was concentrated *in vacuo* and the crude azomethine imine was dissolved in CH_2Cl_2 (5 mL). *N*-(methoxymethyl)-*N*-(trimethylsilylmethyl)benzylamine (90% purity, 249 µL, 0.876 mmol) was added and then TFA (0.5 M in CH_2Cl_2, 130 µL) and the reaction mixture was stirred at 22 °C for 2 h. The mixture was diluted with EtOH (10 mL) and added 10% Pd/C (265 mg, 0.249 mmol). The reaction mixture was stirred under a H_2-atosphere for another 16 h. The suspension was filtered through a celite plug and concentrated *in vacuo*. The crude product was purified by flash column chromatography (EtOAc/heptane/Et_3N

60:20:1) to give the title compounds **2.209** (26.0 mg, 11%) and **2.210** (11.0 mg, 5%) both as brown oils.

Data for 2.209: $\boldsymbol{R_f}$ = 0.27 (EtOAc/heptane 60:20:1); **^{1}H NMR** (400 MHz, CD_3OD) δ 7.51 – 7.35 (m, 5H), 5.02 (dd, *J* = 12.6, 1.3 Hz, 1H), 4.09 (dd, *J* = 12.7, 1.2 Hz, 1H), 3.79 – 3.65 (m, 1H), 3.61 (t, *J* = 10.3 Hz, 1H), 3.51 (dd, *J* = 10.4, 3.1 Hz, 1H), 3.09 (ddd, *J* = 13.9, 3.1, 1.3 Hz, 1H), 2.97 – 2.78 (m, 2H); **^{13}C NMR** (101 MHz, CD_3OD) δ 162.7, 138.5, 130.0 (2C), 129.7, 128.8 (2C), 125.7 (d, *J* = 276.4 Hz), 74.0, 57.8, 52.8, 50.4 (q, *J* = 2.3 Hz), 46.4 (q, *J* = 29.5 Hz); **^{19}F NMR** (377 MHz, CD_3OD) δ -69.09; **IR** (neat) cm^{-1}: 3302 (br., N–H), 1704 (s, C=O); **HRMS** (ESI) calcd for $[C_{13}H_{15}F_3N_3O]$ $[M+H]^+$ 286.1162, found 286.1162.

Data for **2.210**: $\boldsymbol{R_f}$ = 0.17 (EtOAc/heptane/Et_3N 60:20:1); **^{1}H NMR** (400 MHz, CD_3OD) δ 7.53 – 7.33 (m, 5H), 5.03 (dd, *J* = 12.8, 1.3 Hz, 1H), 4.10 (d, *J* = 12.8 Hz, 1H), 3.93 (qd, *J* = 9.4, 8.4 Hz, 1H), 3.66 (dd, *J* = 10.3, 3.1 Hz, 1H), 3.42 (dd, *J* = 12.3, 8.4 Hz, 1H), 3.23 (dd, *J* = 12.3, 9.6 Hz, 1H), 3.08 (ddd, *J* = 13.9, 3.1, 1.4 Hz, 1H), 2.96 (dd, *J* = 13.9, 10.3 Hz, 1H); **^{13}C NMR** (101 MHz, CD_3OD) δ 164.6 (d, *J* = 2.8 Hz), 139.2, 130.0 (2C), 129.6, 128.8 (2C), 126.2 (q, *J* = 277.4 Hz), 71.8, 56.8, 52.9, 49.6, 45.6 (q, *J* = 28.9 Hz); **^{19}F NMR** (377 MHz, CD_3OD) δ -69.94; **IR** (neat) cm^{-1}: 3307 (br., N–H), 1703 (s, C=O); **HRMS** (ESI) calcd for $[C_{13}H_{15}F_3N_3O]$ $[M+H]^+$ 286.1162, found 286.1172.

Other Scaffolds

tert-Butyl *(E)*-(2-(4,4,4-trifluoro-*N*-methylbut-2-enamido)ethyl)carbamate (2.220)

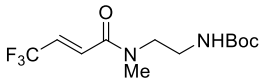

To an ice-cooled solution of (*E*)-4,4,4-trifluorocrotonic acid **2.1** (2.01 g, 14.4 mmol) in CH_2Cl_2 (30 mL) was added DIPEA (7.50 mL, 43.0 mmol), PyBroP (7.36 g, 15.8 mmol), and *tert*-butyl (2-(methylamino)ethyl)carbamate (2.63 g, 15.1 mmol) and the solution was stirred at 22 °C for 2 h. Saturated aqueous $NaHCO_3$ (30 mL) was added and the layers were separated. The aqueous phase was extracted with CH_2Cl_2 (3 × 30 mL) and the combined organic layers were dried over $MgSO_4$, filtered, and concentrated *in vacuo*. The crude product was purified by flash column chromatography (EtOAc/heptane 1:1) to give the title compound as a white solid (2.81 g, 66%). R_f = (EtOAc/heptane 1:1); **m.p.**: 104–106 °C; **^{1}H NMR** (400 MHz, DMSO-d_6) δ 7.29 – 7.11 (m, 1H), 6.94 (t, *J* = 6.0 Hz, 0.6H, major rotamer), 6.83 (t, *J* = 6.0 Hz, 0.4H, minor rotamer), 6.72 (dq, *J* = 14.5, 7.2 Hz, 1H), 3.44 (t, *J* = 5.8 Hz, 1.3H, major rotamer), 3.39 (t, *J* = 6.2 Hz, 0.7H, minor rotamer), 3.14 – 3.01 (m, 3H), 2.89 (s, 2H, major rotamer), 1.36 (s, 3H, minor rotamer), 1.33 (s, 6H, major rotamer); **^{13}C NMR** (101 MHz, DMSO-d_6) δ 163.2 (minor rotamer), 162.9 (major rotamer), 155.90 (major rotamer), 155.87 (minor rotamer), 131.1 (d, *J* = 5.8 Hz, minor rotamer), 130.1 (q, *J* = 6.1 Hz, major rotamer), 126.9 (d, *J* = 33.5 Hz, major rotamer), 126.6 (d, *J* = 38.8 Hz, minor rotamer), 123.32 (d, *J* = 269.6 Hz, major rotamer), 123.28 (d, *J* = 269.8 Hz, minor rotamer) 78.1 (major rotamer), 77.9 (minor rotamer), 49.0 (major rotamer), 47.8 (minor rotamer), 38.1 (major rotamer), 37.5 (minor rotamer), 36.2 (minor rotamer), 33.5 (major rotamer), 28.4 (minor rotamer), 28.3 (major rotamer); **^{19}F NMR** (377 MHz, DMSO-d_6) δ -63.09 (major rotamer), -63.18 (minor rotamer); **IR** (neat) cm^{-1}: 3317 (s, N–H), 1703 (s, C=O), 1622 (s, C=O), 1523 (s, C=C); **HRMS** (ESI) calcd. for $C_{12}H_{20}F_3N_2O_3$ $[M+H]^+$ 297.1421, found 297.1425.

tert-Butyl 4-methyl-2-oxo-1,3,4,6-tetrahydrobenzo[_b_][1,5]diazocine-5(2_H_)-carboxylate (2.234)

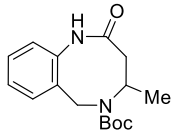

To a suspension of (*E*)-crotonic acid **2.233** (126 mg, 1.46 mmol) in PhMe (10 mL) was added 2-aminobenylamine (393 mg, 3.22 mmol) and the suspension was stirred at reflux for 3 h. Precipitate was collected by filtration was washed with PhMe (3 × 5 mL) to afford the crude Michael addition product.

To a suspension of crude Michael addition product in MeCN (150 mL) was added HATU (655 mg, 1.72 mmol) and Et_3N (0.800 mL, 5.74 mmol) and the reaction mixture was stirred at 22 °C for 18 h. Then, Boc_2O (313 mg, 1.44 mmol) was added and the mixture was stirred for another 8 h. The solution was concentrated *in vacuo* and purified directly by flash column chromatography (EtOAc/heptane 1:1) to give the title compound as a white amorphous solid (320 mg, %).

***R*f** = 0.25 (EtOAc/heptane 1:1); **^{1}H NMR** (400 MHz, $CDCl_3$) δ 8.18 – 7.98 (m, 1H), 7.94 – 7.62 (m, 1H), 7.33 – 6.93 (m, 3H), 5.07 – 4.37 (m, 2H), 3.71 (dd, *J* = 55.4, 14.9 Hz, 1H), 2.60 – 2.27 (m, 3H), 1.57 (s, 5H), 1.46 (s, 5H), 1.33 (s, 2H), 1.32 (s, 2H); **^{13}C NMR** (101 MHz, $CDCl_3$) δ 172.9, 172.7, 154.9, 154.6, 136.1, 135.9, 134.7, 134.4, 132.8, 132.0, 129.1, 128.8, 127.7, 127.4, 124.6, 124.0, 80.7, 80.3, 46.1, 44.7, 41.1, 40.5, 39.60, 39.57, 28.8, 28.6, 16.6, 16.3.

Ethyl (1_S_*,5_S_*)-3-methoxy-5,7-dimethyl-4-oxo-8-oxabicyclo[3.2.1]octa-2,6-diene-6-carboxylate (2.237)

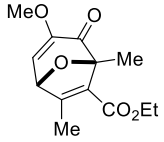

To a suspension of **2.102** (1.52 g, 5.24 mmol) in $CHCl_3$ (6 mL) was added ethyl but-2-ynoate **2.236** (11.8 g, 105 mmol) and *N*,*N*-diisopropylaniline (1.22 mL, 6.29 mmol) and the solution was subjected to microwave heating at 120 °C for 15 min. The reaction mixture was concentrated *in vacuo* and purified directly by flash column chromatography (EtOAc/heptane 1:3) to give the title compound as a yellow oil (379 mg, 29%).

***R*f** = 0.24 (EtOAc/heptane 1:3); **^{1}H NMR** (400 MHz, $CDCl_3$) δ 6.27 (d, *J* = 4.9 Hz, 1H), 5.33 (dt, *J* = 4.9, 0.8 Hz, 1H), 4.25 (qd, *J* = 7.1, 2.5 Hz, 2H), 3.56 (s, 3H), 2.06 (s, 3H), 1.54 (s, 3H), 1.32 (t, *J* = 7.1 Hz, 3H); **^{13}C NMR** (101 MHz, $CDCl_3$) δ 191.3, 163.6, 153.8, 146.2, 139.1, 117.1, 95.7, 77.5, 60.8, 54.8, 16.0, 14.3, 11.1.

Cheminformatics Library Analysis

Cheminformatics library analysis was performed for the 102 (out of 115) fragments that passed quality control and were selected for screening. Principal moment of inertia (PMI) analysis was performed computationally using an algorithm developed by Colomer *et al*.[136] relying on Indigo[352] to convert structures to canonical SMILES format and RDKit[353] to compute the lowest energy conformer of each compound. Normalized PMI ratios (NPRs) were plotted in a triangular graph with coordinates (0;1), (½;½), and (1;1) representing a perfect rod, disc, and sphere, respectively. The NuBBE database of 2712 natural products was the source for natural product data.[135] For an easier visual comparison of libraries, only half of the NuBBE database was plotted in the PMI plot (randomly selected).

The natural product-likeness of molecules was calculated using the open-source and open-data "Natural-Product-Likeness Scorer"[265] based on a previously developed algorithm.[264] This Bayesian measure evaluates how similar a molecule is to the structural space covered by natural products. The algorithm removes small disconnected fragments (*e.g.* counter ions and metals) and divides each compound into smaller substructures, which are compared to two training sets consisting of: 1) 113,425 synthetic lead-like compounds selected from the ZINC database[266] and 2) 58,018 natural products derived from the Traditional Chinese Medicinal Database @ Taiwan[354] and the ChEMBL database (only *Journal of Natural Products* structures selected).[355] On a logarithmic scale, each molecule is assigned a score (typically in the range of -3 to 3) based on the resemblance of its substructures to the two training sets. Positive values indicate higher resemblance to natural products and negative values indicate a more synthetic character. For full experimental details see references.[264,265] The NuBBE database of 2712 natural products was used as the source for natural products.[135]

Other physicochemical properties including AlogP, molecular weight, hydrogen bond acceptors, hydrogen bond donors, chiral centers, polar surface area, and Fsp^3 were calculated using Canvas (v. 3.6.013) by Schrodinger Software Modules. The NPRs and natural product-likeness score of the 3F library along with canonical SMILES can be found in the Supporting Information (Table S1).

General (NMR Screening)

UltraPure™ Tris-HCl buffer (1 M at pH 7.5) was purchased from Invitrogen™. Phosphate-buffered saline (PBS, 137 mM NaCl, 2.7 mM KCl, 8 mM Na_2HPO_4, and 2 mM KH_2PO_4 at pH 7.4) purchased from Sigma-Aldrich. Recombinant full-length human p70S6K1 (9.1 µM) was purchased from SignalChem and supplied in a stock solution of 50 mM sodium phosphate, 300 mM NaCl, 150 mM imidazole, 0.1 mM phenylmethylsulfonyl fluoride (PMSF), 0.25 mM DL-dithiothreitol (DTT), and 25% glycerol. Recombinant full-length human BACE1 (7.8 µM) was purchased from Sino Biological and supplied in neat phosphate buffered saline. p70S6K1 inhibitor PF-4708671 was purchased from Sigma-Aldrich. Proteins were stored at -80 °C and thawed on ice before use.

NMR screening was conducted using either a 600 MHz Bruker AVANCE III spectrometer equipped with a Bruker BBFO SmartProbe, a 700 MHz Bruker AVANCE III HD spectrometer equipped with a 5mm TCI CryoProbe, or an 800 MHz Bruker AVANCE IIIHD spectrometer equipped with a TCI CryoProbe. All experiments were performed in 3 mm NMR tubes at 298 K. ^{1}H chemical shifts are reported relative to the signal for HDO (δ 4.79 ppm for ^{1}H NMR) and ^{19}F chemical shifts are referenced using the deuterium lock-signal with $\delta(CFCl_3) = 0$ ppm. NMR screening data was analyzed using TopSpin 3.5 pl 7 (of April 3 2017) by Bruker BioSpin.

All screening data can be found in the Supporting Information (Figures S10–S50).

Screening Cocktails

Each fragment was stored in DMSO-d_6 at 50 mM and used to prepare premixed cocktails in DMSO-d_6 with each fragment at 1.25 mM. Cocktails were designed to avoid overlap of ^{19}F-NMR signals. All δ ^{19}F are reported in PBS buffer/D_2O 9:1 + 4% DMSO-d_6 (pH = 7.4). Recorded δ^{19}F may differ slightly depending on buffer, pH, and salt concentration. Cocktails 1–5 were screened against HSA, p70S6K1, p38γ, p38α, and BACE1. Cocktails A–D were used against DC-SIGN (for cocktail compositions, see the Supporting Information, Tables S2–S10).

Protein Expression and Purification

Expression and purification of p38α, p38γ, and p38δ

Expression and purification of p38 kinases was performed by collaborators at the CNB/CSIC. Human recombinant p38α, p38γ, and p38δ were expressed as a glutathione-S-transferase (GST) fusion proteins from *E. coli* following a previously reported procedure.[356] GST-p38α/γ/δ were purified by affinity chromatography (glutathione sepharose) in buffer A: 50 mM Tris·HCl (pH 8.0), 0.2 mM EGTA, 0.2 mM EDTA, 0.1% Triton X100, 0.25 M NaCl, 0.1% β-mercaptoethanol, 1.0 mM benzamidine, 0.2 mM PMSF, and 20.0 mM glutathione. The GST

part was removed by incubation with thrombin using 60 µl (60 Units) of thrombin and 1.5 ml GST-p38γ solution (buffer A). Following proteolysis, the protein solution was dialyzed against buffer B: 50 mM Tris·HCl (pH 7.5), 1.0 mM EGTA, 1.0 mM EDTA, 0.1 M NaCl, 0.01% β-mercaptoethanol, 0.01 mM benzamidine, and 0.02 mM PMSF. The GST part was removed by affinity chromatography (glutathione sepharose) to provide solutions of p38α (19.8), p38γ (22.8 µM), and p38δ (26.4 µM) in buffer B.

Expression and purification of DC-SIGN

Expression and purification of DC-SIGN was performed by collaborators at the Max-Planck Institute of Colloids and Interfaces. DC-SIGN was expressed and purified according to a previously reported procedure.[293]

Screening

Protein and ligand concentrations were based on reported recommendations for each experiment type.[194] Generally, as protein size increases, ligands experience a larger effect when bound, which in turn decreases the protein concentration needed. All screening was performed at 298K and screening cocktails were allowed to equilibrate for 20 min. prior to start of each experiment (including 10 min. inside the NMR spectrometer to adjust the temperature).

^{19}F NMR screening

A T_2 CPMG pulse sequence with adiabatic decoupling scheme[47,48] was used for primary ^{19}F NMR screen. Each cocktail was acquired in the absence of protein as a negative control. The longest T_2-relaxation delay used was 200 ms. As most of the fragments only contained CF_3 the sweep width was limited to 50 ppm following the acquisition of a 1D ^{19}F spectrum to verify that these were the only resonances present. The spectra were processed using a 1 Hz exponential line broadening. The apparent binding of fragment **2.115** in all assays was attributed chemical instability and the fragment was treated as a false positive in all cases.

STD NMR

Standard STD pulse sequences were used.[43,357] Several protein irradiation frequencies outside the region of ligand resonances were acquired based on the presence of protein resonances. Included was always a reference spectrum with irradiation at -40 ppm. The spectra were processed using a 1 Hz exponential line broadening.

WaterLOGSY NMR

WaterLOGSY was performed a standard sequence.[358,359] WaterLOGSY was performed by irradiation of bulk water at 4.701 ppm. The spectra were processed using a 1 Hz exponential line broadening and phased with the binders being positive and non-binders being negatives.

p70S6K1

^{19}F NMR screening:

Screening was performed with p70S6K1 at 2.25 µM and fragments at 25 µM using cocktails 1–5. In an Eppendorf tube, p70S6K1 (9.1 µM, 45 µL), PBS (50 mM with 0.2 mM dithiothreitol, 113 µL), D_2O (18 µL), and premixed cocktail (1.25 mM in DMSO-d_6, 3.6 µL) were gently and thoroughly mixed and then transferred to a 3 mm NMR tube for screening in a 600 MHz spectrometer. Then, the competitor inhibitor PF-4708671[272] (K_i = 20 nM, 5.0 mM in DMSO-d_6, 1.8 µL) was added and the experiment was repeated.

^{1}H NMR validation:

Validation was performed with p70S6K1 at 4.5 µM and fragments at 200 µM. ^{19}F NMR fragment hits were pooled in smaller cocktails with each fragment at 10 mM: 1) **2.114** and **2.120**; 2) **2.191**. In an Eppendorf tube, p70S6K1 (9.1 µM, 90.0 µL), PBS (50 mM with 0.2 mM dithiothreitol, 68 µL), D_2O (18 µL), and ^{1}H NMR fragment cocktail (10 mM in DMSO-d_6, 3.6 µL) were gently and thoroughly mixed and then transferred to a 3 mm NMR tube for screening. STD NMR was perform by irradiation of resonance frequencies of p70S6K1 at 1.49 ppm, 0.85 ppm, 0.77 ppm, -0.2 ppm, and -1.3 ppm, respectively.

p38 kinases

^{19}F NMR screening:

Screening was performed with p38α/γ/δ at 5.7 µM and fragments at 25 µM using cocktails 1–5. In an Eppendorf tube, p38α (19.8 µM, 51.8 µL) or p38γ (22.8 µM, 45 µL) or p38δ (26.4 µM, 39.0 µM), D_2O (18 µL), premixed cocktail (1.25 mM, 3.6 µL), and Tris-HCl (50 mM, fill up to 180 µL), were gently and thoroughly mixed and then transferred to a 3 mm NMR tube for screening in a 600 MHz spectrometer.

^{1}H NMR validation:

Validation was performed with p38γ at 11.4 µM and fragments at 200 µM. ^{19}F NMR fragment hits were pooled in smaller cocktails with each fragment at 10 mM: 1) **2.43**, **2.49**, **2.114**, and **2.191**; 2) **2.32**, **2.120**, and **2.190**; 3) **2.42**, **2.170**, **2.198**, , and **2.209**. In an Eppendorf tube, p38γ (22.8 µM, 90 µL), Tris-HCl (50 mM, 68 µL), D_2O (18 µL), and ^{1}H NMR fragment cocktail (10 mM, 3.6 µL) were gently and thoroughly mixed and then transferred to a 3 mm NMR tube for screening.

STD NMR was perform by irradiation of resonance frequencies of p38γ at 8.156 ppm, 0.339 ppm, and -0.577 ppm, respectively.

Enzymatic assays

Enzymatic assays were performed by collaborators at CNB/CSIC. Following a previously reported radioactive kinase assay,[360] p38γ kinase activity of hits was evaluated with either activating transcription factor 2 (ATF2) or Myelin Basic Protein (MBP, Ala-Pro-Arg-Thr-Pro-Gly-Gly-Arg-Arg) as substrate. The pan-p38 kinase inhibitor BIRB-796 was used as a positive control.

Differential chemical shift perturbation

For the four fragments exhibiting *in vitro* inhibition of p38γ (**2.42**, **2.43**, **2.114**, and **2.191**), binding affinities were estimated using a differential chemical shift perturbation (dCSP) experiment. The ligand-observed ^{19}F NMR experiment gives a fair estimation of K_d (<1 mM) by comparing $\Delta\delta^{19}F$ or $\Delta\nu_{1/2}$ (full width at half maximum) at two different ligand concentrations ($[L]_1$ and $[L]_2$) assuming $[L]_0 >> [P]_0$:[286]

$$K_d = \frac{\gamma[L]_1 - [L]_2}{1-\gamma}$$

where

$$\gamma = \frac{v_1 - v_{ref}}{v_2 - v_{ref}} \; or \; \gamma = \frac{\Delta v_{\frac{1}{2},1} - \Delta v_{\frac{1}{2},ref}}{\Delta v_{\frac{1}{2},2} - \Delta v_{\frac{1}{2},ref}}$$

The experiment was performed in the same buffer as described for the primary ^{19}F NMR screening assay.

Table 4.1. Determination of K_d using differential chemical shift perturbation. Measurements were performed at 600 MHz with p38γ at 5.7 µM. No line broadening was used.

Hit	Concentrations (µM)	$\Delta\delta^{19}F_1$ or $\Delta_{w1/2}$ (Hz)	$\Delta\delta^{19}F_2$ or $\Delta_{w1/2}$ (Hz)	K_d (µM)[a]	LE[b]
2.42	-	-	-	ND[e]	-
2.43	50/200	53.4[c]	45.2	750	0.19
2.114	50/200	467.9[c]	348.0	400	0.23
2.191	100/200	0.073[d]	0.056	250	0.25

[a] Rounded to nearest 50 µM. [b] Including fluorine as a heavy atom. [c] $\Delta\delta^{19}F_1$ used. [d] $\Delta_{w1/2}$ used. [e] The uncertainty of these measurements were larger and partly inconclusive. A clear shift of both $\delta^{19}F$ and $\Delta_{w1/2}$ was observed upon addition of protein but no K_d-value could be determined. LE = ligand efficiency; ND = not determined

BACE1

^{19}F NMR screening:

Screening was performed with BACE1 at 2.8 µM and fragments at 25 µM using cocktails 1–5. In an Eppendorf tube, BACE1 (7.8 µM, 64 µL), PBS (50 mM, 94 µL), D_2O (18 µL), and premixed cocktail (1.25 mM, 3.6 µL) were gently and thoroughly mixed and then transferred to a 3 mm NMR tube for screening in a 600 MHz spectrometer (cocktail 1 was screened in a 800 MHz spectrometer).

^{1}H NMR validation:

Validation was performed with BACE1 at 5.6 µM and fragments at 200 µM. ^{19}F NMR fragment hits were pooled in smaller cocktails with each fragment at 10 mM: 1) **2.120**, **2.147**, and **2.168**; 2) **2.26**, **2.121**, and **2.198**; 3) **2.105**. In an Eppendorf tube, BACE1 (7.8 µM, 128 µL), PBS (50 mM, 30 µL), D_2O (18 µL), and ^{1}H NMR fragment cocktail (10 mM, 3.6 µL) were gently and thoroughly mixed and then transferred to a 3 mm NMR tube for screening.

STD NMR was perform by irradiation of resonance frequencies of p38γ at 7.222 ppm, 0.423 ppm, 0.840, and -0.033 ppm, respectively.

DC-SIGN

All work related to DC-SIGN was performed by collaborators at MPI.

^{19}F NMR screening:

Screening was performed with DC-SIGN at 10 µM and fragments at 25 µM using cocktails A–D. In an Eppendorf tube, DC-SIGN (20 µM, 90 µL) and premixed cocktail (50 µM in 20 mM Tris-HCl, pH 7.8 with 150 mM NaCl, 0.5mM EDTA, 20% D_2O, and 200 µM TFA, 90 µL) were gently and thoroughly mixed and then transferred to a 3 mm NMR tube for screening in a 700 MHz spectrometer. Then, Ca^{2+} ($CaCl_2$) was added to a final screening concentration of 10 mM and the experiment was repeated.

Affinity data by NMR

Affinity data on hits against DC-SIGN was obtained with a ^{19}F R_2-filtered NMR assay using a previously reported experimental setup with propargyl-2-deoxy-2-2',2',2'-trifluoroacetamido-α-D-mannopyranoside (**2.224**) as reporter molecule.[287] For the most potent hit, fragment **2.114**, further validation was performed by ^{1}H–^{15}N HSQC NMR to determine K_d and binding site using a previously reported procedure.[288] Both experiments were performed on a 700 MHz spectrometer.

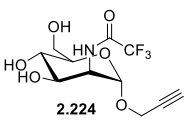

2.224

Table 4.2. Affinity data for DC-SIGN hits. K_i was measured with ^{19}F R_2-filtered NMR. K_d and binding site for **2.114** was determined using $^{1}H–^{15}N$ HSQC NMR.

Ligand	K_i (mM)	LE (K_i)[a]	K_d (mM)	LE (K_d)[a]	Binding site
Mannose	2.34 ± 0.00	0.30	6.4 ± 0.3	0.25	carbohydrate
2.43	2.68 ± 0.02	0.17	ND	-	ND
2.56	4.08 ± 0.02	0.14	ND	-	ND
2.66	3.33 ± 0.01	0.15	ND	-	ND
2.114	1.69 ± 0.01	0.19	0.150 ± 0.05	0.26	III[b]
2.170	12.9 ± 0.3	0.13	ND	-	ND
2.188	3.22 ± 0.02	0.23	ND	-	ND

[a] Including fluorine as a heavy atom. [b] Binding to residues 270Met, 310Ser, and 374Phe (see reference[288]). ND = not determined.

4.2. Part III

General

Commercially available reagents were used without further purification and all solvents were freshly distilled. THF was distilled from CaH_2 and $LiAlH_4$ in the presence of triphenyl methane. CH_2Cl_2, MeOH, PhMe, MeCN, and petroleum ether were distilled from CaH_2. Unless otherwise stated, reactions were carried out as open-system reactions and were monitored by thin layer chromatography (TLC) conducted on Merck TLC Silica gel 60 F_{254} on glass plates. The plates were either visualized under UV-light or stained by dipping in a developing agent followed by heating. $KMnO_4$ [3 g in water (300 mL) along with K_2CO_3 (20 g) and 5% aq. NaOH (5 mL)] or ninhydrin [0.1 g in AcOH (0.5 mL) and acetone (100 mL)] were used as developing agents. Flash column chromatography was performed using Merck 9385 Kieselgel 60 silica gel. All new compounds were characterized by ^{1}H NMR, ^{13}C NMR, IR, HRMS (ESI), and melting point (byproducts were not fully characterized).

NMR data were acquired at 298 K using either a 400 MHz Bruker AVANCE III HD spectrometer equipped with a Smart probe, a 500 MHz Bruker AVANCE III HD spectrometer equipped with a DCH Cryoprobe, or a 600 MHz Bruker AVANCE III spectrometer equipped with a inverse broadband probe. The chemical shifts (δ) are reported in parts per million (ppm) and the coupling constants (*J*) in Hz. For spectra recorded in DMSO-d_6, chemical shifts are reported relative to the signal for DMSO-d_5 (δ 2.50 ppm for ^{1}H NMR and δ 39.52 ppm for ^{13}C NMR). For spectra recorded in $CDCl_3$, chemical shifts are reported relative to the signal for $CHCl_3$ (δ 7.26 ppm for ^{1}H NMR and δ 77.16 ppm for ^{13}C NMR). For spectra recorded in CD_3OD, chemical shifts are reported relative to the signal for CHD_2O(D/H) (δ 3.31 ppm for ^{1}H NMR and δ 49.00 ppm for ^{13}C NMR). For spectra recorded in D_2O, ^{1}H chemical shifts are reported relative to the signal for HDO (δ 4.79 ppm for ^{1}H NMR) and ^{13}C chemical shifts are referenced using the deuterium lock-signal from solvent with δ (TMS) = 0 ppm. NMR data was analyzed using MestReNova (v11.0.0-17609) by Mestrelab Research S.L.

IR analysis was performed on a Perkin-Elmer Spectrum One spectrometer with internal referencing as neat films. In the reporting of IR, s = strong signal, m = medium signal, w = weak signal, and br. = broad signal. Melting points were obtained using a Büchi Melting Point B-545 melting point apparatus and are uncorrected. Analytical LC-HRMS (ESI) analysis was performed on a Micromass QTOF mass spectrometer or a Waters LCT Premier Time of Flight mass spectrometer.

Building Block Synthesis

2-Methyl-2-(prop-2-yn-1-yl)cyclopentane-1,3-dione (3.3)

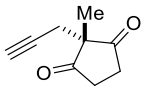

To a suspension of 2-methylcyclopentane-1,3-dione **3.2** (10.0 g, 89.2 mmol) in H_2O (100 mL) was added NaOH (3.92 g, 98.1 mmol) and propargyl bromide (10.6 mL, 98.1 mmol) and the reaction mixture was stirred at 65 °C for 18 h. The aqueous layer was extracted with CH_2Cl_2 (3 × 100 mL) and the combined organic layers were washed with brine (1 × 100 mL), dried over $MgSO_4$, filtered, and concentrated *in vacuo*. The crude product was purified by flash column chromatography (EtOAc/petroleum ether 1:4) to give the title compound as a white solid (10.7 g, 88%).

***R*f** = 0.29 (EtOAc/petroleum ether 1:4); **m.p.**: 68–70 °C; **^{1}H NMR** (400 MHz, $CDCl_3$) δ 2.91 – 2.72 (m, 4H), 2.46 (d, *J* = 2.6 Hz, 2H), 1.97 (t, *J* = 2.6 Hz, 1H), 1.13 (s, 3H); **^{13}C NMR** (101 MHz, $CDCl_3$) δ 215.1 (2C), 78.8, 70.8, 55.3, 35.8 (2C), 24.3, 19.4; **IR** (neat) cm^{-1}: 3280 (m, C≡C–H), 1723 (C=O). Spectroscopic data were consistent with those reported in the literature.[347]

syn-3-Hydroxy-2-methyl-2-(prop-2-yn-1-yl)cyclopentan-1-one (*syn*-3.1) and *anti*-3-hydroxy-2-methyl-2-(prop-2-yn-1-yl)cyclopentan-1-one (*anti*-3.1)

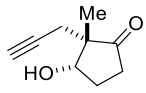

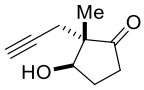

To a solution of **3.3** (10.7 g, 71.2 mmol) in DME (145 mL) at -60 °C was added $NaBH_4$ (1.40 g, 37.0 mmol) portion wise and the reaction mixture was stirred under an atmosphere of N_2 at -60 °C for 24 h. Then, 1 M aq. HCl (145 mL) was added and the mixture was allowed to warm to 22 °C. The aqueous phase was extracted with EtOAc (3 × 300 mL) and the combined organic layers were dried over $MgSO_4$, filtered and concentrated *in vacuo*. The crude products were purified by flash column chromatography (EtOAc/petroleum ether 7:3) to give *syn*-**3.1** (4.08 g, 38%) and *anti*-**3.1** (2.93 mg, 27%) both as colorless oils.

Data for *syn*-**3.1**: R_f = 0.19 (EtOAc/hexane 1:4); **^{1}H NMR** (400 MHz, $CDCl_3$) δ 4.26 (dd, *J* = 4.6, 1.9 Hz, 1H), 2.55 – 2.32 (m, 4H), 2.22 (dddd, *J* = 13.8, 10.2, 9.2, 4.6 Hz, 1H), 2.13 (s, 1H), 2.08 – 2.00 (m, 2H), 1.12 (s, 3H); **^{13}C NMR** (101 MHz, $CDCl_3$) δ 219.7, 81.2, 76.9, 70.8, 53.3, 34.2, 27.6, 21.0, 20.1; **IR** (neat) cm^{-1}: 3435 (br., O–H), 3289 (m, C≡C–H), 1729 (s, C=O). Spectroscopic data were consistent with those reported in the literature.[347]

Data for *anti*-**3.1**: ***R*f** = 0.17 (EtOAc/hexane 1:4); **^{1}H NMR** (400 MHz, $CDCl_3$) δ 4.41 (dd, *J* = 8.9, 6.4 Hz, 1H), 2.54 – 2.44 (m, 1H), 2.40 – 2.25 (m, 3H), 2.24 – 2.06 (m, 2H), 2.05 (t, *J* = 2.7 Hz, 1H), 1.92 – 1.79 (m, 1H), 1.06 (s, 3H); **^{13}C NMR** (101 MHz, $CDCl_3$) δ 218.5, 80.8, 75.5, 71.3, 51.9, 35.0, 27.3, 25.1, 15.2; **IR** (neat) cm^{-1}: 3439 (br., O–H), 3287 (m, C≡C–H), 1731 (s, C=O). Spectroscopic data were consistent with those reported in the literature.[347]

***syn*-3-((*tert*-Butyldimethylsilyl)oxy)-2-methyl-2-(prop-2-yn-1-yl)cyclopentan-1-one (3.27)**

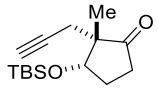

To a solution of *syn*-**3.1** (2.60 g, 17.1 mmol) in anhydrous DMF (60 mL) was added TBSCl (10.3 g, 68.3 mmol) and imidazole (9.30 g, 37 mmol) and the reaction mixture was stirred under an atmosphere of N_2 at 22 °C for 24 h. Water (200 mL) was added and the aqueous phase was extracted with petroleum ether (3 × 200 mL). The combined organic layers were dried over Na_2SO_4, filtered, and concentrated *in vacuo*. The crude product was purified by flash column chromatography (EtOAc/petroleum ether 4:96) to give the title compound as a colorless oil (4.50 g, 99%).

R_f = 0.34 (EtOAc/petroleum ether 4:96); **^{1}H NMR** (400 MHz, $CDCl_3$) δ 4.15 (dd, *J* = 4.0, 2.3 Hz, 1H), 2.47 – 2.26 (m, 4H), 2.19 – 2.08 (m, 1H), 1.97 – 1.90 (m, 2H), 1.09 (s, 3H), 0.87 (s, 9H), 0.12 (s, 3H), 0.10 (s, 3H); **^{13}C NMR** (100 MHz, $CDCl_3$) δ 219.5, 81.8, 77.0, 70.3, 53.8, 33.8, 28.2, 25.9 (3C), 20.7, 19.4, 18.1, -4.4, -4.9; **IR** (neat) cm^{-1}: 3307 (s, C≡C–H), 1744 (s, C=O); **HRMS** (ESI) calcd for $C_{15}H_{27}O_2Si$ $[M+H]^+$ 267.1775, found 267.1775.

***anti*-3-((*tert*-Butyldimethylsilyl)oxy)-2-methyl-2-(prop-2-yn-1-yl)cyclopentan-1-one (3.28).**

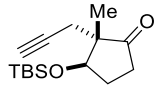

To a solution of *anti*-**3.1** (2.99 g, 19.7 mmol) in anhydrous DMF (65 mL) was added TBSCl (11.8 g, 78.6 mmol) and imidazole (10.7 g, 157 mmol) and the reaction mixture was stirred under an atmosphere of N_2 at 22 °C for 24 h. Water (200 mL) was added and the aqueous phase was extracted with petroleum ether (3 × 200 mL). The combined organic layers were dried over Na_2SO_4, filtered, and concentrated *in vacuo*. The crude product was purified by flash column chromatography (EtOAc/petroleum ether 4:96) to give the title compound as a colorless oil (5.04 g, 96%).

R_f = 0.34 (EtOAc/petroleum ether 4:96); **^{1}H NMR** (400 MHz, $CDCl_3$) δ 4.52 – 4.40 (m, 1H), 2.53 – 2.36 (m, 2H), 2.23 – 2.06 (m, 3H), 1.96 (t, *J* = 2.7 Hz, 1H), 1.89 – 1.77 (m, 1H), 0.96 (s, 3H), 0.90 (s, 9H), 0.11 (s, 3H), 0.10 (s, 3H); **^{13}C NMR** (100 MHz, $CDCl_3$) δ 218.7, 80.7, 74.4, 70.7, 53.1, 35.6, 28.5, 25.9 (3C), 24.5, 18.1, 16.2, -4.3, -4.8; **IR** (neat) cm^{-1}: 3309 (s, C≡C–H), 1747 (s, C=O); **HRMS** (ESI) calcd for $C_{15}H_{27}O_2Si$ $[M+H]^+$ 267.1775, found 267.1775.

Anti Building Block Chemistry

(1*R,2*S**,3*R**)-1-Allyl-3-((*tert*-butyldimethylsilyl)oxy)-2-methyl-2-(prop-2-yn-1-yl)cyclopentan-1-ol (3.29) and (1*S**,2*S**,3*R**)-1-allyl-3-((*tert*-butyldimethylsilyl)oxy)-2-methyl-2-(prop-2-yn-1-yl)cyclopentan-1-ol (3.30)**

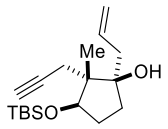

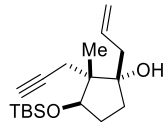

To an ice-cooled solution of **3.28** (444 mg, 1.67 mmol) in anhydrous THF (35 mL) was added allylmagnesium bromide (1.0 M in THF, 1.67 mL, 1.67 mmol) dropwise and the reaction mixture was stirred under an atmosphere of N_2 at 0 °C for 2 h. SiO_2 (3.5 g) was added and the mixture was concentrated *in vacuo* and purified directly by flash column chromatography (EtOAc/petroleum ether 3:97) to give **3.29** (321 mg, 62%) and **3.30** (110 mg, 21%) both as colorless oils.

Data for **3.29**: R_f = 0.26 (EtOAc/petroleum ether 3:97); **^{1}H NMR** (400 MHz, $CDCl_3$) δ 5.99 (ddt, *J* = 17.4, 10.5, 7.1 Hz, 1H), 5.12 – 5.07 (m, 1H), 5.07 – 5.05 (m, 1H), 4.30 (d, *J* = 5.6 Hz, 1H), 4.05 (d, *J* = 1.9 Hz, 1H), 2.29 (dd, *J* = 13.7, 7.2 Hz, 1H), 2.16 (dd, *J* = 16.7, 2.7 Hz, 1H), 2.06 – 1.95 (m, 4H), 1.87 (ddt, *J* = 13.0, 7.2, 3.4 Hz, 2H), 1.79 – 1.70 (m, 1H), 1.17 (s, 3H), 0.89 (s, 11H), 0.08 (s, 7H); **^{13}C NMR** (101 MHz, $CDCl_3$) δ 134.9, 117.0, 83.8, 81.4, 81.3, 71.0, 51.8, 39.8, 36.3, 30.6, 25.9, 25.8, 18.0 (3C), 14.2, -4.7, -5.0; **IR** (neat) cm^{-1}: 3511 (br., O–H), 3311 (s, C≡C–H), 1639 (s, C=C), 1462 (s, C=CH_2); **HRMS** (ESI) calcd for $C_{18}H_{33}O_2Si$ $[M+H]^+$ 309.2245, found 309.2241.

Data for **3.30**: R_f = 0.15 (EtOAc/petroleum ether 3:97); **^{1}H NMR** (400 MHz, $CDCl_3$) δ 5.89 (dddd, *J* = 15.1, 11.7, 8.5, 6.3 Hz, 1H), 5.27 – 5.07 (m, 2H), 4.16 (t, *J* = 8.0 Hz, 1H), 2.66 (dd, *J* = 13.8, 8.5 Hz, 1H), 2.47 (dd, *J* = 17.1, 2.8 Hz, 1H), 2.34 (ddt, *J* = 13.8, 6.3, 1.3 Hz, 1H), 2.22 (dd, *J* = 17.1, 2.8 Hz, 1H), 2.02 (t, *J* = 2.8 Hz, 1H), 2.00 – 1.86 (m, 2H), 1.83 (s, 1H), 1.57 – 1.37 (m, 2H), 0.95 (s, 3H), 0.88 (s, 9H), 0.04 (s, 3H), 0.03 (s, 3H); **^{13}C NMR** (101 MHz, $CDCl_3$) δ 134.0, 119.4, 83.5, 82.1, 78.0, 70.8, 50.3, 42.1, 35.0, 29.2, 26.0 (3C), 23.2, 18.1, 14.9, -4.2, -4.8; **IR** (neat) cm^{-1}: 3486 (br., O–H), 3311 (s, C≡C–H), 1638 (s, C=C), 1463 (s, C=CH_2); **HRMS** (ESI) calcd for $C_{18}H_{33}O_2Si$ $[M+H]^+$ 309.2245, found 309.2248.

(1*R,3a*R**,7a*S**)-7a-Methyl-6-vinyl-1,2,3,4,7,7a-hexahydro-3a*H*-indene-1,3a-diol (3.31)**

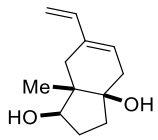

To a solution of **3.29** (39.0 mg, 0.126 mmol) in anhydrous CH_2Cl_2 (25 mL) was added Grubbs II catalyst (10.7 mg, 12.6 µmol) and the reaction mixture was stirred under an ethylene atmosphere at 22 °C for 4 h. The mixture was concentrated *in vacuo* and dissolved in anhydrous THF (3 mL). TBAF (1.0 M in THF, 0.253 mL, 0.253 mmol) was added and the reaction mixture was stirred under an atmosphere of N_2 at 22 °C for 2 h. The mixture was concentrated *in vacuo* and purified directly by flash column chromatography (EtOAc/petroleum ether 2:3) to give the title compound as a white amorphous solid (16.3 mg, 66%).

***R*f** = 0.35 (EtOAc/petroleum ether 2:3); **^{1}H NMR** (600 MHz, $CDCl_3$) δ 6.36 (dd, *J* = 17.5, 10.8 Hz, 1H), 5.60 (dt, *J* = 5.4, 2.6 Hz, 1H), 5.01 (d, *J* = 17.5 Hz, 1H), 4.92 (d, *J* = 10.8 Hz, 1H), 3.89 (t, *J* = 6.3 Hz, 1H), 2.58 (d, *J* = 7.2 Hz, 1H), 2.53 (s, 1H), 2.45 (ddd, *J* = 18.8, 5.4, 2.1 Hz, 1H), 2.40 – 2.29 (m, 1H), 2.26 (d, *J* = 18.8 Hz, 1H), 2.05 (d, *J* = 17.6 Hz, 1H), 1.87 – 1.78 (m, 3H), 1.69 (d, *J* = 17.6 Hz, 1H), 1.07 (s, 3H); **^{13}C NMR** (151 MHz, $CDCl_3$) δ 139.4, 133.2, 126.2, 110.9, 82.0, 81.9, 46.5, 36.1, 34.8, 34.5, 31.3, 14.7; **IR** (neat) cm^{-1}: 3353 (br., O–H), 1647 (m, C=C), 1607 (m, C=C), 1460 (s, C=CH_2); **HRMS** (ESI) calcd for $C_{12}H_{19}O_2$ $[M+H]^+$ 193.1229, found 193.1229.

(4a*S,5*R**,7a*R**,8a*R**)-5,7a-Dihydroxy-4a-methyl-4,4a,5,6,7,7a,8,8a-octahydro-s-indacen-2(1*H*)-one (3.32) and (4a*S**,5*R**,7a*R**,8a*S**)-5,7a-dihydroxy-4a-methyl-4,4a,5,6,7,7a,8,8a-octahydro-s-indacen-2(1*H*)-one (3.33)**

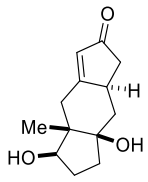

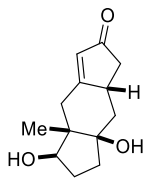

To a solution of $Co_2(CO)_8$ (68.0 mg, 0.195 mmol) in anhydrous CH_2Cl_2 (5 mL) was added a solution of **3.29** (50.0 mg, 0.162 mmol) in anhydrous CH_2Cl_2 (1 mL) and the reaction mixture was stirred under an atmosphere of N_2 at 22 °C for 2 h. Then, 4-methylmorpholine *N*-oxide (190 mg, 1.62 mmol) was added portion wise and the mixture was stirred for another 18 h. Violet Co precipitate was removed by filtration through a short plug of silica (washed with CH_2Cl_2/MeOH 19:1) and the filtrate was concentrated *in vacuo*. The crude Pauson-Khand product was dissolved in anhydrous THF (3.5 mL), added TBAF (1.0 M in THF, 0.325 mL, 0.324 mmol), and stirred under an atmosphere of N_2 at 22 °C for 1 h. The mixture was then concentrated *in vacuo* and purified by flash column chromatography (EtOAc) to give **3.32** (15.0 mg, 42%) and **3.33** (6.0 mg, 17%) both as colorless oils.

Data for **3.32**: ***R*f** = 0.29 (EtOAc); **^{1}H NMR** (400 MHz, CD_3OD) δ 5.92 (d, *J* = 1.8 Hz, 1H), 3.81 (d, *J* = 5.9 Hz, 1H), 3.01 – 2.90 (m, 1H), 2.62 (dd, *J* = 18.9, 6.4 Hz, 1H), 2.47 (d, *J* = 13.9 Hz, 1H), 2.41 – 2.30 (m, 2H), 2.25 – 2.12 (m, 2H), 2.07 (dd, *J* = 18.9, 1.8 Hz, 1H), 1.97 – 1.86 (m, 2H), 1.39 (t, *J* = 12.8 Hz, 1H), 1.00 (s, 3H); **^{13}C NMR** (101 MHz, CD_3OD) δ 211.7, 184.9,

129.8, 83.1, 82.9, 51.9, 43.1, 40.6, 40.0, 39.6, 35.5, 31.8, 14.7; **IR** (neat) cm^{-1}: 3385 (br., O–H), 1704 (s, C=O), 1620 (s, C=C); **HRMS** (ESI) calcd for $C_{13}H_{19}O_3$ $[M+H]^+$ 223.1329, found 223.1341.

Data for **3.33**: R_f = 0.28 (EtOAc); **^{1}H NMR** (400 MHz, $CDCl_3$) δ 5.93 (t, *J* = 1.8 Hz, 1H), 3.88 (q, *J* = 8.0 Hz, 1H), 3.01 (dt, *J* = 12.0, 5.6 Hz, 1H), 2.78 (d, *J* = 14.6 Hz, 1H), 2.59 (ddd, *J* = 18.8, 6.6, 0.7 Hz, 1H), 2.31 (d, *J* = 14.7 Hz, 1H), 2.13 – 2.01 (m, 2H), 1.97 – 1.84 (m, 2H), 1.67 – 1.60 (m, 1H), 1.55 – 1.48 (m, 1H), 1.32 (t, *J* = 13.5 Hz, 1H), 1.06 (s, 3H); **^{13}C NMR** (101 MHz, $CDCl_3$) δ 208.8, 181.7, 128.9, 78.1, 73.6, 49.4, 44.3, 41.8, 37.1, 36.1, 34.9, 28.5, 15.8; **IR** (neat) cm^{-1}: 3391 (br., O–H), 1704 (s, C=O), 1618 (s, C=C); **HRMS** (ESI) calcd for $C_{13}H_{19}O_3$ $[M+H]^+$ 223.1329, found 223.1341.

(1*R,2*S**,3*R**)-1-Allyl-2-methyl-2-(prop-2-yn-1-yl)cyclopentane-1,3-diol (3.34)**

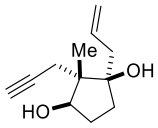

To a solution of **3.29** (45.0 mg, 0.146 mmol) in anhydrous THF (3 mL) was added TBAF (1.0 M in THF, 0.291 mL, 0.219 mmol) and the reaction mixture was stirred under an atmosphere of N_2 at 22 °C for 2 h. The mixture was concentrated *in vacuo* and purified directly by flash column chromatography (EtOAc/petroleum ether 1:3) to give the title compound as a colorless oil (24.6 mg, 87%).

R_f = 0.41 (EtOAc/petroleum ether 1:2); **^{1}H NMR** (400 MHz, $CDCl_3$) δ 5.90 (dddd, *J* = 16.9, 10.2, 8.0, 6.7 Hz, 1H), 5.21 – 5.10 (m, 2H), 4.15 (t, *J* = 6.7 Hz, 1H), 2.95 (d, *J* = 8.0 Hz, 1H), 2.67 (s, 1H), 2.26 (ddt, *J* = 13.6, 8.0, 1.1 Hz, 1H), 2.19 – 2.06 (m, 3H), 2.03 (t, *J* = 2.7 Hz, 1H), 1.96 – 1.78 (m, 4H), 1.21 (s, 3H); **^{13}C NMR** (101 MHz, $CDCl_3$) δ 133.8, 119.1, 84.0, 81.3, 80.3, 71.2, 51.6, 40.1, 35.9, 30.6, 25.9, 13.7; **IR** (neat) cm^{-1}: 3366 (br., O–H), 3303 (s, C≡C–H), 1639 (s, C=C).

***anti*-3-((*tert*-Butyldimethylsilyl)oxy)-2-methyl-5-methylene-2-(prop-2-yn-1-yl)cyclopentan-1-one (3.40)**

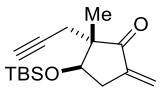

To a solution of *anti*-**3.1** (550 mg, 2.06 mmol) in CH_2Cl_2 (10 mL) was added CH_2Br_2 (0.868 mL, 12.4 mmol) and Et_2NH (2.56 mL, 24.8 mmol) and the reaction mixture was subjected to μW heating at 125 °C for 20 min. The mixture was diluted with Et_2O (150 mL) and precipitate was removed by filtration. The filtrate was concentrated *in vacuo* and purified by flash column chromatography (EtOAc/petroleum ether 3:97) to give the title product as a colorless oil (389 mg, 68%).

R_f = 0.20 (EtOAc/petroleum ether 3:97); **^{1}H NMR** (400 MHz, $CDCl_3$) δ 6.11 (ddd, *J* = 3.1, 2.0, 1.1 Hz, 1H), 5.37 (ddd, *J* = 3.1, 2.0, 1.1 Hz, 1H), 4.46 (dd, *J* = 8.0, 6.9 Hz, 1H), 2.89 (ddt, *J* = 16.5, 6.9, 2.0 Hz, 1H), 2.60 – 2.49 (m, 1H), 2.48 (dd, *J* = 16.9, 2.7 Hz, 1H), 2.23 (dd, *J* = 16.9, 2.7 Hz, 1H), 1.95 (t, *J* = 2.7 Hz, 1H), 1.02 (s, 3H), 0.90 (s, 9H), 0.11 (s, 6H); **^{13}C NMR** (101 MHz, $CDCl_3$) δ 206.2, 142.2, 119.6, 80.7, 72.0, 70.8, 53.4, 36.4, 25.9 (3C), 24.3, 18.1, 16.4, -

4.3, -4.8; **IR** (neat) cm^{-1}: 3313, (m, C≡C–H), 1730 (s, C=O), 1641 (s, C=C), 1462 (m, C=CH_2); **HRMS** (ESI) calcd for $C_{16}H_{27}O_2Si$ $[M+H]^+$ 279.1775, found 279.1767.

Ethyl (5*S,7*S**,8*R**)-8-((*tert*-butyldimethylsilyl)oxy)-7-methyl-6-oxo-7-(prop-2-yn-1-yl)-2-oxa-3-azaspiro[4.4]non-3-ene-4-carboxylate (3.42)**

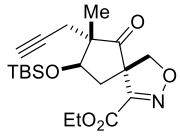

To a vigorously solution of **3.40** (86.0 mg, 0.309 mmol) and Et_3N (52.0 µL, 0.371 mmol) in anhydrous CH_2Cl_2 (5 mL) was added drop wise a solution of 1-ethyl oxalyl chloride 2-oxime (56.2 mg, 0.371 mmol) in anhydrous CH_2Cl_2 (5 mL) over 1 h under an atmosphere of N_2 at 22 °C. The mixture was then concentrated *in vacuo* and purified directly by flash column chromatography (EtOAc/petroleum ether 1:9) to give the title compound as a colorless oil (85.0 mg, 70%).
R_f = 0.33 (EtOAc/petroleum ether 1:9); **^{1}H NMR** (400 MHz, $CDCl_3$) δ 4.55 (t, *J* = 5.5 Hz, 1H), 4.34 (q, *J* = 7.1 Hz, 2H), 3.49 (d, *J* = 18.0 Hz, 1H), 3.14 (d, *J* = 18.0 Hz, 1H), 2.61 (dd, *J* = 14.4, 5.5 Hz, 1H), 2.45 (dd, *J* = 17.1, 2.6 Hz, 1H), 2.28 (dd, *J* = 17.1, 2.6 Hz, 1H), 2.14 – 2.04 (m, 2H), 1.36 (t, *J* = 7.1 Hz, 3H), 1.11 (s, 3H), 0.89 (s, 9H), 0.11 (s, 6H); **^{13}C NMR** (101 MHz, $CDCl_3$) δ 213.3, 160.1, 150.7, 90.1, 79.1, 72.0, 71.8, 62.4, 52.7, 42.8, 42.6, 25.9 (3C), 25.1, 18.1, 16.7, 14.2, -4.4, -4.8; **IR** (neat) cm^{-1}: 3297 (m, C≡C–H), 1752 (s, C=O), 1721 (s, C=O), 1597 (m, C=N); **HRMS** (ESI) calcd for $C_{20}H_{32}NO_5Si$ $[M+H]^+$ 394.2044, found 394.2044.

Ethyl (5*S,7*S**,8*R**)-8-hydroxy-7-methyl-6-oxo-7-(prop-2-yn-1-yl)-2-oxa-3-azaspiro[4.4]non-3-ene-4-carboxylate (3.43)**

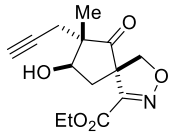

To a solution of **3.42** (29.0 mg, 73.7 µmol) in anhydrous THF (1.5 mL) was added TBAF (1.0 M in THF, 0.111 mL, 0.111 mmol) and the reaction mixture was stirred at 22 °C under an atmosphere of N_2 for 1 h. The mixture was concentrated *in vacuo* and purified directly by flash column chromatography (EtOAc/petroleum ether 2:3) to give the title compound as a colorless oil (9.0 mg, 44%).
R_f = 0.42 (EtOAc/petroleum ether 1:1); **^{1}H NMR** (600 MHz, $CDCl_3$) δ 4.60 (ddd, *J* = 8.1, 6.1, 3.3 Hz, 1H), 4.35 (qd, *J* = 7.2, 0.7 Hz, 2H), 3.53 (d, *J* = 18.0 Hz, 1H), 3.17 (d, *J* = 18.0 Hz, 1H), 2.70 (dd, *J* = 14.4, 6.1 Hz, 1H), 2.49 – 2.40 (m, 2H), 2.12 (t, *J* = 2.7 Hz, 1H), 2.10 (d, *J* = 3.3 Hz, 1H), 2.08 – 2.03 (m, 1H), 1.36 (t, *J* = 7.2 Hz, 3H), 1.18 (s, 3H); **^{13}C NMR** (151 MHz, $CDCl_3$) δ 212.5, 160.0, 150.9, 90.1, 79.8, 73.0, 71.9, 62.5, 51.0, 41.1, 40.8, 25.9, 15.9, 14.3; **IR** (neat) cm^{-1}: 3506 (br. O–H), 3281 (m, C≡C–H), 1752 (s, C=O), 1721 (s, C=O), 1598 (m, C=N); **HRMS** (ESI) calcd for $C_{14}H_{17}NO_5Na$ $[M+H]^+$ 302.0999, found 302.1002.

(3*S,4*R**)-4-((*tert*-Butyldimethylsilyl)oxy)-3,6',6'-trimethyl-3-(prop-2-yn-1-yl)tetrahydro-3'*H*-spiro[cyclopentane-1,2'-pyrrolo[1,2-*b*]isoxazol]-2-one (3.44)**

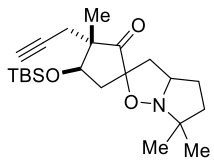

To a solution of **3.40** (27.0 mg, 97.0 µmol) in THF (0.5 mL) was added 5,5-dimethyl-1-pyrroline *N*-oxide (32.3 µL, 291 µmol) and the reaction mixture was stirred at 60 °C for 10 min. The mixture was concentrated *in vacuo* and purified directly by flash column chromatography (EtOAc/petroleum ether 1:7) to give the title compound as a colorless oil (21.0 mg, 55%).

***R*f** = 0.27 (EtOAc/petroleum ether 1:7); **^{1}H NMR** (600 MHz, $CDCl_3$) δ 4.35 (t, *J* = 5.6 Hz, 1H), 3.75 (dddd, *J* = 9.0, 7.4, 5.3, 1.9 Hz, 1H), 2.47 – 2.40 (m, 1H), 2.39 – 2.34 (m, 1H), 2.28 – 2.20 (m, 2H), 2.11 – 2.07 (m, 1H), 1.96 – 1.83 (m, 5H), 1.41 (ddd, *J* = 13.2, 9.4, 4.8 Hz, 1H), 1.16 (s, 3H), 0.95 (s, 3H), 0.94 (s, 3H), 0.77 (s, 9H), -0.01 (s, 3H), -0.02 (s, 3H); **^{13}C NMR** (151 MHz, $CDCl_3$) δ 217.5, 84.8, 80.0, 72.3, 71.1, 68.9, 65.6, 52.3, 47.3, 44.1, 35.8, 30.7, 27.4, 25.9 (3C), 25.3, 24.3, 18.1, 16.9, -4.4, -4.9; **IR** (neat) cm^{-1}: 3313 (m, C≡C–H), 1752 (s, C=O), 1377 (s, C–$(CH_3)_2$); **HRMS** (ESI) calcd for $C_{22}H_{38}NO_3Si$ $[M+H]^+$ 392.2621, found 392.2611.

(5*S,7*S**,8*R**)-2-Benzyl-8-((*tert*-butyldimethylsilyl)oxy)-7-methyl-7-(prop-2-yn-1-yl)-2-azaspiro[4.4]nonan-6-one (3.46) and (5*R**,7*S**,8*R**)-2-benzyl-8-((*tert*-butyldimethylsilyl) oxy)-7-methyl-7-(prop-2-yn-1-yl)-2-azaspiro[4.4]nonan-6-one (3.47)**

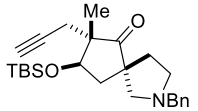

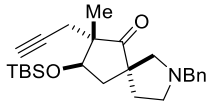

To an ice-cooled solution of **3.40** (99.0 mg, 0.356 mmol) in CH_2Cl_2 (7 mL) was added *N*-(methoxymethyl)-*N*-(trimethylsilylmethyl) benzyl-amine (90%, 0.122 mL, 0.427 mmol) and TFA (0.1 M in CH_2Cl_2, 0.355 mL, 35.6 µmol) and the reaction mixture was stirred at 0 °C for 1 h. The mixture was concentrated *in vacuo* and purified directly by flash column chromatography (EtOAc/petroleum ether 1:9) to give **3.46** (89.9 mg, 61%) and **3.47** (47.5 mg, 32%) both as yellow oils.

Data for **3.46**: ***R*f** = 0.54 (EtOAc/petroleum ether 1:4); **^{1}H NMR** (400 MHz, $CDCl_3$) δ 7.37 – 7.19 (m, 5H), 4.37 (dd, *J* = 8.4, 6.1 Hz, 1H), 3.72 – 3.56 (m, 2H), 2.85 (td, *J* = 8.4, 7.5, 4.2 Hz, 1H), 2.64 – 2.50 (m, 3H), 2.39 (dd, *J* = 16.9, 2.7 Hz, 1H), 2.31 (dd, *J* = 13.0, 6.1 Hz, 1H), 2.22 (ddd, *J* = 12.5, 8.0, 4.2 Hz, 1H), 2.13 (dd, *J* = 16.9, 2.7 Hz, 1H), 1.90 (dd, *J* = 13.0, 8.4 Hz, 1H), 1.84 – 1.73 (m, 2H), 0.98 (s, 3H), 0.90 (s, 9H), 0.10 (s, 3H), 0.08 (s, 3H); **^{13}C NMR** (101 MHz, $CDCl_3$) δ 221.9, 139.1, 128.8 (2C), 128.4 (2C), 127.1, 80.9, 72.4, 70.8, 64.0, 59.8, 54.5, 54.4, 53.5, 44.5, 37.2, 25.9 (3C), 25.0, 18.2, 17.1, -4.3, -4.8; **IR** (neat) cm^{-1}: 3311 (m, C≡C–H), 1737 (s, C=O); **HRMS** (ESI) calcd for $C_{25}H_{38}NO_2Si$ $[M+H]^+$ 412.2667, found 412.2667.

Data for **3.47**: ***R*f** = 0.36 (EtOAc/petroleum ether 1:4); **^{1}H NMR** (400 MHz, $CDCl_3$) δ 7.37 – 7.16 (m, 5H), 4.44 (dd, *J* = 7.8, 5.9 Hz, 1H), 3.70 (d, *J* = 12.8 Hz, 1H), 3.58 (d, *J* = 12.8 Hz, 1H), 2.86 (ddd, *J* = 9.0, 7.3, 4.2 Hz, 1H), 2.68 (d, *J* = 2.4 Hz, 2H), 2.55 (dt, *J* = 9.0, 7.8 Hz,

1H), 2.42 (dd, *J* = 16.9, 2.7 Hz, 1H), 2.25 – 2.08 (m, 3H), 2.02 – 1.92 (m, 2H), 1.64 (dt, *J* = 12.6, 7.5 Hz, 1H), 0.94 (s, 3H), 0.86 (s, 9H), 0.08 (s, 3H), 0.07 (s, 3H); **^{13}C NMR** (101 MHz, $CDCl_3$) δ 221.7, 139.1, 128.9 (2C), 128.4 (2C), 127.1, 81.0, 72.2, 70.9, 64.2, 60.2, 54.4, 54.1, 53.6, 44.6, 37.5, 25.9 (3C), 25.1, 18.1, 16.9, -4.3, -4.8; **IR** (neat) cm^{-1}: 3311 (m, C≡C–H), 1737 (s, C=O); **HRMS** (ESI) calcd for $C_{25}H_{38}NO_2Si$ $[M+H]^+$ 412.2667, found 412. 2666.

(5*S,7*S**,8*R**)-2-Benzyl-8-hydroxy-7-methyl-7-(prop-2-yn-1-yl)-2-azaspiro[4.4]nonan-6-one (3.48)**

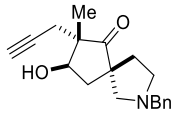

To a solution of **3.46** (67.0 mg, 0.163 mmol) in anhydrous THF (3.5 mL) was added TBAF (1.0 M in THF, 0.326 mL, 0.326 mmol) and the reaction mixture was stirred under an atmosphere of N_2 at 22 °C for 1 h. The mixture was concentrated *in vacuo* and purified directly by flash column chromatography (EtOAc, R_f = 0.28) to give the title compound as a colorless oil (46.0 mg, 95%).

***R*$_f$** = 0.28 (EtOAc); **^{1}H NMR** (600 MHz, $CDCl_3$) δ 7.35 – 7.28 (m, 4H), 7.24 (ddt, *J* = 8.6, 5.4, 2.7 Hz, 1H), 4.32 (dd, *J* = 9.9, 6.5 Hz, 1H), 3.65 (d, *J* = 13.0 Hz, 1H), 3.61 (d, *J* = 13.0 Hz, 1H), 2.93 – 2.85 (m, 1H), 2.60 – 2.53 (m, 2H), 2.46 (dd, *J* = 12.9, 6.5 Hz, 1H), 2.41 (d, *J* = 9.3 Hz, 1H), 2.38 – 2.27 (m, 3H), 2.24 (dt, *J* = 8.2, 4.4 Hz, 1H), 1.93 (t, *J* = 2.6 Hz, 1H), 1.87 (dd, *J* = 12.9, 9.9 Hz, 1H), 1.79 (dt, *J* = 12.9, 7.7 Hz, 1H), 1.05 (s, 3H); **^{13}C NMR** (151 MHz, $CDCl_3$) δ 221.8, 154.6, 128.8 (2C), 128.4 (2C), 127.2, 81.0, 73.4, 71.2, 64.3, 59.8, 54.4, 54.4, 52.1, 43.4, 36.7, 25.6, 16.0; **IR** (neat) cm^{-1}: 3370 (br. s, O–H), 3291 (m, C≡C–H), 1735 (s, C=O); **HRMS** (ESI) calcd for $C_{19}H_{24}NO_2$ $[M+H]^+$ 298.1802, found 298.1805.

(5*R,7*S**,8*R**)-2-Benzyl-8-hydroxy-7-methyl-7-(prop-2-yn-1-yl)-2-azaspiro[4.4]nonan-6-one (3.49)**

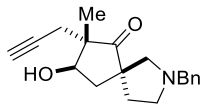

To a solution of **3.47** (43.0 mg, 0.104mmol) in anhydrous THF (2 mL) was added TBAF (1.0 M in THF, 0.209 mL, 0.209 mmol) and the reaction mixture was stirred under an atmosphere of N_2 at 22 °C for 1 h. The mixture was concentrated *in vacuo* and purified directly by flash column chromatography (EtOAc) to give the title compound as a colorless oil (24.5 mg, 79%).

***R*$_f$** = 0.22 (EtOAc); **^{1}H NMR** (400 MHz, $CDCl_3$) δ 7.36 – 7.28 (m, 4H), 7.27 – 7.21 (m, 1H), 4.43 (dd, *J* = 9.6, 6.4 Hz, 1H), 3.72 – 3.58 (m, 2H), 2.83 (ddd, *J* = 9.2, 7.1, 4.5 Hz, 1H), 2.76 (d, *J* = 9.6 Hz, 1H), 2.66 (d, *J* = 9.6 Hz, 1H), 2.57 (dt, *J* = 9.2, 7.4 Hz, 1H), 2.39 – 2.31 (m, 3H), 2.10 (br. s, 1H), 2.06 – 1.89 (m, 3H), 1.68 (dt, *J* = 12.5, 7.4 Hz, 1H), 1.01 (s, 3H); **^{13}C NMR** (100 MHz, $CDCl_3$) δ 221.3, 139.1, 128.8 (2C), 128.4 (2C), 127.1, 81.1, 72.9, 71.3, 63.7, 60.1, 54.2, 54.0, 52.1, 43.5, 38.0, 25.7, 15.8; **IR** (neat) cm^{-1}: 3331 (br. s, O–H), 3285 (m, C≡C–H), 1735 (s, C=O); **HRMS** (ESI) calcd for $C_{19}H_{25}NO_2$ $[M+H]^+$ 298.1802, found 298.1799.

(5*S,7*S**,8*R**)-8-Hydroxy-7-methyl-7-propyl-2-azaspiro[4.4]nonan-6-one (3.50)**

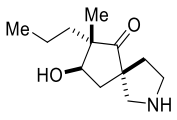

To a solution of **3.48** (30.0 mg, 0.101 mmol) in EtOH (2 mL) was added 10% Pd/C (21.5 mg, 20.2 µmol) and the resulting suspension was stirred under an atmosphere of H_2 at 40 °C for 4 h. The mixture was filtered through a pad of celite and concentrated *in vacuo* to give the title compound as an off-white amorphous solid (20.8 mg, 98%).

^{1}H NMR (400 MHz, CD_3OD) δ 4.15 (dd, *J* = 7.2, 5.9 Hz, 1H), 3.09 (ddd, *J* = 11.4, 8.3, 5.6 Hz, 1H), 3.00 (dt, *J* = 11.4, 7.4 Hz, 1H), 2.88 (d, *J* = 11.5 Hz, 1H), 2.76 (d, *J* = 11.5 Hz, 1H), 2.29 (dd, *J* = 13.2, 5.9 Hz, 1H), 2.12 (ddd, *J* = 13.0, 8.3, 6.9 Hz, 1H), 1.95 (dd, *J* = 13.2, 7.2 Hz, 1H), 1.83 (ddd, *J* = 13.0, 7.7, 5.6 Hz, 1H), 1.45 – 1.30 (m, 4H), 1.24 – 1.14 (m, 1H), 0.99 (s, 3H), 0.91 (t, *J* = 7.0 Hz, 3H); **^{13}C NMR** (101 MHz, CD_3OD) δ 226.0, 73.8, 58.3, 56.4, 55.1, 47.7, 42.1, 39.9, 39.0, 18.5, 16.7, 15.0; **IR** (neat) cm^{-1}: 3299 (br. s, O–H), 1727 (s, C=O); **HRMS** (ESI) calcd for $C_{12}H_{22}NO_2$ $[M+H]^+$ 212.1651, found 212.1648.

(5*R,7*S**,8*R**)-8-Hydroxy-7-methyl-7-propyl-2-azaspiro[4.4]nonan-6-one (3.51)**

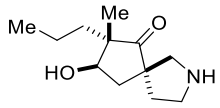

To a solution of **3.49** (20.0 mg, 67.3 µmol) in EtOH (1.5 mL) was added 10% Pd/C (14.3 mg, 13.5 µmol) and the resulting suspension was stirred under an atmosphere of H_2 at 40 °C for 4 h. The mixture was filtered through a pad of celite and concentrated *in vacuo* to give the title compound as an off-white amorphous solid (14.0 mg, 99%).

^{1}H NMR (400 MHz, CD_3OD) δ 4.19 (t, *J* = 5.4 Hz, 1H), 3.49 – 3.35 (m, 3H), 3.26 (d, *J* = 12.1 Hz, 1H), 2.41 (dd, *J* = 13.6, 5.4 Hz, 1H), 2.19 – 1.97 (m, 3H), 1.49 – 1.40 (m, 2H), 1.38 – 1.20 (m, 2H), 1.02 (s, 3H), 0.92 (t, *J* = 7.2 Hz, 3H); **^{13}C NMR** (101 MHz, CD_3OD) δ 223.0, 73.9, 55.6, 55.0, 54.0, 46.3, 40.4, 39.0, 36.5, 18.5, 16.2, 14.9; **IR** (neat) cm^{-1}: 3364 (br. s, O–H), 1733 (s, C=O); **HRMS** (ESI) calcd for $C_{12}H_{22}NO_2$ $[M+H]^+$ 212.1651, found 212.1645.

(2*R,3*R**)-2-((*tert*-Butyldimethylsilyl)oxy)-3-methyl-3-(prop-2-yn-1-yl)-1,2,3,9,10,10a-hexahydrobenzo[*b*]cyclopenta[*e*][1,4]diazepine (3.58)**

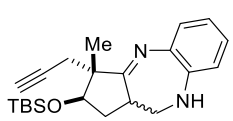

To a solution of **3.40** (52.0 mg, 0.187 mmol) in EtOH (2 mL) was added *o*-phenylenediamine (40.4 mg, 0.373 mmol) and AcOH (10 µL, 0.215 mmol) and subjected to µW heating at 140 °C for 15 min. The mixture was concentrated *in vacuo* and purified directly by flash column chromatography (EtOAc/petroleum ether 1:9) to give the title compound as a colorless oil (26.0 mg, 38%, 55:45 mixture of diastereomers). R_f = 0.30 (EtOAc/petroleum ether 1:9)

(3a*S,5*S**,6*R**,6a*R**)-2-Benzyl-6-((*tert*-butyldimethylsilyl)oxy)-5-methyl-5-(prop-2-yn-1-yl)hexahydrocyclopenta[*c*]pyrrol-4(1*H*)-one (3.62) and (3a*R**,5*S**,6*R**,6a*S**)-2-benzyl-6-((*tert*-butyldimethylsilyl)oxy)-5-methyl-5-(prop-2-yn-1-yl)hexahydrocyclopenta-[*c*]-pyrrol-4(1*H*)-one (3.63)**

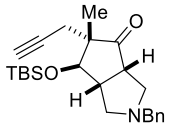

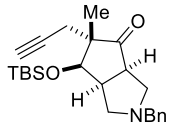

To a solution of **3.28** (180 mg, 0.676 mmol) in PhF/DMSO (2:1, 5 mL) was added IBX (30%, 2.52 g, 2.70 mmol) and the reaction mixture was stirred under an atmosphere of N_2 at reflux for 62 h. The mixture was diluted with Et_2O (35 mL) and washed successively with sat. aq. $NaHCO_3$ (1 × 35 mL), water (1 × 35 mL), and brine (1 × 35 mL). The organic layer was dried over $MgSO_4$, filtered, and concentrated *in vacuo*. The crude α,β-unsaturated product was dissolved in CH_2Cl_2 (13 mL) and added *N*-(methoxymethyl)-*N*-(trimethylsilylmethyl)benzylamine (90%, 0.259 mL, 0.909 mmol) and TFA (0.1 M in CH_2Cl_2, 0.673 mL, 35.6 μmol). The reaction mixture was stirred at 22 °C for 1 h, then concentrated *in vacuo*, and purified directly by flash column chromatography (EtOAc/petroleum ether 1:19) to give **3.62** (31.5 mg, 12%, brsm = 30%) and **3.63** (25.0 mg, 10%, brsm = 25%) both as yellow oils.

Data for **3.62**: R_f = 0.46 (EtOAc/petroleum ether 1:9); **^{1}H NMR** (400 MHz, $CDCl_3$) δ 7.33 – 7.15 (m, 5H), 4.37 (d, *J* = 6.3 Hz, 1H), 3.69 (d, *J* = 13.4 Hz, 1H), 3.46 (d, *J* = 13.4 Hz, 1H), 3.19 (d, *J* = 9.2 Hz, 1H), 3.00 (t, *J* = 9.2 Hz, 2H), 2.90 (d, *J* = 9.2 Hz, 1H), 2.64 – 2.54 (m, 2H), 2.31 – 2.23 (m, 2H), 2.16 (dd, *J* = 16.9, 2.7 Hz, 1H), 2.01 (t, *J* = 2.7 Hz, 1H), 1.02 (s, 3H), 0.88 (s, 9H), 0.07 (s, 3H), -0.01 (s, 3H); **^{13}C NMR** (100 MHz, $CDCl_3$) δ 219.3, 139.3, 128.3 (2C), 128.3 (2C), 127.0, 81.1, 78.6, 70.5, 58.8, 58.5, 56.3, 55.3, 49.7, 46.0, 25.9 (3C), 23.5, 18.2, 17.5, -4.0, -4.5; **IR** (neat) cm^{-1}: 3309 (m, C≡C–H), 1745 (s, C=O); **HRMS** (ESI) calcd for $C_{24}H_{36}NO_2Si$ $[M+H]^+$ 398.2510, found 392.2526.

Data for **3.63**: R_f = 0.35 (EtOAc/petroleum ether 1:9); **^{1}H NMR** (400 MHz, $CDCl_3$) δ 7.37 – 7.21 (m, 5H), 4.73 (d, *J* = 8.3 Hz, 1H), 3.66 (d, *J* = 13.2 Hz, 1H), 3.55 (d, *J* = 13.2 Hz, 1H), 3.41 (dd, *J* = 9.8, 2.6 Hz, 1H), 3.22 (d, *J* = 8.9 Hz, 1H), 3.06 – 2.94 (m, 1H), 2.69 (ddd, *J* = 8.9, 6.2, 1.1 Hz, 1H), 2.54 (dd, *J* = 16.7, 2.6 Hz, 1H), 2.38 (dd, *J* = 8.9, 6.2 Hz, 1H), 2.31 – 2.17 (m, 2H), 1.96 (t, *J* = 2.6 Hz, 1H), 1.19 (s, 3H), 0.94 (s, 9H), 0.16 (s, 3H), 0.13 (s, 3H); **^{13}C NMR** (101 MHz, $CDCl_3$) δ 222.5, 139.0, 128.5 (2C), 128.3 (2C), 127.0, 81.4, 73.9, 70.4, 59.8, 58.3, 53.1, 53.0, 52.8, 43.4, 26.7, 25.9 (3C), 18.3, 18.2, -4.4, -4.8; **IR** (neat) cm^{-1}: 3308 (m, C≡C–H), 1740 (s, C=O); **HRMS** (ESI) calcd for $C_{24}H_{36}NO_2Si$ $[M+H]^+$ 398.2510, found 392.2528.

(3a*S,5*S**,6*R**,6a*R**)-2-Benzyl-6-hydroxy-5-methyl-5-(prop-2-yn-1-yl)hexahydrocyclopenta[*c*]pyrrol-4(1*H*)-one (3.64)**

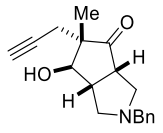

To a solution of **3.62** (22.0 mg, 55.3 µmol) in anhydrous THF (1.5 mL) was added TBAF (1.0 M in THF, 0.111 mL, 0.111 mmol) and the reaction mixture was stirred under an atmosphere of N_2 at 22 °C for 1 h. The mixture was concentrated *in vacuo* and purified directly by flash column chromatography (EtOAc/petroleum ether/Et_3N 35:65:1) to give the title compound as a colorless amorphous solid (13.4 mg, 90%).

***R*f** = 0.25 (EtOAc/petroleum ether/Et_3N 35:65:1); **^{1}H NMR** (600 MHz, $CDCl_3$) δ 7.34 – 7.22 (m, 5H), 4.12 (d, *J* = 6.8 Hz, 1H), 3.64 (d, *J* = 13.2 Hz, 1H), 3.52 (d, *J* = 13.2 Hz, 1H), 3.18 (d, *J* = 9.1 Hz, 1H), 3.05 – 3.00 (m, 2H), 2.66 (dt, *J* = 10.5, 6.8 Hz, 1H), 2.46 (dd, *J* = 17.1, 2.7 Hz, 1H), 2.36 (dd, *J* = 17.1, 2.7 Hz, 1H), 2.30 (dd, *J* = 9.4, 5.9 Hz, 1H), 2.22 (t, *J* = 9.1 Hz, 1H), 2.11 (t, *J* = 2.7 Hz, 1H), 1.16 (s, 3H); **^{13}C NMR** (151 MHz, $CDCl_3$) δ 219.1, 138.9, 128.5 (2C), 128.4 (2C), 127.1, 81.4, 80.6, 71.3, 59.2, 58.8, 56.1, 53.4, 48.7, 44.7, 24.3, 16.1; **IR** (neat) cm^{-1}: 3470 (br., O–H), 3293 (m, C≡C–H), 1739 (s, C=O); **HRMS** (ESI) calcd for $C_{18}H_{22}NO_2$ $[M+H]^+$ 284.1645, found 284.1644

(3a*R,5*S**,6*R**,6a*S**)-2-Benzyl-6-hydroxy-5-methyl-5-(prop-2-yn-1-yl)hexahydrocyclopenta[*c*]pyrrol-4(1*H*)-one (3.65)**

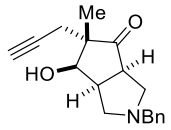

To a solution of **3.63** (25.0 mg, 62.9 µmol) in anhydrous THF (1.5 mL) was added TBAF (1.0 M in THF, 0.126 mL, 0.126 mmol) and the reaction mixture was stirred under an atmosphere of N_2 at 22 °C for 1 h. The mixture was concentrated *in vacuo* and purified directly by flash column chromatography (EtOAc/petroleum ether/Et_3N 35:65:1, R_f = 0.25) to give the title compound as a (14.8 mg, 83%).

***R*f** = 0.25 (EtOAc/petroleum ether/Et_3N 35:65:1); **^{1}H NMR** (400 MHz, $CDCl_3$) δ 7.39 – 7.22 (m, 5H), 5.27 (s, 1H), 4.15 (d, *J* = 5.7 Hz, 1H), 3.71 (d, *J* = 12.8 Hz, 1H), 3.60 (d, *J* = 12.8 Hz, 1H), 3.27 (d, *J* = 9.5 Hz, 1H), 3.19 (d, *J* = 9.3 Hz, 1H), 3.12 (dt, *J* = 9.5, 5.7 Hz, 1H), 3.00 (dd, *J* = 10.6, 9.3 Hz, 1H), 2.42 – 2.33 (m, 2H), 2.29 (t, *J* = 2.9 Hz, 2H), 2.10 (t, *J* = 2.9 Hz, 1H), 1.27 (s, 3H); **^{13}C NMR** (100 MHz, $CDCl_3$) δ 219.8, 137.4, 128.7 (2C), 128.7 (2C), 127.7, 79.2, 76.2, 71.7, 59.2, 57.5, 55.5, 55.3, 48.0, 40.2, 25.4, 14.7; **IR** (neat) cm^{-1}: 3297 (br., O–H), 3280 (m, C≡C–H), 1738 (s, C=O); **HRMS** (ESI) calcd for $C_{18}H_{22}NO_2$ $[M+H]^+$ 284.1645, found 284.1644

(2*S,3*R**,5*R**)-5-Allyl-3-((*tert*-butyldimethylsilyl)oxy)-2-methyl-2-(prop-2-yn-1-yl)cyclopentan-1-one (*syn*-3.66)**

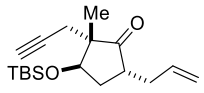

To a solution of **3.28** (222 mg, 0.833 mmol) in anhydrous THF (17 mL) was added LiHMDS (1.0 M in PhMe, 1.00 mL, 1.00 mmol) at -78 °C and the mixture was stirred under an atmosphere of N_2 for 30 min. Then, cooling was removed and the mixture was allowed to warm to 22 °C. After stirring 30 min at 22 °C, the mixture was cooled to 0 °C and added allyl bromide (86.4 µL, 1.00 mmol) and the reaction mixture was stirred at 0 °C for 1 h. SiO_2 (2.5 g) was added and the mixture was concentrated *in vacuo* and purified directly by flash column chromatography (EtOAc/petroleum ether 2:98) to give the title compound as a 69:22:9 mixture of the *R*-allyl, *S*-allyl, and diallyl products, respectively (158 mg, 62%, 64% purity). $\boldsymbol{R_f}$ = 0.52 (EtOAc/petroleum ether 1:19)

(2*S,3*R**,5*S**)-5-Allyl-3-((*tert*-butyldimethylsilyl)oxy)-2-methyl-2-(prop-2-yn-1-yl)cyclopentan-1-one (*anti*-3.66)**

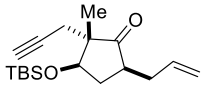

To a solution of CuI (59.4 mg, 0.312 mmol) in anhydrous THF (4 mL) at -78 °C was added vinylmagnesium bromide (0.7 M in THF, 0.632 mL, 0.442 mmol) and the mixture was stirred under an atmosphere of N_2 for 30 min. **3.40** (56.0 mg, 0.201 mmol) was added and the reaction mixture was stirred at -78 °C for another 30 min. Then, the mixture was allowed to warm to 22 °C, added SiO_2 (900 mg), concentrated *in vacuo*, and purified directly by flash column chromatography (EtOAc/petroleum 2:98) to give the title compound as a 3:1 mixture of the *S*-allyl and *R*-allyl (55.6 mg, 89%). $\boldsymbol{R_f}$ = 0.52 (EtOAc/petroleum ether 1:19)

(2*S,3*R**)-5,5-Diallyl-3-((*tert*-butyldimethylsilyl)oxy)-2-methyl-2-(prop-2-yn-1-yl)cyclopentan-1-one (3.67)**

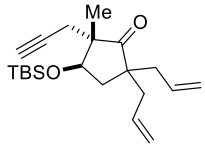

To an ice-cooled solution of **3.28** (117 mg, 0.439 mmol) in anhydrous THF (9 mL) was added NaH (60% in mineral oil, 70.3 mg, 1.76 mmol) and the suspension was stirred under an atmosphere of N_2 at 0 °C for 1 h. Then, allyl bromide (0.150 mL, 1.76 mmol) was added and the reaction mixture was stirred at 22 °C under an atmosphere of N_2 for 16 h. The mixture was concentrated *in vacuo* and purified directly by flash column chromatography (EtOAc/petroleum ether 3:197) to give the title compound as a colorless oil (57.0 mg, 38%).

$\boldsymbol{R_f}$ = 0.32 (EtOAc/petroleum ether 2:98); **^{1}H NMR** (400 MHz, $CDCl_3$) δ 5.79 – 5.61 (m, 2H), 5.15 – 5.00 (m, 4H), 4.53 (dd, *J* = 9.1, 6.6 Hz, 1H), 2.47 (dd, *J* = 16.9, 2.6 Hz, 1H), 2.33 (ddt, *J* = 13.8, 6.7, 1.3 Hz, 1H), 2.26 – 2.11 (m, 4H), 2.02 – 1.90 (m, 2H), 1.81 (dd, *J* = 13.0, 9.1 Hz, 1H), 0.92 (s, 3H), 0.90 (s, 9H), 0.10 (s, 6H); **^{13}C NMR** (101 MHz, $CDCl_3$) δ 220.5, 133.9,

133.7, 118.9, 118.8, 81.4, 71.8, 70.8, 53.8, 52.1, 40.4, 39.5, 37.5, 25.9 (3C), 24.8, 18.2, 16.9, -4.3, -4.7; **IR** (neat) cm^{-1}: 3311 (m, C≡C–H), 1738 (s, C=O), 1639 (m, C=C), 1462 (s, C=CH_2); **HRMS** (ESI) calcd for $C_{21}H_{35}O_2Si$ $[M+H]^+$ 347.2401, found 347.2414.

(1*S,6*R**,8*R**)-8-Hydroxy-1-methyl-3-vinylbicyclo[4.2.1]non-3-en-9-one (3.68)**

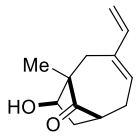

To a solution of **3.66** (61.2 mg, 64% purity, 0.128 mmol) in anhydrous PhMe (40 mL) was added Hoveyda-Grubbs 2nd generation catalyst (12.5 mg, 20.0 µmol) and the reaction mixture was stirred under an ethylene atmosphere at reflux for 3 h. The mixture was concentrated *in vacuo* and filtered through a short plug of silica. The crude RCEYM product was dissolved in anhydrous THF (3 mL) and added TBAF (1.0 M in THF, 0.103 mL, 0.103 mmol), and the reaction mixture was stirred at 22 °C for 2 h. The mixture was concentrated *in vacuo* and purified directly by flash column chromatography (EtOAc/petroleum ether 1:2) to give the title compound as a colorless oil (8.0 mg, 33%)
R_f = 0.45 (EtOAc/petroleum ether 1:1); **^{1}H NMR** (600 MHz, $CDCl_3$) δ 6.30 (dd, *J* = 17.5, 11.0 Hz, 1H), 5.69 (dd, *J* = 6.6, 3.2 Hz, 1H), 5.06 (d, *J* = 17.5 Hz, 1H), 4.93 (d, *J* = 11.0 Hz, 1H), 4.06 (dd, *J* = 6.9, 2.4 Hz, 1H), 2.77 (dt, *J* = 9.0, 4.0 Hz, 1H), 2.47 (d, *J* = 18.4 Hz, 1H), 2.43 – 2.32 (m, 2H), 2.15 (ddd, *J* = 14.5, 6.9, 4.0 Hz, 1H), 2.03 – 1.98 (m, 1H), 1.96 (ddd, *J* = 14.5, 9.0, 2.5 Hz, 1H), 1.61 (br. s, 1H), 1.22 (s, 3H); **^{13}C NMR** (151 MHz, $CDCl_3$) δ 206.3, 142.8, 135.7, 129.4, 110.9, 76.3, 53.3, 44.6, 37.3, 35.5, 33.3, 17.1; **IR** (neat) cm^{-1}: 3397 (br., O–H), 1733 (s, C=O); **HRMS** (ESI) calcd for $C_{12}H_{17}O_2$ $[M+H]^+$ 193.1223, found 193.1229.

(((1*R,2*S**)-2-Methyl-2-(prop-2-yn-1-yl)cyclopent-3-ene-1,3-diyl)bis(oxy))bis(tert-butyldimethylsilane) (3.71)**

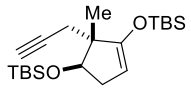

To a solution of **3.28** (100 mg, 0.375 mmol) in anhydrous MeCN (4 mL) was added TBSOTf (0.129 mL, 0.563 mmol) and Et_3N (0.157 mL, 1.13 mmol) and the reaction mixture was stirred under an atmosphere of N_2 at reflux for 2 h. The mixture was concentrated *in vacuo* and purified directly by flash column chromatography (heptane) to give the title compound as a colorless oil (148 mg, >95%).
R_f = 0.95 (EtOAc/heptane 1:9); **^{1}H NMR** (400 MHz, $CDCl_3$) δ 4.40 – 4.31 (m, 2H), 2.40 (ddd, *J* = 14.2, 7.5, 2.7 Hz, 1H), 2.34 – 2.13 (m, 2H), 2.13 – 2.02 (m, 1H), 1.91 (t, *J* = 2.7 Hz, 1H), 0.95 (s, 3H), 0.93 (s, 9H), 0.89 (s, 9H), 0.16 (d, *J* = 4.1 Hz, 6H), 0.07 (d, *J* = 5.3 Hz, 6H).

Syn Building Block Chemistry

O-(Mesitylenesulfonyl)hydroxylamine (3.74)

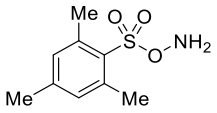

Following a reported procedure.[361] To an ice-cooled solution of ethyl *N*-hydroxyacetamidate (2.88 g, 27.9 mmol) and Et_3N (3.69 mL, 26.5 mmol) in anhydrous DMF (14 mL) was added 2-mesitylenesulfonyl chloride (6.10 g, 27.9 mmol) portion wise and the reaction mixture was stirred under an atmosphere of N_2 at 0 °C for 30 min. The mixture was diluted with Et_2O (250 mL) and washed with H_2O (5 ×125 mL). The organic layer was dried over $MgSO_4$, filtered, and concentrated *in vacuo* to give crude ethyl-*O*-(mesitylenesulfonyl)acetohydroxamate (5.02 g) that was used directly in the next step without further purification.

To an ice-cooled solution of the crude ethyl-*O*-(mesitylenesulfonyl)acetohydroxamate (5.02 g) in dioxane (7 mL) was added perchloric acid (70%, 2.20 mL) drop wise and the reaction mixture was stirred at 0 °C for 15 min. The mixture was poured into ice water (250 mL) and extracted with Et_2O (3 × 75 mL). The combined organic layers were washed with brine (2 × 125 mL), dried/neutralized over K_2CO_3, and filtered. The organic layer was concentrated to a volume of 20 mL and then poured into ice-cold petroleum ether (50 mL). After crystallization, the title compound was collected by filtration as a white crystalline solid (1.50 g, 27%).

R_f = 0.32 (EtOAc/hexane 1:4); **m.p.**: 93–95 °C (Lit. 90–91 °C); **^{1}H NMR** (400 MHz, $CDCl_3$) δ 6.99 (dd, *J* = 1.4, 0.7 Hz, 2H), 5.74 (s, 2H), 2.64 (s, 6H), 2.32 (s, 3H); **^{13}C NMR** (101 MHz, $CDCl_3$) δ 143.9, 141.1, 131.8, 129.2, 22.9, 21.2; **IR** (neat) cm^{-1}: 3469, 3198 (m, N–H stretch), 1603 (s, N–H bend), 1170 (s, S=O). Spectroscopic data were consistent with those reported in the literature.[362]

(5*S**,6*S**)-5-((*tert*-Butyldimethylsilyl)oxy)-6-methyl-6-(prop-2-yn-1-yl)piperidin-2-one (3.19)

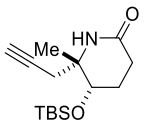

To an ice-cooled solution of **3.27** (827 mg, 3.10 mmol) in anhydrous CH_2Cl_2 (10 mL) was added MSH (1.49 g, 6.92 mmol) and the reaction mixture was stirred under an atmosphere of N_2 at 0 °C for 20 min. Cooling was removed and the mixture was stirred for another 18 h at 22 °C. Then, $BF_3{\cdot}Et_2O$ (1.23 mL, 9.93 mmol) was added and the mixture was stirred for 1 h. The mixture was diluted with CH_2Cl_2 (150 mL) and washed with sat. aq. $NaHCO_3$ (2 × 200 mL). The combined aqueous phases were extracted with CH_2Cl_2 (2 × 200 mL) and the combined organic layers were dried over $MgSO_4$, filtered, and concentrated *in vacuo*. The crude product was purified by flash column chromatography (EtOAc/petroleum ether 2:1) to give the title compound as a white solid (735 mg, 84%, 81:19 mixture of isomers, 70% purity).

R_f = 0.26 (EtOAc/petroleum ether 2:1); **^{1}H NMR** (400 MHz, $CDCl_3$) δ 6.32 (br. s, 1H), 3.80 (dd, *J* = 6.9, 2.8 Hz, 1H), 2.69 – 2.47 (m, 2H), 2.45 – 2.20 (m, 2H), 2.08 (t, *J* = 2.7 Hz, 1H), 1.99 – 1.82 (m, 2H), 1.34 (s, 3H), 0.89 (s, 9H), 0.09 (s, 6H); **^{13}C NMR** (101 MHz, $CDCl_3$) δ 171.2, 79.9, 72.4, 70.8, 58.2, 28.1, 27.1, 26.6, 25.9 (3C), 25.3, 18.1, -4.2, -4.9; **IR** (neat) cm^{-1}: 3252 (s, C≡C–H), 1663 (s, C=O); **HRMS** (ESI) calcd for $C_{15}H_{28}NO_2Si$ $[M+H]^+$ 282.1884, found 282.1885.

(5*S,6*S**)-5-Hydroxy-6-methyl-6-(prop-2-yn-1-yl)tetrahydro-2*H*-pyran-2-one (3.76)**

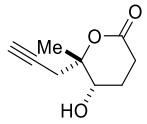

To a solution of **3.27** (110 mg, 0.413 mmol) in anhydrous CH_2Cl_2 was added $KHCO_3$ (82.7 mg, 0.826 mmol) and mCPBA (<77%, 1.02 g, 4.13 mmol) and the reaction mixture was stirred under an atmosphere of N_2 at reflux for 40 h. The mixture was concentrated *in vacuo* and filtered through a short plug of silica. The crude Baeyer–Villiger oxidation product was dissolved in anhydrous THF (5 mL), added TBAF (1.0 M in THF, 0.657 mL, 0.657 mmol), and stirred under an atmosphere of N_2 at 22 °C for 2 h. The mixture was concentrated *in vacuo* and purified directly by flash column chromatography (EtOAc/petroleum ether/AcOH 50:50:2) to give the title compound as a colorless oil (20.2 mg, 29%).

R_f = 0.36 (EtOAc/petroleum ether 1:1); **^{1}H NMR** (400 MHz, $CDCl_3$) δ 4.56 (dd, *J* = 7.9, 7.2 Hz, 1H), 2.64 – 2.50 (m, 4H), 2.29 (dddd, *J* = 12.9, 9.9, 9.2, 7.9 Hz, 2H), 2.18 (dddd, *J* = 12.9, 9.9, 7.2, 4.5 Hz, 1H), 2.08 (t, *J* = 2.7 Hz, 1H), 1.27 (s, 3H); **^{13}C NMR** (101 MHz, $CDCl_3$) δ 177.2, 83.6, 79.8, 72.4, 71.6, 30.2, 29.0, 22.1, 21.7; **IR** (neat) cm^{-1}: 3452 (br., O–H), 3285 (s, C≡C–H), 1754 (s, C=O); **HRMS** (ESI) calcd for $C_9H_{13}O_3$ $[M+H]^+$ 169.0859, found 235.0865.

(8*S,8a*S**)-8-((*tert*-Butyldimethylsilyl)oxy)-8a-methyl-6,7,8,8a-tetrahydroindolizin-5(1*H*)-one (3.20)**

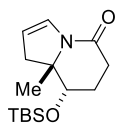

$InCl_3$ (224 mg, 1.01 mmol) was introduced into a Schlenk flask and heated with a heat gun under vacuum for 2 min. After cooling to 22 °C, anhydrous THF (3 mL) was added and the mixture was stirred for 10 min and cooled to -65 °C. DIBAL-H (1.2 M in PhMe, 0.755 mL, 0.906 mmol) was added dropwise and the mixture was stirred at -65 °C for 40 min. Compound **3.19** (170 mg, 0.604 mmol) was then added followed by Et_3B (1.0 M in THF, 0.393 mL, 0.393 mmol) and the mixture was stirred at -70 °C for 4 h. A solution of I_2 (920 mg, 3.62 mmol) in anhydrous THF (1.5 mL) was added and the mixture was stirred another 1 h at -70°C. The mixture was then poured onto sat. aq. $NaHCO_3$ (20 mL) and added $Na_2S_2O_3$ until complete decoloration. The aqueous phase was extracted with EtOAc (5 × 20 mL) and the combined organic layers were dried over $MgSO_4$, filtered, and concentrated *in vacuo* to give the crude allyl iodide.

CuI (46.0 mg, 0.241 mmol) and Cs_2CO_3 (236 mg, 0.724 mmol) were introduced into a Schlenk flask and kept under vacuum for 1 h. Under an atmosphere of N_2, anhydrous PhMe (4 mL) was added followed by *N,N'*-dimethylethane-1,2-diamine (42.6 mg, 0.483 mmol) and the crude allyl iodide and the mixture was stirred under an atmosphere of N_2 at 85 °C for 24 h. SiO_2 (3 g) was added and the mixture was concentrated *in vacuo* and purified directly by flash column chromatography (EtOAc/petroleum ether 1:1) to give the title compound as a white solid (86.8 mg, 73%).

***R*f** = 0.50 (EtOAc/petroleum ether 3:1); **^{1}H NMR** (400 MHz, $CDCl_3$) δ 6.92 – 6.81 (m, 1H), 5.13 (dt, *J* = 5.0, 2.7 Hz, 1H), 3.89 (t, *J* = 2.7 Hz, 1H), 3.08 (dt, *J* = 15.5, 2.7 Hz, 1H), 2.49 (ddd, *J* = 18.5, 10.0, 8.7 Hz, 1H), 2.34 (ddd, *J* = 18.5, 8.7, 1.7 Hz, 1H), 2.19 – 2.02 (m, 2H), 1.85 (dddd, *J* = 14.4, 8.7, 3.5, 1.7 Hz, 1H), 1.22 (s, 3H), 0.84 (s, 9H), 0.07 (d, *J* = 4.5 Hz, 6H); **^{13}C NMR** (101 MHz, $CDCl_3$) δ 166.6, 128.2, 109.3, 69.0, 66.6, 40.3, 25.8 (3C), 25.7, 25.6, 25.4, 18.2, -4.2, -4.9. **IR** (neat) cm^{-1}: 1664 (s, C=O), 1629 (s, C=C); **HRMS** (ESI) calcd for $C_{15}H_{28}NO_2Si$ $[M+H]^+$ 282.1884, found 282.1882

(8*S,8a*S**)-8-Hydroxy-8a-methyl-6,7,8,8a-tetrahydroindolizin-5(1*H*)-one (3.78)**

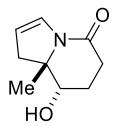

To a solution of **3.20** (36.6 mg, 0.128 mmol) in anhydrous THF (2.5 mL) was added TBAF (1.0 M in THF, 0.192 mL, 0.192 mmol) and the reaction mixture was stirred under an atmosphere of N_2 at 22 °C for 1 h. The mixture was concentrated *in vacuo* and purified directly by flash column chromatography (EtOAc/MeOH 19:1) to give the title compound as a white amorphous solid (21.2 mg, 98%).

***R*f** = 0.25 (EtOAc/MeOH 19:1); **^{1}H NMR** (400 MHz, CD_3OD) δ 6.83 (p, *J* = 2.0 Hz, 1H), 5.36 (dt, *J* = 5.1, 2.6 Hz, 1H), 3.94 (t, *J* = 3.0 Hz, 1H), 3.24 (dt, *J* = 16.1, 2.6 Hz, 1H), 2.56 – 2.33 (m, 2H), 2.33 – 2.20 (m, 2H), 1.96 (dddd, *J* = 14.5, 8.7, 3.0, 2.0 Hz, 1H), 1.29 (s, 3H); **^{13}C NMR** (101 MHz, CD_3OD) δ 169.1, 128.1, 112.7, 68.2, 67.7, 40.7, 26.0, 25.7, 25.7; **IR** (neat) cm^{-1}: 3375 (br., O–H), 1621 (m, C=O), 1592 (s, C=C); **HRMS** (ESI) calcd for $C_{18}H_{32}NO_2Si$ $[M+H]^+$ 168.1019, found 168.1026.

(5*S,6*S**)-1-Allyl-5-((*tert*-butyldimethylsilyl)oxy)-6-methyl-6-(prop-2-yn-1-yl)piperidin-2-one (3.79)**

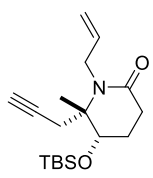

To an ice-cooled solution of **3.19** (343 mg, 70% purity, 1.22 mmol) in anhydrous DMF (12 mL) was added NaH (60% in mineral oil, 58.5 mg, 1.46 mmol) and the mixture was stirred at under an atmosphere of N_2 at 22 °C for 30 min. Then, allyl bromide (0.126 mL, 1.46 mmol) was added and the reaction mixture was stirred for another 2 h. The mixture was diluted with EtOAc (200 mL) and was washed with H_2O (2 × 150 mL) and brine (1 × 150 mL), dried over $MgSO_4$,

filtered, and concentrated *in vacuo*. The crude product was purified by flash column chromatography (EtOAc/petroleum ether 1:2) to give the title compound as a colorless oil (22.6 mg, 76%).

***R*f** = 0.32 (EtOAc/petroleum ether 2:3); **^{1}H NMR** (400 MHz, $CDCl_3$) δ 5.85 (ddt, *J* = 17.3, 10.3, 4.9 Hz, 1H), 5.20 – 5.01 (m, 2H), 4.16 (ddt, *J* = 16.5, 4.9, 2.0 Hz, 1H), 4.00 – 3.85 (m, 2H), 2.72 – 2.52 (m, 3H), 2.39 (dt, *J* = 17.9, 6.7 Hz, 1H), 2.09 – 1.87 (m, 3H), 1.34 (s, 3H), 0.90 (s, 9H), 0.12 (s, 3H), 0.11 (s, 3H); **^{13}C NMR** (151 MHz, $CDCl_3$) δ 169.9, 135.2, 115.5, 81.2, 71.9, 71.8, 63.1, 44.8, 28.3, 26.1, 25.9 (3C), 24.9, 24.6, 18.2, -4.0, -5.0; **IR** (neat) cm^{-1}: 3296 (s, C≡C–H), 1638 (m, C=C), 1620 (s, C=O); **HRMS** (ESI) calcd for $C_{18}H_{32}NO_2Si$ $[M+H]^+$ 322.2197, found 322.2193.

(1*S**,9a*S**)-1-Hydroxy-9a-methyl-8-vinyl-1,2,3,6,9,9a-hexahydro-4*H*-quinolizin-4-one (3.80)

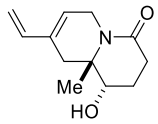

To a solution of **3.79** (55.0 mg, 0.171 mmol) in anhydrous CH_2Cl_2 (34 mL) was added Hoveyda-Grubbs 2nd generation catalyst (10.7 mg, 17.1 µmol) and the reaction mixture was stirred under an ethylene atmosphere at 22 °C for 2 h. The mixture was concentrated *in vacuo* and the crude RCEYM product was dissolved in anhydrous THF (4 mL). TBAF (1.0 M in THF, 0.257 mL, 0.257 mmol) was added and the reaction mixture was stirred at 22 °C for 2 h. The mixture was concentrated *in vacuo* and purified directly by flash column chromatography (EtOAc/MeOH 19:1) to give the title compound as a colorless oil (29.7 mg, 84%).

***R*f** = 0.39 (EtOAc/MeOH 9:1); **^{1}H NMR** (400 MHz, CD_3OD) δ 6.47 (dd, *J* = 17.5, 10.8 Hz, 1H), 5.75 (dt, *J* = 4.9, 3.1 Hz, 1H), 5.19 (d, *J* = 17.5 Hz, 1H), 5.03 (d, *J* = 10.8 Hz, 1H), 4.75 (dt, *J* = 20.2, 3.1 Hz, 1H), 3.82 (dd, *J* = 8.1, 3.0 Hz, 1H), 3.61 (d, *J* = 20.2 Hz, 1H), 2.69 – 2.54 (m, 2H), 2.43 – 2.32 (m, 1H), 2.19 (dt, *J* = 16.9, 1.4 Hz, 1H), 2.09 – 1.88 (m, 2H), 1.33 (s, 3H); **^{13}C NMR** (101 MHz, CD_3OD) δ 171.5, 139.7, 134.5, 124.0, 112.1, 72.4, 59.8, 41.2, 31.5, 29.6, 25.1, 24.1; **IR** (neat) cm^{-1}: 3370 (br., O–H), 1611 (s, C=O), 1600 (s, C=C) , 1408 (s, O–H); **HRMS** (ESI) calcd for $C_{12}H_{18}NO_2$ $[M+H]^+$ 208.1332, found 208.1328.

(3a*R**,9*S**,9a*S**)-9-((*tert*-Butyldimethylsilyl)oxy)-9a-methyl-3a,4,8,9,9a,10-hexahydrocyclopenta[*b*]quinolizine-2,6(3*H*,7*H*)-dione (3.140)

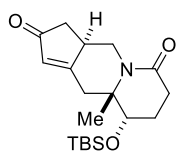

To a solution of $Co_2(CO)_8$ (95.7 mg, 0.280 mmol) in anhydrous CH_2Cl_2 (8 mL) was added a solution of **3.79** (72.0 mg, 0.224 mmol) in anhydrous CH_2Cl_2 (2 mL) and the reaction mixture was stirred under an atmosphere of N_2 at 22 °C for 2 h. Then, 4-methylmorpholine *N*-oxide (262 mg, 2.24 mmol) was added portion wise and the mixture was stirred for another 18 h. Violet Co precipitate was removed by filtration through a short plug of silica (washed with CH_2Cl_2/MeOH 19:1) and the

filtrate was concentrated *in vacuo*. The crude product was purified by flash column chromatography (EtOAc/petroleum ether 2:1) to give the title compound as a colorless amorphous solid (50.1 mg, 95%).

R_f = 0.23 (EtOAc/petroleum ether 2:1); **^{1}H NMR** (400 MHz, $CDCl_3$) δ 6.01 (t, *J* = 1.7 Hz, 1H), 5.09 (dd, *J* = 13.0, 6.6 Hz, 1H), 3.78 (dd, *J* = 7.0, 2.4 Hz, 1H), 2.91 (d, *J* = 13.6 Hz, 1H), 2.81 – 2.62 (m, 2H), 2.61 – 2.32 (m, 4H), 2.09 – 1.96 (m, 2H), 1.89 (dq, *J* = 13.0, 6.2 Hz, 1H), 1.23 (s, 3H), 0.92 (s, 9H), 0.13 (s, 3H), 0.12 (s, 3H); **^{13}C NMR** (101 MHz, $CDCl_3$) δ 207.5, 179.5, 169.2, 130.3, 72.8, 62.1, 43.8, 40.6, 39.0, 37.8, 28.4, 25.9 (3C), 25.1, 23.7, 18.2, -4.1, -4.8; **IR** (neat) cm^{-1}: 1704 (s, C=O), 1624 (m, C=O); **HRMS** (ESI) calcd for $C_{19}H_{32}NO_3Si$ $[M+H]^+$ 350.2146, found 350.2159.

(3a*R,9*S**,9a*S**)-9-Hydroxy-9a-methyl-3a,4,8,9,9a,10-hexahydrocyclopenta[*b*]quinolizine-2,6(3*H*,7*H*)-dione (3.81)**

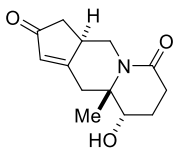

To a solution of **3.140** (28.0 mg, 80.1 µmol) in anhydrous THF (3 mL) was added TBAF (1.0 M in THF, 0.120 mL, 0.120 mmol) and the reaction mixture was stirred under an atmosphere of N_2 at 22 °C for 2 h. The mixture was concentrated *in vacuo* and purified directly by flash column chromatography (EtOAc/MeOH 9:1) to give the title compound as a colorless oil (17.2 mg, 91%).

R_f = 0.22 (EtOAc/MeOH 9:1); **^{1}H NMR** (600 MHz, CD_3OD) δ 6.07 (t, *J* = 1.7 Hz, 1H), 4.99 (dd, *J* = 13.1, 6.7 Hz, 1H), 3.82 (dd, *J* = 7.6, 2.7 Hz, 1H), 3.03 (d, *J* = 13.8 Hz, 1H), 2.88 – 2.82 (m, 1H), 2.70 (d, *J* = 13.8 Hz, 1H), 2.69 – 2.54 (m, 3H), 2.44 – 2.36 (m, 1H), 2.15 – 2.05 (m, 2H), 2.02 – 1.94 (m, 1H), 1.31 (d, *J* = 0.8 Hz, 3H); **^{13}C NMR** (151 MHz, CD_3OD) δ 210.5, 183.0, 171.9, 130.6, 72.1, 63.1, 44.6, 41.7, 39.7, 37.8, 29.4, 25.3, 23.7; **IR** (neat) cm^{-1}: 3377 (br., O–H), 1670 (s, C=O), 1625 (s, C=O), 1412 (s. O–H); **HRMS** (ESI) calcd for $C_{13}H_{18}NO_3$ $[M+H]^+$ 236.1281, found 236.1277.

(5*S,6*S**)-5-Hydroxy-6-methyl-6-(prop-2-yn-1-yl)piperidin-2-one (3.82)**

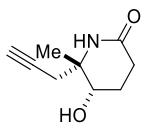

To a solution of **3.19** (31.5 mg, 0.112 mmol) in anhydrous THF (2.5 mL) was added TBAF (1.0 M in THF, 0.168 mL, 0.168 mmol) and the reaction mixture was stirred at 22 °C for 1 h. The mixture was concentrated *in vacuo* and purified directly by flash column chromatography (EtOAc/MeOH 19:1) to give the title compound as a colorless oil (17.5 mg, 94%).

R_f = 0.36 (EtOAc/MeOH 9:1); **^{1}H NMR** (400 MHz, CD_3OD) δ 3.84 (dd, *J* = 6.3, 4.3 Hz, 1H), 2.54 (d, *J* = 2.7 Hz, 2H), 2.55 – 2.43 (m, 1H), 2.43 (t, *J* = 2.7 Hz, 1H), 2.32 (dt, *J* = 18.2, 6.3 Hz, 1H), 2.06 – 1.97 (m, 2H), 1.36 (s, 3H); **^{13}C NMR** (101 MHz, CD_3OD) δ 174.2, 80.9, 72.8,

70.0, 58.6, 28.1, 27.9, 26.5, 25.6; **IR** (neat) cm^{-1}: 3360 (br. O–H), 3272 (s. N–H), 1627 (s, C=O); **HRMS** (ESI) calcd for $C_9H_{14}NO_2$ $[M+H]^+$ 168.1019, found 168.1021.

(3a*R,4*S**,6a*R**)-4-((*tert*-Butyldimethylsilyl)oxy)-2,3a-dimethyloctahydrocyclopenta[*b*] pyrrole (3.89)**

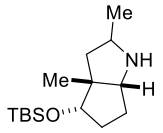

To a solution of **3.27** (111 mg, 0.417 mmol) in anhydrous EtOH (3.6 mL) was added AcOH (0.4 mL) and allylamine (0.312 mL, 4.17 mmol) and the reaction mixture was subjected to µW heating at 140 °C for 20 min. The mixture was cooled to 0 °C and added $NaBH_4$ (31.6 mg, 0.834 mmol). After 1 h, cooling was removed and the mixture was stirred another 15 h. SiO_2 (800 mg) was added and the mixture was concentrated *in vacuo* and purified by flash column chromatography (EtOAc/petroleum ether/Et_3N 4:96:2) to give the product as a colorless oil (19.0 mg, 15%).

***R*f** = 0.31 (EtOAc/petroleum ether/ Et_3N 5:95:2); **^{1}H NMR** (400 MHz, $CDCl_3$) δ 5.92 (dddd, *J* = 17.3, 10.2, 7.6, 5.9 Hz, 1H), 5.15 (dq, *J* = 17.3, 1.6 Hz, 1H), 5.07 (dtt, *J* = 10.2, 2.2, 1.4 Hz, 1H), 3.53 (dd, *J* = 10.4, 5.9 Hz, 1H), 3.39 (ddt, *J* = 14.1, 5.9, 1.4 Hz, 1H), 2.99 (ddt, *J* = 14.1, 7.6, 1.1 Hz, 1H), 2.69 – 2.56 (m, 1H), 2.56 – 2.48 (m, 1H), 1.79 – 1.66 (m, 2H), 1.58 (dtt, *J* = 11.7, 5.9, 1.1 Hz, 1H), 1.44 (dd, *J* = 13.2, 6.5 Hz, 1H), 1.39 – 1.29 (m, 1H), 1.25 – 1.19 (m, 1H), 1.07 (d, *J* = 5.9 Hz, 3H), 1.05 (s, 3H), 0.87 (s, 9H), 0.02 (s, 6H).

Methyl (*E*)-2-((3a*S,6a*S**)-3a-methyl-4-oxohexahydro-2*H*-cyclopenta[*b*]furan-2-ylidene) acetate (3.94)**

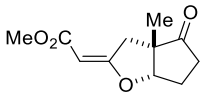

To a solution of $Pd(CH3CN)_2Cl_2$ (30.2 mg, 0.117 mmol) and *p*-benzoquinone (277 mg, 2.57 mmol) in anhydrous MeOH (30 mL) was introduced a CO atmosphere. The mixture was cooled to -50 °C and then added a solution of *syn*-**3.1** (355 mg, 2.33 mmol) in anhydrous MeOH (15 mL) dropwise. The reaction mixture was stirred under a CO atmosphere at -50 °C for 16 h. The mixture was allowed to warm to 22 °C then diluted with CH_2Cl_2 (200 mL). The mixture was washed with 1 M NaOH (1 × 200 mL), dried over $MgSO_4$, filtered and concentrated *in vacuo*. The crude product was purified by flash column chromatography (EtOAc/petroleum ether 1:4) to give the title compound as a colorless oil (160 mg, 33%).

***R*f** = 0.40 (EtOAc/petroleum ether 3:7); **^{1}H NMR** (600 MHz, $CDCl_3$) δ 5.26 (dd, *J* = 2.3, 1.5 Hz, 1H), 4.72 (dd, *J* = 4.2, 1.0 Hz, 1H), 3.67 – 3.62 (m, 4H), 2.86 (dd, *J* = 18.9, 2.3 Hz, 1H), 2.43 – 2.34 (m, 3H), 2.18 – 2.10 (m, 1H), 1.22 (s, 3H); **^{13}C NMR** (151 MHz, $CDCl_3$) δ 219.4, 174.0, 168.4, 91.0, 90.6, 54.2, 51.0, 42.0, 34.5, 25.0, 18.0; **IR** (neat) cm^{-1}: 1741 (s, C=O), 1701 (s, C=O), 1637 (s, C=C); **HRMS** (ESI) calcd for $C_{11}H_{15}O_4$ $[M+H]^+$ 211.0965, found 211.0972.

(1*S,2*S**)-2-Methyl-3-oxo-2-(prop-2-yn-1-yl)cyclopentyl acrylate (3.95)**

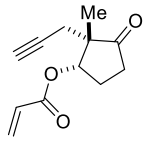

To an ice-cooled solution of *syn*-**3.1** (136 mg, 0.894 mmol), acrylic acid (82.8 µL, 1.21 mmol), and DMAP (16.4 mg, 0.134 µmol) in anhydrous CH_2Cl_2 (9 mL) was added DCC (249 mg, 1.21 mmol) and the reaction mixture was stirred under an atmosphere of N_2 at 22 °C for 16 h. Then, precipitate was filtered off and the mixture was concentrated *in vacuo* and purified by flash column chromatography (EtOAc/petroleum ether 1:8) to give the title compound as a colorless oil (93.7 mg, 51%).

***R*$_f$** = 0.42 (EtOAc/petroleum ether 1:4); **^{1}H NMR** (400 MHz, $CDCl_3$) δ 6.39 (dd, *J* = 17.3, 1.4 Hz, 1H), 6.10 (dd, *J* = 17.3, 10.5 Hz, 1H), 5.86 (dd, *J* = 10.5, 1.4 Hz, 1H), 5.32 (dd, *J* = 4.5, 2.1 Hz, 1H), 2.49 – 2.38 (m, 4H), 2.31 (dddd, *J* = 14.8, 10.5, 8.6, 4.5 Hz, 1H), 2.13 (dddd, *J* = 14.8, 7.5, 5.7, 2.1 Hz, 1H), 1.93 (t, *J* = 2.7 Hz, 1H), 1.20 (s, 3H); **^{13}C NMR** (101 MHz, $CDCl_3$) δ 218.0, 165.2, 131.5, 128.3, 80.1, 78.6, 70.4, 52.0, 34.1, 25.6, 21.3, 20.2;
IR (neat) cm^{-1}: 3279 (m, C≡C–H), 1743 (s, C=O), 1720 (s, C=O), 1636 (s, C=C); **HRMS** (ESI) calcd for $C_{12}H_{15}O_3$ $[M+H]^+$ 207.1016, found 207.1016.

(3*R,8a*S**,11a*S**)-8a-Methyl-3,4,5,8,8a,10,11,11a-octahydro-3,7-methanocyclopenta [*b*]oxecine-2,9-dione (3.97)**

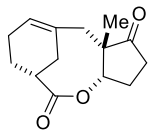

To a solution of **3.96** (38.0 mg, 0.184 mmol) in anhydrous PhMe (37 mL) was added Hoveyda-Grubbs 2nd generation catalyst (11.6 mg, 18.4 µmol) and the reaction mixture was stirred under an ethylene atmosphere at reflux for 4 h. The mixture was concentrated *in vacuo* and purified directly by flash column chromatography (EtOAc/petroleum ether 1:8) to give the title compound as a colorless oil (37.5 mg, 87%).

***R*$_f$** = 0.42 (EtOAc/petroleum ether 1:4); **^{1}H NMR** (400 MHz, $CDCl_3$) δ 5.70 (ddd, *J* = 8.0, 3.8, 1.6 Hz, 1H), 5.08 (t, *J* = 2.9 Hz, 1H), 3.11 (dt, *J* = 14.2, 1.6 Hz, 1H), 2.99 – 2.90 (m, 1H), 2.44 – 2.36 (m, 2H), 2.35 – 2.15 (m, 4H), 2.15 – 2.05 (m, 1H), 1.88 (d, *J* = 14.2 Hz, 1H), 1.81 – 1.68 (m, 2H), 1.55 – 1.45 (m, 1H), 0.94 (s, 3H); **^{13}C NMR** (101 MHz, $CDCl_3$) δ 219.2, 178.9, 137.8, 126.5, 85.2, 57.9, 44.0, 39.7, 38.7, 34.7, 26.0, 23.6, 23.2, 22.5; **IR** (neat) cm^{-1}: 1729 (s, C=O); **HRMS** (ESI) calcd for $C_{14}H_{19}O_3$ $[M+H]^+$ 235.1329, found 235.1334.

(1*S,2*S**)-2-Methyl-3-oxo-2-(prop-2-yn-1-yl)cyclopentyl 2-azidoacetate (3.98)**

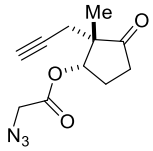

To an ice-cooled solution of *syn*-**3.1** (298 mg, 1.96 mmol), 2-azidoacetic acid (0.198 mL, 2.64 mmol), and DMAP (35.9 mg, 0.294 mmol) in anhydrous CH_2Cl_2 (10 mL) was added DCC (545 mg, 2.64 mmol) and the reaction mixture was stirred under an atmosphere of N_2 at 22 °C for 16 h. Then, precipitate was filtered off and the mixture was concentrated *in vacuo* and purified by flash column chromatography (EtOAc/petroleum ether 1:5) to give the title compound as a colorless oil (448 mg, 97%).

***R*$_f$** = 0.38 (EtOAc/petroleum ether 1:4); **^{1}H NMR** (600 MHz, $CDCl_3$) δ 5.38 (dd, *J* = 4.6, 2.0 Hz, 1H), 3.89 (q, *J* = 17.2 Hz, 2H), 2.50 – 2.42 (m, 2H), 2.38 (d, *J* = 2.7 Hz, 2H), 2.38 – 2.28 (m, 1H), 2.13 (dddd, *J* = 14.5, 8.1, 4.1, 2.0 Hz, 1H), 1.96 (t, *J* = 2.7 Hz, 1H), 1.21 (s, 3H); **^{13}C NMR** (151 MHz, $CDCl_3$) δ 217.3, 167.5, 80.2, 80.0, 70.62, 52.0, 50.5, 34.1, 25.7, 21.5 20.3; **IR** (neat) cm^{-1}: 3273 (s, C≡C–H), 2106 (s, N=N=N), 1735 (m, C=O); **HRMS** (ESI) calcd for $C_{11}H_{14}N_3O_3$ $[M+H]^+$ 236.1030, found 236.1030.

(1*S,2*S**)-2-Methyl-3-oxo-2-(prop-2-yn-1-yl)cyclopentyl 4-azidobutanoate (3.12)**

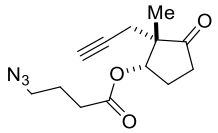

To an ice-cooled solution of *syn*-**3.1** (92.0 mg, 0.605 mmol), 4-azidobutanoic acid (97.6 mg, 0.756 mmol), and DMAP (11.1 mg, 90.7 µmol) in anhydrous CH_2Cl_2 (6 mL) was added DCC (168 mg, 0.816 mmol) and the reaction mixture was stirred under an atmosphere of N_2 at 22 °C for 16 h. Then, precipitate was filtered off and the mixture was concentrated *in vacuo* and purified by flash column chromatography (EtOAc/petroleum ether 1:5) to give the title compound as a colorless oil (142 mg, 89%).

***R*$_f$** = 0.41 (EtOAc/petroleum ether 1:4); **^{1}H NMR** (400 MHz, $CDCl_3$) δ 5.30 – 5.21 (m, 1H), 3.35 (t, *J* = 6.8 Hz, 2H), 2.46 – 2.38 (m, 4H), 2.36 (d, *J* = 2.7 Hz, 2H), 2.33 – 2.22 (m, 1H), 2.10 – 2.01 (m, 1H), 1.94 (t, *J* = 2.7 Hz, 1H), 1.90 (p, *J* = 6.8 Hz, 2H), 1.17 (s, 3H); **^{13}C NMR** (101 MHz, $CDCl_3$) δ 217.9, 171.7, 80.2, 78.6, 70.4, 51.9, 50.6, 34.1, 31.4, 25.6, 24.3, 21.3, 20.1; **IR** (neat) cm^{-1}: 2099 (s, N=N=N), 1732 (m, C=O); **HRMS** (ESI) calcd for $C_{13}H_{18}N_3O_3$ $[M+H]^+$ 264.1343, found 264.1343.

(7a*S,10a*S**)-10a-Methyl-8,9,10a,11-tetrahydrocyclopenta[*g*][1,2,3]triazolo[1,5-*d*][1,4] oxazocine-6,10(5*H*,7a*H*)-dione (3.99)**

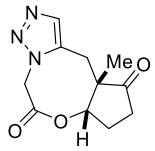

To a solution of **3.98** (43.0 mg, 0.183 mmol) in PhMe (180 mL) was added Cp*RuCl(cod) (13.9 mg, 36.6 µmol) and the reaction mixture was stirred under an atmosphere of N_2 at reflux for 16 h. The mixture was concentrated *in vacuo* and purified directly by flash column chromatography (CH_2Cl_2/MeOH 96:4) to give the title compound as a colorless oil (38.0 mg, 88%).

***R*$_f$** = 0.38 (CH_2Cl_2/MeOH 19:1); **^{1}H NMR** (400 MHz, CD_3OD) δ 7.61 (s, 1H), 5.44 (d, *J* = 17.8 Hz, 1H), 5.34 (d, *J* = 17.8 Hz, 1H), 3.92 (dd, *J* = 4.2, 2.3 Hz, 1H), 2.88 (d, *J* = 15.4 Hz, 1H), 2.80 (d, *J* = 15.4 Hz, 1H), 2.41 – 2.31 (m, 2H), 2.25 – 2.13 (m, 1H), 1.86 (dddd, *J* = 14.1, 7.6, 4.6, 2.3 Hz, 1H), 0.94 (s, 3H); **^{13}C NMR** (101 MHz, CD_3OD) δ 221.9, 169.1, 137.2, 134.6, 76.7, 54.7, 49.8, 34.1, 28.8, 24.9, 19.9; **IR** (neat) cm^{-1}: 1736 (m, C=O); **HRMS** (ESI) calcd for $C_{11}H_{12}N_3O_3$ $[M–H]^-$ 234.0884, found 234.0879.

(1*R,2*R**)-3-(Allylimino)-2-methyl-2-(prop-2-yn-1-yl)cyclopentan-1-ol (3.104)**

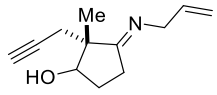

To a solution of *syn*-**3.1** (92.0 mg, 0.605 mmol) in anhydrous pyridine (6 mL) was added methanesulfonyl chloride (0.140 mL, 1.81 mmol) and the reaction mixture was stirred under an atmosphere of N_2 at 22 °C for 2 h. The mixture was diluted with 1 N HCl (60 mL) and extracted with EtOAc (2 × 60 mL). The combined organic layers were dried over $MgSO_4$, filtered, and concentrated *in vacuo*. The crude mesylate product was dissolved in anhydrous DMSO (6 mL), added allylamine (0.452 mL, 6.04 mmol), and subjected to µW heating at 100 °C for 4 h. The mixture was diluted with brine (60 mL) and extracted with EtOAc (2 × 60 mL). The combined organic layers were dried over Na_2SO_4, filtered, and concentrated *in vacuo*. The crude product was purified by flash column chromatography (EtOAc/petroleum ether 1:9) to give the product as a colorless oil (68.0 mg, 59%).

***R*$_f$** = 0.27 (EtOAc/petroleum ether 1:9); **^{1}H NMR** (400 MHz, $CDCl_3$) δ 5.94 (ddt, *J* = 17.2, 10.3, 5.3 Hz, 1H), 5.13 (dq, *J* = 17.2, 1.9 Hz, 1H), 5.07 (dq, *J* = 10.3, 1.9 Hz, 1H), 4.39 – 4.30 (m, 1H), 4.04 – 3.81 (m, 2H), 2.66 – 2.37 (m, 5H), 2.34 (td, *J* = 8.9, 4.6 Hz, 1H), 2.28 – 2.18 (m, 1H), 1.97 (t, *J* = 2.7 Hz, 1H), 1.23 (s, 3H); **^{13}C NMR** (101 MHz, $CDCl_3$) δ 179.1, 135.3, 115.1, 81.8, 69.9, 68.2, 55.6, 52.2, 30.9, 26.1, 25.7, 23.3.

(2*S,3*S**)-3-Azido-2-methyl-2-(prop-2-yn-1-yl)cyclopentan-1-one (3.18)**

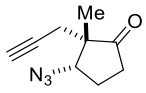

To a solution of *syn*-**3.1** (230 mg, 1.51 mmol) in anhydrous pyridine (7.5 mL) was added methanesulfonyl chloride (0.351 mL, 4.53 mmol) and the reaction mixture was stirred under an atmosphere of N_2 at 22 °C for 2 h. The mixture was diluted with 1 N HCl (75 mL) and extracted with EtOAc (2 × 75 mL). The combined organic layers were dried over $MgSO_4$, filtered, and concentrated *in vacuo*. The crude mesylate product was dissolved in anhydrous DMSO (10 mL), added NaN_3 (393 mg, 6.04 mmol), and stirred under an atmosphere of N_2 at 85 °C for 24 h. The mixture was diluted with brine (75 mL) and extracted with EtOAc (2 × 75 mL). The combined organic layers were dried over $MgSO_4$, filtered, and concentrated *in vacuo*. The crude product was purified by flash column chromatography (EtOAc/petroleum ether 1:12) to give the product as a light yellow oil (168 mg, 63%).
R_f = 0.56 (EtOAc/petroleum ether 1:4); **^{1}H NMR** (400 MHz, $CDCl_3$) δ 4.28 (dd, *J* = 9.2, 6.6 Hz, 1H), 2.54 – 2.41 (m, 2H), 2.41 – 2.32 (m, 1H), 2.31 – 2.14 (m, 2H), 2.04 (t, *J* = 2.6 Hz, 1H), 1.93 (ddt, *J* = 12.6, 9.9, 9.2 Hz, 1H), 1.00 (s, 3H); **^{13}C NMR** (101 MHz, $CDCl_3$) δ 216.3, 79.8, 71.6, 64.7, 52.6, 35.6, 25.2, 25.0, 16.9; **IR** (neat) cm^{-1}: 3295 (s, C≡C–H), 2104 (s, N=N=N), 1745 (s, C=O); **HRMS** (ESI) calcd for $C_9H_{12}N_3O$ $[M+H]^+$ 178.0975, found 178.0975.

***tert*-Butyl ((1*S**,2*S**)-2-methyl-3-oxo-2-(prop-2-yn-1-yl)cyclopentyl)carbamate (3.106)**

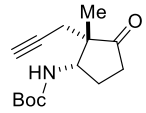

To a solution of **3.18** (444 mg, 2.51 mmol) in THF (25 mL) was added PPh_3 (1.97 g, 7.52 mmol) and the reaction mixture was stirred at 22 °C for 2 h. Water (3 mL) was added and the mixture was stirred another 16 h. Then, Et_3N (1.05 mL, 7.52 mmol) and Boc_2O (1.64 g, 7.52 mmol) were added and the mixture was stirred for 1 h. The mixture was concentrated *in vacuo* and purified directly by flash column chromatography (EtOAc/petroleum ether 1:3) to give the title compound as a white solid (369 mg, 59%).
R_f = 0.30 (EtOAc/petroleum ether 1:3); **^{1}H NMR** (400 MHz, $CDCl_3$) δ 4.63 – 4.36 (m, 2H), 2.51 – 2.28 (m, 4H), 2.20 (ddd, *J* = 18.8, 11.8, 8.9 Hz, 1H), 1.99 (s, 1H), 1.60 (qd, *J* = 11.8, 8.6 Hz, 2H), 0.93 (s, 3H); **^{13}C NMR** (101 MHz, $CDCl_3$) δ 218.0, 155.5, 80.6, 79.9, 70.9, 54.3, 51.1, 36.7, 28.5 (3C), 26.4, 25.7, 16.6; **IR** (neat) cm^{-1}: 3277 (s, C≡C–H), 3141 (s, N–H), 1738 (s, C=O), 1701 (m, C=O); **HRMS** (ESI) calcd for $C_{14}H_{22}NO_3$ $[M+H-C_5H_8O_2]^+$ 152.1070, found 152.1073 (loss of Boc).

***tert*-Butyl ((1*S**,2*S**)-4,4-diallyl-2-methyl-3-oxo-2-(prop-2-yn-1-yl)cyclopentyl)carbamate (3.108)**

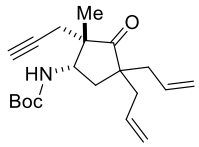

To a solution of **3.106** (124 mg, 0.493 mmol) in anhydrous DMF (10 mL) was added NaH (60% in mineral oil, 21.7 mg, 0.543 mmol) and the mixture was stirred under an atmosphere of N_2 at 22 °C for 30 min. The mixture was cooled to 0 °C, added allyl bromide (51.2 µL, 0.592 mmol), and stirred for 1 h. The mixture was diluted with EtOAc (50 mL) and washed with H_2O (2 × 50 mL) and brine (2 × 50 mL). The combined organic layer was dried over $MgSO_4$, filtered, and concentrated *in vacuo*. The crude product was purified by flash column chromatography (EtOAc/petroleum ether 1:8) to give the title compound as a colorless oil (71.0 mg, 87%). $\boldsymbol{R}_\mathbf{f}$ = 0.30 (EtOAc/petroleum ether 1:8)

***tert*-Butyl (4a*S**,7a*S**)-4a-methyl-5-oxo-4,4a,5,6,7,7a-hexahydro-1*H*-cyclopenta[*b*] pyridine-1-carboxylate (3.109) and *tert*-butyl ((1*S**,2*S**)-2-methyl-3-oxo-2-(2-oxopropyl) cyclopentyl)carbamate (3.110)**

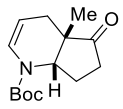

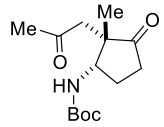

To a solution of **3.106** (47.0 mg, 0.187 mmol) and EtOH (54.6 µL, 0.935 mmol) in anhydrous DCE (2 mL) at 40 °C was added a solution of SPhosAu(MeCN)SbF_6 (8.3 mg, 9.4 µmol) in anhydrous DCE (1 mL) dropwise and the reaction mixture was stirred under an atmosphere of N_2 at 40 °C for 2 h. The mixture was concentrated *in vacuo* and purified directly by flash column chromatography (EtOAc/petroleum ether 1:9 to 2:5) to give **3.109** as a white amorphous solid (6.8 mg, 15%) and **3.110** as a colorless oil (33.2 mg, 71%).

Data for **3.109**: $\boldsymbol{R}_\mathbf{f}$ = 0.67 (EtOAc/petroleum ether 1:3); **^{1}H NMR** (600 MHz, $CDCl_3$) δ 6.76 (d, *J* = 8.2 Hz, 1H), 4.90 – 4.75 (m, 1H), 3.36 (dd, *J* = 12.2, 6.3 Hz, 1H), 2.82 (s, 1H), 2.62 – 2.51 (m, 1H), 2.28 (ddd, *J* = 21.9, 12.2, 9.6 Hz, 1H), 2.22 – 2.11 (m, 2H), 1.98 (dd, *J* = 17.3, 5.5 Hz, 1H), 1.51 (s, 9H), 0.97 (d, *J* = 0.8 Hz, 3H); **^{13}C NMR** (151 MHz, $CDCl_3$) δ 218.0, 158.1, 127.5, 103.9, 81.4, 59.5, 48.0, 35.3, 31.1, 28.5 (3C), 25.3, 14.9; **IR** (neat) cm^{-1}: 1745 (s, C=O), 1701 (m, C=O), 1641 (s, C=C); **HRMS** (ESI) calcd for $C_{14}H_{22}NO_3$ $[M+H-C_5H_8O_2]^+$ 152.1070, found 152.1071 (loss of Boc).

Data for **3.110**: $\boldsymbol{R}_\mathbf{f}$ = 0.20 (EtOAc/petroleum ether 1:3); **^{1}H NMR** (400 MHz, $CDCl_3$) δ 4.62 – 4.28 (m, 2H), 2.95 (d, *J* = 18.4 Hz, 1H), 2.79 (d, *J* = 18.4 Hz, 1H), 2.65 (ddd, *J* = 18.8, 12.5, 9.4 Hz, 1H), 2.37 (dd, *J* = 18.8, 8.7 Hz, 1H), 2.33 – 2.23 (m, 1H), 2.09 (s, 3H), 1.61 – 1.44 (m, 1H), 1.42 (s, 9H), 0.81 (s, 3H); **^{13}C NMR** (101 MHz, $CDCl_3$) δ 219.3, 206.8, 155.7, 79.6, 53.4, 50.1, 49.2, 36.2, 29.8, 28.4 (3C), 26.0, 17.0; **IR** (neat) cm^{-1}: 3353 (s, C≡C–H), 3141 (s, N–H), 1738 (s, C=O), 1701 (m, C=O); **HRMS** (ESI) calcd for $C_{14}H_{23}NO_4Na$ $[M+H]^+$ 292.1519, found 292.1515.

Ethyl 4-(((1*S,2*S**)-2-((*tert*-butyldimethylsilyl)oxy)-1-methyl-5-oxocyclopentyl)methyl) isoxazole-3-carboxylate (3.112) and ethyl 5-(((1*S**,2*S**)-2-((*tert*-butyldimethyl-silyl)oxy)-1-methyl-5-oxocyclopentyl)methyl)isoxazole-3-carboxylate (3.113)**

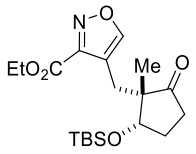

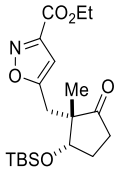

To a solution of **3.27** (147 mg, 0.552 mmol), Et_3N (0.104 mL, 0.745 mmol), and Cp*RuCl(cod) (21.0, 55.2 µmol) in anhydrous DCE (6 mL) at 80 °C was added a solution of ethyl (*Z*)-2-chloro-2-(hydroxy-imino)acetate (209 mg, 1.38 mmol) in anhydrous DCE (5 mL) dropwise over 2 h. The mixture was concentrated *in vacuo* and purified directly by flash column chromatography (EtOAc/petroleum ether 1:7) to give the title compounds as an inseparable 7:5 mixture (108 mg, 51%, brsm = 90%).

***R*f** = 0.60 (EtOAc/petroleum ether 1:4); **^{1}H NMR** (400 MHz, $CDCl_3$) δ 8.37 (d, *J* = 0.8 Hz, 1H), 6.47 (d, *J* = 0.7 Hz, 0.8H), 4.46 – 4.34 (m, 3.6H), 4.22 (t, *J* = 3.4 Hz, 0.8H), 4.10 – 4.03 (m, 1H), 3.15 – 2.91 (m, 3H), 2.79 (d, *J* = 15.1 Hz, 1H), 2.57 – 2.28 (m, 3H), 2.22 – 1.88 (m, 5H), 1.40 (td, *J* = 7.1, 0.9 Hz, 6H), 0.93 – 0.89 (m, 15H), 0.87 (s, 7H), 0.14 – 0.08 (m, 9.6H); **^{13}C NMR** (101 MHz, $CDCl_3$) δ 219.1, 218.6, 172.8, 160.9, 160.2, 159.0, 156.5, 154.3, 116.3, 104.0, 79.1, 77.5, 62.2, 62.0, 54.0, 52.5, 34.9, 33.1, 28.2, 28.1, 27.7, 25.91 (3C), 25.89 (3C), 22.5, 19.11, 19.09, 18.18, 18.16, 14.29, 14.25, -4.1, -4.2, -4.7, -4.8.

Building Block Derivatives

2-(cyclopropylmethyl)cyclopentane-1,3-dione (3.116)

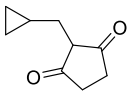

To a suspension of cyclopentane-1,3-dione (638 mg, 6.50 mmol), cyclopropane-carboxaldehyde (1.46 mL, 19.5 mmol), and Hantzsch ester (1.66 g, 6.57 mmol) in anhydrous CH_2Cl_2 (25 mL) was added L-proline (37.4 mg, 0.325 mmol) and reaction mixture was stirred at under an atmosphere of N_2 at 22 °C for 24 h. The mixture was concentrated *in vacuo* and purified by flash column chromatography (EtOAc/petroleum ether/AcOH 90:10:2) to give the title compound as a light orange solid (899 mg, 91%).

R_f = 0.38 (EtOAc/AcOH 98:2); **^{1}H NMR** (400 MHz, DMSO-d_6) δ 11.45 (s, 1H), 2.35 (s, 4H), 1.93 (d, J = 6.6 Hz, 2H), 0.88 – 0.71 (m, 1H), 0.35 – 0.19 (m, 2H), 0.06 – -0.02 (m, 2H); **^{13}C NMR** (101 MHz, DMSO-d_6) δ 115.9, 25.0, 9.9, 4.2 (2C) (4x C in cyclopentadione were not observed); **IR** (neat) cm^{-1}: 2500 (br., O–H), 1673 (s, C=O); **HRMS** (ESI) calcd for $C_9H_{13}O_2$ $[M+H]^+$ 153.0916, found 153.0918.

2-(Cyclopropylmethyl)-2-(prop-2-yn-1-yl)cyclopentane-1,3-dione (3.117)

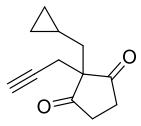

To a suspension of **3.116** (416 mg, 2.73 mmol) in H_2O (30 mL) was added NaOH (6.0 M, 0.456 mL, 2.73 mmol) and propargyl bromide (0.295 mL, 2.73 mmol) and the reaction mixture was stirred at 60 ºC for 16 h. The aqueous layer was extracted with CH_2Cl_2 (3 × 30 mL) and the combined organic layers were washed with brine (30 mL), dried over $MgSO_4$, filtered, and concentrated *in vacuo*. The crude product was purified by flash column chromatography (EtOAc/petroleum ether 1:6) to give the title compound as a colorless oil (336 mg, 65%).

R_f = 0.32 (EtOAc/petroleum ether 1:6); **^{1}H NMR** (400 MHz, $CDCl_3$) δ 2.92 – 2.67 (m, 4H), 2.41 (d, J = 2.6 Hz, 2H), 1.91 (t, J = 2.6 Hz, 1H), 1.55 (d, J = 7.1 Hz, 2H), 0.59 – 0.41 (m, 1H), 0.42 – 0.32 (m, 2H), 0.06 – -0.05 (m, 2H); **^{13}C NMR** (101 MHz, $CDCl_3$) δ 216.5 (2C), 78.9, 70.7, 60.1, 40.5, 37.1 (2C), 23.9, 6.9, 4.9 (2C); **IR** (neat) cm^{-1}: 3278 (s, C≡C–H), 1719 (s, C=O); **HRMS** (ESI) calcd for $C_{12}H_{15}O_2$ $[M+H]^+$ 191.1072, found 191.1071.

***syn*-2-(Cyclopropylmethyl)-3-hydroxy-2-(prop-2-yn-1-yl)cyclopentan-1-one (*syn*-3.118) and *anti*-2-(cyclopropylmethyl)-3-hydroxy-2-(prop-2-yn-1-yl)cyclopentan-1-one (*anti*-3.118)**

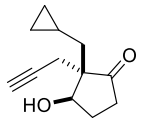

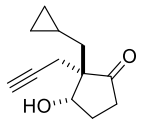

To a solution of **3.117** (320 mg, 1.68 mmol) in DME (9 mL) at -60 °C was added $NaBH_4$ (35.0 mg, 0.925 mmol) portion wise and the reaction mixture was stirred under an atmosphere of N_2 at -60 °C for 24 h. Then, 1 M aq. HCl (10 mL) was added and the mixture was allowed to warm to 22 °C. The aqueous phase was extracted with EtOAc (3 × 10 mL) and the combined organic layers were dried over $MgSO_4$, filtered and concentrated *in vacuo*. The crude products were purified by flash column chromatography (CH_2Cl_2/EtOAc 99:1 to 95:5) to give *syn*-**3.118** (62.6 mg, 19%) and *anti*-**3.118** (174.2 mg, 54%) both as colorless oils.

Data for *syn*-**3.118**: $\boldsymbol{R_f}$ = 0.37 (CH_2Cl_2/EtOAc 9:1); **^{1}H NMR** (400 MHz, $CDCl_3$) δ 4.34 (dq, *J* = 5.0, 3.0 Hz, 1H), 2.70 (dd, *J* = 17.3, 2.7 Hz, 1H), 2.56 – 2.24 (m, 4H), 2.12 (d, *J* = 3.6 Hz, 1H), 2.09 – 1.99 (m, 2H), 1.58 (dd, *J* = 14.5, 5.9 Hz, 1H), 1.43 (dd, *J* = 14.5, 7.8 Hz, 1H), 0.65 (qq, *J* = 7.9, 5.1 Hz, 1H), 0.55 – 0.39 (m, 2H), 0.18 (dtd, *J* = 7.9, 4.8, 3.5 Hz, 1H), -0.01 (dtd, *J* = 10.0, 4.8, 3.5 Hz, 1H); **^{13}C NMR** (151 MHz, $CDCl_3$) δ 219.0, 81.6, 75.5, 71.0, 57.4, 37.9, 35.0, 27.7, 19.0, 6.2, 5.0, 4.6; **IR** (neat) cm^{-1}: 3453 (br., O–H), 3303 (s, C≡C–H), 1732 (s, C=O); **HRMS** (ESI) calcd for $C_{12}H_{17}O_2$ $[M+H]^+$ 193.1229, found 193.1224.

Data for *anti*-**3.118**: $\boldsymbol{R_f}$ = 0.41 (CH_2Cl_2/EtOAc 9:1); **^{1}H NMR** (400 MHz, $CDCl_3$) δ 4.42 (ddd, *J* = 9.8, 7.0, 3.0 Hz, 1H), 2.67 (dd, *J* = 17.0, 2.6 Hz, 1H), 2.51 (ddd, *J* = 19.3, 10.0, 2.6 Hz, 1H), 2.38 – 2.23 (m, 3H), 2.23 – 2.08 (m, 1H), 2.06 (t, *J* = 2.7 Hz, 1H), 1.97 (dq, *J* = 12.5, 9.8 Hz, 1H), 1.74 (dd, *J* = 14.7, 5.4 Hz, 1H), 1.40 (dd, *J* = 14.7, 8.3 Hz, 1H), 0.71 (dtt, *J* = 13.3, 8.3, 5.1 Hz, 1H), 0.56 – 0.36 (m, 2H), 0.14 (dtd, *J* = 8.0, 4.8, 3.5 Hz, 1H), 0.06 (d, *J* = 3.2 Hz, 1H); **^{13}C NMR** (101 MHz, $CDCl_3$) δ 218.0, 81.3, 76.5, 71.5, 55.2, 35.1, 33.4, 27.1, 23.3, 5.9, 5.4, 4.8; **IR** (neat) cm^{-1}: 3452 (br., O–H), 3287 (s, C≡C–H), 1729 (s, C=O); **HRMS** (ESI) calcd for $C_{12}H_{17}O_2$ $[M+H]^+$ 193.1229, found 193.1225.

(4a*S,7a*S**)-4a-(Cyclopropylmethyl)-4a,6,7,7a-tetrahydrocyclopenta[*b*]pyran-5(4*H*)-one (3.119)**

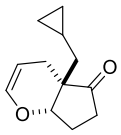

To a solution of *syn*-**3.118** (39.0 mg, 0.203 mmol), *N*-hydroxysuccinimide (11.7 mg, 0.101 mmol), $NaHCO_3$ (8.5 mg, 0.101 mmol), and Bu_4NPF_6 (10.2 mg, 26.4 µmol) in anhydrous DMF (4 mL) was added $Cp^*Ru(PPh_3)_2Cl$ (16.2 mg, 20.3 µmol) and PPh_3 (10.6 mg, 40.6 µmol) and the reaction mixture was stirred under an atmosphere of N_2 at 80 °C for 18 h. The mixture was filtered through a plug of celite and diluted with EtOAc (20 mL). The solution was washed with H_2O (2 × 20 mL) and brine (1 × 20 mL), dried over $MgSO_4$, filtered, and concentrated *in vacuo*. The crude product was purified by flash column chromatography to give the title compound as a colorless oil (19.1 mg, 70%). R_f = 0.46 (EtOAc/petroleum ether 1:9); **^{1}H NMR** (400 MHz, $CDCl_3$) δ 6.31 (dt, *J* = 6.3, 2.1 Hz, 1H), 4.64 (dt, *J* = 6.3, 3.7 Hz, 1H), 4.48 (t, *J* = 4.0 Hz, 1H), 2.45 (ddd, *J* = 18.1, 9.2, 6.7 Hz, 1H), 2.37 – 2.30 (m, 1H), 2.30 – 2.18 (m, 2H), 2.11 – 2.01 (m, 1H), 1.95 (dddd, *J* = 17.7, 4.0, 2.1, 0.7 Hz, 1H), 1.40 (d, *J* = 6.7 Hz, 2H), 0.67 (dddt, *J* = 14.3, 8.4, 6.9, 4.9 Hz, 1H), 0.52 – 0.40 (m, 2H), 0.10 – -0.04 (m, 2H); **^{13}C NMR** (101 MHz, $CDCl_3$) δ 217.3, 142.3, 98.2, 77.6, 51.5, 39.1, 33.5, 25.7, 22.8, 6.1, 4.9, 4.8; **IR** (neat) cm^{-1}: 3066 (m, C=C–H), 1740 (s, C=O), 1660 (s, C=C), 1236 (s, C=C–O–C), 1063 (s, C=C–O–C); **HRMS** (ESI) calcd for $C_{12}H_{17}O_2$ $[M+H]^+$ 193.1223, found 193.1232.

Chemoinformatic Library Analysis

Chemoinformatic Library Analysis was carried out using the same procedures and software as reported in the experimentals for Part II (see p. 238). The NPRs and natural product-likeness score of the QF library (including deprotected versions of **3.64** and **3.65**) along with canonical SMILES can be found in the Supporting Information (Figure S51 and Table S11).

References

[1] N. S. Troelsen, E. Shanina, D. Gonzalez-Romero, D. Danková, I. S. A. Jensen, K. J. Sniady, H. Zhang, C. Rademacher, A. Cuenda, C. H. Gotfredsen and M. H. Clausen, The 3F Library: Fluorinated Fsp3-rich Fragments for Expeditious 19F NMR-based Screening, *Angew. Chem., Int. Ed.*, **2020**, *59*, 2204–2210.

[2] D. E. Scott, A. G. Coyne, S. A. Hudson and C. Abell, Fragment based approaches in drug discovery and chemical biology, *Biochemistry*, **2012**, *51*, 4990–5003.

[3] D. A. Erlanson, S. W. Fesik, R. E. Hubbard, W. Jahnke and H. Jhoti, Twenty years on: the impact of fragments on drug discovery, *Nat. Rev. Drug Discov.*, **2016**, *15*, 605–619.

[4] P. N. Mortenson, D. A. Erlanson, I. J. P. De Esch, W. Jahnke and C. N. Johnson, Fragment-to-Lead Medicinal Chemistry Publications in 2017, *J. Med. Chem.*, **2018**, *62*, 3857–3872.

[5] R. Macarron, M. N. Banks, D. Bojanic, D. J. Burns, D. A. Cirovic, T. Garyantes, D. V. S. Green, R. P. Hertzberg, W. P. Janzen, J. W. Paslay and U. Schopfer, Impact of high-throughput screening, *Nature*, **2011**, *10*, 188–195.

[6] A. Barker, J. G. Kettle, T. Nowak and J. E. Pease, Expanding medicinal chemistry space, *Drug Discov. Today*, **2013**, *18*, 298–304.

[7] G. M. Keserü and G. M. Makara, The influence of lead discovery strategies on the properties of drug candidates, *Nat. Rev. Drug Discovery*, **2009**, *8*, 203–212.

[8] A. Schuffenhauer, S. Ruedisser, A. Marzinzik, W. Jahnke, P. Selzer and E. Jacoby, Library Design for Fragment Based Screening, *Curr. Top. Med. Chem.*, **2005**, *5*, 751–762.

[9] D. A. Erlanson, Introduction to Fragment-Based Drug Discovery, *Top. Curr. Chem.*, **2012**, 1–32.

[10] G. M. Keseru, D. A. Erlanson, G. G. Ferenczy, M. M. Hann, C. W. Murray and S. D. Pickett, Design Principles for Fragment Libraries: Maximizing the Value of Learnings from Pharma Fragment-Based Drug Discovery (FBDD) Programs for Use in Academia, *J. Med. Chem.*, **2016**, *59*, 8189–8206.

[11] M. M. Hann, A. R. Leach and G. Harper, Molecular Complexity and Its Impact on the Probability of Finding Leads for Drug Discovery, *J. Chem. Inf. Comput. Sci.*, **2001**, *41*, 856–864.

[12] C. Lipinski and A. Hopkins, Navigating chemical space for biology and medicine, *Nature*, **2004**, *432*, 855–861.

[13] R. S. Bohacek, C. McMartin and W. C. Guida, The art and practice of structure-based drug design: a molecular modeling perspective, *Rev. Med. Res.*, **1996**, *16*, 3–50.

[14] P. Ertl, Cheminformatics analysis of organic substituents: Identification of the most common substituents, calculation of substituent properties, and automatic identification of drug-like bioisosteric groups, *J. Chem. Inf. Comput. Sci.*, **2003**, *43*, 374–380.

[15] L. Ruddigkeit, R. Van Deursen, L. C. Blum and J. L. Reymond, Enumeration of 166 billion organic small molecules in the chemical universe database GDB-17, *J. Chem. Inf. Model.*, **2012**, *52*, 2864–2875.

[16] W. P. Jencks, On the attribution and additivity of binding energies, *Proc. Natl. Acad. Sci. U.S.A.*, **1981**, *78*, 4046–4050.

[17] C. L. Verlinde, G. Rudenko and W. G. Hol, In search of new lead compounds for trypanosomiasis drug design: a protein structure-based linked-fragment approach, *J. Comput. Aided Mol. Des.*, **1992**, *6*, 131–147.

[18] S. B. Shuker, P. J. Hajduk, R. P. Meadows and S. W. Fesik, Discovering High-Affinity Ligands for Proteins: SAR by NMR, *Science*, **1996**, *274*, 1531–1534.

[19] V. L. Nienaber, P. L. Richardson, V. Klighofer, J. J. Bouska, V. L. Giranda and J. Greer, Discovering novel ligands for macromolecules using X-ray crystallographic screening, *Nat. Biotechnol.*, **2000**, *18*, 1105–1108.
[20] T. L. Blundell, H. Jhoti and C. Abell, High-throughput crystallography for lead discovery in drug design, *Nat. Rev. Drug Discovery*, **2002**, *1*, 45–54.
[21] A. G. Coyne, D. E. Scott and C. Abell, Drugging challenging targets using fragment-based approaches., *Curr. Opin. Chem. Biol.*, **2010**, *14*, 299–307.
[22] A. Ciulli and C. Abell, Fragment-based approaches to enzyme inhibition, *Curr. Opin. Biotechnol.*, **2007**, *18*, 489–496.
[23] L. Chen, E. Cressina, F. J. Leeper, A. G. Smith and C. Abell, A fragment-based approach to identifying ligands for riboswitches., *ACS Chem. Biol.*, **2010**, *5*, 355–358.
[24] E. Cressina, L. H. Chen, C. Abell, F. J. Leeper and A. G. Smith, Fragment screening against the thiamine pyrophosphate riboswitch thiM., *Chem. Sci.*, **2011**, *2*, 157–165.
[25] N. Abdel-Rahman, A. Martinez-Arias and T. L. Blundell, Probing the druggability of protein-protein interactions: Targeting the Notch-1 receptor ankyrin domain using a fragmentbased approach., *Biochem. Soc. Trans.*, **2011**, *39*, 1327–1333.
[26] E. Valkov, T. Sharpe, S. Marsh, M., Greive and M. Hyvonen, Targeting protein-protein interactions and fragment-based drug discovery., *Top. Curr. Chem.*, **2012**, *317*, 145–179.
[27] N. Basse, J. L. Kaar, G. Settanni, A. C. Joerger, T. J. Rutherford and A. R. Fersht, Toward the rational design of p53-stabilizing drugs: Probing the surface of the oncogenic Y220C mutant, *Chem. Biol.*, **2010**, *17*, 46–56.
[28] C. W. Murray, M. G. Carr, O. Callaghan, G. Chessari, M. Congreve, S. Cowan, J. E. Coyle, R. Downham, E. Figueroa, M. Frederickson, B. Graham, R. McMenamin, M. A. O'Brien, P. S., T. R. Phillips, G. Williams, A. J. Woodhead and A. J. Woolford, Fragment-based drug discovery applied to Hsp90. Discovery of two lead series with high ligand efficiency., *J. Med. Chem.*, **2010**, *53*, 5942–5955.
[29] A. J. Woodhead, H. Angove, M. G. Carr, G. Chessari, M. Congreve, J. E. Coyle, J. Cosme, B. Graham, P. J. Day, R. Downham, L. Fazal, R. Feltell, E. Figueroa, M. Frederickson, J. Lewis, R. McMenamin, C. W. Murray, M. A. O'Brien, L. Parra, S. Patel, T. Phillips, D. C. Rees, S. Rich, D. M. Smith, G. Trewartha, M. Vinkovic, B. Williams and A. J. Woolford, Discovery of (2,4-dihydroxy-5-isopropylphenyl)-[5-(4-methylpiperazin-1-ylmethyl)-1,3-dihydroisoindol-2-yl]methanone (AT13387), a novel inhibitor of the molecular chaperone Hsp90 by fragment based drug design., *J. Med. Chem.*, **2010**, *53*, 5956–5969.
[30] P. A. Brough, X. Barril, J. Borgognoni, P. Chene, N. G. Davies, B. Davis, M. J. Drysdale, B. Dymock, S. A. Eccles, C. Garcia-Echeverria, C. Fromont, A. Hayes, R. E. Hubbard, A. M. Jordan, M. R. Jensen, A. Massey, A. Merrett, A. Padfield, R. Parsons, T. Radimerski, F. I. Raynaud, A. Robertson, S. D. Roughley, J. Schoepfer, H. Simmonite, S. Y. Sharp, A. Surgenor, M. Valenti, S. Walls, P. Webb, M. Wood, P. Workman and L. Wright, Combining hit identification strategies: Fragment-based and in silico approaches to orally active 2-aminothieno[2,3-d]pyrimidine inhibitors of the Hsp90 molecular chaperone., *J. Med. Chem.*, **2009**, *52*, 4794–4809.

[31] G. Bollag, P. Hirth, J. Tsai, J. Zhang, P. N. Ibrahim, H. Cho, W. Spevak, C. Zhang, Y. Zhang, G. Habets, E. A. Burton, B. Wong, G. Tsang, B. L. West, B. Powell, R. Shellooe, A. Marimuthu, H. Nguyen, K. Y. J. Zhang, D. R. Artis, J. Schlessinger, F. Su, B. Higgins, R. Iyer, K. Dandrea, A. Koehler, M. Stumm, P. S. Lin, R. J. Lee, J. Grippo, I. Puzanov, K. B. Kim, A. Ribas, G. A. McArthur, J. A. Sosman, P. B. Chapman, K. T. Flaherty, X. Xu, K. L. Nathanson and K. Nolop, Clinical efficacy of a RAF inhibitor needs broad target blockade in BRAF-mutant melanoma, *Nature*, **2010**, *467*, 596–599.

[32] J. Tsai, J. T. Lee, W. Wang, J. Zhang, H. Cho, S. Mamo, R. Bremer, S. Gillette, J. Kong, N. K. Haass, K. Sproesser, L. Li, K. S. Smalley, D. Fong, Y. L. Zhu, A. Marimuthu, H. Nguyen, B. Lam, J. Liu, I. Cheung, J. Rice, Y. Suzuki, C. Luu, C. Settachatgul, R. Shellooe, J. Cantwell, S. H. Kim, J. Schlessinger, K. Y. Zhang, B. L. West, B. Powell, G. Habets, C. Zhang, P. N. Ibrahim, P. Hirth, D. R. Artis, M. Herlyn and G. Bollag, Discovery of a selective inhibitor of oncogenic B-Raf kinase with potent antimelanoma activity., *Proc. Natl. Acad. Sci. U.S.A.*, **2008**, *105*, 3041–3046.

[33] E. D. Deeks, Venetoclax: First Global Approval, *Drugs*, **2016**, *76*, 979–987.

[34] C. W. Murray, D. R. Newell and P. Angibaud, A successful collaboration between academia, biotech and pharma led to discovery of erdafitinib, a selective FGFR inhibitor recently approved by the FDA, *MedChemComm*, **2019**, *10*, 1509–1511.

[35] M. Congreve, R. Carr, C. Murray and H. Jhoti, 'Rule of Three' for fragment-based lead discovery, *Drug Discov. Today*, **2003**, *8*, 876–877.

[36] H. Jhoti, G. Williams, D. C. Rees and C. W. Murray, The 'rule of three' for fragment-based drug discovery: where are we now?, *Nat. Rev. Drug Discovery*, **2013**, *12*, 644–644.

[37] C. A. Lipinski, F. Lombardo, B. W. Dominy and P. J. Feeney, Experimental and computational approaches to estimate solubility and permeability in drug discovery and development settings, *Adv. Drug Delivery Rev.*, **2001**, *46*, 3–26.

[38] H. Köster, T. Craan, S. Brass, C. Herhaus, M. Zentgraf, L. Neumann, A. Heine and G. Klebe, A small nonrule of 3 compatible fragment library provides high hit rate of endothiapepsin crystal structures with various fragment chemotypes, *J. Med. Chem.*, **2011**, *54*, 7784–7796.

[39] I. D. Kuntz, K. Chen, K. A. Sharp and P. A. Kollman, The maximal affinity of ligands, *Proc. Natl. Acad. Sci. U.S.A.*, **1999**, *96*, 9997–10002.

[40] R. E. Hubbard, in *Fragment-based Drug Discovery: Lessons and Outlook*, eds. D. A. Erlanson and W. Jahnke, Wiley-VCH, Weinheim, 1., **2016**, pp. 3–36.

[41] C. A. Lepre, in *Methods in Enzymology*, eds. J. N. Abelson and M. I. Simon, Elsevier Inc., San Diego, USA, 1st Ed., **2011**, pp. 220–239.

[42] M. J. Harner, A. O. Frank and S. W. Fesik, Fragment-based drug discovery using NMR spectroscopy, *J. Biomol. NMR*, **2013**, *56*, 65–75.

[43] M. Mayer and B. Meyer, Characterization of ligand binding by saturation transfer difference NMR spectroscopy, *Angew. Chemie - Int. Ed.*, **1999**, *38*, 1784–1788.

[44] C. Dalvit, P. Pevarello, M. Tato, M. Veronesi, A. Vulpetti and M. Sundström, Identification of compounds with binding affinity to proteins via magnetization transfer from bulk water, *J. Biomol. NMR*, **2000**, *18*, 65–68.

[45] C. Dalvit, Theoretical Analysis of the Competition Ligand-Based Fragment Screening and Selected Applications to NMR Experiments and Binding Constant Measurements, *Concepts Magn. Reson. Part A*, **2008**, *32A*, 341–372.

[46] A. Viegas, J. Manso, F. L. Nobrega and E. J. Cabrita, Saturation-Transfer Difference (STD) NMR: A Simple and Fast Method for Ligand Screening and Characterization of Protein Binding, *J. Chem. Educ.*, **2011**, *88*, 990–994.

[47] H. Y. Carr and E. M. Purcell, Effects of Diffusion on Free Precession in Nuclear Magnetic Resonance Experiments, *Phys. Rev.*, **1954**, *94*, 630–638.
[48] S. Meiboom and D. Gill, Modified Spin-Echo Method for Measuring Nuclear Relaxation Times, *Rev. Sci. Instrum.*, **1958**, *29*, 688–691.
[49] P. J. Hajduk, E. T. Olejniczak and S. W. Fesik, One-dimensional relaxation- and diffusion-edited NMR methods for screening compounds that bind to macromolecules, *J. Am. Chem. Soc.*, **1997**, *119*, 12257–12261.
[50] C. Dalvit, Ligand- and substrate-based 19F NMR screening: Principles and applications to drug discovery, *Prog. Nucl. Magn. Reson. Spectrosc.*, **2007**, *51*, 243–271.
[51] C. Dalvit, P. E. Fagerness, D. T. A. Hadden, R. W. Sarver and B. J. Stockman, Fluorine-NMR experiments for high-throughput screening: Theoretical aspects, practical considerations, and range of applicability, *J. Am. Chem. Soc.*, **2003**, *125*, 7696–7703.
[52] C. Dalvit, M. Flocco, M. Veronesi and B. J. Stockman, Fluorine-NMR Competition Binding Experiments for High-Throughput Screening of Large Compound Mixtures, *Comb. Chem. High Throughput Screening*, **2002**, *5*, 605–611.
[53] J. Klages, M. Coles and H. Kessler, NMR-based screening: a powerful tool in fragment-based drug discovery, *Analyst*, **2007**, *132*, 392–705.
[54] A. M. Petros, J. Dinges, D. J. Augeri, S. A. Baumeister, D. A. Betebenner, M. G. Bures, S. W. Elmore, P. J. Hajduk, M. K. Joseph, S. K. Landis, D. G. Nettesheim, S. H. Rosenberg, W. Shen, S. Thomas, X. Wang, I. Zanze, H. Zhang and S. W. Fesik, Discovery of a potent inhibitor of the antiapoptotic protein Bcl-X L from NMR and parallel synthesis, *J. Med. Chem.*, **2006**, *49*, 656–663.
[55] A. E. Eakin, O. Green, N. Hales, G. K. Walkup, S. Bist, A. Singh, G. Mullen, J. Bryant, K. Embrey, N. Gao, A. Breeze, D. Timms, B. Andrews, M. Uria-Nickelsen, J. Demeritt, J. T. Loch, K. Hull, A. Blodgett, R. N. Illingworth, B. Prince, P. A. Boriack-Sjodin, S. Hauck, L. J. MacPherson, H. Ni and B. Sherer, Pyrrolamide DNA gyrase inhibitors: Fragment-based nuclear magnetic resonance screening to identify antibacterial agents, *Antimicrob. Agents Chemother.*, **2012**, *56*, 1240–1246.
[56] P. J. Hajduk, J. Dinges, G. F. Miknis, M. Merlock, T. Middleton, D. J. Kempf, D. A. Egan, K. A. Walter, T. S. Robins, S. B. Shuker, T. F. Holzman and S. W. Fesik, NMR-based discovery of lead inhibitors that block DNA binding of the human papillomavirus E2 protein, *J. Med. Chem.*, **1997**, *40*, 3144–3150.
[57] T. G. Davies and I. J. Tickle, Fragment Screening Using X-Ray Crystallography, *Top Curr Chem*, **2012**, *317*, 33–59.
[58] J. Blaney, V. Nienaber and S. K. Burley, *Fragment-based Lead Discovery and Optimization Using X-Ray Crystallography, Computational Chemistry, and High-throughput Organic Synthesis*, Wiley-VCH, Weinheim, 1st edn., **2006**, vol. 34.
[59] D. J. Wood, J. D. Lopez-Fernandez, L. E. Knight, I. Al-Khawaldeh, C. Gai, S. Lin, M. P. Martin, D. C. Miller, C. Cano, J. A. Endicott, I. R. Hardcastle, M. E. M. Noble and M. J. Waring, FragLites - Minimal, Halogenated Fragments Displaying Pharmacophore Doublets. An Efficient Approach to Druggability Assessment and Hit Generation, *J. Med. Chem.*, **2019**, *62*, 3741–3752.
[60] J. Blaney, V. Nienaber and S. K. Burley, in *Fragment-based Approaches in Drug Discovery*, eds. W. Jahnke and D. A. Erlanson, Wiley-VCH Verlag GmbH & Co. KGaA, Weinheim, Germany, **2006**, pp. 215–248.
[61] A. M. Davis, S. A. St-Gallay and G. J. Kleywegt, Limitations and lessons in the use of X-ray structural information in drug design, *Drug Discov. Today*, **2008**, *13*, 831–841.

[62] C. R. Søndergaard, A. E. Garrett, T. Carstensen, G. Pollastri and J. E. Nielsen, Structural artifacts in protein-ligand X-ray structures: Implications for the development of docking scoring functions, *J. Med. Chem.*, **2009**, *52*, 5673–5684.
[63] M. A. Cooper, Optical biosensors in drug discovery, *Nat. Rev. Drug Discovery*, **2002**, *1*, 515–528.
[64] I. Navratilova and A. L. Hopkins, Fragment screening by surface plasmon resonance, *ACS Med. Chem. Lett.*, **2010**, *1*, 44–48.
[65] M. Hennig, A. Ruf and W. Huber, Combining Biophysical Screening and X-Ray Crystallography for Fragment-Based Drug Discovery, *Top Curr Chem*, **2012**, *317*, 115–144.
[66] R. L. Rich and D. G. Myszka, Grading the commercial optical biosensor literature-class of 2008: 'The mighty binders', *J Mol Recognit*, **2008**, *23*, 1–64.
[67] J. E. Ladbury and B. Z. Chowdhrv2, Sensing the heat: the application of isothermal titration calorimetry to thermodynamic studies of biomolecular interactions, *Chem. Biol.*, **1996**, *3*, 791–801.
[68] 2bind, Isothermal Titration Calorimetry, https://2bind.com/itc/, (accessed 4 December 2018).
[69] S. A. Hofstadler and K. A. Sannes-Lowery, Applications of ESI-MS in drug discovery: Interrogation of noncovalent complexes, *Nat. Rev. Drug Discovery*, **2006**, *5*, 585–595.
[70] V. V. Hannah, C. Atmanene, D. Zeyer, A. Van Dorsselaer and S. Sanglier-Cianférani, Native MS: an 'ESI' way to support structureand fragment-based drug discovery, *Futur. Med. Chem.*, **2009**, *2*, 35–49.
[71] D. A. Erlanson, J. A. Wells and A. C. Braisted, Tethering: fragment-based drug discovery, *Annu Rev Biophys Biomol Struct*, **2004**, *33*, 199–223.
[72] D. A. Erlanson, A. C. Braisted, D. R. Raphael, M. Randal, R. M. Stroud, E. M. Gordon and J. A. Wells, Site-directed ligand discovery, *Proc. Natl. Acad. Sci. U.S.A.*, **2000**, *97*, 9367–9372.
[73] J. K. Kranz and C. Schalk-Hihi, in *Methods Enzymol.*, ed. L. C. Kuo, Elsevier Inc., 1st edn., **2011**, vol. 493, pp. 277–298.
[74] F. H. Niesen, H. Berglund and M. Vedadi, The use of differential scanning fluorimetry to detect ligand interactions that promote protein stability, *Nat. Protoc.*, **2007**, *2*, 2212–2221.
[75] Y. Bian and X.-Q. Xie, Computational Fragment-Based Drug Design: Current Trends, Strategies, and Applications, *AAPS J.*, **2018**, *20*, 59.
[76] V. Zoete, A. Grosdidier and O. Michielin, Docking, virtual high throughput screening and in silico fragment-based drug design, *J. Cell. Mol. Med.*, **2009**, *13*, 238–248.
[77] M. Jerabek-Willemsen, C. J. Wienken, D. Braun, P. Baaske and S. Duhr, Molecular interaction studies using microscale thermophoresis, *Assay Drug Dev. Technol.*, **2011**, *9*, 342–353.
[78] P. Linke, K. Amaning, M. Maschberger, F. Vallee, V. Steier, P. Baaske, S. Duhr, D. Breitsprecher and A. Rak, An Automated Microscale Thermophoresis Screening Approach for Fragment-Based Lead Discovery, *J. Biomol. Screen.*, **2016**, *21*, 414–421.
[79] Nanotemper, Microscale Thermophoresis, https://nanotempertech.com/, (accessed 18 October 2016).
[80] C. Austin, S. N. Pettit, S. K. Magnolo, J. Sanvoisin, W. Chen, S. P. Wood, L. D. Freeman, R. J. Pengelly and D. E. Hughes, Fragment screening using capillary electrophoresis (CEfrag) for hit identification of heat shock protein 90 ATPase inhibitors, *J. Biomol. Screen.*, **2012**, *17*, 868–876.

[81] E. Farcaş, C. Bouckaert, A. C. Servais, J. Hanson, L. Pochet and M. Fillet, Partial filling affinity capillary electrophoresis as a useful tool for fragment-based drug discovery: A proof of concept on thrombin, *Anal. Chim. Acta*, **2017**, *984*, 211–222.
[82] E. Farcaş, J. Hanson, L. Pochet and M. Fillet, Capillary electrophoretic mobility shift displacement assay for the assessment of weak drug-protein interactions, *Anal. Chim. Acta*, **2018**, *1034*, 214–222.
[83] S. Shibata, Z. Zhang, K. V. Korotkov, J. Delarosa, A. Napuli, A. M. Kelley, N. Mueller, J. Ross, F. H. Zucker, F. S. Buckner, E. A. Merritt, C. L. M. J. Verlinde, W. C. Van Voorhis, W. G. J. Hol and E. Fan, Screening a fragment cocktail library using ultrafiltration, *Anal. Bioanal. Chem.*, **2011**, *401*, 1589–1595.
[84] E. Meiby, H. Simmonite, L. Le Strat, B. Davis, N. Matassova, J. D. Moore, M. Mrosek, J. Murray, R. E. Hubbard and S. Ohlson, Fragment screening by weak affinity chromatography: Comparison with established techniques for screening against HSP90, *Anal. Chem.*, **2013**, *85*, 6756–6766.
[85] M. Saur, M. J. Hartshorn, J. Dong, J. Reeks, G. Bunkoczi, H. Jhoti and P. A. Williams, Fragment-based drug discovery using cryo-EM, *Drug Discov. Today*, **2020**, DOI:10.1016/j.drudis.2019.12.006.
[86] P. J. Hajduk, SAR by NMR: putting the pieces together, *Mol. Interv.*, **2006**, *6*, 266–272.
[87] P. J. Hajduk and J. Greer, A decade of fragment-based drug design: Strategic advances and lessons learned, *Nat. Rev. Drug Discovery*, **2007**, *6*, 211–219.
[88] E. T. Olejniczak, P. J. Hajduk, P. A. Marcotte, D. G. Nettesheim, R. P. Meadows, R. Edalji, T. F. Holzman and S. W. Fesik, Stromelysin inhibitors designed from weakly bound fragments: Effects of linking and cooperativity, *J. Am. Chem. Soc.*, **1997**, *119*, 5828–5832.
[89] T. Oltersdorf, S. W. Elmore, A. R. Shoemaker, R. C. Armstrong, D. J. Augeri, B. A. Belli, M. Bruncko, T. L. Deckwerth, J. Dinges, P. J. Hajduk, M. K. Joseph, S. Kitada, S. J. Korsmeyer, A. R. Kunzer, A. Letai, C. Li, M. J. Mitten, D. G. Nettesheim, S. C. Ng, P. M. Nimmer, J. M. O'Connor, A. Oleksijew, A. M. Petros, J. C. Reed, W. Shen, S. K. Tahir, C. B. Thompson, K. J. Tomaselli, B. Wang, M. D. Wendt, H. Zhang, S. W. Fesik and S. H. Rosenberg, An inhibitor of Bcl-2 family proteins induces regression of solid tumours, *Nature*, **2005**, *435*, 677–681.
[90] A. M. Petros, J. Dinges, D. J. Augeri, S. A. Baumeister, D. A. Betebenner, M. G. Bures, S. W. Elmore, P. J. Hajduk, M. K. Joseph, S. K. Landis, D. G. Nettesheim, S. H. Rosenberg, W. Shen, S. Thomas, X. Wang, I. Zanze, H. Zhang and S. W. Fesik, Discovery of a Potent Inhibitor of the Antiapoptotic Protein Bcl-xL from NMR and Parallel Synthesis, *J. Med. Chem.*, **2006**, *49*, 656–663.
[91] C. Tse, A. R. Shoemaker, J. Adickes, M. G. Anderson, J. Chen, S. Jin, E. F. Johnson, K. C. Marsh, M. J. Mitten, P. Nimmer, L. Roberts, S. K. Tahir, Y. Xiao, X. Yang, H. Zhang, S. Fesik, S. H. Rosenberg and S. W. Elmore, ABT-263: A potent and orally bioavailable Bcl-2 family inhibitor, *Cancer Res.*, **2008**, *68*, 3421–3428.
[92] J. J. Barker, O. Barker, S. M. Courtney, M. Gardiner, T. Hesterkamp, O. Ichihara, O. Mather, C. A. G. N. Montalbetti, A. Müller, M. Varasi, M. Whittaker and C. J. Yarnold, Discovery of a novel Hsp90 inhibitor by fragment linking, *ChemMedChem*, **2010**, *5*, 1697–1700.

[93] S. Howard, V. Berdini, J. A. Boulstridge, M. G. Carr, D. M. Cross, J. Curry, L. A. Devine, T. R. Early, L. Fazal, A. L. Gill, M. Heathcote, S. Maman, J. E. Matthews, R. L. McMenamin, E. F. Navarro, M. A. O'Brien, M. O'Reilly, D. C. Rees, M. Reule, G. Williams, D. Tisi, M. Vinković and P. G. Wyatt, Fragment-Based Discovery of the Pyrazol-4-yl Urea (AT9283), a Multitargeted Kinase Inhibitor with Potent Aurora Kinase Activity, *J. Med. Chem.*, **2009**, *52*, 379–388.

[94] R. Tanaka, M. S. Squires, S. Kimura, A. Yokota, R. Nagao, T. Yamauchi, M. Takeuchi, H. Yao, M. Reule, T. Smyth, J. F. Lyons, N. T. Thompson, E. Ashihara, O. G. Ottmann and T. Maekawa, Activity of the multitargeted kinase inhibitor, AT9283, in imatinib-resistant BCR-ABL-positive leukemic cells, *Blood*, **2010**, *116*, 2089–2095.

[95] B. Vormoor, G. J. Veal, M. J. Griffin, A. V. Boddy, J. Irving, L. Minto, M. Case, U. Banerji, K. E. Swales, J. R. Tall, A. S. Moore, M. Toguchi, G. Acton, K. Dyer, C. Schwab, C. J. Harrison, J. D. Grainger, D. Lancaster, P. Kearns, D. Hargrave and J. Vormoor, A phase I/II trial of AT9283, a selective inhibitor of aurora kinase in children with relapsed or refractory acute leukemia: challenges to run early phase clinical trials for children with leukemia, *Pediatr. Blood Cancer*, **2017**, *64*, 1–4.

[96] R. E. Hubbard, Fragment approaches in structure-based drug discovery, *J. Synchrotron Radiat.*, **2008**, *15*, 227–230.

[97] I. J. Chen and R. E. Hubbard, Lessons for fragment library design: Analysis of output from multiple screening campaigns, *J. Comput. Mol. Des.*, **2009**, *23*, 603–620.

[98] D. R. Davies, B. Mamat, O. T. Magnusson, J. Christensen, M. H. Haraldsson, R. Mishra, B. Pease, E. Hansen, J. Singh, D. Zembower, H. Kim, A. S. Kiselyov, A. B. Burgin, M. E. Gurney and L. J. Stewart, Discovery of leukotriene A4 hydrolase inhibitors using metabolomics biased fragment crystallography, *J. Med. Chem.*, **2009**, *52*, 4694–4715.

[99] I. Akritopoulou-Zanze and P. J. Hajduk, Kinase-targeted libraries: The design and synthesis of novel, potent, and selective kinase inhibitors, *Drug Discov. Today*, **2009**, *14*, 291–297.

[100] W. F. Lau, J. M. Withka, D. Hepworth, T. V. Magee, Y. J. Du, G. A. Bakken, M. D. Miller, Z. S. Hendsch, V. Thanabal, S. A. Kolodziej, L. Xing, Q. Hu, L. S. Narasimhan, R. Love, M. E. Charlton, S. Hughes, W. P. Van Hoorn and J. E. Mills, Design of a multi-purpose fragment screening library using molecular complexity and orthogonal diversity metrics, *J. Comput.-Aided Mol. Des.*, **2011**, *25*, 621–636.

[101] N. Baurin, F. Aboul-Ela, X. Barril, B. Davis, M. Drysdale, B. Dymock, H. Finch, C. Fromont, C. Richardson, H. Simmonite and R. E. Hubbard, Design and characterization of libraries of molecular fragments for use in NMR screening against protein targets, *J. Chem. Inf. Comput. Sci.*, **2004**, *44*, 2157–2166.

[102] N. Blomberg, D. A. Cosgrove, P. W. Kenny and K. Kolmodin, Design of compound libraries for fragment screening, *J. Comput.-Aided Mol. Des.*, **2009**, *23*, 513–525.

[103] J. Fejzo, C. A. Lepre, J. W. Peng, G. W. Bemis, Ajay, M. A. Murcko and J. M. Moore, The SHAPES strategy: An NMR-based approach for lead generation in drug discovery, *Chem. Biol.*, **1999**, *6*, 755–769.

[104] C. W. Murray and D. C. Rees, Opportunity Knocks: Organic Chemistry for Fragment-Based Drug Discovery (FBDD), *Angew. Chemie - Int. Ed.*, **2016**, *55*, 488–492.

[105] G. M. Rishton, Nonleadlikeness and leadlikeness in biochemical screening, *Drug Discov. Today*, **2003**, *8*, 86–96.

[106] J. B. Baell and G. A. Holloway, New substructure filters for removal of pan assay interference compounds (PAINS) from screening libraries and for their exclusion in bioassays, *J. Med. Chem.*, **2010**, *53*, 2719–2740.

[107] J. Baell and M. A. Walters, Chemical con artists foil drug discovery, *Nature*, **2014**, *513*, 481–483.
[108] W. R. J. D. Galloway, A. . Bender, M. Welch and D. R. Spring, The discovery of antibacterial agents using diversity-oriented synthesis, *Chem. Commun.*, **2009**, *14*, 2446–2462.
[109] W. R. J. D. Galloway, A. Isidro-Llobet and D. R. Spring, Diversity-oriented synthesis as a tool for the discovery of novel biologically active small molecules, *Nat. Commun.*, **2010**, *1*, 1–13.
[110] M. D. Burke and S. L. Schreiber, A planning strategy for diversity-oriented synthesis, *Angew. Chem., Int. Ed.*, **2004**, *43*, 46–58.
[111] M. D. Burke, E. M. Berger and S. L. Schreiber, Generating diverse skeletons of small molecules combinatorially, *Science*, **2003**, *302*, 613–618.
[112] W. H. B. Sauer and M. K. Schwarz, Molecular shape diversity of combinatorial libraries: A prerequisite for broad bioactivity, *J. Chem. Inf. Comput. Sci.*, **2003**, *43*, 987–1003.
[113] W. R. J. D. Galloway and D. R. Spring, Is synthesis the main hurdle for the generation of diversity in compound libraries for screening?, *Exp. Opin. Drug Discov.*, **2009**, *4*, 467–472.
[114] A. A. Shelat and R. K. Guy, Scaffold composition and biological relevance of screening libraries, *Nat. Chem. Biol.*, **2007**, *3*, 442–446.
[115] R. N. Daniels, C. W. Lindsley, J. P. Kennedy, L. Williams, T. M. Bridges and D. Weaver, Application of Combinatorial Chemistry Science on Modern Drug Discovery, *J. Comb. Chem.*, **2008**, *10*, 345–354.
[116] I. Paterson and E. Anderson, The Renaissance of Natural Products as Drug Candidates, *Science*, **2005**, *310*, 451–453.
[117] B. Over, S. Wetzel, C. Grütter, Y. Nakai, S. Renner, D. Rauh and H. Waldmann, Natural-product-derived fragments for fragment-based ligand discovery, *Nature Chem.*, **2013**, *5*, 21–28.
[118] A. D. Morley, A. Pugliese, K. Birchall, J. Bower, P. Brennan, N. Brown, T. Chapman, M. Drysdale, I. H. Gilbert, S. Hoelder, A. Jordan, S. V. Ley, A. Merritt, D. Miller, M. E. Swarbrick and P. G. Wyatt, Fragment-based hit identification: Thinking in 3D, *Drug Discov. Today*, **2013**, *18*, 1221–1227.
[119] J. Meyers, M. Carter, N. Yi Mok and N. Brown, On the origins of three-dimensionality in drug-like molecules, *Futur. Med. Chem.*, **2016**, *8*, 1753–1767.
[120] N. C. Firth, N. Brown and J. Blagg, Plane of best fit: A novel method to characterize the three-dimensionality of molecules, *J. Chem. Inf. Model.*, **2012**, *52*, 2516–2525.
[121] F. Lovering, J. Bikker and C. Humblet, Escape from Flatland: Increasing Saturation as an Approach to Improving Clinical Success, *J. Med. Chem.*, **2009**, *52*, 6752–6756.
[122] F. Lovering, Escape from Flatland 2: complexity and promiscuity, *MedChemComm*, **2013**, *4*, 515.
[123] S. Kortagere, M. D. Krasowski and S. Ekins, The importance of discerning shape in molecular pharmacology, *Trends Pharmacol. Sci.*, **2009**, *30*, 138–147.
[124] D. C. Kombo, K. Tallapragada, R. Jain, J. Chewning, A. A. Mazurov, J. D. Speake, T. A. Hauser and S. Toler, 3D molecular descriptors important for clinical success, *J. Chem. Inf. Model.*, **2013**, *53*, 327–342.
[125] S. L. Kidd, T. J. Osberger, N. Mateu, H. F. Sore and D. R. Spring, Recent Applications of Diversity-Oriented Synthesis Toward Novel, 3-Dimensional Fragment Collections, *Front. Chem.*, **2018**, *6*, 460.

[126] P. A. Clemons, N. E. Bodycombe, H. A. Carrinski, J. A. Wilson, A. F. Shamji, B. K. Wagner, A. N. Koehler and S. L. Schreiber, Small molecules of different origins have distinct distributions of structural complexity that correlate with protein-binding profiles, *Proc. Natl. Acad. Sci. U.S.A.*, **2010**, *107*, 18787–18792.
[127] K. Kingwell, Medicinal chemistry: Exploring the third dimension, *Nat Rev Drug Discov*, **2009**, *8*, 931.
[128] A. Y. Meyer, Molecular mechanics and molecular shape. III. Surface area and cross-sectional areas of organic molecules, *J. Comput. Chem.*, **1986**, *7*, 144–152.
[129] R. Todeschini and V. Consonni, *Molecular Descriptors for Chemoinformatics*, Wiley-VCH, Weinheim, 2nd edn., **2009**.
[130] L. B. Kier and L. H. Hall, in *Reviews in Computational Chemistry*, eds. K. B. Lipkowitz and D. B. Boyd, VCH Publishers, New York, 1st edn., **1991**, pp. 367–422.
[131] D. T. Stanton and P. C. Jurs, Development and Use of Charged Partial Surface Area Structural Descriptors in Computer-Assisted Quantitative Structure-Property Relationship Studies, *Anal. Chem.*, **1990**, *62*, 2323–2329.
[132] Merriam-Webster, Moment of Inertia, https://www.merriam-webster.com/dictionary/moment of inertia, (accessed 21 January 2019).
[133] Y. H. Zhao, M. H. Abraham and A. M. Zissimos, Fast Calculation of van der Waals Volume as a Sum of Atomic and Bond Contributions and Its Application to Drug Compounds, *J. Org. Chem.*, **2003**, *68*, 7368–7373.
[134] N. A. Meanwell, Fluorine and Fluorinated Motifs in the Design and Application of Bioisosteres for Drug Design, *J. Med. Chem.*, **2018**, *61*, 5822–5880.
[135] M. Valli, R. N. dos Santos, L. D. Figueira, C. H. Nakajima, I. Castro-Gamboa, A. D. Andricopulo and V. S. Bolzani, Development of a Natural Products Database from the Biodiversity of Brazil, *J. Nat. Prod.*, **2013**, *76*, 439–444.
[136] I. Colomer, C. J. Empson, P. Craven, Z. Owen, R. G. Doveston, I. Churcher, S. P. Marsden and A. Nelson, A divergent synthetic approach to diverse molecular scaffolds: assessment of lead-likeness using LLAMA, an open-access computational tool, *Chem. Commun.*, **2016**, *52*, 7209–7212.
[137] L. A. Thompson and J. A. Ellman, Synthesis and applications of small molecule libraries, *Chem. Rev.*, **1996**, *96*, 555–600.
[138] S. L. Schreiber, Target-oriented and diversity-oriented organic synthesis in drug discovery, *Science*, **2000**, *287*, 1964–1969.
[139] D. Lee, J. K. Sello and S. L. Schreiber, Pairwise Use of Complexity-Generating Reactions in Diversity-Oriented Organic Synthesis, *Org. Lett.*, **2000**, *2*, 709–712.
[140] D. Pizzirani, T. Kaya, P. A. Clemons and S. L. Schreiber, Stereochemical and skeletal diversity arising from amino propargylic alcohols, *Org. Lett.*, **2010**, *12*, 2822–2825.
[141] G. L. Thomas, R. J. Spandl, F. G. Glansdorp, M. Welch, A. Bender, J. Cockfield, J. A. Lindsay, C. Bryant, D. F. J. Brown, O. Loiseleur, H. Rudyk, M. Ladlow and D. R. Spring, Anti-MRSA agent discovery using diversity-oriented synthesis, *Angew. Chemie - Int. Ed.*, **2008**, *47*, 2808–2812.
[142] D. Morton, S. Leach, C. Cordier, S. Warriner and A. Nelson, Synthesis of natural-product-like molecules with over eighty distinct scaffolds, *Angew. Chemie - Int. Ed.*, **2009**, *48*, 104–109.
[143] T. E. Nielsen and S. L. Schreiber, Towards the optimal screening collection: A synthesis strategy, *Angew. Chemie - Int. Ed.*, **2008**, *47*, 48–56.
[144] S. Wetzel, R. S. Bon, K. Kumar and H. Waldmann, Biology-oriented synthesis, *Angew. Chemie - Int. Ed.*, **2011**, *50*, 10800–10826.

[145] A. Nören-Müller, I. Reis-Corrêa, H. Prinz, C. Rosenbaum, K. Saxena, H. J. Schwalbe, D. Vestweber, G. Cagna, S. Schunk, O. Schwarz, H. Schiewe and H. Waldmann, Discovery of protein phosphatase inhibitor classes by biology-oriented synthesis, *Proc. Natl. Acad. Sci. U.S.A.*, **2006**, *103*, 10606–10611.
[146] S. Oh and S. B. Park, A design strategy for drug-like polyheterocycles with privileged substructures for discovery of specific small-molecule modulators, *Chem. Commun.*, **2011**, *47*, 12754–12761.
[147] A. Nadin, C. Hattotuwagama and I. Churcher, Lead-oriented synthesis: A new opportunity for synthetic chemistry, *Angew. Chemie - Int. Ed.*, **2012**, *51*, 1114–1122.
[148] R. Doveston, S. Marsden and A. Nelson, Towards the realisation of lead-oriented synthesis, *Drug Discov. Today*, **2014**, *19*, 813–819.
[149] A. W. Hung, A. Ramek, Y. Wang, T. Kaya, J. A. Wilson, P. A. Clemons and D. W. Young, Route to three-dimensional fragments using diversity-oriented synthesis, *Proc. Natl. Acad. Sci. U.S.A.*, **2011**, *108*, 6799–6804.
[150] D. J. Foley, R. G. Doveston, I. Churcher, A. Nelson and S. P. Marsden, A systematic approach to diverse, lead-like scaffolds from α,α-disubstituted amino acids, *Chem. Commun.*, **2015**, *51*, 11174–11177.
[151] D. J. Foley, P. G. E. Craven, P. M. Collins, R. G. Doveston, A. Aimon, R. Talon, I. Churcher, F. von Delft, S. P. Marsden and A. Nelson, Synthesis and Demonstration of the Biological Relevance of sp3-rich Scaffolds Distantly Related to Natural Product Frameworks, *Chem. - A Eur. J.*, **2017**, *23*, 15227–15232.
[152] S. Haftchenary, S. D. Nelson, L. Furst, S. Dandapani, S. J. Ferrara, Ž. V. Bošković, S. Figueroa Lazú, A. M. Guerrero, J. C. Serrano, D. K. Crews, C. Brackeen, J. Mowat, T. Brumby, M. Bauser, S. L. Schreiber and A. J. Phillips, Efficient Routes to a Diverse Array of Amino Alcohol-Derived Chiral Fragments, *ACS Comb. Sci.*, **2016**, *18*, 569–574.
[153] J. Mayol-Llinàs, W. Farnaby and A. Nelson, Modular synthesis of thirty lead-like scaffolds suitable for CNS drug discovery, *Chem. Commun.*, **2017**, *53*, 12345–12348.
[154] Y. Wang, J. Y. Wach, P. Sheehan, C. Zhong, C. Zhan, R. Harris, S. C. Almo, J. Bishop, S. J. Haggarty, A. Ramek, K. N. Berry, C. O'Herin, A. N. Koehler, A. W. Hung and D. W. Young, Diversity-Oriented Synthesis as a Strategy for Fragment Evolution against GSK3β, *ACS Med. Chem. Lett.*, **2016**, *7*, 852–856.
[155] H. Hassan, S. P. Marsden and A. Nelson, Design and synthesis of a fragment set based on twisted bicyclic lactams, *Bioorg. Med. Chem.*, **2018**, *26*, 3030–3033.
[156] N. Mateu, S. L. Kidd, L. Kalash, H. F. Sore, A. Madin, A. Bender and D. R. Spring, Synthesis of Structurally Diverse N-Substituted Quaternary-Carbon-Containing Small Molecules from α,α-Disubstituted Propargyl Amino Esters, *Chem. - A Eur. J.*, **2018**, *24*, 13681–13687.
[157] D. G. Twigg, K. Kondo, S. L. Mitchell, W. R. J. D. Galloway, H. F. Sore, A. Madin and D. R. Spring, Partially Saturated Bicyclic Heteroaromatics as an sp3-Enriched Fragment Collection, *Angew. Chem., Int. Ed.*, **2016**, *55*, 12479–12483.
[158] O. A. Davis, R. A. Croft and J. A. Bull, Synthesis of diversely functionalised 2,2-disubstituted oxetanes: Fragment motifs in new chemical space, *Chem. Commun.*, **2015**, *51*, 15446–15449.
[159] H. Grünewald, *Nobel Lectures, Chemistry 1901-1921*, Elsevier Publishing Company, Amsterdam, **1966**.
[160] M. Jaccaud, R. Faron, D. Devilliers and R. Romano, in *Ullmann's Encyclopedia of Industrial Chemistry*, Wiley-VCH, Weinheim, Germany, 7th edn., **2012**.

[161] C. D. Murphy, C. Schaffrath and D. O'Hagan, Fluorinated natural products: The biosynthesis of fluoroacetate and 4-fluorothreonine in Streptomyces cattleya, *Chemosphere*, **2003**, *52*, 455–461.
[162] P. Bazzini and C. G. Wermuth, in *The Practice of Medicinal Chemistry*, eds. C. G. Wermuth, D. Aldous, P. Raboisson and D. Rognan, Elsevier Ltd, 4th edn., **2015**.
[163] M. Pettersson, X. Hou, M. Kuhn, T. T. Wager, G. W. Kauffman and P. R. Verhoest, Quantitative Assessment of the Impact of Fluorine Substitution on P-Glycoprotein (P-gp) Mediated Efflux, Permeability, Lipophilicity, and Metabolic Stability, *J. Med. Chem.*, **2016**, *59*, 5284–5296.
[164] T. Yamazaki, T. Taguchi and I. Ojima, in *Fluorine in Medicinal Chemistry and Chemical Biology*, ed. I. Ojima, John Wiley & Sons, West Sussex, 1st edn., **2009**.
[165] K. Goss, Thermodynamic Estimate of p K a Values of the Carboxylic Ac-, *Environ. Sci. Technol.*, **2008**, *42*, 456–458.
[166] B. E. Smart, Fluorine substituent effects (on bioactivity), *J. Fluorine Chem.*, **2001**, *109*, 3–11.
[167] Q. A. Huchet, B. Kuhn, B. Wagner, N. A. Kratochwil, H. Fischer, M. Kansy, D. Zimmerli, E. M. Carreira and K. Müller, Fluorination Patterning: A Study of Structural Motifs That Impact Physicochemical Properties of Relevance to Drug Discovery, *J. Med. Chem.*, **2015**, *58*, 9041–9060.
[168] E. P. Gillis, K. J. Eastman, M. D. Hill, D. J. Donnelly and N. A. Meanwell, Applications of Fluorine in Medicinal Chemistry, *J. Med. Chem.*, **2015**, *58*, 8315–8359.
[169] S. Wolfe, Gauche effect. Stereochemical consequences of adjacent electron pairs and polar bonds., *Acc. Chem. Res.*, **1972**, *5*, 102–111.
[170] L. Pauling, *The Nature of the Chemical Bond*, Cornell University Press, New York, 3rd edn., **1960**.
[171] F. Leroux, Atropisomerism, biphenyls, and fluorine: A comparison of rotational barriers and twist angles, *ChemBioChem*, **2004**, *5*, 644–649.
[172] J. D. Hepworth, J. A. Hudson, D. A. Ibbitson and G. Hallas, A Dipole Moment Study of the Electrical Effect of the Trifluoromethyl Group, *J. Chem. Soc., Perkin Trans. 2*, **1972**, 1905–1908.
[173] E. V. Anslyn and D. A. Dougherty, *Modern Physical Chemistry*, University Science Books, USA, 1st edn., **2006**.
[174] J. E. True, T. D. Thomas, R. W. Winter and G. L. Gard, Electronegativities from core-ionization energies: Electronegativities of SF5and CF3, *Inorg. Chem.*, **2003**, *42*, 4437–4441.
[175] P. A. Champagne, J. Desroches and J. F. Paquin, Organic fluorine as a hydrogen-bond acceptor: Recent examples and applications, *Synthesis*, **2015**, *47*, 306–322.
[176] C. Dalvit, C. Invernizzi and A. Vulpetti, Fluorine as a hydrogen-bond acceptor: Experimental evidence and computational calculations, *Chem. - A Eur. J.*, **2014**, *20*, 11058–11068.
[177] J. A. K. Howeard, V. J. Hoy, D. O'Hagan and G. T. Smith, How Good is Fluorine as a Hydrogen Bond Acceptor?, *Tetrahedron*, **1996**, *52*, 12613–12622.
[178] B. Kuhn, E. Gilberg, R. Taylor, J. Cole and O. Korb, How Significant Are Unusual Protein–Ligand Interactions? Insights from Database Mining, *J. Med. Chem.*, **2019**, *62*, 10441–10455.
[179] K. Eskandari and M. Lesani, Does fluorine participate in halogen bonding?, *Chem. - A Eur. J.*, **2015**, *21*, 4739–4746.
[180] X. García-Llinás, A. Bauzá, S. K. Seth and A. Frontera, Importance of R-CF3···O Tetrel Bonding Interactions in Biological Systems, *J. Phys. Chem. A*, **2017**, *121*, 5371–5376.

[181] C. Bhatia, W. W. Yue, F. Niesen, E. Pilka, E. Ugochukwu, P. Savitsky, V. Hozjan, A. K. Roos, P. Filippakopoulos, F. Von Delft, T. Heightman, C. Arrowsmith, J. Weigelt, A. Edwards, C. Bountra and U. Opperman, *Protein Data Bank*, **2009**.
[182] J. Fried and E. F. Sabo, 9α-Fluoro Derivatives of Cortisone and Hydrocortisone, *J. Am. Chem. Soc.*, **1954**, *76*, 1455–1456.
[183] A. Vulpetti and C. Dalvit, Fluorine local environment: from screening to drug design, *Drug Discov. Today*, **2012**, *17*, 890–897.
[184] S. Purser, P. R. Moore, S. Swallow and V. Gouverneur, Fluorine in medicinal chemistry, *Chem. Soc. Rev.*, **2008**, *37*, 320–330.
[185] W. K. Hagmann, The Many Roles for Fluorine in Medicinal Chemistry, *J. Med. Chem.*, **2008**, *51*, 4359–4369.
[186] K. B. Park, N. R. Kitteringham and P. M. O'Neill, Metabolism of Flourine-Containing Drugs, *Annu. Rev. Pharmacol. Toxicol.*, **2001**, *41*, 443–470.
[187] H. S. Gutowsky, B. R. McCall, B. R. Mcgarvey and L. H. Meyer, Electron Distribution in Molecules. I. F19 Nuclear Magnetic Shielding and Substituent Effects in Some Benzene Derivatives, *J. Am. Chem. Soc.*, **1952**, *74*, 4809–4817.
[188] W. R. Dolbier Jr, *Guide to fluorine NMR for organic chemists*, John Wiley & Sons, Inc., Hoboken, New Jersey, 1st edn., **2009**.
[189] J. T. Gerig, Fluorine nuclear magnetic resonance of fluorinated ligands, *Methods Enzymol.*, **1989**, *177*, 3–23.
[190] C. Dalvit and M. Piotto, 19F NMR transverse and longitudinal relaxation filter experiments for screening: a theoretical and experimental analysis, *Magn. Reson. Chem.*, **2017**, *55*, 106–114.
[191] T. Tengel, T. Fex, H. Emtenäs, F. Almqvist, I. Sethson and J. Kihlberg, Use of 19F NMR spectroscopy to screen chemical libraries for ligands that bind to proteins, *Org. Biomol. Chem.*, **2004**, *2*, 725–731.
[192] C. Dalvit and S. Knapp, 19F NMR isotropic chemical shift for efficient screening of fluorinated fragments which are racemates and/or display multiple conformers, *Magn. Reson. Chem.*, **2017**, 1091–1095.
[193] C. Dalvit and A. Vulpetti, Ligand-Based Fluorine NMR Screening: Principles and Applications in Drug Discovery Projects, *J. Med. Chem.*, **2019**, *62*, 2218–2244.
[194] A. D. Gossert and W. Jahnke, NMR in drug discovery: A practical guide to identification and validation of ligands interacting with biological macromolecules, *Prog. Nucl. Magn. Reson. Spectrosc.*, **2016**, *97*, 82–125.
[195] A. Vulpetti, U. Hommel, G. Landrum, R. Lewis and C. Dalvit, Design and Application of LEF , a library of chemical fragments with different Local Environment of Fluorine, *J. Am. Chem. Soc.*, **2009**, *131*, 12949–12959.
[196] LifeChemicals, Fluorine Fragment Cocktails, https://lifechemicals.com/screening-libraries/fragment-libraries, (accessed 14 March 2017).
[197] A. Divakaran, S. E. Kirberger and W. C. K. Pomerantz, SAR by (Protein-Observed) 19F NMR, *Acc. Chem. Res.*, **2019**, *52*, 3407–3418.
[198] R. Vorberg, E. M. Carreira and K. Müller, Aqueous Instability of δ-Fluorobutylpiperidines, *ChemMedChem*, **2017**, *12*, 431–437.
[199] M. Janjetovic, A. Ekebergh, A. M. Träff and G. Hilmersson, Catalytic Iodination of the Aliphatic C–F Bond by YbI3(THF)3: Mechanistic Insight and Synthetic Utility, *Org. Lett.*, **2016**, *18*, 2804–2807.
[200] M. Janjetovic, A. M. Träff and G. Hilmersson, Mild and selective activation and substitution of strong aliphatic C-F bonds, *Chem. - A Eur. J.*, **2015**, *21*, 3772–3777.

[201] A. M. Träff, M. Janjetovic, L. Ta and G. Hilmersson, Selective C-F bond activation: Substitution of unactivated alkyl fluorides using YbI3, *Angew. Chemie - Int. Ed.*, **2013**, *52*, 12073–12076.
[202] Y. Mizukami, Z. Song and T. Takahashi, Halogen Exchange Reaction of Aliphatic Fluorine Compounds with Organic Halides as Halogen Source, *Org. Lett.*, **2015**, *17*, 5942–5945.
[203] R. Hemelaere, P. A. Champagne, J. Desroches and J. F. Paquin, Faster initiation in the Friedel-Crafts reaction of benzyl fluorides using trifluoroacetic acid as activator, *J. Fluorine Chem.*, **2016**, *190*, 1–6.
[204] P. A. Champagne, Y. Benhassine, J. Desroches and J. F. Paquin, Friedel-crafts reaction of benzyl fluorides: Selective activation of C-f bonds as enabled by hydrogen bonding, *Angew. Chemie - Int. Ed.*, **2014**, *53*, 13835–13839.
[205] A. Vulpetti and C. Dalvit, Design and generation of highly diverse fluorinated fragment libraries and their efficient screening with improved 19F NMR methodology, *ChemMedChem*, **2013**, *8*, 2057–2069.
[206] W. A. Sheppard, Arylsulfur Trifluorides and Pentafluorides, *J. Am. Chem. Soc.1*, **1960**, *82*, 4751–4752.
[207] A. Zawadzka-Kazimierczuk, M. Somlyay, H. Kaehlig, G. Iakobson, P. Beier and R. Konrat, 19F multiple-quantum coherence NMR spectroscopy for probing protein–ligand interactions, *RSC Adv.*, **2018**, *8*, 40687–40692.
[208] A. Harsanyi and G. Sandford, Organofluorine chemistry: Applications, sources and sustainability, *Green Chem.*, **2015**, *17*, 2081–2086.
[209] C. N. Neumann and T. Ritter, Late-stage fluorination: Fancy novelty or useful tool?, *Angew. Chemie - Int. Ed.*, **2015**, *54*, 3216–3221.
[210] N. Al-Maharik and D. O'Hagan, Organofluorine chemistry. Deoxyfluorination reagents for C-F bond synthesis, *Aldrichim. Acta*, **2011**, *44*, 65–75.
[211] P. K. Guha, R. Poi and A. Bhattacharyya, An Imide from the Pods of Butea-Monosperma, *Phytochemistry*, **1990**, *29*, 2017.
[212] M. Suzuki, M. Daitoh, C. S. Vairappan, A. Tsuyoshi and M. Masuda, Novel halogenated metabolites from the Malaysian Laurencia pannosa, *J. Nat. Prod.*, **2001**, *64*, 597–602.
[213] S. M. Waraszkiewicz, H. H. Sun, K. L. Erickson, J. Finer and J. Clardy, C15 Halogenated Compounds from the Hawaiian Marine Alga Laurencia nidifica. Maneonenes and Isomaneonenes, *J. Org. Chem.*, **1978**, *43*, 3194–3204.
[214] Y. Li and J. E. Casida, Cantharidin-Binding Protein: Identification as Protein Phosphatase 2A, *Proc. Natl. Acad. Sci. U.S.A.*, **1992**, *89*, 11867–11870.
[215] O. Diels and K. Alder, Synthesen in der hydroaromatischen Reihe, *Justus Liebigs Ann. Chem.*, **1928**, *460*, 98–122.
[216] E. T. McBee, C. G. Hsu and C. W. Roberts, Stereochemistry of the Diels-Alder Reaction. I. 4,4,4-Trifluorocrotonic Acid as Dienophile, *J. Am. Chem. Soc.*, **1956**, *78*, 3389–3392.
[217] W. J. Zuercher, M. Hashimoto and R. H. Grubbs, Tandem ring opening-ring closing metathesis of cyclic olefins, *J. Am. Chem. Soc.*, **1996**, *118*, 6634–6640.
[218] S. B. Garber, J. S. Kingsbury, B. L. Gray and A. H. Hoveyda, Efficient and recyclable monomeric and dendritic Ru-based metathesis catalysts, *J. Am. Chem. Soc.*, **2000**, *122*, 8168–8179.
[219] V. VanRheenen, R. C. Kelly and D. Y. Cha, An improved catalytic OsO4 oxidation of olefins to cis-1,2-glycols using tertiary amine oxides as the oxidant., *Tetrahedron Lett.*, **1976**, *23*, 1973–1976.

[220] O. Mitsunobu and M. Yamada, Preparation of Esters of Carboxylic and Phosphoric Acid via Quaternary Phosphonium Salts, *Bull. Chem. Soc. Jpn.*, **1967**, *40*, 2380–2382.
[221] W. L. Jorgensen and J. Gao, Cis-Trans Energy Difference for the Peptide Bond in the Gas Phase and in Aqueous Solution, *J. Am. Chem. Soc.*, **1988**, *110*, 4212–4216.
[222] T. F. Spande, H. M. Garraffo, M. W. Edwards, H. J. C. Yeh, L. Pannell and J. W. Daly, Epibatidine: A Novel (Chloropyridyl)azabicycloheptane with Potent Analgesic Activity from an Ecuadoran Poison Frog, *J. Am. Chem. Soc.*, **1992**, *114*, 3475–3478.
[223] B. Badio, H. M. Garraffo, C. V. Plummer, W. L. Padgett and J. W. Daly, Synthesis and nicotinic activity of epiboxidine: an isoxazole analogue of epibatidine, *Eur. J. Pharmacol.*, **1997**, *321*, 189–194.
[224] D. Sesardic, A. R. Boobis, B. P. Murray, S. Murray, J. Segura, R. Delatorre and D. S. Davies, Furafylline is a Potent and Selective Inhibitor of Cytochrome-P450IA2 in Man, *Br. J. Clin. Pharmacol.*, **1990**, *29*, 651–663.
[225] G. Grynkiewicz and M. Gadzikowska, Tropane alkaloids as medicinally useful natural products and their synthetic derivatives as new drugs, *Pharmacol. Reports*, **2008**, *60*, 439–463.
[226] Z. Mucsi, B. Viskolcz and I. G. Csizmadia, A quantitative scale for the degree of aromaticity and antiaromaticity: A comparison of theoretical and experimental enthalpies of hydrogenation, *J. Phys. Chem. A*, **2007**, *111*, 1123–1132.
[227] J. Gonzalez, J. I. Koontz, L. M. Hodges, K. R. Nilsson, M. Sabat, W. D. Harman, L. K. Neely and W. H. Myers, Osmium-Promoted Dipolar Cycloadditions with Pyrroles: An Efficient, Stereoselective Synthesis of 7-Azanorbornanes, *J. Am. Chem. Soc.*, **1995**, *117*, 3405–3421.
[228] A. T. Murray, E. Packard, A. Nortcliffe, W. Lewis, D. Hamza, G. Jones and C. J. Moody, Synthesis of Epibatidine Analogues by Pyrrole Diels–Alder Reactions: Rapid Access to Azabicyclo[2.2.1]heptane and 3,8-Diazabicyclo[3.2.1]octane Scaffolds for Library Synthesis, *Eur. J. Org. Chem.*, **2017**, *2017*, 138–148.
[229] A. O. King, R. D. Larsen and E. Negishi, in *Handbook of Organopalladium Chemistry for Organic Synthesis*, ed. E. Negishi, John Wiley & Sons, Inc., 1st edn., **2002**, pp. 2719–2752.
[230] J. B. He, J. Luo, L. Zhang, Y. M. Yan and Y. X. Cheng, Sesquiterpenoids with new carbon skeletons from the resin of Toxicodendron vernicifluum as new types of extracellular matrix inhibitors, *Org. Lett.*, **2013**, *15*, 3602–3605.
[231] H. Ogura, H. Takayanagi, A. Yoshino and T. Okamoto, Ambrosic Acid, a New Irritant Principle from Ambrosia arthemisiifolia, *Chem. Pharm. Bull.*, **1974**, *22*, 1435–1437.
[232] J. Y. Su, Y. Y. Kuang and L. M. Zeng, Two new marine sesquiterpenes, *Acta Chim. Sin.*, **2003**, *61*, 1097–1100.
[233] Z. Y. Jiang, J. Zhou, C. G. Huang, Q. F. Hu, X. Z. Huang, W. Wang, L. Z. Zhang, G. P. Li and F. T. Xia, Two novel antiviral terpenoids from the cultured Perovskia atriplicifolia, *Tetrahedron*, **2015**, *71*, 3844–3849.
[234] K. E. O. Ylijoki and J. M. Stryker, [5 + 2] Cycloaddition Reactions in Organic and Natural Product Synthesis, *Chem. Rev.*, **2013**, *113*, 2244–2266.
[235] C. Meck, N. Mohd and R. P. Murelli, An oxidopyrylium cyclization/ring-opening route to polysubstituted α-hydroxytropolones, *Org. Lett.*, **2012**, *14*, 5988–5991.
[236] E. Nogueira, E. Guitián, L. Castedo and A. Castiñeiras, Tandem Benzyne Cycloadditions Leading to Polycyclic Compounds, *Aust. J. Chem.*, **1997**, *50*, 751–754.
[237] P. G. Sammes, L. J. Street and P. Kirby, Preparation and properties of some phytotoxic 2-benzyloxy-8-oxa bicycle[3.2.1]octane derivatives, *J. Chem. Soc. Perkin Trans. 1*, **1983**, 2729–2734.

[238] P. A. Wender and J. L. Mascarenas, Preparation and cycloadditions of a 4-methoxy-3-oxidopyrylium ylid: A reagent for the synthesis of highly substituted seven-membered rings and tetrahydrofurans, *Tetrahedron Lett.*, **1992**, *33*, 2115–2118.
[239] S. Fakih, M. Podinovskaia, X. Kong, H. L. Collins, U. E. Schaible and R. C. Hider, Targeting the lysosome: Fluorescent iron(III) chelators to selectively monitor endosomal/ lysosomal labile iron pools, *J. Med. Chem.*, **2008**, *51*, 4539–4552.
[240] J. L. Mascarenas, I. Perez, A. Rumbo and L. Castedo, A New [5 + 2] Annulation Method for the Synthesis of 8-Oxabicyclo[3.2.1]octanes from Pyrones, *J. Org. Chem.*, **1997**, *1*, 81–82.
[241] H. Guo, D. Roman and C. Beemelmanns, Tropolone natural products, *Nat. Prod. Rep.*, **2019**, *36*, 1137–1155.
[242] V. Grignard, Sur quelques nouvelles combinaisons organométaliques du magnésium et leur application à des synthèses d'alcools et d'hydrocabures, *Compt. Rend.*, **1900**, *130*, 1322–1325.
[243] K. Takasu, M. Ueno, K. Inanaga and M. Ihara, Catalytic [2+2]-Cycloaddition Reactions of Silyl Enol Ethers. A Convenient and Stereoselective Method for Cyclobutane Ring Formation, *J. Org. Chem.*, **2004**, *69*, 517–521.
[244] M. Kashiwabara, T. Kamo, H. Makabe, H. Shibata and M. Hirota, Repraesentins D, E and F, New Plant Growth Promoters from Lactarius repraesentaneus, *Biosci., Biotechnol., Biochem.*, **2006**, *70*, 1502–1505.
[245] Y. Shiono, H. Akasaka, F. Hiramatsu, K. Sato, T. Murayama and M. Ikeda, Three sesquiterpenoids, fascicularones E, F, and G produced by the fungus Hypholoma fasciculare, *Zeitschrift Fûr Naturforsch. B*, **2005**, *60*, 880–884.
[246] K. Kurata, M. Suzuki, K. Shiraishi and K. Taniguchi, Diterpenes With Biological Activity From the Brown Alga Dilophus Okamurai, *Phytochemistry*, **1988**, *27*, 1321–1324.
[247] K. Ohashi, M. Kawai, N. Ninomiya, C. Taylor and Y. Kurebayashi, Effect of a new α2δ ligand PD-217014 on visceral hypersensitivity induced by 2,4,6-trinitrobenzene sulfonic acid in rats, *Pharmacology*, **2008**, *81*, 144–150.
[248] M. Franck-Neumann, M. Miesch and L. Gross, The bicyclo [2.1.0] pentane way to the diquinane alcohol part of natural triquinanes. A high yield access starting from trimethylsilyloxycyclopentene., *Tetrahedron Lett.*, **1990**, *31*, 5027–5030.
[249] Y. Okazaki, A. Ishizuka, A. Ishihara, T. Nishioka and H. Iwamura, New dimeric compounds of avenanthramide phytoalexin in oats, *J. Org. Chem.*, **2007**, *72*, 3830–3839.
[250] A. Yang, L. Si, Z. Shi, L. Tian, D. Liu, D. Zhou, P. Proksch and W. Lin, Nitrosporeusines A and B, unprecedented thioester-bearing alkaloids from the arctic streptomyces nitrosporeus, *Org. Lett.*, **2013**, *15*, 5366–5369.
[251] S. Brooks, G. Jacobs, P. de Boer, J. Kent, L. Van Nueten, G. van Amerongen, R. Zuiker, I. Kezic, R. Luthringer, P. van der Ark, J. van Gerven and W. Drevets, The selective orexin-2 receptor antagonist seltorexant improves sleep: An exploratory double-blind, placebo controlled, crossover study in antidepressant-treated major depressive disorder patients with persistent insomnia, *J. Psychopharmacol.*, **2019**, *33*, 202–209.
[252] W. E. Sweeney, P. Frost and E. Avner, Tesevatinib ameliorates progression of polycystic kidney disease in rodent models of autosomal recessive polycystic kidney disease, *World J. Nephrol.*, **2017**, *6*, 188–200.
[253] L. M. Blair and J. Sperry, Natural Products Containing a Nitrogen−Nitrogen Bond, *J. Nat. Prod.*, **2013**, *76*, 794–812.

[254] R. Kirsten, K. H. Molz, I. Tzonev and K. Nelson, Clinical-Evaluation of Muzolimine and Indapamide During Treatment for Essential-Hypertension, *Zeitschrift Fur Kardiol.*, **1985**, *74*, 66–72.
[255] R. A. Maurya, J. S. Kapure, P. R. Adiyala, P. S. Srikanth, D. Chandrasekhar and A. Kamal, Catalyst-free stereoselective cyclopropanation of electron deficient alkenes with ethyl diazoacetate, *RSC Adv.*, **2013**, *3*, 15600–15603.
[256] J. Riss, J. Cloyd, J. Gates and S. Collins, Benzodiazepines in epilepsy: Pharmacology and pharmacokinetics, *Acta Neurol. Scand.*, **2008**, *118*, 69–86.
[257] M. Chaffman and R. N. Brogden, Diltiazem : A Review of its Pharmacological Properties and Therapeutic Efficacy, *Drugs*, **1985**, *29*, 387–454.
[258] P. J. Zhao, G. H. Li and Y. M. Shen, New chemical constituents from the endophyte Streptomyces species LR4612 cultivated on Maytenus hookeri, *Chem. Biodivers.*, **2006**, *3*, 337–342.
[259] W. Maison, in *Amine N-Oxides, Haloamines, Hydroxylamines and Sulfur Analogues, and Hydrazines*, eds. D. Enders and E. Schaumann, George Thieme Verlag KG, **2009**, pp. 1211–1252.
[260] T. Tobin, S. Chay, S. Kamerling, W. E. Woods, T. J. Weckman, J. W. Blake and P. Lees, Phenylbutazone in the horse : a review, *J. Vet. Pharmacol. Ther.*, **1986**, *9*, 1–25.
[261] C. J. Jones, The pharmacology and pharmacokinetics of azapropazone - a review, *Curr Med Res Opin.*, **1976**, *4*, 3–16.
[262] S. Lin, M. Li, Z. Dong, F. Liang and J. Zhang, Hypervalent iodine(III)-mediated cyclopropa(e)nation of alkenes/alkynes under mild conditions, *Org. Biomol. Chem.*, **2014**, *12*, 1341–1350.
[263] G. W. Bemis and M. A. Murcko, The Properties of Known Drugs. 1. Molecular Frameworks, *J. Med. Chem.*, **1996**, *39*, 2887–2893.
[264] P. Ertl, S. Roggo and A. Schuffenhauer, Natural Product-likeness Score and Its Application for Prioritization of Compound Libraries, *J. Chem. Inf. Model.*, **2008**, *48*, 68–74.
[265] K. V Jayaseelan, P. Moreno, A. Truszkowski, P. Ertl and C. Steinbeck, Natural product-likeness score revisited: an open-source, open-data implementation, *BMC Bioinforma.*, **2012**, *13*, 106–111.
[266] J. J. Irwin and B. K. Shoichet, ZINC - A free database of commercially available compounds for virtual screening., *J. Chem. Inf. Model.*, **2005**, *45*, 177–182.
[267] C. Dalvit, D. Caronni, N. Mongelli, M. Veronesi and A. Vulpetti, NMR-Based Quality Control Approach for the Identification of False Positives and False Negatives in High Throughput Screening, *Curr. Drug Discovery Technol.*, **2006**, *3*, 115–124.
[268] U. Kragh-Hansen, V. T. G. Chuang and M. Otagiri, Practical Aspects of the Ligand-Binding and Enzymatic Properties of Human Serum Albumin, *Biol. Pharm. Bull.*, **2002**, *25*, 695–704.
[269] R. Anjum and J. Blenis, The RSK family of kinases: emerging roles in cellular signalling., *Nat. Rev. Mol. cell Biol.*, **2008**, *9*, 747–58.
[270] N. Pullen and G. Thomas, The modular phosphorylation and activation of p70(s6k), *FEBS Lett.*, **1997**, *410*, 78–82.
[271] C. K. M. Ip and A. S. T. Wong, Exploiting p70 S6 kinase as a target for ovarian cancer., *Expert Opin. Ther. Targets*, **2012**, *16*, 619–660.
[272] Z.-X. Qiu, R.-F. Sun, X.-M. Mo and W.-M. Li, The p70S6K Specific Inhibitor PF-4708671 Impedes Non-Small Cell Lung Cancer Growth, *PLoS One*, **2016**, *11*, 1–11.

[273] K. D. Rice, M. H. Kim, J. Bussenius, N. K. Anand, C. M. Blazey, O. J. Bowles, L. Canne-Bannen, D. S. M. Chan, B. Chen, E. W. Co, S. Costanzo, S. C. Defina, L. Dubenko, S. Engst, M. Franzini, P. Huang, V. Jammalamadaka, R. G. Khoury, R. R. Klein, A. D. Laird, D. T. Le, M. B. Mac, D. J. Matthews, D. Markby, N. Miller, J. M. Nuss, J. J. Parks, T. H. Tsang, A. L. Tsuhako, Y. Wang and W. Xu, Pyrazolopyrimidines as dual Akt/p70S6K inhibitors, *Bioorganic Med. Chem. Lett.*, **2012**, *22*, 2693–2697.

[274] A. D. Abdullahi, A. M. Abdualkader, N. H. A. Samat, F. Mohamed, B. Y. Muhammad, H. A. Mohammed, A. Aljarbou and A. Kasmuri, Novel insight into the structural requirements of P70S6K inhibition using group-based quantitative structure activity relationship (GQSAR), *J. Appl. Pharm. Sci.*, **2014**, *4*, 16–24.

[275] A. Cuenda and J. J. Sanz-Ezquerro, p38γ and p38δ: From Spectators to Key Physiological Players, *Trends Biochem. Sci.*, **2017**, *42*, 431–442.

[276] D. J. Selkoe and J. Hardy, The amyloid hypothesis of Alzheimer's disease at 25 years, *EMBO Mol. Med.*, **2016**, *8*, 595–608.

[277] R. Yan and R. Vassar, Targeting the β secretase BACE1 for Alzheimer's disease therapy, *Lancet Neurol.*, **2014**, *13*, 319–329.

[278] H. Cai, Y. Wang, D. McCarthy, H. Wen, D. R. Borchelt, D. L. Price and P. C. Wong, BACE1 is the major β-secretase for generation of Ab peptides by neurons, *Nat. Neurosci.*, **2001**, *4*, 233–234.

[279] A. K. Ghosh and H. L. Osswald, BACE1 (β-secretase) inhibitors for the treatment of Alzheimer's disease, *Chem. Soc. Rev.*, **2014**, *43*, 6765–6813.

[280] T. B. H. Geijtenbeek, R. Torensma, S. J. Van Vliet, G. C. F. Van Duijnhoven, G. J. Adema, Y. Van Kooyk and C. G. Figdor, Identification of DC-SIGN, a novel dendritic cell-specific ICAM-3 receptor that supports primary immune responses, *Cell*, **2000**, *100*, 575–585.

[281] J. J. García-Vallejo, J. M. Ilarregui, H. Kalay, S. Chamorro, N. Koning, W. W. Unger, M. Ambrosini, V. Montserrat, R. J. Fernandes, S. C. M. Bruijns, J. R. T. van Weering, N. J. Paauw, T. O'Toole, J. van Horssen, P. van der Valk, K. Nazmi, J. G. M. Bolscher, J. Bajramovic, C. D. Dijkstra, B. A. 't Hart and Y. van Kooyk, CNS myelin induces regulatory functions of DC-SIGN-expressing, antigen-presenting cells via cognate interaction with MOG, *J. Exp. Med.*, **2014**, *211*, 1465–1483.

[282] N. Cox, D. Pilling, R. H. Gomer and J. V. Ravetch, DC-SIGN activation mediates the differential effects of SAP and CRP on the innate immune system and inhibits fibrosis in mice, *Proc. Natl. Acad. Sci. U.S.A.*, **2015**, *112*, 8385–8390.

[283] P. Conde, M. Rodriguez, W. van der Touw, A. Jimenez, M. Burns, J. Miller, M. Brahmachary, H. M. Chen, P. Boros, F. Rausell-Palamos, T. J. Yun, P. Riquelme, A. Rastrojo, B. Aguado, J. Stein-Streilein, M. Tanaka, L. Zhou, J. Zhang, T. L. Lowary, F. Ginhoux, C. G. Park, C. Cheong, J. Brody, S. J. Turley, S. A. Lira, V. Bronte, S. Gordon, P. S. Heeger, M. Merad, J. Hutchinson, S. H. Chen and J. Ochando, DC-SIGN(+) Macrophages Control the Induction of Transplantation Tolerance, *Immunity*, **2015**, *42*, 1143–1158.

[284] T. B. Geijtenbeek, D. S. Kwon, R. Torensma, S. J. van Vliet, G. C. van Duijnhoven, J. Middel, I. L. Cornelissen, H. S. Nottet, V. N. KewalRamani, D. R. Littman, C. G. Figdor and Y. van Kooyk, DC-SIGN, a dendritic cell-specific HIV-1-binding protein that enhances trans-infection of T cells, *Cell*, **2000**, *100*, 587–597.

[285] Y. Kuma, G. Sabio, J. Bain, N. Shpiro, R. Márquez and A. Cuenda, BIRB796 inhibits all p38 MAPK isoforms in vitro and in vivo, *J. Biol. Chem.*, **2005**, *280*, 19472–19479.

[286] J. B. Jordan, L. Poppe, X. Xia, A. C. Cheng, Y. Sun, K. Michelsen, H. Eastwood, P. D. Schnier, T. Nixey and W. Zhong, Fragment Based Drug Discovery: Practical Implementation Based on 19 F NMR Spectroscopy, *J. Med. Chem.*, **2012**, *55*, 678–687.
[287] E. C. Wamhoff, J. Hanske, L. Schnirch, J. Aretz, M. Grube, D. Varón Silva and C. Rademacher, 19F NMR-Guided Design of Glycomimetic Langerin Ligands, *ACS Chem. Biol.*, **2016**, *11*, 2407–2413.
[288] J. Aretz, H. Baukmann, E. Shanina, J. Hanske, R. Wawrzinek, V. A. Zapol'skii, P. H. Seeberger, D. E. Kaufmann and C. Rademacher, Identification of Multiple Druggable Secondary Sites by Fragment Screening against DC-SIGN, *Angew. Chemie - Int. Ed.*, **2017**, *56*, 7292–7296.
[289] J. A. Johnson, C. A. Nicolaou, S. E. Kirberger, A. K. Pandey, H. Hu and W. C. K. Pomerantz, Evaluating the Advantages of Using 3D-Enriched Fragments for Targeting BET Bromodomains, *ACS Med. Chem. Lett.*, **2019**, *10*, 1648–1654.
[290] S. J. Pollack, K. S. Beyer, C. Lock, I. Müller, D. Sheppard, M. Lipkin, D. Hardick, P. Blurton, P. M. Leonard, P. A. Hubbard, D. Todd, C. M. Richardson, T. Ahrens, M. Baader, D. O. Hafenbradl, K. Hilyard and R. W. Bürli, A comparative study of fragment screening methods on the p38α kinase: New methods, new insights, *J. Comput.-Aided Mol. Des.*, **2011**, *25*, 677–687.
[291] Y. Sen Wang, C. Strickland, J. H. Voigt, M. E. Kennedy, B. M. Beyer, M. M. Senior, E. M. Smith, T. L. Nechuta, V. S. Madison, M. Czarniecki, B. A. McKittrick, A. W. Stamford, E. M. Parker, J. C. Hunter, W. J. Greenlee and D. F. Wyss, Application of fragment-based NMR screening, X-ray crystallography, structure-based design, and focused chemical library design to identify novel μM leads for the development of nM BACE-1 (β-site APP cleaving enzyme 1) inhibitors, *J. Med. Chem.*, **2010**, *53*, 942–950.
[292] J. R. M. Coimbra, D. F. F. Marques, S. J. Baptista, C. M. F. Pereira, P. I. Moreira, T. C. P. Dinis, A. E. Santos and J. A. R. Salvador, Highlights in BACE1 inhibitors for Alzheimer's disease treatment, *Front. Chem.*, **2018**, *6*, 178.
[293] J. Aretz, E. C. Wamhoff, J. Hanske, D. Heymann and C. Rademacher, Computational and experimental prediction of human C-type lectin receptor druggability, *Front. Immunol.*, **2014**, *5*, 323.
[294] E. J. Corey, Catalytic Enantioselective Diels-Alder Reactions: Methods, Mechanistic Fundamentals, Pathways, and Applications, *Angew. Chem., Int. Ed.*, **2002**, *41*, 1650–1667.
[295] K. Shibatomi, F. Kobayashi, A. Narayama, I. Fujisawa and S. Iwasa, A Diels-Alder approach to the enantioselective construction of fluoromethylated stereogenic carbon centers, *Chem. Commun.*, **2012**, *48*, 413–415.
[296] T. Hashimoto and K. Maruoka, Recent Advances of Catalytic Asymmetric 1,3-Dipolar Cycloadditions, *Chem. Rev.*, **2015**, *115*, 5366–5412.
[297] K. Gao, Y. G. Zhang, Z. Wang and H. Ding, Recent development on the [5+2] cycloadditions and their application in natural product synthesis, *Chem. Commun.*, **2019**, *55*, 1859–1878.
[298] D. Enders, C. Wang and J. X. Liebich, Organocatalytic asymmetric aza-Michael additions, *Chem. - A Eur. J.*, **2009**, *15*, 11058–11076.
[299] P. Hu, H. M. Chi, K. C. DeBacker, X. Gong, J. H. Keim, I. T. Hsu and S. A. Snyder, Quaternary-centre-guided synthesis of complex polycyclic terpenes, *Nature*, **2019**, *569*, 703–707.
[300] Y. Liu, S. J. Han, W. B. Liu and B. M. Stoltz, Catalytic Enantioselective Construction of Quaternary Stereocenters: Assembly of Key Building Blocks for the Synthesis of Biologically Active Molecules, *Acc. Chem. Res.*, **2015**, *48*, 740–751.

[301] C. Li, S. S. Ragab, G. Liu and W. Tang, Enantioselective formation of quaternary carbon stereocenters in natural product synthesis: a recent update, *Nat. Prod. Rep.*, **2020**, DOI:10.1039/c9np00039a.
[302] C. J. Douglas and L. E. Overmant, Catalytic asymmetric synthesis of all-carbon quaternary stereocenters, *Proc. Natl. Acad. Sci. U.S.A.*, **2004**, *101*, 5363–5367.
[303] H. Zheng, Y. Wang, C. Xu, X. Xu, L. Lin, X. Liu and X. Feng, Stereodivergent synthesis of vicinal quaternary-quaternary stereocenters and bioactive hyperolactones, *Nat. Commun.*, **2018**, *9*, 1968–1974.
[304] D. W. Brooks, P. G. Grothaus and W. L. Irwin, Chiral Cyclopentanoid Synthetic Intermediates via Asymmetric Microbial Reduction of Prochiral 2,2-Disubstituted Cyclopentanediones, *J. Org. Chem.*, **1982**, *47*, 2820–2821.
[305] B. Sun and X. Xu, General synthetic approach to bicyclo[9.3.0]tetradecenone: A versatile intermediate to clavulactone and clavirolides, *Tetrahedron Lett.*, **2005**, *46*, 8431–8434.
[306] C. L. Hugelshofer and T. Magauer, A Divergent Approach to the Marine Diterpenoids (+)-Dictyoxetane and (+)-Dolabellane V, *Chem. - A Eur. J.*, **2016**, *22*, 15125–15136.
[307] A. R. Hanby, N. S. Troelsen, T. Osberger, S. L. Kidd, K. T. Mortensen and D. R. Spring, Fsp3-Rich and Diverse Fragments Inspired by Natural Products as a Collection to Enhance Fragment-Based Drug Discovery, *Chem. Commun.*, **2020**, *56*, 2280–2283.
[308] I. U. Khand, G. R. Knox, P. L. Pauson, W. E. Watts and M. I. Foreman, Organocobalt complexes II. Reaction of acetylenehexacarbonyl dicobalt complexes, (RC2R1)Co2(CO)6 with norbornene and its derivatives, *J. Chem. Soc., Perkin Trans. 1*, **1973**, 977–981.
[309] M. Ahmar, F. Antras and B. Cazes, Pauson-Khand reaction of activated olefins, *Tetrahedron Lett.*, **1999**, *40*, 5503–5506.
[310] T. Holm, Use of Competition Kinetics with Fast Reactions of Grignard Reagents, *J. Org. Chem.*, **2000**, *65*, 1188–1192.
[311] C. Mannich and W. Krösche, Ueber ein Kondensationsprodukt aus Formaldehyd, Ammoniak und Antipyrin, *Arch. der Pharm.*, **1912**, *250*, 647–667.
[312] Y. S. Hon, T. R. Hsu, C. Y. Chen, Y. H. Lin, F. J. Chang, C. H. Hsieh and P. H. Szu, Dibromomethane as one-carbon source in organic synthesis: Microwave-accelerated α-methylenation of ketones with dibromomethane and diethylamine, *Tetrahedron*, **2003**, *59*, 1509–1520.
[313] S. J. Danishefsky and T. Kitahara, Useful diene for the Diels-Alder reaction, *J. Am. Chem. Soc.*, **1974**, *96*, 7807–7808.
[314] L. Zhang, X. Chen, P. Xue, H. H. Y. Sun, I. D. Williams, K. B. Sharpless, V. V. Fokin and G. Jia, Ruthenium-Catalyzed Cycloaddition of Alkynes and Organic Azides, *J. Am. Chem. Soc.*, **2005**, *127*, 15998–15999.
[315] K. C. Nicolaou, T. Montagnon, P. S. Baran and Y. L. Zhong, Iodine(V) reagents in organic synthesis. Part 4. o-Iodoxybenzoic acid as a chemospecific tool for single electron transfer-based oxidation processes, *J. Am. Chem. Soc.*, **2002**, *124*, 2245–2258.
[316] E. Beckmann, Zur Kenntniss der Isonitrosoverbindungen, *Berichte der Dtsch. Chem. Gesellschaft*, **1886**, *19*, 988–993.
[317] L. G. Donaruma and W. Z. Heldt, The Beckmann rearrangement, *Org. React.*, **1960**, *11*, 1–156.
[318] A. Baeyer and V. Villiger, Einwirkung des Caro'schen Reagens auf Ketone, *Berichte der Dtsch. Chem. Gesellschaft*, **1899**, *32*, 3625–3633.

[319] J. Mendiola, C. Mateos, J. F. Soriano, J. A. Rincón, Ó. De Frutos, J. K. Niemeier and E. M. Davis, Preparation, Use and Safety of O-Mesitylenesulfonylhydroxylamine (MSH), *Org. Process Res. Dev.*, **2009**, *13*, 263–267.
[320] S. Nicolai, C. Piemontesi and J. Waser, A palladium-catalyzed aminoalkynylation strategy towards bicyclic heterocycles: Synthesis of (±)-trachelanthamidine, *Angew. Chemie - Int. Ed.*, **2011**, *50*, 4680–4683.
[321] K. Takami, H. Yorimitsu and K. Oshima, Trans-Hydrometalation of Alkynes by a Combination of InCl3 and DIBAL-H: One-Pot Access to Functionalized (Z)-Alkenes, *Org. Lett.*, **2002**, *4*, 2993–2995.
[322] L. Jiang, G. E. Job, A. Klapars and S. L. Buchwald, Copper-catalyzed coupling of amides and carbamates with vinyl halides, *Org. Lett.*, **2003**, *5*, 3667–3669.
[323] G. Wittig and U. Schöllkopf, Über Triphenyl-phosphin-methylene als olefinbildende Reagenzien I, *Chem. Ber.*, **1954**, *87*, 1318–1330.
[324] G. Wittig and W. Haag, Über Triphenyl-phosphin-methylene als olefinbildende Reagenzien II, *Chem. Ber.*, **1955**, *88*, 1654–1666.
[325] G. Wittig and G. Geissler, Zur Reaktionsweise des Pentaphenyl-phosphors und einiger Derivate, *Justus Liebigs Ann. der Chemie*, **1953**, *580*, 44–57.
[326] L. Horner, H. Hoffmann and H. G. Wippel, Phosphororganische Verbindungen, XII. Phosphinoxyde als Olefinierungsreagenzien, *Chem. Ber.*, **1958**, *91*, 61–63.
[327] L. Horner, H. Hoffmann and H. G. Wippel, Phosphororganische Verbindungen, XX. Phosphinoxyde als Olefinierungsreagenzien, *Chem. Ber.*, **1959**, *92*, 2499–2505.
[328] D. H. Wadsworth and W. D. Emmons, The utility of phosphonate carbanions in olefin synthesis, *J. Am. Chem. Soc.*, **1961**, *83*, 1733–1738.
[329] M. Sono, T. Shoji, T. Tamaki, S. Kishi and M. Tori, The Stereochemistry of Electrolysis and Samarium Diiodide-Induced Cyclization between Carbonyl and Enone System in Inter- and Intramolecular Coupling, *Heterocycles*, **2007**, *72*, 517–528.
[330] K. Kato, A. Nishimura, Y. Yamamoto and H. Akita, Improved method for the synthesis of (E)-cyclic-β-alkoxyacrylates under mild conditions, *Tetrahedron Lett.*, **2001**, *42*, 4203–4205.
[331] J. Bredt, J. Houben and P. Levy, Ueber isomere Dehydrocamphersäuren, Lauronolsäuren und Bihydrolauro-Lactone, *Ber. Dtsch. Chem. Ges.*, **1902**, *35*, 1286–1292.
[332] J. Bredt, Über sterische Hinderung in Brückenringen (Bredtsche Regel) und über die meso-trans-Stellung in kondensierten Ringsystemen des Hexamethylens, *Justus Liebigs Ann. Chem.*, **1924**, *437*, 1–13.
[333] J. Y. W. Mak, R. H. Pouwer and C. M. Williams, Natural products with anti-bredt and bridgehead double bonds, *Angew. Chemie - Int. Ed.*, **2014**, *53*, 13664–13688.
[334] K. P. Kaliappan, V. Ravikumar and S. A. Pujari, Synthesis of a bicyclo[5.3.1]undecene by a facile domino enyne cross-metathesis/IMDA, *Tetrahedron Lett.*, **2006**, *47*, 981–984.
[335] V. V. Betkekar, A. A. Sayyad and K. P. Kaliappan, A domino enyne/IMDA approach to the core structure of (-) vinigrol, *Org. Lett.*, **2014**, *16*, 5540–5543.
[336] C. W. Tornøe, C. Christensen and M. Meldal, Peptidotriazoles on Solid Phase: [1,2,3]-Triazoles by Regiospecific Copper(I)-Catalyzed 1,3-Dipolar Cycloadditions of Terminal Alkynes to Azides, *J. Org. Chem.*, **2002**, *67*, 3057–3064.
[337] V. V. Rostovtsev, L. G. Green, V. V. Fokin and K. B. Sharpless, A stepwise huisgen cycloaddition process: Copper(I)-catalyzed regioselective 'ligation' of azides and terminal alkynes, *Angew. Chemie - Int. Ed.*, **2002**, *41*, 2596–2599.

[338] C. Baumgartner, S. Ma, Q. Liu and B. M. Stoltz, Efforts toward rapid construction of the cortistatin A carbocyclic core via enyne-ene metathesis, *Org. Biomol. Chem.*, **2010**, *8*, 2915–2917.
[339] H. Staudinger and J. Meyer, Über neue organische Phosphorverbindungen III. Phosphinmethylenderivate und Phosphinimine, *Helvetica*, **1919**, *2*, 635–646.
[340] S. Fustero, I. Ibáñez, P. Barrio, M. A. Maestro and S. Catalán, Gold-catalyzed intramolecular hydroamination of o-alkynylbenzyl carbamates: A route to chiral fluorinated isoindoline and isoquinoline derivatives, *Org. Lett.*, **2013**, *15*, 832–835.
[341] D. B. Ramachary and M. Kishor, Direct amino acid-catalyzed cascade biomimetic reductive alkylations: Application to the asymmetric synthesis of Hajos-Parrish ketone analogues, *Org. Biomol. Chem.*, **2008**, *6*, 4176–4187.
[342] B. M. Trost and Y. H. Rhee, A Ru catalyzed divergence: Oxidative cyclization vs. cycloisomerization of bis-homopropargylic alcohols, *J. Am. Chem. Soc.*, **2002**, *124*, 2528–2533.
[343] G. Karageorgis, D. J. Foley, L. Laraia and H. Waldmann, Principle and Design of Pseudo-Natural Products, *Nature Chem.*, **2020**, DOI: 10.1038/s41557-019-0411-x.
[344] K. Nakamura, R. Yamanaka, T. Matsuda and T. Harada, Recent developments in asymmetric reduction of ketones with biocatalysts, *Tetrahedron Asymmetry*, **2003**, *14*, 2659–2681.
[345] H. C. Brown, P. Ramachandran and P. Veeraraghavan, Asymmetric reduction with chiral organoboranes based on α-pinene, *Acc. Chem. Res.*, **1992**, *25*, 16–24.
[346] B. T. Cho, Recent advances in the synthetic applications of the oxazaborolidine-mediated asymmetric reduction, *Tetrahedron*, **2006**, *62*, 7621–7643.
[347] D. W. Brooks, H. Mazdiyasni and P. G. Grothaus, Asymmetric microbial reduction of prochiral 2,2,-disubstituted cycloalkanediones, *J. Org. Chem.*, **1987**, *52*, 3223–3232.
[348] G. M. Sheldrick, A short history of SHELX, *Acta Crystallogr.*, **2008**, *A64*, 112–122.
[349] O. Y. Lee, K. L. Law and D. Yang, Secondary amine formation from reductive amination of carbonyl compounds promoted by lewis acid using the InCl3 Et3SiH system, *Org. Lett.*, **2009**, *11*, 3302–3305.
[350] A. Palma, M. Artelsmair, G. Wu, X. Lu, S. J. Barrow, N. Uddin, E. Rosta, E. Masson and O. A. Scherman, Cucurbit[7]uril as a Supramolecular Artificial Enzyme for Diels–Alder Reactions, *Angew. Chemie - Int. Ed.*, **2017**, *56*, 15688–15692.
[351] Y. Nakajima, T. Inoue, K. Nakai, K. Mukoyoshi, H. Hamaguchi, K. Hatanaka, H. Sasaki, A. Tanaka, F. Takahashi, S. Kunikawa, H. Usuda, A. Moritomo, Y. Higashi, M. Inami and S. Shirakami, Synthesis and evaluation of novel 1H-pyrrolo[2,3-b]pyridine-5-carboxamide derivatives as potent and orally efficacious immunomodulators targeting JAK3, *Bioorg. Med. Chem.*, **2015**, *23*, 4871–4883.
[352] EPAM Systems, Indigo Toolkit, version 1.3.0 Beta, http://lifescience.opensource.epam.com/indigo/, (accessed 4 February 2019).
[353] G. Landrum, RDKit: Open-Source Cheminformatics Software, https://www.rdkit.org/, (accessed 4 February 2019).
[354] C. Y. C. Chen, TCM Database @ Taiwan: The World Largest Traditional Chinese Medicine Database for Drug Screening In Silico., *PLoS One*, **2011**, *6*, e15939.
[355] J. Gaulton, L. J. Bellis, A. P. Bento, J. Chambers, M. Davies, A. Hersey, Y. Light, S. McGlinchey, D. Michalovich, B. Al-Lazikani and J. P. Overington, ChEMBL: a large-scale bioactivity database for drug discovery, *Nucleic Acids Res.*, **2012**, *40*, 1100–1107.
[356] J. Bain, H. McLauchlan, M. Elliott and P. Cohen, The specificities of protein kinase inhibitors: An update, *Biochem. J.*, **2003**, *371*, 199–204.

[357] T. L. Hwang and A. J. Shaka, Water Suppression That Works. Excitation Sculpting Using Arbitrary Wave-Forms and Pulsed-Field Gradients, *J. Magn. Reson. Ser. A*, **1995**, *112*, 275–279.
[358] C. Dalvit, Efficient multiple-solvent suppression for the study of the interactions of organic solvents with biomolecules, *J. Biomol. NMR*, **1998**, *11*, 437–444.
[359] C. Dalvit, G. Fogliatto, A. Stewart, M. Veronesi and B. Stockman, WaterLOGSY as a method for primary NMR screening: practical aspects and range of applicability, *J. Biomol. NMR*, **2001**, *21*, 349–359.
[360] S. P. Davies, H. Reddy, M. Caivano and P. Cohen, Specificity and mechanism of action of some commonly used protein kinase inhibitors, *Biochem. J.*, **2000**, *351*, 95–105.
[361] C. E. Elliott, D. O. Miller and D. J. Burnell, Synthesis of 6-Alkyl Analogues of the 1-Azabicyclo[4.3.0]nonan-2-one System by a Strategy of Geminal Acylation and Beckmann Rearrangement., *J. Chem. Soc., Perkin Trans. 1*, **2002**, 217–226.
[362] G. J. Bernardes, J. M. Chalker, J. C. Errey and B. G. Davis, Facile conversion of cysteine and alkyl cysteines to dehydroalanine on protein surfaces: Versatile and switchable access to functionalized proteins, *J. Am. Chem. Soc.*, **2008**, *130*, 5052–5053.
[363] L. P. Bejcek, A. K. Garimallaprabhakaran, D. M. Suyabatmaz, A. Greer, W. H. Hersh, M. Greer, E and R. P. Murelli, Maltol- and Allomaltol-Derived Oxidopyrylium Ylides: Methyl Substitution Pattern Kinetically Influences [5+3] Dimerization versus [5+2] Cycloaddition Reactions, *J. Org. Chem.*, **2019**, *84*, 14670–14678.
[364] S. Jehle, H. Kovacs, T. Kuehn and A. Gossert, Fragment Screening by Ligand Observed NMR, https://www.theresonance.com/fragment-screening-by-ligand-observed-nmr/, (accessed 14 January 2019).

Appendix

Publications